STATE OF CALIFORNIA • DEPARTMENT OF TRANSPORTATION

TECHNICAL REPORT DOCUMENTATION PAGE

TR-0003 (REV 04/2024)

Lock Form

1. REPORT NUMBER	2. GOVERNMENT ASSOCIATION NUMBER	3. RECIPIENT'S CATALOG NUMBER
CA24-3917	N/A	N/A

4. TITLE AND SUBTITLE	5. REPORT DATE
Re-inventing Airport Land Use Planning in California: A Strategy for Updating the California Airport Land Use Planning Handbook Recommendations for Update of California Airport Land Use Handbook	05/31/2024
	6. PERFORMING ORGANIZATION CODE University of California, Berkeley
7. AUTHOR	8. PERFORMING ORGANIZATION REPORT NO.
Jasenka Rakas, Ph.D., and Sarah Lindbergh, Ph.D.	N/A
9. PERFORMING ORGANIZATION NAME AND ADDRESS University of California, Berkeley Institute for Transportation Studies 109 McLaughlin Hall, Berkeley, CA 94720	10. WORK UNIT NUMBER N/A
	11. CONTRACT OR GRANT NUMBER 65A0963 (Task 3917)
12. SPONSORING AGENCY AND ADDRESS California Department of Transportation P.O. Box 942873, MS #83 Sacramento, CA 94273-0001	13. TYPE OF REPORT AND PERIOD COVERED June 2022 to May 2024
	14. SPONSORING AGENCY CODE Caltrans

15. SUPPLEMENTARY NOTES

Principal Investigator Jasenka Rakas, Ph.D.
Lead Researcher Sarah Lindbergh, Ph.D.

16. ABSTRACT

This report is written in response to the State of California Department of Transportation (Caltrans), Division of Aeronautics, relating to the need to update the 2011 version of the California Airport Land Use Planning (ALUP) Handbook. The purpose of this technical report and its supplementary materials is to provide a robust scientific foundation for the final Handbook update publication for airport land use compatibility planning, which will be created soon by Caltrans.

In this study, optimized are visualizations of spatial distribution patterns of aviation accidents across 259 airports in California. Accident data by geographic coordinates are derived from the National Transportation Safety Board (NTSB) for 2008-2022. The accident database is analyzed through Geographic Information Systems (GIS) overlay and point pattern analysis. Results highlight a notable concentration of accidents near the borders between Zones 5 and 6, suggesting potential expansions of Zone 5 into Zone 6. This research contributes to airport land use compatibility strategies by proposing data-driven modifications to safety zones, enhancing their effectiveness in protecting airport vicinities from accidents.

17. KEY WORDS	18. DISTRIBUTION STATEMENT	
Unmanned Aircraft System (UAS), Urban Air Mobility (UAM), Land Use Planning, California Airport Land Use Planning Handbook, electric Vertical Take-off and Landing vehicles (eVTOLs), Safety, Risk, midair collisions, Drone incidents, Wildlife Strikes, Noise Exposure, Environmental Justice, Wind Analysis, Safety Zones Accident Density, Land Use Compatibility	No restrictions.	
19. SECURITY CLASSIFICATION *(of this report)*	20. NUMBER OF PAGES	21. COST OF REPORT CHARGED
Unclassified		N/A

Reproduction of completed page authorized.

ADA Notice This document is available in alternative accessible formats. For more information, please contact the Forms Management Unit at (279) 234-2284, TTY 711, in writing at Forms Management Unit, 1120 N Street, MS-89, Sacramento, CA 95814, or by email at Forms.Management.Unit@dot.ca.gov.

DISCLAIMER STATEMENT

This document is disseminated in the interest of information exchange. The contents of this report reflect the views of the authors who are responsible for the facts and accuracy of the data presented herein. The contents do not necessarily reflect the official views or policies of the State of California or the Federal Highway Administration. This publication does not constitute a standard, specification or regulation. This report does not constitute an endorsement by the Department of any product described herein.

For individuals with sensory disabilities, this document is available in alternate formats. For information, call (916) 654-8899, TTY 711, or write to California Department of Transportation, Division of Research, Innovation and System Information, MS-83, P.O. Box 942873, Sacramento, CA 94273-0001.

Re-inventing Airport Land Use Planning in California: A Strategy for Updating the California Airport Land Use Planning Handbook

Version 1.0 (2023)

Principal Investigator
Jasenka Rakas, Ph.D.

Lead Researcher
Sarah Lindbergh, Ph.D.

Graduate Student Researchers
Rukia Hassoun
Lee Keslerwest
Yingjie Hu
Sungmin Sohn
Moise B. Tchivwila

Project Manager: Adam Cohen

University of California, Berkeley
Institute for Transportation Studies
The FAA Consortium in Aviation Operations Research (NEXTOR III)

December 29, 2023

VERSION HISTORY

Version 1.0 – December 29, 2023

ACKNOWLEDGEMENTS

There are many individuals who have contributed to the successful compilation of this report.

First and foremost, we would like to thank our Caltrans sponsors and mentors: Matthew Friedman, for his vision and funding initiatives; Tony Sordello for providing his expertise and deep knowledge of the 2011 CA ALUP Handbook; and Tiffany Martinez for coordinating the project. Your patience, guidance, inputs, resources and support throughout the duration of the project were invaluable.

We would also like to acknowledge the additional Caltrans' managerial help provided by Johnathan Huff, Gabrielle Sefranek, Nathan Loebs and Keith Holowecky. In addition, we very much appreciate the engineering and safety comments, discussions and advice about the Airport Zone 5 design from Patrick Kyo, Parvin Bijani, Patrick Miles and Christopher Brooks.

Our work on noise analysis was assisted by a number of experts from industry and government, including David Schleicher from ATAC; Kyle Titlow and Justyna Goworowska from the U.S. Department of Transportation - Bureau of Transportation Statistics; Juliet Page, Alexandria Salton and Michael James from Blue Ridge Research; Christopher J. Roof from VOLPE; and Raquel Girvin, Donald Scata and David A. Senzig from the Federal Aviation Administration.

Lastly, we would like to thank our colleagues at UC Berkeley, Kendra Levine for providing necessary bibliographical references, Adam Cohen for managing the UCB side of the project and Prof. Mark Hansen for helping with the initial scope of the proposal.

This work would have not been possible without their assistance.

I. INTRODUCTION

This report is written in response to the State of California Department of Transportation (Caltrans), Division of Aeronautics, relating to the need to update the 2011 version of the California Airport Land Use Planning (ALUP) Handbook. The project was led by the University of California Berkeley, Institute of Transportation Studies, and The FAA Consortium in Aviation Operations Research (NEXTOR III) under the sponsorship and supervision of Caltrans Aeronautics between July 2022 and December 2023.

To support creating a new ALUP Handbook for the 21st century, our research identified the Handbook's sections that have to be updated, and provided studies on new areas that have to be added to address emerging technologies and new aviation concepts across diverse topics centered on safety and the environment. Additional databases have been examined in this report and used to develop safety and environmental metrics that are relevant to airport land use planning. As a result, new safety and environmental metrics have been proposed concerning aircraft accidents, wildlife strikes, drone intrusions, midair-collisions, hazardous wind, noise exposure, and environmental justice focused on geographic information systems (GIS).

The purpose of this technical report and its supplementary materials is to provide a robust scientific foundation for the final Handbook update publication for airport land use compatibility planning, which will be created soon by Caltrans. Our report innovates as it was designed for a diverse range of airport planning stakeholders to incorporate our methods and datasets so that they can be adjusted to each ALUC's needs and managerial and technical capacities, as well as progressively updated as new safety data is released. Data across multiple and complex topics were compiled and assessed for more than 200 California airports structured by topic and organized in data dictionaries. Our data are made available in their raw form, their pre-processed form, and their results, so that all the steps of our analysis are accessible for reproduction at different spatial scales and time frames. Therefore, instead of providing static information, which was a norm to creating previous ALUP Handbooks, we provide a flexible and dynamic method that can help airport land use planners meet their local and regional planning needs.

The Division of Aeronautics is responsible for creating the final ALUP Handbook with essential elements for the State's Airport Land Use Commission (ALUC) preparation of their Airport Land Use Compatibility Plan. The research provided in our report offers a new perspective and methods to help create the new Handbook, that is intended to:

1. provide information to ALUCs, their staffs, airport proprietors, cities, counties, consultants, and the public,
2. identify the requirements and procedures for preparing effective compatibility planning documents,
3. define exemptions where applicable,
4. protect the functionality of airports, and
5. facilitate planning that works in a complimentary activity to guide local development that supports airports and leverages airport activities to benefit the economic and communal functions within airport influence areas.

On the specific topic of safety, this work provides a new foundation for analyzing the validity of Airport Safety Zones by offering a GIS-oriented and data-rich approach to defining and studying accident risk. Because of the increased volume of spatially accurate datasets, we innovate by creating GIS models of generic safety zones for 259 airports in

the state of California. A newly-developed risk metric will make the Handbook more valuable by expanding accident risk into two dimensions: (1) hazard (accident density) and (2) exposure (potential consequences). The accident density provides a more robust metric for assessing accident spatial patterns, and the potential consequences are based on different classes of urban or developed land use and land cover.

II. REPORT ORGANIZATION

This report consolidates the strategy for updating the Airport Land Use Planning Handbook based on multiple tasks developed between July 2022 and December 2023 [Task 10]. For organizational purposes, the original tasks numbers were maintained and the most critical tasks for safety and environmental topics were consolidated in the Main Report, followed by an Appendix with memorandums, and a Supplementary Material folder organized below.

The Main Report consolidates tasks related to critical airport land use planning safety topics such as the accident analysis based on the National Transportation Safety Bureau (NTSB) data; emerging technologies risk based on electric vertical take-off and landing (eVTOLs) midair collision overview and the Federal Aviation Administration (FAA) drone incident data analysis; and and the FAA wildlife strikes data analysis. The Main Report also includes critical environmental airport land use planning such as noise exposure and environmental justice analysis as well as a hazardous wind analysis. Finally, the Main Report concludes with a deep dive into the NTSB and wildlife strike accident implications for safety zones dimension validation and land use compatibility. This final section also includes critical information regarding the uncertainties and limitations of the methods developed here and next steps for improving safety zone risk analysis.

The Appendix consolidated the memorandums on the literature review, on the identification of emerging transportation modes and technologies and their implication for the ALUP Handbook update, and on the digitization strategy for disseminating and creating open-source GIS platform with the datasets and results developed in this report.

The Supplementary Materials correspond to other documents, tables, and datasets so that the methods, data, and literature used in this report are accessible and cross-referenced based on their tasks number.

Main Report [Task 10]

- Task 4.1. Safety and Risk: NTSB Data Accident Spatiotemporal Analysis
- Task 4.1.1 (1) Safety & Risk with Emerging Technologies. Subtask 1: eVTOLs midair collisions
- Task 4.1.1.(2) Safety and Risk with Emerging Technologies: Subtask 2: Drone incidents
- Task 4.1.2. Wildlife Strikes
- Task 4.2. Noise Exposure and Environmental Justice
- Task 4.3. Wind Analysis
- Task 8. Safety Zones Accident Density & Land Use Compatibility Update
- Task 11. Spatial Distribution Analysis of Aircraft Accident in Airport Safety Zones

Appendix [Task 10]

[10.A1] APPENDIX 1. Memorandum: Literature Review (based on original Task 2)
[10.A2] APPENDIX 2. Memorandum: Identify emerging transportation modes and technologies and determine their contributions to the ALUP handbook (based on original Task 5)
[10.A3] APPENDIX 3. Memorandum: Digitization Strategy (original Task 9)

Supplementary Materials [Task 10]

Task 1b. Acceptance Criteria
Task 2. Literature Review Repository
Task 3. Preliminary databases, gaps, and methodologies
Task 4.1. Safety & Risk Supplementary Materials
Task 4.2. Noise Exposure Supplementary Materials
Task 4.3. Wind Analysis Supplementary Materials
Task 8. Safety Zones Update Supplementary Materials
Task 9. Digitization Strategy Supplementary Materials

Task 4.1. Safety and Risk Analysis: NTSB Accident Data Spatio-temporal Analysis

Task goals (from Acceptance Criteria Task 1b): detailed information on retrieval of NTSB accident database; data filtering criteria and process; data analysis methods:

a. *reproduction of the 1993 ITS methodology used for the 2011 handbook (2000-2009 accidents data) for the 2008-2022 accident data updates. The results will be further organized in arrival/departure; phase of operation; aircraft type; pilot control, visibility, time of day; airport proximity; distance from runway end/centerline; airport safety zones; impact types, if possible they can also be organized based on land use/land cover types.*
b. *proposal of new geospatial methodologies covering accidents from 2000-2022 (or earlier if data compatibility allows) based on point pattern analysis and spatial decomposition (i.e., hot spot analysis, interpolation, etc.).*

[4.1] 1.Introduction

The National Transportation Safety Board (NTSB) is required by Public Law 93-633 to investigate and determine the probable cause of all civil aviation accidents in the United States and report its findings in writing. The publicly available Census of US Civil Aviation Accidents (henceforth NTSB accident database) is used for these activities and is the most reliable and continuous data source for the California's ALUP handbook safety and accident analysis updates.

The NTSB Accident/Incident original data was pre-processed for two goals: (1) is updating the safety analysis with new accident information from 2008 - December 2022 for comparison purposes with the 2011 handbook results (2000-2009 accidents); and (2) is to expand the analysis methods by taking advantage of richer and more accurate geospatial accident data availability. Two datasets are created from the original NTSB accident data:

(1) Temporal-only: a complete accident dataset from 1983-2022 with minor data selection to filter California-relevant accidents for the longest time series available to provide a richer temporal analysis

(2) Spatiotemporal: a spatial accident dataset more rigorously pre-processed to filter spatially reliable accident events for geospatial statistics

Section 2 describes the NTSB accident database pre-processing, starting with key definitions and an evolution of the accident analysis methods from California's first Airport Land Use Planning handbook in 1983, to the latest handbook in 2011. Then it describes the detailed data processing of the accident and other GIS information used in the spatiotemporal analysis. Results on temporal and spatiotemporal statistics of the accident datasets are available in Section 3.

1.1. Definitions

The Government Information Locator Service (GILS) Aviation Accident Database provides the following definitions:

Accidents are "an occurrence associated with the operation of an aircraft which takes place between the time any person boards the aircraft with the intention of flight and all such persons have disembarked, and in which any person suffers death or serious injury, or in which the aircraft receives substantial damage."

Incidents are "an occurrence other than an accident, associated with the operation of an aircraft, which affects or could affect the safety of operations…incidents typically do not involve the level of injury or damage characteristic of an accident". Following previous ALUP handbooks, NTSB incident events have been purposefully excluded from the accident analysis because of lower accuracy and fewer events registered when compared to accidents. The FAA Accident/Incident Data System (AIDS) is considered the most reliable incident database in use since 1974, although commercial aviation incidents were not included until 1978, and standardized from Jan. 1st, 2001 (FAA form 8020-5). According to the NTSB (2002, p6-7) "*Because of its broad reporting criteria, the AIDS database contains many different kinds of incidents, ranging from airport events involving collisions between aircraft and catering trucks to the loss of a cabin door in flight. The database does not contain reports of near-midair collisions, which are handled through separate reporting procedures and are contained in a separate database called the Near Midair Collision System (NMACS)"*

1.2. Accident data assessment evolution from previous handbooks

- **1983 handbook** uses NTSB data from 1970-1979, sometimes with data up to 1982 in all of the U.S. A total of 363 accidents are assessed (98 arrivals, 41 departures, 152 in-flight, and 72 taxi or static), out of which 57 involved fatalities.
- **1993 handbook** uses the UC Berkeley ITS report methodology published in 1993, covering all 50 states, from 1983-1991, accident only data, with a total of 400 accidents (190 arrivals and 210 departures) out of 12,700 accident and incident events. Uses NTSB Factual Reports and validates the usefulness of the NTSB data based on multiple sources (managers of individual airports, local newspapers, local police and fire department records, state aeronautic offices, aircraft owners and pilots' association, and aircraft insurance companies). For all types of general aviation airplanes, excluding airline aircraft, helicopters, or other aircraft types like ultralight, blimps, etc.).
- **2002 handbook** uses UC Berkeley 1993 methodology, covering accidents from the previous handbook (1983-1991) and adds accident data up to 1998 with a total of 873 (445 arrivals and 428 departures) accidents in the U.S. assessed (all 50 states).
- **2011 handbook** changes the methodology to cover California only accidents from 2000-2009. A total of 17,000 accidents were assessed in the U.S.; and 1,800 in CA. However only 154 accidents were considered in analysis after specific selection criteria (off runway, not during cruise, within 5 miles of airport, only fixed wing aircrafts). An issue

was identified when there was a large overlap of accident events with runway midpoint, resulting in the refinement of the database to only 70 accidents with reliable geolocation based on the investigation of accident narratives.

The 1983, 1993, 2002 and 2011 ALUP Handbooks, and the technical report developed in 1993 by the UC Berkeley Institute of Transportation Studies for the 1993 Handbook were uploaded as supplementary material under Task 4.1. Called “ALUP Handbook Series_1983-2011”

[4.1] 2. Data & methods for the 2023 ALUP handbook update

A large part of the NTSB accident data analysis was devoted to the data cleaning and pre-processing in order to develop new datasets that are temporally and spatially significant for statistical analysis, as well as reliable and relevant for ALUP handbook update goals. The accident data pre-processing and cleaning is described in section 2.1. and 2.2.; downloaded directly from the NTSB public repository with over 88,000 accident entries with over 200 relational variables for each entry. Section 2.3 describes how other auxiliary Geographic Information System datasets such as airport boundaries, runways and runway safety zones were created for the spatially-relevant accident analysis.
Spatial statistics methods used focus on describing accident density based on point pattern analysis and spatial interpolation using ArcGIS software further described in the spatial statistics results (section 3.2). Data preprocessing and other statistical analysis also relied on Python and Microsoft Excel software.

2.1. NTSB dataset pre-processing and compatibility issues

NTSB Accident/Incident public data[1] repository provides accident data from 1968 to the current date, with weekly updates, downloaded on February 24, 2023. Changes on the way accident data has been collected and stored requires careful processing to maintain temporal and relational compatibility. Temporal compatibility pertains to the ability of comparing the accident events through time and relational compatibility refers to the ability to cross reference the various attributes in the NTSB dataset based on a unique identifier (documented under “*eadmspub.pdf*” Figure 1).

Important compatibility considerations for this accident analysis are described below:

[1] Metadata and further information regarding the NTSB accident dataset can be found on the Government Information Locator Service (GILS) Aviation Accident Database. NTSB number unique to each accident event can be used through the CAROL (Case Analysis and Reporting Online), Query Tool to find information about investigations and recommendations. The ACRP guidelines on Enhancing Airport Land Use Compatibility and its appendix on Aircraft Accident Data Sources and Trends as well as the NTSB report on Transportation Safety Databases (2002) were also used as a methodological reference.

- Three distinct sub-databases span three time periods: 1948 -1981 (“*PRE1982.zip”*, Figure 1), 1982, and 1983 - present. NTSB considers that “most data fields, though similar in purpose among the three sub-databases, are incompatible” across these three sub-datasets. In California only two accident events were found between 1948-1981 sub-database; and 382 accidents in the 1982 sub-database. We combined the 1982 and the 1983-present events for this study (“*Pre2008.zip*” and “*avall.zip*” Figure 1) but we subdivided the data based on geospatial attribute availability and accuracy as will be explained further.
- The NTSB explains that in 1989 accident events started to contain a narrative description of the probable cause of the accident, in 1994-today this description is available within five days from the accident occurrence. The narrative was sometimes used to validate assumptions about temporal and relational consistency between the datasets.
- A newly designed accident database was revised and implemented in a relational database format (Microsoft Access) on Jan 1st, 2001 by the NTSB. A new software program was also developed to facilitate data entry with standard fields also available to the incident database maintained by the FAA under the Accident/Incident Data System (AIDS). Incident data was not used for this report due to the small number of events and even less spatial information.
- Relational database inconsistencies found during our data processing (non-documented by the NTSB manuals or data dictionary):
    - According to an email exchange with NTSB data manager, Latlon attribute started being registered in 2001, however our for California accident dataset only shows consistent Latlon data from 2008 onwards.
    - The phase of flight was consistently registered under “Occurence_result” tab and “Phase_of_Flight” column until 2007, with well documented code references in the NTSB data manual (“*codman.pdf*” Figure 1). However we noticed that most recent accident events (after 2008) have no data under this attribute. For events after 2008 “Sequence_of_Events_results” “phase_no” is used as phase of flight information.

File name	Date created	File size	File link
avall.zip	4/3/2023 8:13:22 PM	78630487	avall.zip
codman.pdf	9/15/2021 3:32:50 PM	124029	codman.pdf
eadmspub.pdf	9/15/2021 3:33:48 PM	58852	eadmspub.pdf
eadmspub_legacy.pdf	9/15/2021 3:33:48 PM	19112	eadmspub_legacy.pdf
PRE1982.zip	10/27/2020 3:52:46 PM	39353261	PRE1982.zip
Pre2008.zip	9/30/2020 12:51:56 PM	144454739	Pre2008.zip

Figure 1. NTSB data repository structure and links used for this study: https://data.ntsb.gov/avdata

2.2. Accident datasets pre-processing for spatiotemporal analysis

This section explains the step-by step data pre-processing and how the different variables of the NTSB original dataset were used to develop richer temporal and spatiotemporal accident datasets. Four accident datasets were created and are detailed in this section:

1 - Baseline accident dataset that results from the combination of two NTSB accident datasets of all the U.S. (**US_NTSB_1948-2023_raw**) with a total of 88,184 accidents from 1948- Jan 2023. This dataset was processed to contain all the auxiliary information from Microsoft Access format to Microsoft Excel format. There are 20 different tabs, however the main tabs used to assess accident data include: aircraft_result, engines_result, events_result, Events_Sequence_result, and narratives_result. The tab with legend information for the NTSB data is eADMSPUB_DataDictionary_result.

2- California temporal dataset selects accidents in California state based on the US_NTSB_1948-2023_raw dataset using the "ev_state" field to create the the longest and continuous accident time-series possible for the state and applying ALUP basic selection criteria, resulting in of 40 years of data between 1982-2022 (**CA_NTSB_temporal_82-22**) with a total of 8,550 events in shapefile format. From this dataset only 1,897 have geospatial information, which will be further filtered for the spatially-relevant datasets below. All GIS datasets are projected in the coordinate system North American Datum 1983 California Teale Albers (in US Feet).

3- Spatiotemporal datasets: Three different methods were applied to create spatially-relevant and ALUP-relevant datasets for accidents with a 15 year series from 2008-2022:

(1) Largest number of spatially-relevant accidents method (**CA_NTSB_spatialLargest_08-22**) with a total of 1,355 events out of 1,897.
(2) Reproduction of 2011 handbook method (**CA_spatial2011Method_08-22**) with a total of 292 events (495 when including those outside the 5 mile buffer of airport boundaries)
(3) Highest spatial-accuracy criteria method (**CA_spatialAccuracy_08-22)** with a total of 466 events.

2.2.1. Baseline accident dataset pre-processing

- **US_NTSB_1948-2023_raw:** Concatenated version of *"Pre2008.mdb"* (1948-2008) and "*avail.mdb"* (2008- today) from NTSB database covering events from 1948-Jan 2023 (downloaded data available in Feb 2023). Event identification numbers (IDs) for each accident were used to check if there were any duplicates between the two databases. The databases were first converted to .xlsx file format. Then, the whole sheets in two databases were compared and cross-checked. There were no duplicates. Accordingly, the two databases were combined through the concatenation function on Python. This is

the baseline NTSB database with a total of 88,184 accidents from which more complex filters will be applied for the temporal dataset and the spatiotemporal datasets (Figure 2).

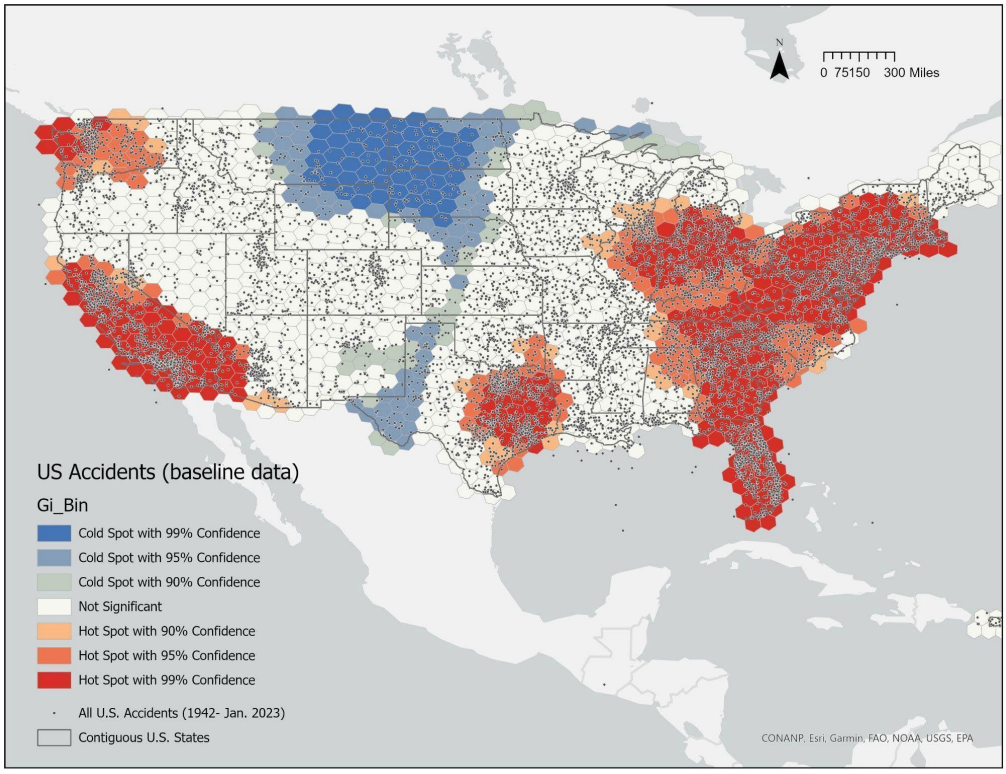


Figure 2. Overview of accident baseline dataset across the contiguous U.S. (1942- Jan 2023) with high spatial clusters (hot spots) and low clusters (cold spots) of accident.

2.2.2. Temporal accident dataset pre-processing

- **CA_NTSB_temporal_82-22:** Attribute and spatial selection of all accidents in California, only for the "event_results" tab. This dataset is intended to be used for temporal analysis only (non-spatial dependencies). Starting from the US_NTSB_1948-2023_raw it simply filters CA events based on the attribute table.

  From US_NTSB_1948-2023_raw:
  1) Selected "ev_Country" = USA (attribute table); total of 88,184 accidents
  2) To reproduce the selection criteria from the previous handbook, the multiple tabs from the original finalNTSB_db.xls were joined based on the *event_id*. Tables 1 - 4 provide details on the tabs and variables used for accident data selection defined on the 2011 handbook:
     a) Only accidents
     b) Only fixed wing
     c) Occurred during takeoff, climb, approach, and landing
     d) Only powered aircrafts

3) Selected "ev_State" = CA (attribute table); total of 8,564 accidents
4) Spatial select events that intersect with CA state boundary = 14 accidents in CA under different state in attribute table. The blue points in Figure 3 indicate events that are geolocated in or within 5 miles of CA but classified under AZ (6), ID (1), MT (1), NV (5), and OR (1). Only 7 are retained based on the measured accuracy of their geolocation.



Figure 3. Accidents registered in other states but included in this analysis due to their location being in California (blue points).

5) Merge attribute selection + spatial selection = 8,558 accidents in California from 1963-2023
6) Delete events from before 1982 (only 2 events) and after 2022 (only 6 events in Jan 2023) = 8,550 accidents in California from 1982-2022

7) After applying all the selection criteria from Table 1, **CA_NTSB_temporal_82-22 = 8,550 accident data points** for the largest temporal series dataset.

*This dataset is the baseline for all spatiotemporal datasets detailed below.

Table 1. Selection criteria for all accident database (temporal and spatial datasets)

Tab name	Attribute name	Selection criteria/ utility for this analysis
All tabs	**event_id**	10-11 digit alphanumeric code used to reference all database records to each unique event (relational key)
event_result	**ev_type**	Selection criteria: accident only events (ACC)
event_result	**ev_state**	Selection criteria: CA (14 events were added from other states based on their geolocation inside CA or within 5 miles of the state border)
event_result	**ev_country**	Selection criteria: U.S.
aircraft_result	**acft_category**	Selection criteria for powered aircraft & fixed wing: Include: AIR, WSFT, ULTR, RCKT Exclude: HELI, BALL, PPAR, GYRO, GLI WSFT: weight-shift controlled ultralight aircraft (15

		accidents) AIR: airplane (7,078 accidents) GLI: glider (221 accidents) ULTR: ultralight aircraft (37 accidents) RCKT: rocket-powered aircraft (1 accident) HELI: helicopter (1,089 accidents) BALL: balloon (57 accidents) PPAR: powered parachute (4 accidents) GYRO: gyrocopter (31 accidents)
Occurence_result	**Phase_of_Flight** * this variable only covers events up to 2007	Selection criteria: only accidents occurred during takeoff, climb, approach, and landing. Include:(in green) 520-523, 530, 531, 542, 550-553, 560-569, 570-576, 580-583, 590-592 Exclude: 500-505, 510-514, 540, 541, 600, 610 (6,592 accidents with these variables) Code used for phase of operations statistics (p 15 of NTSB Code Manual): ● Standing (500-505) = 79 accidents ● Taxi (510-514) = 189 accidents ● Takeoff (520-523) = 1,087 accidents ● Climb (530-531) = 210 accidents ● Cruise (540-541) = 1,063 accidents ● Descent (550-553) = 420 accidents ● Approach (560-569) = 774 accidents ● Landing (570-576) = 1,827 accidents ● Maneuvering (542; 580-583) = 799 accidents ● Hover (590-592) = 75 accidents ● Other (600) = 10 accidents ● Unknown (610) = 59 accidents ● N/A data: 1,958 accidents
Events_Sequence_result	**Defining_ev** *this variable only covers events from 2008 onwards	Used to filter “TRUE” phase_no variable for each event since most accidents have multiple phase_no describing their sequence
Events_Sequence_result	**Phase_no** *this variable only covers events from 2008 onwards	Selection criteria: only accidents occurred during takeoff, climb, approach, and landing. Included: 300xxx, 350xxx, 400xxx-405xxx, 450xxx-453xxx, 500xxx-509xxx, 550xxx-552xxx, 600xxx, 650xxx, 700xxx, 750xxx; xxx090-xxx093, xxx440, xxx470, xxx490, xxx500 (1,692 accidents with these variables as “TRUE” Defining_ev) *A total of 140 variables were classified as belonging to these critical phases of flight categories, Details are available in Appendix A.

2.2.3. Spatiotemporal accident data pre-processing for California

To reflect the most accurate spatial data whilst being most efficient with the available data points, we created three types of spatiotemporal datasets based on different criteria described below. Table 2 provides a list of the selection criteria from the original NTSB dataset allowing the spatial refinement of the three following datasets:

(a) Largest number of spatially-relevant events in California (2008-2022): **CA_NTSB_spatialLargest_08-22**, total accident events = 1,355 This method benefits the most from spatial accuracy information (GPS measured Latlon data) that became available in 2008 and provides the dataset with the largest number of spatially-relevant events. The tradeoff is the potential APR-colocation error that is corrected in the 2011 method and the highest spatial-accuracy dataset.

(b) Reproduction of 2011 handbook method: **CA_NTSB_2011Method_08-22**, total accident events = 292. This provides the closest reproduction of the 2011 handbook methodology. It removes all accidents located outside the 5 mile buffer of the airport's centroid, all accidents within the Primary Surface, and all accidents with the APR-Latlon co-location error. The advantage is that this dataset can be used for comparison purposes, however it does not optimize the use of richer geospatial information available since 2008 and has a very small number of events.

(c) Highest spatial-accuracy criteria **CA_NTSB_spatialAccuracy_08-22**, total accident events = 466. This method reproduces the 2011 methodology but further benefits from richer information on geospatial accuracy. It refines the APR co-location error by filtering only accidents that have "measured" Latlon accuracy. This represents the strictest spatial accuracy criteria, but the tradeoff is the small number of events to process.

Detailed processing below:

- **CA_NTSB_spatialLargest_08-22:** Breaks from the 2011 handbook methodology to optimize the use of increased geolocation information of accident data that was not available before 2008.

  From CA_NTSB_temporal_82-22 attribute selection of "latlon_ac" = MEAS.
  Deletion of 3,897 accidents
  = 1,355 accidents with GPS measurement of Latlon attributes in California

- **CA_NTSB_spatial2011Method_08-22:** This provides the closest reproduction of the 2011 handbook methodology by further processing of CA full accident data to retrieve events with spatial accuracy.

  From CA_NTSB_temporal_82-22 dataset:
  1) Attribute filter: Selected only events with geospatial attribution = deletion of 4,358 events. Only events after 2008 remain = 899 accidents

2) Spatial filter: Selected only events that intersect with California state with a margin of 5 miles outwards = deletion of 3 events; 896 accidents remaining.
3) Exclude 171 accidents within the primary surface (between 50- 200 meters off the runway centerline according to FAA Part 77, see Figure 4.) =725 accidents remaining
4) Exclude 197 accidents outside the 5 mile buffer of airport's centroid. = 528 accidents remaining

5) Strategy to mitigate error related to registering accident events on the Airport Points of Reference (APR):
    a) Dissolve primary surfaces from civilian airports based on loc_ID (airport ID) to obtain one polygon feature per airport.
    b) Use the dissolved primary surfaces layer to calculate the APR as the approximate runway center point, or the mean of the latitudes and longitudes of a runway's ends (NGS, NOAA)
    c) Spatial select all accident events within 50m distance from APR= 230 accidents
    d) Delete 230 accidents that intersect with APR **= 292 accidents** considered as spatially reliable (2008-2022)

- **CA_NTSB_spatialAccuracy_08-22:** Reproduces the 2011 methodology without deleting events within the Primary Surface or those outside the 5 mile buffer of the airport's centroid. This method further benefits from richer data concerning geospatial accuracy by correcting only for the APR Latlon co-location error and further selecting accidents based on the accuracy of the Latlon data.

  From the CA_2spatial011Method_08-22 attribute selection of "latlon_ac" = MEAS. Deletion of 317 events that have empty or "EST" latlon_ac.
  = 466 accidents with high spatial accuracy (2008-2022)

Table 2. Selection criteria for spatial dataset

Tab	Attribute name	Selection criteria/ utility for this analysis
event_result	**latlong_acq**	Selection criteria for highly accurate events where Latlon is measured with GPS
event_result	**dec_latitude**	Selection criteria: only events with Latitude data for spatial analysis (transformed to North American Datum, 1983, Teale Albers, CA, Projected Coordinate System for higher California-state level accuracy)
event_result	**dec_longitude**	Selection criteria: only events with Longitude data for spatial analysis (transformed to North American Datum, 1983, Teale Albers, CA Projected Coordinate System for higher California-state level accuracy)

Table 3. Definition of variables used as selection criteria all accident databases (source: NTSB accident dataset, tab “eADMSPUB_DataDictionary_result”)

Tab	Attribute name	NTSB Definition
event_result	**ev_type**	Refers to a regulatory definition of the event severity. The severity of a general aviation accident or incident is classified as the combination of the highest level of injury sustained by the personnel involved (that is, fatal, serious, minor, or none) and level of damage to the aircraft involved (that is, destroyed, substantial, minor, or none). The NTSB is responsible for investigating aircraft accidents. The FAA investigates incidents, and the NTSB database includes few incident event records. Additional incident information is available from the FAA incident database at http://nasdac.faa.gov/internet/.
event_result	**ev_state**	The state in which the event occurred (if in the US)
event_result	**ev_country**	The country in which the event took place.
event_result	**latlong_acq**	Indicates whether the reported Latitude/Longitude coordinates represent a measurement from GPS or other official source, or whether they were estimated. NEW VARIABLE- With the implementation of eADMS in 2006, this field/variable was added to clarify the accuracy of reported latitude/longitude data.
event_result	**dec_latitude & dec_longitude** *only consistently available from 2008 onwards for CA accidents	Event Location Latitude. Latitude and longitude are entered for the event site in degrees, minutes of arc, and seconds of arc. If the event occurred at an airport, the published coordinates for that airport can be entered. If the event was not at an airport, position coordinates may be obtained using Global Positioning System equipment. Latitude should be entered in the format DD:MM:SS N/S. For example, 37°43’09”N should be entered as 374309N.
aircraft_result	**acft_category**	The category of the involved aircraft. In this case, the definition of aircraft category is the same as that used with respect to the certification, ratings, privileges, and limitations of airmen. Also note that there is some overlap of category and class in the available choices.
aircraft_result	**Fixed_retractable**	Indicate whether the accident aircraft had either fixed or retractable landing gear.
Occurence_result	**Phase_of_Flight**	All occurrences include information about the phase of flight in which the occurrence took place. Phase of flight refers to the point in the aircraft operation profile in which the event occurred. *For simplicity purposes we opted to use this “Phase_of_Flight” variable, but there are occurrences with more than one phase of flight code, in this case codes are assigned a sequential seq_event_no (in seq_events table) to distinguish between multiple codes.).

Events_Sequence_result	**Defining_ev**	For each accident, one of the events cited in the events_sequence timeline is further identified as the "defining event". This is meant to group accidents of similar type and is not meant to indicate or suggest cause.NEW VARIABLE with the implementation of eADMS in 2006, the "Events_Sequence" table will replace the "Occurrences" table and the "Findings" table will replace the "Seq_of_events" table.
Events_Sequence_result	**phase_no**	Used to identify the phase of flight associated with discrete events in the accident event sequence timeline. NEW VARIABLE with the implementation of eADMS in 2006, the "Events_Sequence" table will replace the "Occurrences" table and the "Findings" table will replace the "Seq_of_events" table.

Table 4. Other attributes used for statistical analysis

Tab	Attribute	Other analysis function
event_result	ev_date	Temporal statistics
event_result	ev_dow	Day of week statistics
event_result	ev_time	Time of day statistics
event_result	ev_year	Temporal statistics
event_result	ev_month	Temporal statistics
event_result	mid_air	Midair collision statistics (Y/N)
event_result	on_ground_collision	On-ground collision statistics (Y/N)
event_result	light_cond	Light conditions statistics (dawn, day, dusk, night, unknown)
event_result	ev_highest_injury	Highest level of injury statistics (fatal, serious, minor, and none)
event_result	inj_f_grnd	Statistics for fatal injuries on-ground (#)
event_result	inj_m_grnd	Statistics for minor injuries on-ground (#)
event_result	inj_s_grnd	Statistics for serious injuries on-ground (#)
event_result	inj_tot_f	Statistics for fatal injuries (#)
event_result	inj_tot_m	Statistics for minor injuries (#)
event_result	inj_tot_n	Statistics for “none” injuries (#)
event_result	inj_tot_s	Statistics for serious injuries (#)

event_result	inj_tot_t	Statistics for total injuries (#)
aircraft_result	dest_apt_id	Destination Airport Code was used to attribute each accident event to an airport in the statistical analysis
aircraft_result	dprt_apt_id	Departure Airport Code was used to attribute each accident event to an airport in the statistical analysis
aircraft_result	rwy_num	Runway Number was used to attribute each accident event to a specific runway end and calculate the global departure and arrival accident densities in relationship with runway ends

2.3. Other GIS data pre-processing

2.3.1. Airport Boundaries (parcels)

The total airport population used in this report is 259 covering civil and general aviation facilities in California with the necessary runway information from the Bureau of Transportation Safety (BTS). The original Caltrans open source GIS dataset provides 221 airport boundaries[2] (parcels) (from Feb 16 2022), however only 216 airports had the runway data necessary from the BTS[3]. These 216 airport boundaries are considered of public use based on Caltrans Open GIS data description. To complete the airport boundary dataset of the remaining runways digitized based on the BTS runway end dataset, 43 airport boundaries were digitized manually based on the land use parameters of OpenStreetMap (A table of the 259 airport boundaries used in this report and the 43 manually digitized boundaries is available in Appendix B together with other data cleaning details). There is no attribute table for these extra 43 airports and they might not be considered public use airports. The airport names were retrieved from OpenStreetMap.

2.3.2. Runway Safety Zones

To create the runway safety zones, different runway open source GIS were examined: Caltrans, FAA Aeronautical Data Delivery Service (ADDS), and the Bureau of Transportation Statistics (BTS) part of the U.S. Department of Transportation (USDOT) National Transportation Atlas Database (NTAD). The BTS runway end table (created on July, 16, 2020) was the most appropriate due to the detailed attribute table with runway end points and the obstruction identification surface codes necessary for determining the runway's primary surfaces according to the Federal Aviation Regulations Part 77.The values described in Figure 4 for the definition of the primary surface were applied based on runway visibility parameters (i.e. visual runways, non-precision instrument runways, and precision instrument runways).

[2] SCK (Stockton Metropolitan Airport) and SFO (San Francisco International Airport) had conflicting sets of boundaries that needed correction, details available in Appendix B

[3] A total of five airports from Caltrans airport boundary dataset lacked BTS runway data and were therefore excluded from this analysis: KINGDON AIRPARK AIRPORT (O20), LOST HILLS-KERN COUNTY AIRPORT (L84); LODI AIRPARK AIRPORT (L53); RIALTO MUNICIPAL/ART SCHOLL MEMORIAL FIELD AIRPORT (L67); and WOODLAKE AIRPORT (O42).

After defining the runway's primary surface, the geometries for the 6 generic safety zones (civil aviation), were applied based on the BTS runway length, approach visibility minimums, and the type of general aviation or large air carrier runway (see Figures 5 -7). For informational purposes Figure 8 describes Accident Potential Zones of military runways of large aircrafts. Detailed runway data selection and process are described below:

Runway data selection:

a. Has defined attribute 'Base_End_Control_Object_Affect_' or 'Recip_End_Control_Object_Affect' in BTS data or is at a military airport (excludes generally small private airports without this definition, military airport Loc_Id 7CL4, NID, EDW, 9L2, NJK, SUU, HGT, AHC, NRS, NLC, VBG, SLI, BAB, NFG, PMD, NTD, NUC, NKX, NZY, NSI, NXP)
b. Attribute 'State_Post_Office_Code' = CA

Process:

1. Determine primary surface (from part 2) if non-military
2. Define safety zones based on primary surface and 2011 handbook diagrams (general aviation), or military zones if military airport (EPSG:2870 for conversion to feet)
3. If runway is PIR, define zones 3L and 5L as zones 3 and 5 for "Large air carrier runways"
4. Split primary surfaces, zones 1, 2, and 4 into civilian and military airports
5. Combined zones for all runways (including military, where each zone is the lowest numbered zone for the entire state, primary surface = zone 0) in zone_#_2011_exclusive

Output Dataset

Geometric Features:

- Zones 1-2,4: 391 multi-polygons (based on Figure 5 - from the 2011 ALUP Handbook p. 3-17
- Zones 3, 5, 6: 357 multi-polygons (based on Figure 5 - from the 2011 ALUP Handbook p. 3-17
- Zones 3L, 5L: 54 multi-polygons (based on Figure 7 - from the 2011 ALUP Handbook p. 3-19)
- Exclusive zones: 7 multi-polygons (1 per zone) (based on Figure 5 - from the 2011 ALUP Handbook p. 3-17)

Attributes: Same as BTS data (none in exclusive zones)

According to the 2011 ALUP handbook (pp. 3-19 and 3-20) "The intent of the set of zones depicted for each example is that risk levels be relatively uniform across each zone, but distinct from the other zones." and that they are "intended just as a starting place for the development of zones appropriate for a particular airport. In some cases, the zones might be quite suitable, however in most airports, some degree of adjustment of the generic zones is necessary in recognition of the physical and operational characteristics of the airport."

Based on the former ALUP handbook, we also considered that where the zones of two or more runways overlap, the lower numbered zone takes over. For runways designed for multiple aircraft operations (i.e., general aviation and large air carriers) the largest critical aircraft zoning is predominant. The intention is to reflect the risk of highest potential consequences and not probability, since the impact of a large commercial airliner would have greater potential damage than that of a single engine aviation aircraft (ALUP, 1983). Based on the available attributes of the BTS runway dataset, the Safety Zones geometries were created for General Aviation for all the 259 airports in this study using only the standards from Figure 5 (or Figure 3-A, (p.3-17 from the 2011 ALUP Handbook). General Aviation runways are distinguished between short, medium and long. Safety Zones geometries used in this study are available and organized within a metadata for Task 9.

Figure 9 illustrates the generic safety zones in the southern San Francisco Bay Area and Figure 10 the generic safety zones of Sacramento Executive Airport. Runway safety zones are created with the goal to maintain “undeveloped land clear of objects in accordance with FAA standards” (ALUP 2011 pp.4-31) and is based on the observation that most aircraft accidents occur near runway surfaces and the assumption of decreased risk of damage in case of an accident if open areas are preserved where accidents are observed to occur more regularly. Table 5 explains each runway safety zone, their desirable usable open land percentages, and the percentage of area outside airport boundaries. Table 6 provides the aggregate area of each safety zone for all 259 California airports under study and the surface situated outside and inside airport boundaries. Safety zones located outside airport boundaries likely require more complex land use compatibility studies and stakeholder involvement. According to the 2011 ALUP handbook, useful open lands should be at least 300 ft. long by 75 ft., relatively leveled and free of objects such as structures, overhead lines, and large trees or poles. For urbanized areas, parking lots or recreational areas can be considered as acceptable open lands although not ideal.

Table 5. Characteristics of Primary Runway Zone and Runway Safety Zones (According to ALUP, 2011, pp-4-31, 4-32; and FAA Part 77)

Zone	**Jurisdiction**	**Description**	**Desirable % of Usable Open Land**	**% area outside airport boundaries***
Primary Runway Surface**	FAA	A surface longitudinally centered on a runway, dimensioned according to FAA Part 77(Figure 4)	100%	1.31%
Runway Safety Zone 1	ALUP/FAA	Runway Protection Zone	Clear of objects in accordance with FAA standards	49.74%
Runway Safety	ALUP	Inner	25-30%, especially areas	79.59%

Zone 2		Approach/Departure zones	close to the runway extended centerline	
Runway Safety Zone 3	ALUP	Inner Turning Zone	15-20% minimum	88.39%
Runway Safety Zone 4	ALUP	Outer Approach/Departure Zones	15-20% approximately, with emphasis on areas along the extended runway centerline	97.94%
Runway Safety Zone 5	ALUP	Sideline Zone	25-30% is desirable	26.09%
Runway Safety Zone 6***	ALUP	Traffic Pattern Zone	10% approximately every ¼ to ½ mile should be provided	94.64%

*calculated based on the generic safety zones dimensions for 259 California airport boundaries modeled
**Primary Runway Surfaces are not jurisdictionally allowed outside of the Airport boundaries, this percentage corresponds to the inherent error of generic safety zones and GIS modeling uncertainties from airport boundary digitization. Please refer to Supplementary Materials of Task 4.1. Called “Primary Surface Boundary Error Exploration” for more information.
*** Due to an under dimensioning error of Zone 6, any results associated with this zone area are underestimated, this error does not impact the core results of this analysis. Please refer to Task 8 for further information on the mitigation of this error.

Table 6. Safety zone areas inside and outside airport boundaries (sq. mi)

	Area inside airport boundary	**Area outside airport boundary**	**Total area**
Primary Surface	32.11	0.42	32.54
Z1	26.51	55.86	82.37
Z2	25.60	148.52	174.12
Z3	18.35	135.19	153.54
Z4	2.40	158.15	160.54
Z5	41.48	14.43	55.91
*Z6***	95.94	1617.65	1713.60

OBSTRUCTION IDENTIFICATION SURFACES
FEDERAL AVIATION REGULATIONS PART 77

DIM	ITEM	DIMENSIONAL STANDARDS (FEET)					
		VISUAL RUNWAY		NON - PRECISION INSTRUMENT RUNWAY			PRECISION INSTRUMENT RUNWAY
		A	B	A	B		
					C	D	
A	WIDTH OF PRIMARY SURFACE AND APPROACH SURFACE WIDTH AT INNER END	250	500	500	500	1,000	1,000
B	RADIUS OF HORIZONTAL SURFACE	5,000	5,000	5,000	10,000	10,000	10,000
		VISUAL APPROACH		NON - PRECISION INSTRUMENT APPROACH			PRECISION INSTRUMENT APPROACH
		A	B	A	B		
					C	D	
C	APPROACH SURFACE WIDTH AT END	1,250	1,500	2,000	3,500	4,000	16,000
D	APPROACH SURFACE LENGTH	5,000	5,000	5,000	10,000	10,000	*
E	APPROACH SLOPE	20:1	20:1	20:1	34:1	34:1	*

- A - UTILITY RUNWAYS
- B - RUNWAYS LARGER THAN UTILITY
- C - VISIBILITY MINIMUMS GREATER THAN 3/4 MILE
- D - VISIBILITY MINIMUMS AS LOW AS 3/4 MILE
- * - PRECISION INSTRUMENT APPROACH SLOPE IS 50:1 FOR INNER 10,000 FEET AND 40:1 FOR AN ADDITIONAL 40,000 FEET

Figure 4. Variables used for the definition of the Primary Runway Surface (Source: http://www.ngs.noaa.gov/AERO/oisspec.html)

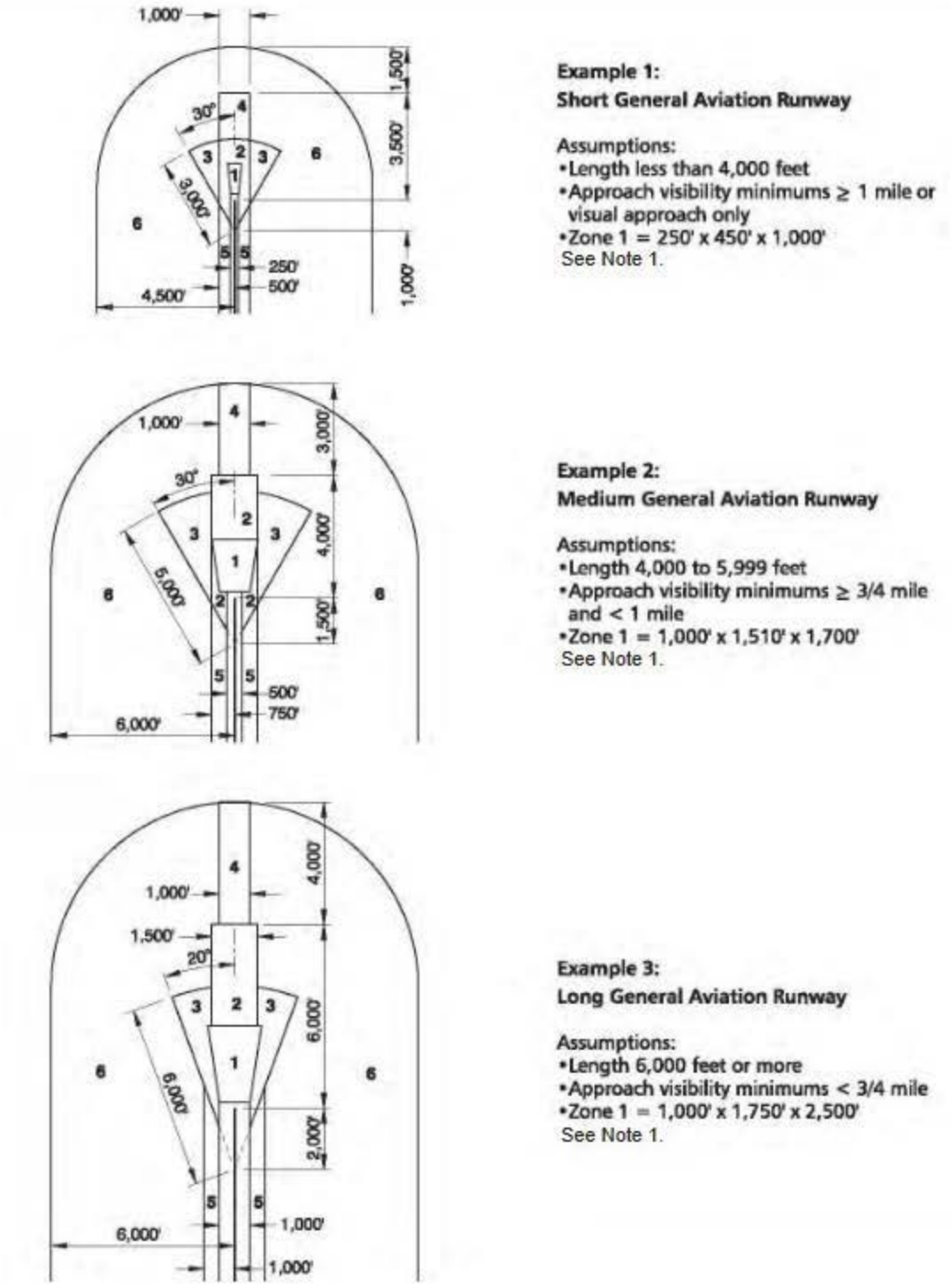
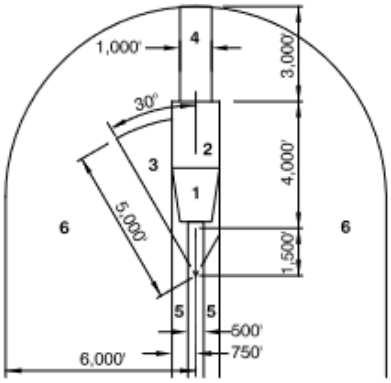


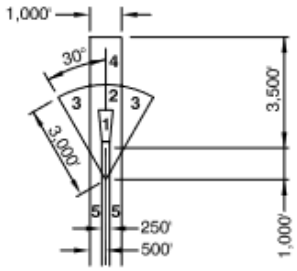
Figure 5. Generic safety zones geometries - Short, Medium, and Long General Aviation (Source: ALUP Handbook 2011, Figure 3-A, p.3-17)



Example 4:
General Aviation Runway with Single-Sided Traffic Pattern

Assumptions:
- No traffic pattern on right
- Length 4,000 to 5,999 feet
- Approach visibility minimums ≥ 3/4 mile and < 1 mile
- Zone 1 = 1,000' x 1,510' x 1,700'

See Note 1.

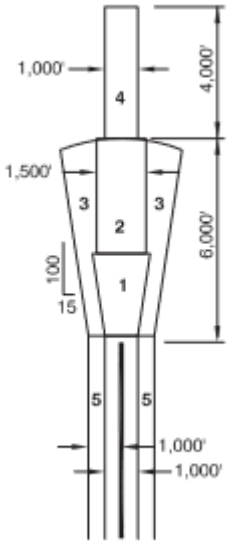


Example 5:
Low-Activity General Aviation Runway

Assumptions:
- Less than 2,000 takeoffs and landings per year at individual runway end.
- Length less than 4,000 feet
- Approach visibility minimums ≥ 1 mile or visual approach only
- Zone 1 = 250' x 450' x 1,000'

See Note 1.

Figure 6. Generic safety zones geometries - Single sided Traffic Pattern and Low Activity General Aviation (Source: ALUP Handbook 2011, Figure 3A p, 3-18)



Legend

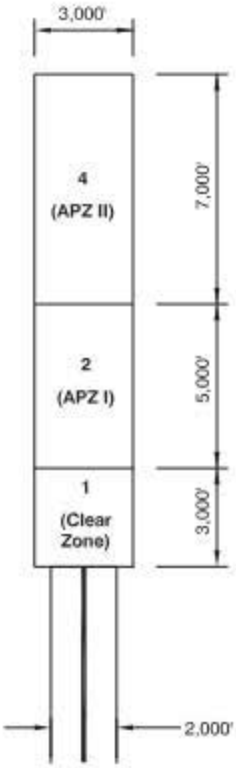
1. Runway Protection Zone
2. Inner Approach/Departure Zone
3. Inner Turning Zone
4. Outer Approach/Departure Zone
5. Sideline Zone
6. Traffic Pattern Zone

Notes:

1. RPZ (Zone 1) size in the large air carrier runway example is as indicated by FAA criteria for the approach type assumed. Adjustment may be necessary if the approach type differs.
2. See Figure 3A for factors to consider regarding other possible adjustments to these zones to reflect characteristics of a specific airport runway.
3. See Figures 4B through 4G for guidance on compatibility criteria applicable with each zone.

These examples are intended to provide general guidance for establishment of airport safety compatibility zones. They do not represent California Department of Transportation standards or policy.

Figure 7. Generic safety zones geometries - Large Air Carrier (Source: ALUP Handbook 2011, Figure 3-B p.3-19)



Military Runway for Large Aircraft

Assumptions:
- Military airport
- Predominately straight-in and straight-out flight routes (must modify for turning routes and traffic pattern activity)

Legend

1. Runway Protection Zone (Clear Zone)
2. Inner Approach/Departure Zone (Accident Potential Zone I)
3. Inner Turning Zone
4. Outer Approach/Departure Zone (Accident Potential Zone II)
5. Sideline Zone

Figure 8. Generic safety zones for Military runways - Large aircraft (Source: ALUP Handbook 2011, Figure 3-B, p.3-19)

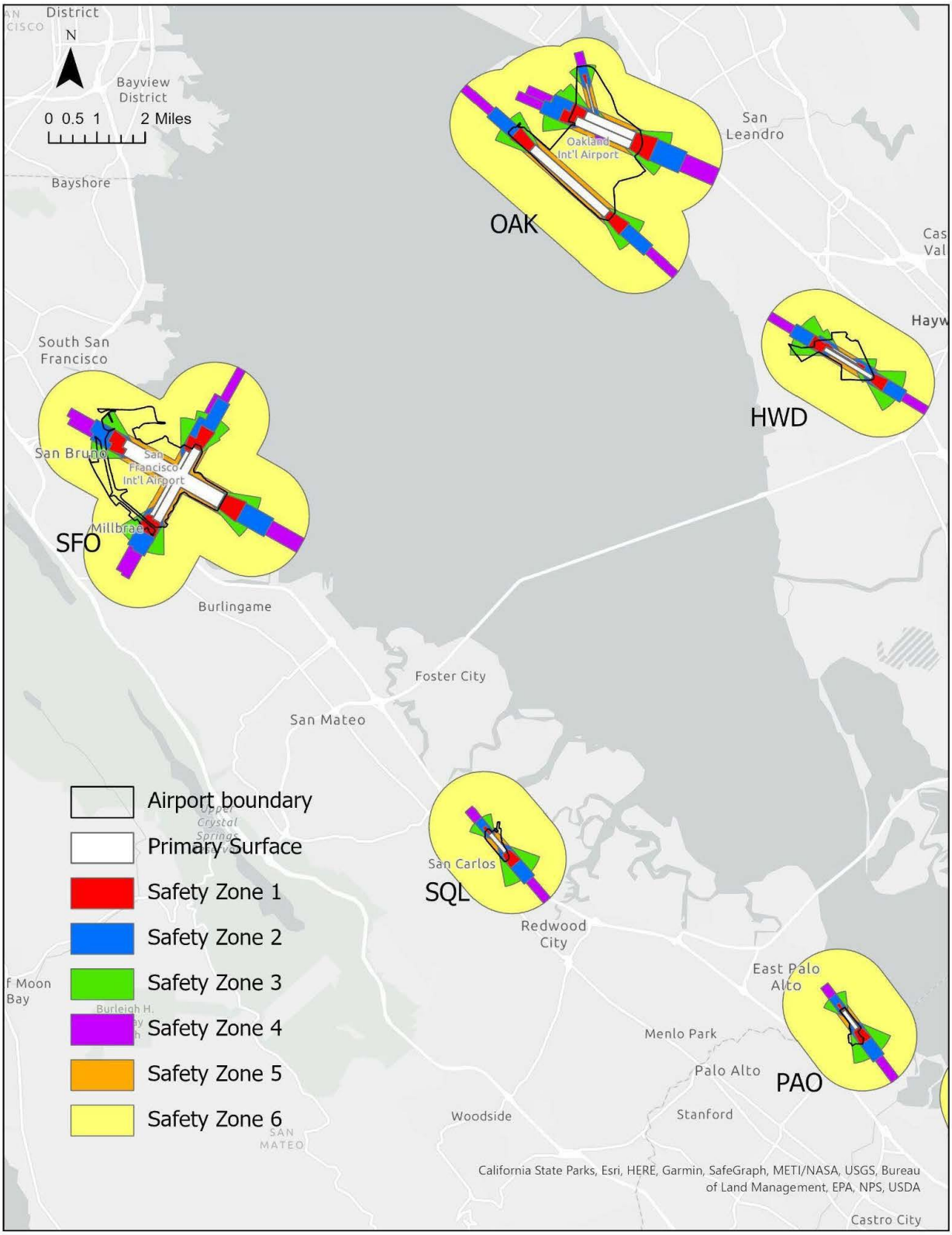


Figure 9. Illustration of generic safety zones in the southern San Francisco Bay Area Airports

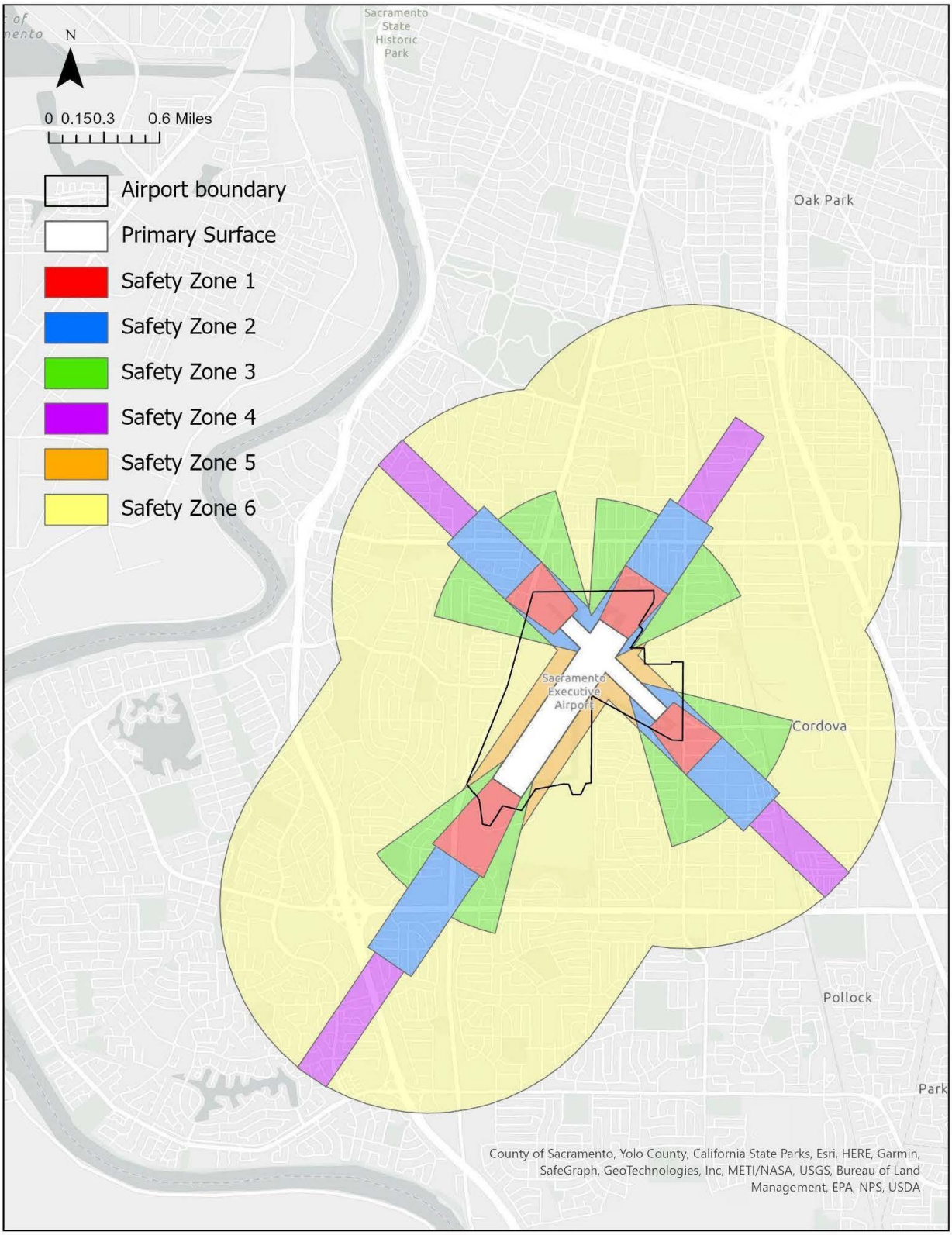


Figure 10. Zoom in Sacramento Executive Airport generic safety zones.

[4.1] 3. Results

The results section is subdivided in 3.1. temporal accident dataset analysis and 3.1. spatial accident dataset analysis.
Results in section 3.1. are derived from the accident data selection criteria that prioritized the collection of the longest possible time-series using NTSB sources (CA_ACC_full_final82-22). It provides a 41-year time series from 1982-2022. It provides basic statistics using spatially-independent information based on California ALUP-relevant accidents (filtered to account for specific aircraft types and phases of flight). The results are organized based on yearly evolution, season, month, day of the week, hour of the day, injury type, and phase of light.
Results in section 3.2. Are derived from the accident datasets created to deliver spatially reliable information covering a 15-year time series from 2008-2022 (CA_spatialLargest_08-22; CA_spatial2011Method_08-22; and CA_spatialAccuracy_08-22). The analysis is subdivided based on accidents located on airport vicinities; located inside airport boundaries, located in safety zones, and cumulative accidents based on distance from runway centerlines.

3.1. Temporal accident dataset analysis: 41 year time-series (1982-2022)

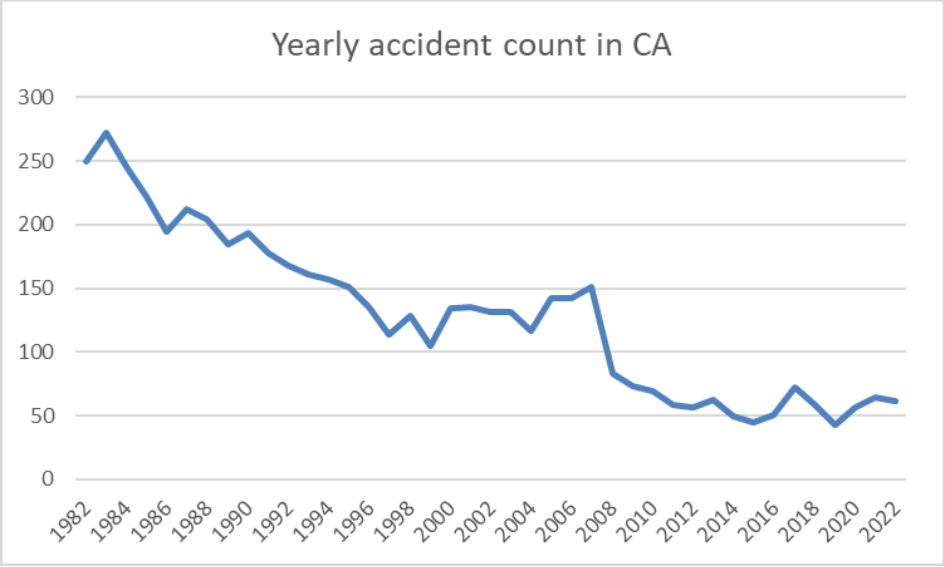


Figure 11. Accident evolution in California

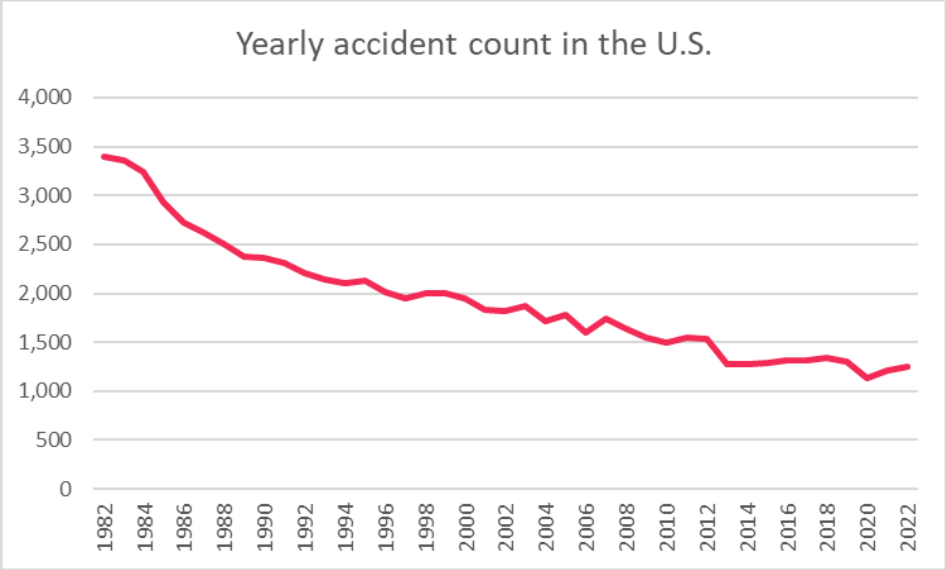


Figure 12. Accident evolution in the U.S. (reference data was not filtered to represent ALUP-relevant accidents based on phase of flight and aircraft type)

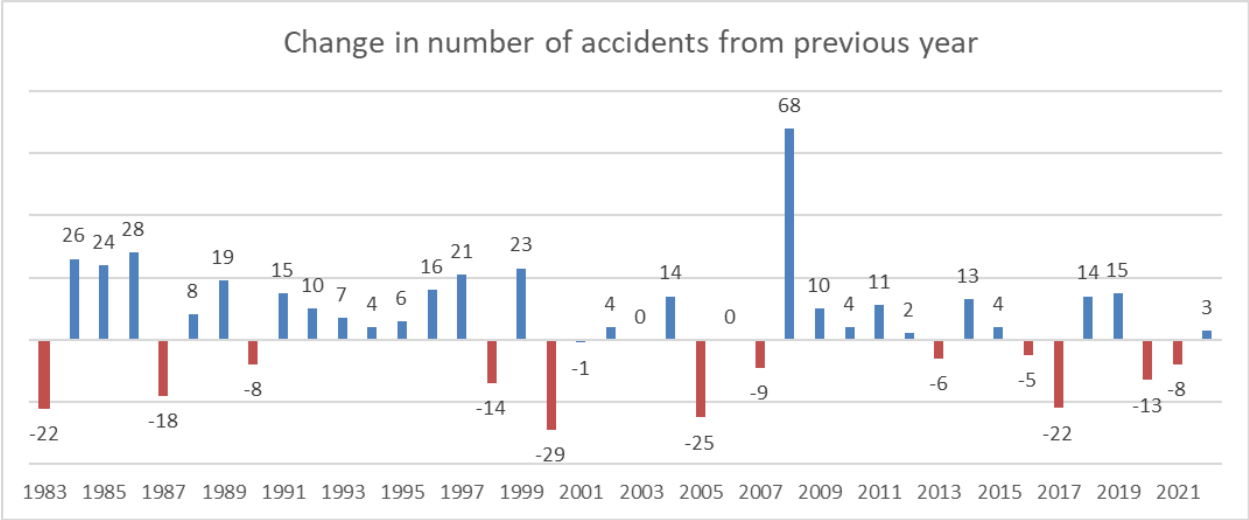
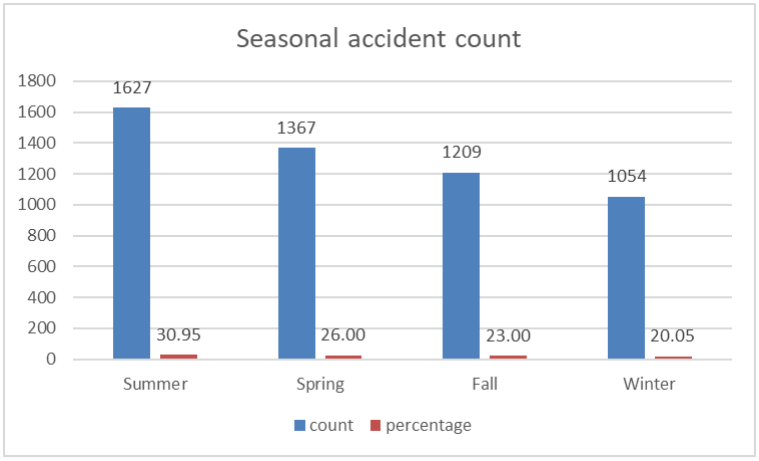
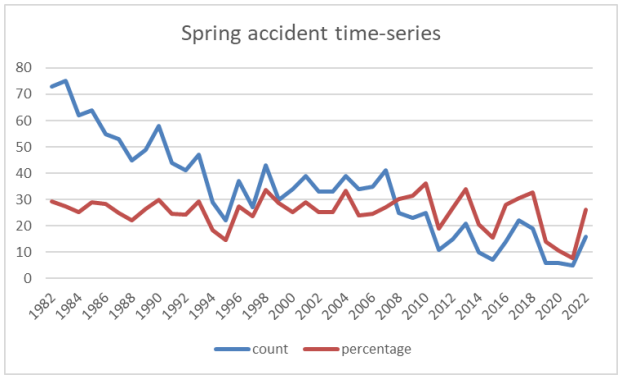
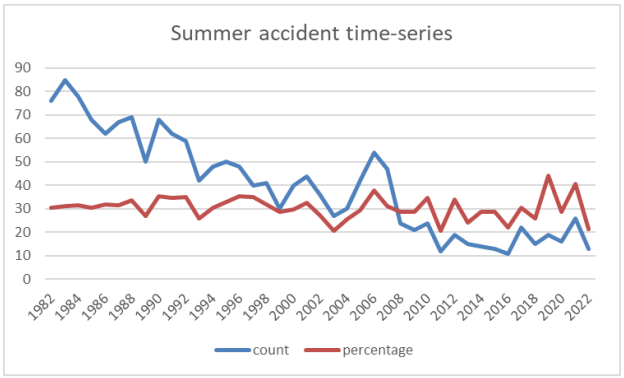


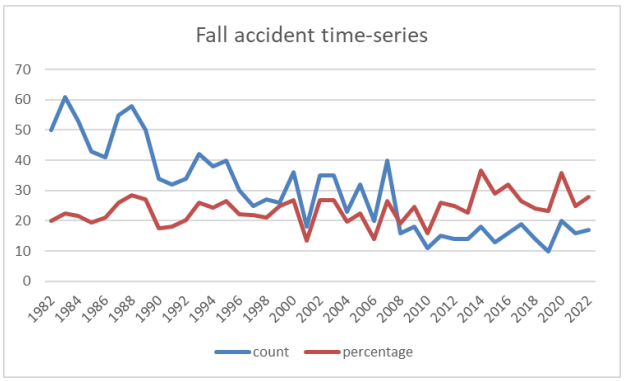
Figure 13. Yearly difference in the number of accidents in California

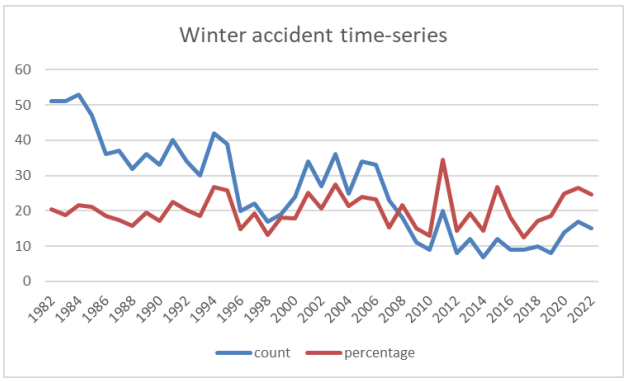
Accident by season in California based on the 1982-2022 dataset (Figure 14)



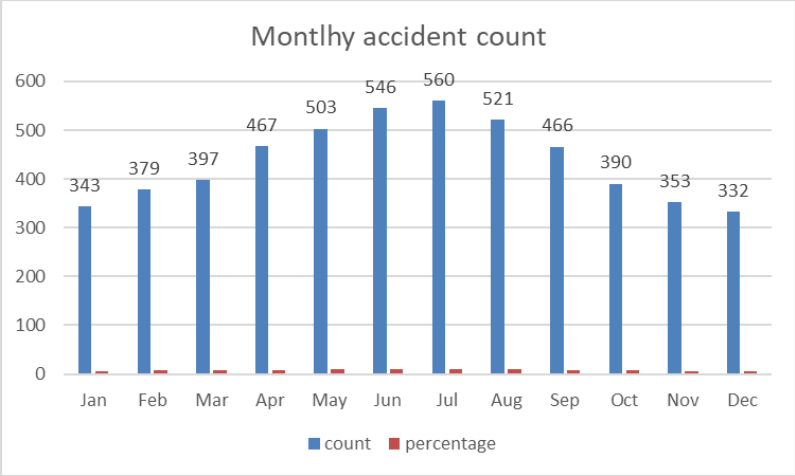


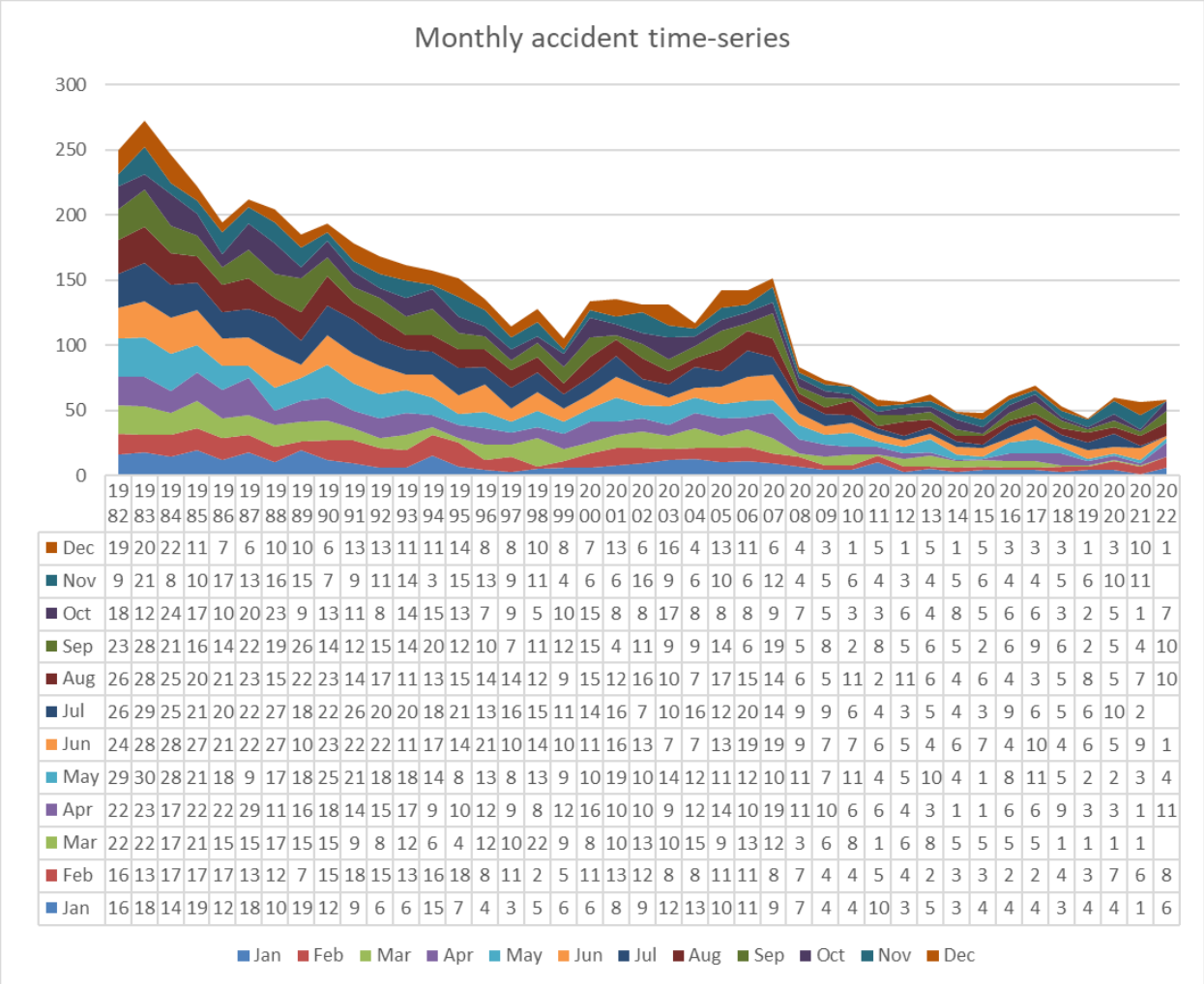






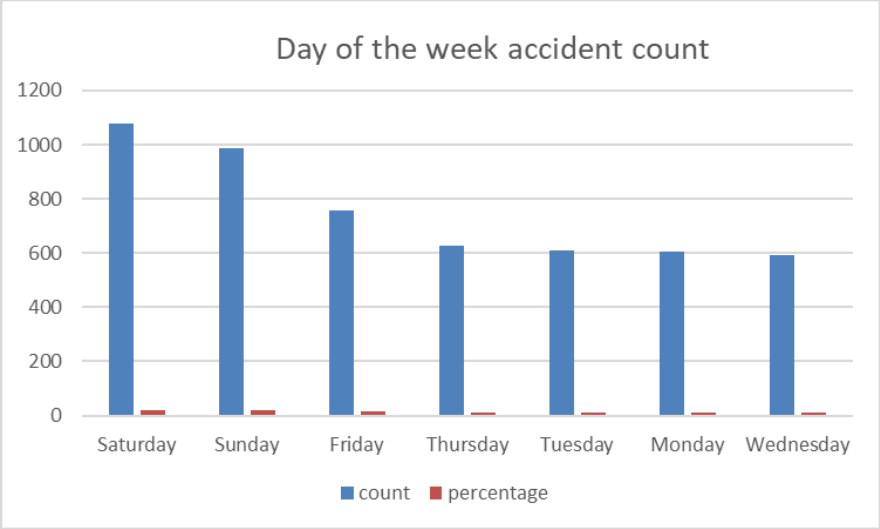
Accidents by month in California based on the 1982-2022 dataset (Figure 15)

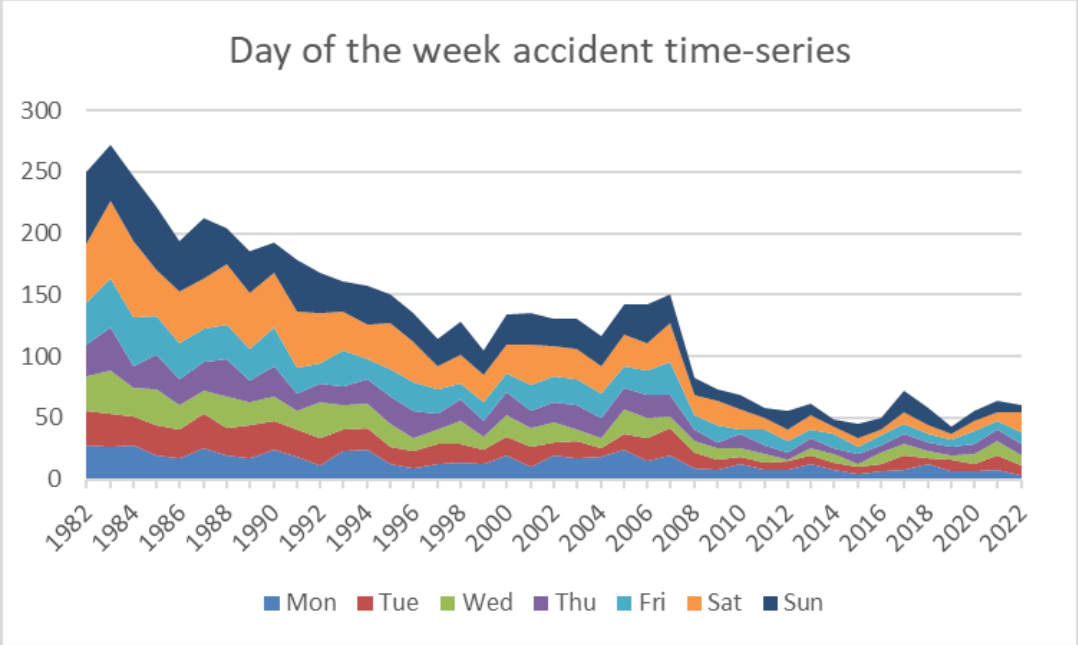




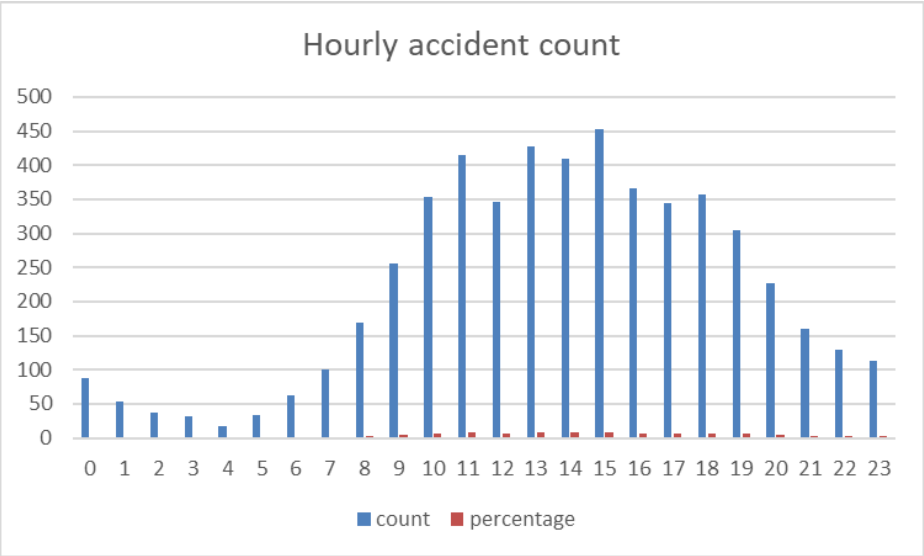
	1982	1983	1984	1985	1986	1987	1988	1989	1990	1991	1992	1993	1994	1995	1996	1997	1998	1999	2000	2001	2002	2003	2004	2005	2006	2007	2008	2009	2010	2011	2012	2013	2014	2015	2016	2017	2018	2019	2020	2021	2022
Dec	19	20	22	11	7	6	10	10	6	13	13	11	11	14	8	8	10	8	7	13	6	16	4	13	11	6	4	3	1	5	1	5	1	5	3	3	3	1	3	10	1
Nov	9	21	8	10	17	13	16	15	7	9	11	14	3	15	13	9	11	4	6	6	16	9	6	10	6	12	4	5	6	4	3	4	5	6	4	4	5	6	10	11	
Oct	18	12	24	17	10	20	23	9	13	11	8	14	15	13	7	9	5	10	15	8	8	17	8	8	8	9	7	5	3	3	6	4	8	5	6	6	3	2	5	1	7
Sep	23	28	21	16	14	22	19	26	14	12	15	14	20	12	10	7	11	12	15	4	11	9	9	14	6	19	5	8	2	8	5	6	5	2	6	9	6	2	5	4	10
Aug	26	28	25	20	21	23	15	22	23	14	17	11	13	15	14	14	12	9	15	12	16	10	7	17	15	14	6	5	11	2	11	6	4	6	4	3	5	8	5	7	10
Jul	26	29	25	21	20	22	27	18	22	26	20	20	18	21	13	16	15	11	14	16	7	10	16	12	20	14	9	9	6	4	3	5	4	3	9	6	5	6	10	2	
Jun	24	28	28	27	21	22	27	10	23	22	22	11	17	14	21	10	14	10	11	16	13	7	7	13	19	19	9	7	7	6	5	4	6	7	4	10	4	6	5	9	1
May	29	30	28	21	18	9	17	18	25	21	18	18	14	8	13	8	13	9	10	19	10	14	12	11	12	10	11	7	11	4	5	10	4	1	8	11	5	2	2	3	4
Apr	22	23	17	22	22	29	11	16	18	14	15	17	9	10	12	9	8	12	16	10	10	9	12	14	10	19	11	10	6	6	4	3	1	1	6	6	9	3	3	1	11
Mar	22	22	17	21	15	15	17	15	15	9	8	12	6	4	12	10	22	9	8	10	13	10	15	9	13	12	3	6	8	1	6	8	5	5	5	5	1	1	1	1	
Feb	16	13	17	17	17	13	12	7	15	18	15	13	16	18	8	11	2	5	11	13	12	8	8	11	11	8	7	4	4	5	4	2	3	3	2	2	4	3	7	6	8
Jan	16	18	14	19	12	18	10	19	12	9	6	6	15	7	4	3	5	6	6	8	9	12	13	10	11	9	7	4	4	10	3	5	3	4	4	4	3	4	4	1	6

Accident by day of the week in California based on the 1982-2022 dataset(Figure 16)





Accidents by the hour in California based on the 1982-2022 dataset (Figure 17)



Accident by injury type in California (Figure 18)

Injury Total Fatal: 2,202

Injury Total Minor: 1,704

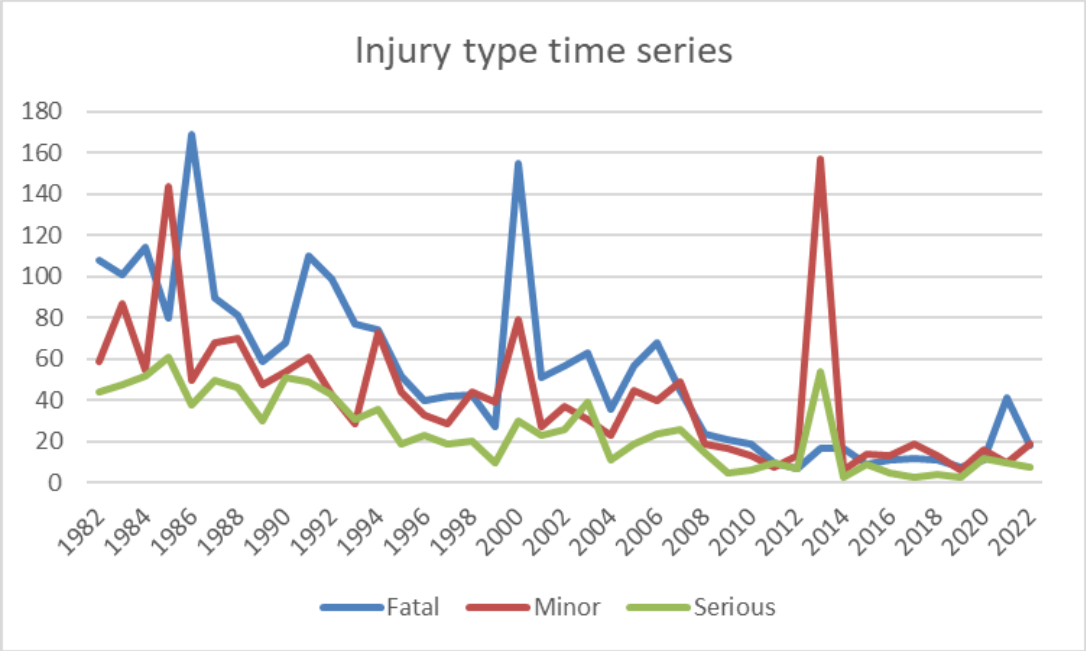
Injury Total Serious: 1,022

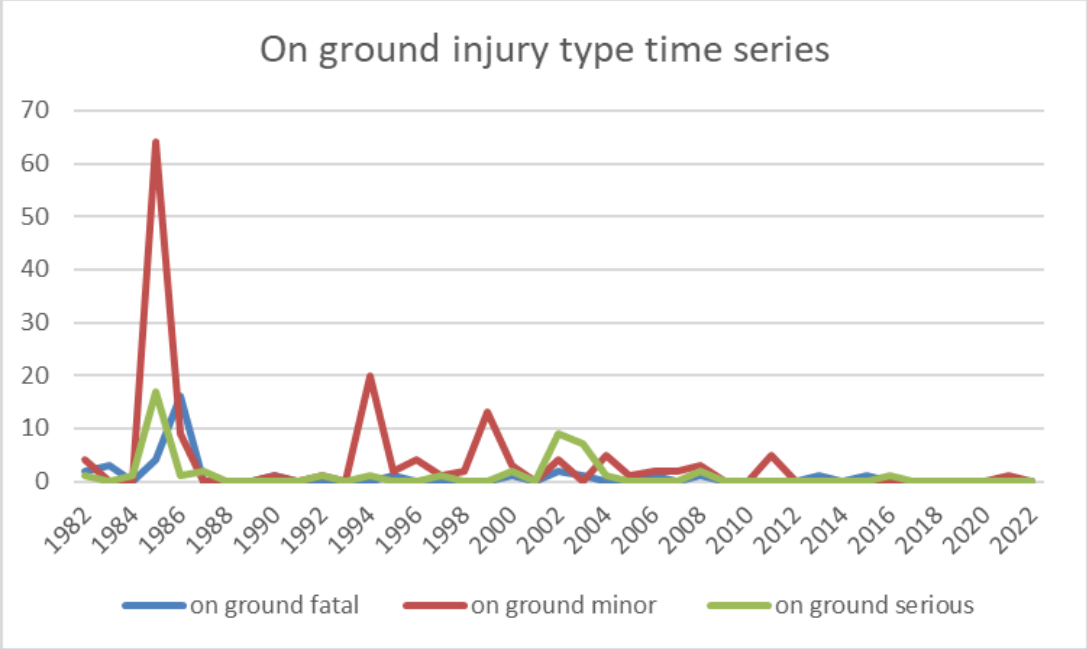
On Ground, Minor Injuries: 147

On Ground, Serious Injuries: 47

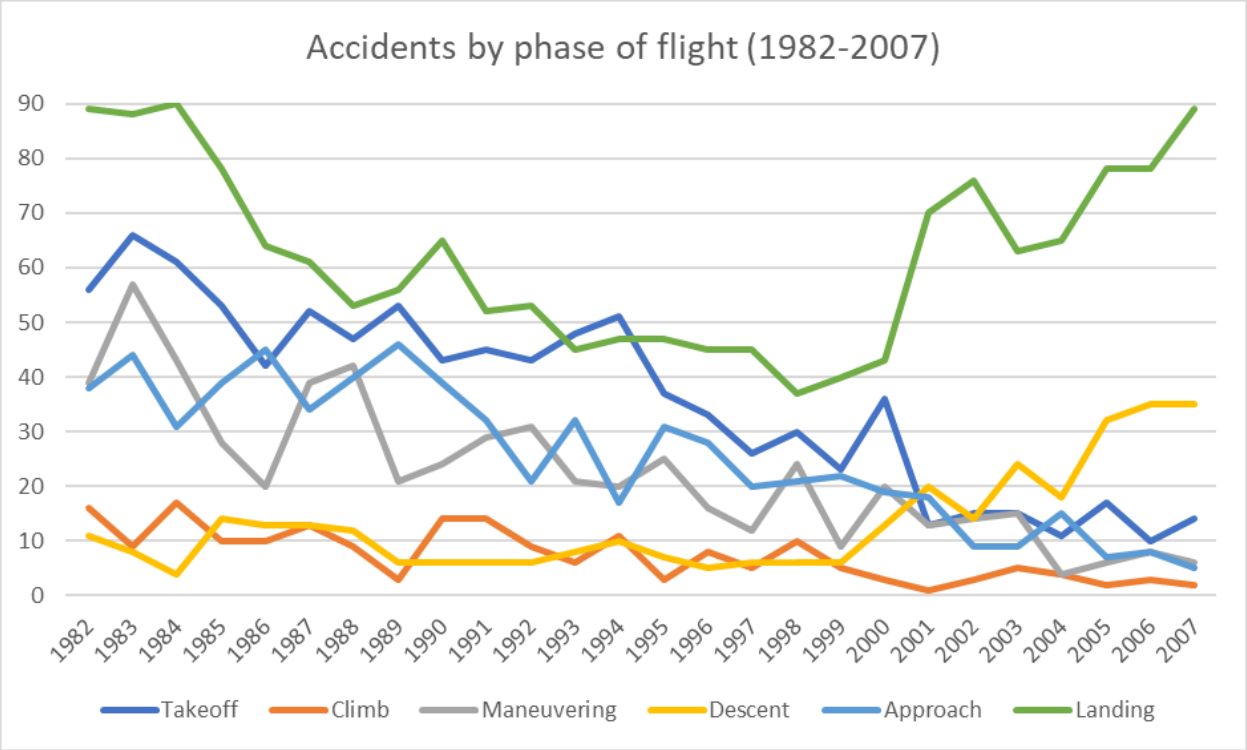
On Ground, Fatal Injuries: 35

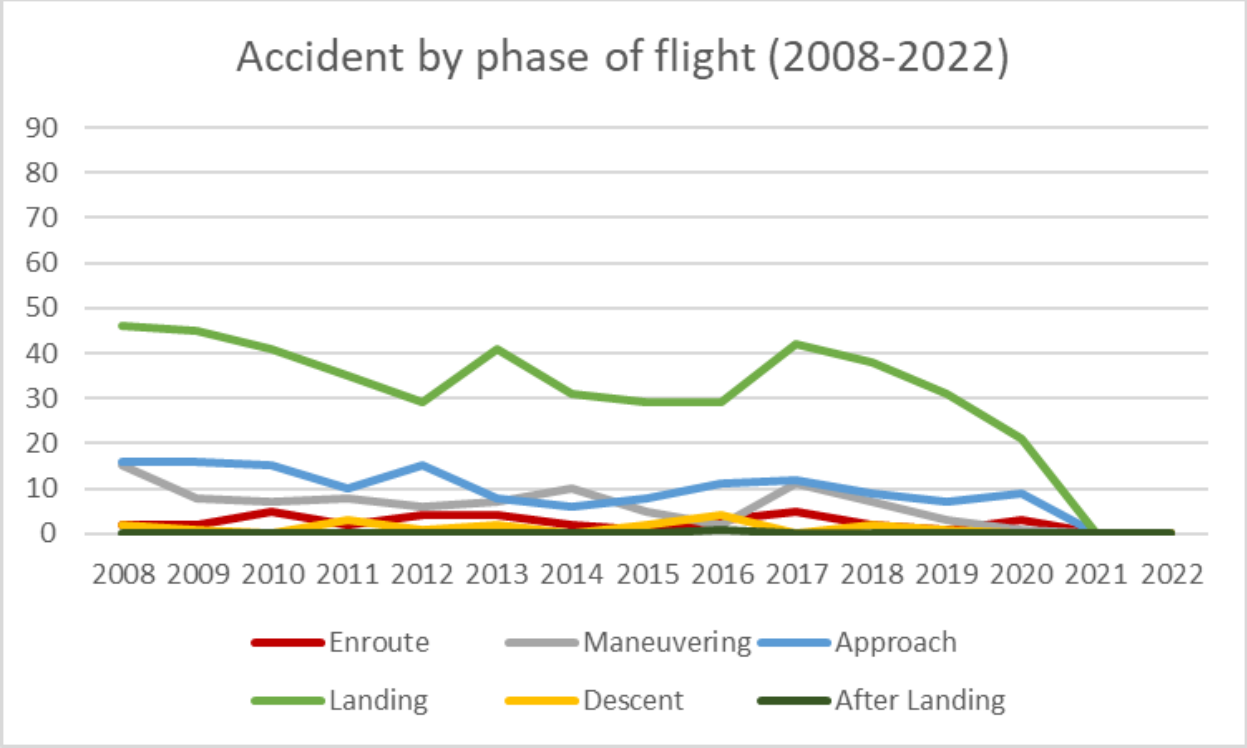
Injury Total All (F+S+M): 7,170





Accident by phase of flight in California (Figure 19)





3.2. Spatiotemporal accident dataset analysis

This section focuses on spatial properties of ALUP-relevant accidents such as location, spatial patterns, spatial arrangement, distance, and a focus on understanding accident density through an exploratory point patterns analysis and interpolation.
Point pattern analysis is done using Getis-Ord General G statistic, which measures the degree of clustering for either high or low values (hot spot analysis) with respective statistical significance. The statistical significance is featured at 99, 95, and 90% confidence levels of high or low spatial clusters taking into consideration the randomization null hypothesis of accident occurrence in a determined area.
Interpolation decomposes point data into line and areal data to help identify spatial patterns, including those of specific accident attributes such as injury type.

For the spatiotemporal accident data analysis, we explore the results across three spatial datasets:

(1) **CA_spatialLargest_08-22**, total accident events = 1,355 representing the dataset with highest number of spatially-relevant events.
(2) **CA_spatial2011Method_08-22**, total accident events = 292 representing the closest reproduction of the 2011 handbook method.
(3) **CA_spatialAccuracy_08-22**, total accident events = 466 representing highest spatial-accuracy criteria.

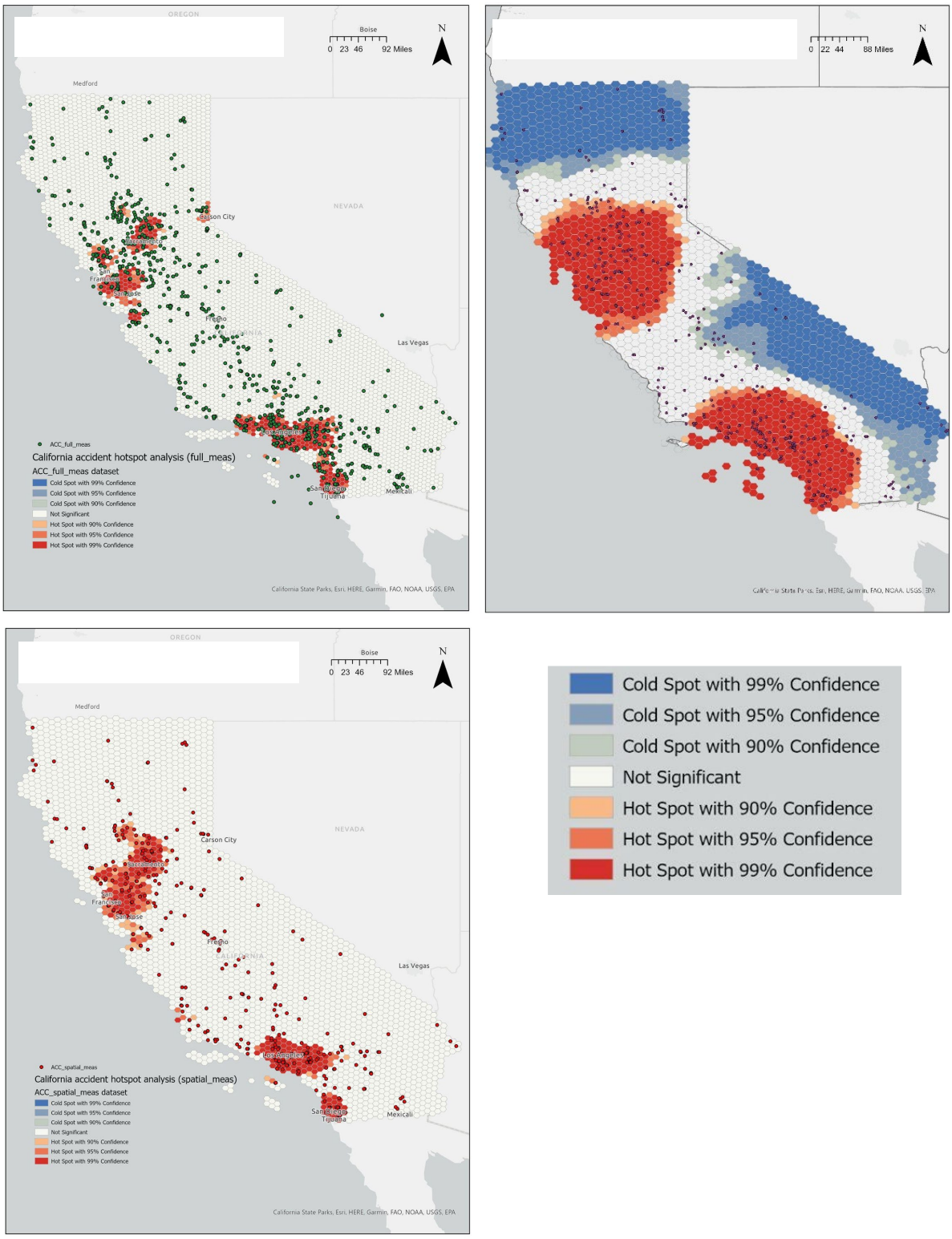
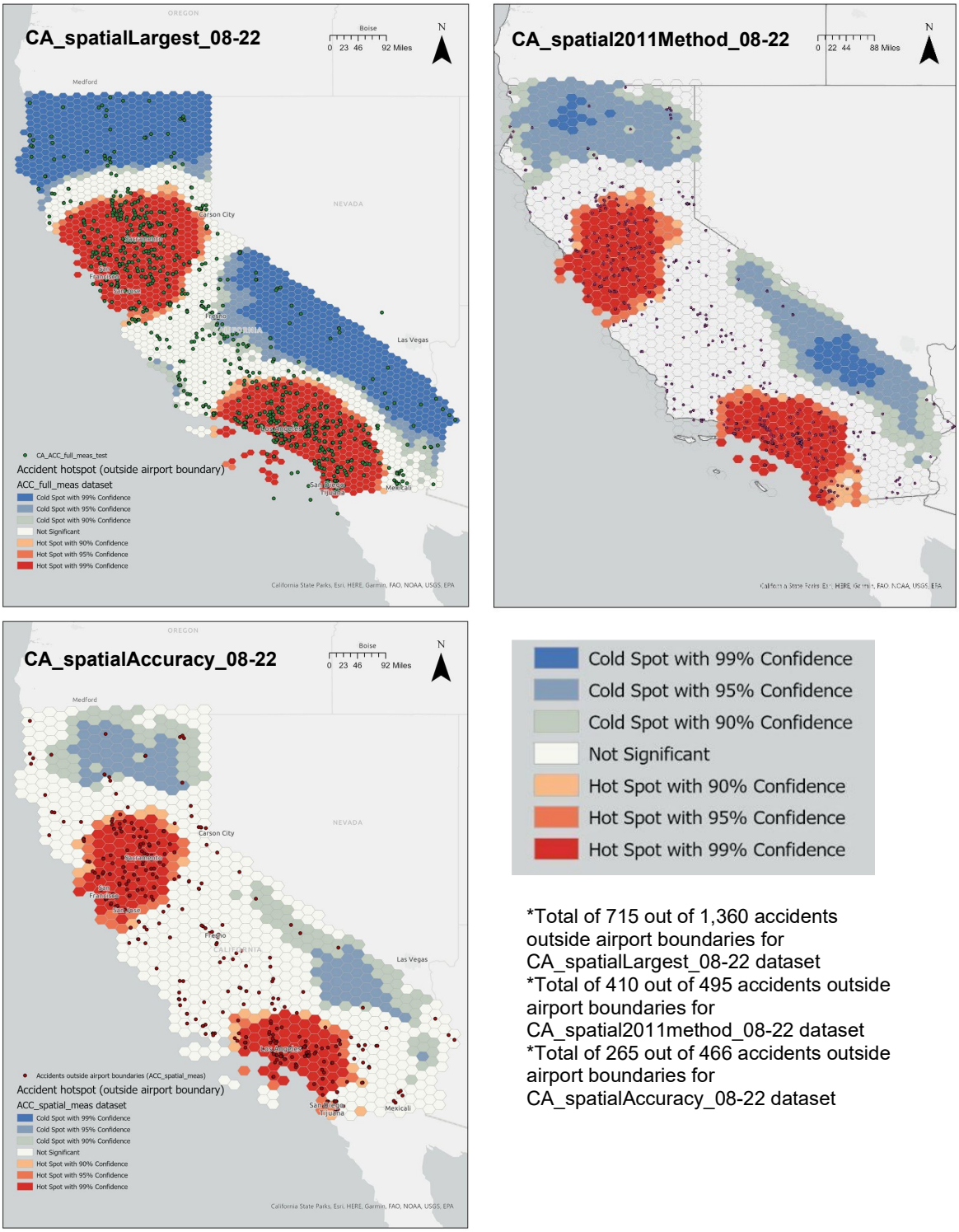


Figure 20. High clustering of accidents: state-level analysis for each spatial dataset



*Total of 715 out of 1,360 accidents outside airport boundaries for CA_spatialLargest_08-22 dataset
*Total of 410 out of 495 accidents outside airport boundaries for CA_spatial2011method_08-22 dataset
*Total of 265 out of 466 accidents outside airport boundaries for CA_spatialAccuracy_08-22 dataset

Figure 21. Hot spot analysis of accidents outside airport boundaries for all spatial accident datasets.

3.2.1. Accident spatial distribution in airport vicinities

Figure 22 identifies the total number of accidents within the 1-5 mile buffer around airport boundaries and the evolution of these accidents from 2008-2022. The hotspot analysis of accidents located solely within 1-5 miles of airport boundaries (Figure 23) indicates that Caltrans northern Districts 3 and 4, and California southern Districts 7,8,11, 12 have the highest clustering of accident events within areas of interest to the ALUCs. The northern clustering Districts concentrate 136 accident events for the CA_spatialAccuracy_08-22 database out of 466. The southern clustering Districts concentrate 175 accident events for the CA_spatialAccuracy_08-22 database out of 466. Tables 7 and 8 rank the airports with the highest number of accidents in their vicinity versus those that have the highest number of accidents within their boundaries.

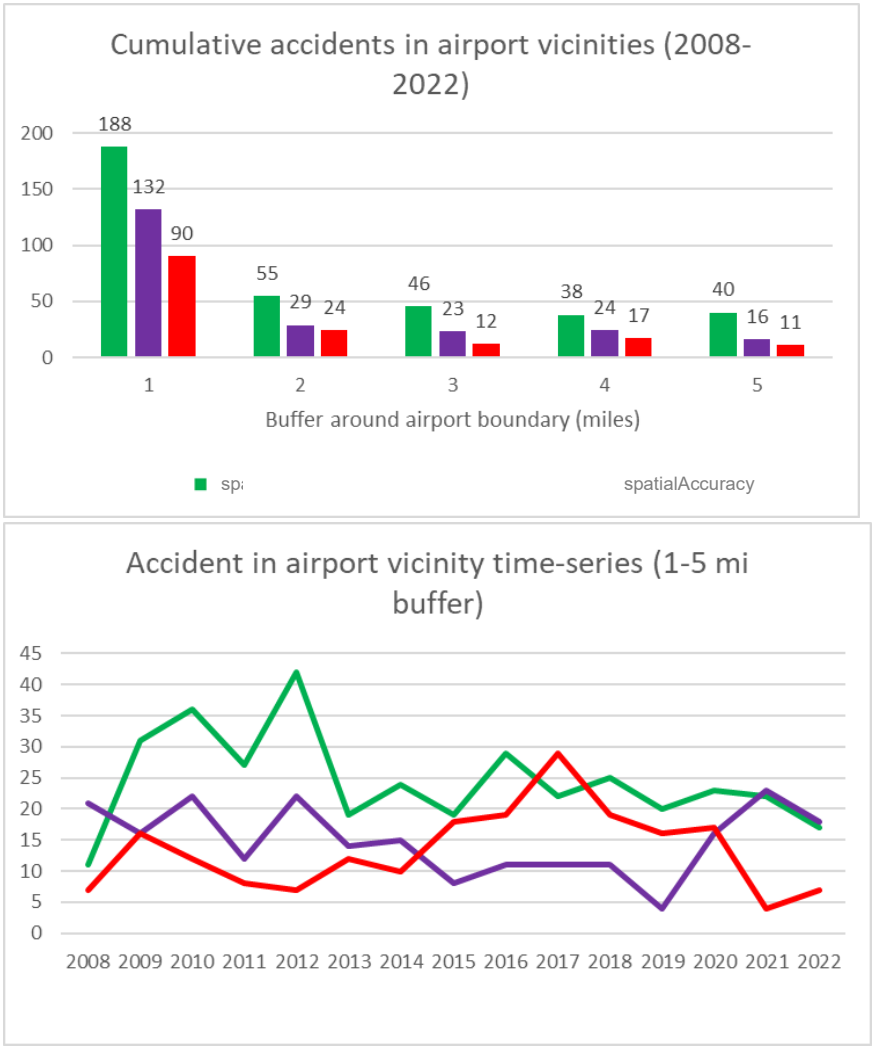


Figure 22. Accident count and evolution in airport vicinities (1-5 mile buffer)

- Total of 367 accidents in 1-5 miles of airports out of 1,355 (CA_spatialLargest_08-22)
- Total of 292 accidents in 1-5 miles of airports out of 495 (CA_spatial2011Method_08-22)

- Total of 201 accidents in 1-5 miles of airports of 466 (CA_spatialAccuracy_08-22)

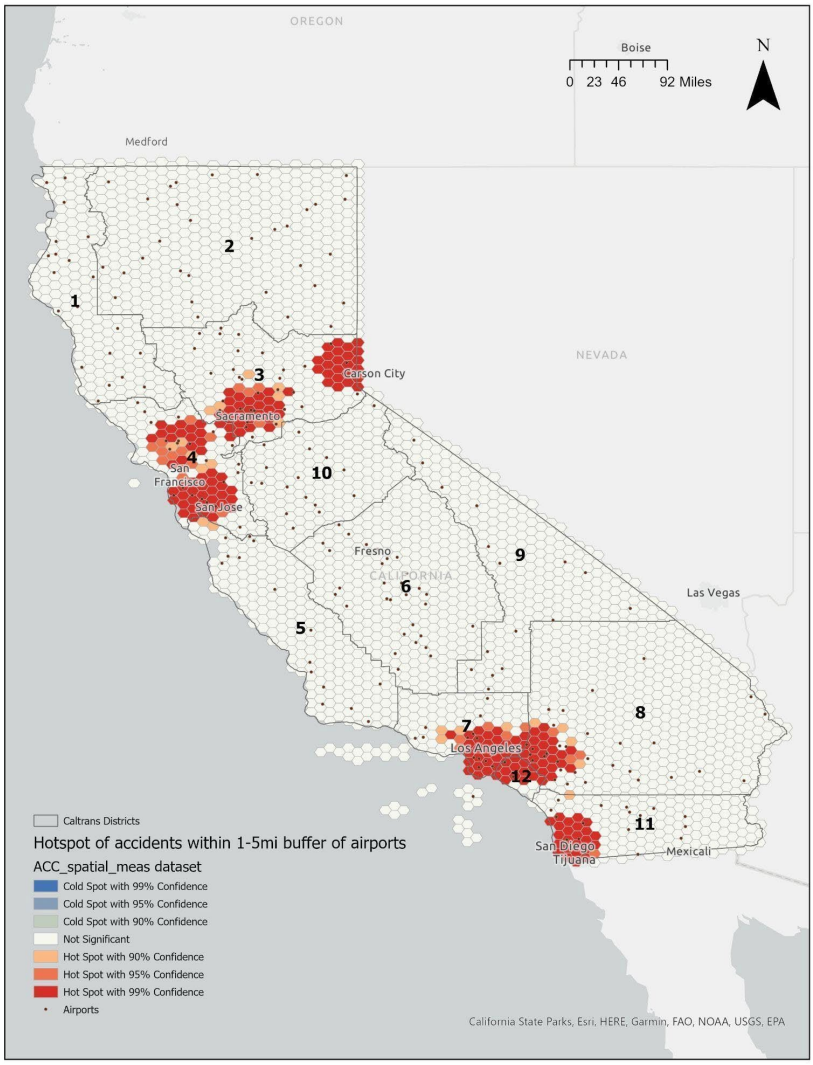
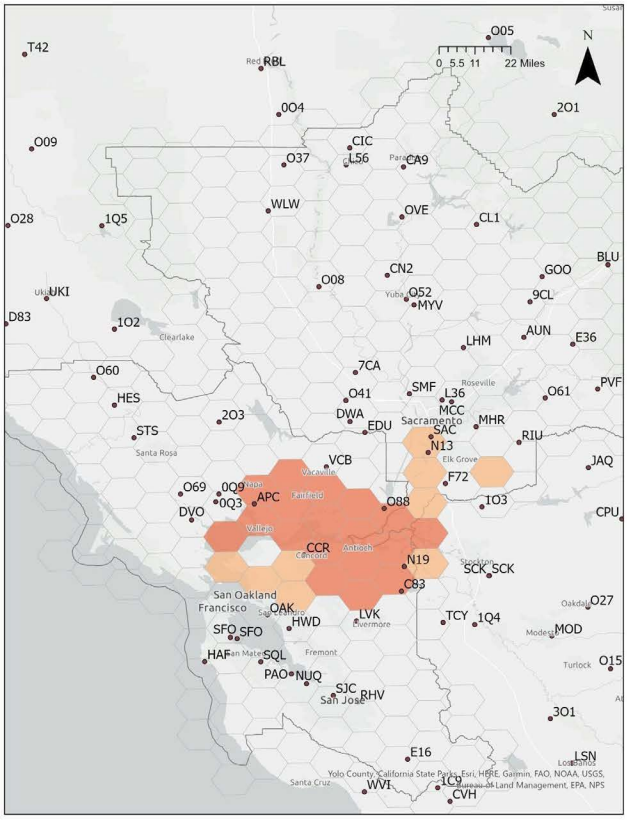
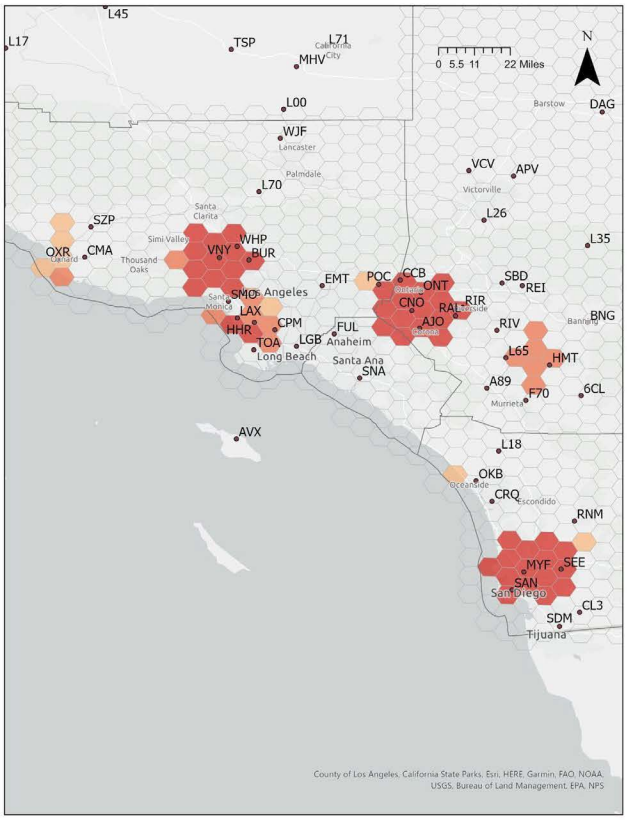


Figure 23. Hotspot analysis of accidents within 1-5 mile buffer of airport boundaries (CA_spatialAccuracy_08-22)





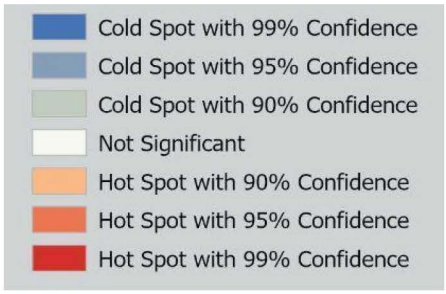


Figure 24. Hot spot analysis of northern (above) and southern (below) Caltrans districts with accident concentration from 1-5 miles airport buffer (CA_spatialAccuracy_08-22).

Table 7. Rank of airports with highest number of accidents outside their boundary (1-5 miles buffer of boundary) for spatial accident datasets (2008-2022).

Rank	Count Spatial Largest		Count 2011 Method		Count Spatial Accuracy	
1	15	BUR	12	AJO	8	AJO
2	15	TRK	10	LAX	6	LAX
3	13	VNY	6	CCB	5	ONT
4	11	LAX	6	ONT	5	WHP
5	11	NUQ	6	RHV	4	BUR
6	10	HHR	6	WHP	4	CCB
7	9	AJO	5	BUR	4	CPM
8	9	CNO	5	CNO	4	LVK
9	8	EDU	5	CPM	4	MYF
10	8	ONT	5	E45	4	NUQ
11	8	WHP	5	LVK	4	PAO
12	7	0Q3	5	MYF	4	RHV
13	7	CCB	5	NUQ	4	SEE
14	7	MYF	5	PAO	3	1O2
15	7	PAO	5	SBD	3	AVX
16	7	SBD	5	SEE	3	CNO
17	7	SEE	5	TRK	3	EDU
18	6	1O2	4	0Q3	3	GOO
19	6	DWA	4	0Q9	3	HHR
20	6	N13	4	AVX	3	N13

Table 8. Rank of airports with highest number of accidents inside their boundary for the spatial datasets (2008-2022). *Includes Primary Surface accidents

Rank	Count Spatial Largest		Count 2011 Method		Count Spatial Accuracy	
1	MYF	16	MYF	11	MYF	10
2	CMA	14	VNY	8	VNY	6
3	FUL	14	C83	8	CNO	6
4	AJO	13	O22	8	SBP	6
5	SEE	13	CNO	7	WVI	5
6	CNO	13	RDD	7	CMA	5
7	VNY	12	SBP	7	O22	5
8	TOA	11	WVI	6	RDD	5
9	RHV	11	STS	5	STS	4
10	WHP	10	APC	5	SNS	4
11	LGB	10	CMA	5	C83	4
12	LHM	9	SBA	5	HMT	4
13	LVK	9	TRM	4	SMX	4
14	WJF	8	TRK	4	TRM	3
15	SQL	8	SNS	4	WLW	3
16	EMT	8	RNM	4	APC	3
17	L18	8	APV	4	RNM	3
18	PSP	8	HMT	4	APV	3
19	LAX	8	LVK	4	L18	3
20	SBA	8	GOO	4	LHM	3

3.2.3. Accident spatial distribution per generic safety zones

Table 9. Total count of accidents within each Safety Zone (2008-2022)

	Accident dataset		
Safety Zones	**Spatial Largest**	**2011 Method**	**Spatial Accuracy**
Primary Surface	503	N/A	138
Z1	34	34	19
Z2	40	28	22
Z3	24	17	13
Z4	4	3	3
Z5	91	57	43
*Z6**	137	77	53
Total in Safety Zones	833	*216	291
Total Accidents	1360	*292	466

*Excludes accidents in Primary Surface and accidents outside the 5 mile buffer of airport's centroid for comparison with 2011 Handbook methodology

** Due to an under dimensioning error of Zone 6, any results associated with this zone area are underestimated, this error does not impact the core results of this analysis. Please refer to Task 8 for further information on the mitigation of this error.

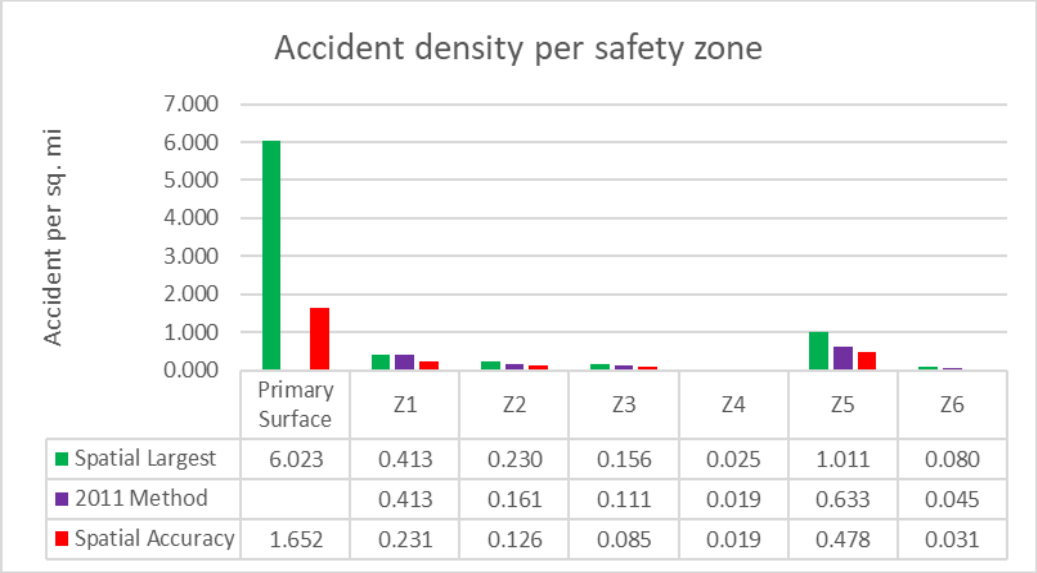


Figure 25. Accident density per safety zone (cumulative accident over 259 California airports assessed). Density formula: $Accidents/Area$

Table 10. Percentage of accident in each safety zone relative to total accidents in California (2008-2022)

Safety Zones	**Spatial Largest**	**Spatial 2011 Method**	**Spatial Accuracy**
Primary Surface	36.99%	N/A	29.61%
Z1	2.50%	11.41%	4.08%
Z2	2.94%	9.40%	4.72%
Z3	1.76%	5.70%	2.79%
Z4	0.29%	1.01%	0.64%
Z5	6.69%	19.13%	9.23%
*Z6**	10.07%	25.84%	11.37%

*Due to an under dimensioning error of Zone 6, any results associated with this zone area are underestimated, this error does not impact the core results of this analysis. Please refer to Task 8 for further information on the mitigation of this error.

Table 11. Percentage of accident in each safety zone relative to total accident within safety zones (2008-2022)

Safety Zones	**Spatial Largest**	***spatial 2011 Method**	**Spatial Accuracy**	**2011 Handbook Metrics****
Primary Surface	60.38%	N/A	47.42%	N/A
Z1	4.08%	15.74%	6.53%	20-21%
Z2	4.80%	12.96%	7.56%	8-22%
Z3	2.88%	7.87%	4.47%	4-8%
Z4	0.48%	1.38%	1.03%	2-6%
Z5	10.92%	26.38%	14.78%	3-5%
*Z6***	16.45%	35.64%	18.21%	18-29%

*Excluding accident in Primary Surface and accidents outside the 5 mile buffer of airport's centroid for comparison with 2011 Handbook methodology **The 2011 Handbook accident metrics correspond to the % of accidents within each safety zone. There is no explicit information on what the % is relative for, we estimate the results refer to the % relative to all accidents within the 2 mile buffer of each airport.

** Due to an under dimensioning error of Zone 6, any results associated with this zone area are underestimated, this error does not impact the core results of this analysis. Please refer to Task 8 for further information on the mitigation of this error.

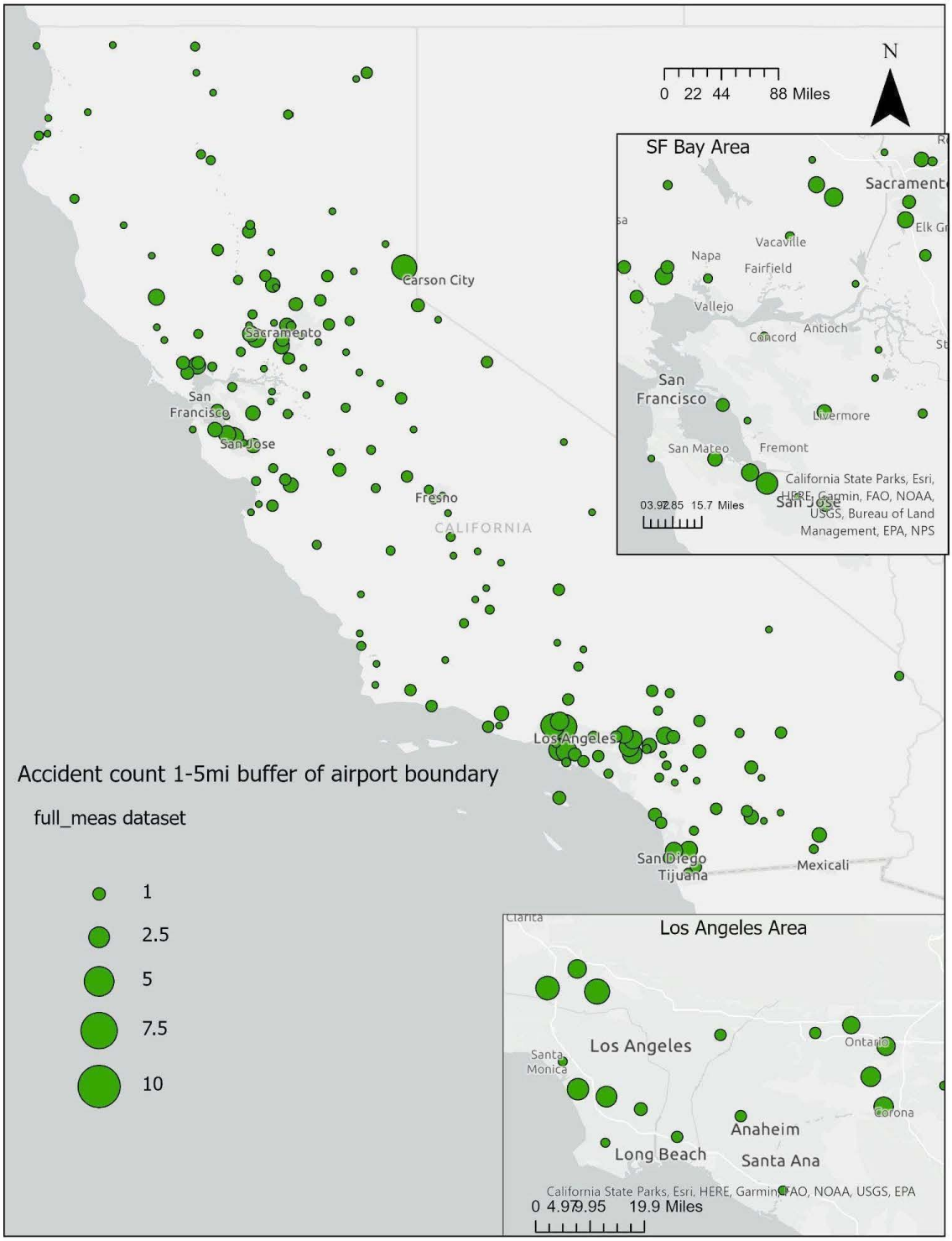


Figure 26. Accident count within 1-5 mi buffer of airports in California (CA_spatialLargest_08-22 dataset). Excludes accidents inside airport parcels.

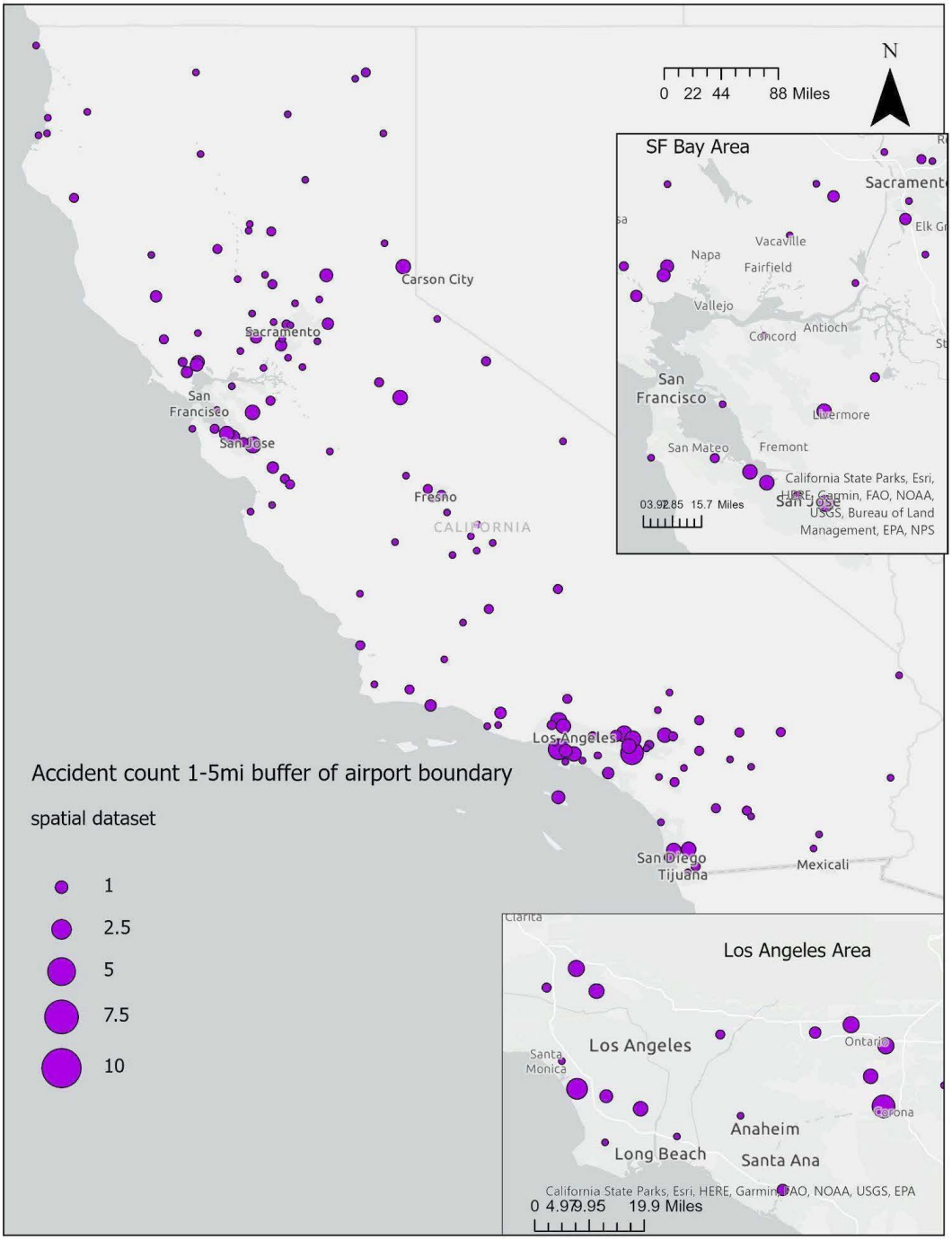


Figure 27. Accident count within 1-5 mi buffer of airports in California (CA_spatial2011Method_08-22 dataset). Excludes accidents inside airport parcels.

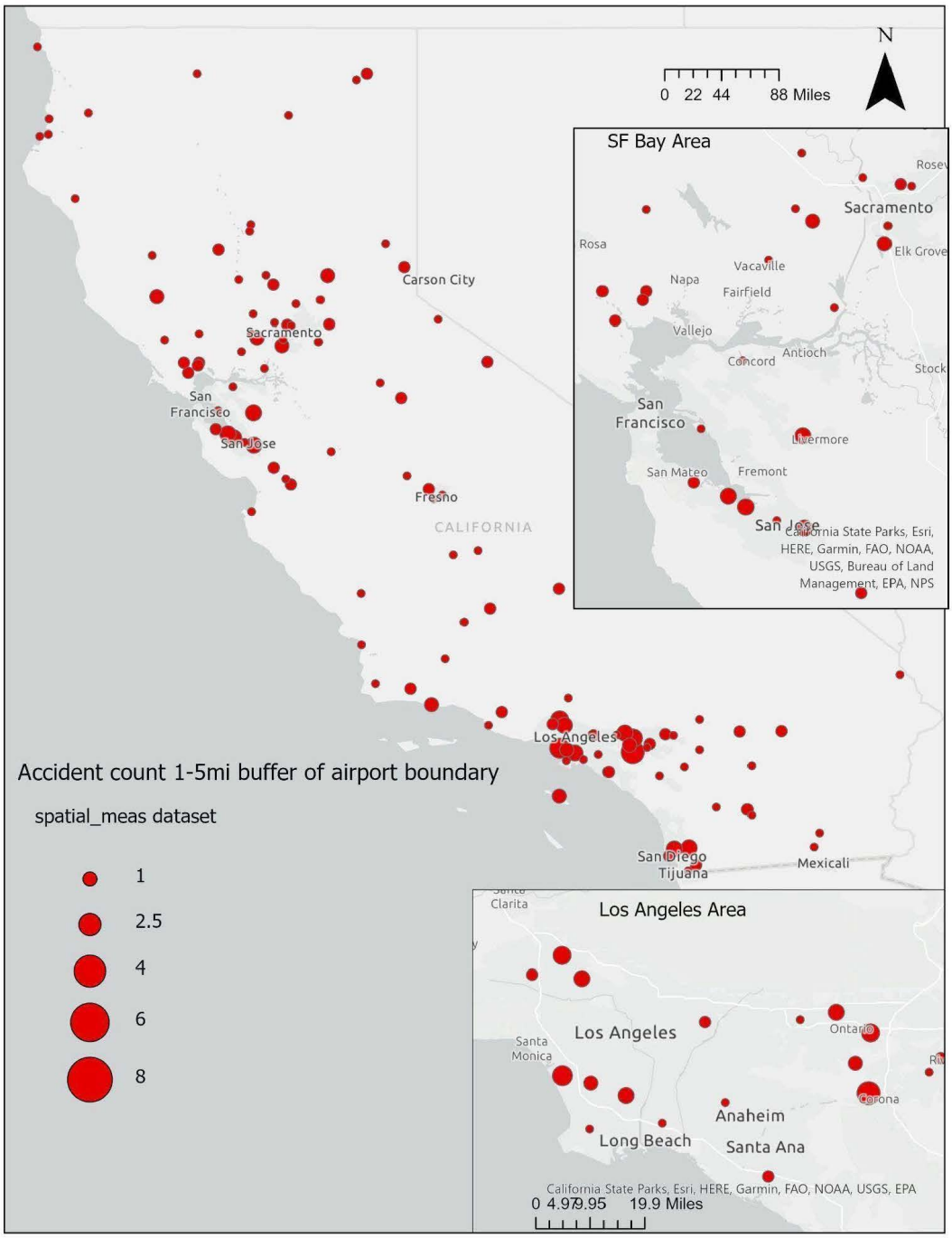


Figure 28. Accident count within 1-5 mi buffer of airports in California (CA_spatialAccuracy_08-22 dataset). Excludes accidents inside airport parcels.



Figure 29. Accident time-series per safety zones across spatiotemporal accident datasets (From top to bottom: Spatial Largest accident dataset; Spatial 2011 Method accident dataset; Spatial Accuracy accident dataset, all from 2008-2022)

3.2.4. Cumulative accident distribution based on distance from runway end

Since the 2002 Handbook, accidents are assessed by the distance relative to the runway end. This section updates this analysis by focusing on the changes of mean and median distance of arrival and departure accidents taking into consideration the 2008-2022 geospatial NTSB accident dataset.

An important way of looking at aircraft accidents is by the distance the accident occurred relative to the runway end associated with the aircraft operation. The 2002 Handbook tabulated these distances in Table 8D. An updated version of this table (Table E1) focuses on the mean and median distances for all categories of accidents, with both the distances from the previous study as well as the current effort. The limited number of records which met the criteria for this study has prevented any valid analysis for the various sub-categories included in the Table 8D of 2002 Handbook (Table E6, below). For arrival accidents, the mean distance from the runway end has decreased by less than 150 feet (-4.8%), while the mean distance for departures has increased by 884 feet (16%). The median distance for arrival accidents has more than doubled from the 2002 study at 1,000 feet to 2,110 feet (111%) in the current study. The median distance for departure accidents has increased by slightly more than 600 feet (13%), from 4,684 feet in the 2002 study to 5,296 feet in the current study.

Table 12. Mean and median distance of accidents from runway end and centerline between 2008-2022

Distance in ft (Distance in the X,Y plot Figures 29-31)	Arrivals	Departures
Mean from runway end	10,470 ft (9,109 ft)	9,452 ft (8,559 ft)
Median from runway end	1,513 ft (-242 ft)	1,594 ft (907 ft)
Mean distance from runway centerline	8,558 ft (-338 ft)	9,594 ft (750 ft)
Median distance from runway centerline	634 ft (-20 ft)	27 (1,307 ft)

Table 13. Mean and median distance of accidents from runway end and centerline between 2000-2009 (2011 ALUP Handbook, p E-7 Table E-1)

This section plots all accidents from the “CA_spatialLargest_08-22” dataset with distances to the nearest end of a runway. Accidents are not reliably linked to runways in the NTSB dataset, so the nearest runway in the BTS dataset was used as a reference. Accidents are first selected for aircraft type (excluding helicopters, balloons, powered parachutes, gyrocopters, and gliders). Accidents are then divided into arrivals (phase codes 404, 405, 500, 501, 502, 503, 504, 505, 506, 507, 508, 509, 550, 551, 552, 600, 650, 750), departures (phase codes 300, 350, 401), and other relevant accidents (phase codes 400, 402, 403, 450, 451, 452, 453, 700, 800, 990).

The nearest runway end is then located within the BTS dataset and coordinates relative to the position and orientation of the runway are calculated. These coordinates are then plotted, and the graph is limited to a certain distance from the runway end.

The plots below cover 212 departures, 392 arrivals, and 296 other relevant accidents remaining after this division. They are plotted at different scales starting at 200,000, 5,000, and 1000 feet from the nearest runway end.
Table 12 provides the mean and median distances from runway end and runway centerline of departure and arrival-related accidents. For arrival accidents, the mean distance from the runway end.

Input Data:

a. Accident data with the largest spatial dataset (CA_spatialLargest_08-22)
b. BTS Runway Lines Data

Process:

1. Select events based on aircraft type (excludes helicopters, balloons, powered parachutes, gyrocopters, and gliders) (964 events remain)
2. Divide data into arrivals (392), departures (212), and other relevant accidents (296).
3. Find nearest runway end in BTS runway lines data.
4. Transform coordinates into coordinates relative to the orientation of the runway and centered on the near end.
5. Plot these transformed coordinates for the 900 remaining events
6. Limit plot to distance from the end of the runway

Output Data:

a. CSV containing coordinates for perpendicular (right is positive) and parallel (away from the runway is positive) to the runway, as well as data from input sheets ‘events’, ‘aircraft’, and ‘Events_Sequence’.
b. Scatter plot as an image file.

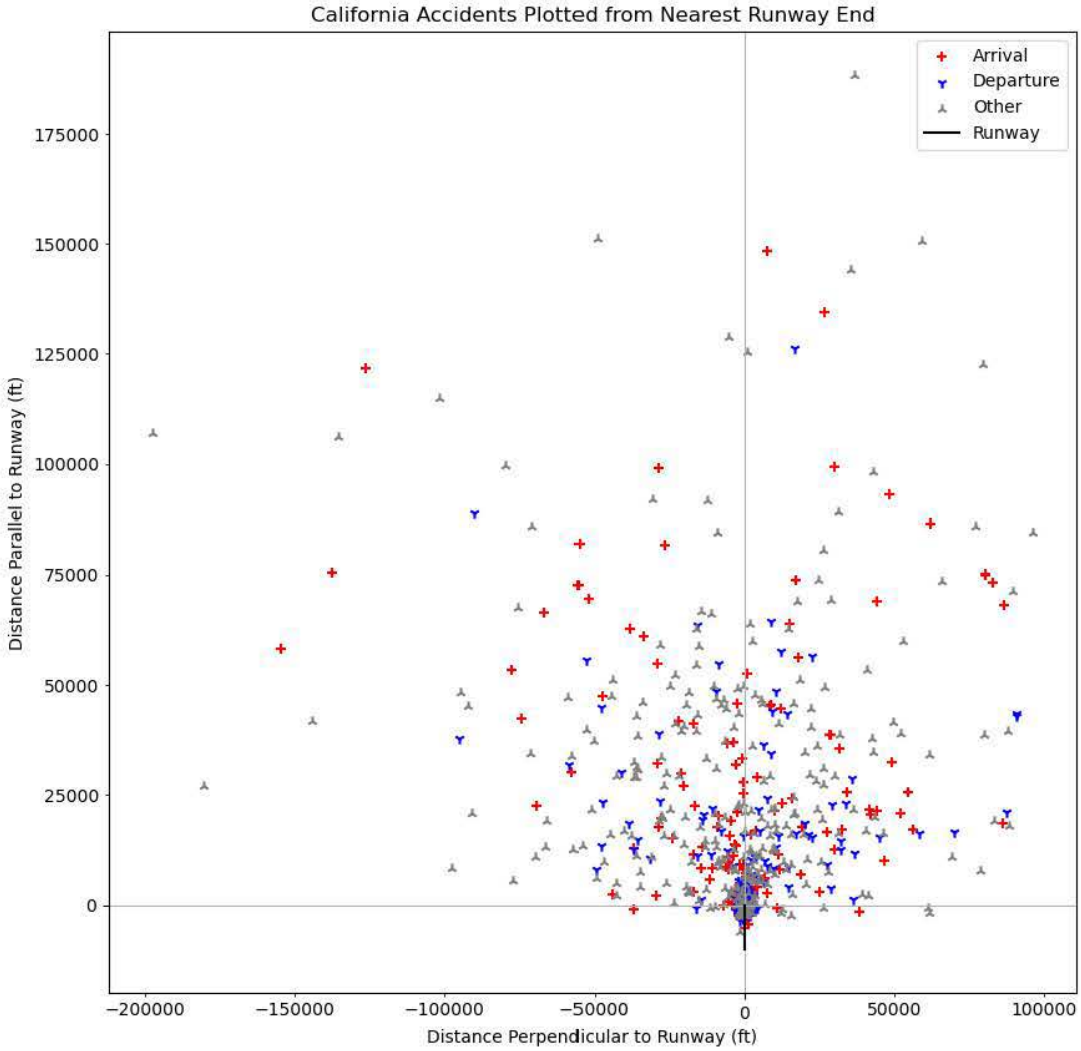


Figure 29. Cumulative accidents at 200,000ft from nearest runway

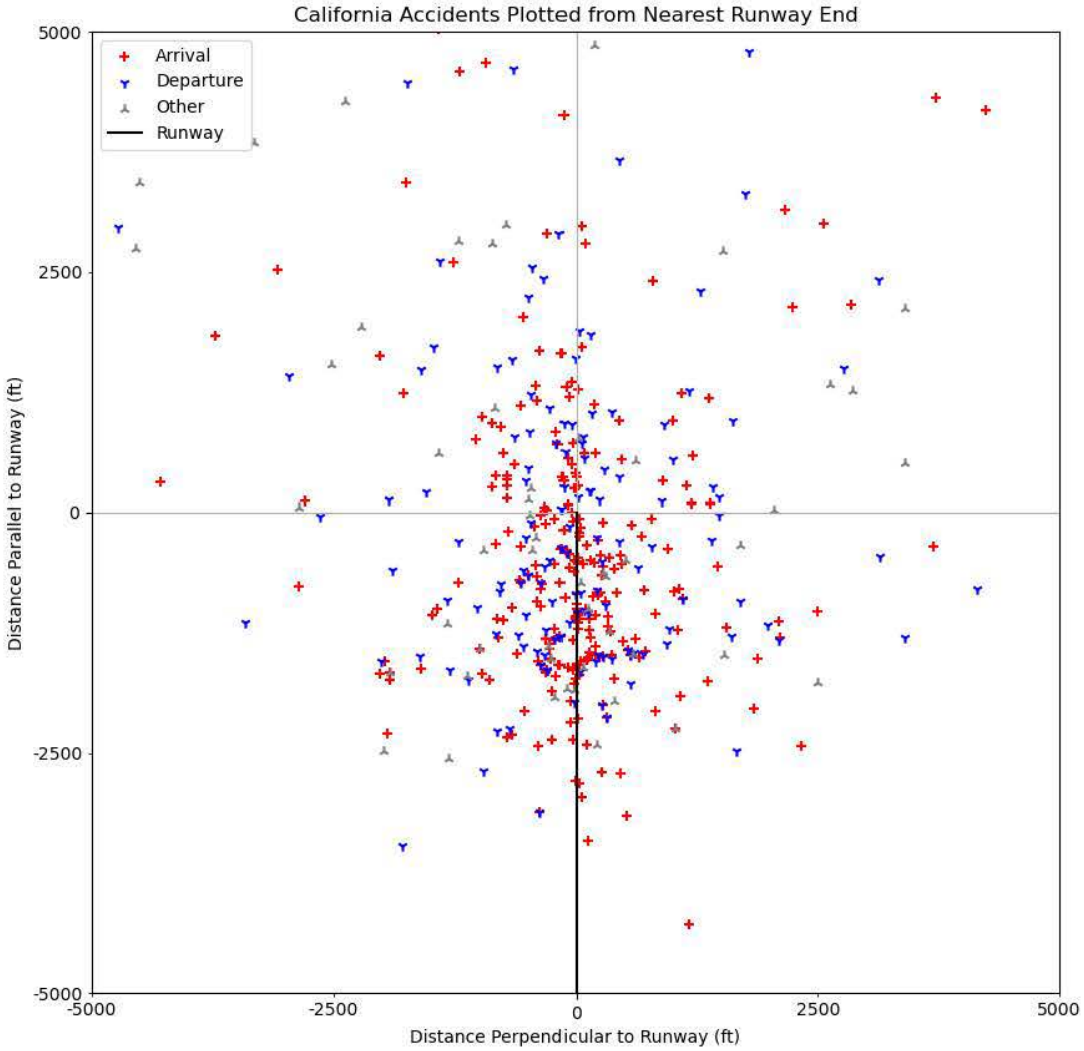


Figure 30. Cumulative accidents at 5,000ft from nearest runway

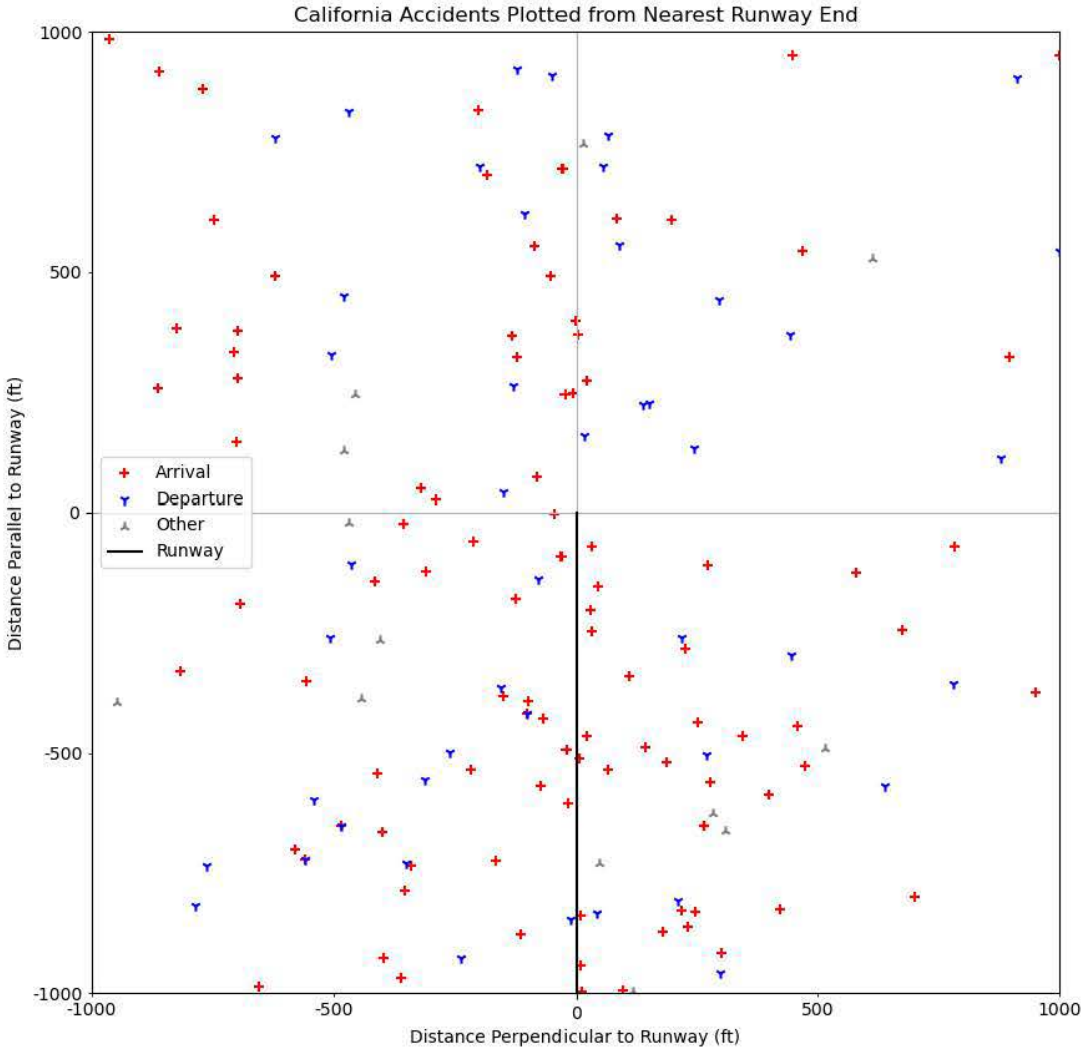


Figure 31. Cumulative accidents at 1,000ft from nearest runway

[4.1] Appendix A. Phase of flight code descriptions and variable selection to correspond to takeoff, climb, approach, and landing.

This classification was done based on Berkeley and Caltrans inputs.

Table A.1. Variables used for the selection criteria of ALUP relevant phases of flight (pertaining to takeoff, climb, approach and landing)

code_iaids	meaning	Takeoff/Landing*
300xxx	Takeoff	T
350xxx	Initial Climb	T
400xxx	Enroute	T
401xxx	Enroute-Climb to cruise	T
402xxx	Enroute-Cruise	N/A
403xxx	Enroute-Change of cruise level	N/A
404xxx	Enroute-Descent	L
405xxx	Enroute-Holding (IFR)	L
450xxx	Maneuvering	N/A
451xxx	Maneuvering-Aerobatics	N/A
452xxx	Maneuvering-Low-alt flying	N/A
453xxx	Maneuvering-Hover	N/A
500xxx	Approach	L
501xxx	Approach-IFR Initial Approach	L
502xxx	Approach-IFR Final Approach	L
503xxx	Approach-Circling (IFR)	L
504xxx	Approach-IFR Missed Approach	L
505xxx	Approach-VFR Pattern Crosswind	L
506xxx	Approach-VFR Pattern Downwind	L
507xxx	Approach-VFR Pattern Base	L
508xxx	Approach-VFR Pattern Final	L
509xxx	Approach-VFR Go-Around	L
550xxx	Landing	L
551xxx	Landing-Flare/Touchdown	L

code_iaids	meaning	Takeoff/Landing*
300xxx	Takeoff	T
350xxx	Initial Climb	T
400xxx	Enroute	T
552xxx	Landing-Landing Roll	L
600xxx	Emergency Descent	L
650xxx	Uncontrolled Descent	L
700xxx	Post-Impact	N/A
750xxx	After Landing	L
xxx090	Abnormal Runway Contact	N/A
xxx091	Tailstrike	N/A
xxx092	Hard landing	L
xxx093	Dragged wing/rotor/float/other	N/A
xxx440	Off-field or emergency landing	L
xxx470	Collision with terr/obj (non-CFIT)	N/A
xxx490	Collision during takeoff/land	N/A
xxx500	Loss of lift	T

*T = Takeoff, L= Landing, N/A not enough information

List A.2. Variables used to exclude accident events that do not pertain to ALUP relevant phases of flight

Code_iaids & meaning

100xxx Prior to Flight
150xxx Standing
151xxx Standing-Engine(s) Not Oper
152xxx Standing-Engine(s) Start-up
153xxx Standing-Engine(s) Operating
154xxx Standing-Engine(s) Shutdown
200xxx Pushback/Towing
201xxx Pushback/Tow-Engine Not Oper
202xxx Pushback/Tow-Engine Start-up
203xxx Pushback/Tow-Engine Oper
204xxx Pushback/Tow-Engine Shutdown
250xxx Taxi
251xxx Taxi-to Runway
252xxx Taxi-into Takeoff Position
253xxx Taxi-from Runway
301xxx Takeoff-Rejected Takeoff
800xxx Other
990xxx Unknown
xxx000 Unknown or undetermined
xxx010 Aircraft loading event
xxx020 Aircraft servicing event
xxx030 Preflight or dispatch event
xxx040 Aircraft maintenance event
xxx050 Aircraft inspection event
xxx060 Attempted remediation/recovery
xxx070 Airport occurrence
xxx080 Ground handling event
xxx081 AC/prop/rotor contact w person

xxx082 Prop/jet/rotor blast/suction
xxx094 Landing gear collapse
xxx095 Landing gear not configured
xxx096 Nose over/nose down
xxx097 Roll over
xxx100 Air traffic event
xxx110 Cabin safety event
xxx120 Control flight into terr/obj
xxx130 Emergency descent initiated
xxx140 Engine shutdown
xxx150 Fire/Smoke (Non-Impact)
xxx160 Explosion (non-impact)
xxx170 Fire/Smoke (Post-Impact)
xxx180 Explosion (post-impact)
xxx190 Fuel Related
xxx191 Fuel starvation
xxx192 Fuel exhaustion
xxx193 Fuel contamination
xxx194 Wrong fuel
xxx200 Ground Collision
xxx210 Icing encounter
xxx220 Low altitude operations
xxx230 Loss of control on ground
xxx231 Dynamic Rollover
xxx232 Ground resonance
xxx240 Loss of control in flight
xxx241 Aerodynamic stall/spin
xxx242 VFR encounter with IMC
xxx243 Retreating blade stall
xxx244 Settling with power/vortex ring state
xxx245 Mast bumping
xxx250 Midair collision
xxx260 Near midair collision
xxx270 Abrupt Maneuver
xxx271 Inflight upset
xxx280 Course deviation
xxx290 Altitude deviation
xxx300 Runway Excursion
xxx310 Runway incursion animal
xxx320 Runway incursion veh/AC/person
xxx330 Sys/Comp malf/fail (non-power)
xxx331 Pressure/environ sys malf/fail
xxx332 Electrical system malf/failure
xxx333 Flight control sys malf/fail
xxx334 Flight instrument malf/fail
xxx335 Nav system malfunction/failure
xxx336 Comm system malf/failure
xxx337 Aircraft structural failure
xxx338 Part(s) separation from AC
xxx340 Powerplant sys/comp malf/fail
xxx341 Loss of engine power (total)
xxx342 Loss of engine power (partial)
xxx343 Uncontained engine failure
xxx350 Security/criminal event
xxx360 Turbulence Encounter
xxx361 Aircraft wake turb encounter
xxx362 Clear air turbulence encounter
xxx370 Landing area undershoot
xxx380 Landing area overshoot
xxx390 Windshear or Thunderstorm
xxx400 Other weather encounter
xxx401 VFR encounter with IMC
xxx402 Loss of visual reference
xxx410 Terrain avoidance alert
xxx420 Collision avoidance alert
xxx430 Stall warn/stick-shaker/pusher
xxx441 Ditching
xxx450 Hazardous material leak/spill
xxx460 Evacuation
xxx480 External load event (Rotorcraft)
xxx510 Glider tow event
xxx600 Simulated/training event
xxx900 Miscellaneous/other
xxx901 Birdstrike
xxx990 Missing aircraft

[4.1] Appendix B. List of 259 California public-use and general aviation airports included in the 2023 ALUP handbook update study

AIRPORTID	FACILITY NAME	Boundary Source
0O2	BAKER AIRPORT	Original Caltrans
0O4	CORNING MUNICIPAL AIRPORT	Original Caltrans
0O9	WARD FIELD AIRPORT	Original Caltrans
0Q3	SONOMA VALLEY AIRPORT	Original Caltrans
0Q4	SELMA AIRPORT	Original Caltrans
0Q5	SHELTER COVE AIRPORT	Original Caltrans
0Q9	SONOMA SKYPARK AIRPORT	Original Caltrans
1C9	FRAZIER LAKE AIRPARK	Original Caltrans
1O2	LAMPSON FIELD AIRPORT	Original Caltrans
1O3	LODI AIRPORT	Original Caltrans
1O5	MONTAGUE-YREKA, ROHRER FIELD	Original Caltrans
1O6	Dunsmuir Muni-Mott Airport	Digitized (OSM)
1Q1	ECKERT FIELD AIRPORT	Original Caltrans
1Q2	SPAULDING AIRPORT	Original Caltrans

1Q4	NEW JERUSALEM AIRPORT	Original Caltrans
1Q5	GRAVELLY VALLEY AIRPORT	Original Caltrans
2O1	GANSNER AIRPORT	Original Caltrans
2O3	PARRETT FIELD AIRPORT	Original Caltrans
2O6	CHOWCHILLA AIRPORT	Original Caltrans
2O7	INDEPENDENCE AIRPORT	Original Caltrans
36S	HAPPY CAMP AIRPORT	Original Caltrans
3O1	GUSTINE AIRPORT	Original Caltrans
3O8	HARRIS RANCH AIRPORT	Original Caltrans
49X	CHEMEHUEVI VALLEY AIRPORT	Original Caltrans
4CL	24CL (Slayer Farms Airport)	Digitized (OSM)
6CL	86CL (Ernst Field)	Digitized (OSM)
7CA	97CA	Digitized (OSM)
8CL	58CL (Borrego Air Ranch Airport)	Digitized (OSM)
9CL	09CL	Digitized (OSM)
A24	CALIFORNIA PINES AIRPORT	Original Caltrans
A26	ADIN AIRPORT	Original Caltrans
A28	FORT BIDWELL AIRPORT	Original Caltrans

A30	SCOTT VALLEY AIRPORT - BUD DAVIS FIELD	Original Caltrans
A32	BUTTE VALLEY AIRPORT	Original Caltrans
A69	CA69 (Avenal Gliderport)	Digitized (OSM)
A89	CA89 (Skylark Field Airport)	Digitized (OSM)
AAT	ALTURAS MUNICIPAL AIRPORT	Original Caltrans
ACV	California Redwood Coast-Humboldt County Airport	Digitized (OSM)
AJO	CORONA MUNICIPAL AIRPORT	Original Caltrans
APC	NAPA COUNTY AIRPORT	Original Caltrans
APV	APPLE VALLEY AIRPORT	Original Caltrans
AUN	AUBURN MUNICIPAL AIRPORT	Original Caltrans
AVX	CATALINA AIRPORT	Original Caltrans
BFL	Meadows Field Airport	Digitized (OSM)
BIH	EASTERN SIERRA REGIONAL AIRPORT	Original Caltrans
BLH	BLYTHE AIRPORT	Original Caltrans
BLU	BLUE CANYON AIRPORT	Original Caltrans
BNG	BANNING MUNICIPAL AIRPORT	Original Caltrans
BUR	BOB HOPE AIRPORT	Original Caltrans
BWC	BRAWLEY MUNICIPAL AIRPORT	Original Caltrans

C80	NEW COALINGA MUNICIPAL AIRPORT	Original Caltrans
C83	BYRON AIRPORT	Original Caltrans
CA0	0CA0 (Del Rey Juice Airstrip)	Digitized (OSM)
CA9	CA92 (Paradise Skypark)	Digitized (OSM)
CCB	CABLE AIRPORT	Original Caltrans
CCR	BUCHANAN FIELD AIRPORT	Original Caltrans
CEC	Del Norte County Regional Airport/ McNamara Field	Digitized (OSM)
CIC	Chico Municipal Airport	Digitized (OSM)
CL1	2CL1 (Brownsville Aero Pines Airport)	Digitized (OSM)
CL3	0CL3	Digitized (OSM)
CL35	CL35 (Warmer Springs Gliderport)	Digitized (OSM)
CLR	CLIFF HATFIELD MEMORIAL AIRPORT	Original Caltrans
CMA	CAMARILLO AIRPORT	Original Caltrans
CN2	0CN2	Digitized (OSM)
CNO	CHINO AIRPORT	Original Caltrans
CPM	COMPTON/WOODLEY AIRPORT	Original Caltrans
CPU	CALAVERAS CO./MAURY RASMUSSEN AIRPORT	Original Caltrans
CRO	CORCORAN AIRPORT	Original Caltrans

CRQ	McClellan-Palomar Airport	Digitized (OSM)
CVH	HOLLISTER MUNICIPAL AIRPORT	Original Caltrans
CXL	CALEXICO INTERNATIONAL AIRPORT	Original Caltrans
D63	DINSMORE AIRPORT	Original Caltrans
D83	BOONVILLE AIRPORT	Original Caltrans
D86	SEQUOIA FIELD	Original Caltrans
DAG	BARSTOW-DAGGETT AIRPORT	Original Caltrans
DLO	DELANO MUNICIPAL AIRPORT	Original Caltrans
DVO	GNOSS FIELD AIRPORT	Original Caltrans
DWA	YOLO COUNTY-DAVIS WOODLAND WINTERS AIRPORT	Original Caltrans
E16	SOUTH COUNTY AIRPORT	Original Caltrans
E36	GEORGETOWN AIRPORT	Original Caltrans
E45	PINE MOUNTAIN LAKE AIRPORT	Original Caltrans
E55	OCEAN RIDGE AIRPORT	Original Caltrans
E79	SIERRA SKY PARK AIRPORT	Original Caltrans
EDU	UNIVERSITY AIRPORT	Original Caltrans
EED	NEEDLES AIRPORT	Original Caltrans
EKA	MURRAY FIELD AIRPORT	Original Caltrans

EMT	EL MONTE AIRPORT	Original Caltrans
F34	FIREBAUGH AIRPORT	Original Caltrans
F62	HAYFORK AIRPORT	Original Caltrans
F70	FRENCH VALLEY AIRPORT	Original Caltrans
F72	FRANKLIN FIELD AIRPORT	Original Caltrans
FAT	FRESNO YOSEMITE INTERNATIONAL AIRPORT	Original Caltrans
FCH	FRESNO CHANDLER EXECUTIVE AIRPORT	Original Caltrans
FOT	ROHNERVILLE AIRPORT	Original Caltrans
FUL	FULLERTON MUNICIPAL AIRPORT	Original Caltrans
GOO	NEVADA COUNTY AIRPORT	Original Caltrans
H37	HERLONG AIRPORT	Original Caltrans
H47	HYAMPOM AIRPORT	Original Caltrans
HAF	HALF MOON BAY AIRPORT	Original Caltrans
HES	HEALDSBURG MUNICIPAL AIRPORT	Original Caltrans
HHR	JACK NORTHROP FIELD/HAWTHORNE MUNICIPAL AIRPORT	Original Caltrans
HJO	HANFORD MUNICIPAL AIRPORT	Original Caltrans
HMT	HEMET-RYAN AIRPORT	Original Caltrans
HWD	HAYWARD EXECUTIVE AIRPORT	Original Caltrans

IPL	Imperial County Airport	Digitized (OSM)
IYK	Inyokern-Kern County Airport	Digitized (OSM)
IZA	SANTA YNEZ AIRPORT	Original Caltrans
JAQ	WESTOVER FIELD AMADOR COUNTY AIRPORT	Original Caltrans
KIC	MESA DEL REY AIRPORT	Original Caltrans
L00	ROSAMOND SKYPARK AIRPORT	Original Caltrans
L05	KERN VALLEY AIRPORT	Original Caltrans
L06	FURNACE CREEK AIRPORT	Original Caltrans
L08	BORREGO VALLEY AIRPORT	Original Caltrans
L09	STOVEPIPE WELLS AIRPORT	Original Caltrans
L17	TAFT AIRPORT	Original Caltrans
L18	FALLBROOK COMMUNITY AIRPARK	Original Caltrans
L19	WASCO-KERN AIRPORT	Original Caltrans
L22	YUCCA VALLEY AIRPORT	Original Caltrans
L26	HESPERIA AIRPORT	Original Caltrans
L35	BIG BEAR CITY AIRPORT	Original Caltrans
L36	RIO LINDA AIRPORT	Original Caltrans
L45	BAKERSFIELD MUNICIPAL AIRPORT	Original Caltrans

L52	OCEANO COUNTY AIRPORT	Original Caltrans
L54	AGUA CALIENTE SPRINGS AIRPORT	Original Caltrans
L56	CL56 (Ranchero Airport)	Digitized (OSM)
L61	SHOSHONE AIRPORT	Original Caltrans
L62	ELK HILLS-BUTTONWILLOW AIRPORT	Original Caltrans
L65	Perris Valley Airport	Digitized (OSM)
L70	Agua Dulce Airport	Digitized (OSM)
L71	CALIFORNIA CITY MUNICIPAL AIRPORT	Original Caltrans
L72	Trona Airport	Digitized (OSM)
L73	POSO-KERN COUNTY AIRPORT	Original Caltrans
L77	CHIRIACO SUMMIT AIRPORT	Original Caltrans
L78	JACUMBA AIRPORT	Original Caltrans
L88	New Cuyama Airport	Digitized (OSM)
L90	OCOTILLO AIRPORT	Original Caltrans
LAX	LOS ANGELES INTERNATIONAL AIRPORT	Original Caltrans
LGB	LONG BEACH AIRPORT DAUGHERTY FIELD	Original Caltrans
LHM	LINCOLN REGIONAL AIRPORT / KARL HARDER FIELD	Original Caltrans
LLR	LITTLE RIVER AIRPORT	Original Caltrans

LPC	Lompoc Airport	Digitized (OSM)
LSN	LOS BANOS MUNICIPAL AIRPORT	Original Caltrans
LVK	LIVERMORE MUNICIPAL AIRPORT	Original Caltrans
M45	ALPINE COUNTY AIRPORT	Original Caltrans
M90	WILLIAM R. JOHNSTON (MENDOTA) AIRPORT	Original Caltrans
MAE	MADERA MUNICIPAL AIRPORT	Original Caltrans
MCC	McCLELLAN AIRFIELD	Original Caltrans
MCE	Merced Regional Airport/ Macready Field	Digitized (OSM)
MER	CASTLE AIRPORT	Original Caltrans
MHR	SACRAMENTO MATHER AIRPORT	Original Caltrans
MHV	MOJAVE AIRPORT	Original Caltrans
MIT	SHAFTER AIRPORT - MINTER FIELD	Original Caltrans
MMH	MAMMOTH YOSEMITE AIRPORT	Original Caltrans
MOD	Modesto City-County Airport	Digitized (OSM)
MPI	MARIPOSA - YOSEMITE AIRPORT	Original Caltrans
MRY	Monterey Regional Airport	Digitized (OSM)
MYF	MONTGOMERY FIELD	Original Caltrans
MYV	YUBA COUNTY AIRPORT	Original Caltrans

N13	CN13 (Borges Clarksburg Airport)	Digitized (OSM)
N19	CN19 (Las Serpientes Airport)	Digitized (OSM)
N37	CN37 (Kelso Valley Airport)	Digitized (OSM)
N64	CN64 (Desert Center Airport)	Digitized (OSM)
NUQ	Moffet Federal Airfield	Digitized (OSM)
O02	NERVINO AIRPORT	Original Caltrans
O05	ROGERS FIELD AIRPORT	Original Caltrans
O08	COLUSA COUNTY AIRPORT	Original Caltrans
O09	ROUND VALLEY AIRPORT	Original Caltrans
O15	TURLOCK MUNICIPAL AIRPORT	Original Caltrans
O16	GARBERVILLE AIRPORT	Original Caltrans
O19	KNEELAND AIRPORT	Original Caltrans
O21	HOOPA AIRPORT	Original Caltrans
O22	COLUMBIA AIRPORT	Original Caltrans
O24	LEE VINING AIRPORT	Original Caltrans
O26	LONE PINE AIRPORT	Original Caltrans
O27	OAKDALE MUNICIPAL AIRPORT	Original Caltrans
O28	WILLITS MUNICIPAL AIRPORT	Original Caltrans

O32	REEDLEY MUNICIPAL AIRPORT	Original Caltrans
O33	EUREKA MUNICIPAL AIRPORT	Original Caltrans
O37	HAIGH FIELD AIRPORT	Original Caltrans
O39	RAVENDALE AIRPORT	Original Caltrans
O41	WATTS - WOODLAND AIRPORT	Original Caltrans
O46	WEED AIRPORT	Original Caltrans
O52	SUTTER COUNTY AIRPORT	Original Caltrans
O54	LONNIE POOL FIELD-WEAVERVILLE	Original Caltrans
O55	SOUTHARD FIELD AIRPORT	Original Caltrans
O57	BRYANT FIELD AIRPORT	Original Caltrans
O59	CEDARVILLE AIRPORT	Original Caltrans
O60	CLOVERDALE MUNICIPAL AIRPORT	Original Caltrans
O61	Cameron Airpark	Digitized (OSM)
O63	EXETER	Original Caltrans
O69	PETALUMA MUNICIPAL AIRPORT	Original Caltrans
O79	SIERRAVILLE DEARWATER AIRPORT	Original Caltrans
O81	Tulelake Municipal Airport	Digitized (OSM)
O85	BENTON FIELD	Original Caltrans

O86	TRINITY CENTER/JAMES E. SWETT AIRPORT	Original Caltrans
O88	RIO VISTA MUNICIPAL AIRPORT	Original Caltrans
O89	FALL RIVER MILLS AIRPORT	Original Caltrans
OAK	METROPOLITAN OAKLAND INTERNATIONAL AIRPORT	Original Caltrans
OAR	MARINA MUNICIPAL AIRPORT	Original Caltrans
OKB	OCEANSIDE MUNICIPAL AIRPORT	Original Caltrans
ONT	ONTARIO INTERNATIONAL AIRPORT	Original Caltrans
OVE	OROVILLE MUNICIPAL AIRPORT	Original Caltrans
OXR	Oxnard Airport	Digitized (OSM)
PAO	Palo Alto Airport	Digitized (OSM)
POC	BRACKETT FIELD AIRPORT	Original Caltrans
PRB	PASO ROBLES MUNICIPAL AIRPORT	Original Caltrans
PSP	PALM SPRINGS INTERNATIONAL AIRPORT	Original Caltrans
PTV	PORTERVILLE MUNICIPAL AIRPORT	Original Caltrans
PVF	PLACERVILLE AIRPORT	Original Caltrans
RAL	RIVERSIDE MUNICIPAL AIRPORT	Original Caltrans
RBL	RED BLUFF MUNICIPAL AIRPORT	Original Caltrans
RDD	Redding Municipal Airport	Digitized (OSM)

REI	REDLANDS MUNICIPAL AIRPORT	Original Caltrans
RHV	REID HILLVIEW AIRPORT	Original Caltrans
RIR	FLABOB AIRPORT	Original Caltrans
RIU	RANCHO MURIETA AIRPORT	Original Caltrans
RIV	March Air Reserve Base	Digitized (OSM)
RNM	RAMONA AIRPORT	Original Caltrans
S51	ANDY MCBETH AIRPORT	Original Caltrans
SAC	SACRAMENTO EXECUTIVE AIRPORT	Original Caltrans
SAN	SAN DIEGO INTERNATIONAL AIRPORT	Original Caltrans
SAS	SALTON SEA AIRPORT	Original Caltrans
SBA	SANTA BARBARA MUNICIPAL AIRPORT	Original Caltrans
SBD	SAN BERNARDINO INTERNATIONAL AIRPORT	Original Caltrans
SBP	San Luis Obispo Regional Airport	Digitized (OSM)
SCK	STOCKTON METROPOLITAN AIRPORT	Original Caltrans
SDM	BROWN FIELD	Original Caltrans
SEE	GILLESPIE FIELD AIRPORT	Original Caltrans
SFO	SAN FRANCISCO INTERNATIONAL AIRPORT	Original Caltrans
SIY	SISKIYOU COUNTY AIRPORT	Original Caltrans

SJC	SAN JOSE INTERNATIONAL AIRPORT, NORMAN Y. MINETA	Original Caltrans
SMF	SACRAMENTO INTERNATIONAL AIRPORT	Original Caltrans
SMO	SANTA MONICA MUNICIPAL AIRPORT	Original Caltrans
SMX	Santa Maria Public Airport	Digitized (OSM)
SNA	JOHN WAYNE AIRPORT, ORANGE CO.	Original Caltrans
SNS	SALINAS MUNICIPAL AIRPORT	Original Caltrans
SQL	SAN CARLOS AIRPORT	Original Caltrans
STS	CHARLES M. SCHULZ, SONOMA COUNTY AIRPORT	Original Caltrans
SVE	SUSANVILLE MUNICIPAL AIRPORT	Original Caltrans
SZP	SANTA PAULA AIRPORT	Original Caltrans
T42	RUTH AIRPORT	Original Caltrans
TCY	TRACY MUNICIPAL AIRPORT	Original Caltrans
TLR	MEFFORD FIELD AIRPORT	Original Caltrans
TNP	TWENTYNINE PALMS AIRPORT	Original Caltrans
TOA	ZAMPERINI FIELD AIRPORT	Original Caltrans
TRK	TRUCKEE-TAHOE AIRPORT	Original Caltrans
TRM	JACQUELINE COCHRAN REGIONAL AIRPORT	Original Caltrans

TSP	TEHACHAPI MUNICIPAL AIRPORT	Original Caltrans
TVL	LAKE TAHOE AIRPORT	Original Caltrans
UDD	BERMUDA DUNES EXECUTIVE AIRPORT	Original Caltrans
UKI	UKIAH MUNICIPAL AIRPORT	Original Caltrans
VCB	NUT TREE AIRPORT	Original Caltrans
VCV	Southern California Logistics Airport	Digitized (OSM)
VIS	Visalia Municipal Airport	Digitized (OSM)
VNY	VAN NUYS AIRPORT	Original Caltrans
WHP	WHITEMAN AIRPORT	Original Caltrans
WJF	GENERAL WILLIAM M FOX AIRPORT	Original Caltrans
WLW	WILLOWS - GLENN COUNTY AIRPORT	Original Caltrans
WVI	WATSONVILLE MUNICIPAL AIRPORT	Original Caltrans

***** SCK and SFO Airport original boundary data from Caltran had conflicting polygons defining the airport boundaries that were excluded. Excluded boundaries are illustrated in blue in Figure B.1. and B.2.)

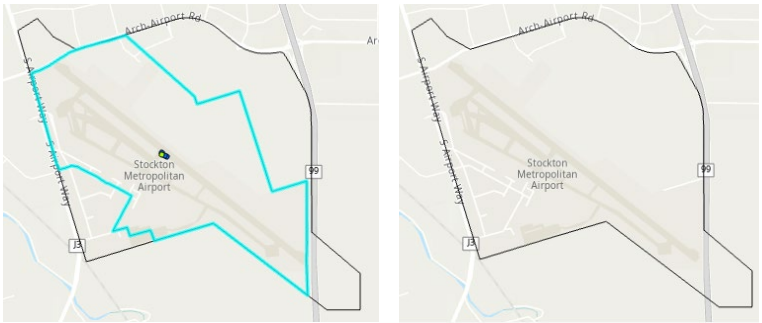


Figure B.1. SCK original Caltrans boundary polygon (left) and the boundary used for the study (right)



Figure B.2. SFO original Caltrans boundary polygon (left) and the boundary used for the study (right)

Other California airports excluded from this analysis due to lack of runway or boundary data are listed below based on the BTS runway end point data Facility Name attribute:
-MCMWTC

[4.1] Appendix C. Which accident dataset should I use?

Five accident datasets were created for this report that are available as GIS data (*.shp*) and table datasets (*.csv*) in the report folder. Depending on the goal of the analysis they each provide different tradeoffs:

1- **US_NTSB_1948-2023** with a total of 88,184 accidents from 1948- Jan 2023 in all the U.S.

This dataset can be useful for users interested in a comparison baseline with results from California or other states. It is derived from the combination of two raw NTSB accident datasets.

2- **CA_ACC_full_final82-22** with a total of 8,550 accidents in California from 1982-2022.

This dataset is the baseline of California's accidents, using the selection criteria from previous handbooks to create the ALUP-relevant accident dataset with the longest time-period possible of 41 years. There are no geospatial criteria for the selection for this dataset and it should therefore not be used for GIS analysis.

3- **CA_spatialLargest_08-22** with a total of 1,355 events in California between 2008-2022, this dataset was selected to provide users with the highest number of spatially-relevant accidents with ALUP-relevant criteria. It can be especially useful if the user is looking to cross specific accident variables that would drastically reduce the available data (i.e., a specific phase of flight and damage type). However, to retain a maximum number of spatially-relevant accidents, this dataset did not exclude events occurring inside the Primary Surface. This dataset is not the best suited for comparison with the 2011 accident analysis, but it benefits from richer geospatial data that former analysis did not have, such as retaining only accident events that have measured Latlon with GPS.

4- **CA_spatial2011Method_08-22** with a total of 292 events in California between 2008-2022, this dataset closely reproduces the 2011 Handbook method for the accident analysis. It is useful for users that seek to compare the accident patterns of

the previous assessment with the current one. This dataset does not take full advantage of the current improvements in geospatial reporting of NTSB accidents, and largely reduces the number of available reliable spatial data.

(1) **CA_spatialAccuracy_08-22** with a total of 466 events in California between 2008-22, this method reproduces the APR Latlon co-locaiton error used in the of 2011 handbook method without deleting the accidents within the Primary Surface or those outside the 5 mile airport buffer to provide a larger accident dataset with the highest spatial-accuracy criteria method.

Task 4.1.1 (1) Safety and Risk with Emerging Technologies. Subtask 1: Discussion on mid-air collision between fixed-wing aircraft and manned eVTOLs

Deliverable: Subtask (1) A high-level discussion on mid-air risk collision between fixed-wing aircraft and manned eVTOLs and mitigation recommendations.

[4.1.1(1)] 1. Introduction

Currently, the aviation industry is undergoing a transformative revolution as it explores the possibilities of integrating electric Vertical Take-off and Landing vehicles (eVTOLs) into the existing airspace. This revolution represents a remarkable shift in urban mobility and promises to provide efficient, environmentally friendly, and congestion-alleviating transportation solutions. However, the coexistence of traditional fixed-wing aircraft and eVTOLs within the same airspace introduces significant challenges, particularly concerning collision risk (Bauranov and Rakas, 2019).

In this section, we address these challenges by discussing the probability of collision between fixed-wing aircraft and eVTOLs. We follow a systematic approach and draw upon concepts and methods from the relevant Federal Aviation Administration (FAA) documents and academic articles in the field. Through this investigation, we aim to provide a clear understanding of the collision risk and its potential implications on the future of urban air mobility.

[4.1.1(1)] 2. Background: Coexistence of Fixed-Wing Aircraft and eVTOLs

Electric Vertical Take-off and Landing vehicles (eVTOLs) are revolutionizing the aviation industry with their vertical take-off and landing capabilities, electric propulsion, and potential for urban air travel. These aircraft represent a promising solution to urban congestion, offering the prospect of rapid point-to-point transportation within metropolitan areas. While the concept of urban air mobility is not entirely new, recent technological advancements in propulsion, avionics, and automation have brought it to the forefront of the industry (Bauranov and Rakas, 2021).

Urban Air Mobility (UAM) encompasses both manned and unmanned aerial vehicles designed for people and cargo transportation at relatively low altitudes in urban and suburban environments. The control and navigation of these aerial vehicles can be facilitated by pilots, remote operators, on-board automation systems, or centralized ground-based automated systems (FAA, 2023; Bauranov and Rakas, 2019). In the near term, pilot-operated flights adhering to existing air traffic control procedures will dominate UAM passenger flights, complying with current airspace rules and regulations provided by the FAA (FAA, 2020).

Nevertheless, as the industry matures, a transition toward higher levels of autonomy is expected. However, manned operations will continue to be part of the evolving ecosystem. Establishing UAM involves collaboration among civil aviation authorities, aircraft manufacturers, and transportation network companies. Yet, the absence of a robust regulatory framework poses a substantial hurdle for the industry's progress. Issues such as the level of regulatory rigor, pilot and technology certification, and the lack of procedures for testing and certifying autonomous systems need to be addressed (FAA, 2020a).

Furthermore, the rights to use urban airspace remain a point of contention. While some regulations restrict low flying operations over cities, exemptions are granted to specific types of aircraft, such as helicopters (FAA, 2020a). The surveillance and control of urban airspace have yet to be assigned. Multiple agencies in the United States are actively engaged in discussions about controlling urban airspace, recognizing the need for a separate air traffic control system to accommodate the expected surge in unmanned aerial operations (Bauranov and Rakas, 2019).

The introduction of eVTOLs into the airspace raises a crucial concern – how can manned and unmanned vehicles safely share the skies? As eVTOLs transition to higher levels of autonomy, questions about pilot reaction to unexpected automation behavior and the potential for increased human errors emerge. The growing demand for UAM flights will undoubtedly intensify pressure on urban airspace capacity (Choo and Yun, 2018; Beard and McLain, 2003, Wand et al., 2007; Goerzen et al., 2010; Bauranov and Rakas 2021), while the diverse mix of air vehicles further complicates the system, potentially exceeding the capabilities of current Air Traffic Management (ATM) systems. This complexity, combined with the novelty of eVTOLs, poses potential safety risks to the system (Bauranov and Rakas, 2019).

In light of these concerns, this section aims to investigate the hazards and safety concerns associated with manned flights in urban airspace, with a specific focus on estimating the probability of collision between fixed-wing aircraft and eVTOLs. Our approach combines insights from diverse sources, which provide relevant information and methods for risk assessment in the context of aviation safety.

[4.4.1.(1)] 3. Methodology: Systemic Approach to Estimating Collision Probability

To estimate the probability of collision between fixed-wing aircraft and eVTOLs, we follow a systematic approach, leveraging the Safety Management Systems (SMS) framework proposed by the FAA (FAA, 2020b; 2022; 2023a).

SMS is a structured method for analyzing and managing safety risk in aviation, and it consists of five phases:

1. Describe the system: Define the key components, stakeholders, and operational characteristics of the aviation system.

2. Identify the hazards: Identify potential safety issues, accidents, and their root causes, including any factors that could lead to collisions.

3. Determine the risk: Calculate the risk by multiplying the probability of an adverse event by the severity of its consequences (Bauranov and Rakas, 2021).

4. Assess and analyze the risk: Evaluate the risk in terms of its significance, considering factors such as probability, severity, and the potential for harm.

5. Mitigate and manage the risk: Develop and implement safety measures and strategies to mitigate the identified risks and ensure safe operations.

Once the system is defined and the hazards have been identified, we can start with the latter phases developed in the subsections below: determining risk (3.1.), assessing risk (3.2.), and mitigating risk (3.3)

3.1. Determining Risk

To ascertain the risk of collision between fixed-wing aircraft and eVTOLs, a comprehensive analysis is essential. This involves quantifying the probability of incidents and evaluating their potential severity. Key considerations include the operational characteristics and behaviors of these aircraft within shared airspace, encompassing take-off and landing profiles, cruise altitudes, and typical flight patterns in urban environments (Pradeep and Wei, 2018).

This phase draws from insights into eVTOL performance and operational features, providing a foundation for estimating collision probabilities. The focus is on understanding how these aircraft navigate airspace and the associated challenges during critical phases such as transitioning from vertical to horizontal flight.

The probabilistic safety assessment (PSA) framework is integral to this phase, enabling the modeling of various accident scenarios. Variables such as aircraft characteristics, pilot behavior, and environmental conditions are considered to derive a nuanced understanding of collision risks. This analytical approach is a fundamental component in the broader context of safety management systems [20].

This systematic determination of risk sets the stage for subsequent phases in the safety management process, allowing for a thorough and data-driven evaluation of the potential hazards associated with the coexistence of fixed-wing aircraft and eVTOLs in shared airspace (Bauranov and Rakas, 2021; 2019).

3.2. Assessing Risk

Assessing the risk involves evaluating the significance of estimated collision probabilities, considering factors such as the severity of potential accidents and the likelihood of their occurrence. Insights from various sources contribute to this assessment, with a focus on both structured and unstructured urban airspace concepts (Dill et al., 2016).

1. Structured Airspace:

Existing Technologies and Realism:

- The first group of proposals (NASA, FAA, SESAR U-Space, DLR U-Space) relies on existing technologies, making them more realistic for immediate implementation (Bauranov and Rakas, 2021).
- These proposals leverage the current air traffic management system for identity registration, weather information, and obstacle data (Bauranov and Rakas, 2021).

Operational Limits:

- Operations are kept below 400 ft in G Class airspace, adhering to existing airspace rules (Bauranov and Rakas, 2021).
- Line-of-sight piloting and adherence to established regulations ensure a controlled and manageable environment (FAA 2023; Hoekstra et al., 2016)

Communication and Traffic Control:

- Operations are kept separate from controlled airspace, using segregated corridors with air traffic control permission if needed.
- The phased implementation approach mitigates risks associated with rapid and complex deployment.

2. Unstructured Airspace:

Degrees of Freedom and User-Preferred Routes:

- Less structured airspace provides air vehicles with more degrees of freedom, enabling them to choose positions, altitudes, headings, and speeds more freely (Bauranov and Rakas, 2021).
- User- preferred routes allow for cost-effective and efficient flight paths, contingent on the autonomy of the vehicles.

Challenges and Risks:

- Autonomy is crucial for user-preferred routes, limiting the applicability of this concept to autonomous vehicles.
- Increased collision risk in less structured airspace, relying heavily on the detect-and-avoid system, poses challenges to safety.

Social and Coordination Challenges:

- Higher levels of coordination and structure are needed, conflicting with the abstraction of the city into a mathematical network.
- Social factors, including community preferences and coordination challenges, are often overlooked in less structured airspace concepts.

Capacity and Safety Trade-offs:

- Trade-offs between traffic density and safety exists, with a reliance on onboard conflict resolution technologies in less structured airspace (Hoekstra et al., 2016)
- Exclusivity of free flight, not considering social factors in route selection, may limit their feasibility in populated urban environments.

The discussion on airspace structure types revolves around the trade-off between freedom and safety in aviation. Less structured airspace offers flexibility but requires advanced technology and raises collision risks. Free flight concepts prioritize user-preferred routes but are constrained to specific geographic areas. Highly structured airspace ensures safety but may limit efficiency. Layered airspace strikes a balance, reducing collision probability through vertical

separation (Sunil et al., 2015). Fig 1. Shows the relationship between airspace and the different design concepts.

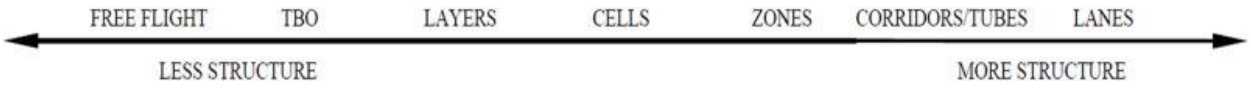


Fig. 1. Airspace structure and design concepts (Bauranov and Rakas, 2021)

Specialized concepts like UAS Traffic Management aim to integrate small drones. Consideration of rotorcraft wake vortex emphasizes the need for tailored structures. In essence, the challenge lies in designing airspace that accommodates diverse aircraft while minimizing risks and maximizing safety (Jang et al., 2017). Fig 2. presents the performance of the different factors for free flight, as well as for the other more complex structures in less- and more-structured environments.

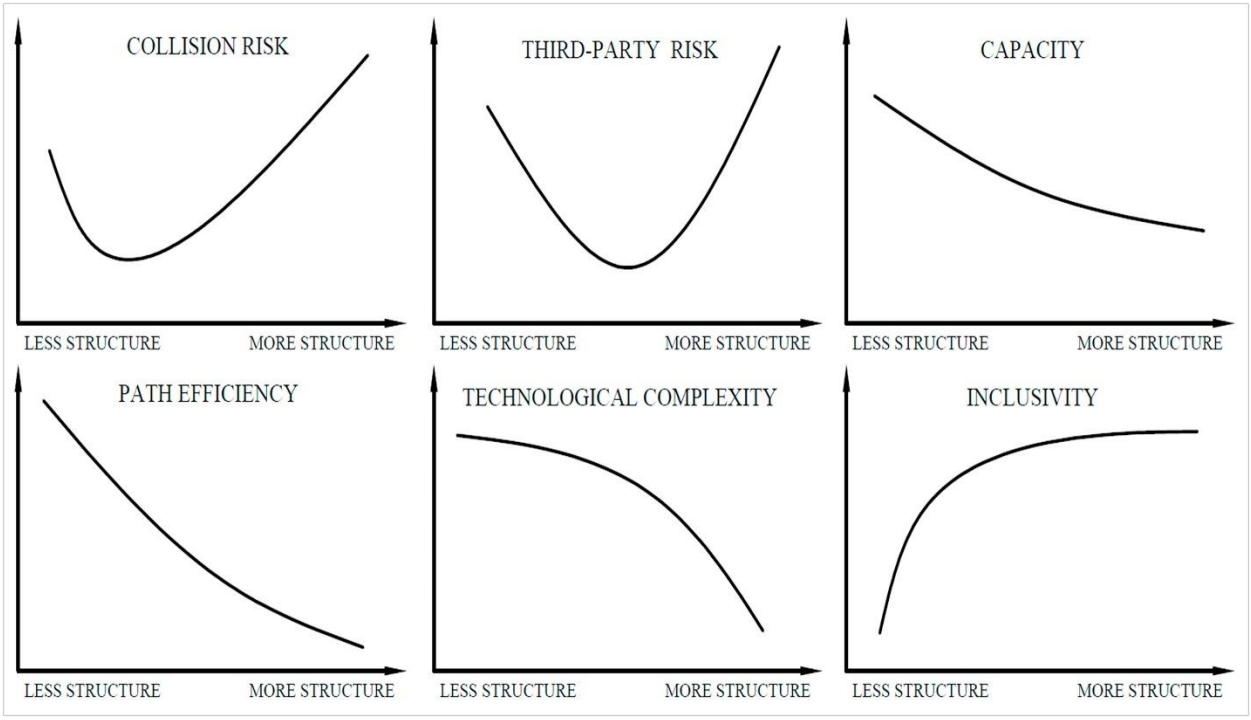


Fig. 2. Performance vs. Airspace structure (Bauranov and Rakas, 2021)

3. Discussion and Future Considerations:

Public Engagement and Regulatory Challenges:

- Early and continuous public engagement is crucial for the success of urban airspace concepts, considering noise impact and other social factors.

- Regulatory challenges, such as the Remote Identification of Unmanned Aircraft Systems Rule, highlight the need for careful policy implementation to balance safety and community interests.

Long-Term Implications:

- Rapid UAM development, especially in passenger transportation, poses potential safety issues and public opposition (Bauranov and Rakas, 2021).
- Careful consideration is necessary to avoid unexpected challenges that could hinder overall UAM development (Jang et al., 2017).

Public Awareness and Education:

- Public awareness and education about UAM are essential for addressing concerns and ensuring public acceptance (Yedavalli et al., 2019).
- Past experiences in aviation noise opposition should guide strategies for handling noise concerns in urban environments.

3.3. Mitigating Risk

Having determined and assessed the potential collision risk between fixed-wing aircraft and eVTOLs, the focus now shifts to implementing effective strategies for risk mitigation. The following strategies are derived from the collective insights provided by the selected articles:

1. Advancements in Avionics and Automation:

Emphasizing the role of cutting-edge avionics and automation becomes imperative in mitigating collision risk. The integration of autonomous systems plays a crucial role in minimizing the likelihood of accidents. Such technologies facilitate collision avoidance and enhance overall safety in shared airspace (Goerzen et al., 2010; Beard et al., 2003).

2. Pilot Training and Safety Protocols:

An essential component of risk mitigation involves prioritizing advanced training programs for eVTOL pilots. Additionally, the implementation of robust safety protocols contributes significantly to reducing the risk associated with emerging aviation technologies. Human factors, including pilot reactions to system failures, are pivotal considerations in this context (Bauranov and Rakas, 2021).

3. Development of Advanced Traffic Management Systems:

Tailoring traffic management systems to the unique demands of urban air mobility is proposed as a key strategy. These advanced systems are designed to optimize traffic flow, alleviate congestion, and bolster collision avoidance measures in shared airspace (Bauranov and Rakas, 2019). Investing in such technology is crucial for enhancing overall safety and efficiency.

By adopting these strategies, the aviation industry can proactively address and mitigate the identified collision risks between fixed-wing aircraft and eVTOLs. Each of these measures contributes to a comprehensive approach that combines technological advancements, human factors considerations, and tailored traffic management systems.

[4.1.1.(1)] 4. Findings

Valuable insights have been integrated into the risk determination, assessment, and mitigation phases of estimating the probability of collision between fixed-wing aircraft and eVTOLs.

1. Vertical Take-Off and Landing (VTOL) Phases: The critical VTOL phases in eVTOL operations emphasize the importance of understanding the transitions between vertical and horizontal flight. This finding can be integrated into the risk determination phase, particularly when estimating the likelihood of accidents during these transitional stages [Rakas and Bauranov, 2021).

2. Automation and Collision Avoidance: It's important to highlight the role of advanced avionics and automation in enhancing safety. Automation and collision avoidance systems are critical elements that can be incorporated into risk mitigation strategies (Alexander at al., 2021).

3. Human Factors: The significance of human factors in aviation safety is crucial. Human behavior plays a critical role in accidents. These insights can be incorporated into the risk assessment phase to evaluate how pilot behavior and reactions may influence collision risks (Bauranov and Rakas, 2019).

4. Advanced Training and Safety Protocols: It is suggested that advanced training for eVTOL pilots and the implementation of effective safety protocols are key strategies for reducing risks associated with new technologies. These findings can be integrated into the risk mitigation phase (Bauranov and Rakas, 2019).

5. Traffic Management Systems: The development of advanced traffic management systems tailored to urban air mobility is suggested. These systems are essential for optimizing traffic flow and enhancing collision avoidance measures in shared airspace (Bauranov and Rakas, 2019).

[4.1.1.(1)] 5. Recommendations for Mitigating Collision Risk

A set of recommendations is presented to mitigate the collision risk between fixed-wing aircraft and eVTOLs. These recommendations are designed to enhance safety and contribute to the coexistence of these aircraft in urban airspace (FAA, 2023): regulatory framework and standards, integration and traffic management, training and education, research and development.

A. Regulatory Framework and Standards

1. Define Clear Separation Standards: Regulatory authorities should collaborate with industry experts to establish clear separation standards between fixed-wing aircraft and eVTOLs. These standards should consider factors such as altitude, speed, and flight paths.

2. Certification and Compliance: Develop comprehensive certification processes for eVTOLs, ensuring rigorous safety standards and requirements are met. Compliance with these standards should be closely monitored and enforced (SESAR, 2018).

B. Integration and Traffic Management

1. Integration Planning: Policymakers should facilitate the development of urban air mobility integration plans. These plans should include designated flight corridors and urban vertiports to segregate fixed-wing and eVTOL traffic where feasible (Bauranov and Rakas, 2021).
2. Advanced Traffic Management Systems: Invest in advanced traffic management systems that utilize automation, artificial intelligence, and real-time data to optimize traffic flow. These systems should provide collision avoidance and rerouting capabilities (Wang et al., 2007).

C. Training and Education

1. Pilot Training: Establish specialized training programs for eVTOL pilots that address the unique challenges posed by these aircraft. This training should encompass both traditional flight skills and eVTOL-specific safety protocols (Bauranov and Rakas, 2021).
2. Public Awareness: Launch public awareness campaigns to educate the general public about the presence of eVTOLs in urban airspace. Awareness among the public can contribute to enhanced safety through responsible behavior (Bauranov and Rakas, 2021).

D. Research and Development

1. Collaborative Research: Encourage collaboration between academia, industry, and regulatory bodies to conduct ongoing research into collision risk modeling and safety enhancements. This research should evolve with the development of new eVTOL technologies (Luxhoj, 2016).
2. Innovative Safety Technologies: Foster innovation in safety technologies, such as advanced collision avoidance systems and eVTOL-specific sensors. Support research and development efforts to enhance the safety of eVTOL operations (Wang et al., 2007).

[4.1.1.(1)] 6. Conclusion

In summary, the integration of eVTOLs into urban airspace, alongside fixed-wing aircraft, holds immense promise for the future of urban air mobility. However, the risk of collision is a significant concern that must be addressed systematically.

The below flowchart has outlined a framework for estimating the probability of collision between these aircraft, leveraging insights from existing research articles and a Safety Management System (SMS) approach. By identifying risks and hazards, conducting quantitative analysis, and formulating recommendations, it is possible to work towards safe coexistence.

The coexistence of these diverse aircraft types presents unique challenges, but with careful planning, regulation, and technology integration, it is possible to ensure safe and efficient urban air mobility. Collaboration among stakeholders and a commitment to safety remain paramount in achieving this vision.

As eVTOL technology evolves, it is essential that safety remains a central focus. The aviation industry, known for its unwavering commitment to safety, must apply this ethos to the expanding field of urban air mobility. By doing so, we can ensure that the skies of tomorrow are not only efficient and accessible but also extremely safe.

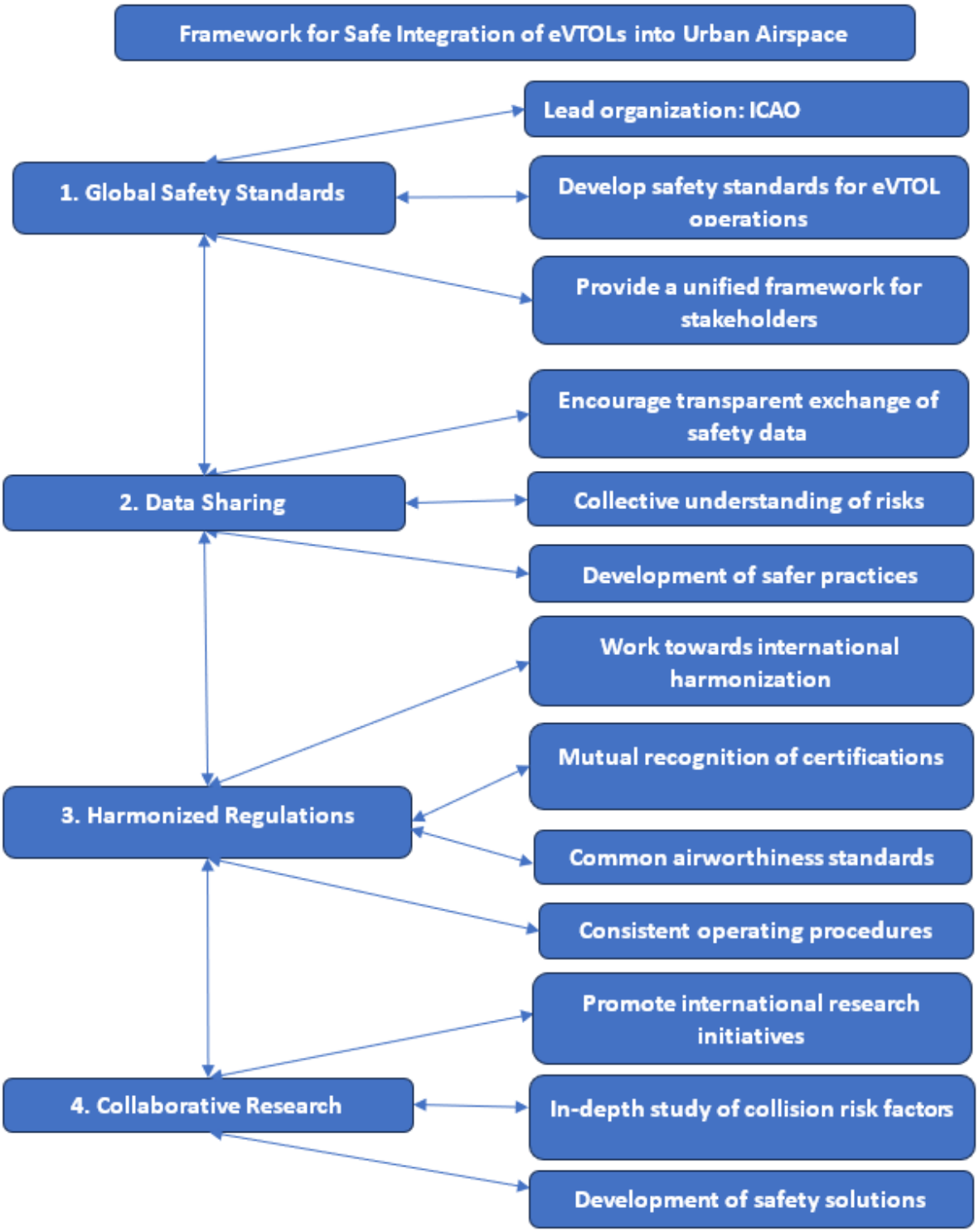


Figure 3. Framework for Safe Integration of eVTOLs into Urban Airspace

[4.1.1.(1)] 7. Citations

Alexander, R. J., Syms, R. A., Johnson, C., & Roberts, J. (2021). A Retrospective and Historical Analysis of Vertical Lift Infrastructure Accidents for the Purpose of Operational Risk Identification and Accident Prevention. In *Vertical Flight Society Forum* (Vol. 77). Vertical Flight Soc.

Bauranov, A., & Rakas, J. (2019, September). Urban air mobility and manned eVTOLs: Safety implications. In 2019 IEEE/AIAA 38th Digital Avionics Systems Conference (DASC) (pp. 1-8). IEEE.

Bauranov, A., & Rakas, J. (2021). Designing airspace for urban air mobility: A review of concepts and approaches. Progress in Aerospace Sciences, 125, 100726. https://doi.org/10.1016/j.paerosci.2021.100726.

Beard, R. W., & McLain, T. W. (2003, December). Multiple UAV cooperative search under collision avoidance and limited range communication constraints. In 42nd IEEE international conference on decision and control (IEEE Cat. No. 03CH37475) (Vol. 1, pp. 25-30). IEEE.

Cho, J., & Yoon, Y. (2018). How to assess the capacity of urban airspace: A topological approach using keep-in and keep-out geofence. Transportation Research Part C: Emerging Technologies, 92, 137-149.

Dill, E. T., Young, S. D., & Hayhurst, K. J. (2016). SAFEGUARD: An assured safety net technology for UAS. In 2016 IEEE/AIAA 35th digital avionics systems conference (DASC) (pp. 1-10). IEEE.

FAA. (2020). The Pilot's Handbook of Aeronautical Knowledge, Federal Aviation Administration, Washington DC [online]. Available: https://www.faa.gov/regulations_policies/handbooks_manuals/aviation/phak/.

FAA. (2020a). Title 14: Aeronautics and Space, Code of Federal Regulations, Federal Aviation Administration, Washington DC [online]. Available: https://www.ecfr.gov/cgi-bin/text-idx?SID=4130cc8c1736ff3b58a8e3f248cf9f25&mc=true&node=se14.2.91_1119&rgn=div8.

FAA. (2020b). Order 8000.369B - Safety Management System, Federal Aviation Administration, Washington DC.

FAA. (2020c) UTM Concept of Operations–v2. 0, Federal Aviation Administration, Washington DC [online]. Available: https://www.faa.gov/researchdevelopment/trafficmanagement/utm-concept-operations-version-20-utm-conops-v20

FAA. (2022). Air Traffic Organization, Safety Management System Manual, Federal Aviation Administration, Washington DC.

FAA. (2023). Urban Air Mobility: Concept of Operations, v2. 0, Federal Aviation Administration, Washington DC.

FAA. (2023a) Safety Management System for Airports, AC 150/5200-37A, Federal Aviation Administration, Washington DC.

Goerzen, C., Kong, Z., & Mettler, B. (2010). A survey of motion planning algorithms from the perspective of autonomous UAV guidance. Journal of Intelligent and Robotic Systems, 57, 65-100.

Hoekstra, J. M., Maas, J., Tra, M., & Sunil, E. (2016, June). How do layered airspace design parameters affect airspace capacity and safety?. In Proceedings of the 7th international conference on research in air transportation (pp. 1-8). ICRAT Philadelphia, USA.

Jang, D. S., Ippolito, C. A., Sankararaman, S., & Stepanyan, V. (2017). Concepts of airspace structures and system analysis for uas traffic flows for urban areas. In AIAA Information Systems-AIAA Infotech@ Aerospace (p. 0449).

Luxhoj, J. T. (2016). System safety modeling of alternative geofencing configurations for small uas. International Journal of Aviation, Aeronautics, and Aerospace, 3(1), 2.

Pradeep, P., & Wei, P. (2018). Energy efficient arrival with RTA constraint for urban eVTOL operations. In 2018 AIAA Aerospace Sciences Meeting (p. 2008).

SESAR, (2018). European ATM Master Plan: Roadmap for the safe integration of drones into all classes of airspace. SESAR Joint Undertaking: Brussels, Belgium.

Sunil, E., Hoekstra, J., Ellerbroek, J., Bussink, F., Nieuwenhuisen, D., Vidosavljevic, A., & Kern, S. (2015, June). Metropolis: Relating airspace structure and capacity for extreme traffic densities. In ATM seminar 2015, 11th USA/EUROPE Air Traffic Management R&D Seminar.

Wang, X., Yadav, V., & Balakrishnan, S. N. (2007). Cooperative UAV formation flying with obstacle/collision avoidance. IEEE Transactions on control systems technology, 15(4), 672-679.

Yedavalli, P., & Mooberry, J. (2019). An assessment of public perception of urban air mobility (UAM). Airbus UTM: Defining Future Skies, 2046738072-1580045281.

Task 4.1.1.(2) Safety and Risk with Emerging Technologies: Subtask 2: Drone incidents

Deliverables of Task 4.1.1.: Summary report focusing on subtask (2) probability of a drone incident (i.e. probability of a drone violating six Airport Safety Zones) at CA airports that are the most impacted by drones.
Acceptance Criteria: A report that includes probability modeling of drone incidents, and summarizes results for most impacted airports. With regard to Task 4.1.1., the deliverables will address and satisfy all of the relevant Task 1 Acceptance Criteria.

[4.1.1(2)] 1.Introduction: Context and Definitions

1.1. UAS technology emergence and context

Unmanned aircraft systems (UAS) are defined as “airborne operations without a pilot on board the aircraft” (GAO, 2019), commonly referred to drones. Drones are also called small UAS weighing less than 55 pounds. UAS technological innovation has disrupted markets, fundamentally changed the way some jobs are performed and has had a substantial impact in the risk reduction and public safety industry with promising economic and societal benefits. The increased investment in UAS operations has created new challenges to their safe and scalable integration into the National Airspace System (NASEM, 2018). Pioneering research to collect data, detect, monitor, assess hazards, and mitigate risk associated with UAS commercialization and operations have been developed in the last five years. Most of this research has relied on ad-hoc methodology, local UAS detection equipment, and the FAA’s UAS registration system and sighting incident reports that went into effect in 2015. In 2015 the U.S. had nearly 138 thousand recreational drones registered, reaching 1,375 million by the end of 2021 (FAA, 2022). With one of the highest concentrations of UAS per capita, California is the state with the highest registration numbers for both recreational and commercial uses (Figure 1) (ASSURE, 2022). From 2006 to August 2023, a total of 27 UAS accidents have been reported in the U.S. according to the National Transportation Safety Board (NTSB) dataset, out of which 7 occurred in California.

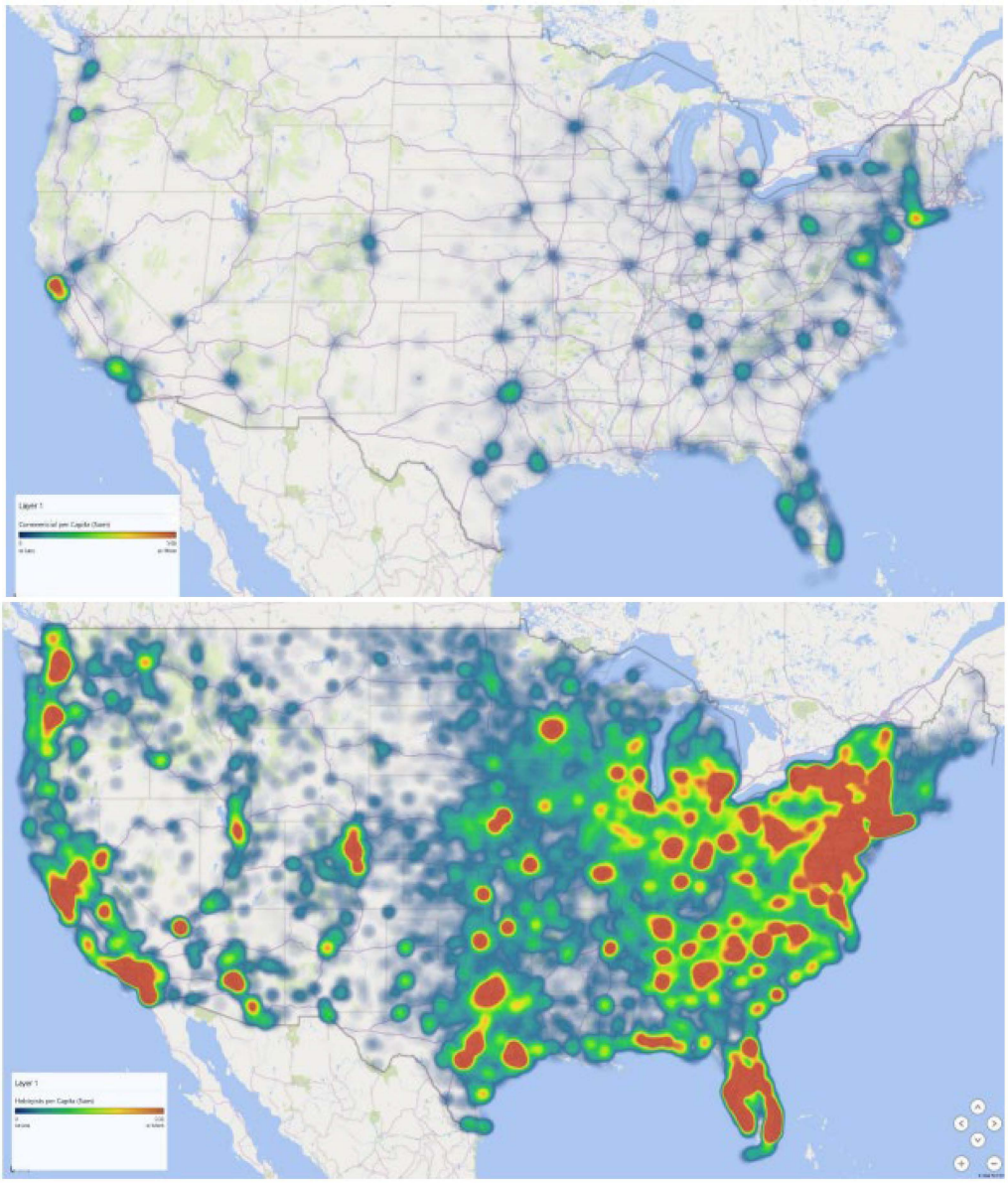


Figure 1. Heatmap of UAS Registration per Capita. Commercial users on top (max score of 3.58 UAS per person); and Recreative users on the bottom (max score of 0.38 UAS per person). Source: ASSESS, 2022: https://www.assureuas.org/projects/integrating-expanded-and-non-segregated-uas-operations-into-the-nas-impact-on-traffic-trends-and-safety/

UAS uses generally fall into three categories and each of them have respective regulatory frameworks that changes ways in which UAS operation violation can be defined:

a. Public safety and government users (i.e. survey of national parks, disaster risk response) who need to register each UAS and follow Part 107 of the Code of Federal Regulations, and follow FAA Advisory Circular 107-2 on “Small Unmanned Aircraft System (Small UAS)”. In some cases, public safety and government users also follow the FAA's Certificate of Authorization.

b. Non-recreational or commercial users (real estate photography, mapping, industrial inspection, etc) who are regulated by Part 107, follow FAA Advisory Circular 107-2 on "Small Unmanned Aircraft System (Small UAS)", and must obtain a remote pilot certificate from the FAA.
c. Recreational users who fly strictly for recreational purposes require a certificate of registration from the FAA and adhere to other specific requirements listed under 49 USC 44809: "Exception for limited recreational operations of unmanned aircraft"[4] .

Current UAS incident data collection methods do not permit distinguishing between these user categories, however there is an assumption that most incidents are associated with recreational flyers.

1.2. UAS incident and accident definition

1.2.1. UAS incident or sighting definition:

UAS incident or sighting definition: UAS operation violations, or intrusions, that can lead to evasive maneuvers, mid-air collisions, runway incursions, and other hazards that could cause incidents or accidents that threaten human and property integrity (ASSURE, 2022). These UAS operation violations are often characterized by the encounters between UAS and aircraft, helicopter, or traffic control tower, and the intrusion of restricted or special use airspace further described below.

Most non-governmental users of UAS must keep their drones within visual line of sight, in controlled airspace, never fly near other aircraft, and are not allowed to fly above 400 feet in uncontrolled airspace (Figure 2).[5] Other UAS operating restrictions that further define drone incidents or sighting studied in this report fall within three major categories according to the FAA[6]:

1) Restricted Airspace: areas where UAS operations is prohibited:
    a. Security sensitive airspace restrictions (designated national security sensitive facilities such as military bases, national landmarks, and nuclear power plants, etc.)
    b. Near airports and controlled airspace (Class B, C, D, and surface Class E, Special Flight Rules Area (SFRA) within a 30-mile radius of Ronald Reagan Washington National Airport in Washington DC)

[4] https://www.faa.gov/uas/recreational_flyers
[5] The FAA's UAS Traffic Management (UTM) has been developing procedures to expand the areas where UAS are allowed to fly by testing and identifying airspace operations requirements to enable safe beyond visual line of sight and Low Altitude Authorization and Notification Capability (LAANC) which flexibilizes the flying options below 400 feet.
[6] https://www.faa.gov/uas/getting_started/where_can_i_fly/airspace_restrictions/tfr

c. Emergency and rescue operations (during wildfires and hurricanes or rescue operations UAS flying is prohibited)

2) Local Restrictions: in some locations drone takeoffs and landings are restricted by state, local, territorial or tribal government agencies
3) Temporary Flight Restrictions: define a certain area of airspace where air travel is limited for a period for different reasons (i.e., near stadiums during particular sporting events, during events of national security importance in specific sites, etc). The FAA provides a safety app with real-time information on airspace restrictions and other flying requirements based on the GPS location (B4UFLY App: https://www.faa.gov/uas/getting_started/b4ufly)

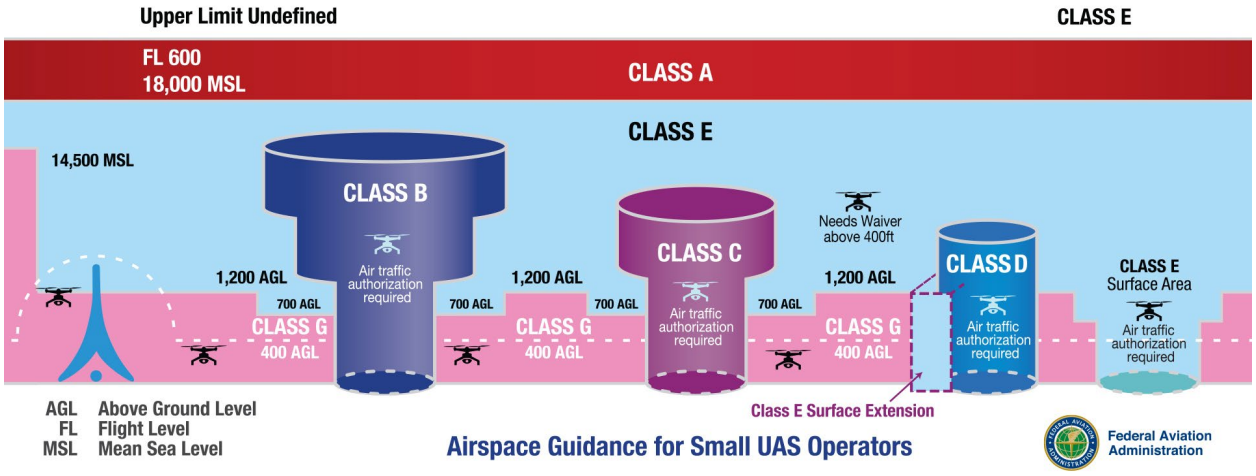


Figure 2. Drone flying zones restrictions: uncontrolled vs. controlled airspace (Source FAA)

1.2.2. UAS accident definition

NTSB regulations define an “unmanned aircraft accident” as an occurrence associated with the operation of any public or civil UAS that takes place between the time that the system is activated with the purpose of flight and the time that the system is deactivated at the conclusion of its mission, in which any person suffers death or serious injury, or the aircraft has a maximum gross takeoff weight of 300 pounds or greater and sustains substantial damage. NTSB regulations contain specific definitions for “serious injury” and “substantial damage” (FAA’s Advisory Circular 107-2A , 2021).

[4.1.1(2)] 2. Methods & Data

2.1. UAS Sighting Data & Data Cleaning Methods

2.1.1. UAS Sighting Data Overview

The FAA UAS sighting dataset covers UAS violations or intrusions reported by pilots, air traffic controllers, airport operators, airport tenants, military personnel, police, or civilians. The dataset has been published as “Sightings Reports” on a 3-month basis since 2015. Due to time constraints, this project only covers UAS incidents reported from July 2020 to June 2021, as the FAA UAS dataset has inconsistencies in data format and content that requires more meticulous data cleaning methods and text analysis. The original dataset is organized under four data fields: Day of Sighting, State, City, and Summary (Figure 3). The “Summary” data field specifically contains text based information that requires more sophisticated data cleaning techniques to identify the incident’s geolocation, notably using the aircrafts cardinal direction, origin-destination pairs, and altitude (further described below). For each individual drone sighting, other key information that is typically described under Summary include: time of day, aircraft type, aircraft altitude, a description of the location, drone color and occasionally other design features, altitude of the UAS in relation to the aircraft at the time of the UAS sighting, as well as any infraction notification.

Day of Sightin	State	City	Summary
7/1/2020	CALIFORNIA	SAUSALITO	FOLLOW UP INFO FROM FAA OPS: SAUSALITO, CA/UAS INCIDENT/1251P/NORCAL TRACON ADVISED CESSNA C525, OAK - RNO, REPORTED A WHITE UAS FROM THE 10 O'CLOCK POSITION WHILE NE BOUND AT 8,600 FEET 6 ENE SAUSALITO VOR. NO EVASIVE ACTION REPORTED. CONTRA COSTA COUNTY SHERIFF NOTIFIED.
7/3/2020	CALIFORNIA	PALM SPRINGS	PRELIM INFO FROM FAA OPS: PALM SPRINGS, CA/UAS INCIDENT/1924P/PIPER PA24, REPORTED AN ORANGE AND BLACK UAS FROM 200 FEET BELOW WHILE E BOUND AT 11,500 FEET 5 N PSP. NO EVASIVE ACTION TAKEN. NO LEO NOTIFICATION REPORTED.

Figure 3: Original FAA UAS Sighting Data

2.1.2. Creating UAS Sighting Data Geolocation

The dataset was initially filtered to only include drone sighting locations within the state of California, obtaining 362 records between July 2020 and June 2021.
Of particular interest to us was the location descriptions, which the dataset typically outlines the location with either 1) the bearing in compass points (N, SW, NNE, etc), and the distance in miles from the nearest airport of VOR equipment, or 2) the distance and/or altitude of the aircraft from the runway on its final approach.
To clean and parse the “Summary” field data we used Regular Expression (Regex), a text pattern recognition. For case 1) Regex allowed to automatically capture the nearby airport/equipment, distance and bearing descriptors from incident summaries. We matched the location descriptor with airport centerpoint coordinate data obtained from FAA’s Airport Data and Information Portal (ADIP). We then use the bearing and distance to arrive at an approximate geolocation of the drone sighting. Geolocations obtained through case 1) inherently contain some limitations on their accuracy: bearing was described in compass points, each 22.5 degrees apart from their nearest compass points. As the distance increases, so too does the length of the arc within the 22.5 degrees. But as we are more concerned with near-airport drone intrusions, this inaccuracy poses less concern. This approach yielded 258 approximate drone sighting geolocations.
Case 2) was more difficult to capture with Regex alone. For this case, we manually read through the descriptions to obtain useful information such as airport/equipment location, the aircraft’s approach runway, and distance and/or altitude on final approach. With this information we manually traced the aircraft’s distance from the runway limit and obtained a coordinate of the drone sighting through satellite imagery and mapping software (Google Earth). We obtained a further 80 drone sighting geolocations through this approach, for a total of 338 drone sightings which we were able to approximate the geolocations.

Based on the incident Summary field below we provide a Regex parsing results example:

> Incident Summary example:
> PRELIM INFO FROM FAA OPS: OAKLAND, CA/UAS INCIDENT/1340P/OAKLAND ATCT ADVISED E75L, SEA - OAK, REPORTED A BLACK UAS OR BALLOON 200 FEET FROM BELOW WHILE S BOUND AT 3,500 FEET 8 E OAK. NO EVASIVE ACTION TAKEN. ALAMEDA PD NOTIFIED.
>
> Airport/equipment: “OAK” in “8 E OAK”, recognized as Oakland International Airport, coordinates 37.72125 (degrees) N, 122.22114 (degrees) W.
> Time of day: “1340P”, read as 1:40 PM Pacific Standard Time
> Drone altitude relative to aircraft: “200 FEET FROM BELOW”, read as -200 (ft)
> Aircraft altitude: “3,500 FEET” read as 3,500 (ft)
> Distance: “8” in “8 E OAK”, read as 8 (miles)
> Bearing: “E” in “8 E OAK”, approximated to bearing 90 (degrees)
> Result approximate drone location and altitude: 37.72116 N, 122.07511 W, 3,300 ft

2.2. GIS data of the controlled and prohibited UAS zones

Due to the lack of information on the specific violation of the UAS operation in the original FAA database, a Geographical Information System (GIS) was gathered and processed to attribute the drone sighting to specific infractions (i.e. which controlled or prohibited zones suffered intrusions) based on the FAA’s B4UFLY application that is used for drone flyers situational awareness (Table 1). This table includes only prohibited and restricted areas with permanent boundaries, which means this does not include temporary flight restrictions (TFR) or other temporary restriction such as Military Training Routes (MTR) that are updated every 8 weeks[7]. Most information was collected from the FAA’s open data GIS: https://udds-faa.opendata.arcgis.com/, with specific restriction details for each layer available on the interactive map of each layer’s link.

Table 1. UAS Controlled Zones Used to Calculate Drone Intrusion Attribution

Layer Name	Description	Source & Date
National Security UAS Flight Restrictions (or Critical Infrastructure) See Figure 4	National security areas or critical infrastructure where UAS operations are prohibited within the airspace defined under NOTAM FDC 7/7282. These areas can be mapped with XY coordinates only.	FAA, Aug. 20, 2023
National Park Service Boundary	National park boundaries where UAS operations are prohibited. These areas can be mapped with XY	National Park Service, Land

[7] To access MTRs GIS: https://adds-faa.opendata.arcgis.com/datasets/faa::mtr-segment-1/about this dataset was not incorporated to calculate drone incidents due to the lack of retroactive restrictions for the July 2020 - June 2021 UAS dataset assessed.

See Figure 5	coordinates only.	Resource Division, Aug. 8, 2023
FAA Controlled Airspace Class See Figure 6	Different airspace classification based on dimensions within which air traffic control service is provided to instrument and visual flight rules (IFR, VFR). Classes range from A-G and their dimensions often require X,Y and Z coordinates because they are layered. For the purposes of this study only classes associated with airports are assessed (Classes B, C, and D)	FAA, Aug 10, 2023
FAA UAS Facility Map See Figures 7 and 8	Identifies permissible altitudes (above ground level) at which UAS can be authorized to fly within the surface areas of controlled airspace (operating under the Small UAS Rule, 14 CFR 107).The ceiling permitting UAS flight ranges from 0 to 400 feet above ground and has associated airport IDs	FAA, Aug. 20, 2023
Airport Boundary	Public airport GIS boundaries used in this study are based on Caltrans open data GIS merged with manual digitization. Details are available in Task 4.1. Typically airport areas and close vicinity (2 mile buffer) have UAS operations restrictions defined by FAA classes and UAS permissions.	See Task 4.1. “Safety and Risk”, Apr. 2023
Airport Safety Zones	Airport Safety Zones GIS was generated for this project (Task 4.1.) and is based on FAA and Caltrans regulations. There are no explicit UAS operation regulations associated with Airport Safety Zones however they typically correspond to the airspace class restrictions and UAS flight ceilings defined by the FAA.	See Task 4.1. “Safety and Risk”, Apr. 2023

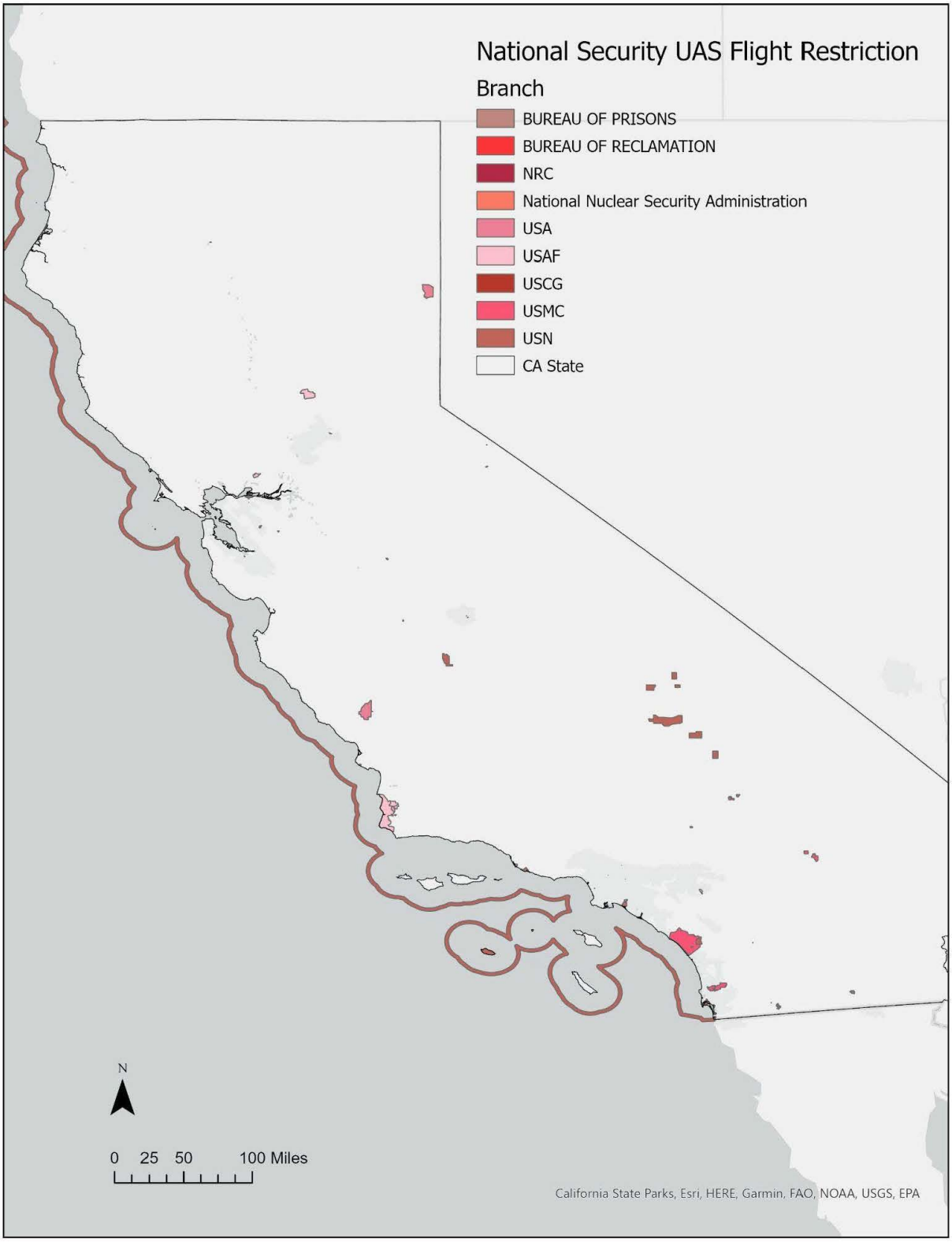


Figure 4: UAS restriction zones based on National Security Zones and Critical infrastructure

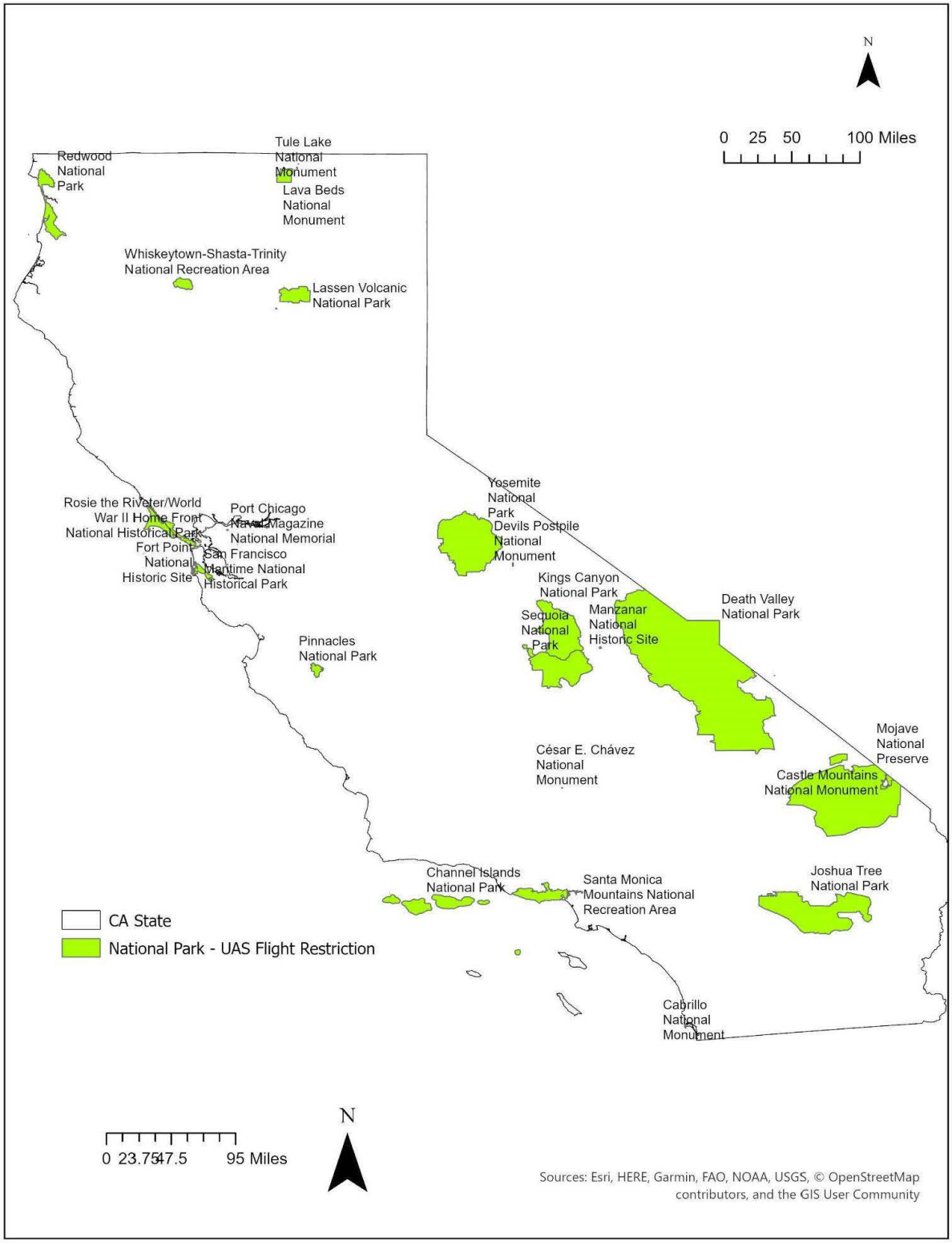


Figure 5: UAS restriction zones based on National Park boundaries

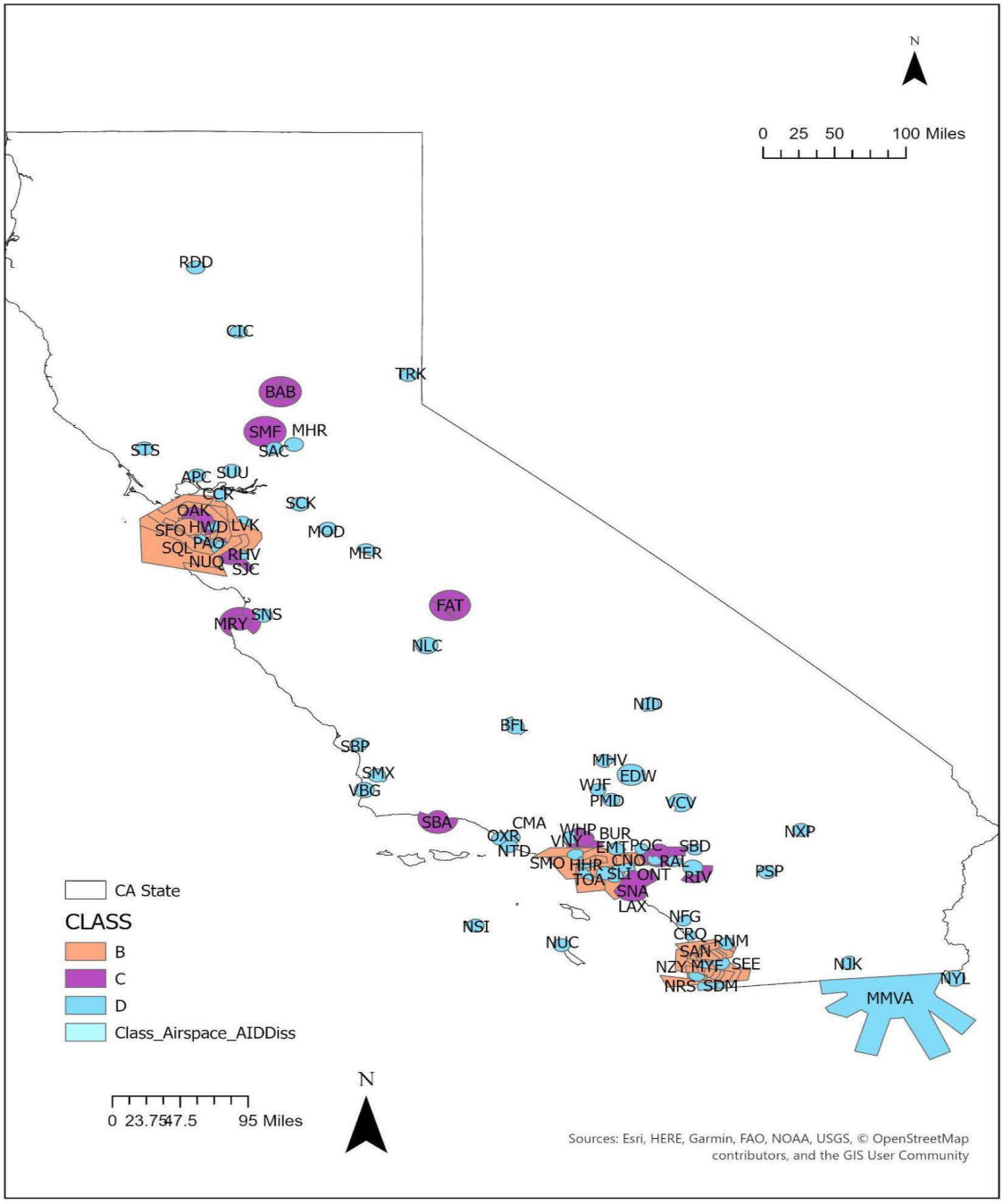


Figure 6. UAS Restricted zones based on FAA Airspace Classes B, C, and D

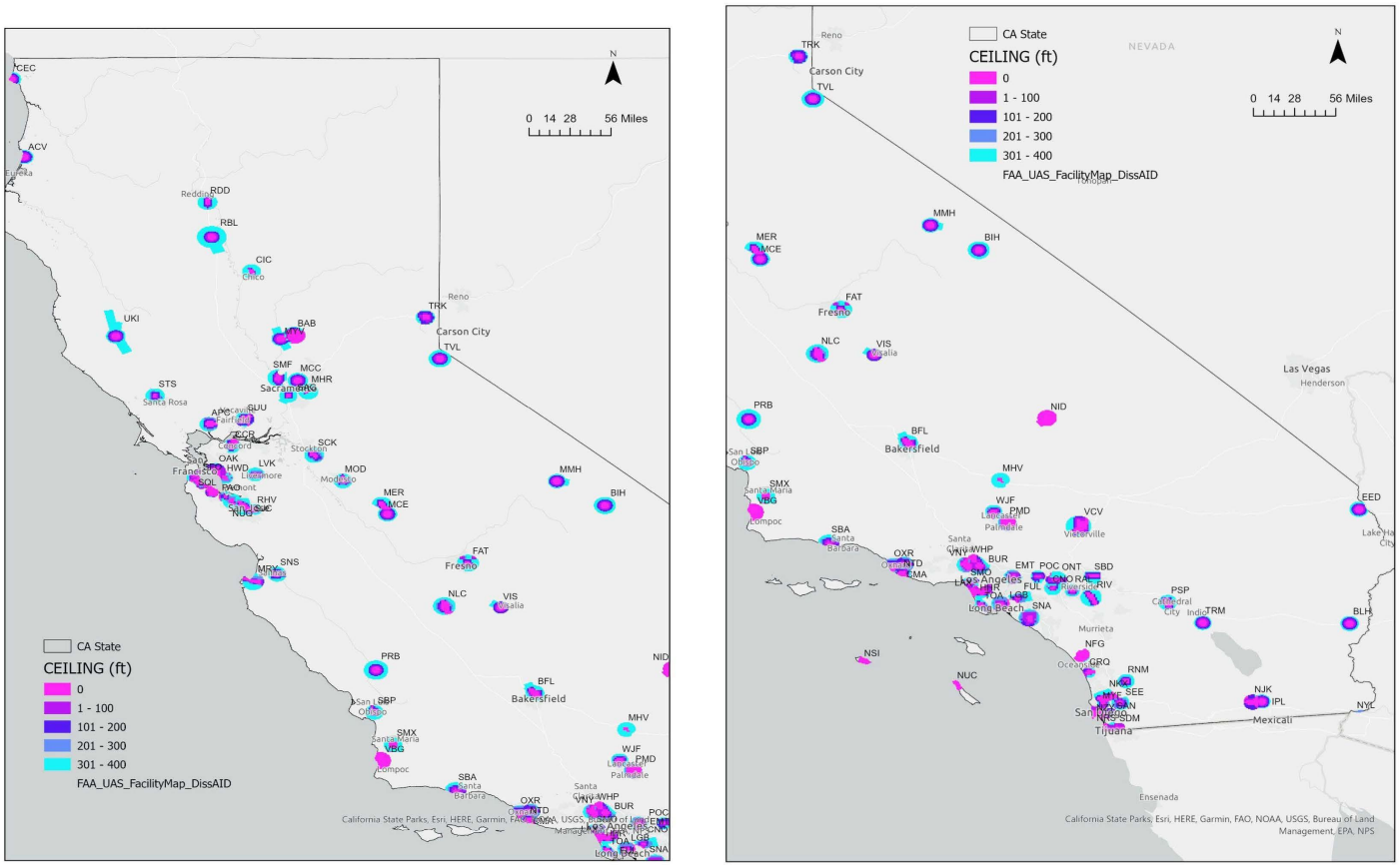


Figure 7. FAA UAS Facility map and ceiling limitations (ft): North CA

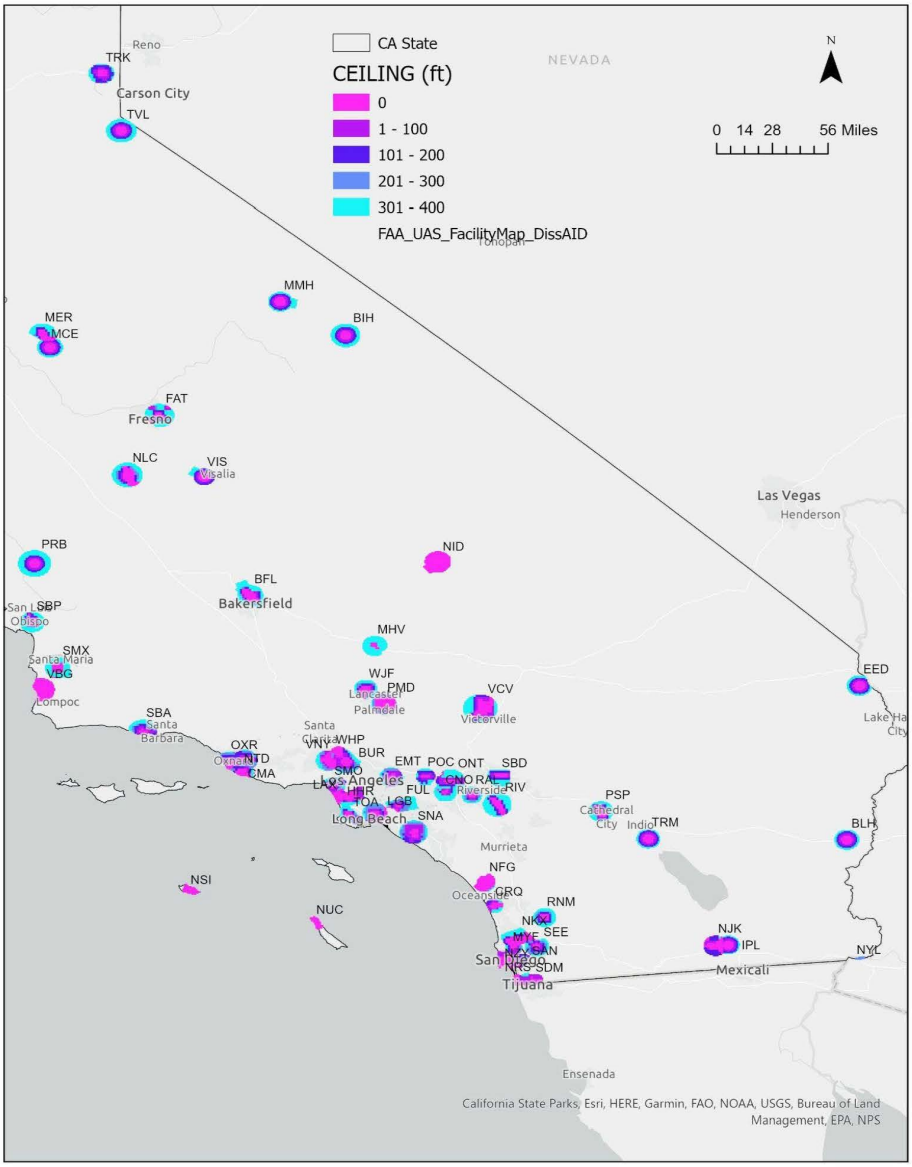


Figure 8. FAA UAS Facility map and ceiling limitations (ft): South CA

[4.1.1(2)] 3. Results

3.1. Overview

3.1.1. Temporal frequency and spatial clusters of drone sighting

Between July 2020 and June 2021 (365 days) a total of 214 days had at least one drone sighting in CA. The number of drone sightings per day in that period ranged from 0 to 10 (Table 2) with 127 days per year with one drone sighting and one day per year with 10 drone sightings. During this period a total of 362 drone sightings were recorded in California, for which 338 were geolocated using text analysis (Figure 9). Most sightings occurred while the sighter was below 3,000 ft (Figure 10). Most drone sighters under 1000 feet correspond to Air Traffic Control Towers while most sighters above 1500 feet correspond to aircrafts. Spatial clusters of drone sightings are located in the Los Angeles, San Francisco Bay, and San Diego regions with very high statistical significance (Figure 11). Results section 3.2. identifies the top areas of concern for drone intrusion based on densities and ranking of airports and airspace intrusion, finishing with the probability of drone intrusion in one year based on the count of sightings per each controlled area and/or airspace identified in Methods section 2.2.

Table 2. Frequency of drone sighting in one day

Frequency of daily drone sighting	Total days in one year
0	151
1	127
2	47
3	27
4	11
6	1 (date: June 11, 2021)
10	1 (date: June 12, 2021)

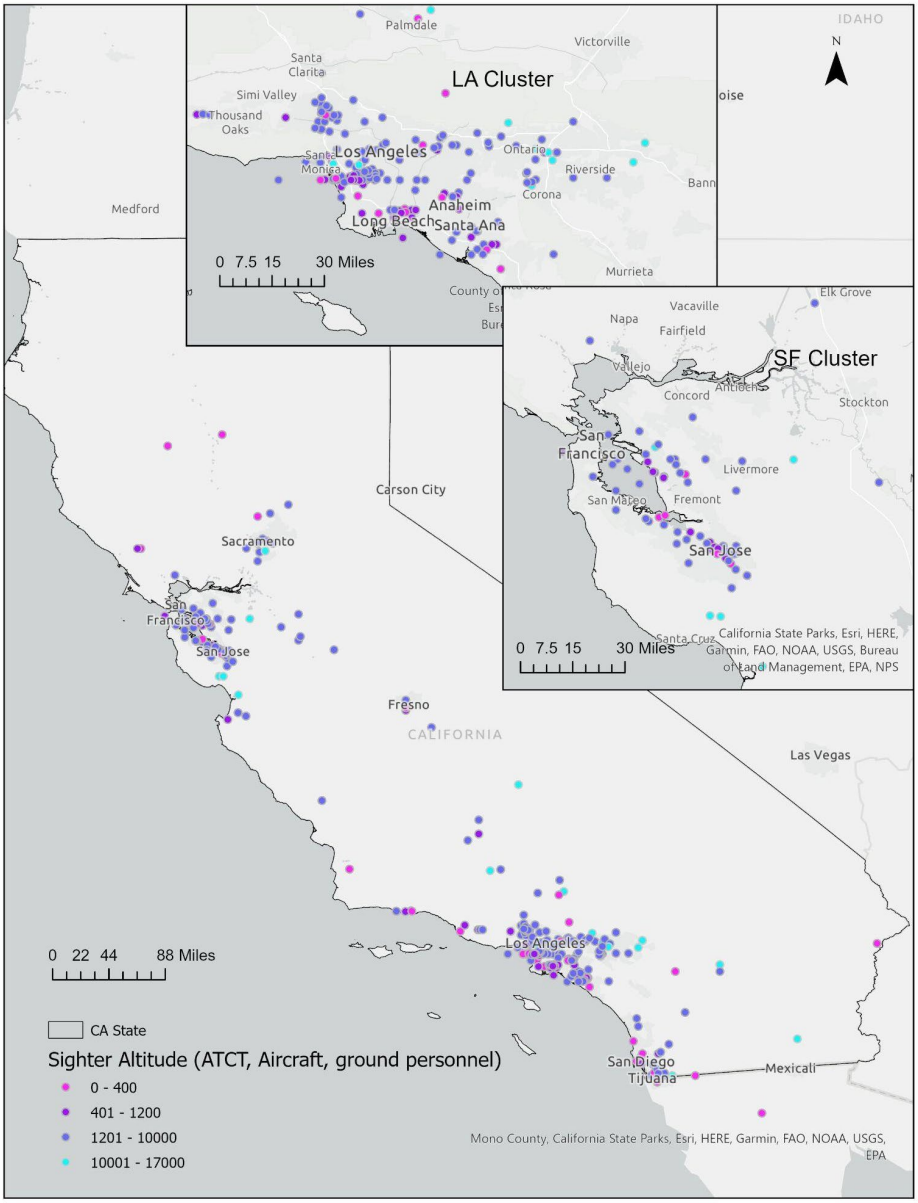


Figure 9. Drone sighting locations and based on sighter's altitude.

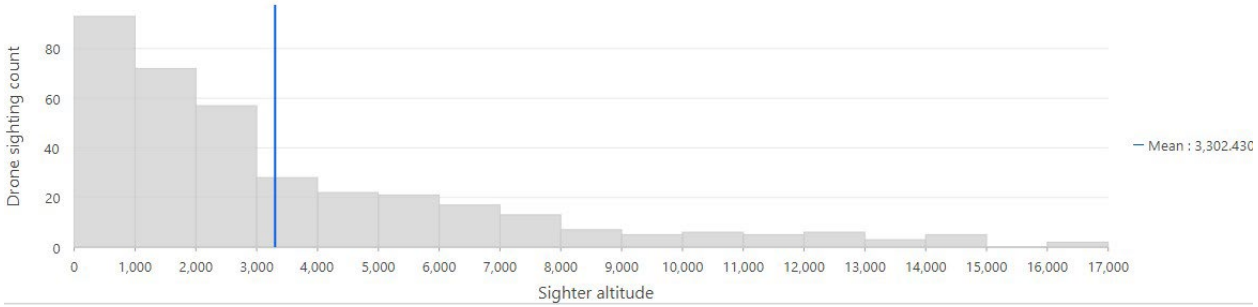


Figure 10. Drone sighter's altitude histogram (ATCT, Aircraft)

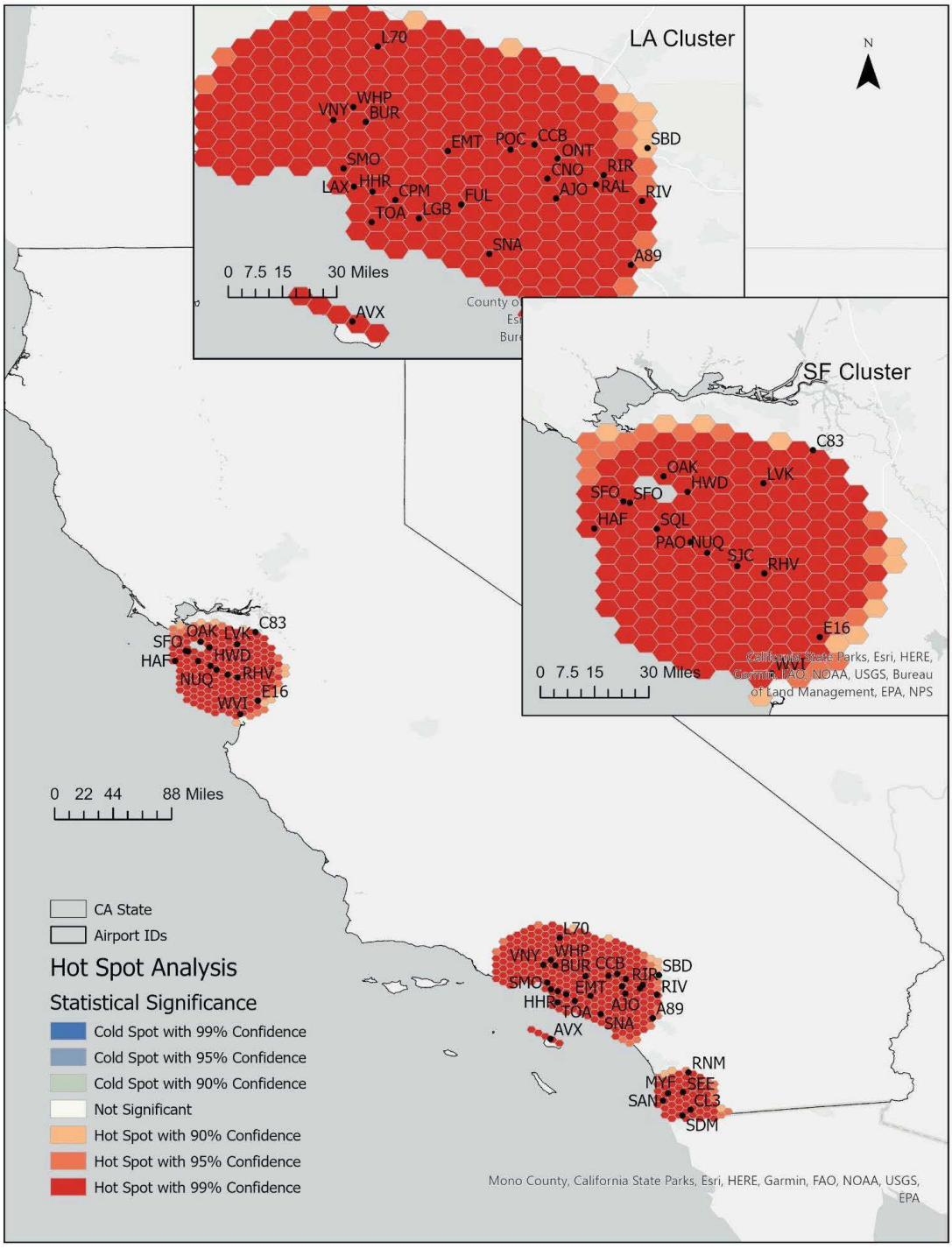

LA Cluster
SF Cluster
N
L70
WHP
VNY
BUR
EMT
POC
CCB
ONT
SBD
SMO
CNO
RIR
LAX
HHR
CPM
AJO
RAL
RIV
FUL
TOA
LGB
SNA
A89
AVX
0 7.5 15 30 Miles
C83
OAK
LVK
SFO
HWD
HAF
SQL
PAO
NUQ
SJC
RHV
E16
WVI
0 22 44 88 Miles
CA State
Airport IDs
Hot Spot Analysis
Statistical Significance
Cold Spot with 99% Confidence
Cold Spot with 95% Confidence
Cold Spot with 90% Confidence
Not Significant
Hot Spot with 90% Confidence
Hot Spot with 95% Confidence
Hot Spot with 99% Confidence
RNM
MYF
SEE
SAN
CL3
SDM
Mono County, California State Parks, Esri, HERE, Garmin, FAO, NOAA, USGS, EPA

Figure 11. Clusters of Drone Sightings/Intrusion (Hot Spots) and Airports of Concern

3.1.2. Airport Safety Zones that intersect with FAA UAS Facilities

FAA UAS facility maps depict the maximum altitude (ceiling) that may be authorized to UAS operators under FAA Part 107. There are 88 FAA UAS facilities in California, out of which 78 intersect with airport boundaries and their respective safety zones (see example Figure 12). Table 3 shows the percentage of each safety zone where UAS operations are not allowed and where they are allowed with authorization, indicating a high % of allowable flight on Zone 4 (Outer Approach/Departure Zones) with 9.29%. Table 4 indicates the detailed surface (square miles) of each with the respective UAS operations ceiling under FAA Part 107.

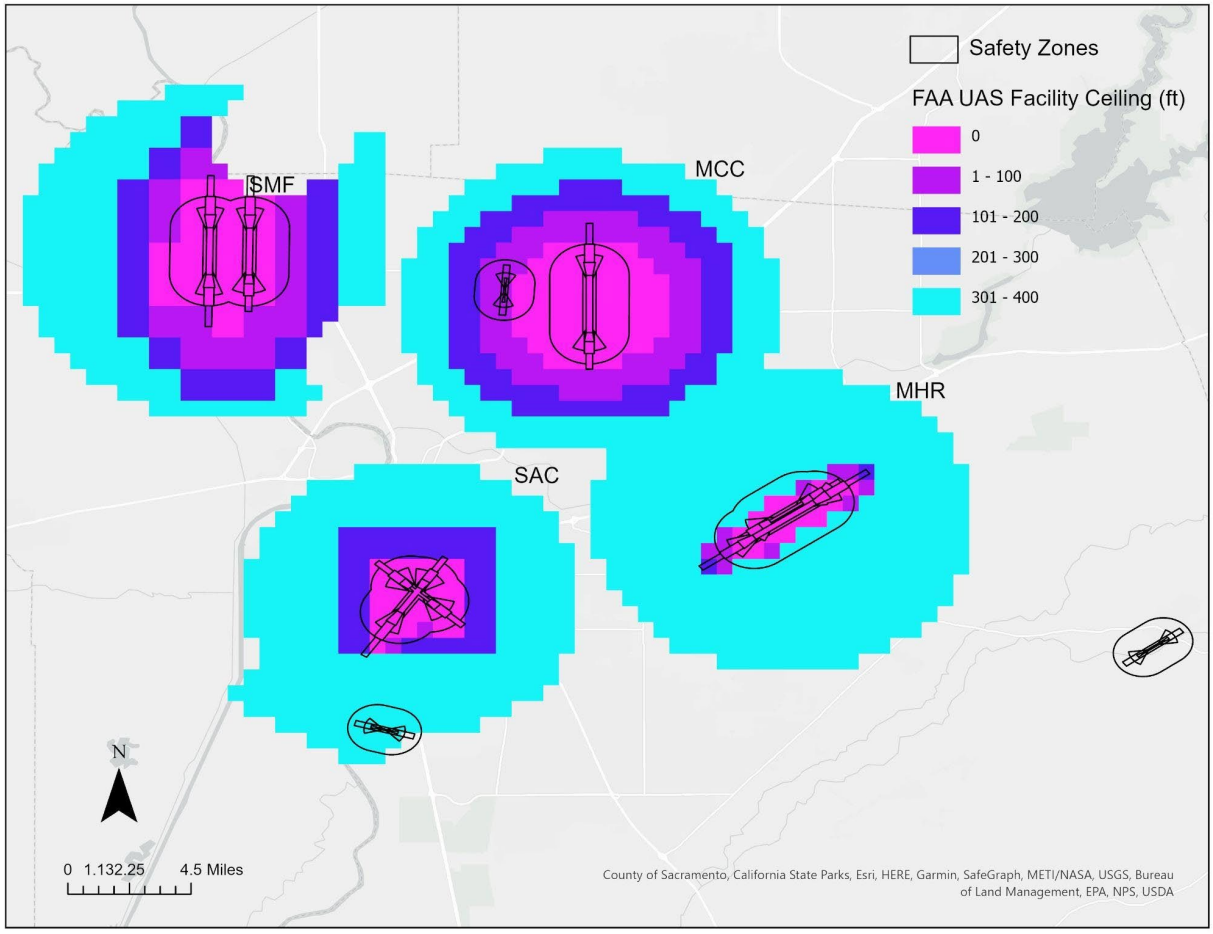


Figure 12. Example of FAA UAS facilities that intersect with airport safety zones near Sacramento.

Table 3. Percentage of Safety Zones that intersect with FAA UAS facilities with allowable operations under FAA Part 107

	Not allowed (%)	**Allowed with authorization (%)**
Primary Surface	72.31	0.14
Z1	65.68	0.18
Z2	52.03	1.66
Z3	47.90	1.05
Z4	44.85	9.29
Z5	52.75	0.40
Z6*	34.14	5.21

** Due to an under dimensioning error of Zone 6, any results associated with this zone area are underestimated, this error does not impact the core results of this analysis. Please refer to Task 8 for further information on the mitigation of this error.

Table 4. Airport Safety Zones that intersect with FAA UAS facilities and the respective ceiling)

Airport Safety Zones (sq. Mi)	**FAA UAS Facility Ceiling (ft)**				
	0	***1-100***	***101-200***	***201-300***	***301-400***
Primary Surface	37.522	0.050	0	0	0.0202

Z1	33.617	0.065	0	0	0.0250
Z2	56.290	1.393	0	0.269	0.130
Z3	45.699	0.818		0.014	0.167
Z4	44.744	5.556	2.894	0.505	0.311
Z5	18.328	0.103	0	0	0.036
Z6*	363.487	38.631	6.867	1.139	8.825
Total Area	599.690	46.619	9.762	1.929	9.515

** Due to an under dimensioning error of Zone 6, any results associated with this zone area are underestimated, this error does not impact the core results of this analysis. Please refer to Task 8 for further information on the mitigation of this error.

3.2. Top Areas of Concern for Drone Intrusion: Densities and Ranking

3.2.1. Drone Sighting Density in Airport Safety Zones and Vicinity (1-5 miles buffer)

Between July 2020 and June 2021 there were 70 drone sightings in the Primary Runway Surface and the Airport Safety Zones 1-6 (Table 5) and a total of 236 sightings in California's airport vicinities with (Table 6). The sighting densities, calculated as *incidents/ total area* indicates if the spatial incidence is homogenous or not. For the airport safety zones, special attention must be given to the primary runway surface with a density of 8.29 e^{-9} drone sightings per sq. mile; followed by Airport Safety Zone 1 and Zone 5 with approximately 5 e^{-9} drone sightings per sq. mile. In terms of airport vicinity, the fist mile buffer outside the airport boundaries presents the highest sighting density of 1,54 e^{-2} sightings per sq. mile followed by the density within airport boundaries. The densities of drone sightings inside the airport boundary are more homogeneous and present a tendency of decreasing incidents as we move further from the airports boundaries.

Table 5. Aggregate drone sighting in airport runway and safety zones

Airport Safety Zones	**Drone Sighting**	**Density (sq.mi)**
Primary Runway Surface	12	8.29 e^{-9}
Z1	8	5.6 e^{-9}

Z2	8	2.65 e^{-9}
Z3	3	1.12 e^{-9}
Z4	4	1.43 e^{-9}
Z5	5	5.16 e^{-9}
Z6*	30	1.01 e^{-9}

** Due to an under dimensioning error of Zone 6, any results associated with this zone area are underestimated, this error does not impact the core results of this analysis. Please refer to Task 8 for further information on the mitigation of this error.

Table 6. Aggregate drone sighting in Airport boundary and vicinity

Airport boundary and vicinity	**Drone Sighting**	**Density (sq.mi)**
Inside airport boundary	26	1,19 e^{-2}
1 mile buffer outside airport	54	1,54 e^{-2}
1 - 2 mile buffer outside airport	51	1,01 e^{-2}
2 - 3 mile buffer outside airport	47	0,07 e^{-2}
3 - 4 mile buffer outside airport	49	0.06 e^{-2}
4 - 5 mile buffer outside airport	35	0.04 e^{-2}

3.2.3. Ranking of Airport and Airspace Areas of Concern

Due to the lack of specification of the violation of each drone intrusion, we assessed the spatial intersection of drone sighting incidents and the controlled UAS areas described in Methods & Data section 2.2. Three different controlled areas of concern are appraised: (1) two mile buffer of airport boundaries, (2) the FAA UAS facilities, and (3) FAA Airspace Class B,C, and D pertaining to airports.

(1) Two mile buffer from airport boundaries: a total of 131 drone sightings were reported within the 2 mile buffer of 42 airports in California (out of 261 public airports assessed in this study).
(2) FAA UAS facilities: a total 222 sightings were reported in 44 FAA UAS facilities out of 88 facilities
(3) FAA Airspace Class B,C, and D: a total of 275 sightings in the airspace of 41 airports out of 75 of B,C, or D classes

Tables 7 to 9 respectively rank the top 10 airports of concern based on the potential violation of each of these three areas of concern perimeters (the full count is available in Appendix A). Table 10 presents a final ranking of the 16 airport IDs associated with these 3 areas of concern violations, with LAX, VNY and SJC as the top three areas of concern.

Table 7: Ranking of drone sighting within 2 mile buffer of airport's boundary

Rank	Airport ID (2 mile buffer)	# Drone sighting/ intrusion
1	LAX	24
2	HHR	18
3	LGB	9
4	VNY	7
5	RHV	7
6	SJC	6
7	SDM	5
8	EMT	4
9	HWD	4
10	SAN	4

Table 8: Ranking of drone sighting within FAA UAS facility perimeters

Rank	Airport ID associated with FAA UAS facility	# Drone sighting/ intrusion
1	LAX	53
2	VNY	16
3	SNA	13
4	LGB	11
5	EMT	10
6	SJC	10
7	ONT	9
8	RHV	8
9	BUR	7

10	SMO	7

Table 9: Ranking of drone sighting within FAA restricted airspace Class B,C and D

Rank	Airport ID associated to Class B, C and D	# Drone sighting/ intrusion
1	LAX	109
2	SFO	38
3	BUR	9
4	SJC	7
5	ONT	7
6	SNA	6
7	VNY	5
8	SAN	4
9	LGB	4
10	EMT	4

Table 10. Final ranking of areas of concern for drone intrusion

Associated Airports	**Score***	**Weight***
LAX	**30**	**3**
VNY	**20**	**3**
SJC	**17**	**3**
LGB	**17**	**3**
SNA	**13**	**2**
BUR	**10**	**2**

ONT	**10**	**2**
RHV	**9**	**2**
EMT	**7**	**2**
SFO	**9**	**1**
HHR	**9**	**1**
SDM	**4**	**1**
SAN	**3**	**1**
SMO	**1**	**1**
HWD	**1**	**1**

* Score is calculated based on the rank number for each of the 3 areas of concern assessed in tables 5 to 7; and the weight represents the number of times each airport appears in the three areas of concern assessed. Rank 1 scores 10, rank 2 scores 9, rank 3 scores 7…rank 10 scores 1. Eg. LAX was ranked 1st 3 times, thus the score is 10 x 3 = 30.

3.3. Probability of Drone Intrusion

The probability of drone intrusion is calculated based on the probability of any given drone to violate the different controlled zones assessed in the study in the period of one year: *total drone sightings/ 365 days.* The limitation of this intrusion probability is that the current drone sighting data is very limited in the description of the drone altitude (Z coordinates) which adds error to the intersection GIS calculation that is only based on X,Y coordinates.

- National Security Areas and Critical Infrastructure: In the study period no intrusions were calculated based on the intersection of drone sighting points and the GIS layers of the National Security and CRitical Infrastructure boundaries.
  Probability = 0

- National Reserve Parks: One drone sighting was identified at the intersection of a national reserve park representing a potential intrusion, however when reading the

summary report there was no clear indication that this represented a violation of a national park, the specification indicates that it was sighted by Burbank ATCT at 5,000 ft.
Probability = 0.00273

- FAA Airspace Class: The probability of a drone to enter any of the B, C and D FAA controlled airspace in the period of a year is *0.98355,* for the probability of each separate class see Table 11. The probability of a drone intruding the FAA restricted airspace class of the top 10 airports with most drone sightings in one year is 0.24102, for the probability of drone intrusion in restricted airspace per airport or ATCT ID see Table 12.
Probability = 0.98355

- FAA UAS facility: The probability of a drone intruding the FAA UAS facilities of the top 10 airports with most drone sightings in one year is *0.30719*, for the probability of drone intrusion per airport FAA UAS facility see Table 13.
Probability = 0.30719

- Two mile buffer of airport boundary: The probability of a drone entering the 2 mile buffer of the top 10 airports' boundaries with most drone sightings in one year is *0.264828*, for the probability of drone intrusion per airport from 1 to 5 mile buffer see Table 14.
Probability = 0.264828

- Airport Safety Zones: The probability of a drone entering any of the Airport Safety Zones, including the Primary Runway Surface is *0.19173*, when removing the Primary Runway Surface the probability decreases to 0.15886. The probability of drone intrusion for each separate zone is described in Table 15.
Probability = 0.19173

Table 11. Probability of intrusion given the aggregate sightings of FAA airspace classes

Class	Description (FAA, Controlled Airspace)	Airport or ATCT IDs	Aggregate Drone Sightings	*Probability*
B	Restricted airspace surrounding US busiest airports, usually formed by layers resembling an upside down wedding cake, with complex geometries that generally covers the surface of 10,000 feet above the airport elevation.	LAX, SAN, SFO	160	0.43835

C	Restricted airspace surrounding airport facilities that have an operational control tower, are serviced by radar approach control and have a certain number of IFR operations or passenger enplanements. Generally, consists of two layers: a 5 NM radius from the surface to 4,000 above the airport elevation and a 10 NM radius shelf area between 1,200 and 4,000 feet above airport elevation	BAB, BUR, FAT, MRY, OAK, ONT, RIV, SMF, SJC, SNA, SBA	96	0.26301
D	Restricted airspace surrounding airport facilities with an operational control tower that generally extends from the surface to 2,500 feet above the airport elevation. Some Class D surface is part-time, meaning that it may revert to class E or Class G airspace during certain times of day and/or year.	APC, BFL, CCR, CIC, CMA, CNO, CRQ, EDW, EMT, FUL, HHR, HWD, LGB, LVK, MER, MHR, MHV, MMVA, MOD, MYF, NFG, NID, NJK, NLC, NRS, NSI, NTD, NUC, NUQ, NXP, NYL, NZY, OXR, PAO, PMD, POC, PSP, RAL, RDD, RHV, BNM, SAC, SBD, SBP, SCK, SDM, SEE, SLI, SMO, SMX, SNS, SQL, STS, SUU, TOA, TRK, VBG, VCV, VNY, WHP, WJF	103	0.28219

Table 12. Probability of intrusion of FAA controlled airspace class per airport

Rank	Airport ID (2 mile buffer)	Probability of drone intrusion
1	LAX	0.06575
2	HHR	0.04931
3	LGB	0.02465

4	VNY	0.01917
5	RHV	0.01917
6	SJC	0.01643
7	SDM	0.01369
8	EMT	0.01095
9	HWD	0.01095
10	SAN	0.01095

- FAA UAS Facility (Table 13)

Rank	Airport ID associated with FAA UAS facility	Probability of drone intrusion
1	LAX	0.14520
2	VNY	0.04383
3	SNA	0.03561
4	LGB	0.03013
5	EMT	0.02739
6	SJC	0.02739
7	ONT	0.02465
8	RHV	0.02465
9	BUR	0.01917
10	SMO	0.01917

- Two miles buffer of airports (including airport boundaries) (Table 14)

Rank	Airport ID (2 mile buffer)	Probability of drone intrusion
1	LAX	0.09315
2	HHR	0.04931
3	LGB	0.02465

4	VNY	0.01917
5	RHV	0.01917
6	SJC	0.016438
7	SDM	0.01369
8	EMT	0.01095
9	HWD	0.01095
10	SAN	0.01095

- Runway and Airport Safety Zones (Table 15)

Airport Safety Zones	**Probability of drone intrusion**
Primary Runway Surface	0.03287
Z1	0.02191
Z2	0.02191
Z3	0.00821
Z4	0.01095
Z5	0.01369
Z6*	0.08219

** Due to an under dimensioning error of Zone 6, any results associated with this zone area are underestimated, this error does not impact the core results of this analysis. Please refer to Task 8 for further information on the mitigation of this error.

[4.1.1(2)] 4. Citations

FAA. (2021). Small Unmanned Aircraft System (Small UAS).
https://www.faa.gov/regulations_policies/advisory_circulars/index.cfm/go/document.information/
documentID/1038977
FAA. (2021). UAS Sightings Report.

https://www.faa.gov/uas/resources/public_records/uas_sightings_report
FAA. (2022a). B4UFLY App. https://www.faa.gov/uas/getting_started/b4ufly
FAA. (2022b). Unmanned Aircraft System (p. 45). https://www.faa.gov/sites/faa.gov/files/2022-06/Unmanned_Aircraft_Systems.pdf
FAA. (2023a). Class Airspace. https://adds-faa.opendata.arcgis.com/datasets/faa::class-airspace/about
FAA. (2023b). FAA UAS FacilityMap Data. https://udds-faa.opendata.arcgis.com/datasets/faa::faa-uas-facilitymap-data/about
FAA. (2023c). FAA's UAS Data Delivery System [dataset]. https://udds-faa.opendata.arcgis.com/
FAA. (2023d). National Security UAS Flight Restrictions. https://udds-faa.opendata.arcgis.com/datasets/faa::national-security-uas-flight-restrictions-1/about
FAA. (2023e). Operating Restrictions. https://www.faa.gov/uas/getting_started/where_can_i_fly/airspace_restrictions/tfr
FAA. (2023f). Recreational Flyers & Community-Based Organizations. https://www.faa.gov/uas/recreational_flyers
FAA. (2023g). Section 2. Controlled Airspace. https://www.faa.gov/air_traffic/publications/atpubs/aim_html/chap3_section_2.html
National Park Service. (2018). National Park Service Land Resources Division Tract and Boundary Service. https://nps.maps.arcgis.com/home/item.html?id=a2848257cf5541338bab9b656440bd0c
Smith, P. (2022). Ntegrating Expanded And Non-Segregated UAS Operations Into The NAS: Impact On Traffic Trends And Safety (A21__A11L.UAS.69) (p. 69). https://www.assureuas.org/projects/integrating-expanded-and-non-segregated-uas-operations-into-the-nas-impact-on-traffic-trends-and-safety/

[4.1.1(2)] Appendix A: Full Rank of Drone Sighting by Airports and their Controlled Airspace in California (July 2020- June 2021)

A.1. Count of drone sightings at 2 mile buffer from airport boundaries

Rank	*Airport ID*	*Drone Sightings*
1	LAX	24
2	HHR	18
3	LGB	9
4	VNY	7
5	RHV	7
6	SJC	6
7	SDM	5
8	EMT	4
9	HWD	4
10	SAN	4
11	ONT	4
12	SMO	3
13	FUL	3

14	NUQ	3
15	PAO	3
16	STS	2
17	SEE	2
18	CNO	2
19	POC	2
20	MYF	2
21	SFO	2
22	SNA	2
23	OAK	2
24	UDD	1
25	0Q3	1
26	TOA	1
27	AJO	1
28	RAL	1
29	CCB	1
30	REI	1
31	FCH	1
32	L45	1
33	LHM	1
34	LVK	1
35	MHR	1
36	SBA	1
37	SFO	1
38	CIC	1
39	L35	1
40	MRY	1
41	OXR	1

42	SMX	1

A.2. Count of drone sightings at FAA UAS facility sites

Rank	*Airport ID*	*Drone Sightings*
1	LAX	53
2	VNY	16
3	SNA	13
4	LGB	11
5	EMT	10
6	SJC	10
7	ONT	9
8	RHV	8
9	BUR	7
10	SMO	7
11	CNO	6
12	FUL	6
13	HWD	5
14	NUQ	5
15	OAK	5
16	SDM	5
17	SAN	4
18	POC	3
19	SBA	3
20	CMA	2
21	HHR	2
22	MCC	2
23	MYF	2

24	NRS	2
25	PAO	2
26	PMD	2
27	SAC	2
28	SEE	2
29	SFO	2
30	STS	2
31	BFL	1
32	CIC	1
33	FAT	1
34	LVK	1
35	MER	1
36	MHR	1
37	MRY	1
38	OXR	1
39	RAL	1
40	RIV	1
41	SMX	1
42	SNS	1
43	SQL	1
44	TOA	1

A.3. Count of drone sightings at FAA Controlled Airspace Class B,C, and D

Rank Airport ID Drone Sightings

1	LAX	109
2	SFO	38
3	BUR	21
4	SJC	19

5	ONT	17
6	SNA	17
7	VNY	14
8	SAN	13
9	LGB	11
10	EMT	10
11	OAK	9
12	RHV	8
13	SMO	7
14	CNO	6
15	FUL	5
16	SDM	5
17	HWD	4
18	NUQ	4
19	SBA	4
20	FAT	3
21	PAO	3
22	POC	3
23	SMF	3
24	HHR	2
25	MRY	2
26	MYF	2
27	PMD	2
28	SAC	2
29	SEE	2
30	STS	2
31	BFL	1
32	CIC	1

33	LVK	1
34	MHR	1
35	NRS	1
36	OXR	1
37	RAL	1
38	RIV	1
39	SMX	1
40	SNS	1
41	TOA	1

Task 4.1.2. Impact of Wildlife Strikes

Deliverables: A summary report that presents (1) bird-strike accidents and incidents at CA airports over all 6 Zones frequency and (probability per airport for the entire period), and (2) bird-strike accidents and incidents (i) by phases of flight, (ii) aircraft damage type, (iii) aircraft speed and altitude and distance/altitude , (iv) aircraft type, (v) seasonality, (vi) bird species, and (vii) weather conditions (visibility, temperature, precipitation).

Acceptance Criteria: A document that includes figures and tables that display frequency of bird-strike accidents and incidents at CA airports over each airport zone.

[4.1.2] 1. Introduction

Wildlife strikes are part of a safety as well as a biodiversity conservation concern in airport land use decision making. In this analysis wildlife strikes are being assessed mostly for safety concerns to provide incident frequency, probability and impact data that can be useful to mitigate strike risk through habitat management and aircraft operation adjustment (FAA, 2022; FAA AC 150/5200-32-C, 2020; ACRP, 2015).

The severity of the wildlife strike depends on multiple factors like the mass and number of wildlife involved in the incident, the location of the strike on the aircraft (engines being the most vulnerable areas) and speed of aircraft.

From January 1st 1990 to April 17th 2023, a total of 20,245 wildlife strikes have been reported in California out of which 401 resulted in substantial damage[8] to the aircraft and 4 resulted in aircraft destruction[9]. During the same period in the U.S. a total of 279,446 incidents were registered, out of which 4,232 resulted in “substantial damage” impact type and 82 resulted in “destruction” impact type. In California there is one recorded incident with one fatality from wildlife strikes on aircrafts, and a total of 19 incidents that caused 23 injuries between 1990-April 2023.

California’s database shows that most wildlife strike incidents involved birds (96,46%). There are some cases of flying mammals strikes with bats, and terrestrial mammals strikes with skunks, rabbits, coyotes, deer and others (2.94%); and very rare cases of terrestrial collisions with reptiles such as snakes and turtles (0.04%).

Direct costs of wildlife strikes for the aviation industry are related to cost of labor and materials of repairs, and in rare cases the most severe accidents cause injuries or fatalities (McKee and

[8] Substantial impact category refers to “when the aircraft incurs damage of structural failure which adversely affects the structure strength performance or flight characteristics of the aircraft and which would normally require major repair or replacement of the affected component. Bent fairings or cowlings, small dents or puncture holes in the skin; damage to wind tips, antenna, tires or brakes; and engine blade damage not requiring blade replacement are specifically excluded.” (Source FAA Wildlife Strike Reference Table: https://wildlife.faa.gov/search)

[9] Destroyed impact category refers to “ when the damage sustained makes it inadvisable to restore the aircraft to an airworthy condition.”(Source FAA Wildlife Strike Reference Table: https://wildlife.faa.gov/search)

all, 2016). Indirect costs are associated with delays, cancellations and other changes to aircraft operations such as aborted takeoffs and precautionary or emergency landings. Other costs include the impact on wildlife welfare and biodiversity, as wildlife strikes are almost always fatal to the wildlife involved, and have been steadily increasing in developed countries and California. The causes of this increase have been attributed to multiple factors such as improvements of reporting and monitoring of aircraft-wildlife collisions or changes in regulation in some countries that made reporting mandatory. Aircraft engine design has become more efficient and quieter with the substitution of the three or four-engine aircraft to two-engine aircraft of commercial air carriers. The hypothesis is that wildlife is less able to detect and avoid modern jet aircraft with quieter turbofan engines (FAA, 2022) resulting in higher rates of wildlife collision. Land use and conservation practices improvements are a very important factor directly affecting wildlife population behavior such as the increasing the number and frequency of wildlife in urban landscape (Kelly & Allan, 2006). In North America for example, most large bird species (with a mean body mass of 1.1kg or more) have increased in the last three decades (FAA, 2022). Section 2 describes how the wildlife strike database for California was used together with runway GIS. Section 3 provides the results of the statistical analysis including the incidents in airports and their respective runway safety zones, and further wildlife strike analysis based on available variables such as phase of flight, aircraft damage type, aircraft speed, altitude and distance from runway end, aircraft type, seasonality, wildlife taxonomy, and weather conditions. A parallel study focusing specifically on bird strike severity prediction is described in Appendix A.

[4.1.2] 2. Data & methods

The bird strike analysis is developed based on the publicly available Federal Aviation Administration (FAA) Wildlife strike database (https://wildlife.faa.gov/home). Wildlife aircraft incidents data assessed in this report spans from 1990 up to April 17th 2023. FAA wildlife strikes are voluntarily reported therefore it cannot be guaranteed that reporting rates are 100%, however report rates are rising according to the FAA's latest report on Wildlife Strikes to Civil Aircraft (FAA, 2022).

2.1. Wildlife strike data

This analysis only focuses on wildlife strikes attributed to California state in the original FAA wildlife strike dataset downloaded on April 17th, 2023. The Lat lon information of the incidents refers mostly to airport centroids and therefore could not be used entirely to locate the occurrence of the all wildlife strikes. The geographical information aiding on the location attribution of each incident includes a combination of airport distance (assuming end of runway as the starting point), phase of flight, height, and runway location. The combination of this geographical data with basic assumptions on aircraft landing and departure paths (i.e five miles straight line for arrivals) allowed for the approximate birds strike location. It is important to highlight that the precision of strike distance from airport and height is low (rounded integers).

Although the total number of reported wildlife strikes in the study period was of 20,245, the number of strikes assessed changes in the statistical analysis based on the variable of interest because not all reported incidents have have valid entries for all variables (i.e. phase of flight, height, wildlife species, etc). A total of 19,873 strikes provide Latlon data for the GIS analysis.

2.2. GIS data: Runway Safety Zones

To create the runway safety zones, different runway open source GIS were examined: Caltrans, FAA Aeronautical Data Delivery Service (ADDS), and the Bureau of Transportation Statistics (BTS) part of the U.S. Department of Transportation (USDOT) National Transportation Atlas Database (NTAD). The BTS runway data (created on July, 16, 2020) was the most appropriate due to the detailed attribute table available with runway end points and the obstruction identification surface codes necessary for determining the runway's primary surfaces according to the Federal Aviation Regulations Part 77. The definition of the primary surface was applied based on runway visibility parameters (i.e. visual runways, non-precision instrument runways, and precision instrument runways). After defining the runway's primary surface, the geometries for the 6 generic safety zones were applied based on the BTS runway length, approach visibility minimums, and the type of general aviation or large air carrier runway (see figure 3A, pp.3-17 and 3-18 of the 2011 Airport Land Use Planning Handbook). For detailed methods see section 2.3.2 of Task 4.1. Safety and Risk.

2.3. Aircraft Characteristics: AAC and ADG

The FAA's Aircraft Approach Category (AAC) (Table 1) and Aircraft Design Group (ADG) (Table 2) from the Airport Design Advisory Circular (AC 150/5300-13A, 2014) are used in this analysis to understand patterns of wildlife strikes based on aircraft characteristics in the results Section 3.8. The FAA's Aircraft Characteristics Data was used to match the identified aircraft models identified in the wildlife strike database to the AAC and ADG categories. Helicopters are considered as a separate AAC category.

Table 1. FAA's Aircraft Approach Categories (AAC)

AAC	V_{REF} / Approach Speed
A	Less than 91 knots
B	91 knots or more but less than 121 knots
C	121 knots or more but less than 141 knots
D	141 knots or more but less than 166
E	166 knots or more

Table 2. FAA's Airplane Design Group (ADG)

Group #	Tail Height (ft[m])	Wingspan (ft [m])
I	< 20' (< 6m)	< 49' (< 15m)
II	20'-< 30' (6 -< 9m)	49' - < 79' (15- < 24m)
III	30'- < 45' (9-<13.5m)	79' - < 118' (24 -< 36m)
IV	45' -< 60' (13.5 -< 18.5m)	118' - <171' (36 - < 52m)
V	60' - < 66' (18.5 - < 20m)	171'- < 124' (52 - < 65m)
VI	66' - < 80' (20- < 24.5m)	214' - < 262' (65 - < 80m)

[4.1.2] 3. Results

Results are organized starting with single- and two-variable analysis, then GIS-relevant results, ending with a multivariable analysis, and a severity analysis in the appendix:

- Sections 3.1 to 3.9 present the single variable analysis, starting with an overview of the strike analysis (evolution by year, engine type, and height). Sections 3.2.-3.8 will then focus on assessing the following single variables: engine type (by damage location and year); height analysis (averages by year and engine type); phase of flight (percentage by phase of flight, yearly evolution, and by engine type); impact type (percentage of each impact category, yearly evolution, and by engine type); seasonality (percentage per season, yearly evolution, and by engine type); by weather conditions (percentage, yearly evolution, and by engine type); by aircraft characteristics, namely Aircraft Approach Category (AAC) and Aircraft Design Group (ADG) (percentages by AAC and ADG, yearly evolution, and by engine types), and by wildlife taxonomy, focused on Order (percentage by Order, yearly evolution, and by engine type)
- Section 3.10 focuses on GIS-relevant results, with a subsection presenting probability by location, percentage of strikes per safety zone, and another subsection focusing on the distance from runway (percent of strikes based on distance from runway, percent of strike based on distance from runway and engine type, and average distance from runway change over time).
- Section 3.11 focuses on two multivariable analysis: the first crosses strikes distances from runway, height and speed; the second crosses wildlife taxonomy, distance, height, and speed.

- Appendix A. Bird Strike Severity Analysis, provides a parallel investigation on the severity of strikes attributed to birds only (over 96% of strikes in California) covering over 6,000 incidents from 2010 to 2019. Logistic regression is applied here to further investigate the statistical relationship of available variables of bird strikes (height, speed, time of day, weather conditions, etc) to strike damage types.

In Section 3.1.Overview, Figure 1 shows that the total number of wildlife strike reports in California has been increasing since 1990, with a total of 20,254 strikes, an average of 609.3 strikes per year and an average yearly increase of 25.6 strikes over 32 years (Figure 2). A total of 56 California public airports have registered wildlife strikes since 1990. Most strikes occur during day time (n = 8.,878); followed by night time (4,383), dusk (n=503) and dawn (n= 471). The most commonly impacted engine type is the turbo fan (Figure 3). From the strikes with height information, the frequency steadily decreases from 1 to 3,000 feet.When excluding incidents occurring at ground-level, we can observe that nearly 50% of strikes occur between 1-401 feet, reaching 90% at 3,500 feet, (Figure 4).

In Section 3.2. Strikes by Engine Type, the most common damage location of strikes occur on the engines for Turbofan engine-type aircrafts, on the wing for reciprocating and turboprop-engine type aircrafts, and on the windshield for turboshaft engine-type aircrafts (Figure 5). Figure 6 shows the evolution of strikes from 1990 to 2022, where we can see that the increase of strikes is mostly attributed to incidents occurring with turbofan -engine-type aircrafts, which surpassed the 100th incident at the start of series in 1990, peaking at 652 strikes in 2019, and with a visible dip to 386 strikes in 2020 (probably due to the decrease of operations during COVID 19 pandemic restrictions) . Strikes to all other engine-type aircrafts are much less frequent, although a very slight increase is visible for reciprocating and turboshaft engine-type aircrafts after 2014.

In Section 3.3. Strike height Analysis, Figure 7 shows that the yearly average strike height between 1990 and 2022 has been between 400 and 1200 feet (taking into consideration the standard errors). In the beginning of the series, from 1990 to 2000 the yearly average height remained low, mostly close to 600 feet. After 2000 there was a significant increase in the average height of strikes, reaching nearly 1,200 feet in 2002, and maintaining averages above 700 feet up to 2022. In Figure 8 we can see that Turboshaft and Turbofan engine-type aircrafts have higher average strike heights, closer to 1000 feet, and reciprocating turbojet, and turboprop have average strikes close to 500 feet.

In Section 3.4. Strike and Phase of Flight Analysis, Figure 9 shows that the majority of strikes occur during approach (43.9%), followed by landing roll (17.4%), climb (16.5%), and take-off run (16%). The evolution of strikes from 1990 to 2022 in Figure 10 shows that independently of the phase of flight, strikes have been steadily increasing over time, with visual dips in incidents during Covid-19 pandemic for the most frequent phases of flight with strike occurrences described above. For most engine-type aircraft incidents, strikes have occurred during approach; including 45% for turbofan, 43% for reciprocating, and 39% for turboprop. Turbojet

engine-types have 40% of their strikes occurring during landing roll, and turboshaft has 67% of strikes occurring en-route (Figure 11).

In Section 3.5. Strike and Impact Analysis, it is possible to see that the majority of strikes cause no damage is reported (87.8%), with no incidents that have destroyed an aircraft, as in inadvisable to restoration. Minor damage was caused by 5.4% of strikes caused (when simple repair or replacements can render the aircraft airworthy, and no extensive inspection is necessary); and 2.8% of incidents caused substantial damage, where the damage affects the structure strength, performance or flight characteristics which normally requires major repair or replacement of the affected component; and 4% of strikes have undetermined damage (damage was incurred but the details of the damage extent are unknown) (Figure 12). The yearly evolution of the different damage categories in Figure 12 show the increase of strikes that cause no damage to aircrafts as well as undetermined damage (especially after 2015). Strikes causing minor and substantial damage have shown a gaslight decrease after 2015. When looking at the damage level based on engine type, strikes affecting turbojet engine-type have the highest substantial damage (20%) as well as the highest unknown damage level (20%), while other engine types have only 1-3% of their strikes causing substantial damage, except for turboshafts that have 8% of strikes causing substantial damage (Figure 13).

In Section 3.6. Strike Seasonality Analysis, shows that winter months have the lowest incidence of strikes (18,4%) while Fall and Summer have the highest incidence (28,4% and 27,8% respectively), followed by Spring (25.5%) (Figure 14). Figure 15 shows the evolution of strikes per season from 1990-2022, where the overall trend of strikes increase is visible for all seasons, it is possible to notice here that the gap between the number of strikes for the Fall, Summer, and Spring and that of winter increases after 2004. When assessing the strike season by engine type in Figure 16, there is no significant change from the overall seasonal incidence described in Figure 14, asides from the observation that turbojet engine has a discrepant percentage of strikes occurring in winter (50%), although it is important to highlight that the total sample for turbojet trikes is very low (6 strikes total).

In Section 3.7. Strike Weather Conditions, Figure 17 shows that most strikes occur when there is no precipitation (92.64% of strikes). More specifically, a total of 62.6% under no cloud and no precipitation; followed by 21.14% occurring under some cloud and no precipitation; and 8,9% under overcast and no precipitation. The yearly evolution of strikes and their weather conditions show that the number of strikes have been increasing for these three major categories (Figure 18) . Especially for strikes under no cloud and no precipitation, the increase of incidents is very steep between 2000 and 2009. Figure 19 shows similar proportions of strikes under these 3 major weather categories independently of engine-types.

In Section 3.8 Strikes by Aircraft Characteristics, we can see that the most affected Aircraft Approach Category (AAC) is C (approach speed between 121-141 knots), with 67% of strikes, while other categories cover approximately 10% of the strikes (Figure 20). The yearly evolution of strikes based on AAC shows the increasing trend of incidents for category C, and category D (approach speed between 141-166 knots), especially after 2010 for the latter. All other

categories have a stable incidence since 1990. Strike distribution based on engine type shows that turbojet and turbofans have the highest percentage category C aircrafts, and 15% of strikes affecting turbofan engine type belong to category D aircrafts (Figure 22). When looking at the strikes distribution based on Airplane Design Group (ADG), category III (tail height between 30'- < 45' feet and wingspan between 79' - < 118') has 59% of strikes, followed by category II with 13,5% (tail height between 20'-< 30' and wingspan between 49' - < 79'), and categories IV and I with approximately 11% (tail height between 45' -< 60' and wingspan between 118' - <171'; and tail height <20' and wingspan <39' respectively) (Figure 23).Figure 24 shows the evolution of strikes based on ADG, illustrating the constant increasing trend for category III, and a more nuanced increasing trend for category I after 2008. Categories II and IV airplanes have an increasing trend from 1990 to 2015 and 2012 respectively, with a slight decreasing trend afterwards. Strike distribution based on engine type shows that turbofans have the highest percentage of category III aircrafts incidents (70%) and turboprop engine types have the highest percentage of category II incidents (72%).

In Section 3.9. Strikes by Taxonomy: Order, for the incidents with Order identification (11,581), birds are the most affected, including Passeriformes with the highest incidence (28.49%), followed by Charadriiformes (16.56%), Columbiformes and Accipitriformes (around 11%), and Anseriformes (7.82%) ranking 5th most incidents. Passeriformes are mostly small land birds like sparrows and swallows that do not surpass 20cm (8in) or 30g (1 oz), however Charadriiformes includes larger birds like Gulls that can reach over 130cm (54in) and surpass 1kg (2.3lbs). Accipitriformes also includes larger bird species such as Turkey Vultures, although the highest incidence is with Red-tailed Hawks, a much smaller species (for more description on Order see Table 3 and a count of incidents by species in Appendix B). Figure 27 shows these prevalent Orders evolution since 1990, where it is possible to see a big jump of impacted Passeriformes starting in 2009, as well as for Charadriiformes Order (although much less prominent). Accipitriformes have spikes where their incidence surpasses Charadriiformes specifically in 2013, 2018, 2020, and 2021. When assessing Order by engine-type, we can see a very diverse pattern. Turbofan and Turboprop engine-type reproduce the Order ranks the closest, with a majority of Passeriformes, followed by Charadriiformes, and Anseriformes. However Reciprocating engine types have a much higher proportion of incidents involving Columbiformes followed by Accipitriformes, and Turbojet engines are exclusively impacted by Accipitriformes Order (Figure 28). It is important to highlight that most wildlife strikes incidents (85.83%) are attributed to one single strike, 12,99% are attributed to 2 - 10 strikes, 0.83% are attributed to 11-100 strikes, and 0.05% are attributed to more than 100 strikes in one incident.

In Section 3.10. GIS-relevant Results uses the 19,873 wildlife data subset with Latlon attributes to assess spatial patterns of wildlife strikes.

Subsection 3.10.1. Strikes Location Shows how the vast majority of strikes between 1990 and April 2023 have occurred inside the airport boundaries (99%), with only 83 strikes occurring outside airport boundaries, out of which 53 were within the 1-5 mile buffers (Figure 29). From the strikes occurring within the airport's vicinity; 19 were counted in the 1st mile buffer, 0 between the 1st-2nd mile buffer, 4 between the 2nd and the 3rd mile buffer, 0 between the 3rd and the 4th mile buffer, and 30 between the 4th

and the 5th mile buffer. Figure 30 identifies hotspots of wildlife strikes taking into consideration the full spatial dataset and points to a statistically significant spatial concentration of strikes in southern California, in the greater Los Angeles area, and another concentration in the San Francisco Bay Area that expands further inland beyond Sacramento. The hotspot analysis with the California boundary (Figure 30) reflects a statistically significant density analysis, but it can be biased by the concentration of airports in those two regions of the state. For this reason we also developed a hotspot analysis of wildlife strikes occurring exclusively outside airport boundaries in Figure 31. This map points to statistically significant concentrations of wildlife strikes in the greater Los Angeles area, where a zoom is provided with the codes of airports belonging to this cluster.

Subsection 3.2.2. Strike Probability by Airport provides a map (Figure 32) and Table 4, identifies the wildlife strike probability for each California airport assessed in this study. Sacramento International Airport (SMF), San Bernardino International Airport (SBD), and Ontario International are the top three airports with the highest probability of wildlife strikes in the state. Table 5 identifies the proposition of each strike in the safety zones, with 56.76% occurring inside the Primary Surface, 39.18% in Zone 6, 4.03% in Zone 5, and 0.02 in Zone 2. From the strikes occurring in these safety zones, only 24 occurred outside airport boundaries.

Subsection 3.2.3. Strike Runway Distance Analysis, Figure 33 shows that 86.2% of incidents occur on the runway centerline (total of 11,738 incidents) with rapidly diminishing frequency as you move away from the runway centerline (Figure 34). Figure 34 presents the yearly evolution of strikes by distance category, illustrating the increasing trend of incidents occurring on the runway and a general increase of other distance categories after 2005, especially those occurring at 1 nautical mile from the runway centerline and those beyond 5 nautical miles of the runway centerline.

Figure 36 presents the yearly evolution of the average distance of wildlife strikes between 1990-2022. It highlights a steep increase in these average distances from 2005 to 2010 that merits further investigation. Before 2005,the yearly averages of strike remained around 1000-3000 feet away from the runways; increasing to approximately 6000 ft distance from the runways between 2007-2009; and spiking at approximately 9,500 feet in 2010, and maintaining an approximate average distance of 7,000 feet after 2010. When assessing patterns based on distance from runway and engine-types, we can observe that turbofan engine aircrafts have a higher proportion of strikes beyond the 5 Nautical Miles of runways and that turboshafts have a higher percentage of strikes in the Safety Zones compared to other engine-types (Figure 37). Figure 38 identifies the average distance from runway centerline of wildlife strikes per engine type:

(a) 11,000 ft for turboshaft (standard error of 950-12,200 ft)
(b) 9,000 ft for turbofan (standard error of 6,000-12,000 ft)
(c) 3,000 ft for turboprop (standard error of 1800-4900 ft)
(d) 2500 ft for reciprocating (standard error of 1800-3800 ft)
(e) 800 ft fir turbojet (standard error 750-950 ft)

In Section 3.11.Multivariable Analysis, it is possible to trace a window of highest strike incidents between 1- 2,000 ft of height and 0-50,000ft of distance from the runway; there is no clear indication that this window has shifted through the years (Figure 39). In Figure 40 two clusters of strikes are observable below 2,000 ft; one at a lower height (approximately between 0-800ft) for aircrafts between 50 and 100 kts in speed, and another cluster between 1 -1800ft in height and 125-160 kt in speed. Again there is no visible sign that these clusters have changed through time. In Figure 41, variables of strike height, distance, and engine type are assessed, similar windows of height and distance as Figure 39 are observed but there are no clear patterns based on the engine type. In Figure 42 we can observe that the first clusters of strikes identified in Figure 40 closely represent reciprocating engine type accidents (lower height and speed) and the second cluster represents turbofan and turboprop incidents (higher heights and speed). The following two figures cross strike height and distance with wildlife Order, as well as strike height and aircraft speed with wildlife Order (Figure 43 and 44 respectively). Both of these figures highlight that Passeriforms (rank 1) and Anseriformes (rank 5) are also predominant in strikes occurring at greater distances from the runway, greater heights, and speed, which is specially concerning for the latter order that encompasses larger birds like Gulls. Other less frequent orders impacting aircrafts in these conditions include Columbiformes (rank 3) and Accipitriformes (rank 4).

3.1. Overview

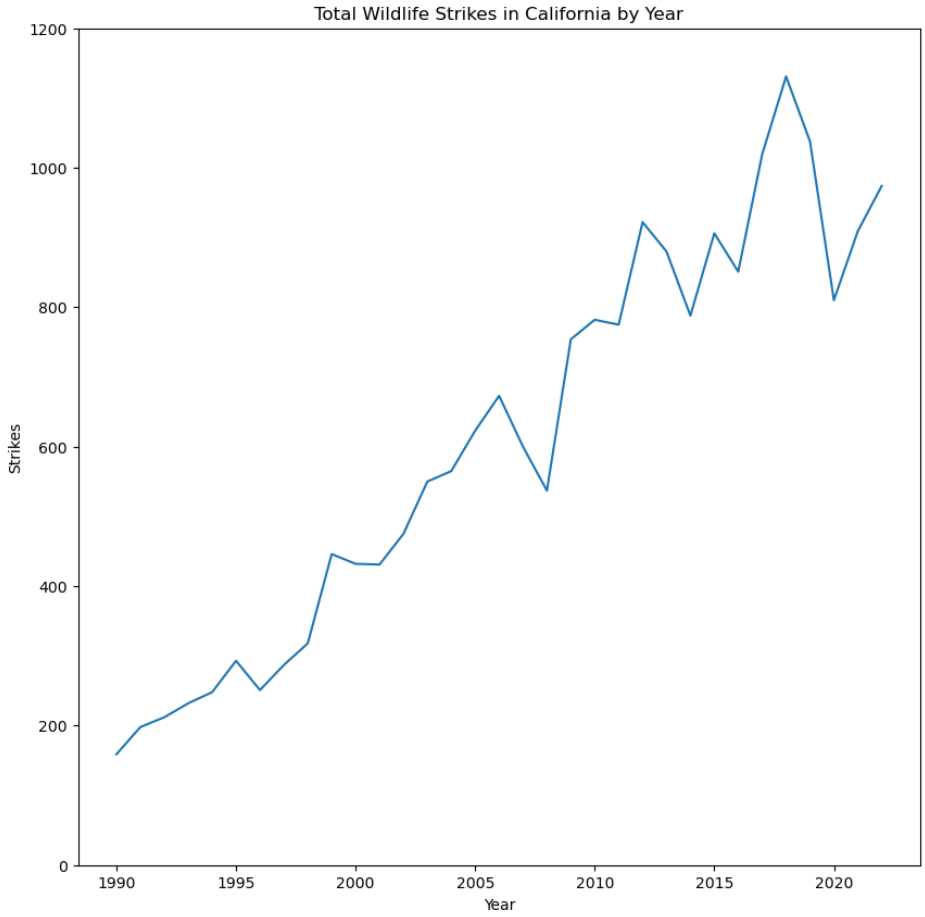


Figure 1. Total Strikes by Year (n = 20,254)

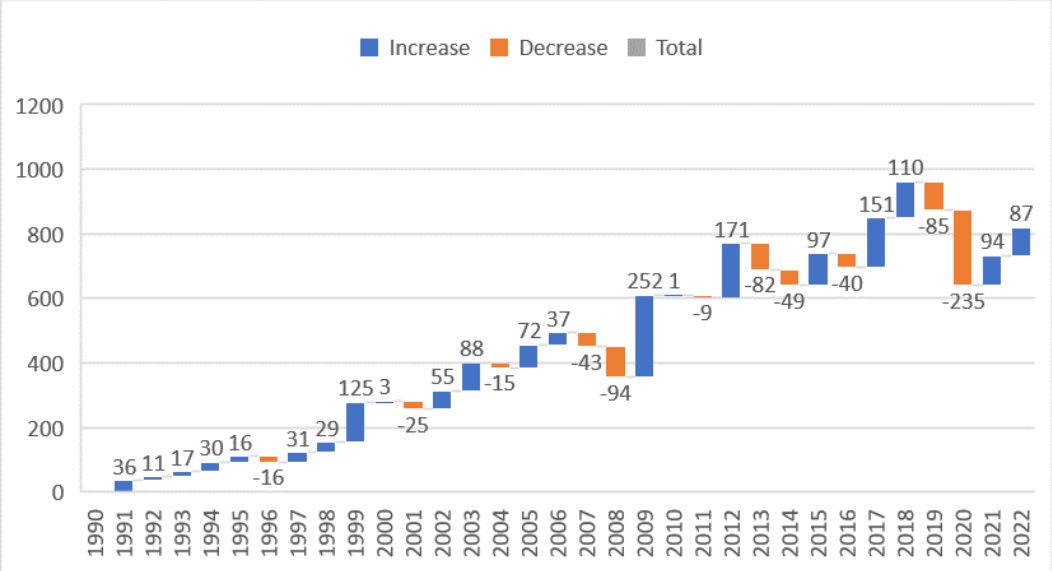


Figure 2. Yearly strike evolution (n = 20,254)

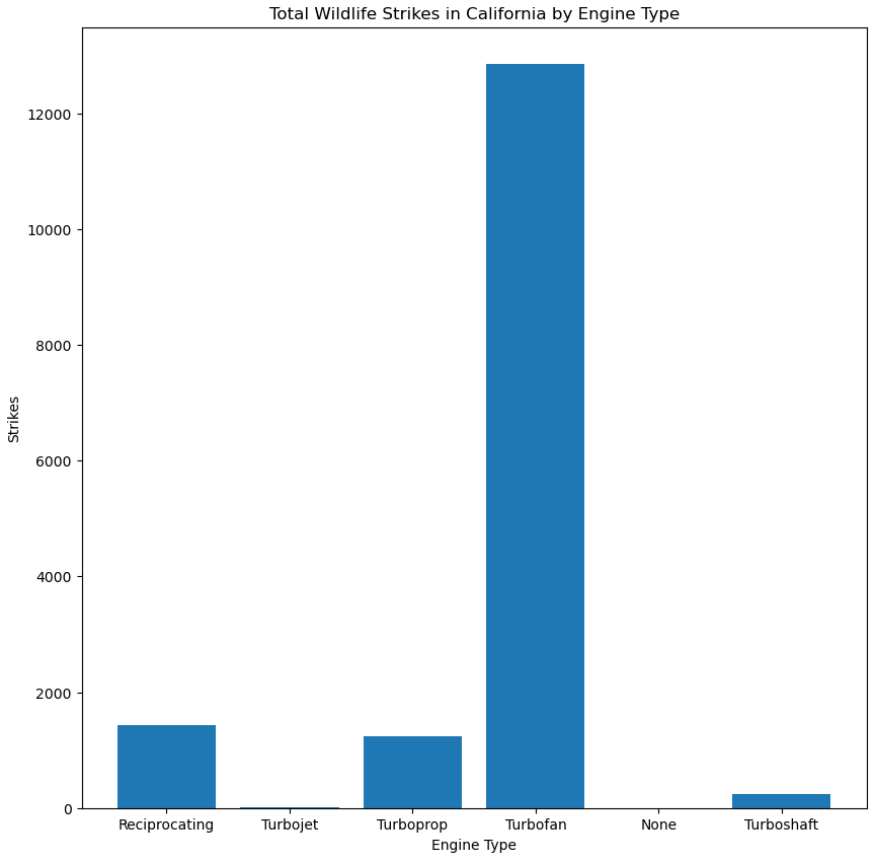


Figure 3. Total Strikes by Engine Type (n = 15,764)

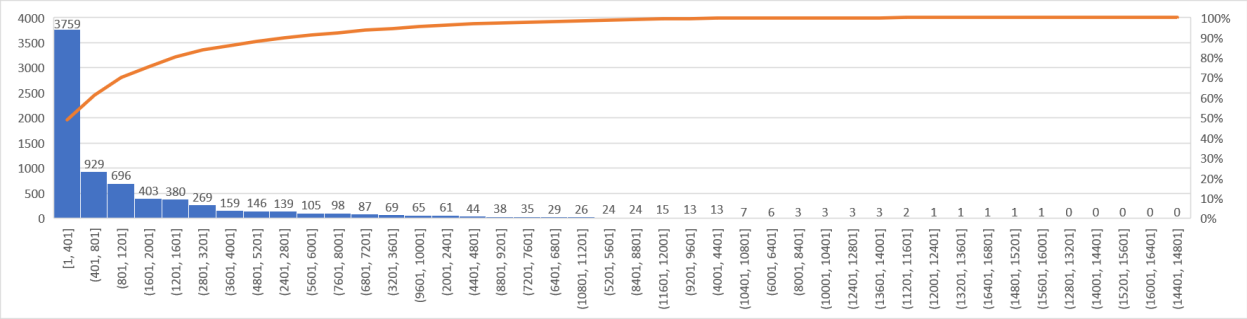


Figure 4. Strike Heights above ground (n = 12,995, for ground-level= 5,337 strikes)

3.2. Strikes by Engine Type

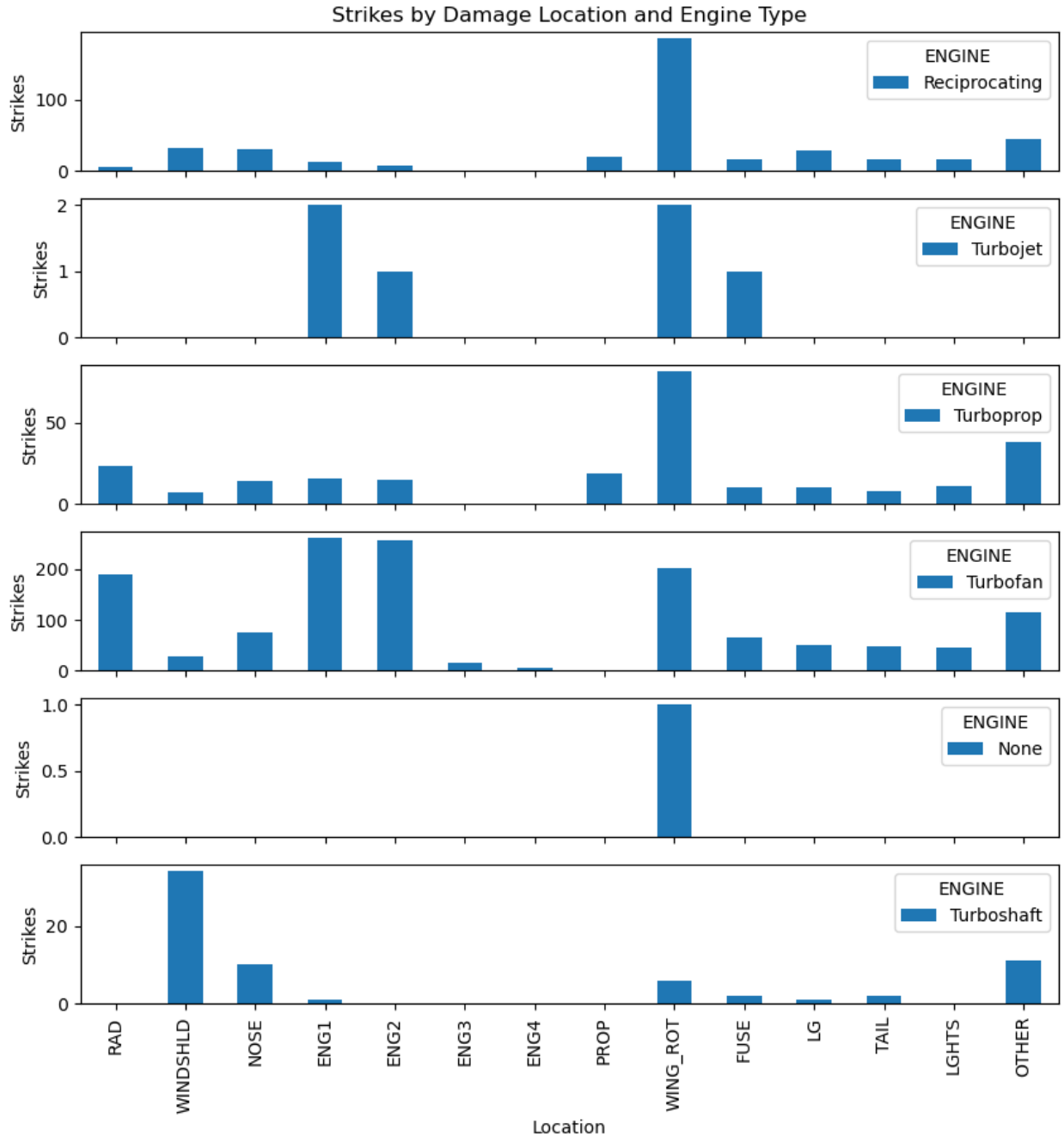


Figure 5. Damage location by engine type aircraft (n = 20,930)

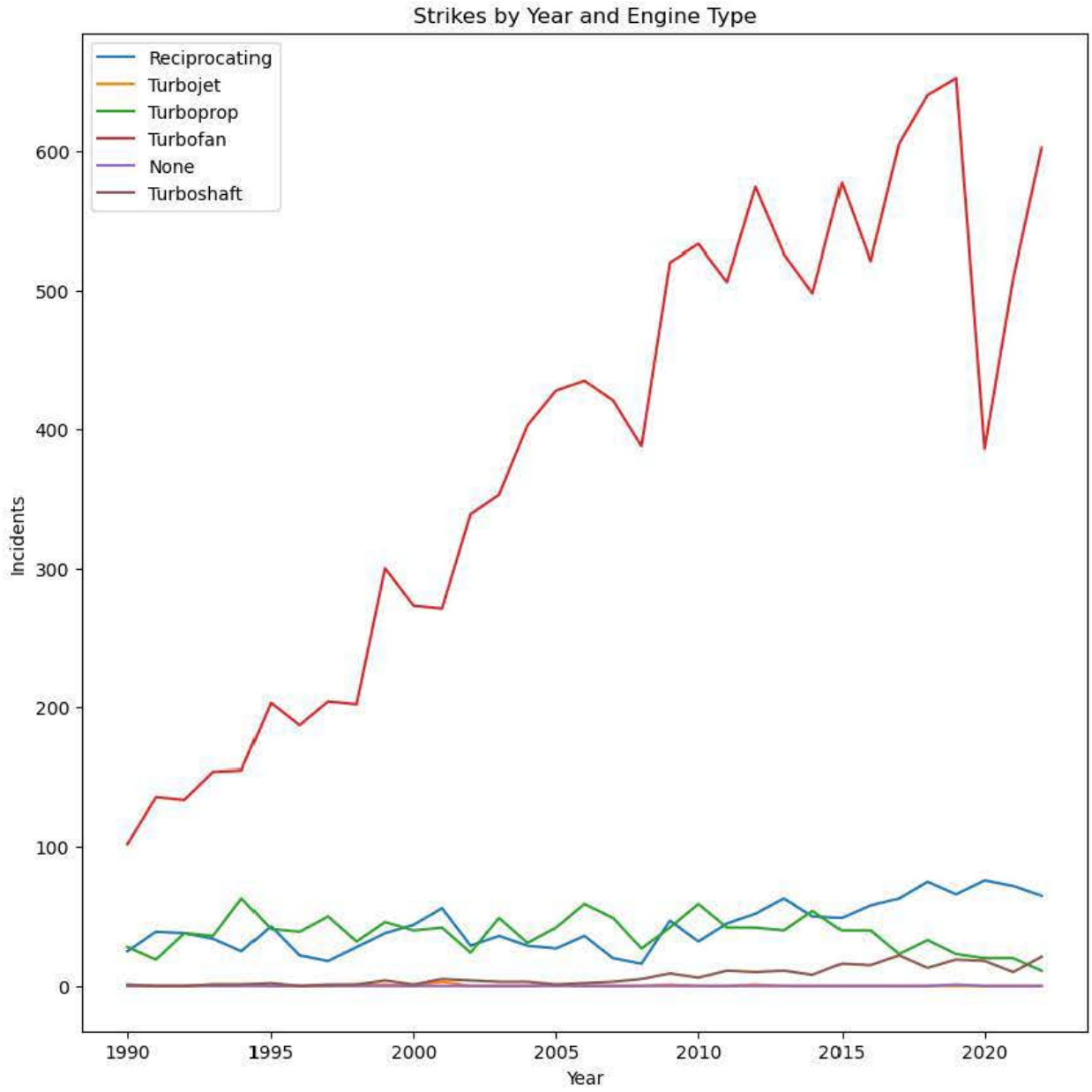


Figure 6. Yearly evolution of strikes by engine type (n = 15,634)

3.3. Strike Height Analysis

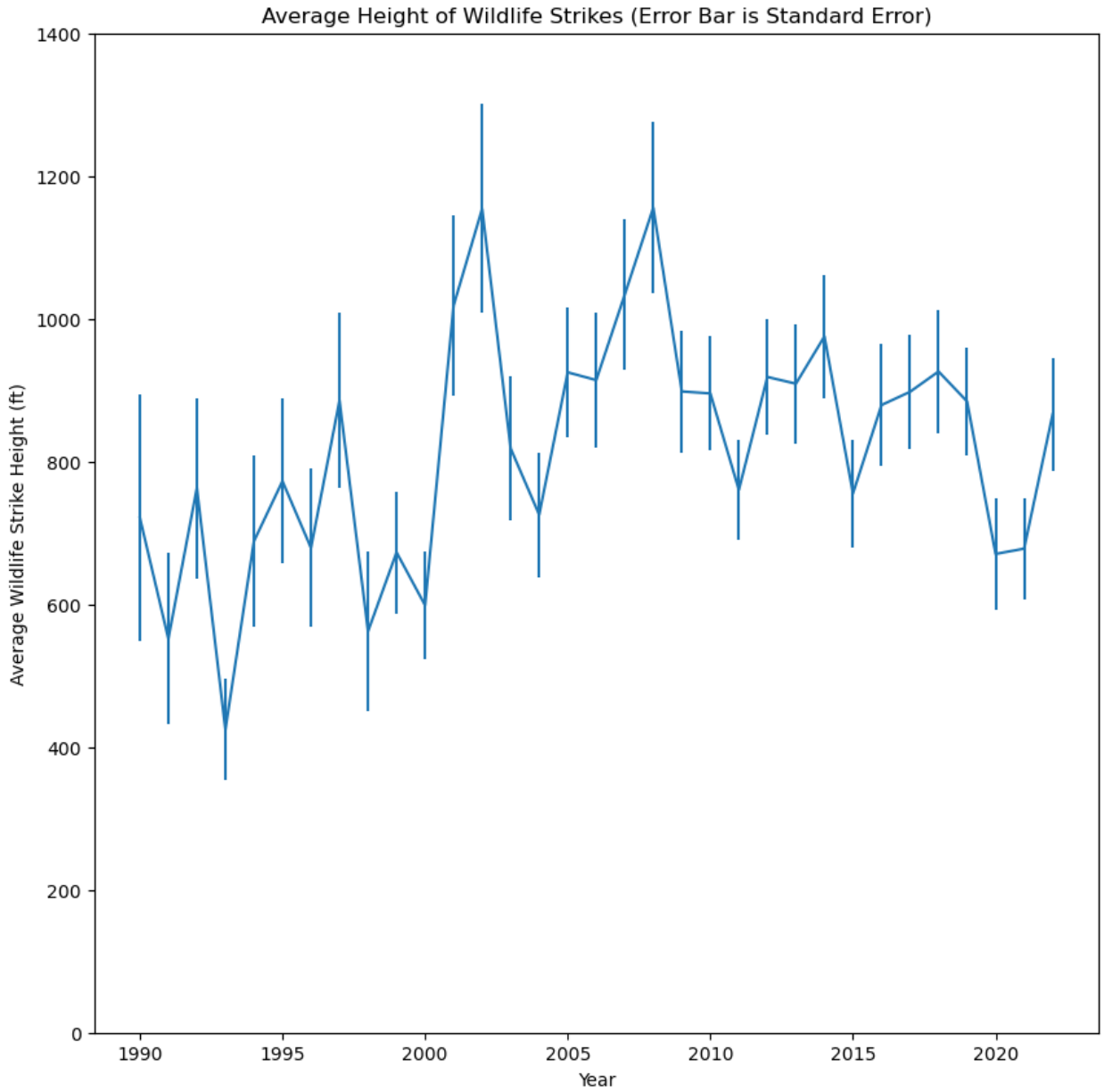


Figure 7. Average Height of Wildlife Strikes by Year, (n = 12,881)

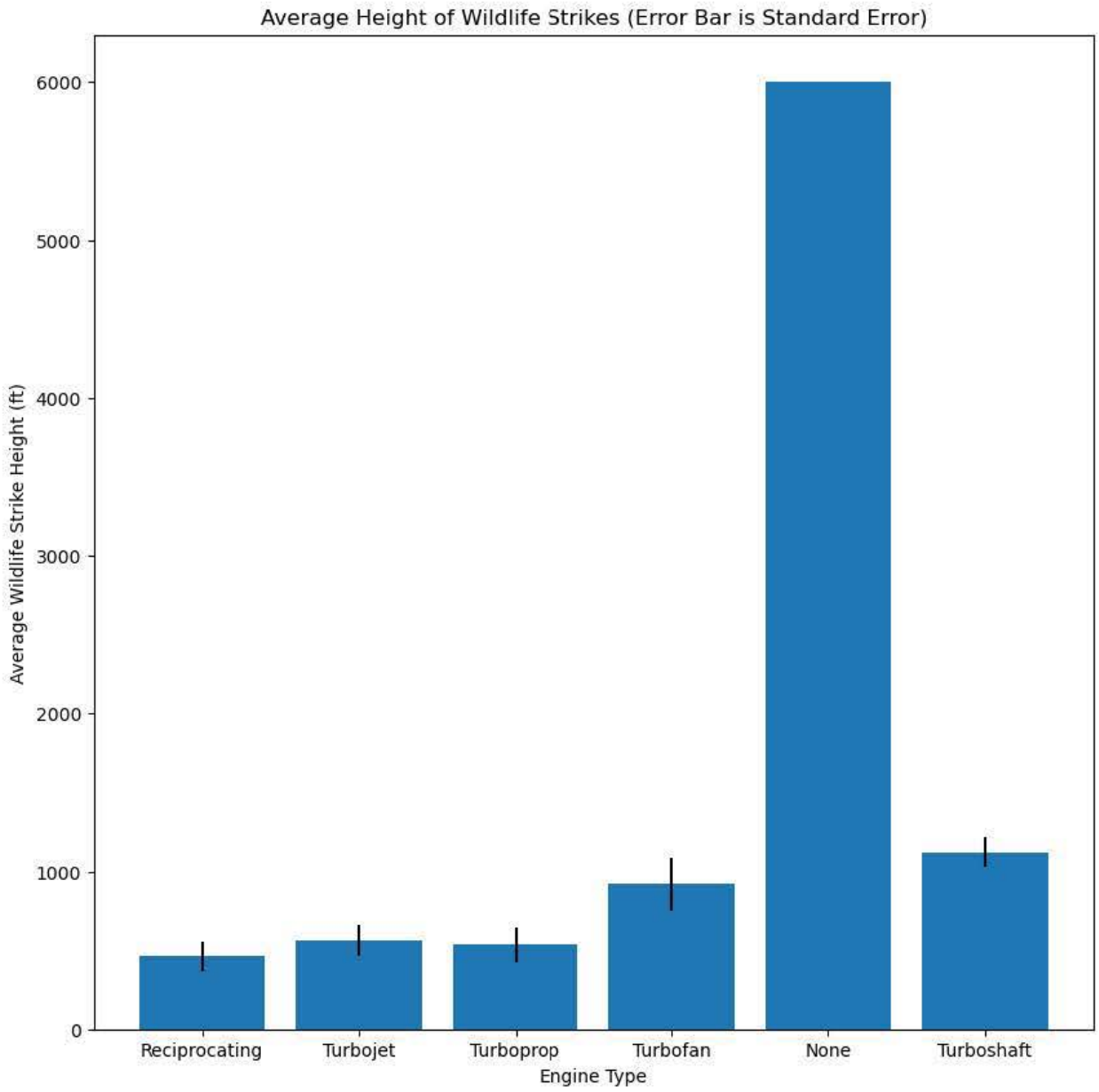


Figure 8. Average Height of Wildlife Strikes by Engine Type (n =12,832. Note only 1 strike from aircraft with no engine)

3.4. Strike and Phase of Flight Analysis

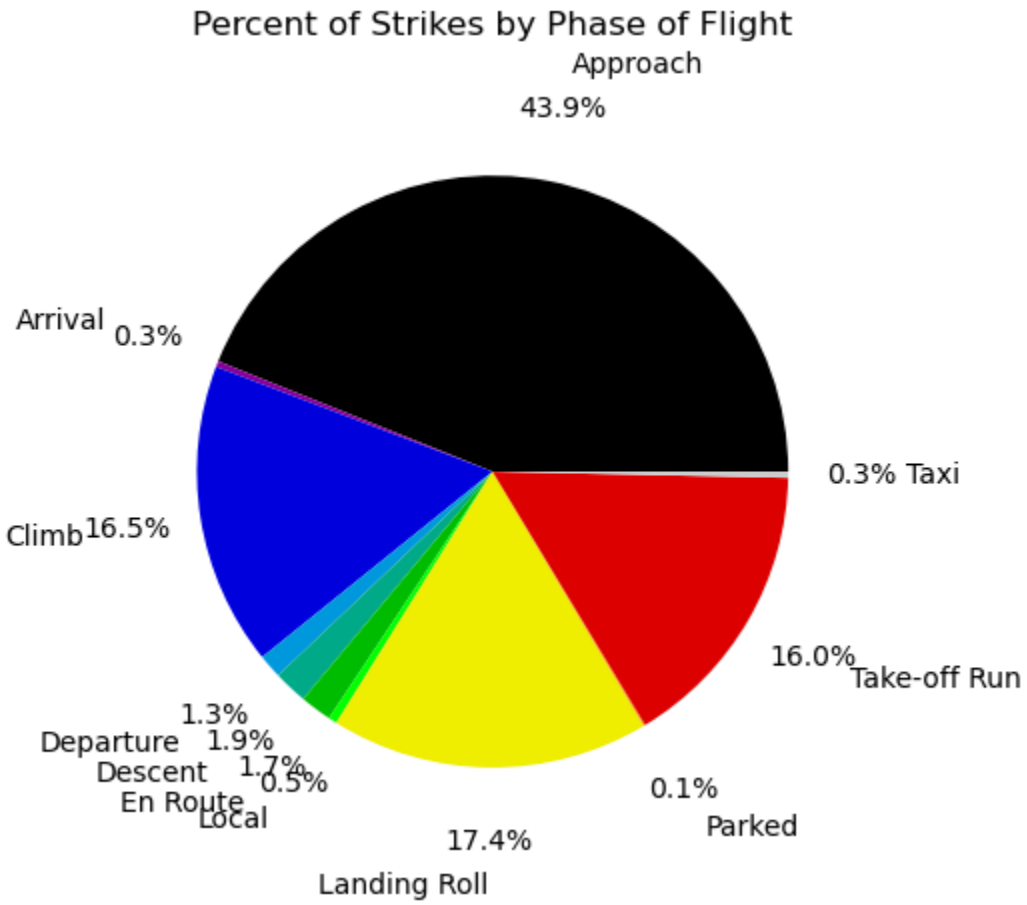


Figure 9. Percent of strikes by Phase of FLight (n = 15,720)

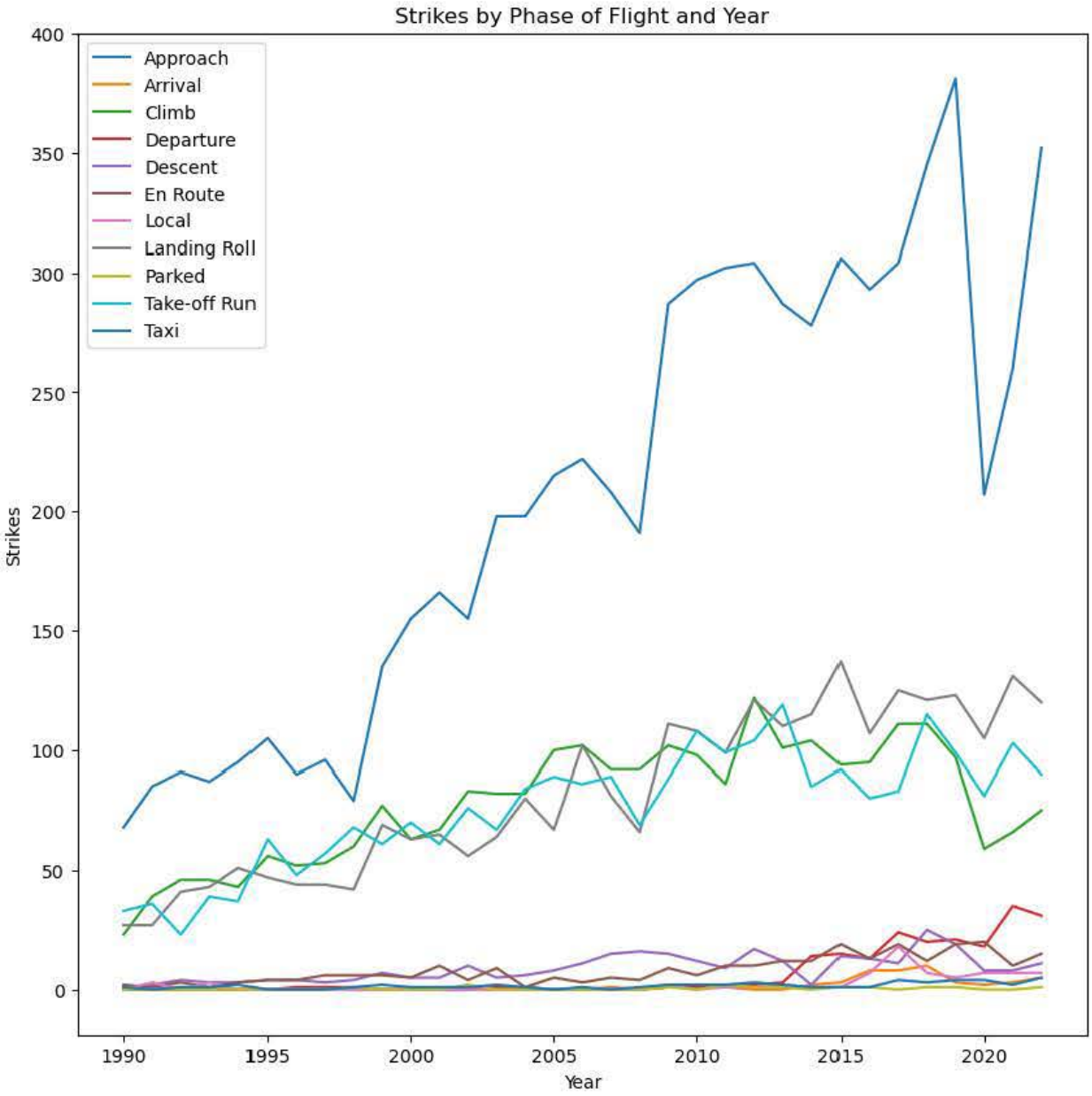


Figure 10. Strikes yearly evolution by phase of flight (n = 15,587)

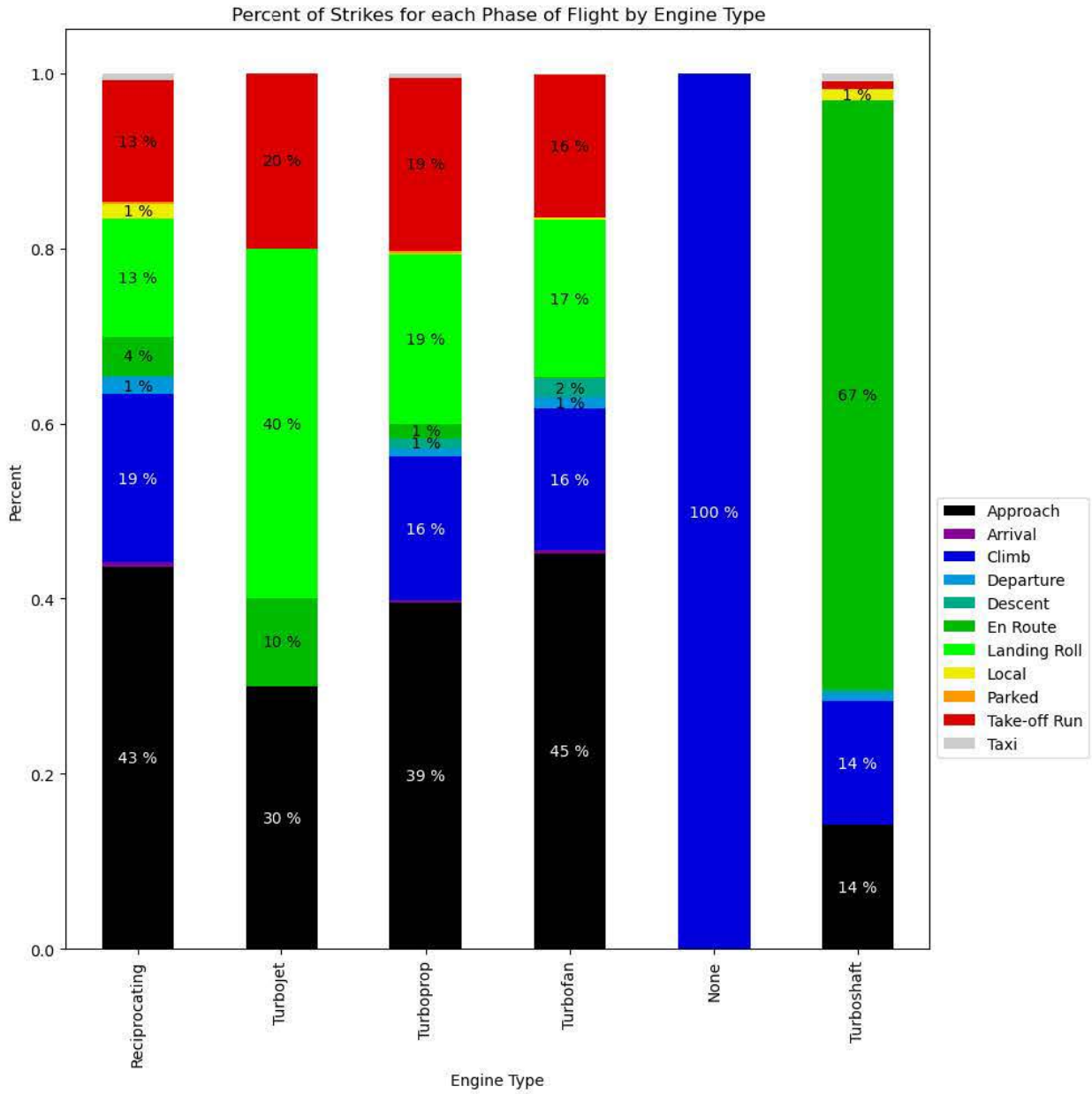


Figure 11. Percentage of strikes by phase of flight and engine type (n= 15504)

3.5. Strike and Impact Analysis

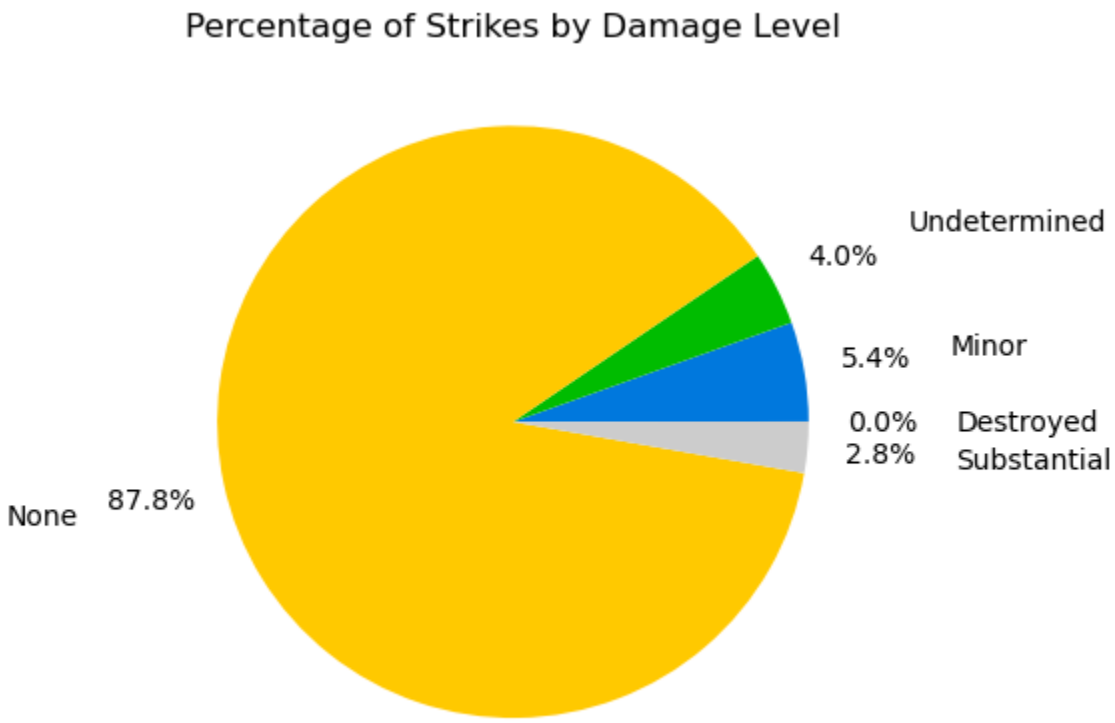


Figure 11. Damage level of strikes (n = 14,491)

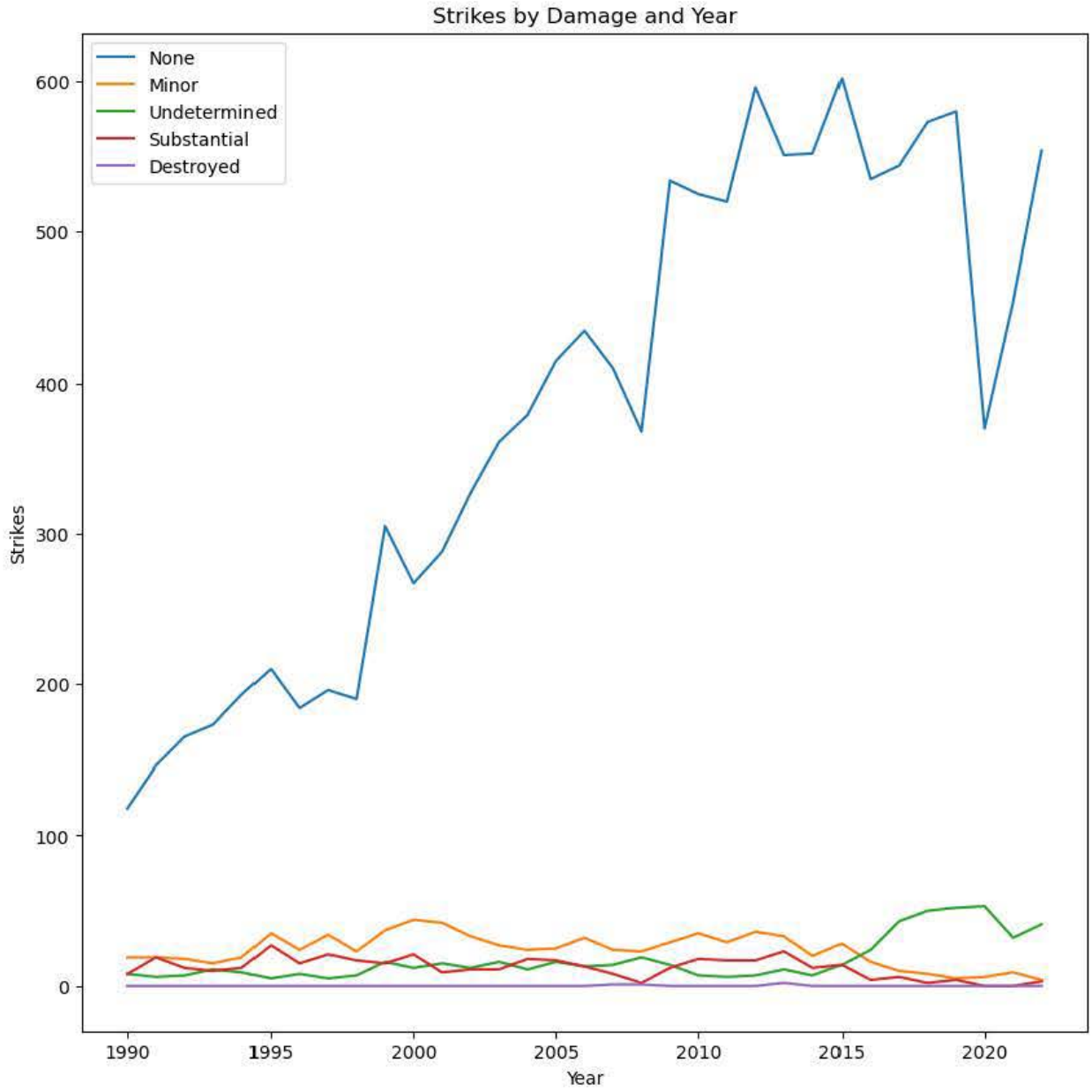


Figure 12. Yearly evolution of strike damage to aircrafts (n = 14,378)

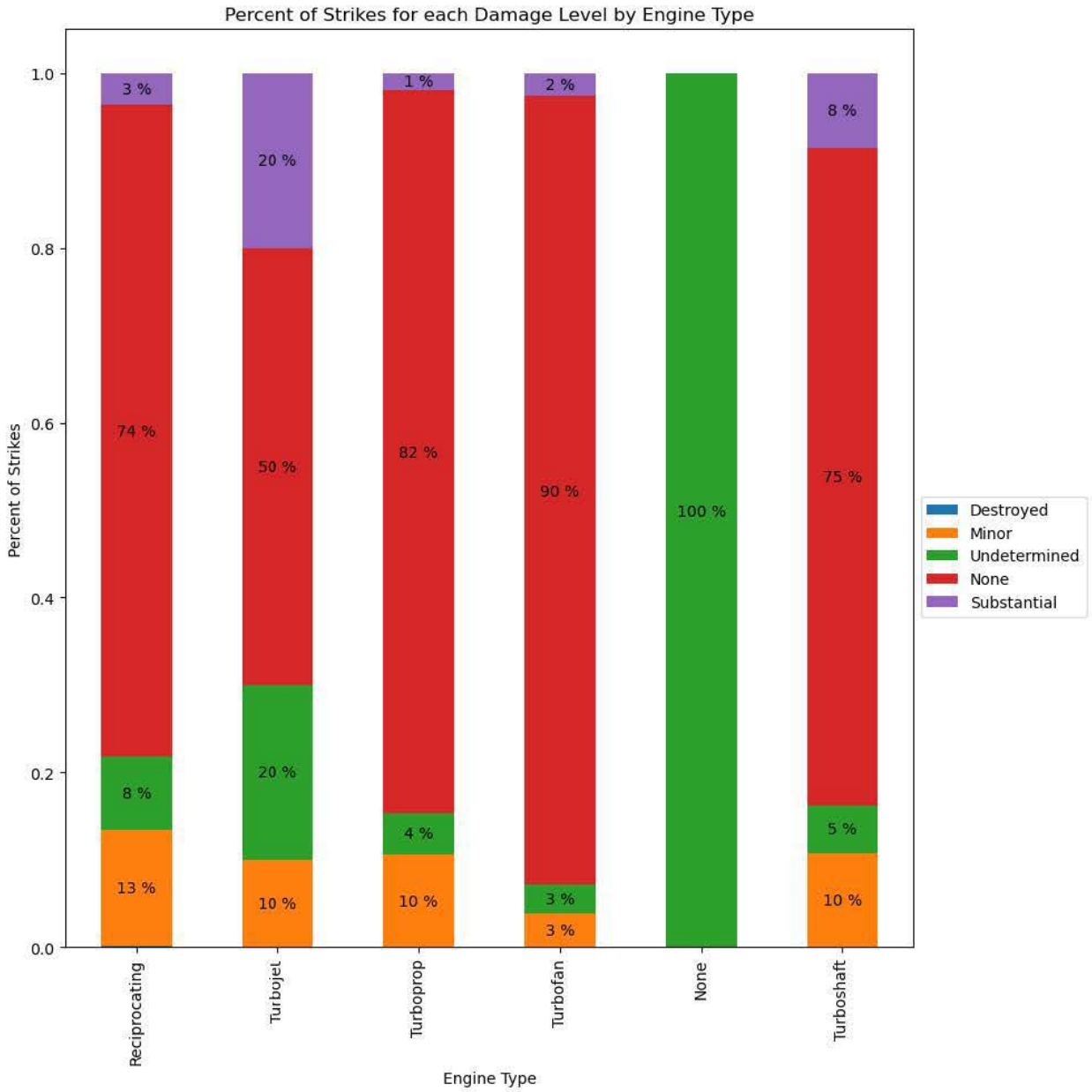


Figure 13. Damage level by engine type (n = 14,338)

3.6. Strike Seasonality Analysis

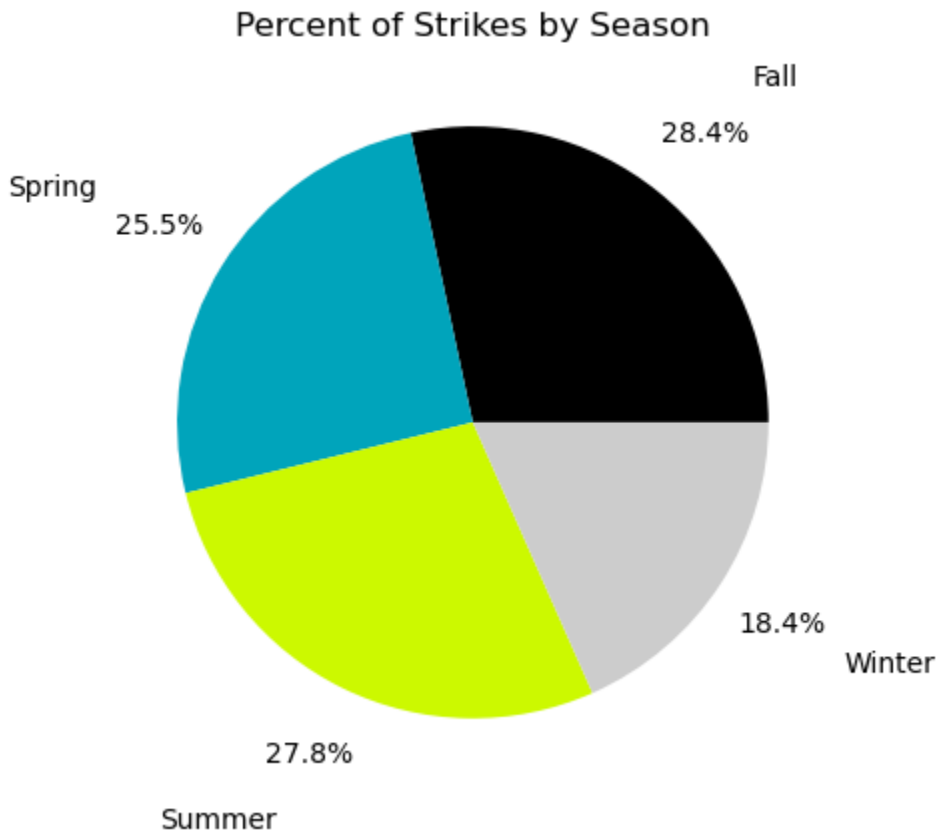


Figure 14. Strikes by season (n = 20,069, does not include 2023)

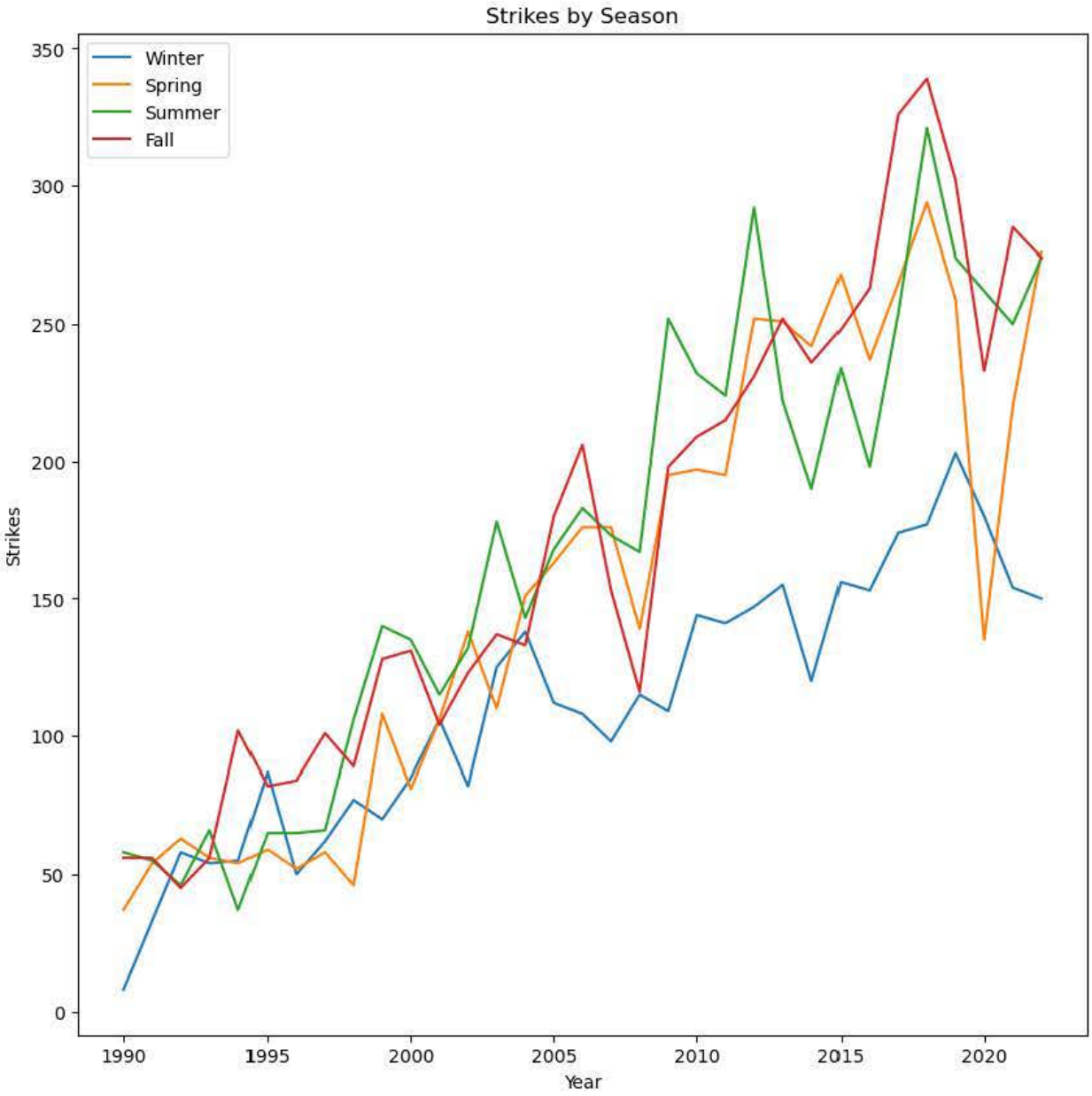


Figure 15. Yearly evolution of strikes by season (n = 20,069)

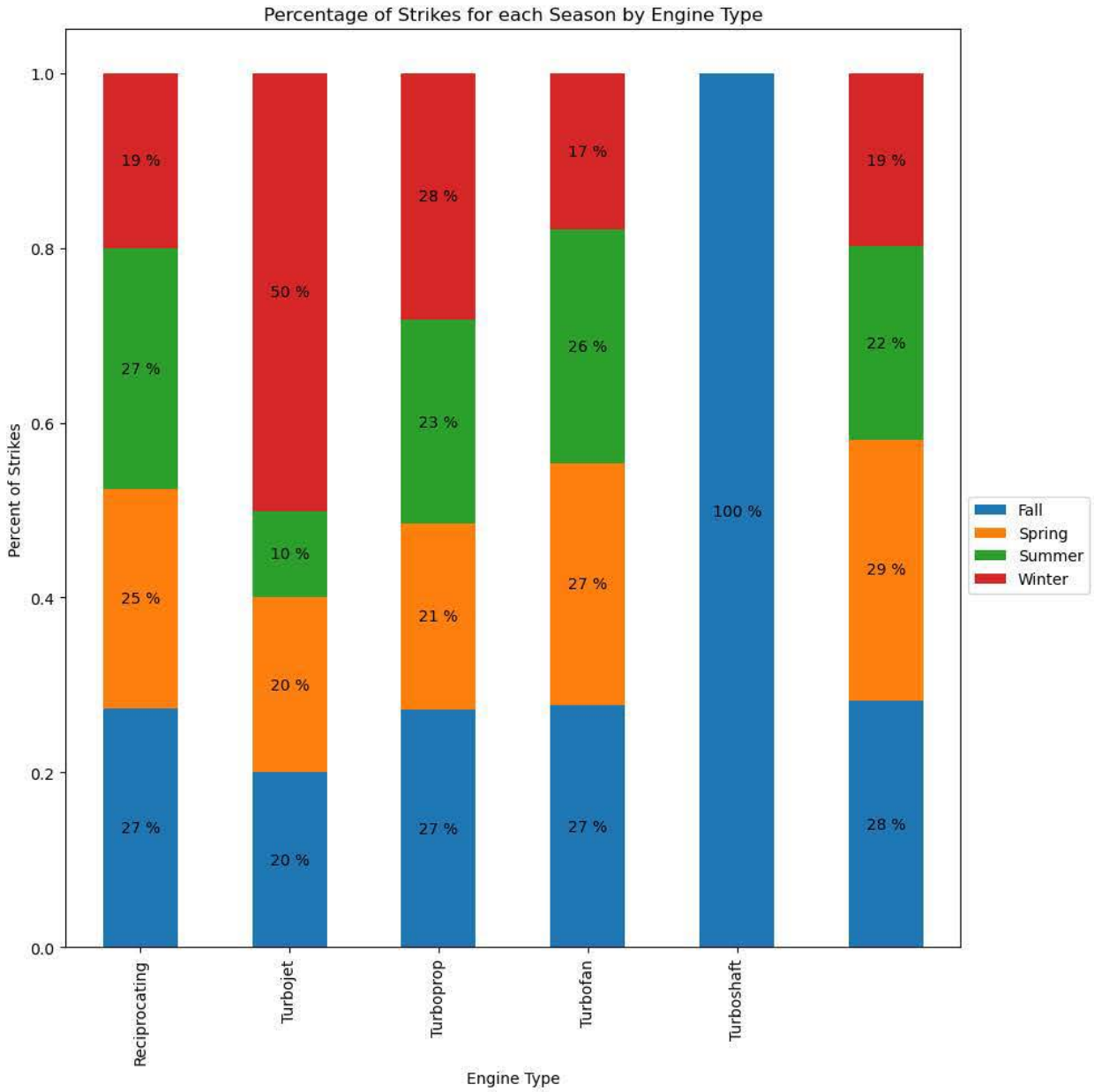


Figure 16. Strikes by season and engine type (n = 15,634)

3.7. Strike and Weather Conditions

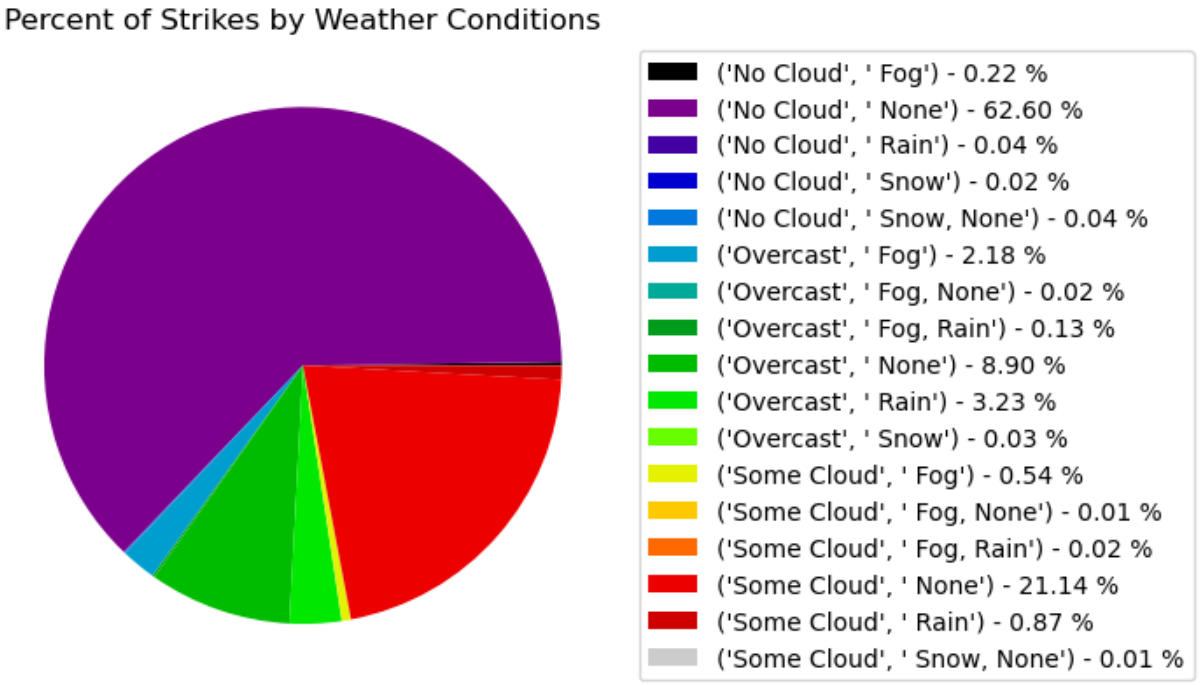


Figure 17. Weather conditions of strikes (n= 11,442)

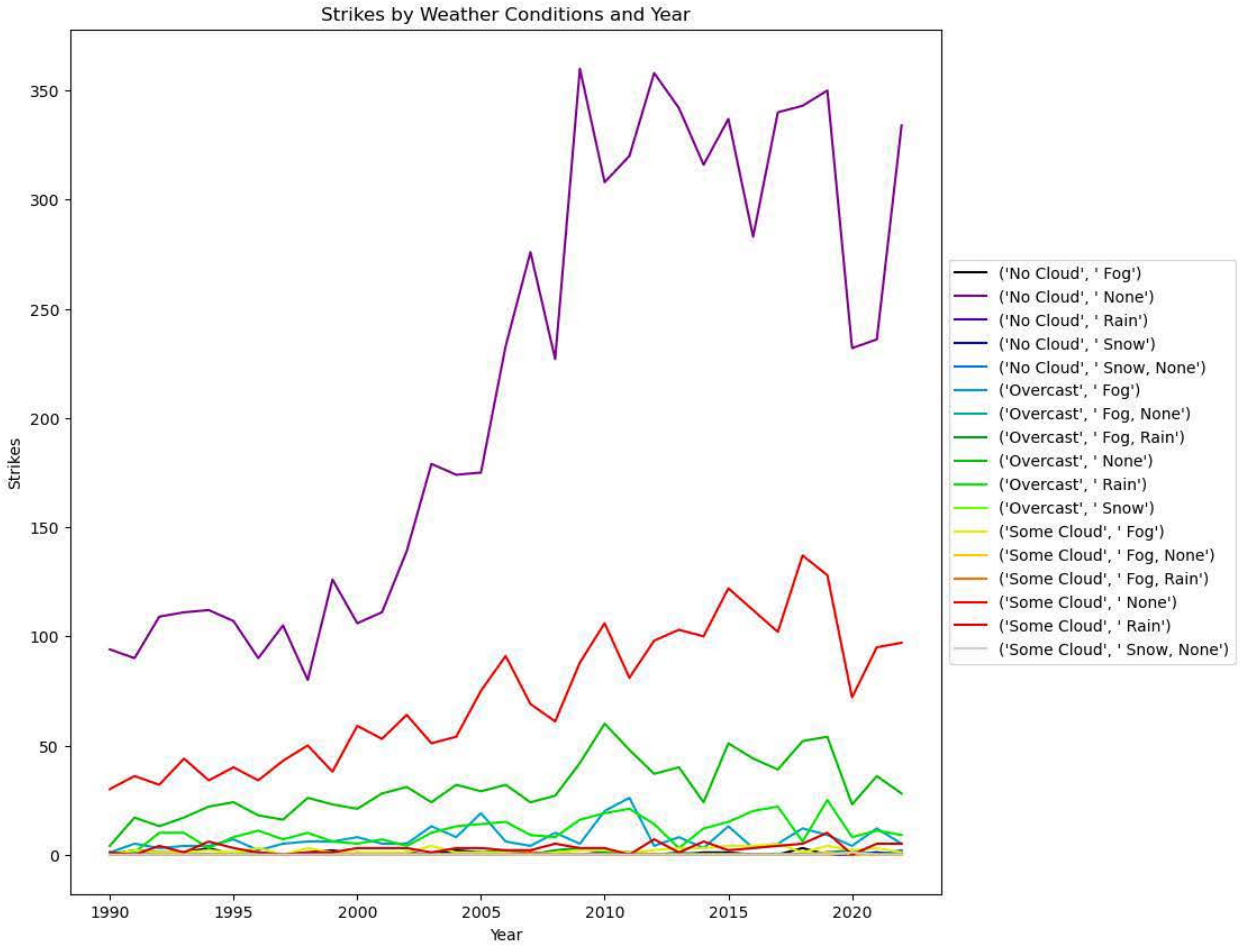


Figure 18. Yearly evolution of strikes based on weather conditions (n = 11,328)

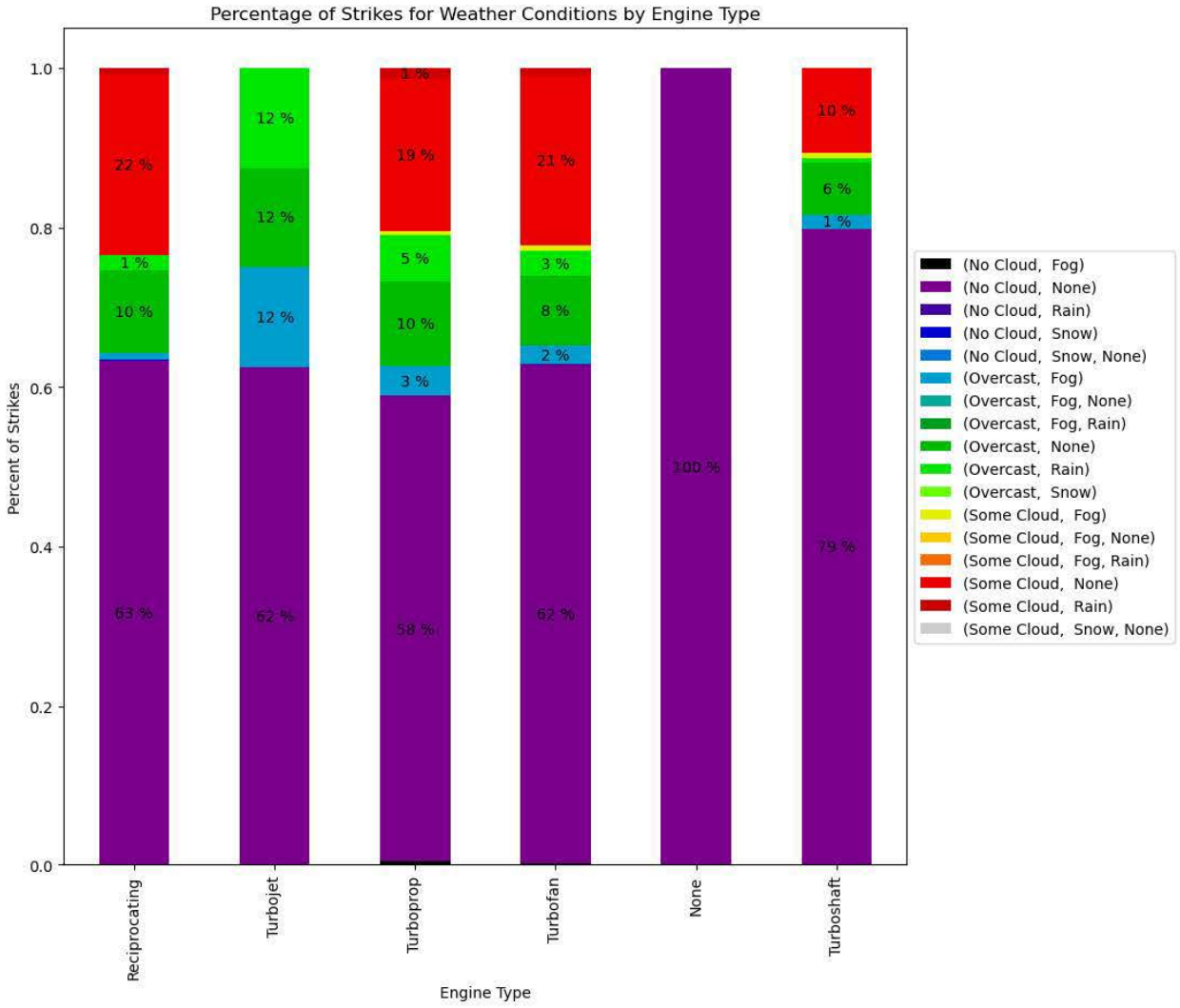


Figure 19. Strikes and weather conditions by engine-type (n = 11,285)

3.8. Strikes by Aircraft Characteristics: Aircraft Approach Category (AAC) and Aircraft Design Group (ADG)

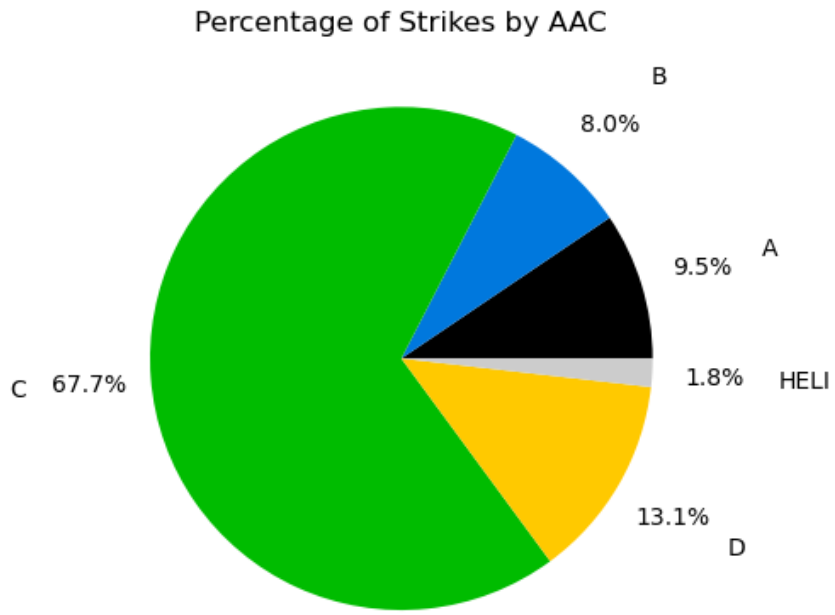


Figure 20. Strikes based on the Aircraft Approach category (AAC) . See Table 1 for the FAA's AAC classification (n = 15,660).

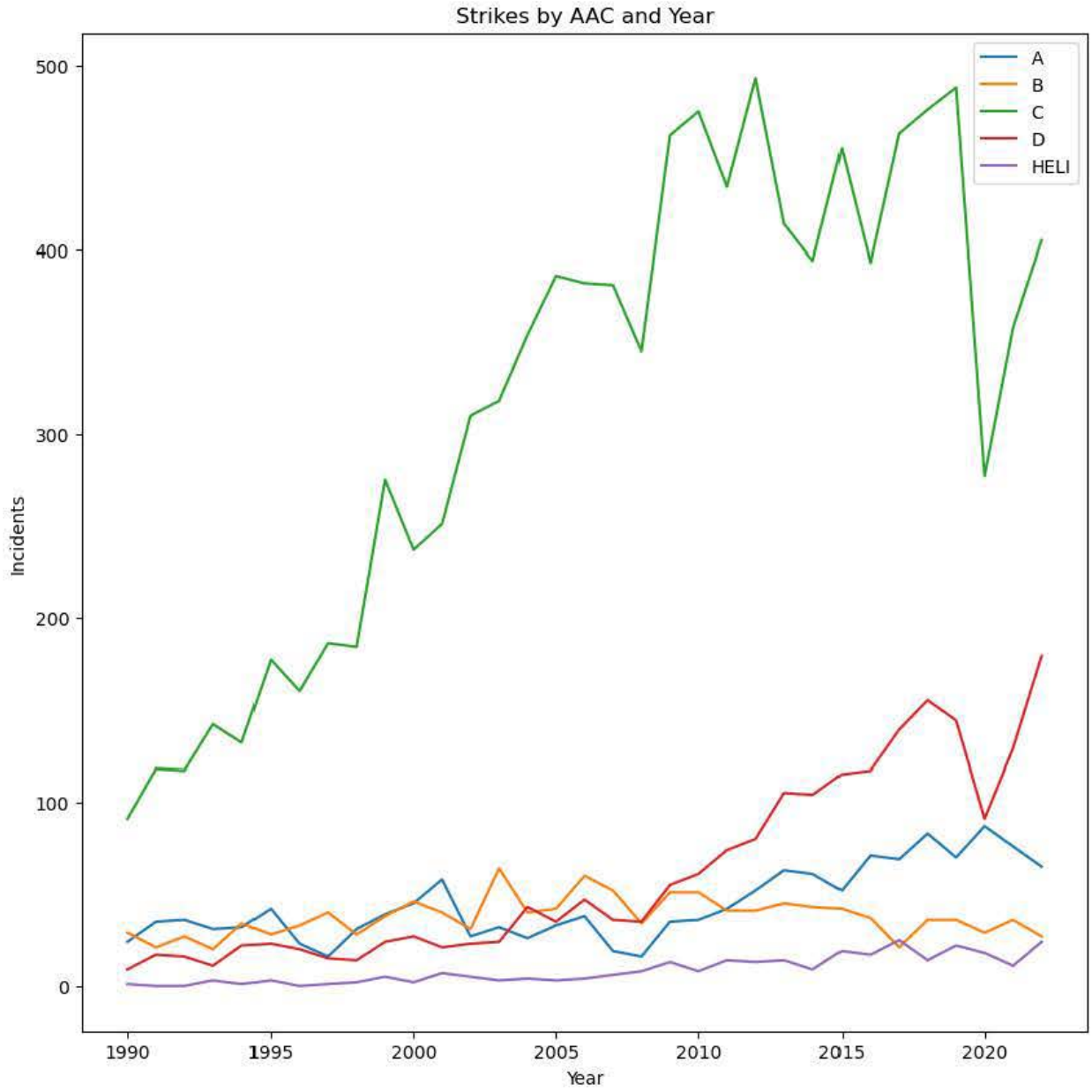


Figure 21. Yearly evolution of strikes based on Aircraft Approach Category (AAC) See Table 1 for the FAA's AAC classification. (n = 15,530)

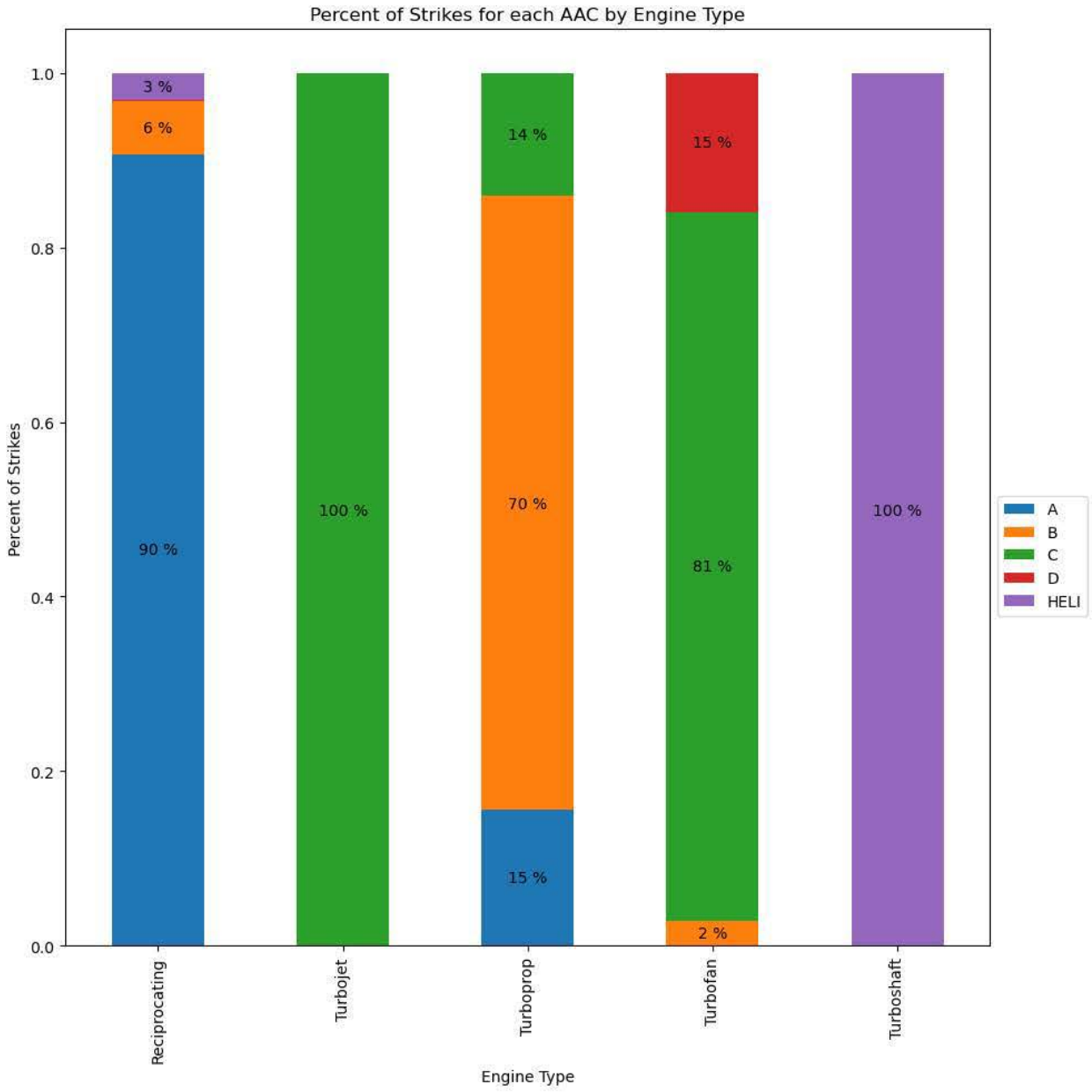


Figure 22. Strikes based on Aircraft Approach Category (AAC) and engine type. See Table 1 for the FAA's AAC classification (n = 15,628)

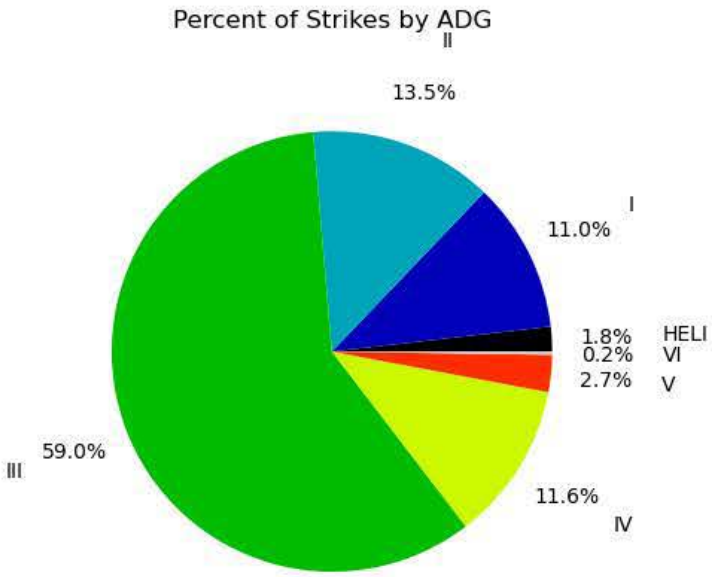


Figure 23. Strikes based on Airplane Design Group (ADG). See Table 2 for the FAA's ADG classification (n = 15,660).

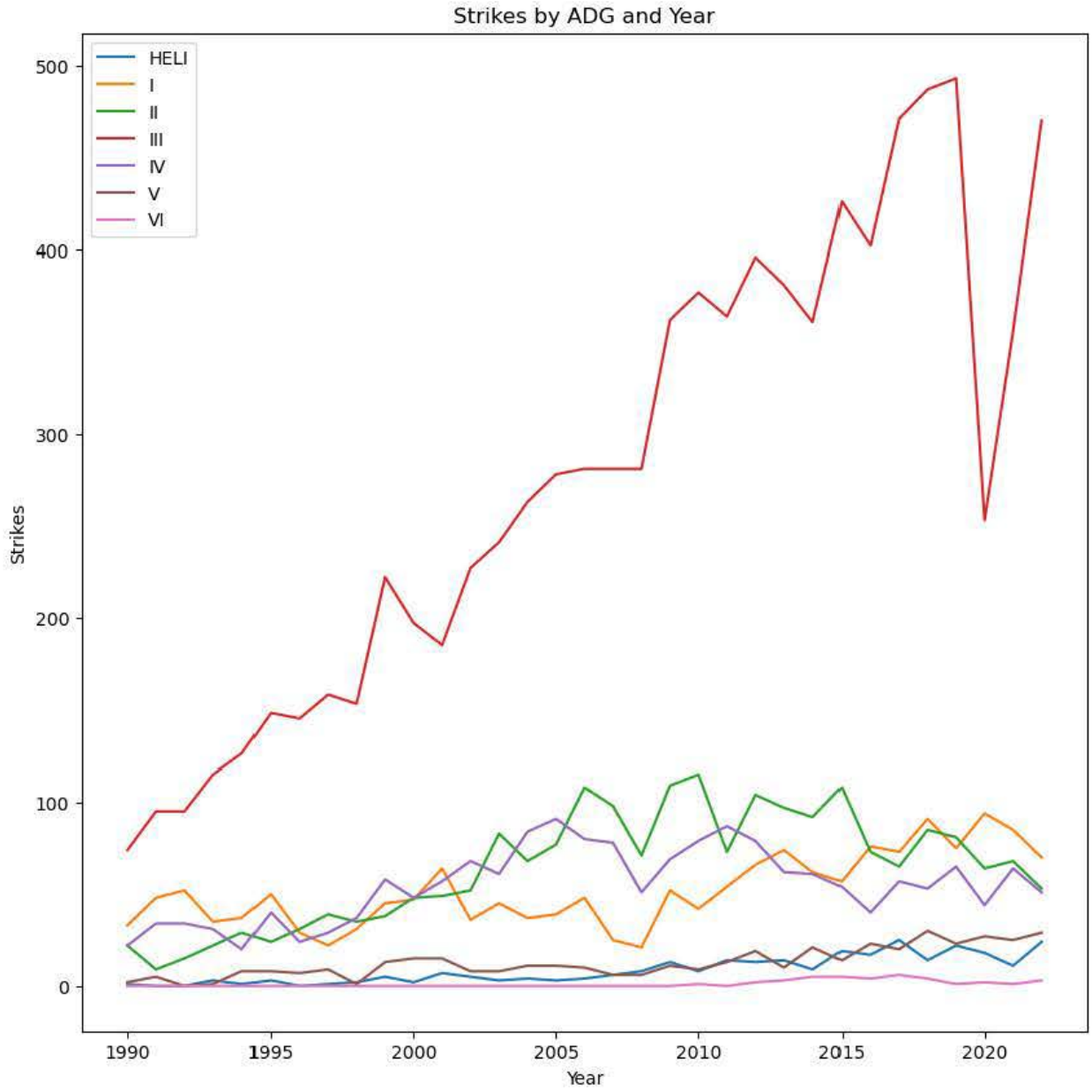


Figure 24. Yearly evolution of strikes based on Airplane Design Group (ADG). See Table 2 for the FAA's ADG classification. (n = 15,530)

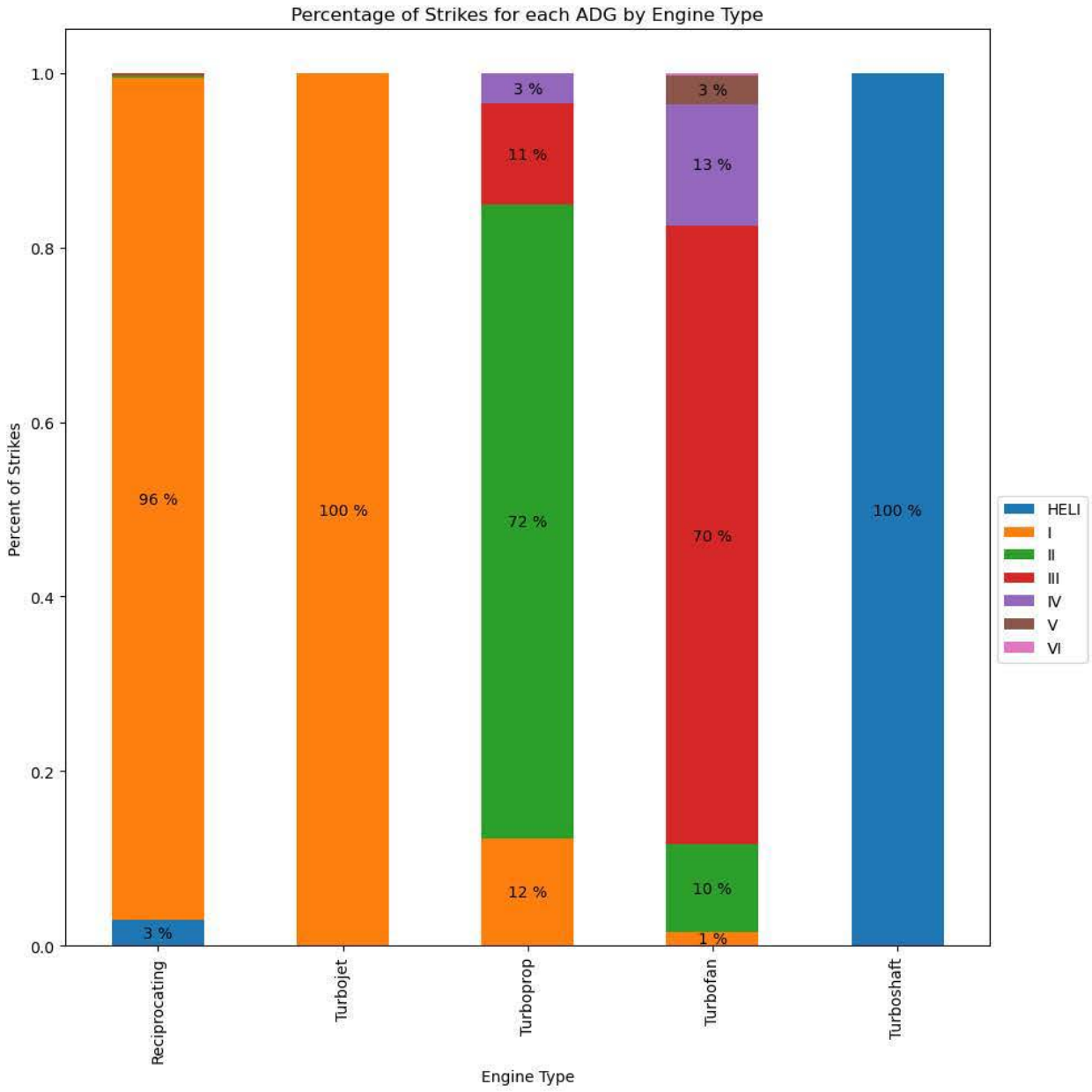


Figure 25. Strikes by Airplane Design group (ADG) and engine type. See Table 2 for the FAA's ADG classification (n = 15,628).

3.9. Strikes by Wildlife Taxonomy: Order

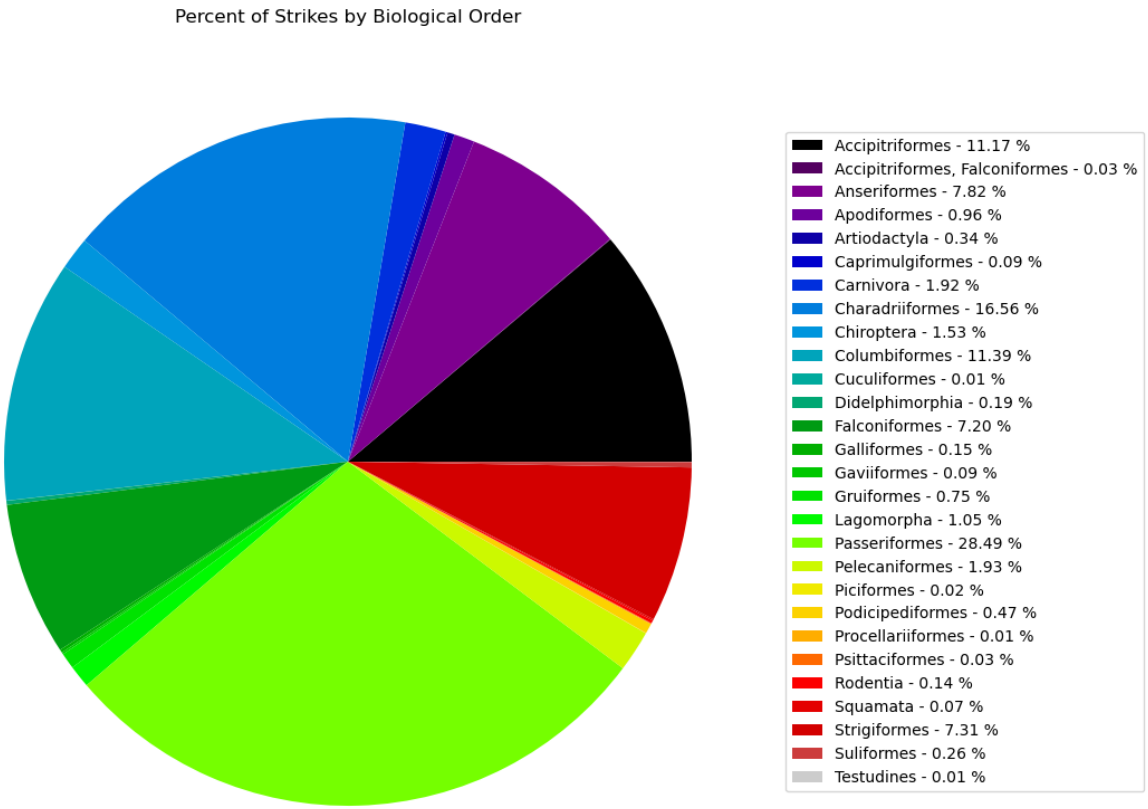


Figure 26. Strikes percentage based on wildlife Order (n = 11,581)

Table 3. Description of wildlife with highest strike incidence based on Order

Order Rank	% of strikes	Examples with highest incidence*	Length Range*	Weight Range*
1. Passeriformes	28.49%	Western Meadowlark, Cliff Swallow, Sparrow, Horned Lark, Barn Swallow	12.5- 20 cm (5 - 8in)	15- 30g (0.5 - 1 oz)
2. Charadriiformes	16.56%	Western Sandpiper, California Gull, Dunlin, Ring-Billed Gull	17- 137cm (6.7- 54in)	30- 1,045g (1.1oz- 2.3lbs)
3. Columbiformes	11.39%	Mourning Dove, Rock Pigeon, Band-Tailed Pigeon, Eurasian Collared Dove	31- 40cm (12 - 16in)	170- 515g (6- 18.2oz
4. Accipitriformes	11.17%	Red -tailed Hawk, Turkey Vulture,	61- 132cm (24-	380- 2,400g

		White-tailed Kite, Red-shouldered Hawk	52in)	(1.51- 5.3lbs)
5. Anseriformes	7.82%	Canada Goose, Gadwall, Green-winged teal, Northern Shoveler, Mallard Duck	37- 114cm (14.5- 45in)	280- 10,900g(10oz- 24lbs)
6. Strigiformes	7.31%	Barn Owl, Burrowing Owl, Great Horned Owl, Short-eared Owl	21- 64cm (9.5- 25in)	240- 1,608gr (8oz- 3.54lbs)
7. Falconiformes	7.2%	American Kestrel, Caracara, Peregrine Falcon, Prairie Falcon	31- 65cm (12.2- 26in)	165- 1,600g (5.82oz - 3.5lbs)
8. Pelecaniformes	1.93%	American White Pelican, Brown Pelican	130- 180cm (50- 70in)	5- 9kg (10- 20lbs)
9. Carnivora	1.92%	Coyote, Red Fox, Raccoon, Domestic Cat, Domestic Dog	25- 135cm (10- 53.1in)	5-18kg (11- 40lbs)
10. Chiroptera	1.53%	Brazilian Free-tailed Bat, Free-tailed Bat, Hoary Bat, Little Brown Bat, Western Red Bat	0.4-9cm (1.6- 3.5in)	9- 220g (0.3- 7.7oz)

* Information compiled from The *National Geographic Field Guide to the Birds of North America, Second Edition (1992)*

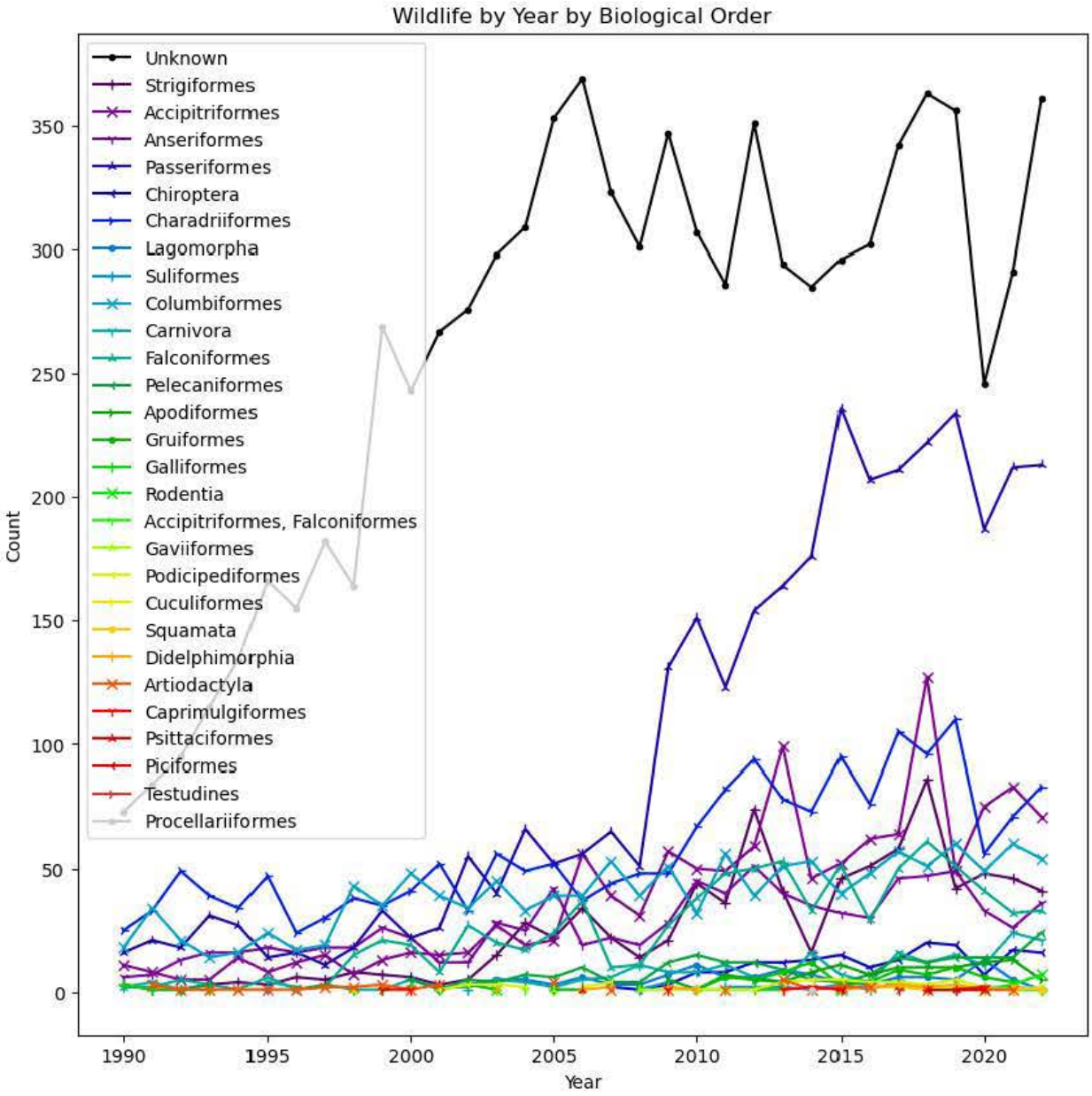


Figure 27. Yearly evolution of wildlife strike by Order (n = 11,466, unknown order: 8603)

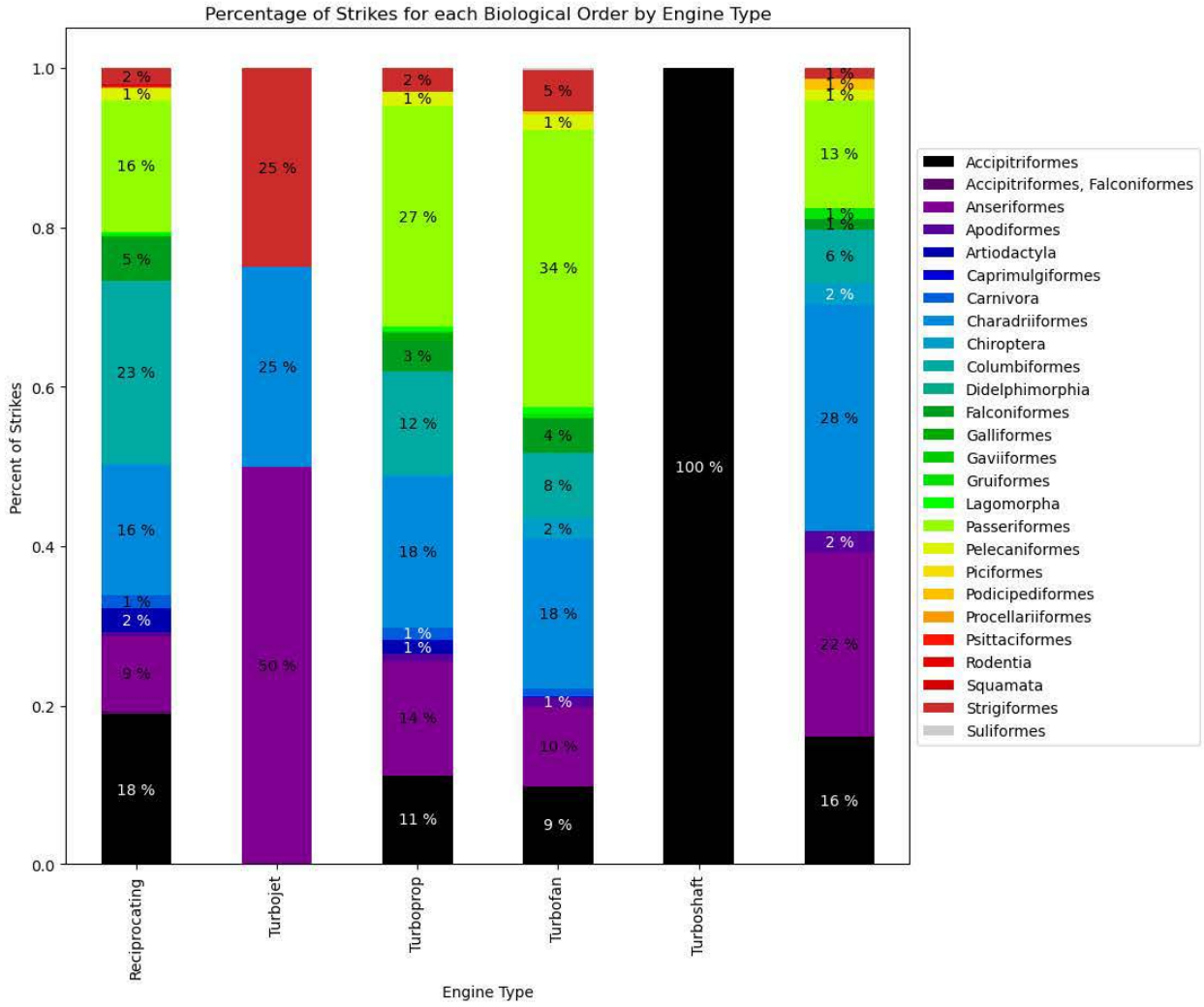


Figure 28. Strikes by wildlife Order and engine-type (n = 7352)

3.10. GIS-relevant Results

3.10.1. Strike Location and Hotspot Analysis

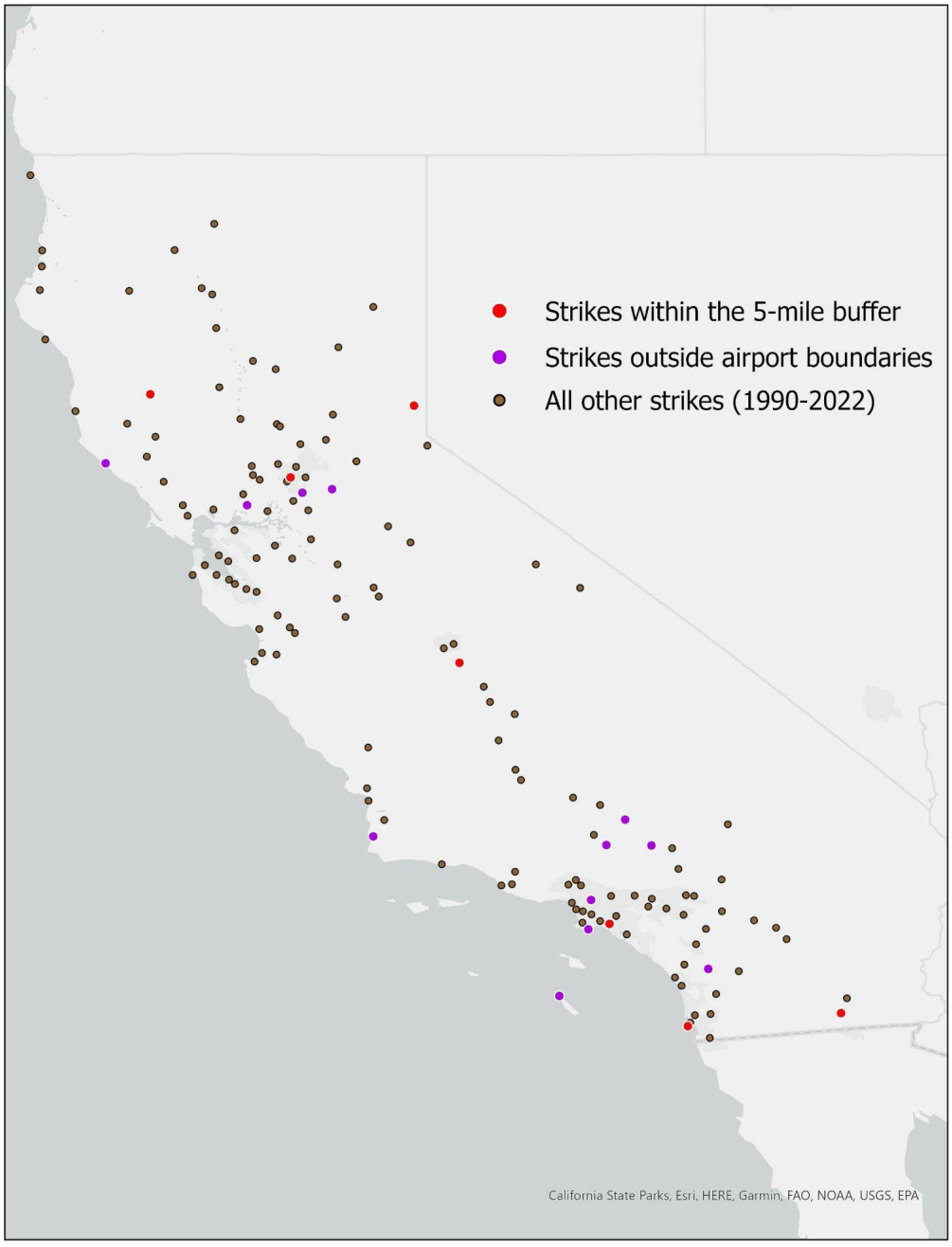


Figure 29. Wildlife strike occurrence in California from 1990- April 2023 (n = 19,873)

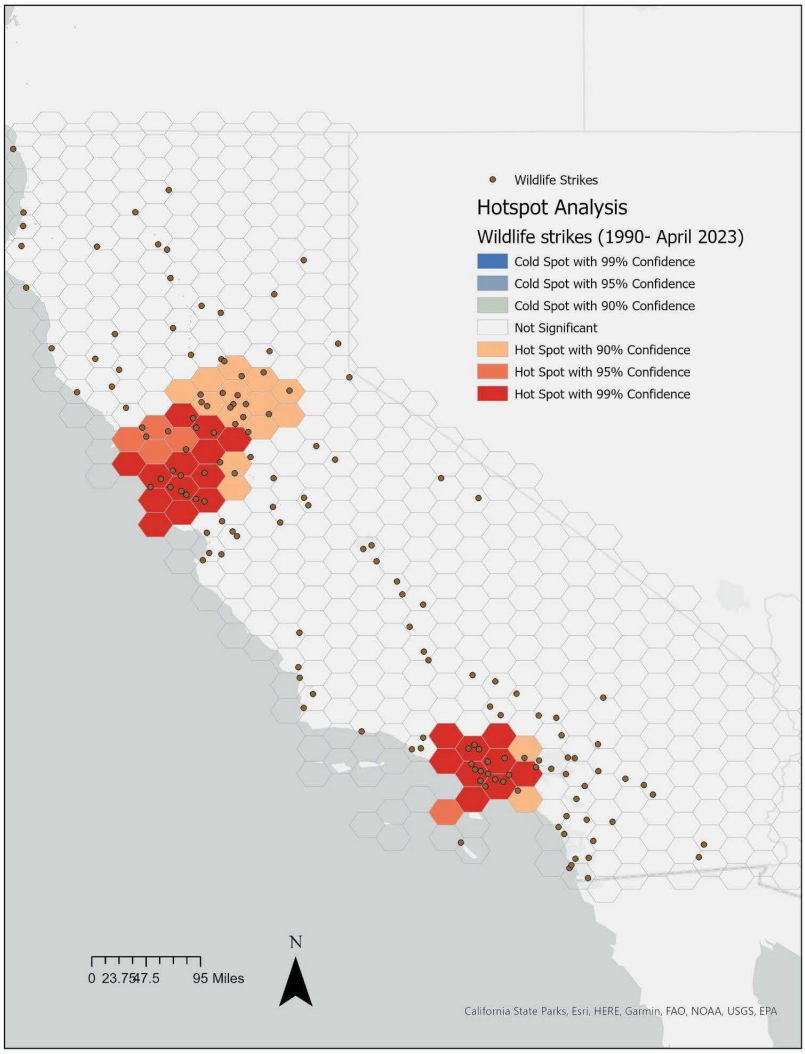

Wildlife Strikes
Hotspot Analysis
Wildlife strikes (1990- April 2023)
Cold Spot with 99% Confidence
Cold Spot with 95% Confidence
Cold Spot with 90% Confidence
Not Significant
Hot Spot with 90% Confidence
Hot Spot with 95% Confidence
Hot Spot with 99% Confidence
0 23.7547.5 95 Miles
N
California State Parks, Esri, HERE, Garmin, FAO, NOAA, USGS, EPA

Figure 30. Wildlife strike hotspots (n = 19,873)

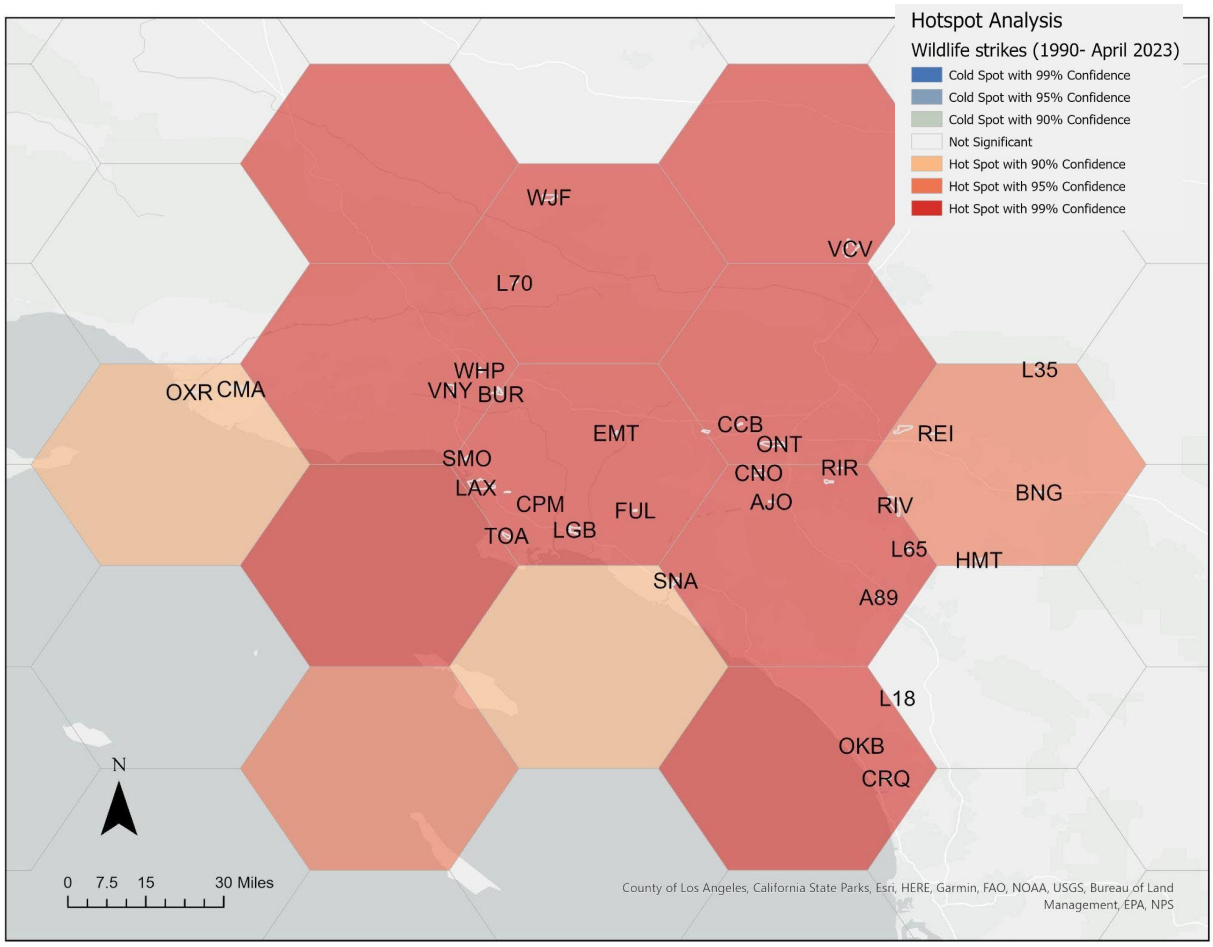


Figure 31. Hotspot analysis of wildlife strikes outside the airport boundaries. Identification of airports within the hotspot zones (90 to 99% confidence) (n= 83)

3.10.2. Strike Probability by Airport

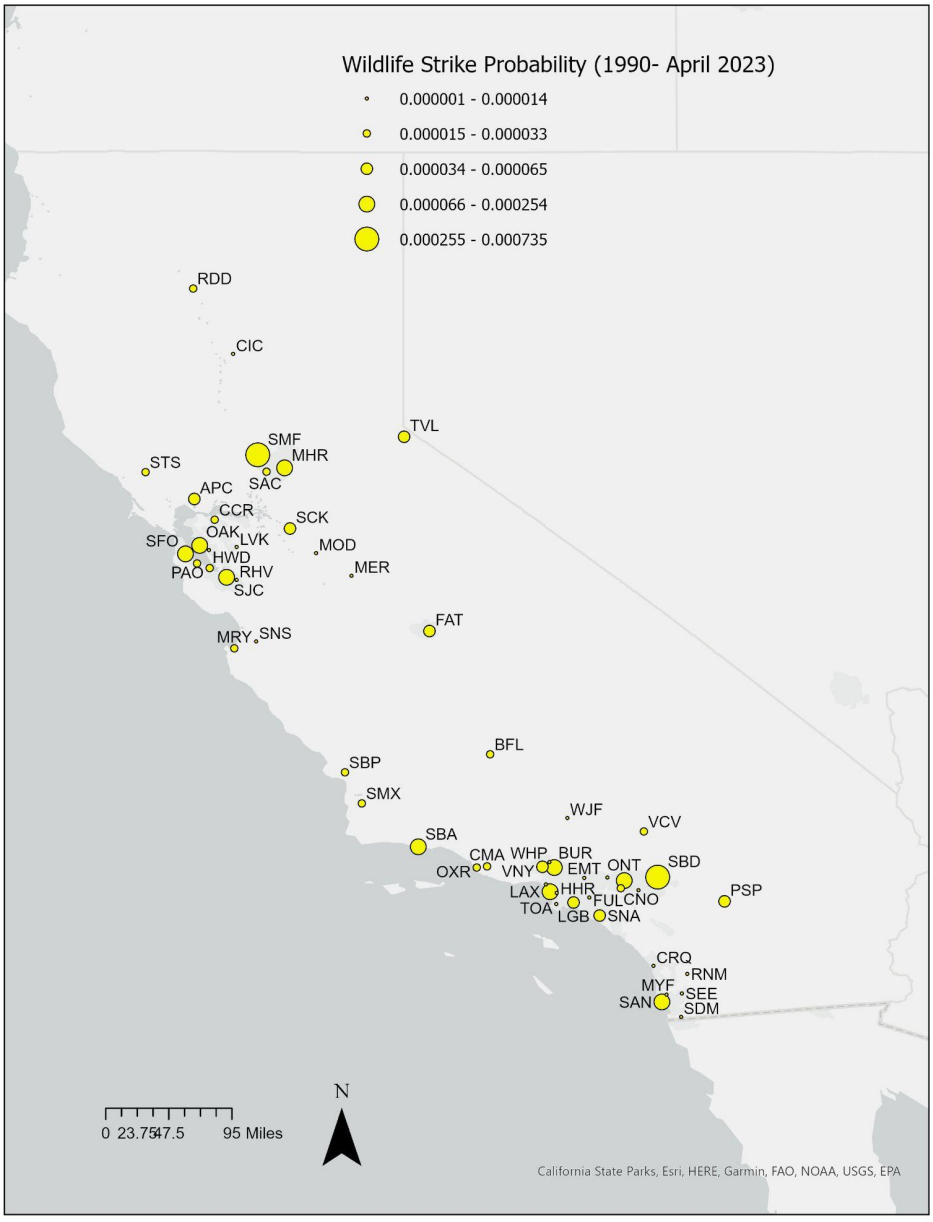


Figure 32. Map of wildlife strike probability of California airports based on air traffic data and wildlife strikes data from 1990- April 2023 (n = 19,873)

Table 4. Top 10 airports for strike probability

Airport	Operations	Strikes	Probability*
1. SMF	4,764,744	3,502	0.000735
2. SBD	80,367	39	0.000485
3. ONT	4,213,543	1,072	0.000254
4. SJC	7,333,453	1,728	0.000236
5. SFO	13,355,398	2,241	0.000168
6. SBA	4,514,849	735	0.000163
7. OAK	10,985,998	1,617	0.000147
8. LAX	21,918,076	2,626	0.00012
9. BUR	5,322,742	575	0.000108
10. MHR	1,903,082	204	0.000107

**Probability = Total strikes/ total air traffic between 1990-2022*

Table 5. Wildlife Strikes per Safety Zone (1990-April 2023) (n= 19,873)

Safety Zone	Number of Wildlife strikes	% of strikes
Primary Surface	11,268	56.76
Zone 1	0	0
Zone 2	4	0.02
Zone 3	0	0
Zone 4	0	0
Zone 5	800	4.03
Zone 6	7,777	39.18

3.10.3. Strike Runway Distance Analysis

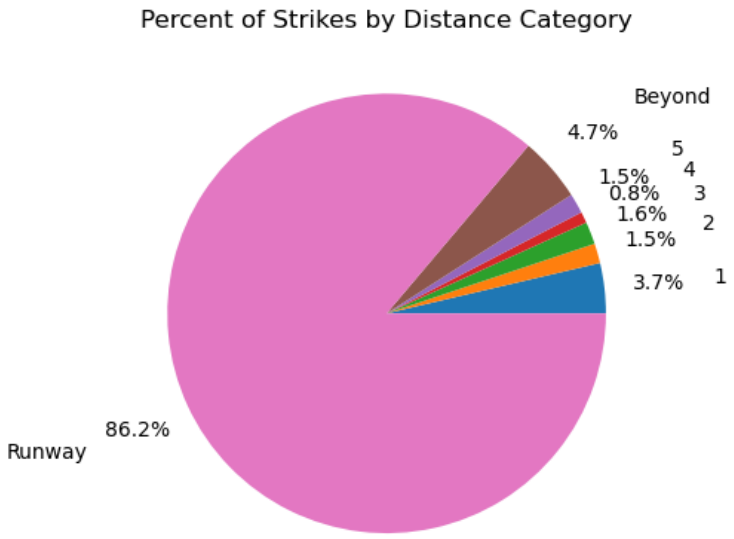


Figure 33. Wildlife strikes based on their distance from the runway . Distances were calculated in Nautical Miles, and categorized as Runway, 0-1 NM, 1-2 NM, 2-3 NM, 3-4 NM, 4-5 NM, >5 NM. (n = 19,873).

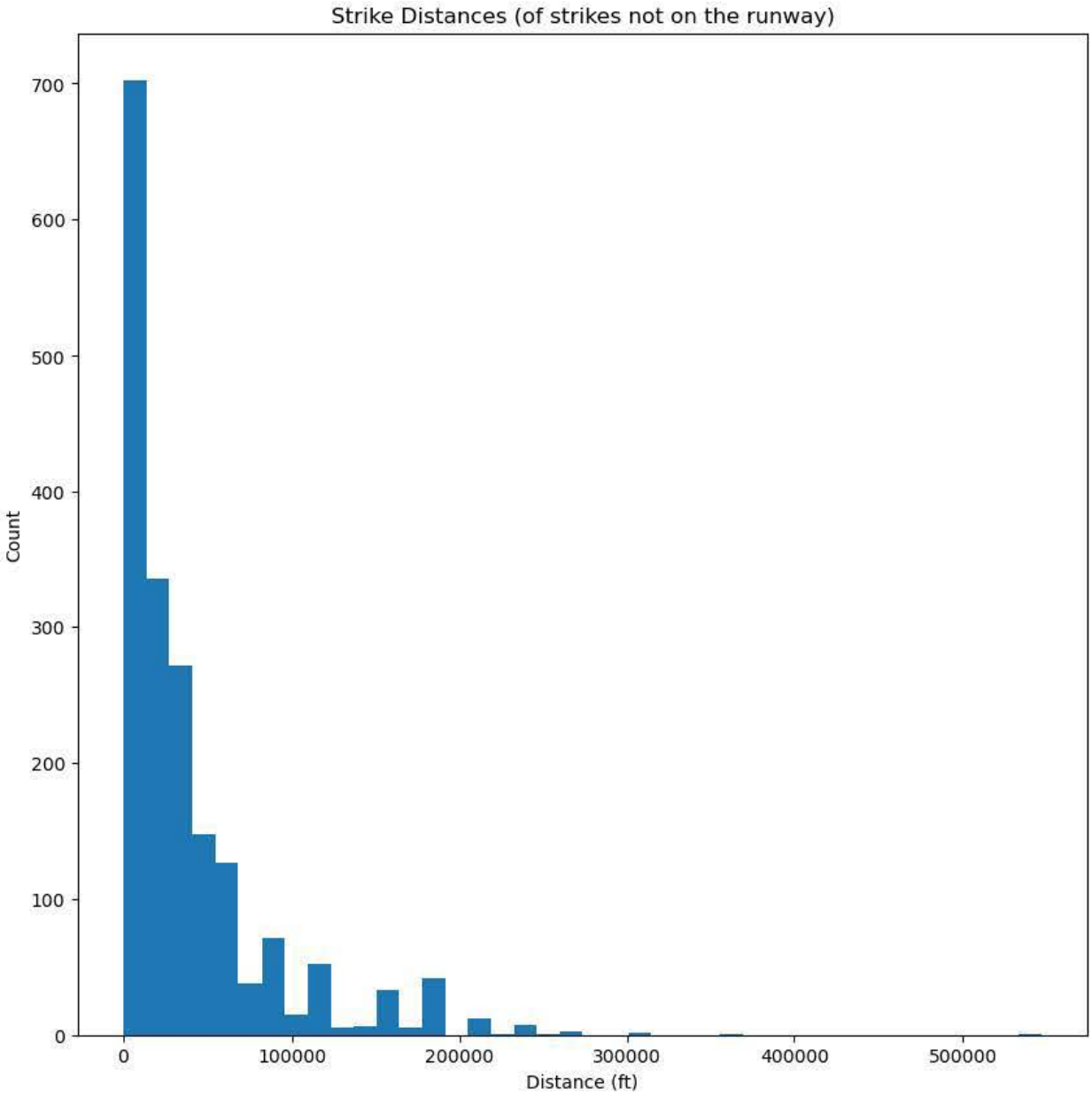


Figure 34. Strike Distances (excluding those in the runway centerline = 11,738) (n = 1,881)

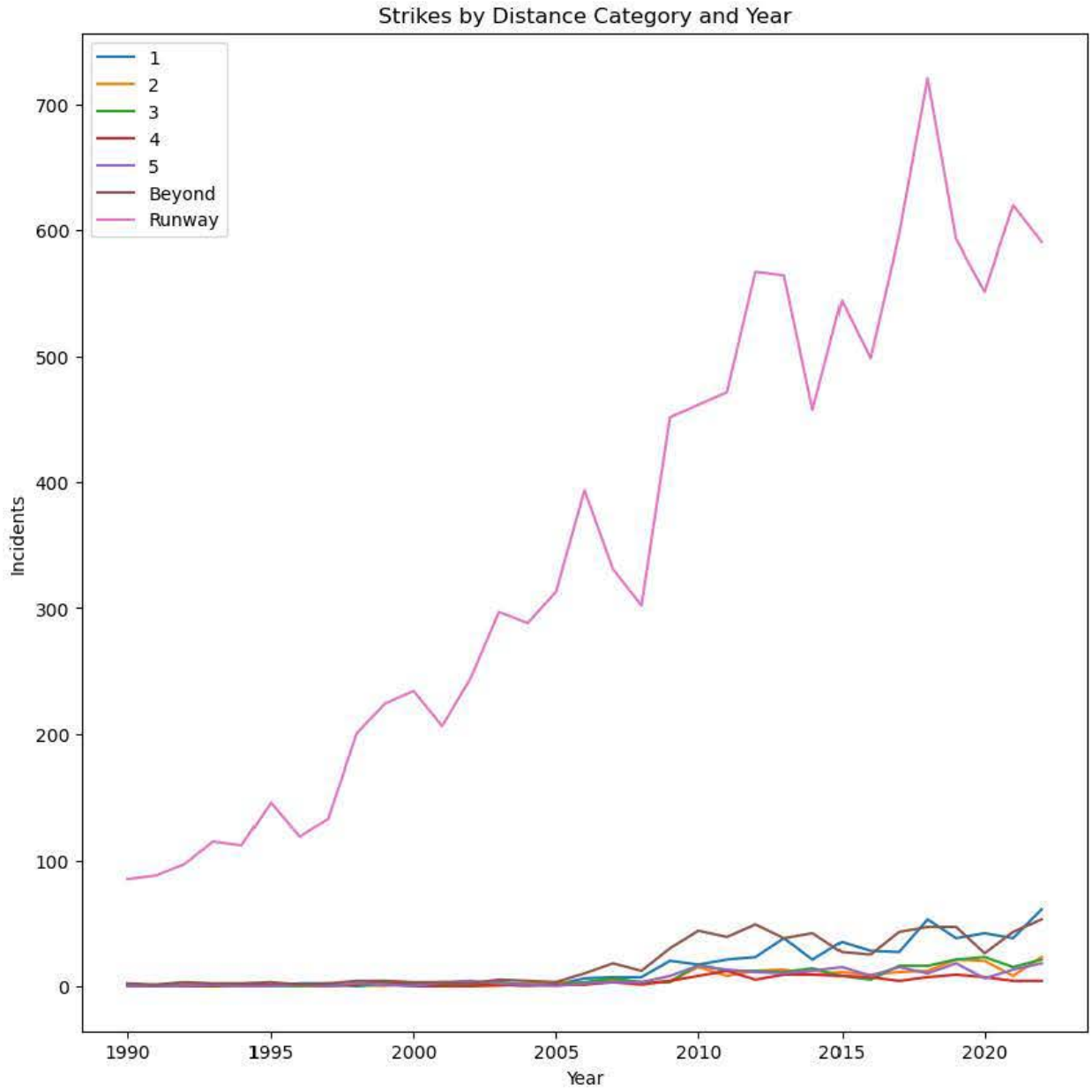


Figure 35. Yearly evolution of strikes by distance category. (n = 13,473)

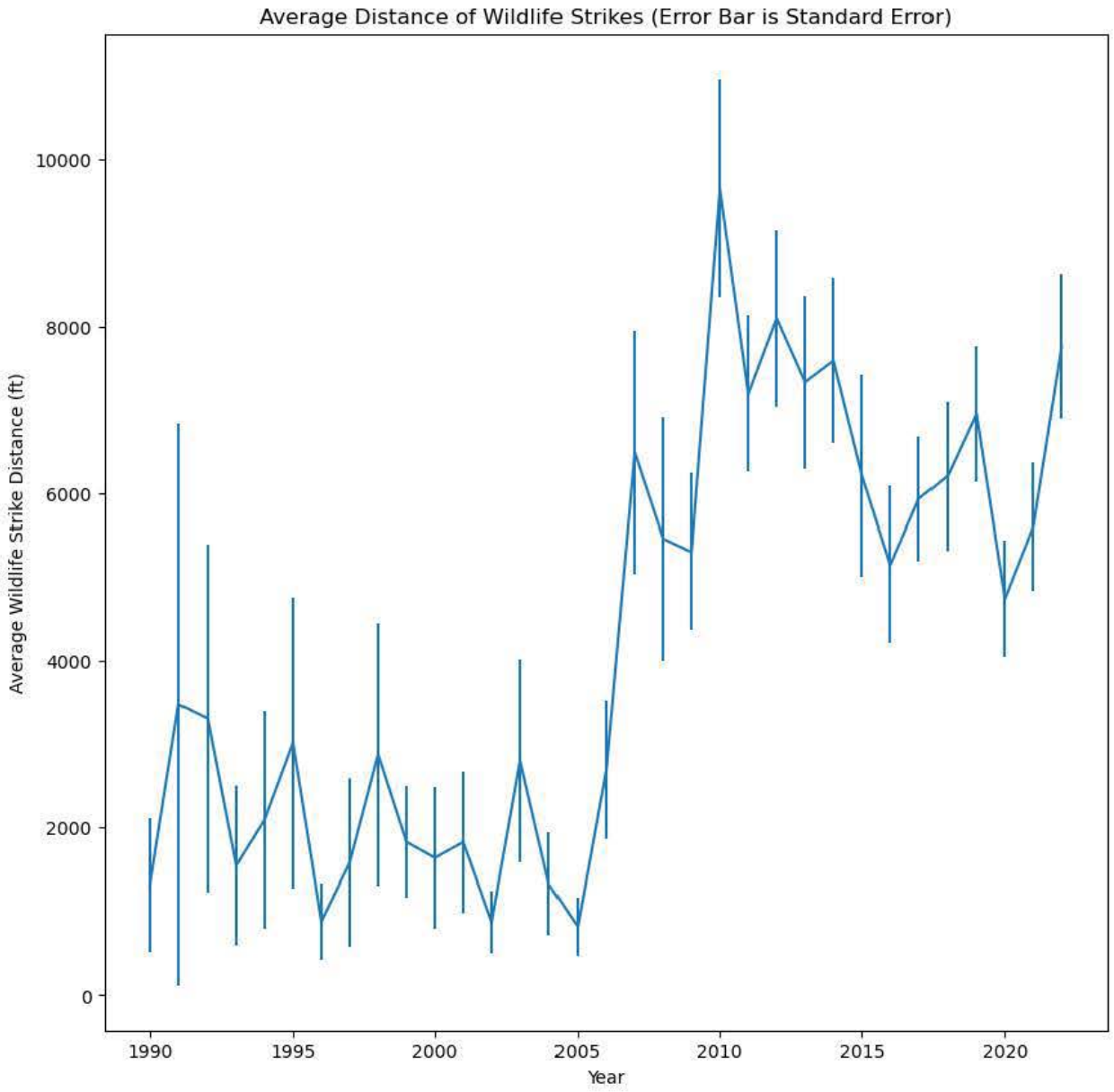


Figure 36. Average strike distance from the runway by year (n = 13,473)

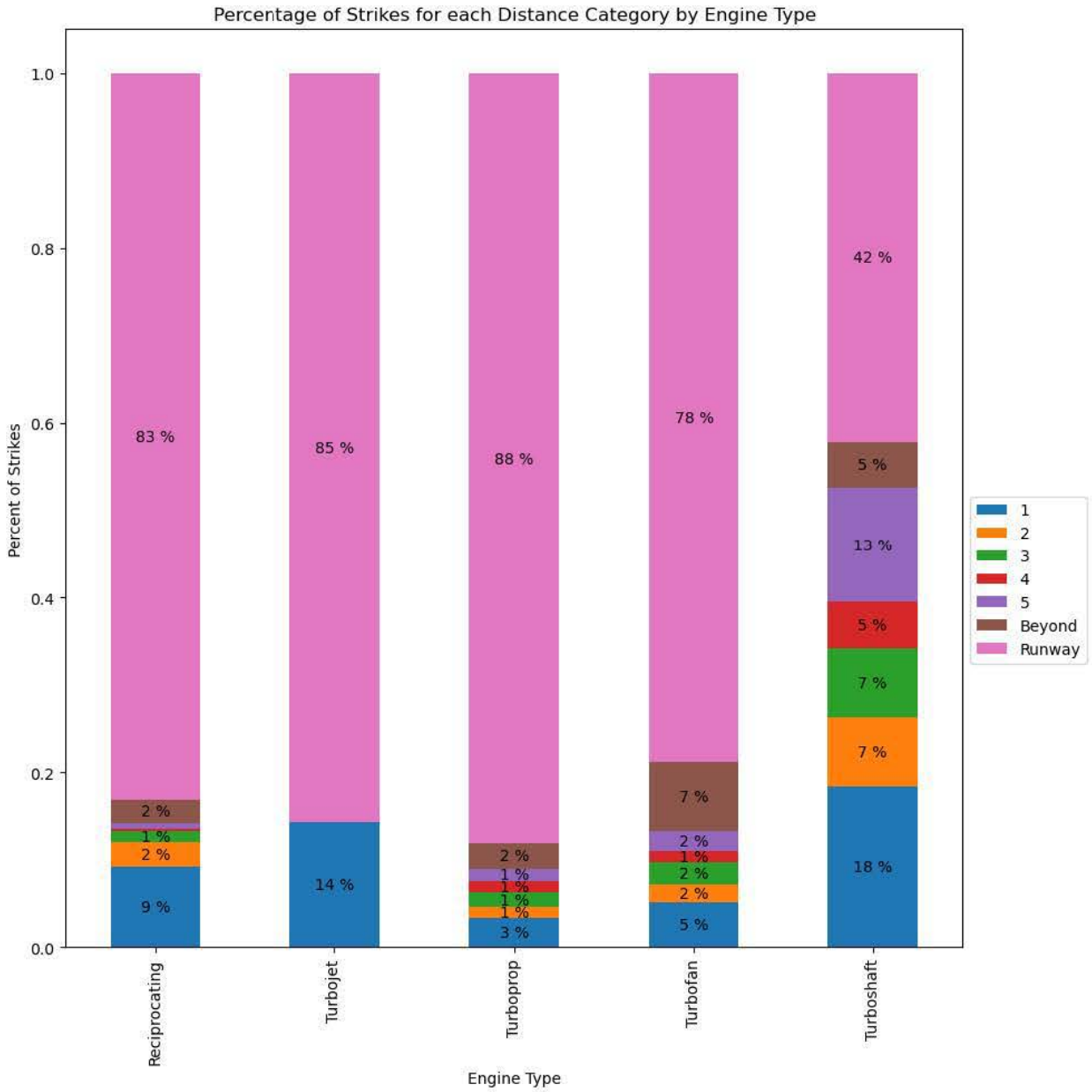


Figure 37. Strikes based on distance from runway and engine-type (n = 9,206)

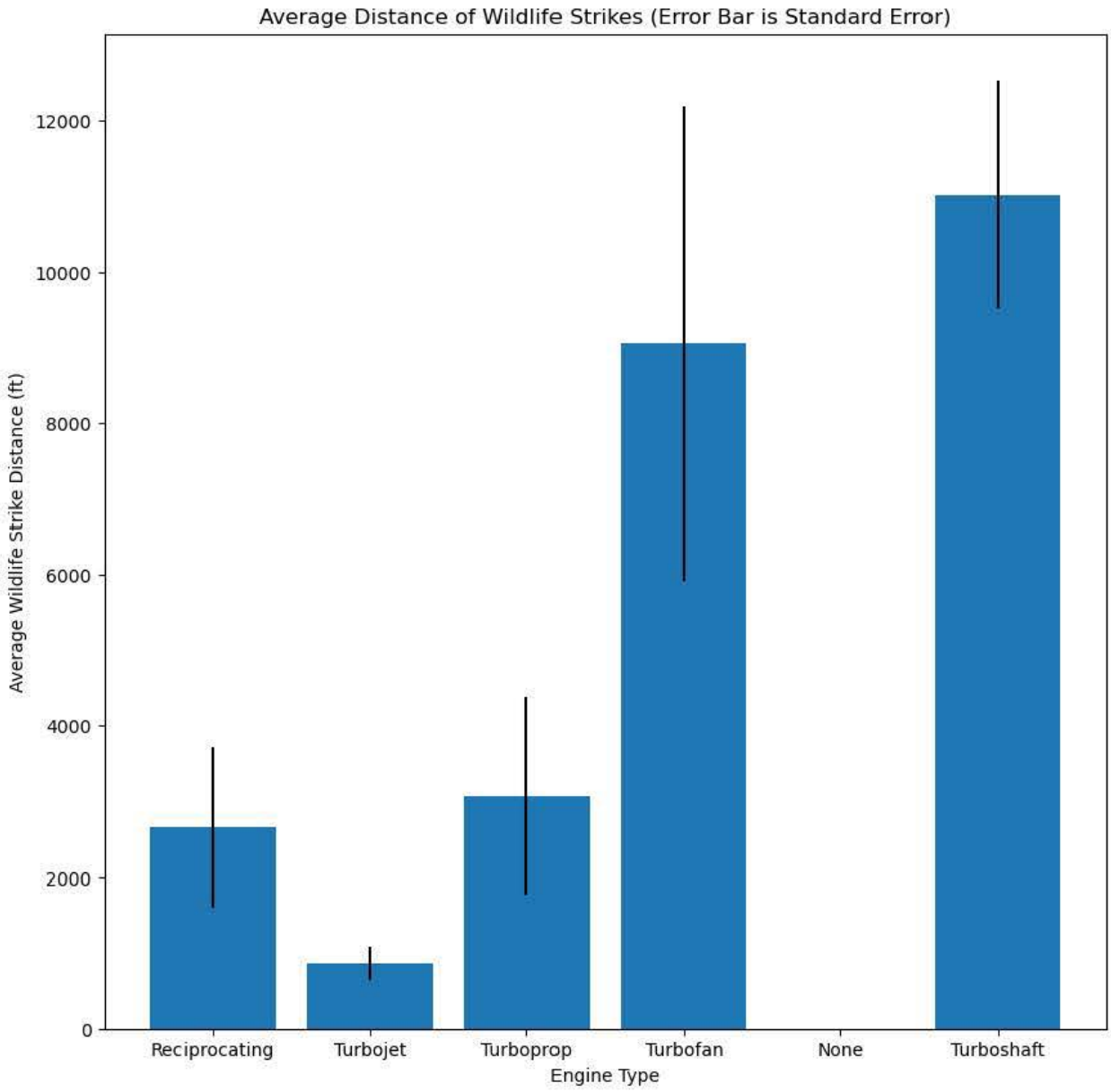


Figure 38. Average strike distance from runway centerline by engine type (n = 9206)

3.11. Multivariable Analysis

3.11.1. Distance, Height, Speed, and Engine Variables

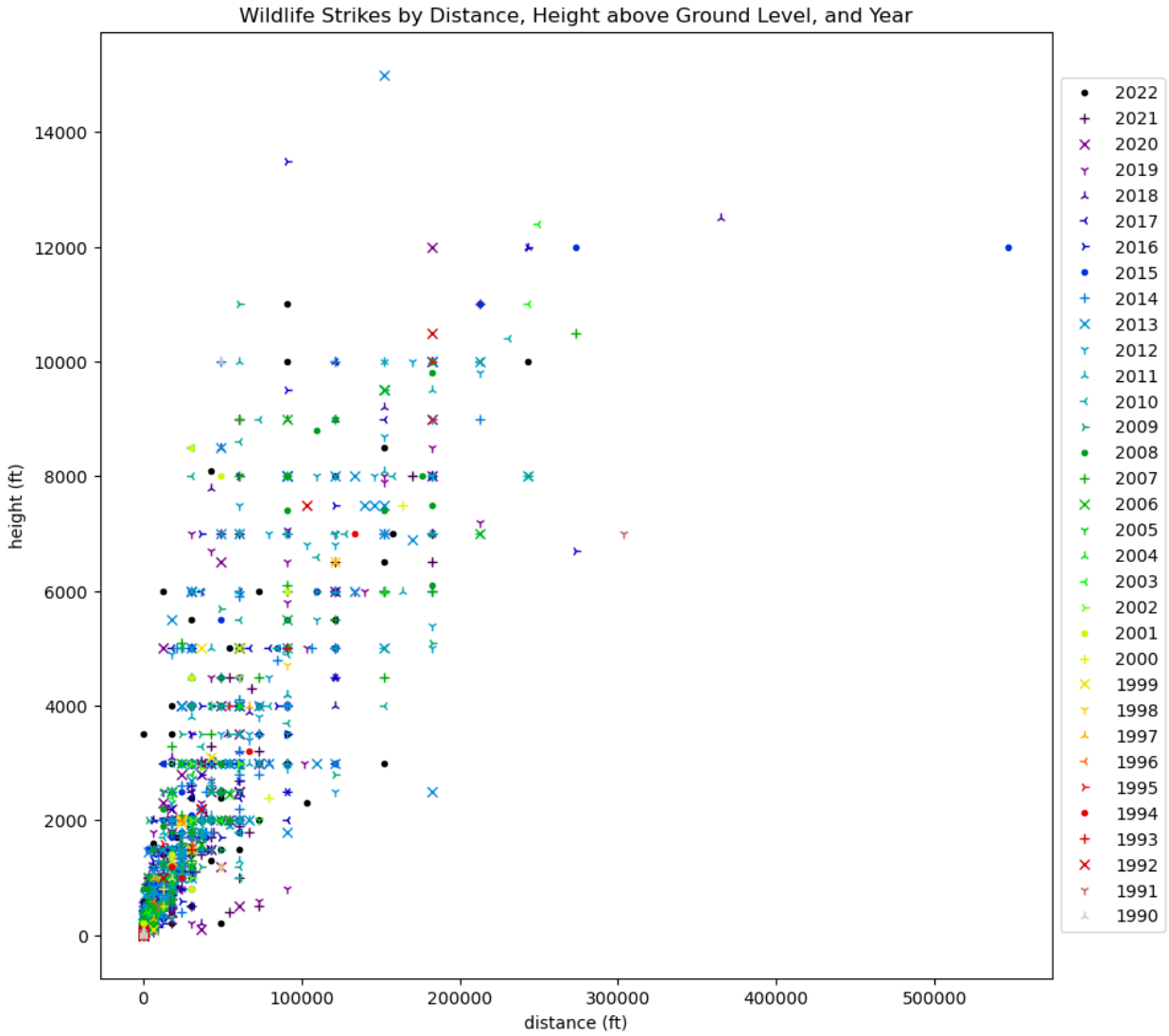


Figure 39. Wildlife strikes based on distance from runway, height, and year (n = 8,550)

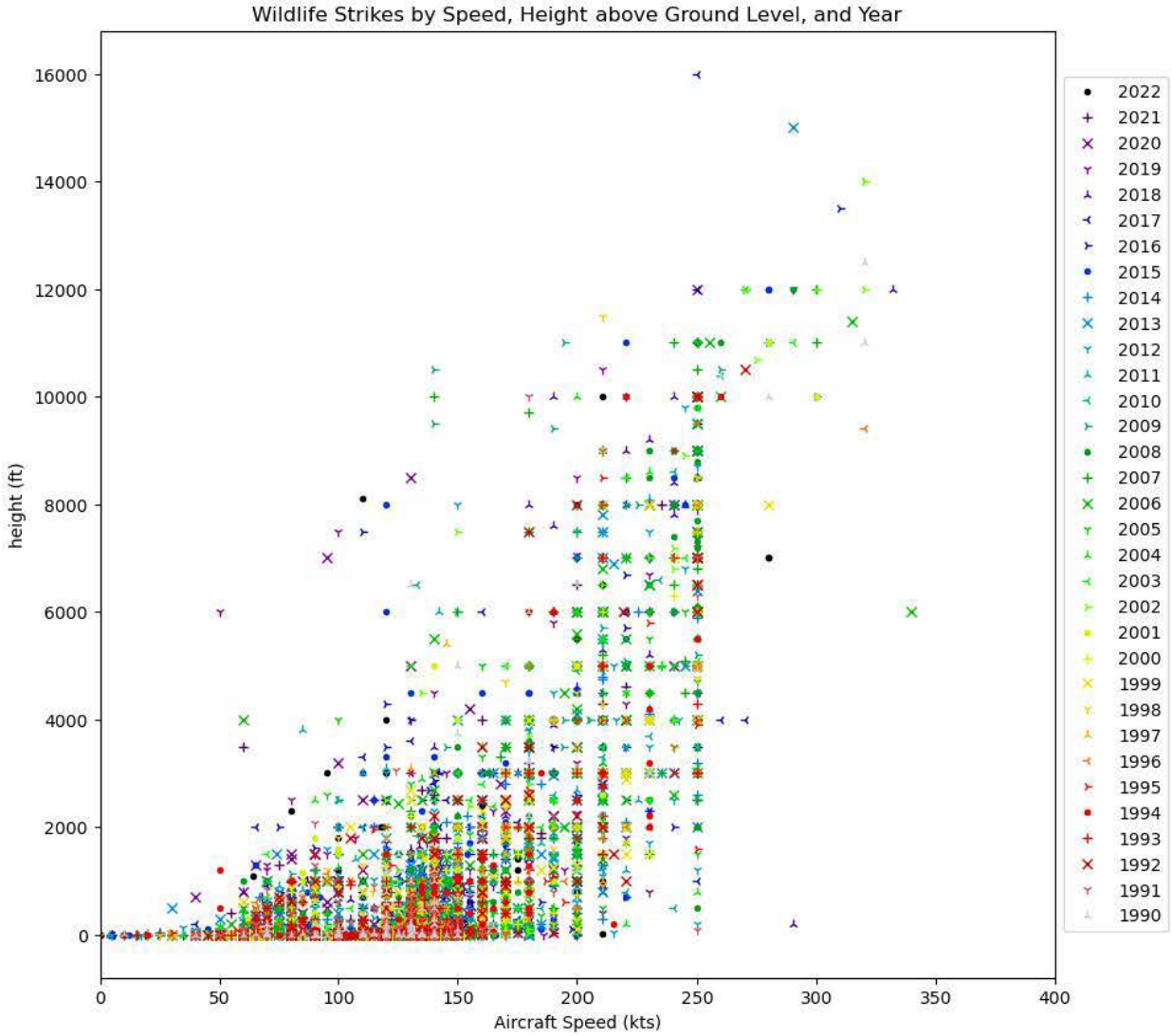


Figure 40. Wildlife strikes based speed, height, and year (n = 8,056)

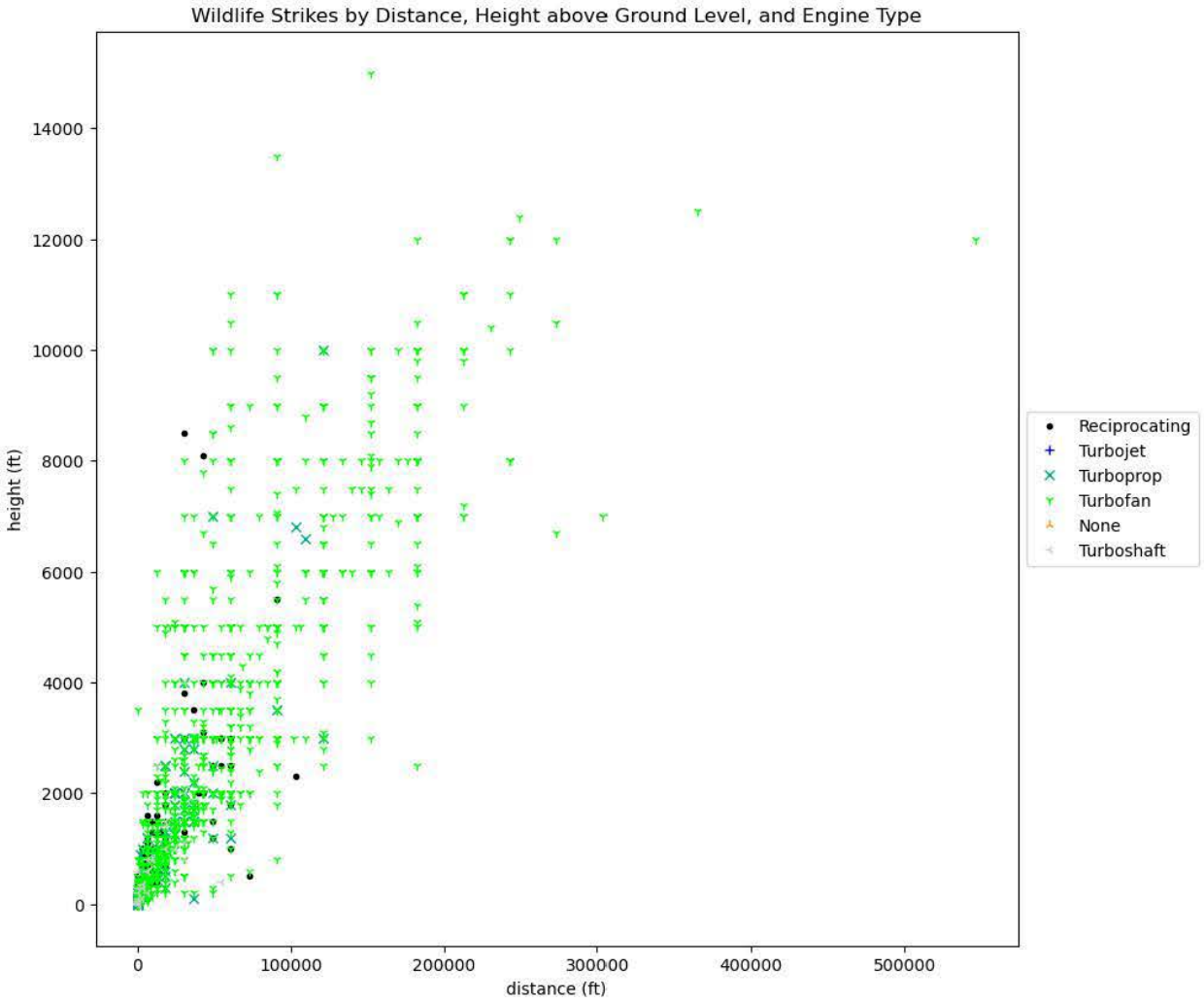


Figure 41. Wildlife strikes based on distance from runway, height, and engine-type (n = 8,517)

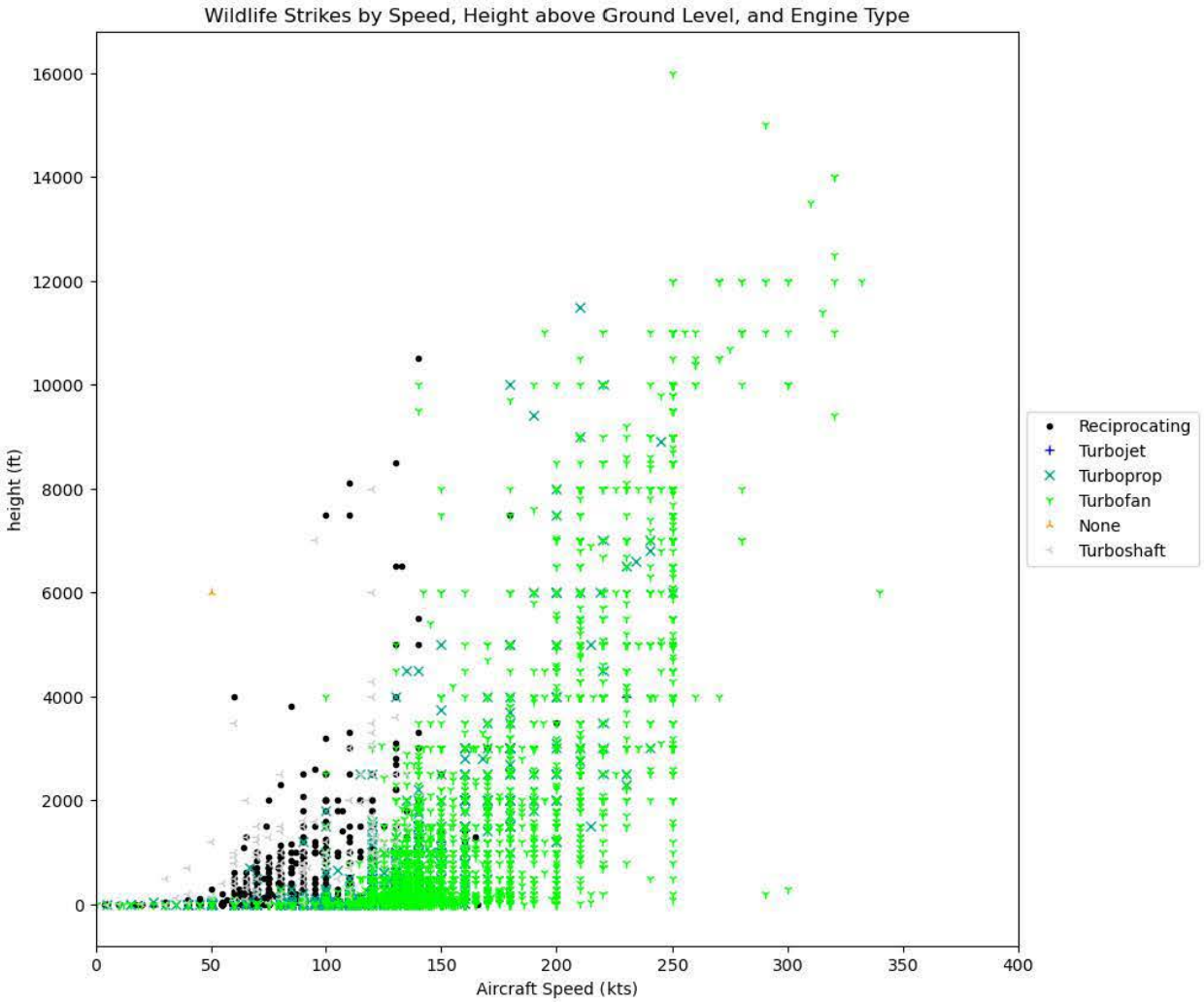


Figure 42. Wildlife strikes based on speed, height, and engine-type (n = 8,064, one strike at around 650 kts excluded)

3.11.2. Wildlife Taxonomy, Distance, Height, and Speed Variables

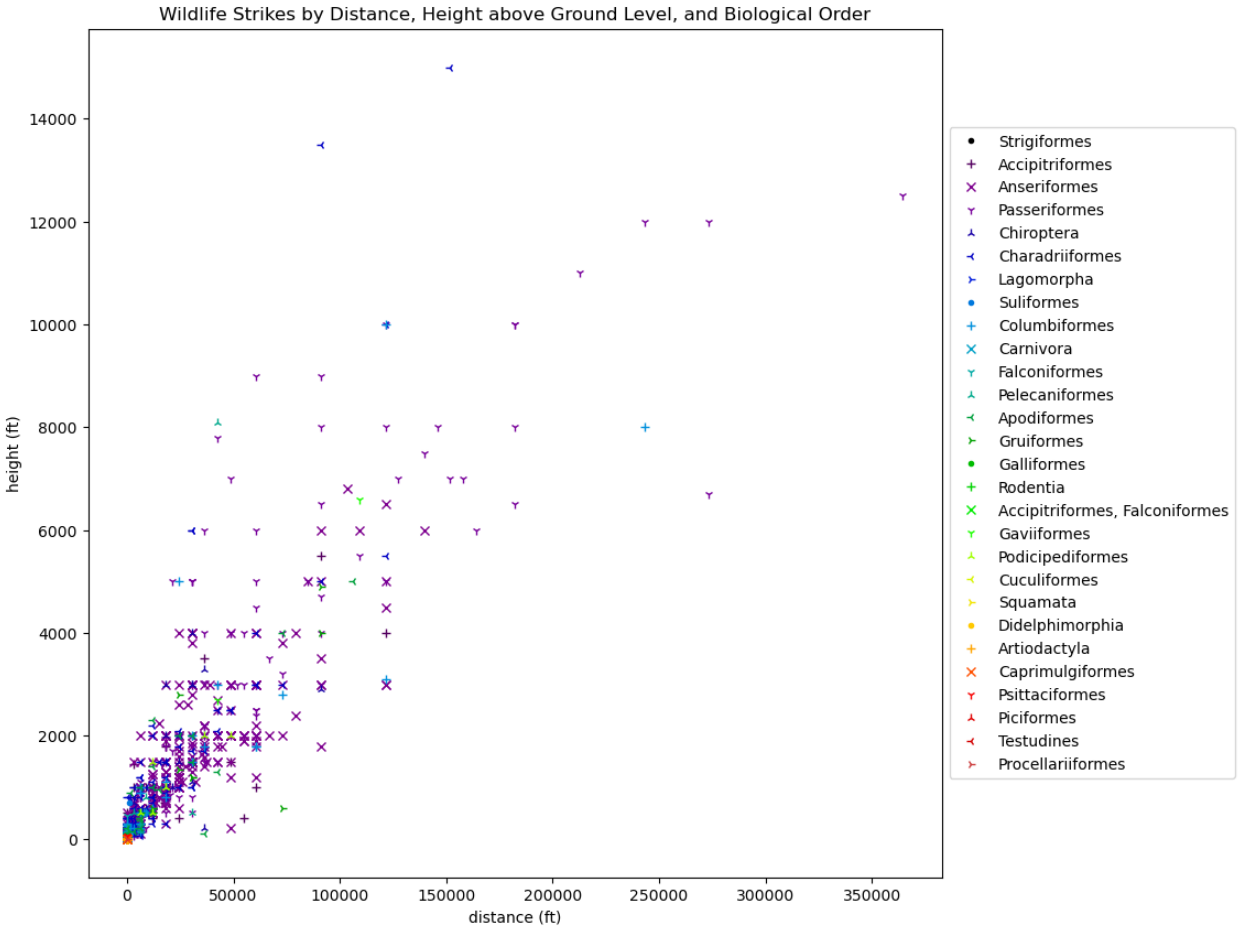


Figure 43. Strikes by height, distance and Order (n = 8,640)

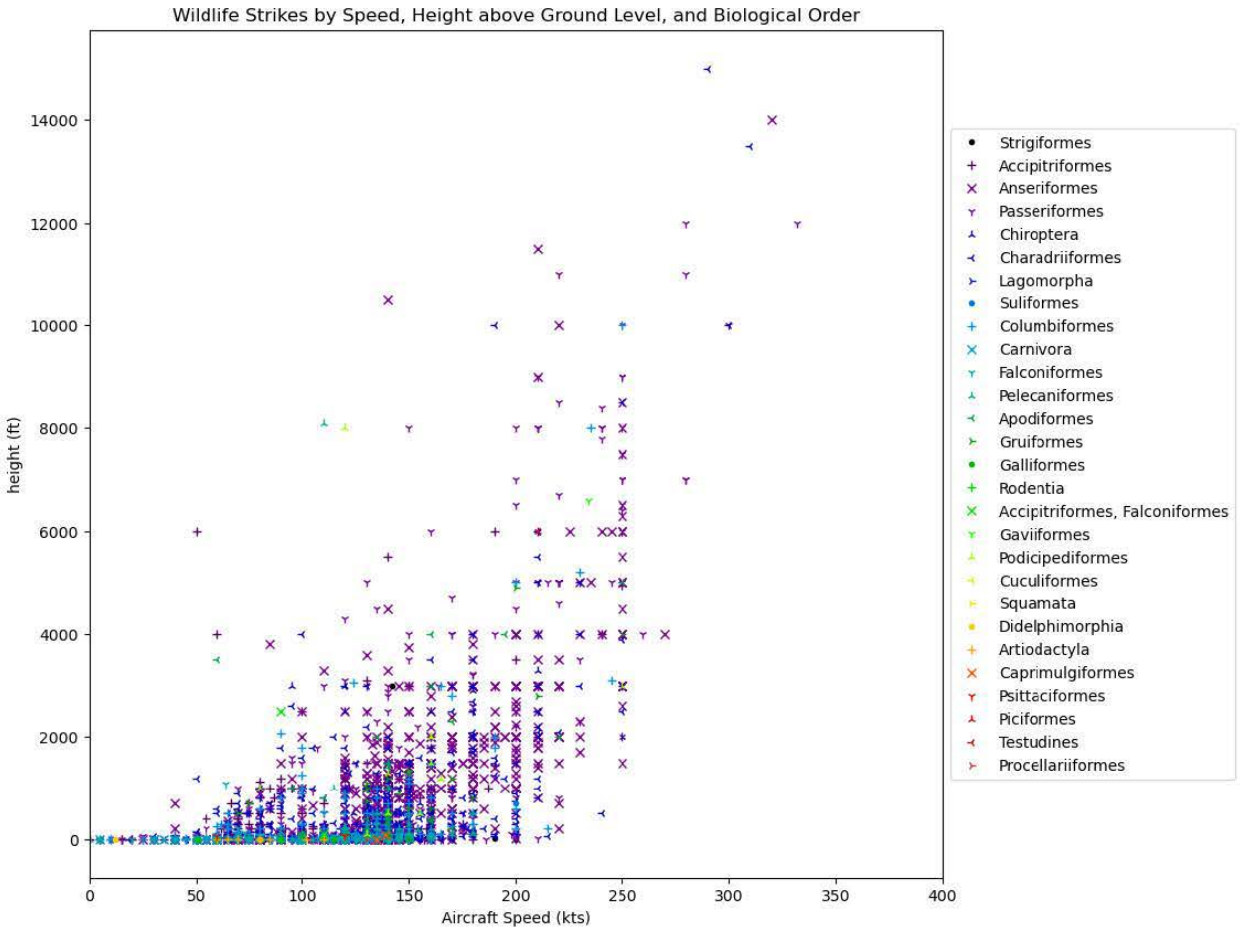


Figure 44. Strikes by height, speed, and Order (n = 8,127 (one strike at around 650 knots excluded, -> 8126)

[4.1.2] 4. Citations

FAA. (2014). *Airport Design*. https://www.faa.gov/documentlibrary/media/advisory_circular/150-5300-13a-chg1-interactive-201705.pdf

FAA. (2020). *Hazardous Wildlife Attractants on or near Airports* (p. 47). https://www.faa.gov/documentLibrary/media/Advisory_Circular/150-5200-33C.pdf

FAA. (2022). *FAA Wildlife Strike Database*. https://wildlife.faa.gov/home

FAA. (2023a). *Aircraft Characteristics Data*. https://www.faa.gov/airports/engineering/aircraft_char_database/data

FAA. (2023b). *Wildlife Strikes to Civil Aircraft in the United States, 1990—2022*. https://www.faa.gov/airports/airport_safety/wildlife/wildlife_strikes_civil_aircraft_united_states_1990_2022

Kelly, T., & Allan, J. (2006). *Ecological effects of aviation*. https://link.springer.com/chapter/10.1007/1-4020-4504-2_1

McKee, J., Shaw, P., Dekker, A., & Patrick, K. (2016). *Approaches to Wildlife Management in Aviation*. https://canadianbirdstrike.ca/wp-content/uploads/2018/02/McKee_et_al_2016.pdf

[4.1.2] APPENDIX A. BIRD STRIKE SEVERITY ANALYSIS (2010 - 2019):

A.1. Introduction

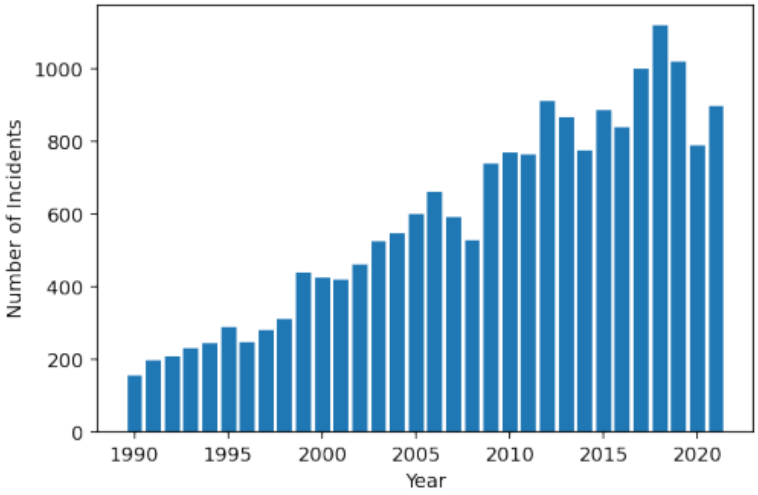
Over 95% of wildlife strikes involve birds in California, therefore a specific discussion of severity of strikes focusing on birds is developed here. This section focuses on bird strikes using logistic regression analysis to understand which variables from the FAA Wildlife Strikes Database can better predict the severity of strikes. The increasing trend of bird strikes from 1990-2021 is available in Figure A.1.The monthly pattern in Figure A.2. identifies two major peaks of bird strike incidence in California from April to June; and from September to November. A clear decrease of incidence is observed between December and March. The Yearly evolution of bird strikes based on the severity is available in Figure A.3. and the severity based on phase of flight in Figure A.4. The FAA dataset classifies the severity of strikes in five classes:

- (N) None: no damage reported
- (M) Minor: when the aircraft can be rendered airworthy by simple repair or replacements and an extensive inspection is not necessary
- (S) Substantial: when the aircraft incurs damage of structural failure which adversely affects the structure strength performance or flight characteristics of the aircraft and which would normally require major repair or replacement of the affected component. Bent fairings or cowlings, small dents or puncture holes in the skin; damage to wind tips, antenna, tires or brakes; and engine blade damage not requiring blade replacement are specifically excluded.
- (D) Destroyed: when the damage sustained makes it inadvisable to restore the aircraft to an airworthy condition.
- (M?) Undetermined Level: the aircraft was damaged but the details as to the extent of the damage is unknown

The majority of bird strikes cause no damage to aircrafts, and the increasing trend of incidents are attributed to this class of severity. We observe a slight decrease of substantial and destroyed severity levels, and an increase of undetermined level that is accentuated from 2015 onwards (Figure A.2). The highest incidence of Substantial damage or Destroyed aircraft severity occurs during Approach and Climb phases of flight (Figure A.4.).

Figure A.5. looks at the height and speed of incidents based on severity, showing that most incidents cluster around a speed of 100 to 150 kts at a relatively low height, while other incidents are relatively uniformly distributed within the speed of 250 kts. Figure A.6. focuses only on incidents with Substantial damage, identifying a similar cluster (up to approximately 800 ft. in height and 100-150 kts in speed) aligning with the concentration of incidents during Approach and Climb phases of flight.

Figure A.1. Trend of bird strikes in California



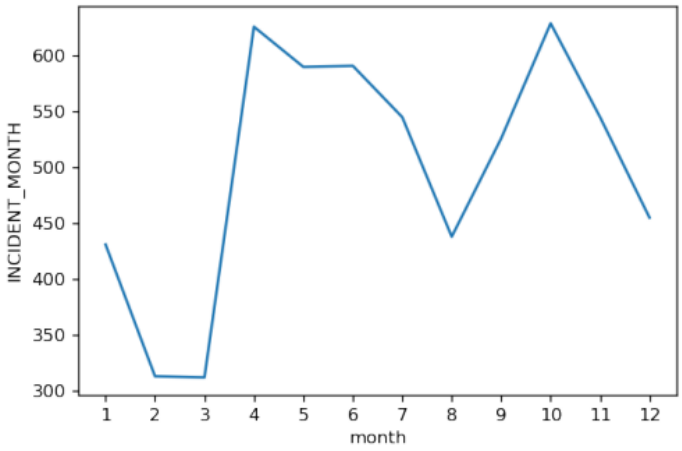


Figure A.3. Bird strikes distribution based on the month (1990-2021)

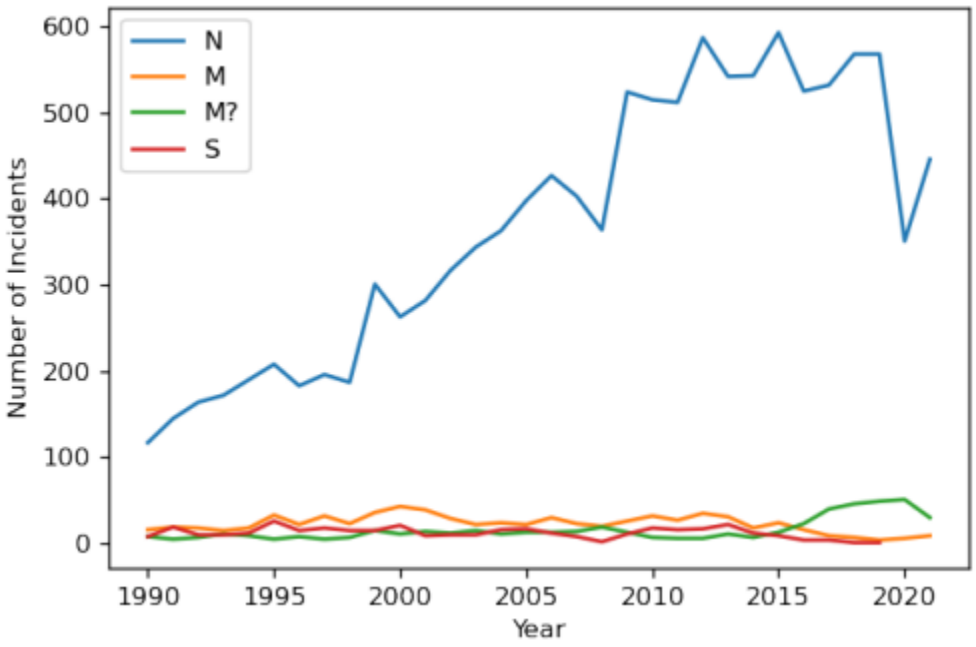


Figure A.3. Yearly evolution of bird strikes based on their severity (1990- 2021)

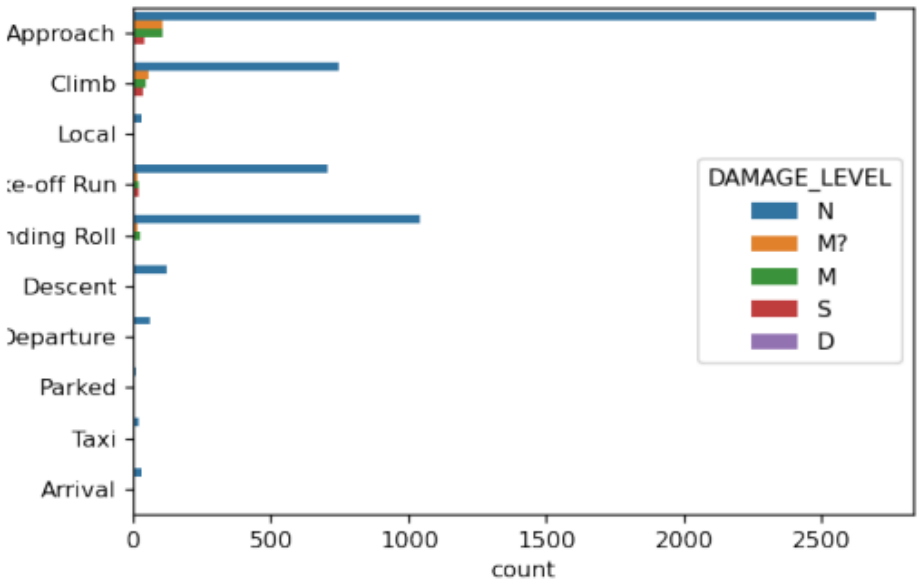


Figure A.4. Bird strike severity based on phase of flight (1990- 2021)

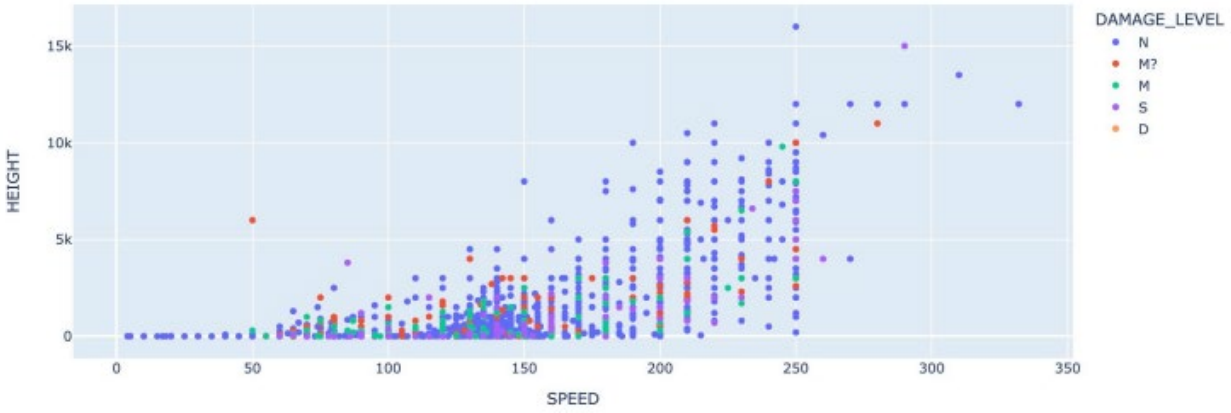


Figure A.5. Distribution of bird strikes by severity based on aircraft height (ft) and speed (kts) (1990-2021)

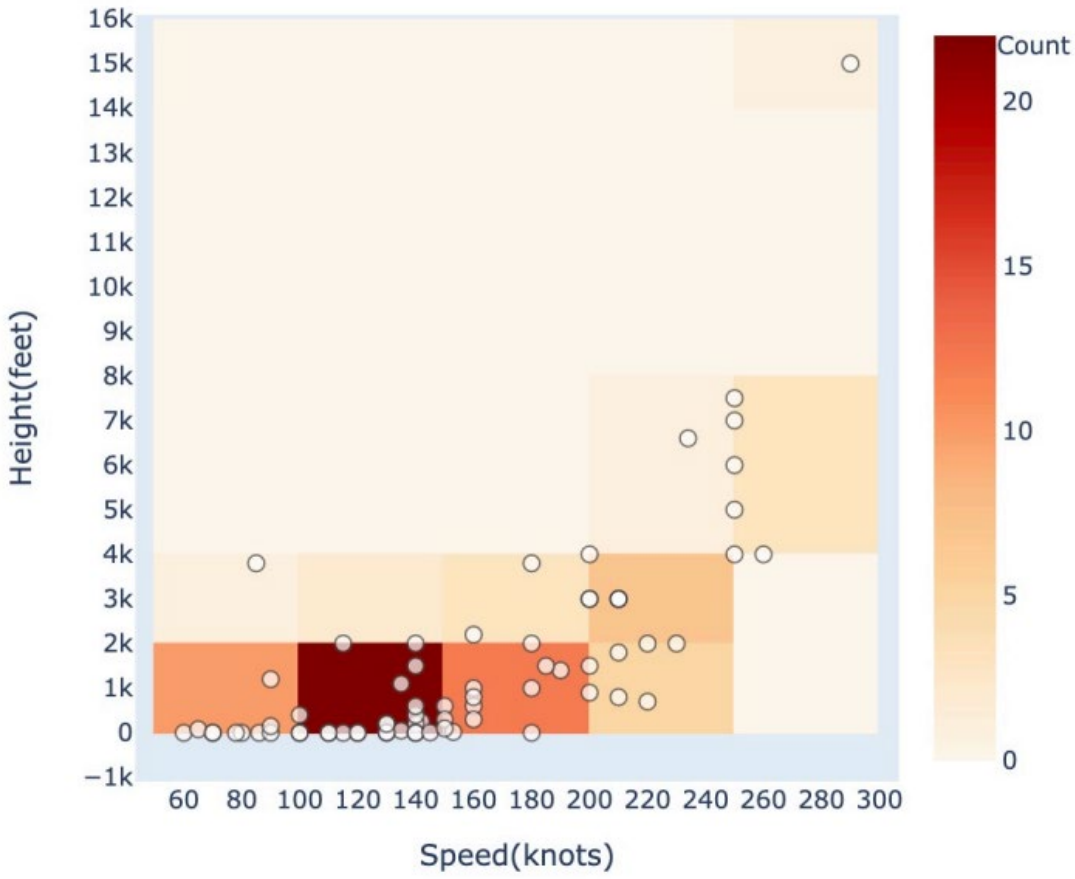


Figure A.6. Distribution of bird strikes with Substantial damage based on aircraft height and (ft) and speed (kts) (1990-2021)

A.2. Methods

A.2.1. Data

The section focusing the correlation analysis uses bird strike data between the 2010 and 2019 in California, resulting in approximately 6000 records. The independent variable *y* is the severity of damage and the dependent variables *x* include 1) month, 2) local time, 3) aircraft mass, 4) speed, 5) height, 6) location, 7) phase of flight, 8) cloud condition, and 9) weather conditions.

A.2.2. Correlation Analysis: Logistic Regression

The severity of a bird strike, or the dependent variable y_i, including Minor, Substantial, and Destruction severity classes labeled as 0, 1, or 2 respectively. In this study, bird strike severity is modeled as a function of *x*, where *x* denotes the various features of that particular bird strike (dependent variables, e.g., the mass of aircraft, local time, etc.). According to the problem setup, the impact of different features can be analyzed using ordinal logistic regression. In other words, the probability that a bird strike severity is at least *i* can be calculated using the formula below[10]:

$$y_i = \frac{1}{1 + e^{-(A^T \vec{x} + b_i)}}, i = 1, 2$$

Where *A* is a vector that represents the weight of each feature.

However, such regression analysis cannot be directly implemented in this study because the independent variable is very biased (over 90% of all occurrences are labeled as ”0”). To mitigate this issue, we applied data augmentation by adding nine copies of data with labels ”1” and ”2” to the original dataset so that the label distribution becomes more even.

While ordinal logistic regression can help find the features related to the severity of the bird strikes, some of the associated features may share a similar piece of information and are thus redundant. A principle component analysis (PCA) is applied therefore to see if the number of inputs (independent variables *x)* could be reduced while maintaining a similar model accuracy. All the dependent variables (21 features in total) that were found related to bird strike severity (significance level < 0.05) were used as the input of PCA. Figure A.6. shows however the explained variance almost increases linearly with respect to the number of principal components. This means that all the features are quite independent of each other. So generally, the benefit of reconstructing the input features to reduce the dimension of the input is not very significant.Therefore all 21 independent variables were maintained in the logistic regression described in Table A.1.

10

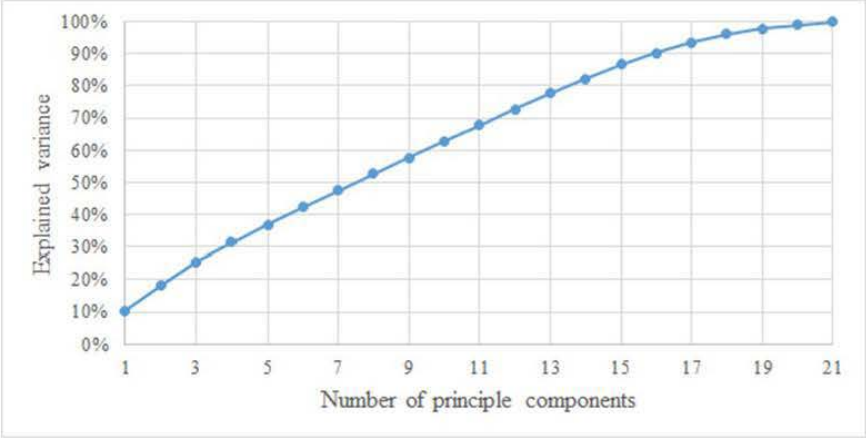


Figure A.6. Principal Component Analysis result

Table A.1. Independent and dependent variables labels

Label			
Notaion	**Meaning**	**Data range**	**Note**
y	Severity of the incident	0/1/2	0: No damage 1: Moderate damage 2: Substantial damage
Features			
Notaion	**Meaning**	**Data range**	**Note**
x1∼x12	Month	0/1	e.g., x5=1 means the month was May.
x13∼x16	Time of day	0/1	x13: Whether it happened in the daytime. x14: Whether it happened in the night. x15: Whether it happened in the dawn. x16: Whether it happened in the dusk.
x17	Aircraft mass	1 to 5	1: less than 2,250 kg 2: 2251-5700 kg: 3: 5,701-27,000 kg; 4: 27,001-272,000 kg: 5: above 272,000 kg Missing data are filled with the average.
x18	Speed	>=0	Missing data are filled with the average.
x19	height	>=0	Missing data are filled with zeros.
x20∼x23	The phase of flight	0/1	x20: Whether the phase was Approach. x21: Whether the phase was Landing Roll. x22: Whether the phase was Climb. x23: Whether the phase was Take-off Run.
x24	The cloud condition	0 to 2	0: No cloud 1: Some cloud 2: Overcast Missing data are filled with the average.
x25	Whether it was raining	0/1	Missing data are filled with zeros.
x26	Whether it was foggy	0/1	Missing data are filled with zeros.

A.3. Results

The regression results are summarized in Table A.2.. According to the results, high velocity, high altitude, denser clouds, and fog can increase the probability of severe damage, while higher mass and rain can decrease the probability of severe damage. In terms of time, severe damage is more likely to happen during winter, dusk, and nights. In terms of the phase of flight, more severe damage tends to occur during the ”climb” phase of flight.

Table A.2. Logistic Regression Results

$ln(y_i/1-y_i) = b_i + a_1x_1 + a_2x_2 + ... + a_nx_n$		Estimation	Significance level	95% confidence interval	
				Lower bound	Upper bound
Thresholds	b1	-0.82	0	-1.143	-0.496
	b2	1.613	0	1.287	1.939
Parameters	a1	-0.091	0.272	-0.254	0.071
	a2	-0.567	0	-0.771	-0.363
	a3	-0.214	0.027	-0.404	-0.024
	a4	-0.787	0	-0.955	-0.62
	a5	-1.195	0	-1.378	-1.012
	a6	-1.605	0	-1.818	-1.393
	a7	-1.07	0	-1.265	-0.875
	a8	-0.993	0	-1.193	-0.794
	a9	-0.819	0	-1	-0.637
	a10	-0.456	0	-0.616	-0.296
	a11	-0.194	0.017	-0.352	-0.035
	a12	0	Note: Redundant variable		
	a13	-0.144	0.102	-0.317	0.028
	a14	0.36	0	0.182	0.538
	a15	0.04	0.773	-0.229	0.309
	a16	0.925	0	0.668	1.183
	a17	-0.396	0	-0.435	-0.357
	a18	0.0014	0.048	1.10E-05	0.003
	a19	8.69E-05	0	5.95E-05	0
	a20	0.447	0	0.24	0.654
	a21	0.047	0.699	-0.191	0.284
	a22	1.099	0	0.882	1.316
	a23	0.819	0	0.581	1.057
	a24	0.252	0	0.188	0.316
	a25	-0.464	0	-0.712	-0.215
	a26	0.437	0	0.212	0.661

[4.1.2] APPENDIX B. Count of Strikes by Species (or closest description)

SPECIES_ID	SPECIES	COUNT
UNKBS	Unknown bird - small	3415
UNKBM	Unknown bird - medium	3221
UNKB	Unknown bird	1664
NE1	Gulls	845
K3302	Red-tailed hawk	761
K5114	American kestrel	761
O2111	Rock pigeon	749
R1101	Barn owl	604
ZT002	Western meadowlark	535
YI009	Cliff swallow	502

O2205	Mourning dove	483
UNKBL	Unknown bird - large	358
YH004	Horned lark	288
ZX3	Sparrows	278
K33	Hawks	213
YI005	Barn swallow	211
NE120	Western gull	181
J21	Ducks	165
N6016	Western sandpiper	163
YL001	European starling	159
N5111	Killdeer	156
NE121	California gull	150
J2204	Canada goose	139
ZC204	American pipit	133
J2104	Northern pintail	130
R2008	Burrowing owl	126
1C2201	Brazilian free-tailed bat	117
Y	Perching birds (y)	111
1F41	Striped skunk	107
J2109	Mallard	106
K1002	Turkey vulture	100
I1102	Great blue heron	97
YI	Swallows	96
1D11	Black-tailed jackrabbit	95
K3101	White-tailed kite	87
YM1102	American crow	86
M7005	American coot	82
ZX303	Savannah sparrow	79
T1009	White-throated swift	72
ZT1	Blackbirds	70
R	Owls	69
NE141	White-headed gull complex	68
J22	Geese	61
1F11	Coyote	56
J2210	Greater white-fronted goose	53
ZX018	House finch	51
K5102	Peregrine falcon	50
N6013	Dunlin	46
N6024	Least sandpiper	44
O22	Doves	44

K3305	Swainson's hawk	42
N5105	Black-bellied plover	42
J2131	Northern shoveler	39
H2002	Brown pelican	37
1G12	Mule deer	36
ZX329	White-/golden-crown sparrow complex	36
J2103	American wigeon	30
I1105	Black-crowned night-heron	29
J2140	Ruddy duck	29
N6	Sandpipers, curlews, phalaropes, allies	29
Z6004	Swainson's thrush	28
ZS009	Yellow-rumped warbler	28
J2106	Green-winged teal	26
J	Ducks, geese, swans	25
NE104	Ring-billed gull	25
R2203	Great horned owl	25
ZX110	Western tanager	25
ZZ201	House sparrow	25
Z6007	American robin	24
1C22	Free-tailed bats	23
1F131	Red fox	23
H4105	Double-crested cormorant	23
1A1	Virginia opossum	22
J2202	Snow goose	22
K3312	Ferruginous hawk	22
Y9018	Pacific-slope flycatcher	22
I1302	Great egret	21
R2004	Short-eared owl	21
Z6014	Hermit thrush	21
ZX315	Song sparrow	21
K3311	Cooper's hawk	20
ZT103	Brewer's blackbird	20
ZD102	Cedar waxwing	19
ZS014	Yellow warbler	19
1C2	Microbats	18
Y9008	Western kingbird	18
YI010	Tree swallow	18
ZT101	Red-winged blackbird	18
NE203	Caspian tern	17

ZS007	Wilson's warbler	17
ZX000	Finches, Euphonias	17
F1002	Western grebe	16
J2134	Gadwall	16
F1009	Western/Clark's grebe complex	15
UNKBB	Unknown bird or bat	15
ZL004	Warbling vireo	15
ZX304	Fox sparrow	15
K2001	Osprey	14
N	Shorebirds	14
O21	Pigeons	14
O2110	Band-tailed pigeon	14
YM1201	Common raven	14
1E3402	California ground squirrel	13
K3502	Northern harrier	13
NE101	Herring gull	13
ZS008	Common yellowthroat	13
ZS020	Townsend's warbler	13
ZT104	Brown-headed cowbird	13
1D2	Rabbits	12
K3206	Golden eagle	12
ZX309	White-crowned sparrow	12
ZX314	Lincoln's sparrow	12
K5105	Merlin	11
1F31	Raccoon	10
N5123	Semipalmated plover	10
N6201	Red-necked phalarope	10
NE2	Terns, Noddies	10
O2203	Eurasian collared dove	10
YI012	Northern rough-winged swallow	10
Z6017	Varied thrush	10
1C2102	Hoary bat	9
I11	Herons	9
I13	Egrets	9
J2136	Canvasback	9
J2139	Lesser scaup	9
T1	Swifts	9
T3003	Anna's hummingbird	9
YM402	Yellow-billed magpie	9
ZS	New World wood-warblers	9

ZS013	Orange-crowned warbler	9
ZX104	Black-headed grosbeak	9
ZX305	White-throated sparrow	9
ZX328	Dark-eyed junco	9
1D22	Desert cottontail	8
1F61	Domestic cat	8
E1001	Common loon	8
K51	Falcons, kestrels, falconets	8
L4201	Ring-necked pheasant	8
N6039	Wilson's snipe	8
F	Grebes	7
F1001	Eared grebe	7
I1306	Snowy egret	7
J2142	Bufflehead	7
K3304	Red-shouldered hawk	7
NE106	Glaucous-winged gull	7
YI011	Violet-green swallow	7
1F12	Domestic dog	6
1F4	Skunks	6
J2216	Snow goose/Ross's goose complex	6
N6033	Greater yellowlegs	6
N6103	Whimbrel	6
T1007	Vaux's swift	6
T3002	Rufous hummingbird	6
Y9009	Ash-throated flycatcher	6
Z5201	Northern mockingbird	6
ZX017	American goldfinch	6
F1003	Pied-billed grebe	5
J2154	Diving duck (Aythya)	5
L6001	Wild turkey	5
N6006	Willet	5
N6019	Sanderling	5
N6034	Long-billed dowitcher	5
N6104	Long-billed curlew	5
N6203	Red phalarope	5
NE217	Least tern	5
O2	Pigeons, doves	5
S5210	Common poorwill	5
Y9007	Say's phoebe	5
Y9017	Hammond's flycatcher	5

YI013	Cave swallow	5
ZS027	MacGillivray's warbler	5
1D	Lagomorphs (rabbits, hares)	4
2D01	Gopher snake	4
H2	Pelicans	4
J2146	Cinnamon teal	4
K5113	Prairie falcon	4
N8203	Black-necked stilt	4
Z6021	Mountain bluebird	4
Z8007	Blue-gray gnatcatcher	4
Z9002	Ruby-crowned kinglet	4
ZT102	Yellow-headed blackbird	4
ZX306	Golden-crowned sparrow	4
1C21	Vesper bats	3
1C2104	Little brown bat	3
1G11	White-tailed deer	3
2D	Snakes	3
F1004	Horned grebe	3
H2003	American white pelican	3
H4107	Brandt's cormorant	3
I1110	Green heron	3
J2113	Greater scaup	3
J2151	Surf scoter	3
J2303	Tundra swan	3
K	Raptors: Hawks, eagles, vultures, kites, osprey, falcons, caracaras	3
N51	Plovers	3
N5106	Snowy plover	3
N8103	American avocet	3
NE115	Bonaparte's gull	3
NE222	Elegant tern	3
S5211	Lesser nighthawk	3
S5213	Common nighthawk	3
T3	Hummingbirds	3
Y9030	Black phoebe	3
YI001	Purple martin	3
Z4003	House wren	3
ZT001	Eastern meadowlark	3
ZX024	Lesser goldfinch	3
ZX313	Chipping sparrow	3

ZX403	California towhee	3
1C2122	Western pipistrelle	2
1F13	Foxes	2
1F132	Common gray fox	2
E1002	Red-throated loon	2
F1006	Clark's grebe	2
H41	Cormorants	2
H4106	Pelagic cormorant	2
I1202	American bittern	2
J2112	Ring-necked duck	2
J2116	Common goldeneye	2
J2118	Hooded merganser	2
J2130	Common merganser	2
J2212	Cackling goose	2
L41	New World quail	2
M4001	Sandhill crane	2
M7001	Sora	2
N6001	Upland sandpiper	2
N6014	Baird's sandpiper	2
N6030	Short-billed dowitcher	2
NE207	Gull-billed tern	2
T3004	Black-chinned hummingbird	2
T3005	Allen's hummingbird	2
T3008	Costa’s hummingbird	2
X6101	Northern flicker	2
Y9006	Acadian flycatcher	2
Y9011	Western wood-pewee	2
YI003	Bank swallow	2
YL101	Common myna	2
YR401	Bushtit	2
Z4001	Marsh wren	2
Z5301	Gray catbird	2
ZH002	Loggerhead shrike	2
ZL005	Red-eyed vireo	2
ZS019	Nashville warbler	2
ZS031	Hermit warbler	2
ZT203	Bullock's oriole	2
ZX109	Scarlet tanager	2
1C2112	Evening bat	1
1C2204	Western mastiff bat	1

1D12	White-tailed jackrabbit	1
1D13	Antelope jackrabbit	1
1D21	Eastern cottontail	1
1E3	Prairie dogs, marmots, squirrels	1
1E33	Tree Squirrels	1
1E3303	Eastern gray squirrel	1
1F1	Canids	1
1F52	American badger	1
2A	Turtles	1
2D10	California kingsnake	1
E1003	Pacific loon	1
G2201	Northern fulmar	1
I1	Herons, egrets, bitterns	1
I1301	Cattle egret	1
I6107	White-faced ibis	1
J2107	Blue-winged teal	1
J2115	Muscovy duck	1
J2141	Redhead	1
J2209	Brant	1
J2214	Egyptian goose	1
J2215	Ross's goose	1
K3102	Black kite	1
K3201	Bald eagle	1
K3310	Sharp-shinned hawk	1
L3202	Rock ptarmigan	1
L4302	Gray partridge	1
M7	Rails	1
N5104	American golden-plover	1
N6028	Semipalmated sandpiper	1
N6035	Red knot	1
NE	Gulls, terns, kittiwakes	1
NE102	Mew gull	1
NE122	Heermann's gull	1
NE204	Common tern	1
NE220	Royal tern	1
NF101	Black skimmer	1
NG102	Pigeon guillemot	1
NG201	Common murre	1
P11	Parrots	1
P1114	Budgerigar	1

P1118	Lilac-crowned parrot	1
P1303	Yellow-chevroned parakeet	1
Q2201	Greater roadrunner	1
R2001	Snowy owl	1
Y9	Tyrant (New World) flycatchers	1
Y9028	Olive-sided flycatcher	1
YM1	Crows, ravens	1
YM403	Black-billed magpie	1
YS104	Pygmy nuthatch	1
Z4	Wrens	1
Z4005	Rock wren	1
Z6	Thrushes	1
Z6001	Western bluebird	1
Z6016	Gray-cheeked thrush	1
Z8006	Wrentit	1
ZL006	Cassin's vireo	1
ZS001	Canada warbler	1
ZS004	Black-and-white warbler	1
ZS028	Yellow-throated warbler	1
ZS029	Black-throated gray warbler	1
ZT107	Tricolored blackbird	1
ZT2	Orioles	1
ZT204	Hooded oriole	1
ZT304	Great-tailed grackle	1
ZX010	Pine siskin	1
ZX013	Purple finch	1
ZX014	Red crossbill	1
ZX034	Lawrence's goldfinch	1
ZX107	Lazuli bunting	1
ZX111	Summer tanager	1
ZX308	Lark sparrow	1
ZX316	Bell's sparrow	1
ZX320	Brewer's sparrow	1
ZX401	Eastern towhee	1
ZX404	Spotted towhee	1
ZX501	Lapland longspur	1

Task 4.2. Noise Exposure and Environmental Justice

Deliverables: Summary report for (1) noise estimations using BTS Noise data at CA airports taking into considerations FAA's new Environmental Survey for noise annoyance levels and Environmental Justice variables; and (2) difference in noise levels with electric (i.e. green aircraft) operating at the noisiest airports and on routes that can accommodate smaller electric/green aircraft.

Acceptance Criteria: A document explaining the outputs for noise contours at CA airports for a base-case scenario (without green/electric aircraft) and a futuristic scenario (with green/electric aircraft). With regard to Task 4.2., the deliverables will address and satisfy all of the relevant Task 1 Acceptance Criteria.

[4.2] 1. Introduction

California has the highest percent of population exposed to transportation noise in the U.S. with a total of 6.5% exposed to 60+ dB LeqA (Seto & Huang, 2023), which includes aviation, road, and rail traffic. Noise has historically been the predominant aviation environmental concern of the public, pioneering policies in the late 1960's and early 1970's to minimize negative environmental impacts associated with aircraft noise while maximizing the benefits of airports and their surrounding communities[11]. Over the past five decades the number of people in the U.S. exposed to aviation noise has dropped substantially even as the number of flights has soared. Population exposure to severe noise levels related to aircrafts declined from seven million people in 1970 to approximately 400 thousand today, (FAA,2023). Two major mechanisms allowed for the effectiveness of noise mitigation policies: hazard reduction and exposure reduction. The most important one was hazard reduction, or reducing noise pollution at the source, with the transition to quieter aircrafts, and the second one was compatibility land use planning (exposure reduction) that has seeked to prevent new residential or other noise sensitive development near airports together with noise mitigation techniques on buildings or noise abatement procedures for flights (CRS, 2021).

Noise pollution and exposure reduction remain the two key strategies to mitigate the negative effects of aircraft noise and they rely on effectively measuring noise as well as correlating the noise metrics to annoyance, or measuring the effect of noise on people and airport communities. Noise metrics are based on physical properties for which sophisticated modeling techniques have been developed over time; and the second is typically determined through rigorous sociological surveys that measure people's reactions to weighted average of noise exposure over time (cumulative metrics). Noise is considered, however, an understudied element in transportation health impact analysis although there is both data and capacity for

[11] The Control and Abatement Act of Aircraft Noise and Sonic Boom Act in 1968 and the Noise Control Act of 1972.

noise-related health analysis and improvement of equity (Fox et al., 2023). With the recent incorporation of environmental justice policies in the U.S. and California, there is a great potential for noise exposure reduction from a qualitative perspective. By focusing on disadvantaged communities and those that are overburdened by overall environmental pollution, a new strategy for reducing the impacts of noise pollution can emerge by focusing on the population's propensity to suffer from health-related adverse effects of noise, or by reducing noise vulnerability.

Section 1 presents an overview of different types of noise metrics and modeling data available (1.1.), then how to define thresholds that gauge noise impact on people considering recommendation thresholds for policy and planning using Day-Night Averages (DNL) or Community Noise Equivalent Levels (CNEL) (1.2.).

Section 2, Methods and Data, recapitulates the noise data used in the exposure analysis (2.1.) and the methods developed to calculate exposure including the environmental justice indicators (2.2.1 and 2.2.2) and airport noise footprints. Section 2.3. Presents the rationale for stipulating the effects of aircraft electrification on noise in the near-future.

Results Section 3, has three major parts; 3.1. presents noise exposure results; 3.2. focuses on GIS assessment of noise contours and environmental justice indicators of exposed census tracts; and 3.3 an assessment of the potential effects of aviation electrification on noise exposure:

- Section 3.1. Uses the National Transportation Noise Map models of 2018 available for 53 airports to update the exposure analysis of airport communities in the state taking into consideration FAA's new dose-response curve to noise annoyance that indicates an increase of the population's sensitivity to noise annoyance thresholds from 65 dBA to 50 dBA in Day-Night Averages(DNL) (subsection 3.1.1). Subsection 3.1.2 shows the airport noise footprint results.
- Section 3.2. Presents an overview of environmental justice emergence in planning policies, then assesses the current noise exposure of the population given their current environmental burden levels and population characteristics available though the Office of Environmental Health Hazard Assessment (OEHHA) CalEnviroScreen Tool. The goal is to evaluate whether sensitive or disadvantaged communities are disproportionately exposed to aviation noise. The assessment of these environmental justice indicators is done at the state level and at the county level.
- Section 3.3 addresses the expected effect of emerging aircraft electrification technology in noise pollution reduction. Insights are drawn from studies focused on the effect of aircraft electrification for emissions reduction and a case study of VNY airport electrification effects on noise. A three-step approach is presented to stipulate which airports have the highest potential for fleet electrification in California, and consequently which airports will more likely see noise footprint reduction directly related to aircraft electrification.

1.1. Measuring Noise and Annoyance Thresholds

1.1.1. Noise Metrics: Magnitude, Frequency and Duration

Magnitude[12], frequency[13] and duration[14] are physical properties of sound that can be directly measured, however there is much discussion on appropriate metrics of sound due to environmental variables as well as human perception or acceptance of noise. Various methods have been developed to measure overall exposure produced by a noise event.

Noise metrics intended specifically for measuring aircraft noise and noise associated with aircraft operations to and from airports use decibels (dB) that are weighted to give value to human frequency hearing ranges, also called A-weighted decibels (dBA). These metrics are generally grouped based on a single noise event[15] or alternatively based on cumulative noise. ALUP Handbooks and other planning documents traditionally focus on the latter in the interest of community planning as they describe weighted averages of measurements of noise over time and better reflect annoyance levels of those that are continuously exposed to noise pollution.

This study uses Equivalent noise level (*Leq*) which represents sound level averages in dB (sound energy) over time that takes into account the cumulative effect of multiple noise events. The more frequent the noise events over the measurement period, the closer *Leq* will be to the maximum sound levels measured for a single noise event (*Lmax*), as opposed to low-activity general aviation airports for example, where *Leq* may not be much higher than the ambient

---

[12] Magnitude or strength of a sound (acoustic energy) is determined by how much air particles are displaced from equilibrium by sound pressure waves. Measured in decibels (tenth of a Bell) or dB and uses a logarithmic scale; and loudness is perceived as a relative rather than an absolute term. Human scale: 0 = faintest sound level a healthy unimpaired human ear can detect to more than 140 dB (120 and above being considered as deafening sounds). A 10 dB increase is perceived as a doubling of loudness at any magnitude. If equal sounds magnitudes are combined doubles the sound energy but only produces a 3 dB increase in magnitude (barely perceptible)

[13] Frequency is the tonal quality, measured by wave lengths, or frequency in cycles per second (hertz, Hz) High pitch sounds have short wavelengths and low-pitch sounds have long wavelengths. More often sounds are a mixture of different frequencies.Human scale: 20 Hz – 20,000 Hz, but we do not hear all frequencies in this range equally well, very low and very high frequency sounds are perceived to be less than mid-range frequency sounds. A-weighted dB scale with measurement units expressed as dBA (Table D1 Handbook 2011).

[14] Duration is the length of time over which it occurs. Sound levels vary over time, therefore dB refers to an instantaneous measurement that is often averaged over time.

[15] Single event metrics:

Instantaneous sound levels (*Lmax)* measured on a continuous basis for each instant during this cycle where a significant point is the max sound level (*Lmax* – determinant of speech interference for example). It provides no information however on the duration of a sound.

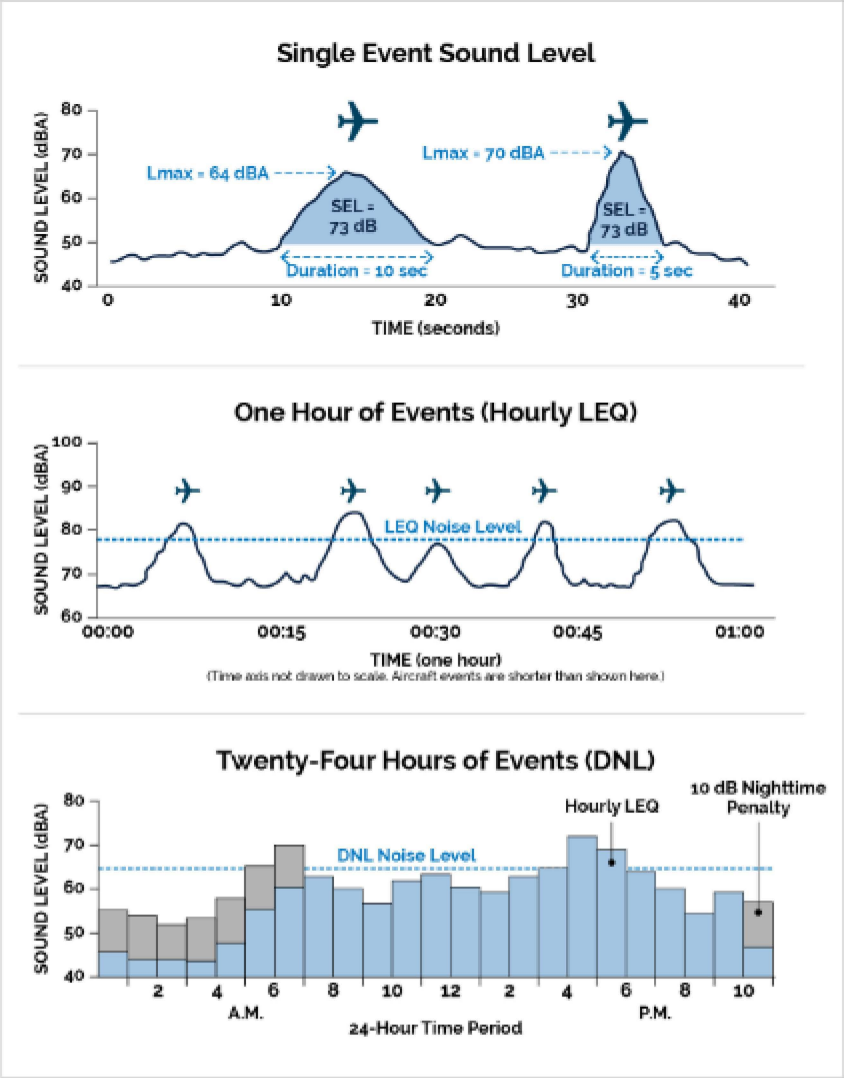
Single-event Noise Exposure Level (SENEL in CA); or *Sound Exposure Level (SEL*, for the FAA) indicates the level of a continuous one-second sound which contains the same amount of energy as the complete noise event. For most aircraft noise events, SENEL is about 5 to 10 dB higher than *Lmax*, the shorter the duration of the noise event the closer the two metrics will be.

noise level (see Figure 1 for a sound level baseline,and Figure 2 comparing cumulative and single-event sound metrics used in this report)

For noise compatibility land use purposes the Federal Aviation Administration (FAA) determined the need to adopt the Day-Night Average Sound Level (*DN*L) (FAA Order 1050.1F, Appendix B), equivalent to the Community Noise Equivalent Level (*CNEL)* in California, which is a time-weighted metric. DNL and CNEL seek to compensate for the increased sensitivity to noise during nighttime hours. This increased sensitivity is commonly associated with the drop in ambient noise levels between daytime and nighttime in a typical community which is highly variable depending on the airport operations and the community characteristics, requiring location specific attributes such as ambient sound level measurements and community annoyance threshold (further discussed in section 1.2.2.)



Figure 1. Comparative Noise Levels (Source: FAA: https://www.faa.gov/regulations_policies/policy_guidance/noise/basics)



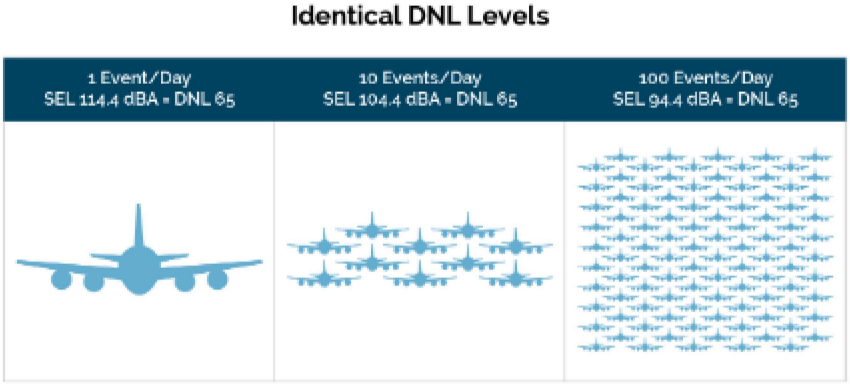


Figure 2. Comparison of Single Event Sound Levels (SEL, or SENEL in California), Equivalent Sound Level (Leq), and Cumulative Sound Level measures in Day-Night Averages (DNL). (Source: FAA, https://faabostonworkshops.com/project-information/aircraft-noise-overview/)

1.1.2. Noise Model: National Transportation Noise Map (NTNM)

The noise model used in this study is the National Transportation Noise Map (NTNM) from the Bureau of Transportation Statistics (BTS). NTNM has been published every 2 years since 2016 and due to the complexity and data processing requirements the publications have one gap year; therefore these noise models exist for 2016, 2018, and 2020. Current FAA policy on noise exempts airport operations from noise analysis when their estimated numbers of propeller and jet operations result in DNL 60 dB contours of less than 1.1 square miles that extend no more than 12,500 feet from start of takeoff roll[16]. Therefore a total of 53 airports in California are captured by the 2018 NTNM (see airport list on Appendix A).

The NTNM is developed using 24 hr equivalent A-weighted sound level (dBA *Leq24*), and the results represent the approximate average noise energy due to aviation operations over a 24 hours period at airports, computed by the Aviation Environmental Design Tool (AEDT[17]). The NTNM report explains that noise levels are calculated at receptor locations in AEDT, for each airport a dynamic gridding approach is used to define the receptor set. The grid refinement uses the linear Integrated Noise Model (INM) approach, which varies per airport, and a manual process of contour review intensifies the refinement levels until a smooth 65 dB contour is produced. The noise level cutoff is at 45 dB(A) *Leq* 24. The model assumes acoustically soft ground, therefore sound levels for large areas with acoustically hard ground (water/ pavement) may be underestimated. Terrain and shielding effects are not included, therefore noise levels may be overestimated in certain landscape configurations. Atmospheric absorption of noise is assumed based on NOAA Global Summary of the Day averaged across a year specific to each airport. Because the AEDT models noise based on measured source data from actual aircraft, the uncertainty on the ground increases as the noise level decreases due to distance from the aircraft and the receptor. This is also due to local effects of shielding, ground type variation, absorption, refraction and scattering from landscape objects that are not included in the model.

The NTNM report states that noise contour modeling (INM) is based on where aircraft fly and how often. For major air carriers and other surrounding metropolitan area airports an extensive amount of data is usually available for creating airport noise contours. For general aviation data may be scarce and use of estimates may become necessary. Sources of data used to produce noise contour include radar flight track data, control tower counts of aircraft operations, airport management records, wind data, interviews with airport personnel, projected airport activity etc. The typical precision of INM is about 3 dB. The NTNM report states that for greater precision,

[16] No noise analysis is needed for projects involving Design Group I and II airplanes (wingspan less than 79 feet) in Approach Categories A through D (landing speed less than 166 knots) operating at airports whose forecast operations3 in the period covered by the National Environmental Policy Act (NEPA) document do not exceed 90,000 annual propeller operations (247 average daily operations) or 700 annual jet operations (2 average daily operations).

[17] The AEDT tool used for the 2018 NTNM is version 3a. The 2018 flight operations data come from an aircraft movement dataset from the FAA Office of Environment and Energy, air traffic counts from the Air Traffic Activity Data System (ATADS), the Air Route Traffic Control Centers (ARTCCs) and major Terminal Radar Approach Control helicopter operations are not included, but military operations at joint-user or commercial airports were included. (TRACON) facilities are also considered.AEDT documentation is available on the AEDT Support website: https://aedt.faa.gov

approximately 1dB, flight track data from radar and/or a permanent noise monitoring system, can be installed.

1.2. Noise Effect on People, Community Annoyance Thresholds, and Policy

Understanding noise effects on people, or human response to noise, is key to determine the thresholds of acceptable and unacceptable sound levels, also known as annoyance levels. These thresholds, further explained in the subsection below, allow the development of strategies for noise mitigation policies such as compatibility planning (i.e. noise ordinances) and noise abatement architectural and engineering solutions (alternate routes, building sound barriers or walls, installing double-pane windows in exposed buildings, etc).

Airport operations noise effects on people are varied and complex, but it is known to be one of several factors producing stress related health effects including annoyance, sleep disturbance, cardiovascular disease (heart disease, high blood pressure, stroke), digestive disorders, and increased risk of cognitive impairment in children in schools.

Three main effects from noise can be identified based on the 2011 ALUP Handbook: physiological, behavioral, and subjective (see below).

- physiological can be temporary or permanent, they include startle reaction, sustained sleep interference, hearing impairment, and the stress-related effects of noise such as cardiovascular diseases and digestive disorders (ulcers).
- behavioral effects refer to the interference with human activities, such as interference on speech, concentration, leisure, and rest. The maximum sound level that will permit a fully intelligible conversation indoors is 45 dB, a satisfactory conversation (95% intelligibility) can be obtained with a sound level of up to 65 dB. The usual design objective for aircrafts operating during normal school hours is Leq of 45 dB, and to mitigate general effects of noise on learning schools are encouraged to
- subjective effects are described in terms of annoyance and are unique to every individual because of the diverse ways people react to the unpleasant aspect of noise, for example, noise duration and how often it occurs, the predictability, tonal qualities of the noise, the demographic and residential dwelling characteristics of the individual, the experience and expectations regarding noise levels in the community, the activity in which the individual in engaged at the time of noise, perceptions regarding the preventability and health effects of noise, etc.

1.2.1. Community Annoyance Thresholds: FAA Neighborhood Environmental Survey (NES)

Current noise policies used in planning and transportation are informed by a dose-response curve also known as the “Schultz Curve”, representing the community response to noise. The Federal Interagency Committee on Noise (FICON) research on human annoyance to noise used a dose-response curve in 1992 to determine that DNL of 65 dB highly annoys 12.3% of persons, making 65 dB a key threshold for noise policies up to today. FAA’s new dose-response curve to noise annoyance that indicates an increase of the population’s sensitivity to noise annoyance thresholds from 65 dBA to 50 or 55 dBA.

The FAA’s most recent effort to quantify the impacts of noise exposure on communities through a multi-year national survey, known as Neighborhood Environmental Survey (NES) updated the scientific evidence on the relationship between aircraft noise exposure and the annoyance of people living near airports (FAA, 2021). It uses the FAA INM version 7.0d to compute the noise exposure of 20 airports sampled to include at least 100 annual average daily jet operations, at least 100 people exposed to DNL greater than or equal to 65 dB and at least 100 people exposed to DNL between 60-65 dB, with a response rate of 40%. including over 10,000 people who responded and completed the survey over a 12 month period.

The results indicate that considerably more people are highly annoyed by aircraft noise exposure compared to the historical FICON data. A total of 42% of respondents were highly annoyed by aviation noise at any DNL, and this % monotonically increases as the DNL increases. 2/3 of people are highly annoyed at 65 dB. The national curve results in approximately 20% being highly annoyed at DNL 50 dB, 66% at 65 dB and 79% at 70 dB (Figures 3 and 4)

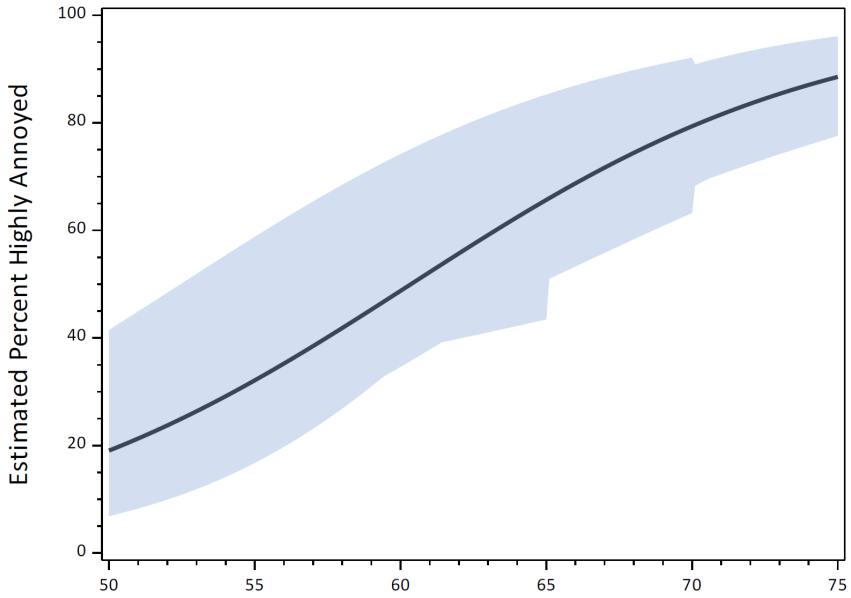


Figure 3. National dose-response curves with the national average (solid line) and the range (shaded area) of the 20 individual airports' response curves to noise. Source: FAA, 2021

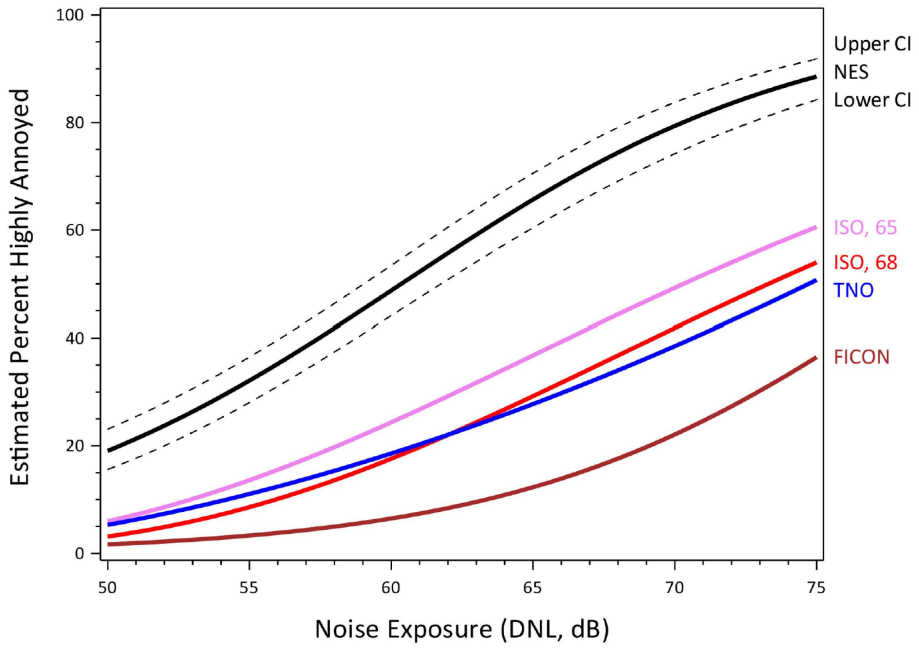


Figure 4. National dose-response curves comparatives: updated curve (NES); former dose-response curve (FICON), and other international standards (ISO: International Standard Organization, TNO: Netherlands Organisation for Applied Scientific Research). Source: FAA, 2021

1.2.2. Noise Acceptability: Community Noise Equivalent Level (CNEL)

California law requires noise metrics to be used in either CNEL or DNL (as specified in §65302(f)), but the State Aeronautics Act for evaluation of noise impact uses CNEL. Cumulative time-weighted noise metrics such as CNEL and DNL compensate for the increased sensitivity to noise during nighttime hours. According to the FAA 1050.1 Desk Reference for Noise and Noise-Compatible Land Use (FAA, 2020), both noise metrics "logarithmically average aircraft sound levels at a location over a complete 24-hour period, with a 10-decibel (dB) adjustment added to those noise events occurring from 10:00 p.m. and up to 7:00 a.m. the following morning. The 10-dB adjustment has been added because of the increased sensitivity to noise during normal night time hours and because ambient (without aircraft) sound levels during nighttime are typically about 10-dB lower than during daytime hours." CNEL exclusively includes a 4.77-dB adjustment added to noise events occurring during the evening from 7:00 p.m. and up to 10:00 p.m.to simulate a penalty of three times the number of operations during the evening. California's General Plan Noise Element Guidelines from the Office of Planning and Research (OPR), rounds the evening penalty to 5 dB (OPR, 2023).

The typical CNEL weights described above is designed for airport communities with summer or year-round operations; urban residential communities (not immediately adjacent to heavily traveled roads and industrial areas); communities with previous exposure to intruding noise but little effort is being made to control the noise, or where the community has not been exposed to

the noise previously, but people are aware that bona fide efforts are being made to control the noise; and no pure tone or impulsive character.

Further adjustment factors for obtaining normalized CNEL are suggested to correct for each airport community specificities such as seasonal corrections; correction for outdoor noise level measured in absence of intruding noise; correction for previous exposure and community attitudes; and pure tone or impulse corrections. Figure 5 shows that the range of CNEL weights based on these airport and its surrounding community characteristics, annoyance threshold can vary from 40 dB to 85 dB. Due these intricacies, CNEL metrics are highly dependent on local noise monitoring systems for airports as well as robust knowledge on community noise perception and annoyance levels driven by surveys and stakeholder engagement.

Below is the formula to calculate CNEL using SENEL as the baseline noise metric from the Handbook of Acoustic Ecology (Trouax, 1999)

$$CNEL = SENEL + 10\ log_{10}\ (N_D + 3N_E + 10N_N) - 49.4\ (dB)$$

where N_D, N_E and N_N are the number of flights during the day (7am to 7pm), evening (7pm to 10pm) and night (10pm to 7am) respectively, and SENEL is the energy mean value of the single event noise exposure level which may be calculated from the equation:

$$SENEL = NL_{max} + 10\ log_{10} t_{ea}\ (dB)$$

where NL_{max} is the maximum noise level in dBA and t_{ea}, is the effective time duration (in seconds) of the noise level (on the A scale) and is approximately equal to one-half of the duration during which the noise level is within 10 dB of the maximum.

The above expressions are simplifications of the actual procedure and only apply to a single type of aircraft and single flight path. An hourly average of the noise level (HNL) including number of flights per hour N is also used and defined as:

$$HNL = SENEL + 10\ log_{10} N - 35.6\ (dB)$$

Figure 6 provides a community noise ordinance threshold for resolution of noise complaints from the California General Plan Guidelines (OPR, 2023), with four classes of noise acceptance: normally acceptable; conditionally acceptable, normally unacceptable, and clearly unanceptable for major land use categories. The lowest level of CNEL for normally unacceptable is 50 dB for auditoriums, concert halls, amphitheaters and sports arena, outdoor spectator sports. The lowest level of CNEL for clearly unacceptable is 70 dB for playgrounds, neighborhood parks. The General Plan Guidelines on noise element further specifies that:

> "*Denotation of a land use as "normally acceptable" implies that the highest noise level in that band is the maximum desirable for existing or conventional construction that does not incorporate any special acoustic treatment. In general, evaluation of land use that*

falls into the "normally acceptable" or "normally unacceptable" noise environments should include consideration of the type of noise source, the sensitivity of the noise receptor, the noise reduction likely to be provided by structures, and the degree to which the noise source may interfere with speech, sleep, or other activities characteristic of the land use" (OPR, 2023, pp.377).

Some limitations to cumulative noise exposure and its relationship to public annoyance include the incorporation of extreme conditions, where there are infrequent loud events for low-activity airports compared to a high-activity airport with relatively many large operations. Cumulative effects also have limitations to capture the different effects on typical daytime vs. nighttime human activities. Weighted averages of nighttime noise will not capture the effects of speech or concentration interference of large operations learning institutions for example that tend to occur in more granular time frames (i.e minutes).

Table 1

Type of Correction	*Description*	*Amount of Correction to be Added to Measured CNEL in dB*
Seasonal Correction	Summer (or year-round operation)	**0**
	Winter only (or windows always closed)	**- 5**
Correction for Outdoor Residual Noise Level	Quiet suburban or rural community (remote from large cities and from industrial activity and trucking).	**+ 10**
	Quiet suburban or rural community (not located near industrial activity).	**+ 5**
	Urban residential community (not immediately adjacent to heavily traveled roads and industrial areas).	**0**
	Noisy urban residential community (near relatively busy roads or industrial areas.	**- 5**
	Very noisy urban residential community.	**- 10**
Correction for Previous Exposure and Community Attitudes	No prior experience with the intruding noise.	**+ 5**
	Community has had some previous exposure to intruding but little effort is being made to control the noise. This correction may also be applied in a situation where the community has not been exposed to the noise previously, but the people are aware that bona fide efforts are being made to control the noise.	**0**
	Community has had considerable previous exposure to the intruding noise and the noise maker's relations with the community are good.	**- 5**
	Community aware that operation causing noise is very necessary and it will not continue indefinitely. This correction can be applied for an operation of limited duration and under emergency circumstances.	**- 10**
Pure Tone or Impulse	No pure tone or impulsive character.	**0**
	Pure Tone or impulsive character present.	**+ 5**

Figure 5. CNEL-specific weighting scheme for sound annoyance thresholds

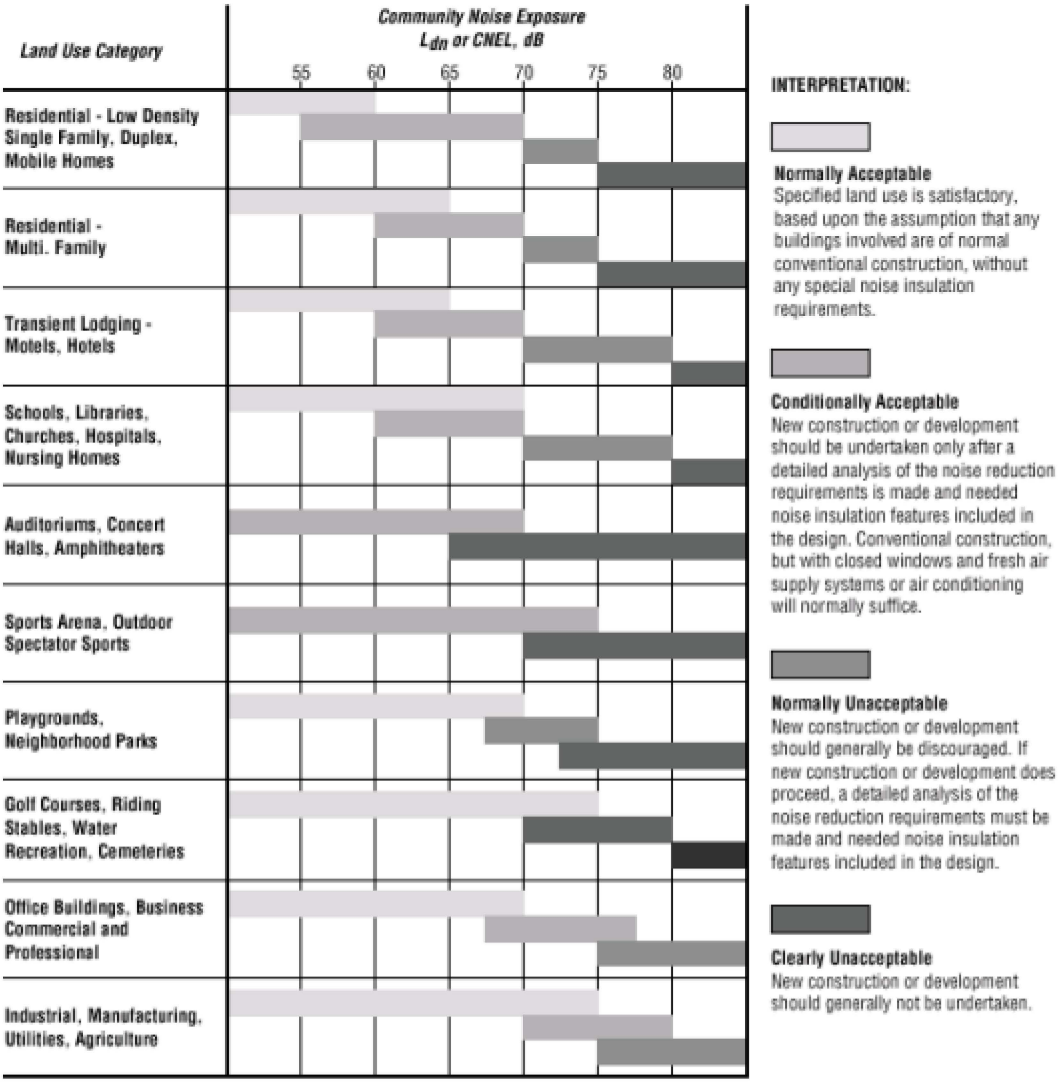


Figure 6. Community noise ordinance threshold for resolution of noise complaints from the California General Plan Guidelines (OPR, 2023)

[4.2] 2. Methods and Data

2.1. Noise Data

The noise model used in this study is the National Transportation Noise Map (NTNM) from the Bureau of Transportation Statistics (BTS) for aviation from 2018. The newest BTS noise model is from 2020, however due to COVID-19 operations anomaly, the 2018 model was chosen. The NTNM noise Geographical Information System (GIS) is a raster model with a 30m spatial resolution. The noise measurement units are in *equivalent noise level* (*Leq*) dBA over 24 hours averaged over a year with a typical precision of 3 dB.

The NTNM covers 53 out of 259 public airports in California, with noise outputs ranging from 45 dBA (minimum cutoff) to 105 dBA. These values were reclassified into 5 dBA intervals to better associate the values to the thresholds of interest identified in the FAA NES (2021) and the 2011 Caltrans ALUP Handbook (Figure 7) .

The BTS dataset, readily available in *Leq* units, underestimates the noise perception and annoyance thresholds described in DNL (based on the NES dose-response curve update) or in CNEL (based on the noise ordinance thresholds). The Leq is a 24 hour cumulative metric that does not take into account the time-related weighting factors from the DNL and CNEL and other community specific threshold adjustments of the CNEL (Figure 5). The inputs used to generate the BTS aggregate noise results uses the FAA AEDT tool, and therefore start with each individual flight and associated timestamp along with other information. After informally reaching out to noise modeling specialists in the U.S. (Blueridge consulting, Volpe, and the FAA), currently available noise data generates more generalized noise outputs for two major reasons: (1) for modeling expediency (modeling every single flight is significantly computationally intensive), and (2) there is sensitivity with some of the FAA's input data sources that require aggregation to keep some level of anonymity. Because of these reasons, as well as for properly accounting for the idiosyncrasies of each community as required in the CNEL weighting scheme (Figure 5), more precise noise modeling for regulatory compliance following DNL and CNEL is recommended to be done at the local level (airport, metropolitan region, etc). (see Table 1 for DNL and CNEL comparative overview)

	Simplified Weighting Scheme (SENEL baseline metric in dB)		
Noise Metric	+10 dB per operation between 10pm -7am	+4.77 dB per operation between 7pm-10pm	-25 dB to + 20 dB depending on airport and community specific characteristics (Figure 5)
DNL	X		
CNEL	X	X	X

Table 1. Comparative overview of DNL and CNEL weighting schemes

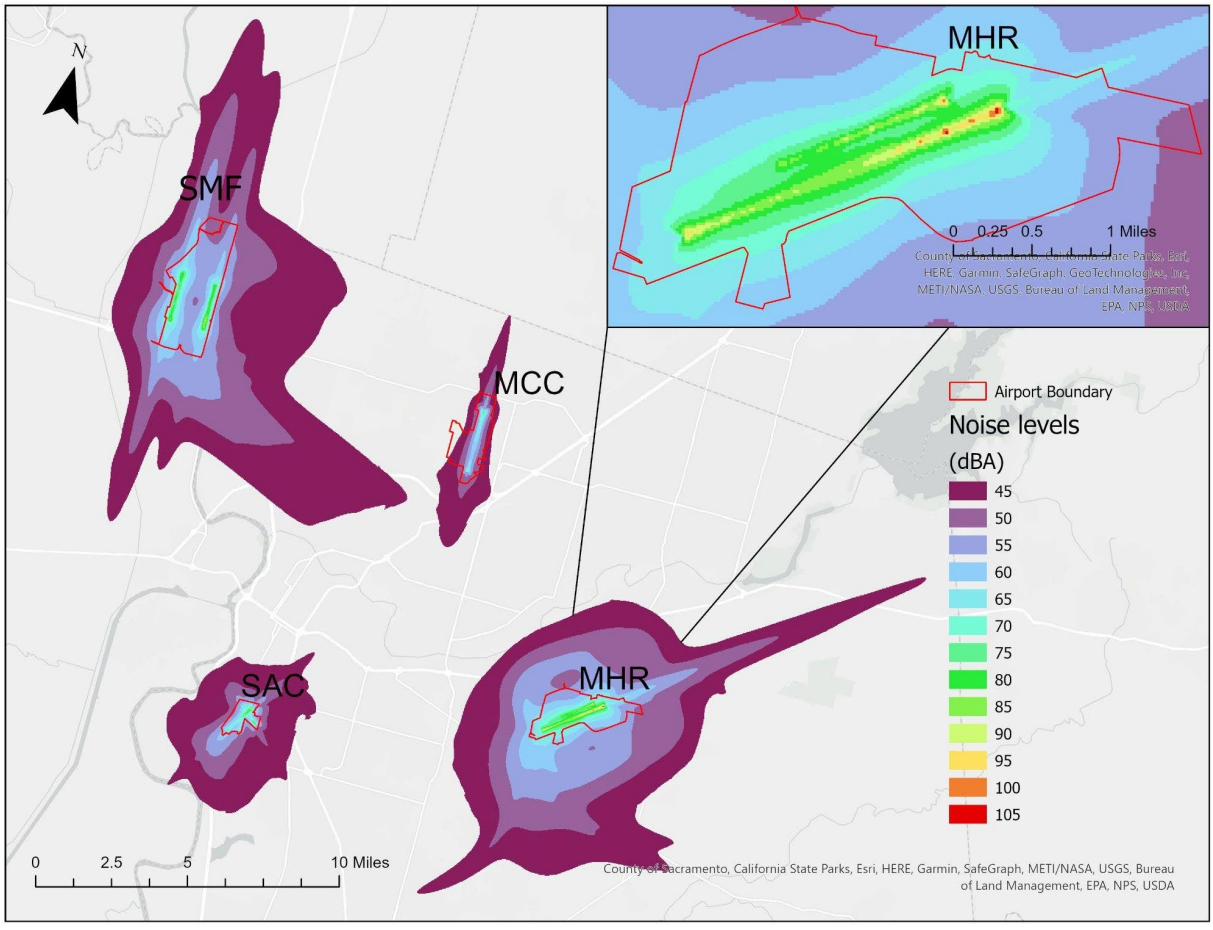


Figure 7. Noise contour examples from the NTNM 2018 aviation dataset for California Airports

2.2. Exposure Calculations and Environmental Justice Data

2.2.1. Environmental Justice Policy Context and Emergency

Environmental justice is a normative principle that is being recently integrated into actionable planning policy in the U.S., notably as an eligibility criteria within the Infrastructure Investment and Jobs Act (Public Law 117-58, 2021) and the Justice40 Initiative (Executive Order 14008, 2021). California is pioneering the integration of environmental justice norms in policy by being the first to codify the concept and incorporate it as a required element in the general plans. According to California's Environmental Protection Agency (CalEPA) “the principles of environmental justice call for fairness, regardless of race, color, national origin or income, and the meaningful involvement of community in the development of laws and regulations that affect every community’s natural surroundings, and the places people live, work, play and learn.”

One of the major efforts to act on environmental justice in policies by targeting disadvantaged communities[18] (those that are disproportionately affected by pollution and those most vulnerable to its effects) to better incorporate them in decision-making as well to lift the unfair burden of cumulative pollution effects. For this, the California’s Office of Environmental Health Hazard Assessment (OEHHA) has developed an Environmental Justice Screen Tool, CalEnviroScreen 4.0 (CES4) which based on Senate Bill 1000 (Levya, 2016), is a tool to help cities and counties incorporate environmental justice policies into their general plans. Key information from CES4 report (OEHHA, 2021) are summarized in the following section.

2.2.2. Environmental Justice Indicators

In this study, population exposure to noise and their environmental justice indicators were calculated based on a spatial overlay of the NTNM raster model for 2018 and the OEHHA CES4 indexes at the census tract level based on census data from 2019, released in October 2021. The goal is to further qualify the areas exposed to noise in terms of their average exposure to other environmental hazards and its population characteristics that render certain areas more vulnerable.

Three indicators from CES4 used in this study are described below:

- Percentiles of the pollution burden (exposure to pollutants and environmental effects): measures the the exposure of a population to a series of pollutants and the adverse

[18] “Disadvantaged communities’ means an area identified by the California Environmental Protection Agency Pursuant to Section 39711 of the Health and Safety Code or an area that is a low-income area that is disproportionately affected by environmental pollution and other hazards that can lead to negative health effects, exposure, or environmental degradation.” (Gov. Code, § 65302, subd. (h)(4)(A)). These communities are specifically targeted for investments such as the state’s Cap-and-Trade Program under Senate Bill 535 (De León, 2012) as well as the eligibility for infrastructure investment funds from the Infrastructure Investment Bill (2021) under the Justice40 Initiative.

environmental effects caused by pollutants. Pollution burden variables are described in Figure 8.



Figure 8. Pollution Burden Indicators (Source: OEHHA, 2021, p21)

- Percentiles of the population characteristics (sensitive population and socioeconomic factors). Sensitive populations are those with physiological conditions that result in increased vulnerability to pollutants; and socioeconomic factors are characteristics that result in increased vulnerability to pollutants. Population characteristics components are described in Figure 9.

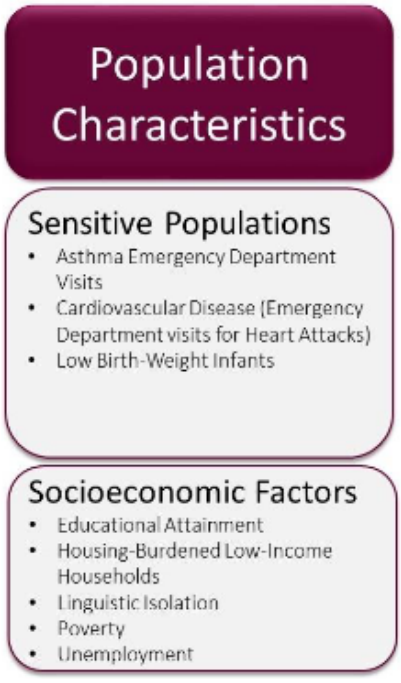
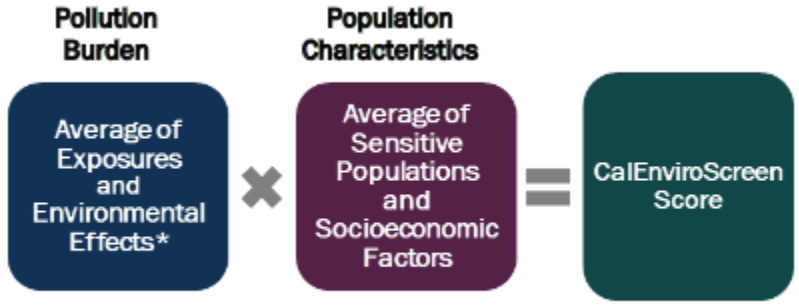


Figure 9. Population Characteristics Indicators (Source: OEHHA, 2021, p21)

- Percentiles of CES4 score (environmental injustice) CES4 score seeks to measure cumulative impacts from pollution, or the overall burden that affects health and quality of life. "*Cumulative impacts means exposures, public health or environmental effects from the combined emissions and discharges, in a geographic area, including environmental pollution from all sources, whether single or multi-media, routinely, accidentally, or otherwise released. Impacts will take into account sensitive populations and socioeconomic factors, where applicable and to the extent data are available.*" The calculation of CES4 score is described in Figure 10.



* The Environmental Effects score was weighted half as much as the Exposures score.

Component Group	Maximum Score*
Pollution Burden	
Exposures and Environmental Effects	10
Population Characteristics	
Sensitive Populations and Socioeconomic Factors	10
CalEnviroScreen Score	**Up to 100 (= 10 × 10)**

* Enough decimal places were retained in the calculation to eliminate ties.

Figure 10. Formula for Calculating CES4 Score (Source: OEHHA, 2021, pp13-14)

These indicators are considered most useful for identifying communities that score highly, which is why we chose to work with the highest percentiles of these indicators. However it is important to remember that a percentile does not describe the magnitude of the difference between two areas, for example; an area ranked in the 30th percentile is not necessarily three times more impacted that an area ranked in the 10th percentile.

One major limitation of these indicators is the spatial resolution being tied to census tracts. This means that the spatial precision of the indicators can be high for small tracts (where there is often high population density) and very low for large tracts (with typically low population densities). Local agencies such as public health departments , water districts, air districts, and metropolitan planning organizations should be contacted to determine if there is more granular information on population characteristics (more detailed than census tracts). OPR also

recommends “early community engagement, particularly with low-income communities, communities of color, sensitive populations, tribal governments , as well as organizations focused on public health and environmental justice. This can help to ensure that the location of disadvantaged communities as well as the nature of their environmental burdens, concerns, and needs are accurately identified”.

Although in this study we only use aggregate indicators (pollution burden, population characteristics and CES4 score), for a more complete analysis we highly recommend further investigating the spatial co-occurrence of noise with other critical environmental justice metrics such as the percentage of Native American, African American, and Hispanic; the percentage of children and elderly; poverty percentile; education percentile; and others.

2.2.3. Population and Census Tracts Exposure Calculation

The noise exposure of the population is calculated based on a GIS overlay of the noise model, reclassified to 5dBA intervals and the CES4 census tracts. Since census tracts have various sizes, and do not align with the noise model contours, it is not possible to accurately estimate the population exposure. In this analysis we assume that the population declared in every census tract that overlays with noise contours is potentially exposed to that noise level modeled.

In Figure 11, we highlighted in pink a census tract that is partially exposed to 45-50 dBA with a total population of 5,416; which means that in our Noise Exposure results (Section 3.1. And 3.2.) we estimate that all of this population is potentially exposed to 45-50 dBA. Some census tracts will be exposed to two different noise thresholds as we can also see in the example below (census that are red and yellow; or red and blue); will also be computed for both categories. Therefore the total population exposed for a specific noise threshold might be an overestimate of the total population exposed, notably for very large census tracts. The population and census tracts exposure assessment is inclusive of upper dBA levels:

All census tracts exposed to “65+ dBA” are exposed to aviation sound levels of a minimum of 65 dBA, i.e. [65[. Because the NTNM model cutoff is at 45 dBA, when looking at the exposure of 45+ dBA this refers to the total noise exposure. Based on the NTNM model, the highest noise level measured outside airport boundaries is 85 dBA (see section 3.1.2.). Figure 12 shows the difference between the precise areas exposed to our noise thresholds and how our overlay computes the census tracts that intersect with those contours.

To identify areas that can be prioritized for aviation noise mitigation programs and noise-related health hazards programs in we provide a hot-spot analysis at the state level focusing only on the CES4 tool environmental justice indicators; and at the county level, where more granular information on the clustering of high scores (environmental injustice) coincide with airport noise contours. Another method developed to identify more specific communities (at the census tract level) is applied by crossing “significant” and “severe” noise exposure thresholds (50 and 65 dBA) with “high” and “severe” environmental injustice burden (75 and 90 percentiles of CES4 score) (Table 2).

Table 2. Method for Identifying Priority Communities for Aviation Noise Mitigation Efforts

Noise Exposure Level	**Environmental Injustice Burden**	**Result**
50 dBA (in *Leq*)	90th percentile of CES4 score	*Community to prioritize*
65 dBA (in *Leq*)	75th percentile of CES4 score	*Community to prioritize*

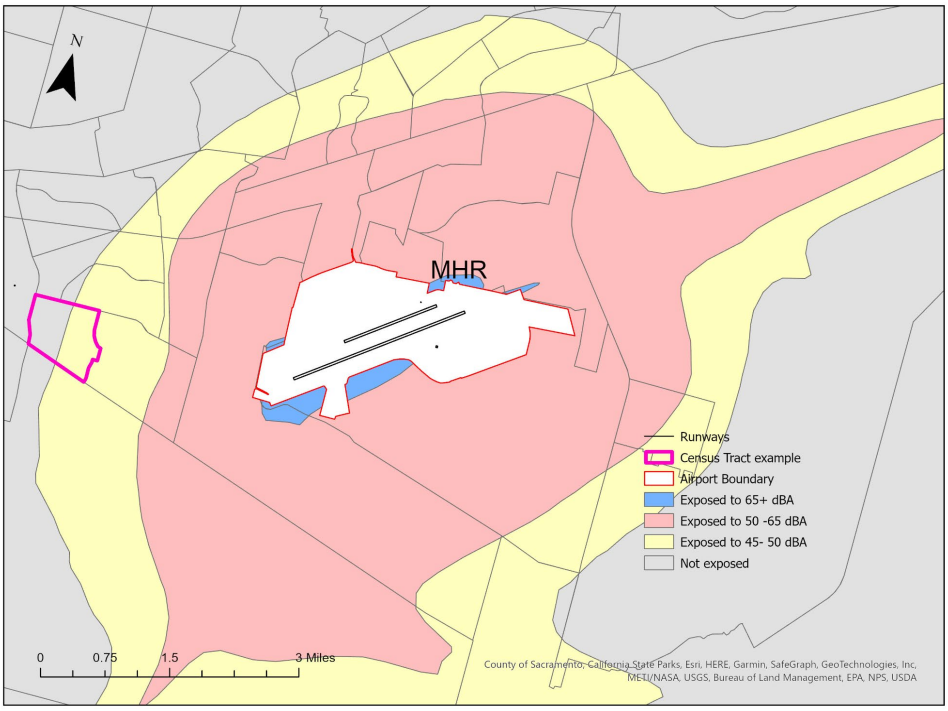


Figure 11. Example of noise contour thresholds of Sacramento Mather Airport (MHR) overlayed with CES4 census tract data.

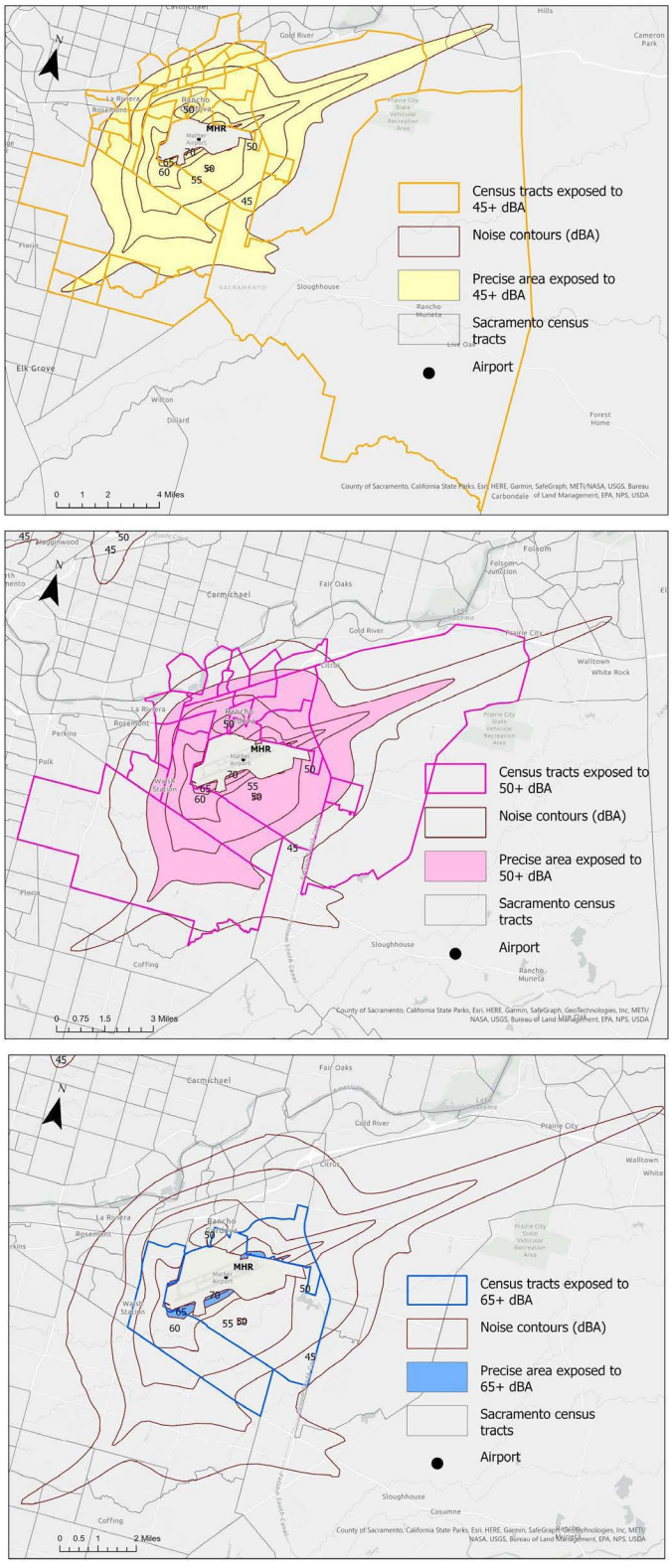


Figure 12. Overlay example and the difference between exposed areas vs. exposed census tracts

2.2.4. Airport Noise Footprint Calculation

The noise footprint is calculated in area (mi^2) for each of the 53 airports, excluding the noise measured inside the airport's boundaries. GIS processing was necessary to associate the noise exposure to a specific airport. Out of 53 airports represented in the NTNM model, 12 airports share noise contour boundaries at some dBA level forming 6 "airport noise source groups" (Table 3). Airport-level noise exposure was equally attributed when the noise level continuously neighbored two or more airports (see examples in Figures 13-16). Examples of noise source groups are the case of OXR and CMA, that share the 45 dBA noise contours (Figure 13); as well as VNY and BUR airport group (Figure 14), who share noise contours from 45 to 50 dBA. There are more complex groups where the noise levels are shared amongst three airports, such as SFO, OAK and HWD, where there is an assumption that the contours up to 50 dBA are shared between the three due to their large surface adjacency with the Bay Area (Figure 15). For the LAX, SMO, and HHR noise source group, Figure 16 shows how they all share 45 dBA noise contours, but only LAX and HHR share up to 50 dBA noise contour.

For airports that share noise contour boundaries an example of noise footprint calculation is described below:

OXR and CMA 45 dBA noise footprint (shared) = 29.86 mi^2
OXR > 45 dBA noise footprint = 3.74 mi^2
CMA > 45 dBA noise footprint = 5.23 mi^2

Total OXR noise footprint = 29.86 + 3.74 mi^2
= 33.06 mi^2

Total CMA noise footprint = 29.86 + 5.23 mi^2
= 35.09 mi^2

Table 3. Airports That Share Noise Contours (Airport Noise Source Groups)

Airport noise source groups	**Shared dBA noise level**
OXR and CMA	45 dBA (Figure 13)
VNY and BUR	45 to 50 dBA (Figure 14)
SFO, OAK, and HWD	45 to 50 dBA (Figure 15)
SJC and NUQ	45 dBA
LAX, SMO, and HHR	45 dBA (Figure 16) 50 dBA for LAX and HHR

ONT and CNO	45 to 50 dBA

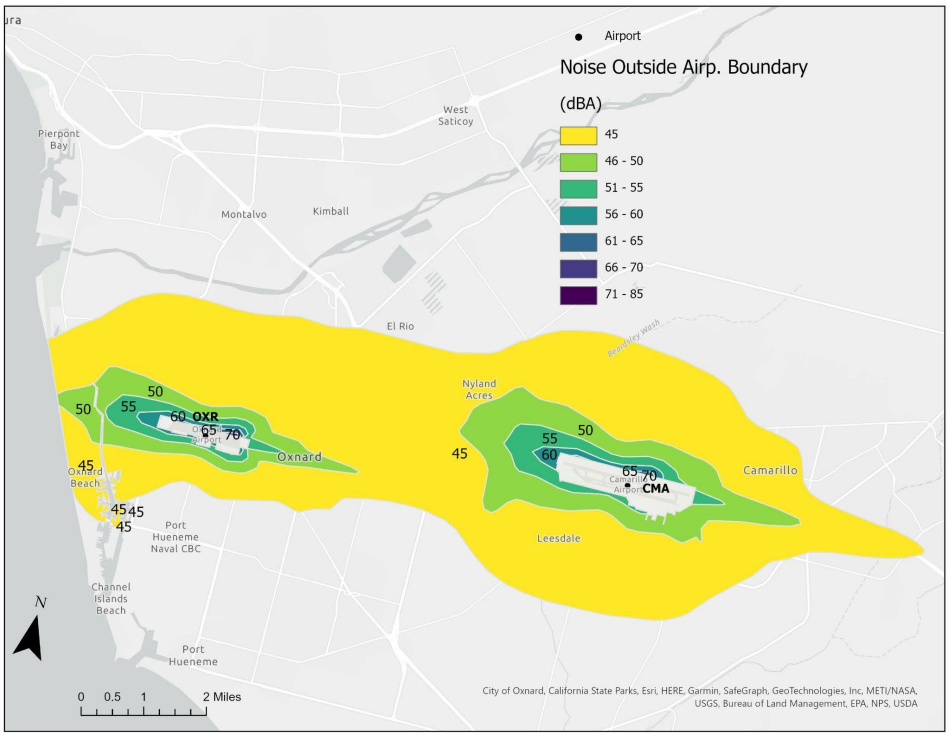


Figure 13. OXR and CMA Airport Noise Source Group Sharing 45 dBA Noise Footprint

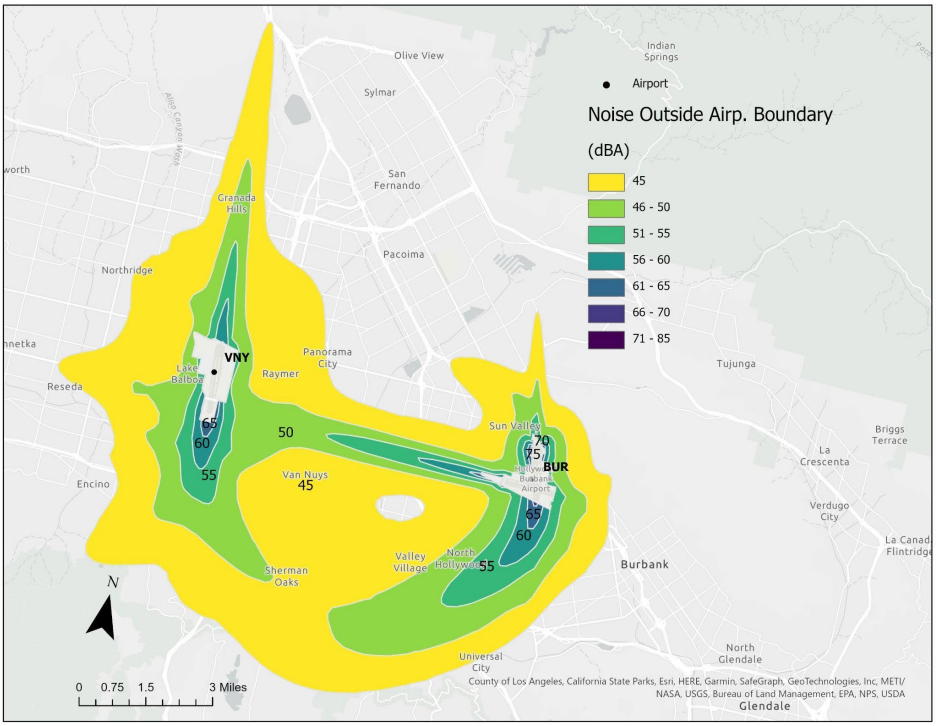


Figure 14. VNY and BUR Airport Noise Source Group Sharing 45 and 50 dBA Noise Footprint

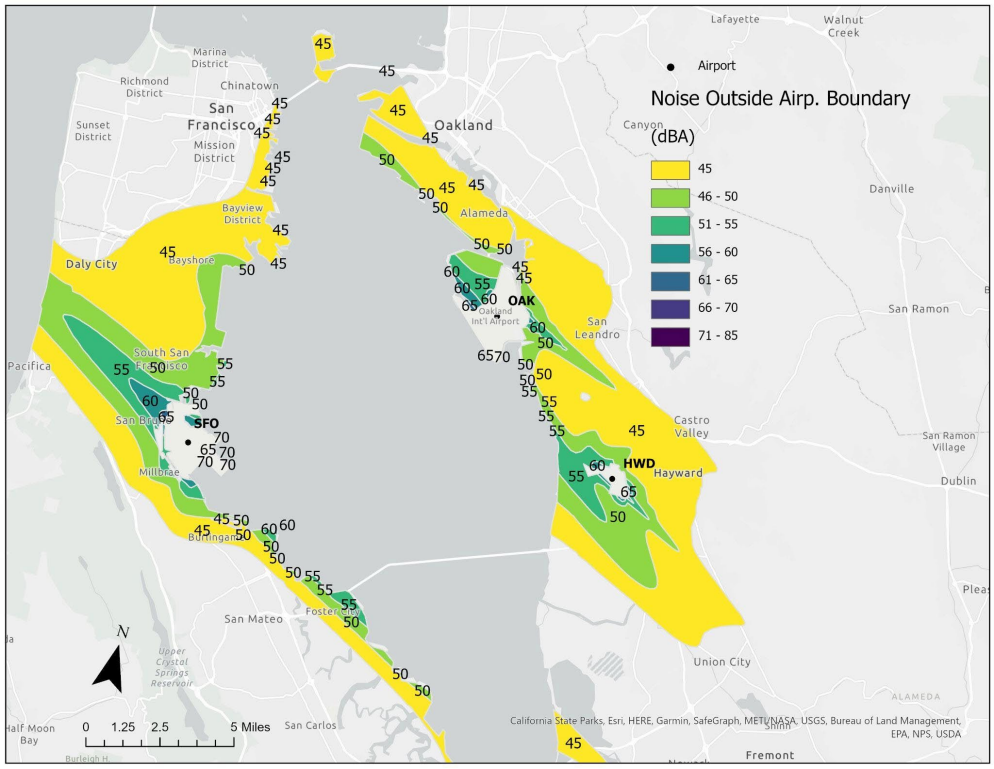


Figure 15. SFO, OAK, and HWD Noise Source GroupSharing 45 and 50 dBA Noise Footprint

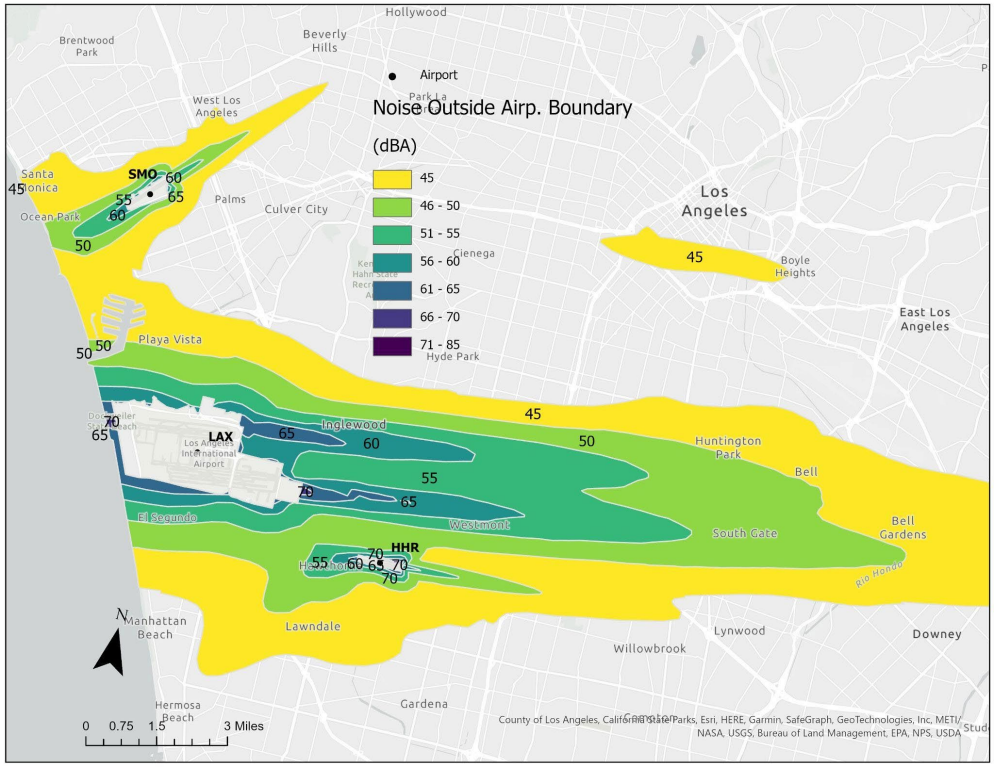


Figure 16. LAX, SMO, HHR Airport Noise Source Group Sharing 45 dbA Noise Footprint (LAX, SMO, and HHR) and 50 dBA Noise Footprint (LAX and HHR)

2.3. Rationale for Stipulating the Impact of Aircraft Electrification on Noise

This section presents the methodology employed to estimate the expected impact of aircraft electrification on noise in the near future (approximately mid-century). First it is necessary to understand aircraft electrification policy and flight replacement trends (subsection 2.3.1.), then in subsection 2.3.2, the rationale to stipulate the expected impact of electric aircraft on noise is presented following three steps:
(a) identifying the potential of electric aircraft replacement in the near future;
(b) understanding the potential electric aircraft market penetration on California airports; and
(c) identifying the potential of these replacements and the new electric aircraft market to impact the current noise levels.

2.3.1. Aircraft Electrification Policy Context and Regional/Commuter Flight Replacement Trends

Decarbonization policies have led to increased interest in aircraft electrification. In 2022, the International Civil Aviation Organization (ICAO) has adopted net-zero[19] 2050 global aspiration for international flights, and California's world-wide pioneering climate action , released the first comprehensive road map to cut air pollution by 71%, reduce fossil fuel consumption by 86%, and achieve carbon neutrality[20] by 2045 (Assembly Bill 1279, Muratsuchi, 2022). One of the results of these decarbonization policies is the intensification of aircraft electrification innovation and deployment, usually using both hybrid and fully electric aircrafts.

2.3.2. Electric Aircraft Selection, Market Penetration California Airports, and the Potential for Noise Reduction

This section borrows the methodology developed in Yee et al., (forthcoming)[21]; assessing the potential of aircrafts to reduce California aviation emissions, which identifies optimal aircraft replacement opportunities based on logistical interests (route distance, feeder load, and total number of aircraft purchases), and environmental interests (total CO2 emissions avoided, energy source for departing and arriving airports for a route, and electric aircraft battery efficiency)

(a) Identifying the potential of electric aircraft replacement in the near future:

[19] Net-zero policies uphold organizations and governments to reduce its absolute emissions across its whole supply chain to support climate mitigation policies, and therefore encompass all emissions that contribute to climate change. It is considered the gold standard for climate action.

[20] Carbon neutrality policies commit organizations and governments to monitor carbon dioxide emissions and finding ways to reduce them combined with compensation policies (ie. reducing CO2 emission elsewhere, contributing to carbon sink holes, cap and trade markets, etc.

[21] Yee, C., Bauranov, A., O'Rourke, M., Chupina, V., Khanykov, I., Rakas, J. (forthcoming) "*Pathways to Aviation Decarbonization: Potential of Electric Aircraft to Reduce Aviation Emissions in California*".

Yee et al,. (forthcoming) researched an array of manufacturers projecting electric aircraft release between 2023 and 2030; which included only those under development for the purposes of commercial and cargo transport. The potential replacement aircrafts was based on how close they are to commercialization (within testing phase or currently in service) and if they are able to hold enough passengers to penetrate commercial airline markets (i.e. greater than 8 passengers). After reviewing potential for electric aircraft models directly within publication from the major manufacturers including Beta, Bye Aerospace, Eviation, Heart Aerospace, Lilium, Pipistrel, Wright, Cranfield Aerospace, Airbus, and Zero Avia; Yee et al, (forthcoming); only two met the requirements of near future commercial use for regional or commuter transportation, with the capacity of at least 8 passengers: Alice aircraft from Eviation, and ZeroAvia (Table 4).

Table 4. Representatives of replacement aircraft selected for this study (Source: Yee at al, forthcoming)

Manufacturer	Aircraft	Type	Year	Range (n.mi.)	Pax	Stage
Eviation (Eviation, 2021; Holland, 2021)	Alice	BE	2024	440	9	Certification Test Flights
ZeroAvia (ZeroAvia, 2021)	ZeroAvia	HFC Powertrain	2024	500	10-20	Testing

(b) Understanding the potential electric aircraft market penetration on California airports:

Widespread electrification of long-haul flights is unlikely to occur in the near future (Brdnik et al., 2022, Epstein et al. 2019). Research quantifying the performance of electric aircraft market, has pointed out that technology innovation trends of batteries limits the ability of aircraft electrification to replace long-range routes and large air-carriers in the near-future (ICCT, 2022, Yee et al., forthcoming). Currently, research estimates that the average range of battery electric aircraft will reach 500 miles (Baumeister et al., 2020), and longer distances require more battery storage capacity ratio compared to current aircrafts maximum takeoff weight[22].This means, in terms of CO2 emission per pax-mile, it will be more effective to first focus on electrifying General Aviation instead of commercial airlines, and that shorter flights are better suited to being replaced by electric propulsion technology.

[22] The International Council on Clean Transportation White Paper on Performance Analysis of Regional Electric Aircraft (ICCT, 2021) states that "*With current battery technology, of 250 watt-hours per kilogram (Wh/kg) the 9Bolt aircraft could fly 140 km missions after accounting for energy reserve requirements. With advanced battery technology (500 Wh/kg), the larger 90Bolt aircraft could cover 280 km missions.*

California's geography and air travel behavior is considered conducive to electric aircraft market for regional and small aircraft carriers, given the state's length of 760 miles and width of 250 miles fitting the range of electric aircraft. Furthermore, California hosts 93 million flights each year, with the SFO - LAX segment being the second most traveled in the country (USDOT, 2023).

Given the current trends for battery technology innovation and deployment, the optimum electric aircraft replacement opportunities are for short-haul flights (500 miles) under regional commercial aviation as well as General Aviation (charter jets) with both battery electric and hydrogen fuel cell electric aircraft with a typical capacity of 20 passengers.

Open-sourced data that can help identify for each airport in California the fleet mix that meets the aircraft replacement requirements expressed in items (a) and (b) can be found in the FAA Aviation System Performance Metrics (ASPM) data. The fleet selection focused only on data from 2019[23] for 30 airports in California and went through a simplified aircraft matching process using the FAA's Aircraft Chart Group, and filtering the Aircraft Approach Category (AAC) to "A" and "B" as well as the Aircraft Design Group (ADG) to "I", resulting mostly in "Small" and "Small+" FAA Weight Class (see Appendix B for detailed aircraft matches). The A-I and B-I fleet mix percentage is used to approximately assess airports with the higher potential of electric aircraft market penetration. For more detailed research it is possible to develop a more detailed matching process including other criteria than the AAC and the ADG depending on the airport electrification market developments.

(c) Identifying the potential of aircraft replacements and the new electric aircraft market to impact the current noise levels.

Steps (a) and (b) help identify airports in California where it is more likely that aircraft electrification will take place in the near future. Step (c) is needed to filter the airports where fleet electrification will effectively reduce current noise levels. This implies (1) removing those airports where the fleet mix includes large commercial operations, and (2) identifying airports with current levels of noise exposure. The first step is necessary because even if there is a replacement for electric aircraft in a fleet mix with large commercial flights, the cumulative noise levels will not change much while commercial aircrafts will remain responsible for most of the currently measured noise levels. The second step is necessary because even if there is an electrification of the majority of the fleet mix for those regional/commuter airports, the baseline exposure to noise was low to begin with, so the environmental gains will mostly be associated with emission reductions. I

[23] 2019 is the most recent year not impacted by the COVID-19 pandemic

[4.2] 3. Results

3.1. Noise Exposure

3.1.1. Noise Exposure by Area and Population

Based on the NTNM noise model, approximately 1,380 sq. mi. are exposed to 45+ dB(A) related to airport operations, with 44 sq. mi. of exposure to 65+ dB(A) (Figure 17). We can see that above 70 dB(A) the percentage of noise exposure predominantly affects areas inside the airport boundaries. For all areas exposed to 70+ dB , 90% or more are located within airport boundaries, and all areas exposed to 90+ dB(A) are completely within airport boundaries. The maximum levels reached outside airport boundaries is 85 dbA. The dB threshold transition occurs at approximately 65 dB(A) where the percentage of areas exposed to this noise level is predominantly inside the airport (62,58%) (Figure 18)

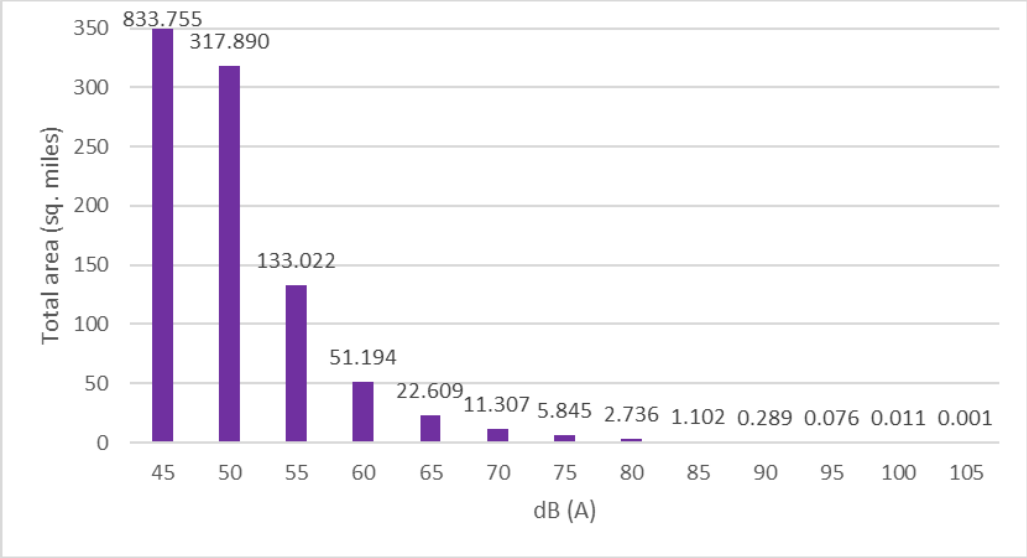


Figure 17. Total area exposed to noise related to airport operations in California in 2018

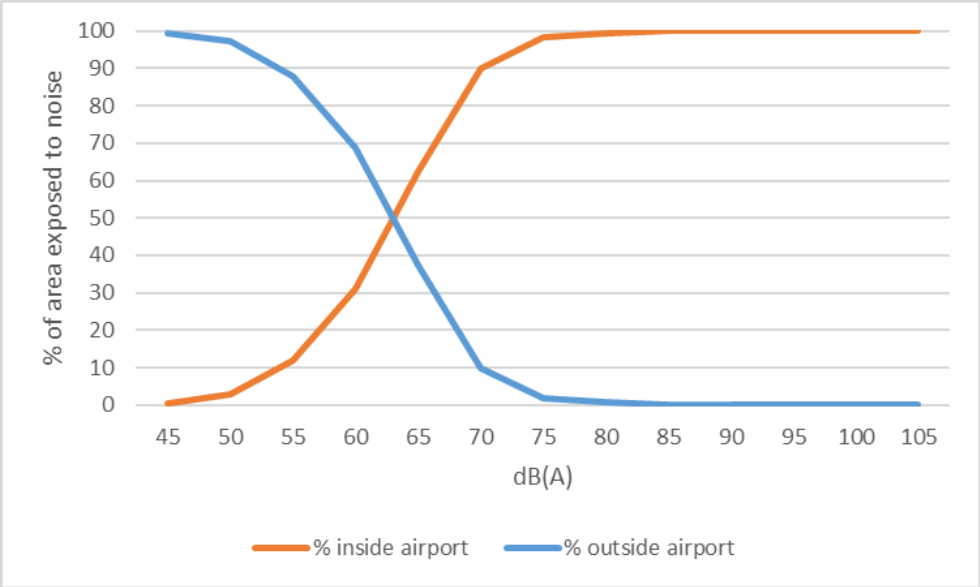


Figure 18. Percentage of area exposed to different dBA levels in *Leq* inside and outside airport boundaries (for a total of 53 airports represented in the NTNM 2018 model)

Based on the 2019 census data from CES4 tool approximately 9,505,677 people (from a total of 39,283,497) registered in 1,935 census tracts (from a total of 8,035) are potentially exposed to aviation noise ranging from 45 to 85 dBA in *Leq* in California. When looking at the noise contours of 50+ dBA in *Leq*, the estimated population exposed decreases to 4,881,579 for a total of 990 census tracts (Figure 19). When looking at noise contours of 65+ dBA, the estimated population exposed decreases to 639,812 for a total of 133 census tracts (Figure 20). The census tracts that are exposed to 65+ dBA are adjacent to 44 out of 53 airports represented in the NTNM 2018 model.

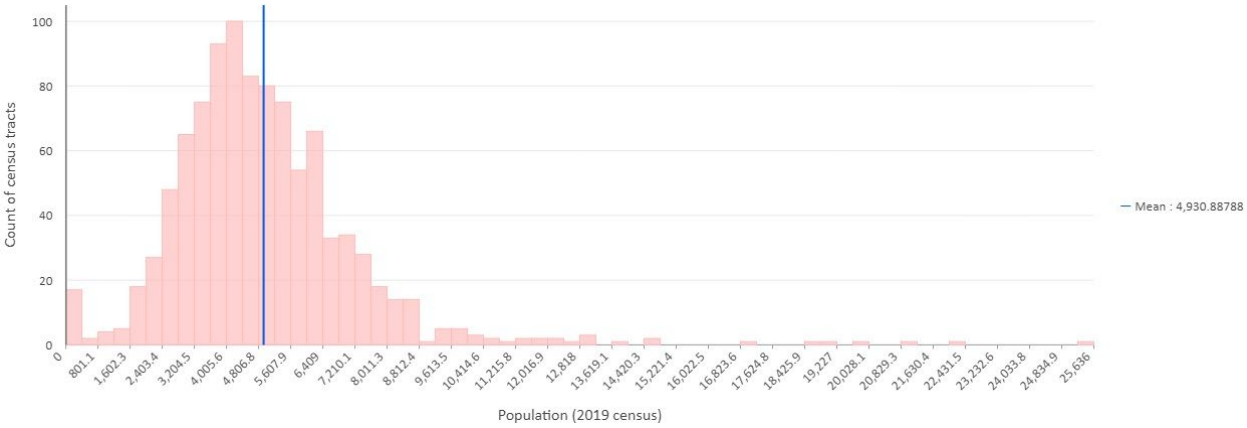


Figure 19. Distribution curve of population in census tracts exposed to aviation noise contours superior to *Leq* of 50 dBA (maximum of 85 dBA).

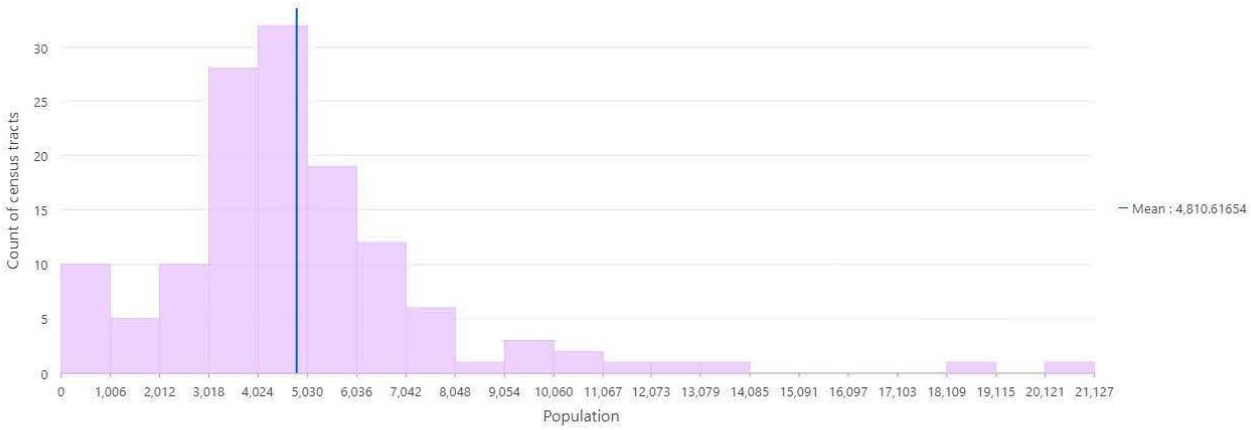


Figure 20. Distribution curve of population in census tracts exposed to aviation noise contours superior to *Leq* of 65 dBA (maximum of 85 dBA)

3.1.2. Airport Noise Footprint

SFO, OAK, and HWD are from the same airport noise source group, and they have the largest noise footprint in California with 112 to 116 mi^2 (for noise levels of 45+ dBA) (Figure 21). LAX and HHR airport noise group follow closely with 101 and 81 mi^2 respectively. Due to the spatial proximity of these airports and their shared noise contour boundaries, it is not possible to accurately discern which airport from the groups contribute the most to the noise footprint with the current NTNM model (see subsection 2.2.3). From the airports not sharing noise contour boundaries, FAT has the largest noise footprint with 78 mi^2. As a reference, the average noise footprint per airport in California is 35 mi^2. And the median is 18 mi^2. The noise footprint is calculated only for the noise measured outside of the airport's boundaries to better inform land use compatibility planning decisions.

From the 53 airports represented in the NTNM model, 44 have portions of their noise footprint that reaches 65 to 85 dBA. The percentage of each airport's noise footprint at these higher levels is however very low (Figure 22). SAN has the higher % of 65+ dBA footprint at 3.75%, followed by IYK with 2.6%. TRK, LAX, SDM,SNA,MMH, FAT, MRY, and UDD all have between 1.1 and 1.7% of their noise footprint at 65+ dBA. The remaining 34 airports all have less than 1% of their noise footprint at the higher noise level measured in the state outside of the airport boundaries..

The airport noise footprint data is available in Appendix C, and the GIS data is available in the supplementary materials "AID_Noisefootprint" in shapefile format.

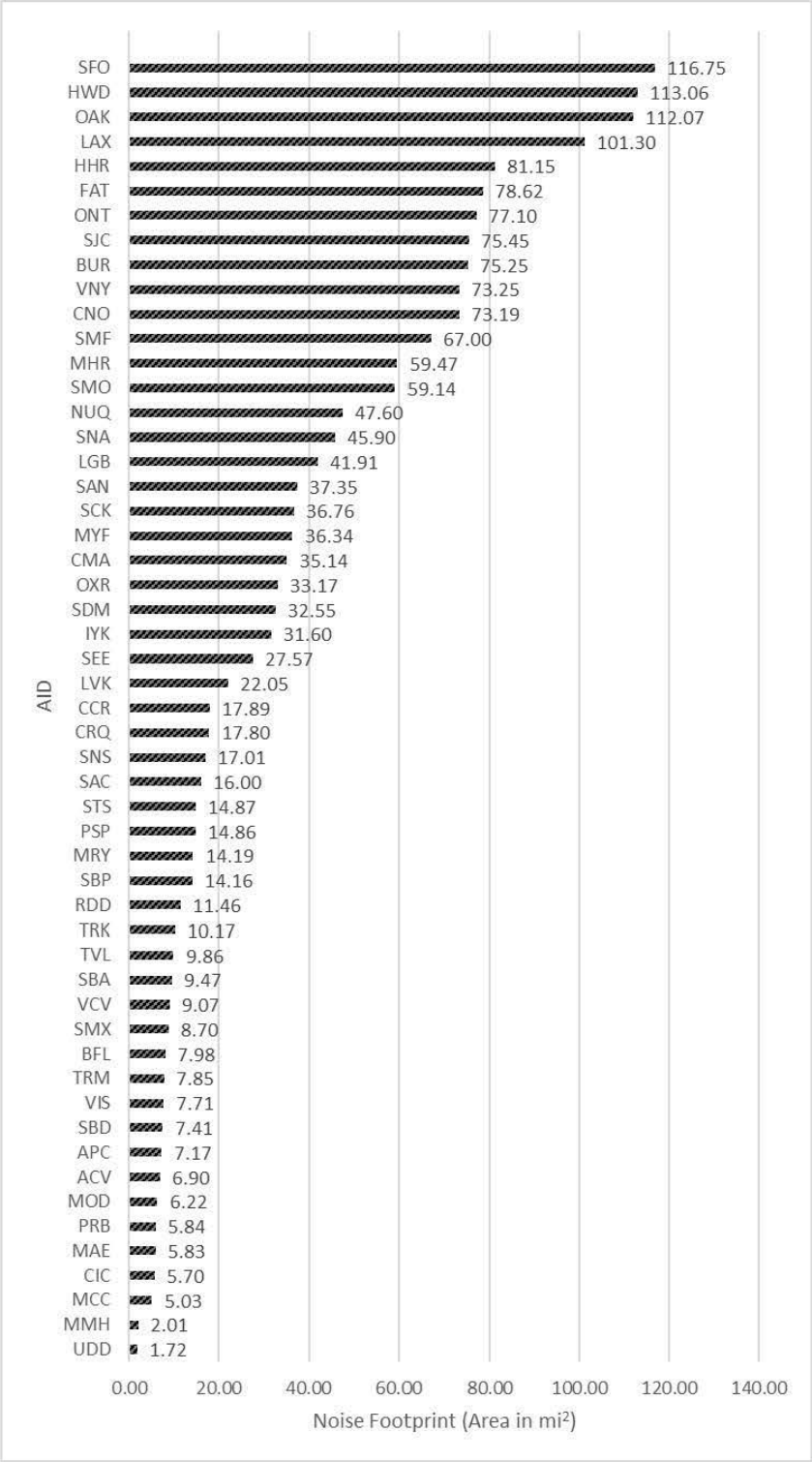


Figure 21. Total Area Exposed to Aviation Noise by Airport (45+ dBA, Outside Airport Boundaries)

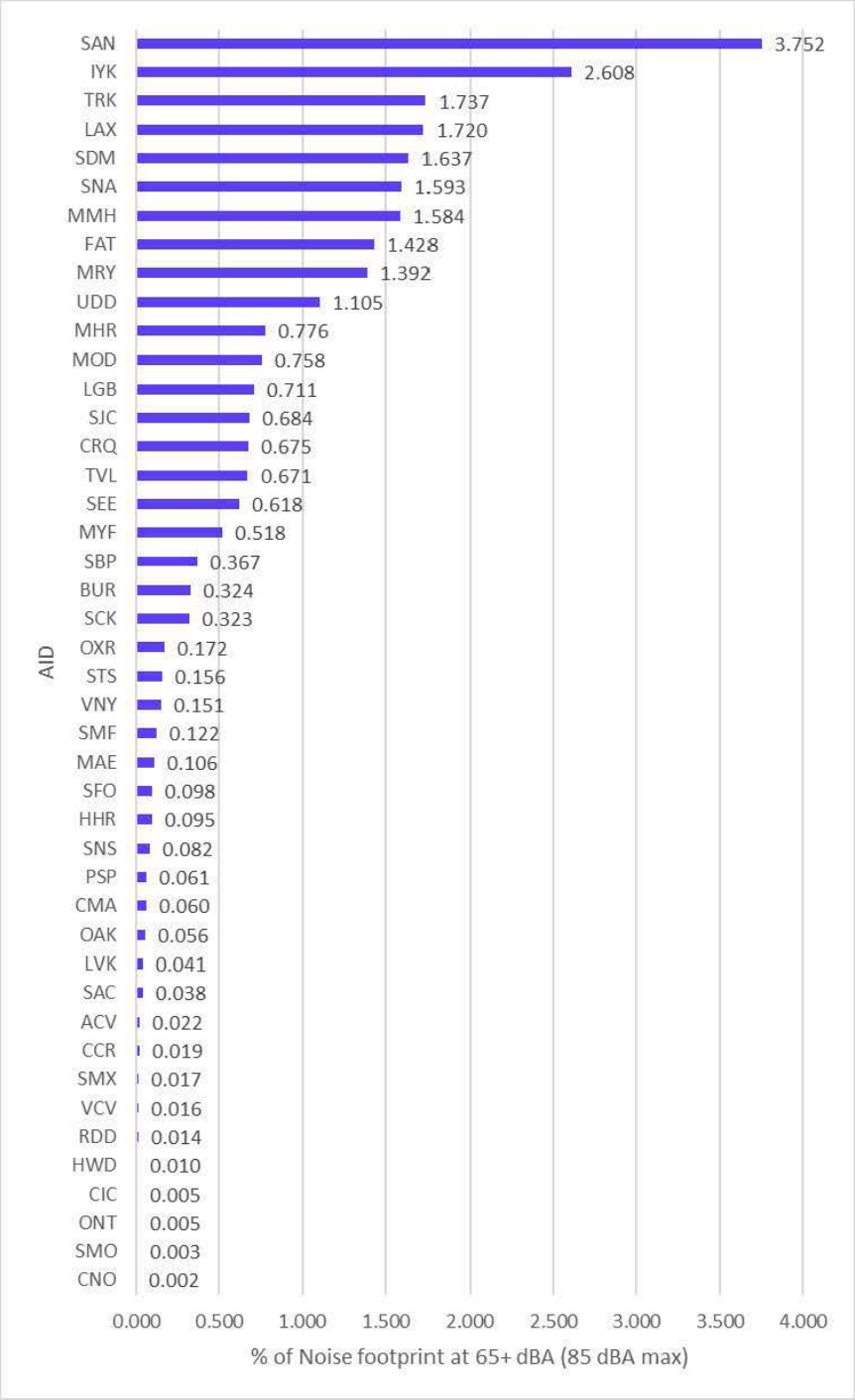


Figure 22. Percentage of Airport Noise Footprint at 65+ dBA (Outside Airport Boundaries)

3.2. Noise Exposure and Environmental Justice

3.2.1. State-level Analysis of Noise Exposure, CES4 Score, Pollution Burden and, Population Characteristics

This section seeks to Identify disproportionately burdened communities that are exposed to aviation noise as a potential health hazard. Understanding the details of environmental burden (pollution exposure) as well as population characteristics that make those exposed to noise more sensitive or vulnerable to environmental health hazards is an important step towards more equitable noise exposure reduction policies that aligns with new normative values being incorporated in Califoprnia's planning documents.

The state's clustering of areas with the highest scores of environmental injustice given their CES4 score (hot spot) is located in the Central Valley extending a bit towards Sacramento, in the Los Angeles Basin, and in South San Diego near the border with Mexico (Figure 23). The airports represented in the NTNM located in the Central Valley/ Sacramento hotspot are BFL, VIS, FAT, E79, MAE, MOD, SCK, SAC, and SMK. The airports represented in the NTNM model located in the LA Basin hot spot are LGB, HHR, LAX, SMO, BUR, VNY, CNO, ONT, SBD, RIV, and SDM near the border with Mexico. State areas with clustering of the lowest scores of environmental injustice (cold spots) are generally located in the coastal areas (except for the LA basin and near the border with Mexico). Similar trends are observed for the pollution burden and the population characteristics except there are hot and cold spots are more concentrated with hot spots present in almost every larger metropolitan area, including for the SF Bay area (Figure 24 and 25).

Based on the overlay results of the aviation noise contours and the environmental justice indicators, we identified that approximately ⅓ of the census tracts in the 75th percentile of the CES4 score (top 25%), the pollution burden, and the population characteristics are exposed to aviation noise of 45+ dBA. An even higher proportion of census tracts at the 90th percentile of the environmental justice indicators are exposed to aviation noise of 45+ dBA. This means that, for the CES4 Score, 37.53% of California's census tracts characterized the top 10% of the most burdened by environmental injustice are also exposed to aviation noise levels. A total of 36.19% of the top 10% of census tracts most burdened by pollution; and a total of 34.76% of those most vulnerable to environmental hazards (population characteristics) are also exposed to aviation noise (Table 5). Given the cutoff of 45 dBA, this threshold does not necessarily translate to annoyance or other hazardous health effects that have been identified with the dose-response curves update for the NES at DNL 50 dBA . However, in view that the applied noise metrics (dBA in *Leq*) tend to underestimate the annoyance potential because they lack time-related weighting of the DNL and CNEL, these results provide an overall quality of the population exposed to all potentially hazardous aviation noise.

The 50+ and 65+ dBA thresholds are more easily associated with noise-related health hazards. For the 50+ DBA levels, there is still a higher percentage of the 90th percentile of tracts

exposed, genelly above 20%. For the 65+ dBA levels, where noise is clearly associated with health hazards, a much smaller percentage of the tracts most burdened by environmental injustice are exposed, ranging between 2-4%.

Table 5. Percentage of California census tracts most burdened by environmental injustice exposed to aviation noise (*Leq*)

CES4 Score	**45+ dBA**	**50+ dBA**	**65+ dBA**
75th pctl (top 25%)	31.70%	17.74%	3.93%
90th pctl (top 10%)	37.53%	22.42%	3.02%
Pollution Burden	**45+ dBA**	**50+ dBA**	**65+ dBA**
75th pctl (top 25%)	33.25%	20.01%	3.33%
90th pctl (top 10%)	36.19%	24.50%	4.35%
Pop Characteristics	**45+ dBA**	**50+ dBA**	**65+ dBA**
75th pctl (top 25%)	30.59%	16.89%	2.02%
90th pctl (top 10%)	34.76%	20.03%	2.14%

Communities most exposed to aviation noise health hazards and those most burdened by environmental injustice indicators overall are identified by crossing the 50+ dBA exposed areas with census tracts at the top 10% of the CES4 score percentile. This identifies communities in census tracts that are potentially exposed to noise-related health hazards associated with aviation and those that are already severely impacted by environmental injustice (90th percentile) (Figure 26). Similarly areas exposed to 65+ dBA, representing communities that are more severely exposed to noise-related health hazards, to census tracts at the top 25% of the CES score percentile, representing those that are highly impacted by environmental justice in California (75th percentile) (Figure 27). Following the General Plan guidelines on Environmental Justice elements, these areas should be further investigated and prioritized for state-level aviation noise mitigation programs or noise-related health hazard programs (See census tract list and all other CES4 Tool indicators for these tracts in Supplementary Materials Data: “Most Burdened and Most Exposed” with data on Figures 26 and 27)

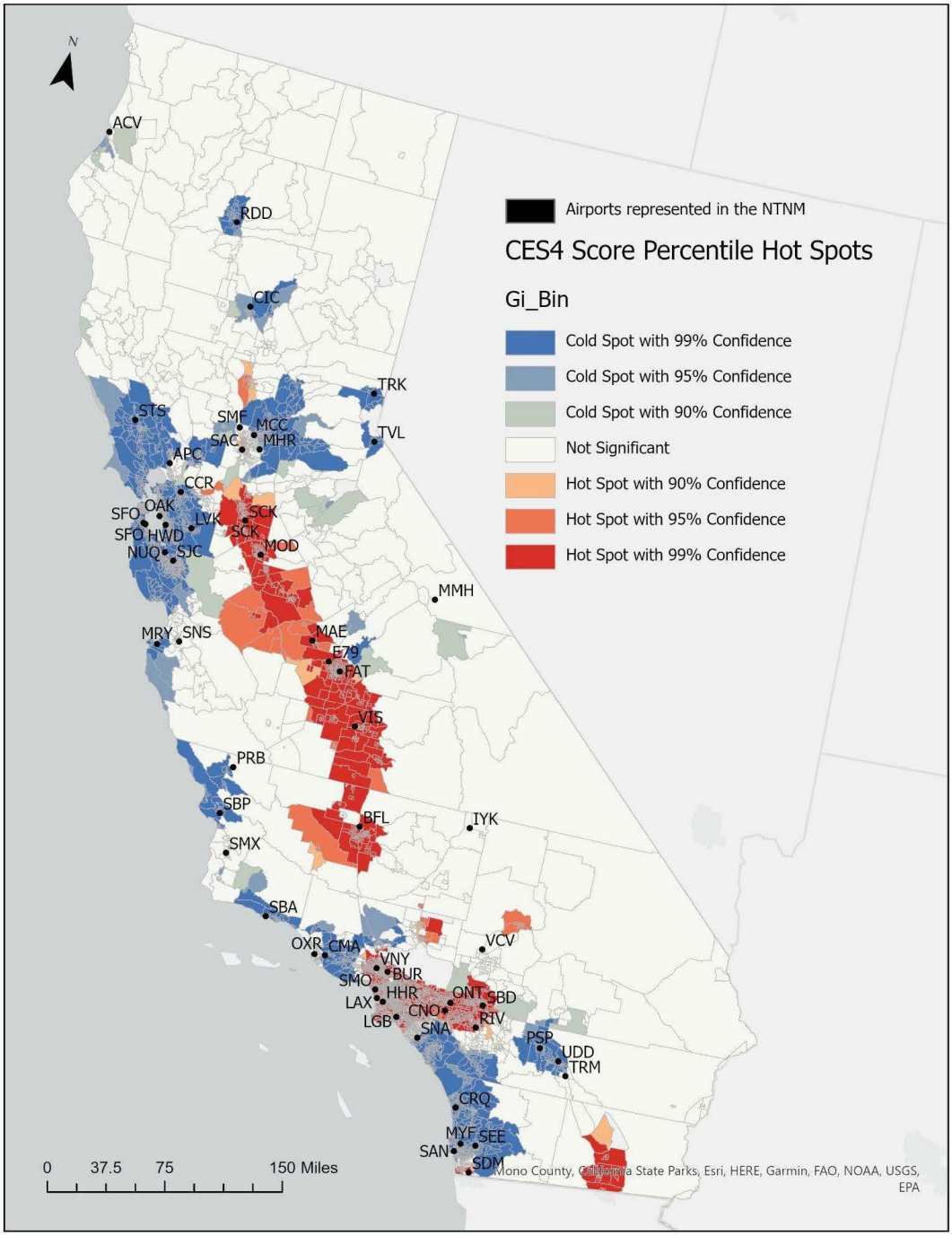


Figure 21. CES4 Score (environmental injustice) State-level Hotspots

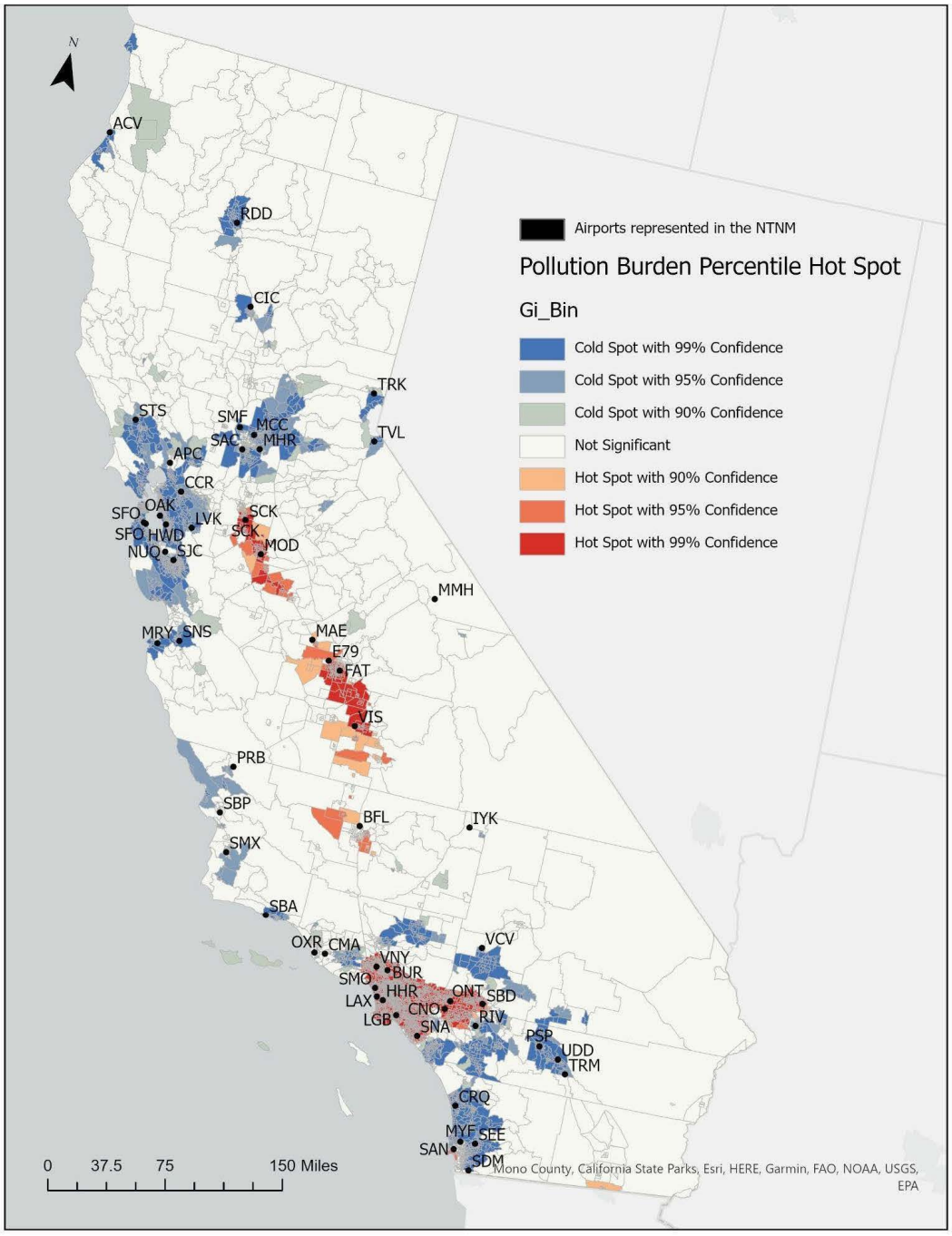


Figure 24. Pollution Burden State-level Hotspots

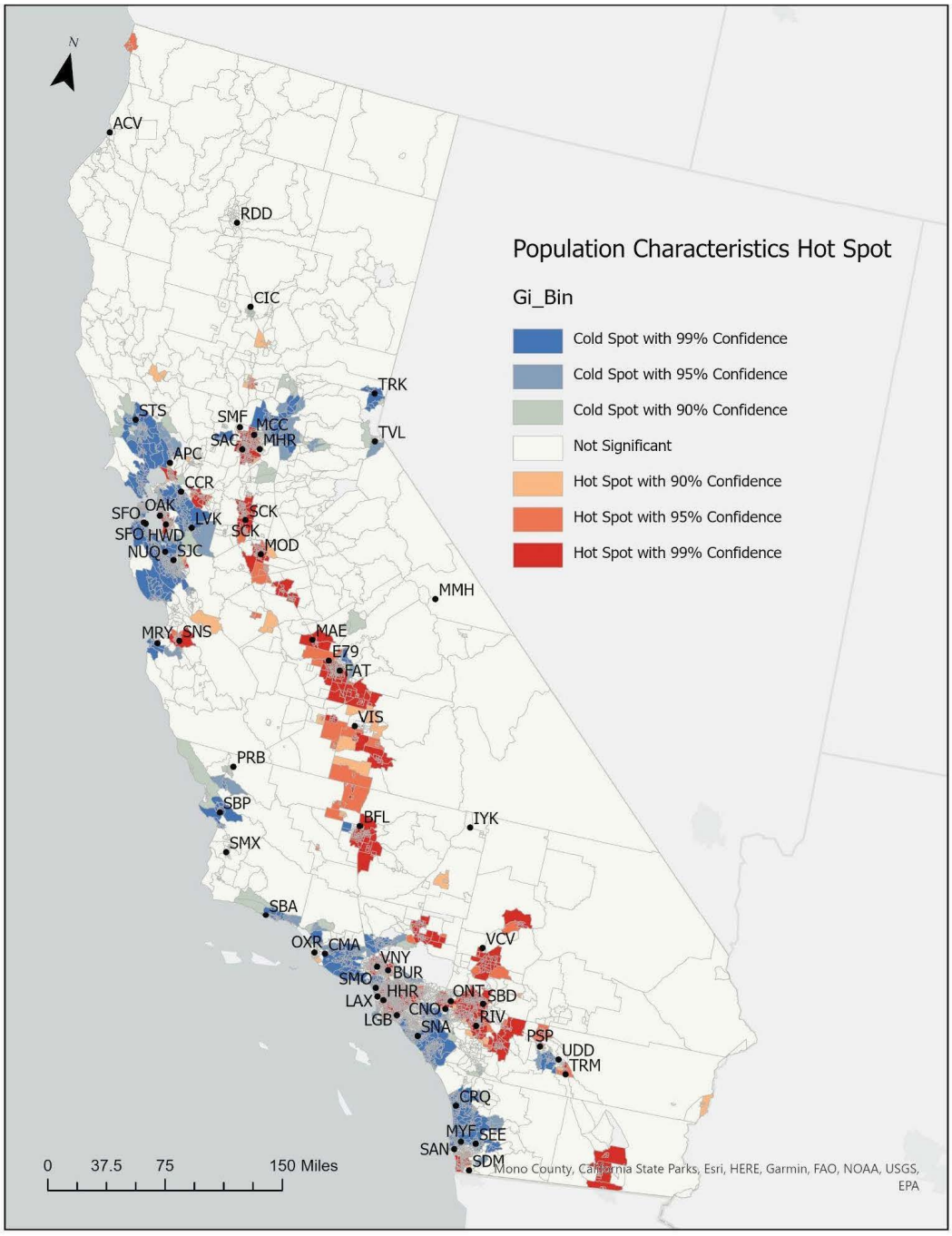


Figure 25. Population Characteristics State-level hotspots

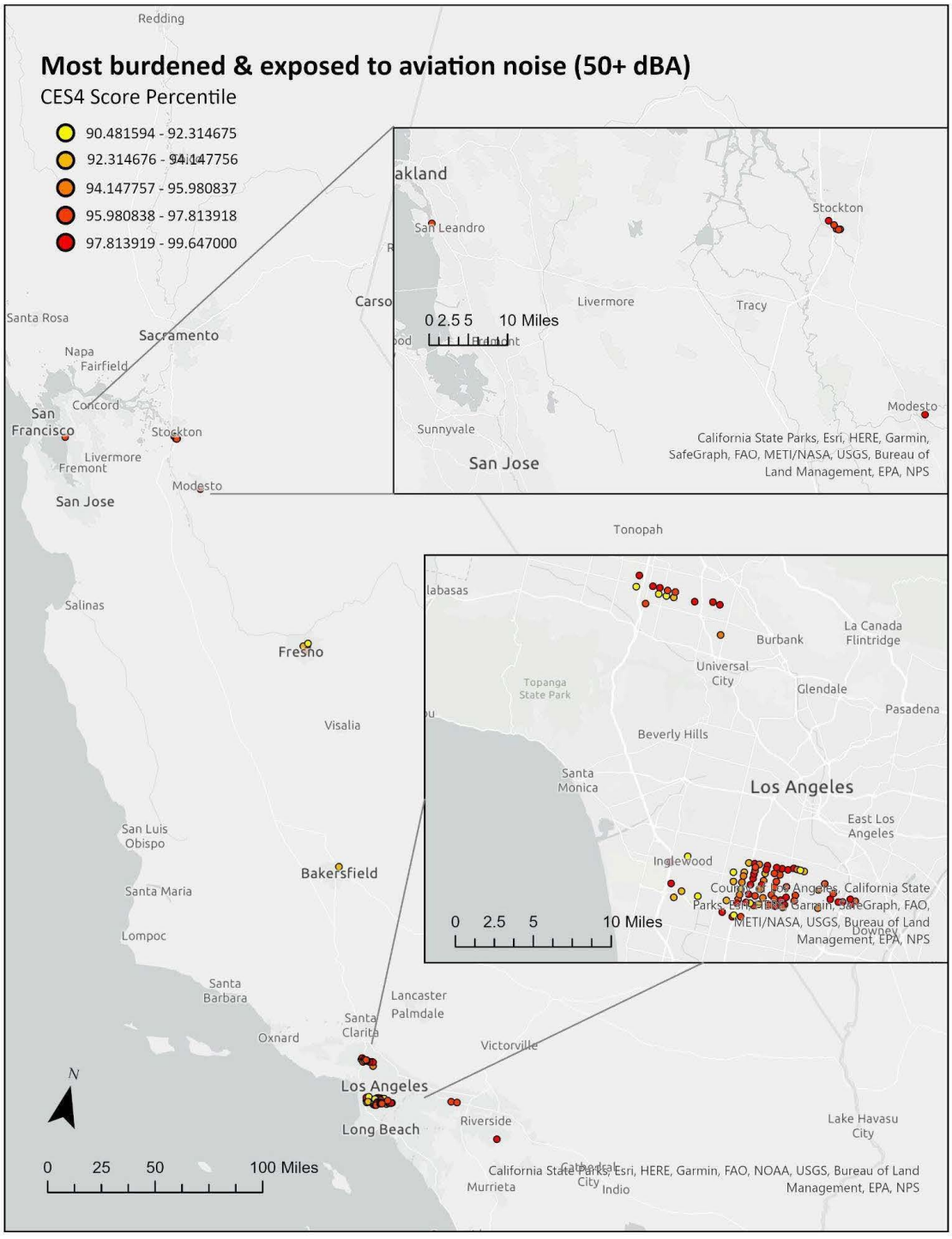


Figure 26. Location of Census Tracts in the Top 10% Most Burdened by Environmental Injustice (CES4 Score) and Exposed to Aviation Noise of 50+ dBA.(See census tract list and all other CES4 Tool indicators for these tracts in Supplementary Materials Data: “Most Burdened and Most Exposed”)

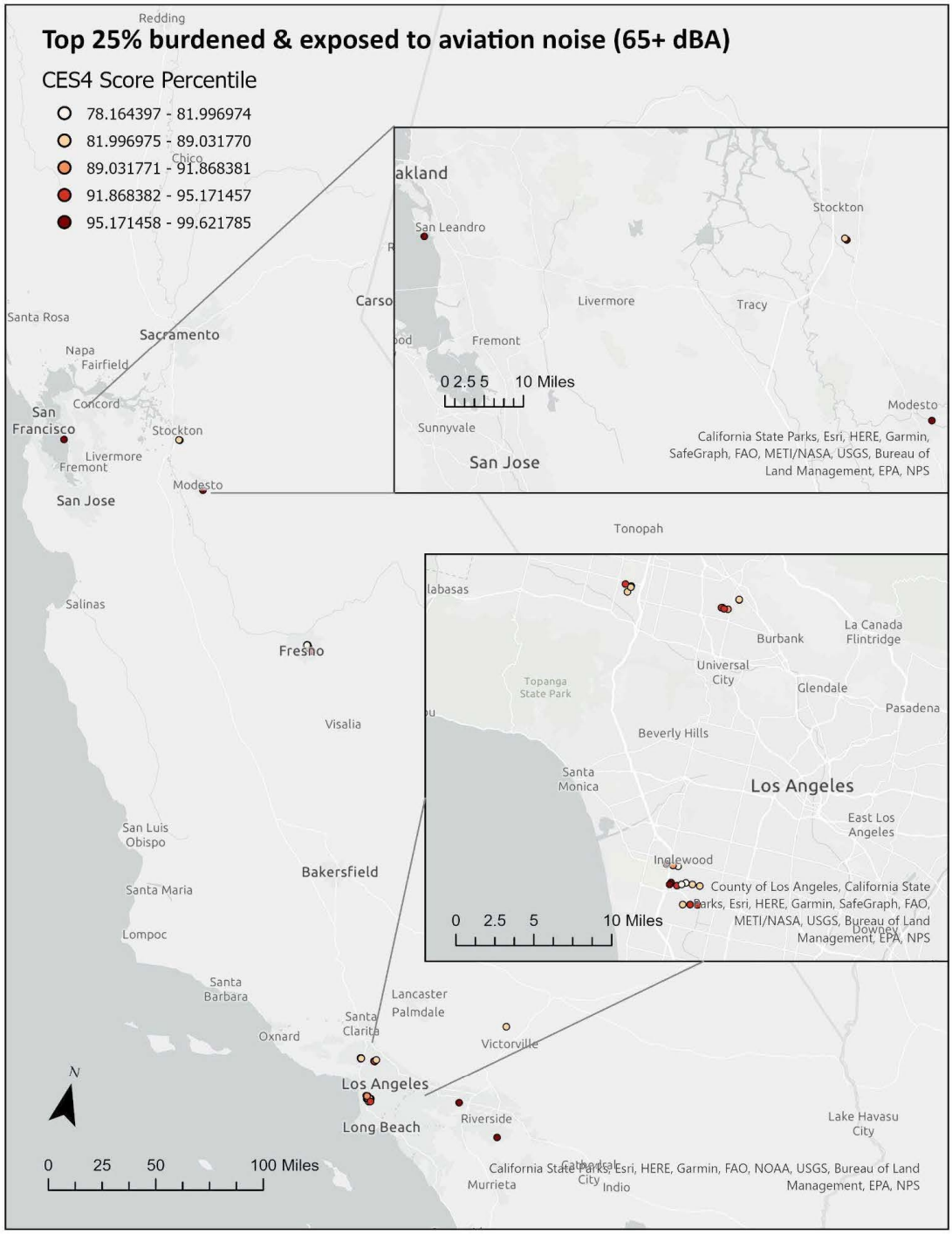


Figure 27. Location of Census Tracts in the Top 25% Most Burdened by Environmental Injustice (CES4 Score) and Exposed to Aviation Noise of 65+ dBA.(See census tract list and all other CES4 Tool indicators for these tracts in Supplementary Materials Data: “Most Burdened and Most Exposed”)

3.2.3. County-Level Analysis of CES4 Score Percentile hotspots and Aviation Noise Contours

The county-level results of the CES4 Score Percentile hot-spot analysis allows to identify areas with statistically significant clustering of high (hot-spot) and low (cold-spot) environmental injustice scores at the county level that are not taken into account when assessing state level clusters. For example, The San Francisco Bay Area is not a hot-spot for CES4 scores when compared to all of the state levels; but if you look closely at Alameda county results it is possible to identify clustering of high scores around OAK and HHW airports (Figure 28). Similarly, while the LA basin was tagged as a hot-spot at the state-level, at the level of the LA county there are much more nuanced results, where clustering of low CES4 scores are found mostly on the coastal fringe and outer eastern census tracts (FIgure 29).

A total of 34 counties are impacted by aviation noise based on the NTNM 2018 model[24]. From these counties, 20 present statistically significant clustering of high and/or low values of CES4 score percentile. Eleven counties have very high spatial co-occurrence of aviation noise and clustering of high scores of environmental injustice (CES4) for 23 airports; and 9 counties have a very high spatial co-occurrence of aviation noise and low scores of environmental injustice for ten airports. Maps of all counties with any statistically significant hotspots or coldspots near aviation noise contours is available in Appendix D. Table 6, presents an overview of all 34 counties exposed to aviation noise with highlighted Airport IDs that have a very high spatial co-occurrence of aviation noise and statistically significant clustering (95% and above confidence) of hot-and cold-spots of CES4 scores .

This complementary analysis at a finer scale can help better inform local policies at the county, airport consortium, metropolitan area, or city-level for noise mitigation and environmental health policies.

[24] Two counties are impacted by aviation noise that sources from outside of California: Siskiyou county, where the noise source is located in Oregon; and Imperial county, where the noise source is located in Arizona.

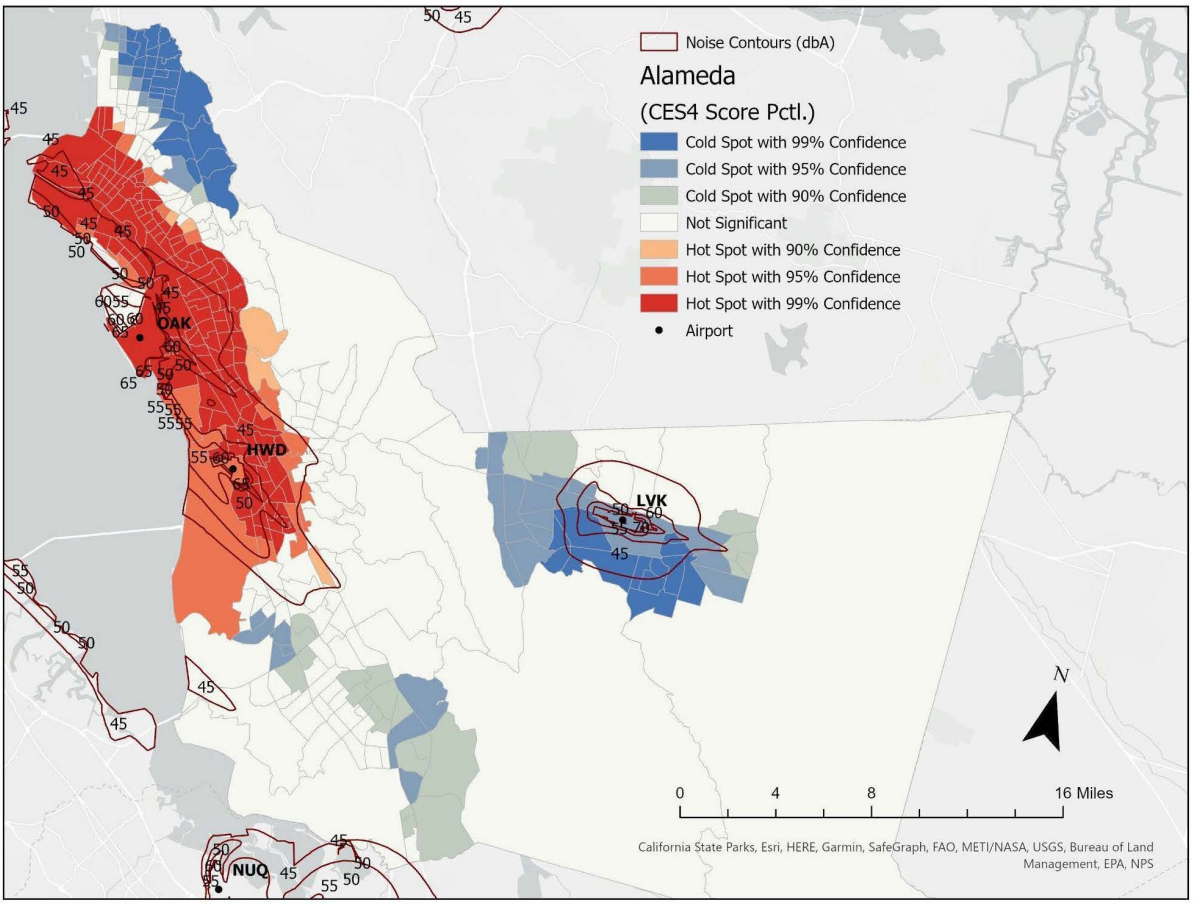


Figure 28. Alameda County Hot Spot Analysis and Noise Contours Outside Airport Boundaries

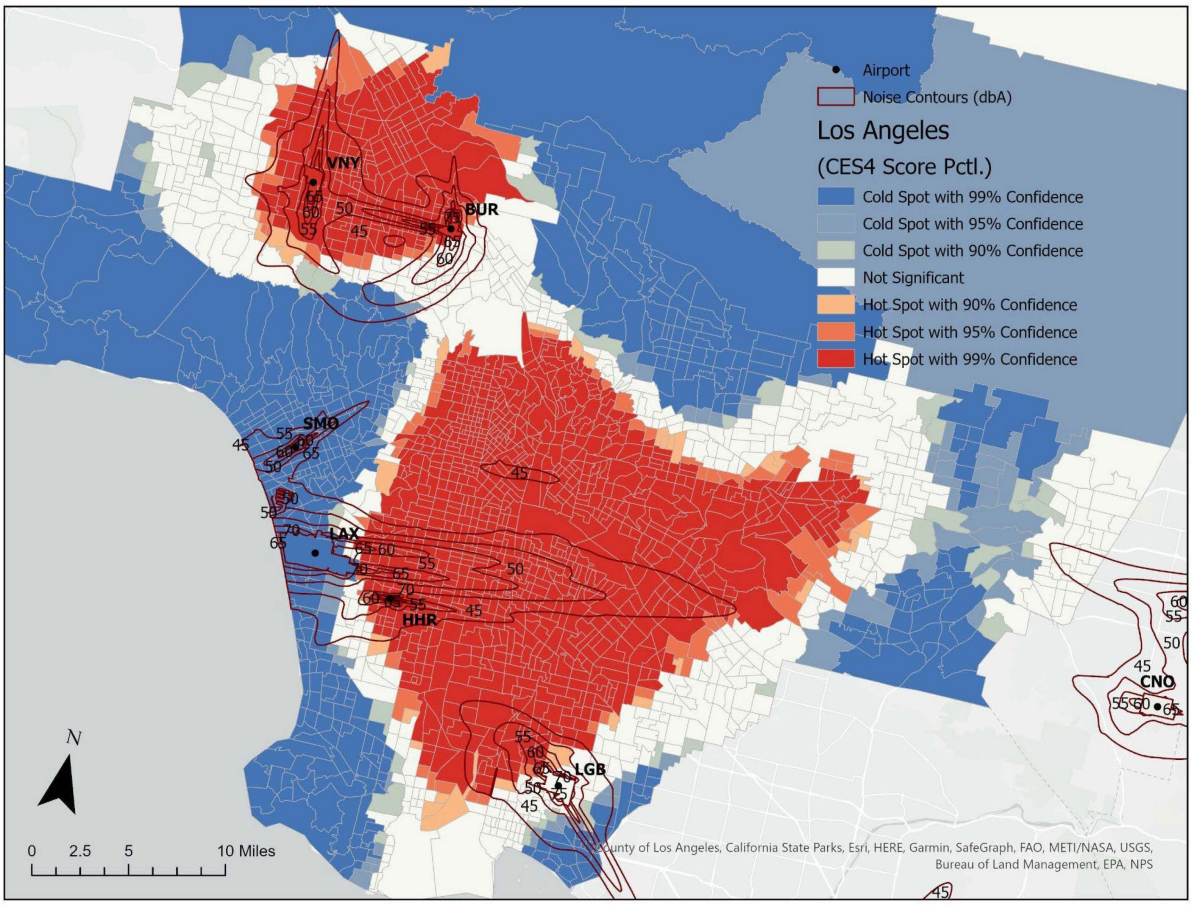


Figure 29. Los Angeles County Hot Spot Analysis and Noise Contours Outside Airport Boundaries

Table 6. Overview of 34 counties exposed to aviation noise (45+ dBA in *Leq*) and their respective airports. Airports highlighted in red and blue show where there is spatial co-occurrence of noise and statistically significant hot-and cold-spots of environmental injustice scores.

County	**AIDs where there is spatial co-occurrence of environmental injustice scores hotspots and aviation noise**	**AIDs where there is spatial co-occurrence of environmental injustice score coldspots and aviation noise**
Alameda	OAK, HWD	LVK
Butte	CIC, No significant spatial clustering of high or low CES4 scores	
Contra Costa	None	CCR
El Dorado	TVL	None

Fresno	FAT	None
Humboldt	ACV, No significant spatial clustering of high or low CES4 scores	
Imperial	Noise source in the State of Arizona. No significant spatial clustering of high or low CES4 scores	
Kern	BFL	None
Los Angeles	VNY, BUR, LAX, HHR, LGB	SMO, LAX
Madera	MAE, No significant spatial clustering of high or low CES4 scores	
Mono	MMH (FAT outside Mono), No significant spatial clustering of high or low CES4 scores	
Monterey	SNS	MRY
Nevada	TRK, No significant spatial clustering of high or low CES4 scores	
Napa	APC, No significant spatial clustering of high or low CES4 scores	
Orange	SNA	SNA
Placer	(TRK, outside Placer), No significant spatial clustering of high or low CES4 scores	
Riverside	(CNO, ONT, outside Riverside)	PSP, UDD
Sacramento	MCC, SAC, MHR	MHR, SMF
San Bernardino	SBD, ONT, CNO	VCV
San Diego	SAN, SDM, SEE, MYF	CRQ, MYF
San Joaquin	SCK	
San Luis Obispo	SBP, PRB, No significant spatial clustering of high or low CES4 scores	
San Mateo	SFO (OAK, HWD outside San Mateo)	SFO (OAK, HWD outside San Mateo)
Santa Barbara	SMX	SBA
Santa Clara	NUQ, SJC	None
San Francisco	(SFO, OAK outside San Francisco)	(SFO, OAK outside San Francisco)

Shasta	RDD, No significant spatial clustering of high or low CES4 scores	
Siskiyou	Noise source in the State of Oregon. No significant spatial clustering of high or low CES4 scores	
Sonoma	STS	None
Stanislau	MOD	None
Tulare	VIS, No significant spatial clustering of high or low CES4 scores	
Ventura	OXR, CMA	None
Yolo	SMF	None

3.2.3. County-Relative Exposure to Aviation Noise at 45+ dBA; 50+ dBA, and 65+ dBA

The estimated population exposure based on the census tract overlay results is of 9,505,677 in California with an average of 279,578 per county for the baseline noise exposure threshold of 45+ dBA. For 50+ dBA the estimated total population decreases to 4,881,579; and for the 65+dBA it totals 639,812. Out of 34 counties exposed to aviation noise, 16 have at least 20% of their population that is potentially exposed to 45+ dBA (Figure 30). San Mateo, Alameda and Fresno are the top counties with 51.1%, 41.25%, and 41.2% of their population exposed to 45+ dBA noise levels.

The proportion of the population potentially exposed to more severe noise levels (65+ dbA) does not surpass 5.98% (Madera) with a median of 1.44%; except for Mono county, with an estimation of 25,84% of their population exposed to more severe noise levels for a total estimate of 3,697 people in the exposed census tracts (Figure 31). Figure 32 helps better understand the number of census tracts counted for each noise threshold and we can see that for Mono, the same census tracts are exposed to both 45+ dBA and 65+ dBA, resulting in the same estimation for the population exposure for both noise levels. Appendix E provides the detailed data reference of this section's results.

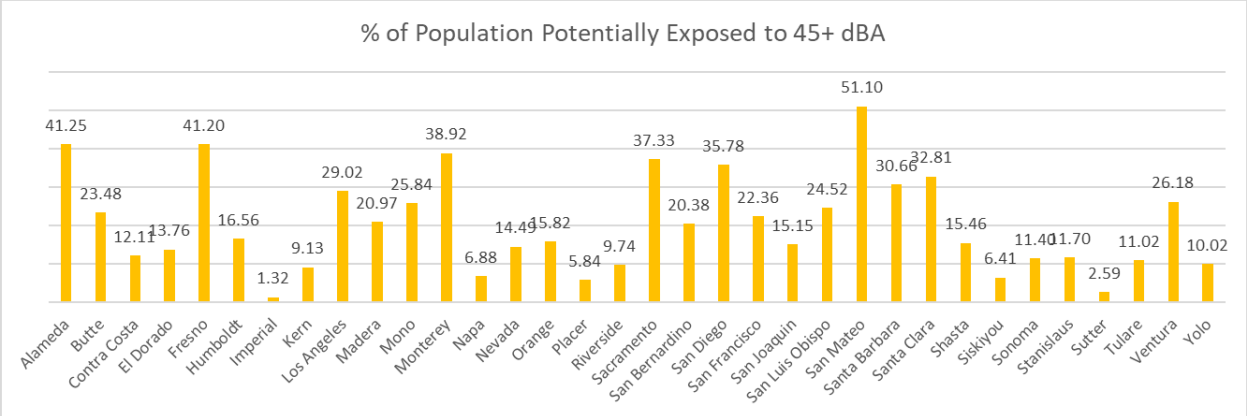


Figure 30. Percentage of potentially exposed population in California's counties to aviation noise levels of 45+ dBA.

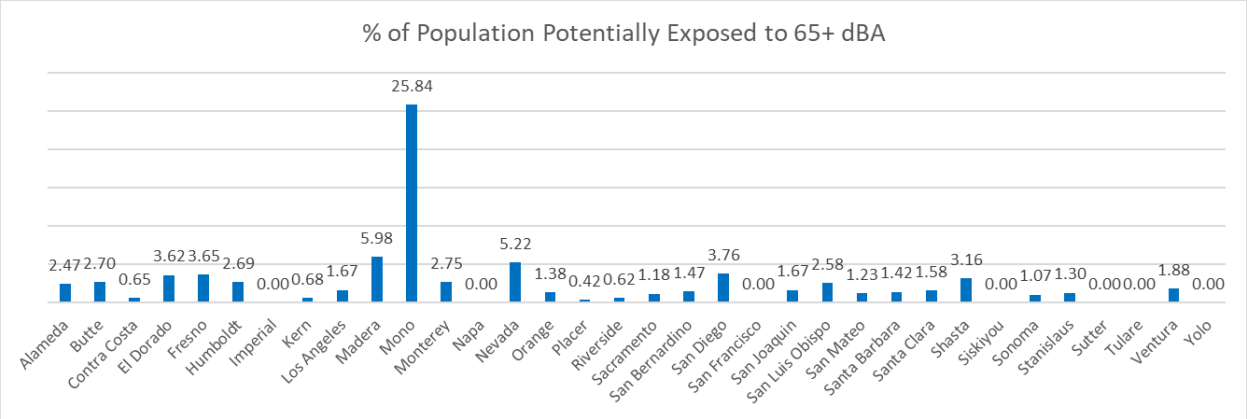


Figure 31. Percentage of potentially exposed population in California's counties to aviation noise levels of 65+ dBA.

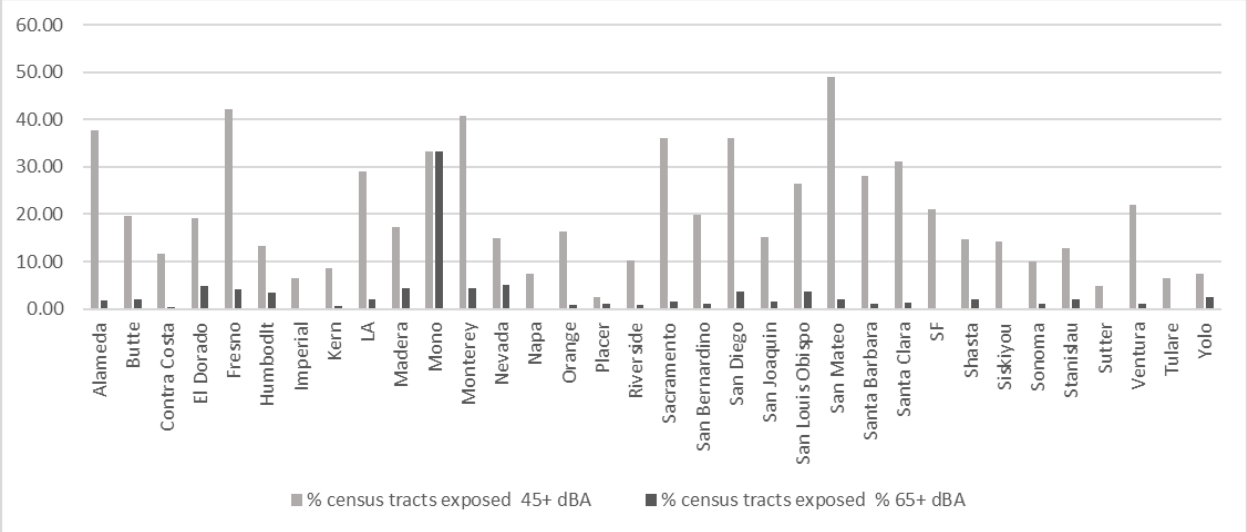


Figure 32. Percentage of census tracts in each county exposed to noise levels of 45 dBA and above; and 65 dBA and above.

3.2.4. County-level Proportion of Most Burdened by Environmental Injustice that are Exposed to Aviation Noise

This section explores the county-level exposure of census tracts at the top 25% (75th percentile) of environmental justice indicators exposed to aviation noise of 45+ dBA and 65+ dBA thresholds. By using each county's baseline count of census tracts environmental injustice score (CES4), pollution burden, and population characteristics; more localized environmental hazard impacts and population vulnerabilities are highlighted and contrasted with noise exposure.

Figure 33 shows that all (100%) of Santa Barbara's census tracts at the 75th percentile of the environmental injustice score (CES4) are also exposed to aviation noise at 45 dBA. There are six counties with nearly half or more of their census tracts most burdened by environmental injustice that are also exposed to potentially hazardous aviation noise: San Francisco, Ventura, San Mateo, Sacramento, Monterey, and Alameda. The proportion of census tracts most burdened by environmental injustice that are exposed to more severe aviation noise (65+ dBA) is however lower overall, with maximum proportions at Madera and Fresno.

Figure 34 identifies 7 counties that have more than half of their census tracts reaching the highest percentiles of pollution burden that are also exposed to aviation noise. Notably San Luis Obispo has 66,67% of its census tracts most burdened by environmental pollution hazards that are also exposed to more severe levels of aviation noise (65+ dbA). Santa Barbara, Santa Clara, San Mateo follow with over 20%, and San Diego with 17%.

Figure 35 highlights San Francisco, with 86,67% of its most vulnerable census tracts (based on population characteristics of vulnerability and sensitivity to environmental health hazards), that are also exposed to potentially hazardous effects of noise coming from aviation. Alameda, Ventura, Monterey and San Mateo reach very high proportions as well between 50-60%. However when looking at more severe noise levels (65+ dbA) the percentage of census tracts with the most vulnerable population characteristics drop considerably, with the highest level at Fresno at 5.77%.

For a more complete analysis of the environmental justice indicators we highly recommend further investigating the spatial co-occurrence of noise exposure and other critical indicators such as the percentage of Native American, African American, and Hispanic; the percentage of children and elderly; poverty percentile; education percentile; and others.

Appendix F provides the detailed data reference of this section's results.

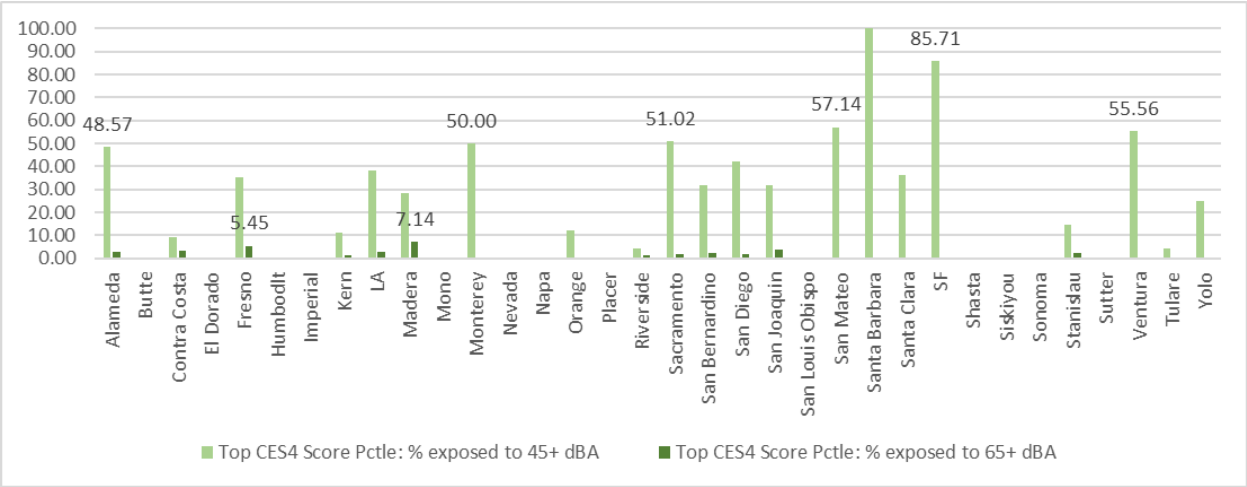


Figure 33. Percentage of the census tracts at 75th percentile for the CES4 score per county exposed to noise levels of 45+ dBA; and 65+ dBA.

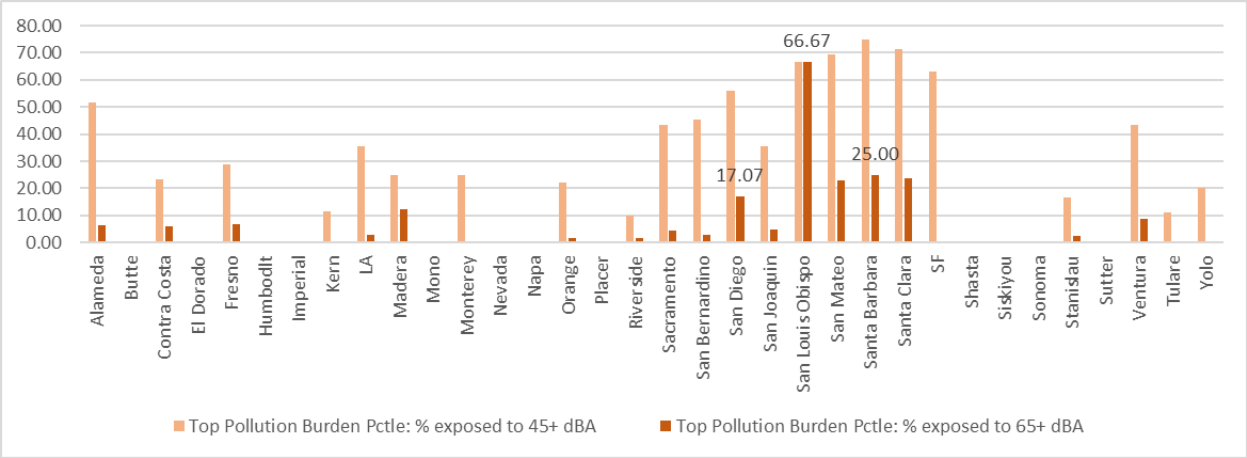


Figure 34. Percentage of the census tracts at 75th percentile for the Pollution Burden indicator per county exposed to noise levels of 45+ dBA; and 65+ dBA.

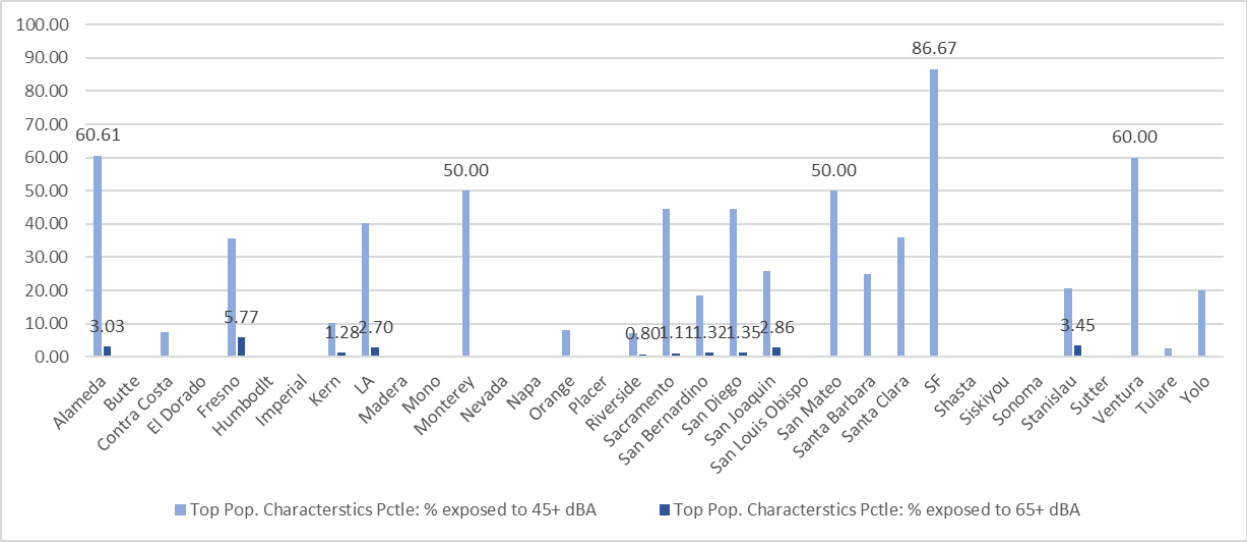


Figure 35. Percentage of the census tracts at 75th percentile for the Population Characteristics index per county exposed to noise levels of 45+ dBA; and 65+ dBA.

3.4. Expected Impact of Electric Aircraft on Noise

3.4.1. California Airports with Replacement Potential of Electric Aircrafts

The expected impact of electric aircraft on noise is stipulated following three steps:
(a) identifying the potential of electric aircraft replacement in the near future;
(b) understanding the potential electric aircraft market penetration on California airports; and
(c) identifying the potential of these replacements and the new electric aircraft market to impact the current noise levels.

Current research on battery technology and market penetration of sustainable aircrafts in commercial and cargo operations indicate that near-term electrification of aircrafts is expected to substitute smaller aircrafts (8-20 passengers) (see section 2.3.). This means that airports currently supporting long-distance flights (> 500 mi) will unlikely see any significant noise footprint reduction from their current levels in the near future (approximately mid century).

For airports with significant noise footprints of 60+ dBA (L*eq*) outside their boundaries, we can estimate that the noise effect of electrifying less than 5% of their fleet will not significantly affect their noise footprints, notably if their dominant commercial airline fleet is unlikely to be replaced by electric aircrafts in the near-future. This assumption does not take into account aeroacoustic and aerodynamic innovations for large-scale aircrafts that can reduce noise pollution at its source independently of electrification technology. Figure 36 shows the typical noise footprints of general aviation aircrafts, where we expect a higher market penetration of near-term aircraft electrification, notably for small and medium-sized propellers airplanes and turboprop airplanes. Figure 37 shows the typical noise footprint of airline jets, which are unlikely to be replaced by electric models in the near-term.

We expect, however, that airports with a higher percentage of regional and commuter flights (fleet mix of A-I and B-I) will have a higher potential of incorporating electric aircraft fleet mix, and of seeing their current noise footprint reduced, especially for those with high percentage of small fixed winged general aviation operations, and those that don't compete with large airline carriers. Figures 38 and 39 call out to SMX, RDD and ACV with 58.71, 35.33, and 33.44% of replaceable fleet mix; followed by BFL, HHR, and TRK with 11.53 to 24.64% of potential replaceable fleet mix[25]. Other regional airports that do not compete with long-haul carriers, or those that have predominantly general aviation operations, can potentially see their medium-sized aircraft operations increase, together with a reduction in their noise footprint. As aircraft electrification, or electric Vertical Take-Off & Landing aircraft (eVTOLs) are approaching certification and the demand for regional or commuter flights is progressively shifting form large-busy airports to regional airports (following emission reduction and passenger demand optimizations Datey, et al, 2023; Yee, et al., forthcoming).

[25] IPL was excluded from this list, with the highest % of replaceable mix, because it is not listed as an airport with noise exposure issues, and therefore the expected impact of fleet electrification on current noise exposure/annoyance is null.

Table 7 lists airports whose communities have high noise exposure, either related to high noise pollution baseline (% of noise footprint of 65+ dBA) or related to a large noise footprint (above the state average of 35 mi2. Airports listed in Table 7 will have a higher potential to see electrification noise effects take place in the surrounding communities. This list includes VNY which is further described in the next subsection to better understand the effects of fleet electrification on airport noise pollution in the near-term. Knowing the current noise exposure levels of airports is key to establish the potential of noise footprint reduction since there are airports like IPL, with the highest % of replaceable fleet mix (Figure 38) that have very low exposure levels. Therefore even if IPL sees a complete replacement of their small to medium aircrafts there would be no effect on the noise exposure.

Table 7. Airports whose Communities Have High Noise Exposure

AID	Tot. Nf.*	65+ dBA Nf.*	% 65+ dBA Nf.
SAN	37.349	1.401	3.75
IYK	31.596	0.824	2.61
TRK	10.169	0.177	1.74
LAX	101.299	1.743	1.72
SDM	32.547	0.533	1.64
SNA	45.903	0.731	1.59
MMH	2.006	0.032	1.58
FAT	78.615	1.123	1.43
MRY	14.187	0.197	1.39
UDD	1.720	0.019	1.10
MHR	59.473	0.462	0.78
LGB	41.915	0.298	0.71
SJC	75.448	0.516	0.68
MYF	36.343	0.188	0.52
BUR	75.253	0.244	0.32
SCK	36.759	0.119	0.32
VNY	73.254	0.110	0.15
SMF	67.002	0.082	0.12
SFO	116.753	0.115	0.10
HHR	81.148	0.077	0.09

AID	Tot. Nf.*	65+ dBA Nf.*	% 65+ dBA Nf.
CMA	35.135	0.021	0.06
OAK	112.069	0.063	0.06
HWD	113.058	0.011	0.01
ONT	77.097	0.004	0.00
SMO	59.139	0.002	0.00
CNO	73.188	0.001	0.00

*Nf = noise footprint in mi^2

By combining the rationale of airports with the highest potential of fleet electrification (Figure 38 and 39) with those of high noise exposure (Table 7), HHR, ONT, and TRK are the top candidates for seeing a reduction in noise exposure based on near-term fleet electrification potential. LAX, OAK, and SMF are also good candidates based on this logic due to their high exposure levels, however they have a slightly less potential for fleet electrification

By combining the airports with the highest potential of fleet electrification (Figure 38 and 39) with those with high co-occurrence of environmental injustice scores (Table 6), SMX, BFL, and HHR are the top three candidates for seeing a a high positive impact on the most vulnerable population from noise pollution reduction based on near-term fleet electrification potential.

HHR airport presents the highest potential for seeing a reduction in overall aviation noise impact due to the high potential of fleet electrification, its high noise exposure, and the high co-occurence of environmental injustice scores in noise exposure areas.

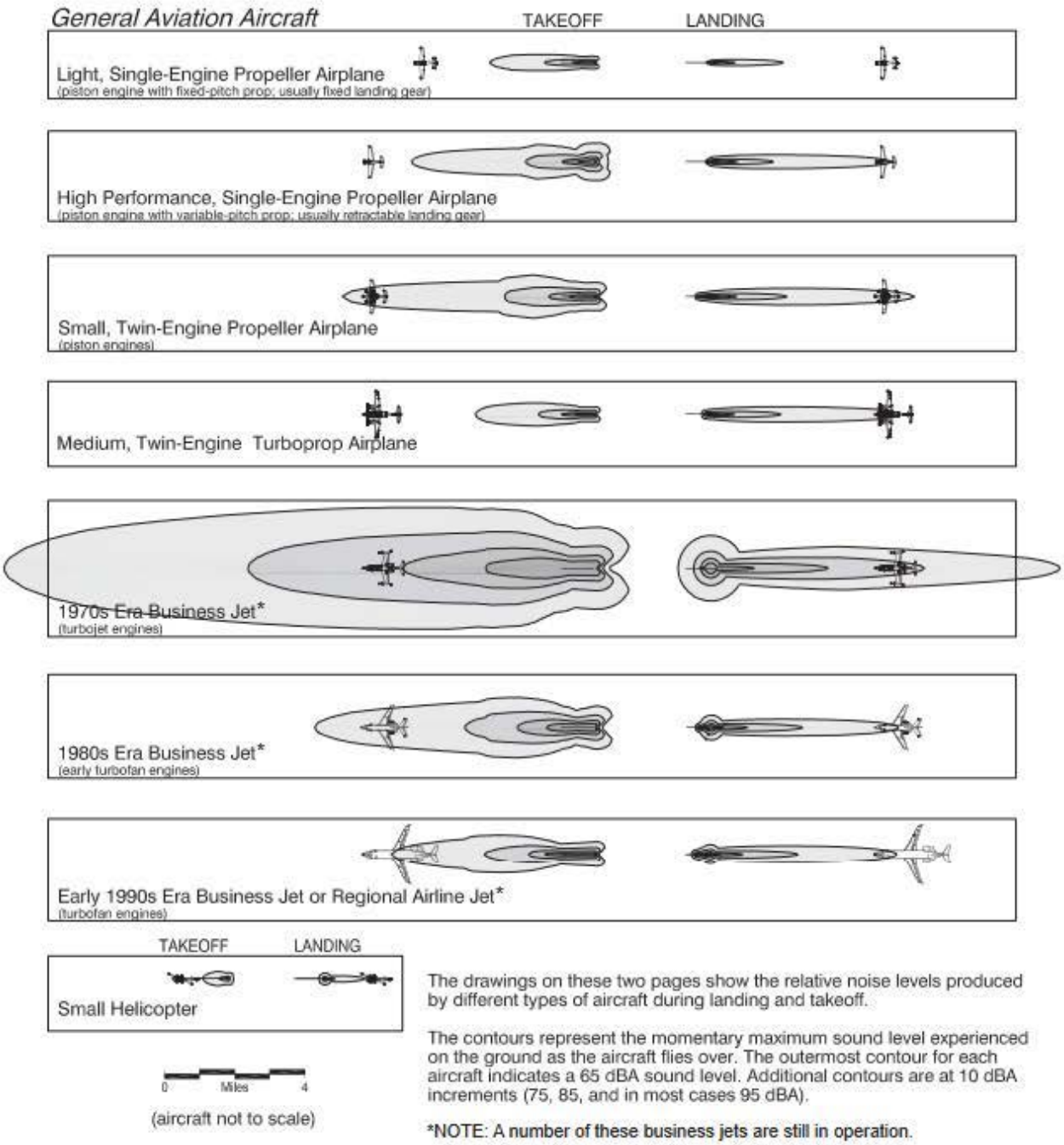


Figure 36. Typical noise footprints of general aviation aircrafts where there is a higher expectation of market penetration of electric aircrafts in the near-term. (Source: 2011 ALUP Handbook, pp.D-5)

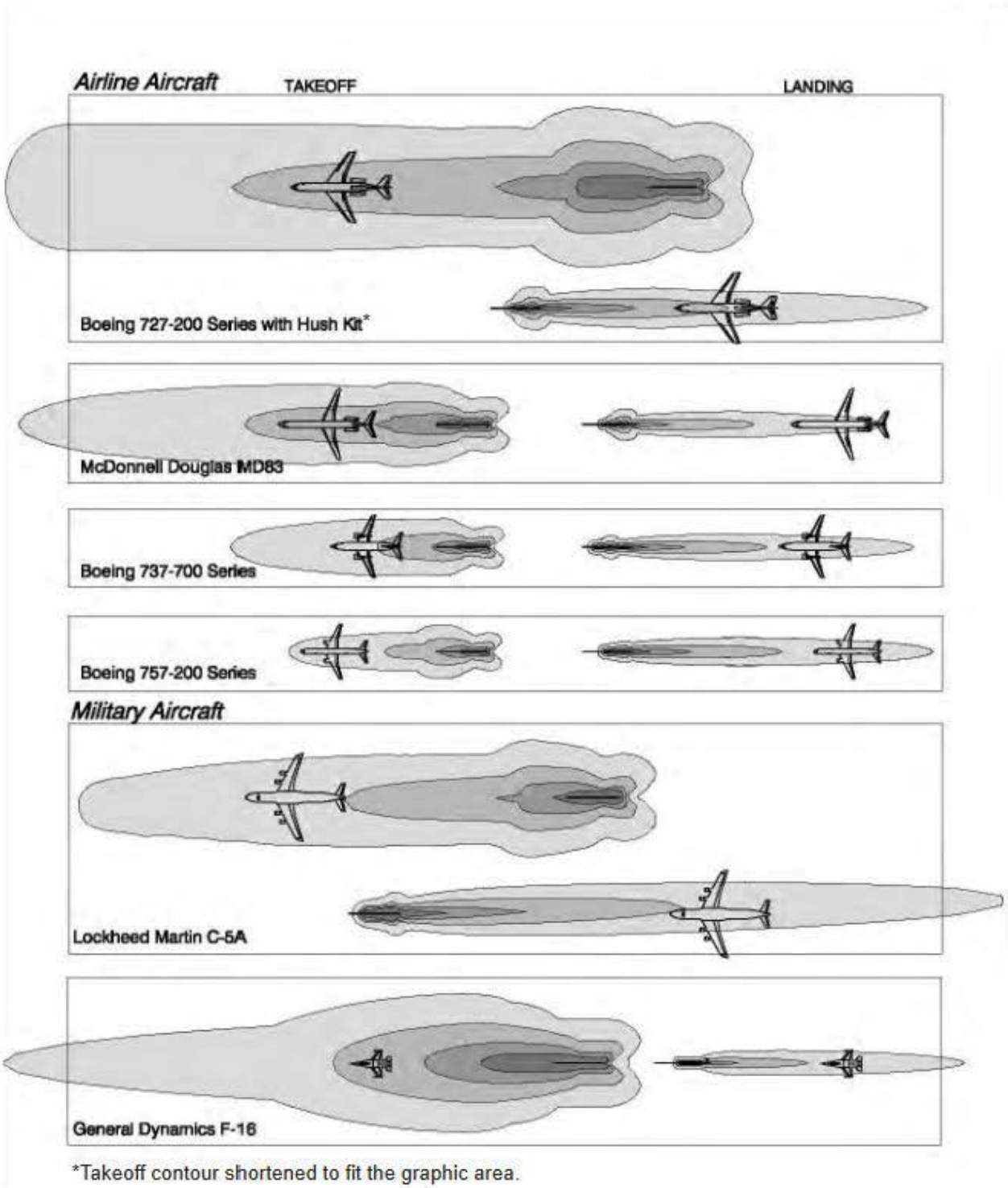


Figure 37. Typical noise footprints of commercial airline jets, which are unlikely to be replaced by electric models in the near-term. (Source: 2011 ALUP Handbook, pp.D-6)

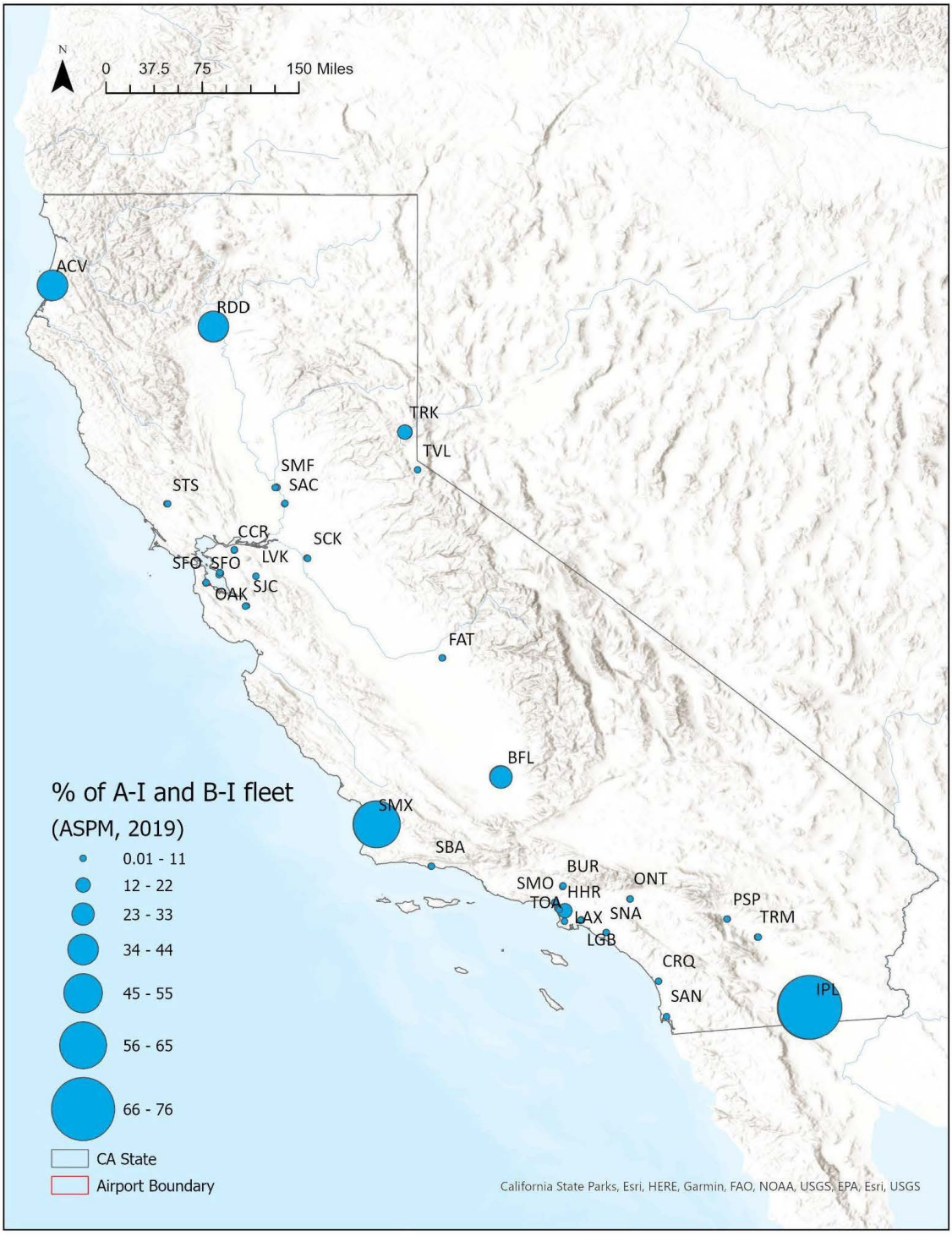


Figure 38. Airports with highest replacement potential of electric aircraft based on current fleet percentage of smaller aircrafts

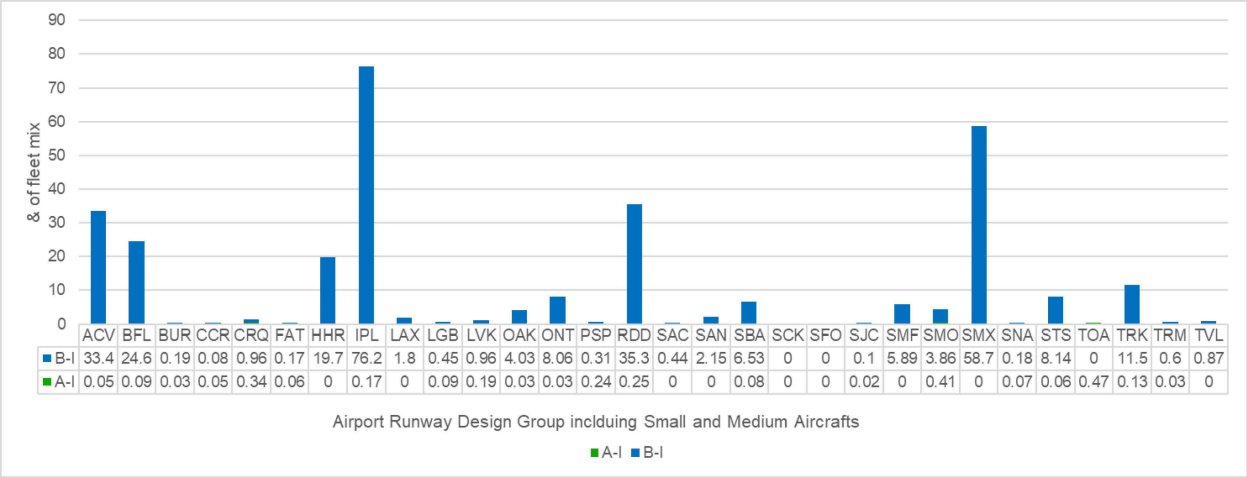


Figure 39. Airports with highest replacement potential of electric aircraft based on current fleet percentage of smaller aircrafts

3.4.2. Overview of Van Nuys Airport (VNY) Research on Noise Footprint of Electric Aviation

A study done in VNY, in the Los Angeles Basin, looks closely at the potential effects of aircraft electrification in regional airports from which we can draw some important trends for the near term impact of aviation electrification in California. Overall, areas with high DNL can be reduced; the percentage of noise reduction is larger in areas with high base case DNL (65+ dB); and, for the VNY case, the number of highly annoyed individuals was estimated to decrease by 7.42% to 14.91% (Datey et al., 2023).

Overview of Methods (Figure 40) : Datey et al., (2023) input data include traffic operations, aircraft trajectories, aircraft path distributions; and EASA Certification Noise Levels. Their noise estimation metrics are in DNL, for one sample day of the year that is representative of the general traffic activity at VNY according to the FAA System Wide Information Management (SWIM) data for 2019. Because a substantial presence of electric aircraft is considered unlikely before 2030, FAA's Terminal Area Forecasts (TAFs) for 2030 is used to scale the future number of operations for the sample day defined as December 30th.

The noise footprint of each operation is done using the input data from the EASA Certification Noise Levels and processed by the publicly available Advanced Acoustic Model (AAM) suite originally developed under the sponsorship of NASA, and currently curanted by the Department of Transportation Volpe Center.

VNY was selected for this study as a representative for the effect of aircraft electrification on noise for two reasons: (1) it airports in California that have predominantly general aviation operations with a fleet mix that is considered as replaceable for eVTOLs in the near future; and (2) knowing the airport current noise levels are detrimental to neighboring communities (has a FAR Part 150 plan for noise mitigation).

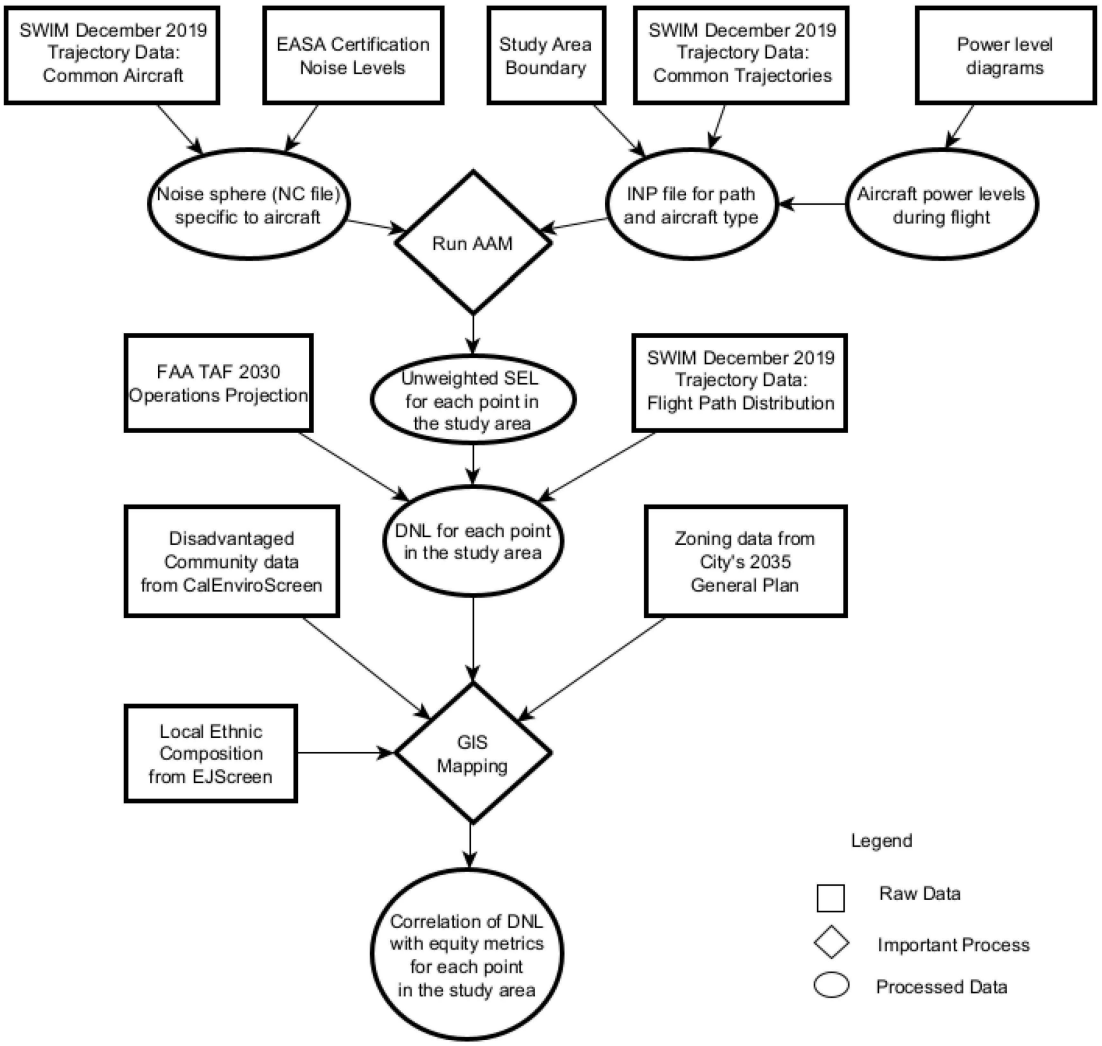


Figure 40. Method used in the VNY case study to estimate noise levels and impact (source, Datey et al., 2023, p 2)

Overview of Results: For two fleet electrification scenarios at VNY (20% and 50% of fleet) the areas exposed to noise decrease (Figure 41), and the highly annoyed population also decreases as can be seen in detail in Table 8 and Figure 42.

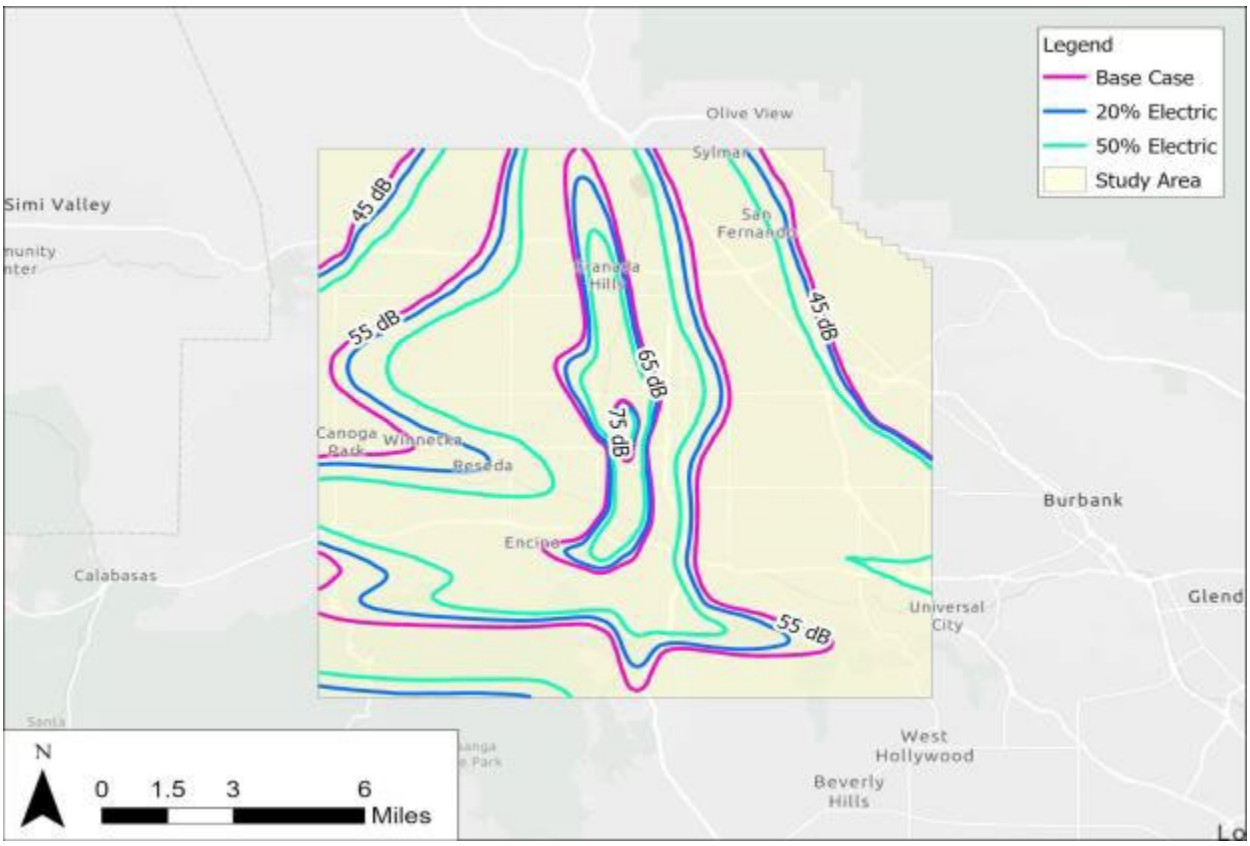


Figure 41. Expected Impact of Fleet Electrification at VNY Noise Contour Lines. Source: Datey et al., 2023, p.8)

Scenario	Number of "Highly Annoyed" Individuals	% Reduction
Base Case	421,110	-
20% Electric	392,028	-7.42%
50% Electric	341,170	-14.91%

Table 8. Expected Reduction of Highly Annoyed Individuals Based on Fleet Electrification Scenarios at VNY (Datey et al., 2023, p.8)

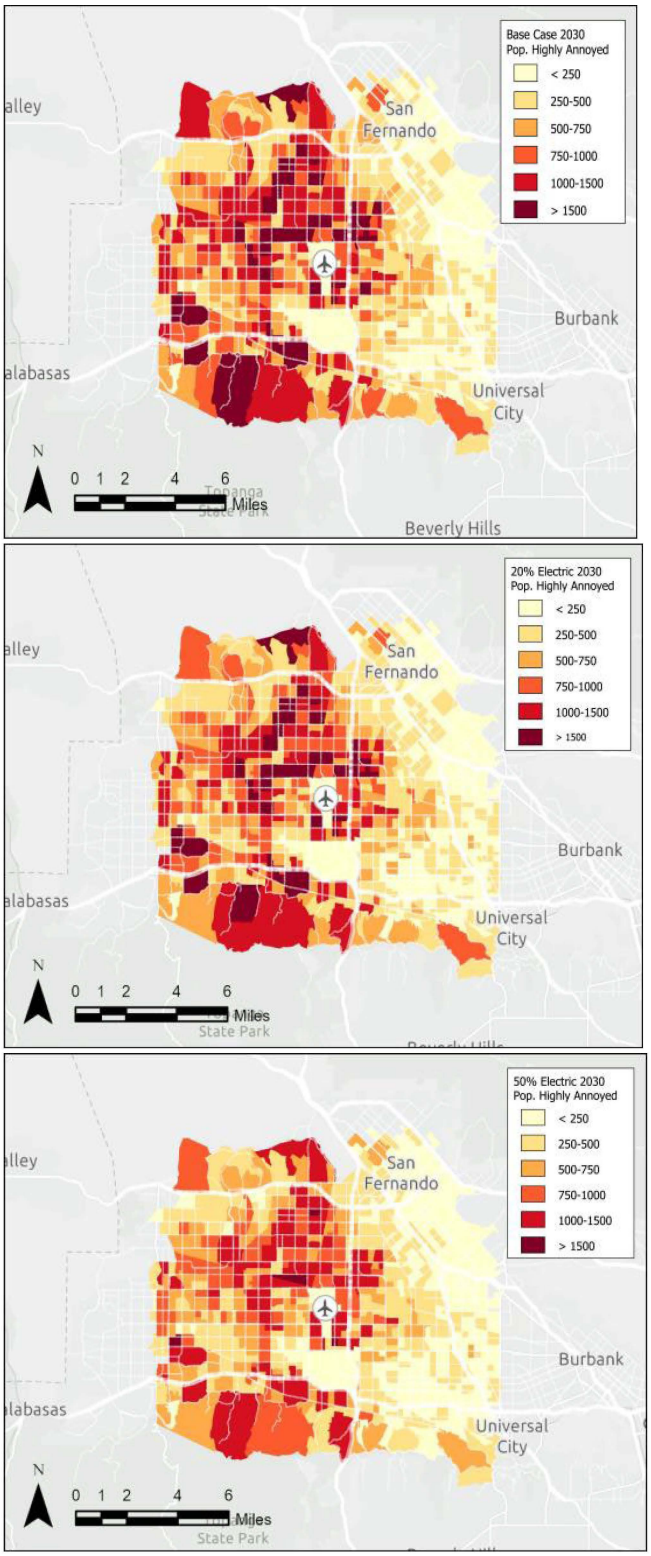


Figure 42. Projected Impact of Fleet Electrification of VNY on Highly Annoyed Population. From top to bottom, the base case scenario, fleet electrification of 20% scenario, and fleet electrification of 50% scenario. (Datey et al., 2023, p.7)

[4.2] 4. Citations

Baumeister, S., Leung, A., & Ryley, T. (2020). The emission reduction potentials of First Generation Electric Aircraft (FGEA) in Finland. Journal of Transport Geography, 85, 102730. https://doi.org/10.1016/j.jtrangeo.2020.102730

Brdnik, P., Kamnik, R., Boˇziˇcnik, S., & Marksel, M. (2022). Ground infrastructure investments for operation of hybrid-electric aircraft. https://iopscience.iop.org/article/10.1088/1757-899X/1226/1/012073/pdf

Caltrans. (2011). ALUP Handbook (p. 455). https://dot.ca.gov/-/media/dot-media/programs/aeronautics/documents/californiaairportlanduseplanninghandbook-a11y.pdf

Congressional Research Service. (2021). Federal Airport Noise Regulations and Programs. https://crsreports.congress.gov/product/pdf/r/r46920

Datey, A., Kao, B., Francisco, R., Moradpour, M., & Kim, R. (2023). Noise Footprint of Electric Aviation at Regional Airports: A Case Study of VNY. https://ieeexplore.ieee.org/document/10124303

Epstein, A. H., & O'Flarity, S. M. (2019). Considerations for Reducing Aviation's CO2 with Aircraft Electric Propulsion. Journal of Propulsion and Power, 35(3), 572–582. https://doi.org/10.2514/1.B37015

FAA. (2015). Environmental Impacts: Policies and Procedures (p. 132). https://www.faa.gov/documentLibrary/media/Order/FAA_Order_1050_1F.pdf

FAA. (2020). Aircraft Noise Overview. https://faabostonworkshops.com/project-information/aircraft-noise-overview/

FAA. (2021). Airport Safety Detail. https://www.airporttech.tc.faa.gov/Products/Airport-Safety-Papers-Publications/Airport-Safety-Detail/ArtMID/3682/ArticleID/2845/Analysis-of-NES

FAA. (2022a). FAA History of Noise. https://www.faa.gov/regulations_policies/policy_guidance/noise/history

FAA. (2022b). Fundamentals of Noise and Sound. https://www.faa.gov/regulations_policies/policy_guidance/noise/basics

Fox, M. A., Sinkar, S., & Bechard, M. (2023). Health and equity in transportation health impact assessments: A retrospective analysis. Journal of Transport & Health, 32, 101675. https://doi.org/10.1016/j.jth.2023.101675

Holland, F. (2021). DHL Express buys electric cargo planes for U.S. package delivery from start-up Eviation. https://www.cnbc.com/2021/08/03/dhl-express-buys-eviation-electric-planes-for-us-package-delivery.html

Mukhopadhaya, J. (2022). PERFORMANCE ANALYSIS OF REGIONAL ELECTRIC AIRCRAFT. https://theicct.org/wp-content/uploads/2022/07/global-aviation-performance-analysis-regional-electric-aircraft-jul22-1.pdf-1.pdf

OPR. (2023). Noise Element Guidelines (p. 14). https://opr.ca.gov/docs/OPR_Appendix_D_final.pdf
Seto, E., & Huang, C.-H. (2023). The National Transportation Noise Exposure Map [Preprint].

Occupational and Environmental Health. https://doi.org/10.1101/2023.02.02.23285396
The California Climate Crisis Act. (2022). 2022—Assembly Bill 1279 (Muratsuchi, Al),. https://ww2.arb.ca.gov/2022-assembly-bill-1279-muratsuchi-al-california-climate-crisis-act-chaptered

Truax, B. (1999). HANDBOOK FOR ACOUSTIC ECOLOGY.
USDOT. (2023). Consumer Airfare Report: Table 1—Top 1,000 Contig. https://data.transportation.gov/Aviation/Consumer-Airfare-Report-Table-1-Top-1-000-Contiguo/4f3n-jbg2/data

[4.2] Appendix A. Airports in California represented in the 2018 NTNM

AID	Facility Name
ACV	CALIFORNIA REDWOOD COAST-HUMBOLDT COUNTY AIRPORT
APC	NAPA COUNTY AIRPORT
BFL	MEADOWS FIELD AIRPORT
BUR	BOB HOPE AIRPORT
CCR	BUCHANAN FIELD AIRPORT
CIC	CHICO MUNICIPAL AIRPORT
CMA	CAMARILLO AIRPORT
CNO	CHINO AIRPORT
CRQ	MCCLELLAN-PALOMAR AIRPORT
FAT	FRESNO YOSEMITE INTERNATIONAL AIRPORT
HHR	JACK NORTHROP FIELD/HAWTHORNE MUNICIPAL AIRPORT
HWD	HAYWARD EXECUTIVE AIRPORT
IYK	INYOKERN-KERN COUNTY AIRPORT
LAX	LOS ANGELES INTERNATIONAL AIRPORT
LGB	LONG BEACH AIRPORT DAUGHERTY FIELD
LVK	LIVERMORE MUNICIPAL AIRPORT
MAE	MADERA MUNICIPAL AIRPORT
MCC	MCCLELLAN AIRFIELD
MHR	SACRAMENTO MATHER AIRPORT
MMH	MAMMOTH YOSEMITE AIRPORT
MOD	MODESTO CITY-COUNTY AIRPORT
MRY	MONTEREY REGIONAL AIRPORT
MYF	MONTGOMERY FIELD
NUQ	MOFFET FEDERAL AIRFIELD
OAK	METROPOLITAN OAKLAND INTERNATIONAL AIRPORT
ONT	ONTARIO INTERNATIONAL AIRPORT
OXR	OXNARD AIRPORT
PRB	PASO ROBLES MUNICIPAL AIRPORT
PSP	PALM SPRINGS INTERNATIONAL AIRPORT
RDD	REDDING MUNICIPAL AIRPORT
SAC	SACRAMENTO EXECUTIVE AIRPORT
SAN	SAN DIEGO INTERNATIONAL AIRPORT
SBA	SANTA BARBARA MUNICIPAL AIRPORT
SBD	SAN BERNARDINO INTERNATIONAL AIRPORT
SBP	SAN LUIS OBISPO REGIONAL AIRPORT
SCK	STOCKTON METROPOLITAN AIRPORT
SDM	BROWN FIELD
SEE	GILLESPIE FIELD AIRPORT
SFO	SAN FRANCISCO INTERNATIONAL AIRPORT
SJC	SAN JOSE INTERNATIONAL AIRPORT, NORMAN Y. MINETA

SMF	SACRAMENTO INTERNATIONAL AIRPORT
SMO	SANTA MONICA MUNICIPAL AIRPORT
SMX	SANTA MARIA PUBLIC AIRPORT
SNA	JOHN WAYNE AIRPORT, ORANGE CO.
SNS	SALINAS MUNICIPAL AIRPORT
STS	CHARLES M. SCHULZ, SONOMA COUNTY AIRPORT
TRK	TRUCKEE-TAHOE AIRPORT
TRM	JACQUELINE COCHRAN REGIONAL AIRPORT
TVL	LAKE TAHOE AIRPORT
UDD	BERMUDA DUNES EXECUTIVE AIRPORT
VCV	SOUTHERN CALIFORNIA LOGISTICS AIRPORT
VIS	VISALIA MUNICIPAL AIRPORT
VNY	VAN NUYS AIRPORT

[4.2] Appendix B. Aircrafts Matched as Potentially Replaceable for Electric Regional/ General Aviation Aircrafts in California Airports (source: FAA Aircraft Characteristics Data)

FAA_ Designator	Manufacturer	Model_FAA	Physical_Class_Engine	AAC	ADG	Class	FAA_ Weight
A5	ICON	Icon A-5	Piston	A	I	Amphibian	Small
AA1	GRUMMAN AMERICAN	Grumman American AA1	Piston	A	I	Fixed-wing	Small
AA5	GRUMMAN AMERICAN	Grumman American AA5	Piston	A	I	Fixed-wing	Small
AC11	ROCKWELL	Rockwell Commander 112	Piston	A	I	Fixed-wing	Small
AC90	GULFSTREAM AEROSPACE-ROCKWELL	Gulfstream 690 Commander 690	Turboprop	B	I	Fixed-wing	Small
AEST	PIPER	Piper Aero Star	Piston	B	I	Fixed-wing	Small
AR11	AERONCA	Aeronca 11 Chief	Piston	A	I	Fixed-wing	Small
B18T	BEECH	Beech 18 (Turbo)	Turboprop	A	I	Fixed-wing	Small
B36T	ALLISON-BEECH	Allison 36 Turbine Bonanza	Piston	A	I	Fixed-wing	Small

BE10	BEECH	Beech King Air 100	Turboprop	B	I	Fixed-wing	Small
BE19	BEECH	Beech B19 Musketeer	Piston	A	I	Fixed-wing	Small
BE23	BEECH	Beech 23 Sundowner	Piston	A	I	Fixed-wing	Small
BE24	BEECH	Beech 24 Sierra	Piston	A	I	Fixed-wing	Small
BE33	BEECH	Beech Bonanza 33	Piston	A	I	Fixed-wing	Small
BE35	BEECH	Beech Bonanza 35	Piston	A	I	Fixed-wing	Small
BE36	BEECH	Beech Bonanza 36	Piston	A	I	Fixed-wing	Small
BE40	RAYTHEON-BEECH-HAWKER	Raytheon/Beech Beechjet 400/T-1 Jayhawk	Jet	B	I	Fixed-wing	Small+
BE50	BEECH	Beechcraft 50 Twin Bonanza	Piston	A	I	Fixed-wing	Small
BE55	BEECH	Beech Baron 55	Piston	B	I	Fixed-wing	Small
BE58	BEECH	Beech 58 Baron	Piston	B	I	Fixed-wing	Small
BE60	BEECH	Beech 60 Duke	Piston	B	I	Fixed-wing	Small
BE65	BEECH	Beech 65 Queen Air	Piston	B	I	Fixed-wing	Small

BE76	BEECH	Beech 76 Duchess	Piston	A	I	Fixed-wing	Small
BE77	BEECH	Beech 77 Skipper	Piston	A	I	Fixed-wing	Small
BE99	BEECH	Beech Airliner 99	Turboprop	B	I	Fixed-wing	Small
BL17	BELLANCA	Bellanca Viking	Piston	A	I	Fixed-wing	Small
BL8	BELLANCA	Bellanca 8 Scout	Piston	A	I	Fixed-wing	Small
BT36	BEECH	Beech 36 Bonanza	Piston	A	I	Fixed-wing	Small
C120	CESSNA	Cessna 120	Piston	A	I	Fixed-wing	Small
C140	CESSNA	Cessna 140	Piston	A	I	Fixed-wing	Small
C150	CESSNA	Cessna 150	Piston	A	I	Fixed-wing	Small
C152	CESSNA	Cessna 152	Piston	A	I	Fixed-wing	Small
C162	CESSNA	Cessna 162 Skycatcher	Piston	A	I	Fixed-wing	Small
C170	CESSNA	Cessna 170	Piston	A	I	Fixed-wing	Small
C172	CESSNA	Cessna Skyhawk 172/Cutlass	Piston	A	I	Fixed-wing	Small
C175	CESSNA	Cessna 175	Piston	A	I	Fixed-wing	Small
C177	CESSNA	Cessna 177 Cardinal	Piston	A	I	Fixed-wing	Small

C180	CESSNA	Cessna 180 Skywagon	Piston	A	I	Fixed-wing	Small
C182	CESSNA	Cessna Skylane 182	Piston	A	I	Fixed-wing	Small
C185	CESSNA	Cessna 185 Skywagon	Piston	A	I	Fixed-wing	Small
C188	CESSNA	Cessna 188	Piston	A	I	Fixed-wing	Small
C195	CESSNA	Cessna 195	Piston	A	I	Fixed-wing	Small
C206	CESSNA	Cessna 206 Stationair	Piston	A	I	Fixed-wing	Small
C207	CESSNA	Cessna 207 Stationair 7	Piston	A	I	Fixed-wing	Small
C210	CESSNA	Cessna 210 Centurion	Piston	A	I	Fixed-wing	Small
C240	CESSNA	Cessna TTx Model T240	Piston	A	I	Fixed-wing	Small
C25M	CESSNA	Cessna Citation M2	Jet	B	I	Fixed-wing	Small
C303	CESSNA	Cessna 303 Crusader	Piston	A	I	Fixed-wing	Small
C310	CESSNA	Cessna 310	Piston	A	I	Fixed-wing	Small
C320	CESSNA	Cessna 320 Skyknight	Piston	A	I	Fixed-wing	Small
C335	CESSNA	Cessna 335	Piston	B	I	Fixed-wing	Small
C340	CESSNA	Cessna 340	Piston	B	I	Fixed-wing	Small

C402	CESSNA	Cessna 401/402	Piston	A	I	Fixed-wing	Small
C404	CESSNA	Cessna 404 Titan	Piston	B	I	Fixed-wing	Small
C414	CESSNA	Cessna Chancellor 414	Piston	B	I	Fixed-wing	Small
C421	CESSNA	Cessna Golden Eagle 421	Piston	B	I	Fixed-wing	Small
C425	CESSNA	Cessna 425 Corsair	Turboprop	B	I	Fixed-wing	Small
C500	CESSNA	Cessna 500/Citation I	Jet	B	I	Fixed-wing	Small
C501	CESSNA	Cessna 1SP	Jet	B	I	Fixed-wing	Small
C510	CESSNA	Cessna Citation Mustang	Jet	B	I	Fixed-wing	Small
C525	CESSNA	Cessna CitationJet/CJ1	Jet	B	I	Fixed-wing	Small
C526	CESSNA	Cessna 526 CitationJet	Jet	B	I	Fixed-wing	Small
C72R	CESSNA	Cessna 172RG Cutlass RG	Piston	A	I	Fixed-wing	Small
C77R	CESSNA	Cessna 177 Cardinal RG	Piston	A	I	Fixed-wing	Small

C82R	CESSNA	Cessna Skylane RG	Piston	A	I	Fixed-wing	Small
CH7A	AERONCA	Aeronca 7AC	Piston	A	I	Fixed-wing	Small
CH7B	BELLANCA	Bellanca 7GCBC Citabria	Piston	A	I	Fixed-wing	Small
COL3	LANCAIR-CESSNA	Lancair LC-40 Columbia 300	Piston	A	I	Fixed-wing	Small
COL4	LANCAIR-CESSNA	Lancair LC-41 Columbia 400	Piston	A	I	Fixed-wing	Small
CRUZ	CZAW	CZAW SportCruiser	Piston	A	I	Fixed-wing	Small
DA40	DIAMOND	Diamond Star DA40	Piston	A	I	Fixed-wing	Small
DA42	DIAMOND	Diamond Twin Star	Piston	A	I	Fixed-wing	Small
DHC2	DEHAVILLAND CANADA	DeHavilland Canada 2 Mk1 Beaver	Piston	A	I	Fixed-wing	Small
DV20	DIAMOND	Diamond 20 Katana	Piston	A	I	Fixed-wing	Small
E50P	EMBRAER	Embraer 500 Phenom 100	Jet	B	I	Fixed-wing	Small
EA50	ECLIPSE	Eclipse 500	Jet	B	I	Fixed-wing	Small
ERCO	ERCO	Ercoupe 415	Piston	A	I	Fixed-wing	Small

EVOT	LANCAIR	Lancair Evolution Turbine	Turboprop	A	I	Fixed-wing	Small
FA10	DASSAULT	Dassault Falcon/Mystère 10	Jet	B	I	Fixed-wing	Small+
FDCT	FLIGHT DESIGN	Flight Design CT	Piston	A	I	Fixed-wing	Small
G164	GRUMMAN AMERICAN	Grumman American G164	Piston	A	I	Fixed-wing	Small
GA7	GULFSTREAM AMERICAN - GRUMMAN AMERICAN	Gulfstream American GA7	Piston	A	I	Fixed-wing	Small
GC1	GLOBE	Globe GC-1 Swift	Piston	A	I	Fixed-wing	Small
HDJT	HONDA	HONDA HA-420 HondaJet	Jet	B	I	Fixed-wing	Small
HUSK	AVIAT	AVIAT Huskey	Piston	A	I	Fixed-wing	Small
KODI	QUEST	Quest Kodiak	Turboprop	A	I	Fixed-wing	Small
L29B	LOCKHEED	Lockheed Jetstar 2/731	Jet	B	I	Fixed-wing	Large
L5	STINTSON	Stintson L5 Sentinel	Piston	A	I	Fixed-wing	Small
L8	LUSCOMBE	Luscombe 8	Piston	A	I	Fixed-wing	Small

LA4	LAKE	Lake LA-4	Piston	A	I	Amphibian	Small
LJ31	LEARJET	Bombardier Learjet 31	Jet	B	I	Fixed-wing	Small+
LNC4	LANCAIR	Lancair IV	Piston	A	I	Fixed-wing	Small
LNP4	LANCAIR	Lancair PropJet IV	Turboprop	A	I	Fixed-wing	Small
M20P	MOONEY	Mooney M-20C Ranger	Piston	A	I	Fixed-wing	Small
M20T	MOONEY	Mooney M20K Encore/M20 M Bravo	Piston	A	I	Fixed-wing	Small
M5	MAULE	Maule M-5	Piston	A	I	Fixed-wing	Small
MU2	MITSUBISHI	Mitsubishi Marquise/Solitaire	Turboprop	B	I	Fixed-wing	Small
MU30	MITSUBISHI	Mitsubishi Diamond/MU300 Diamond	Jet	B	I	Fixed-wing	Small+
NAVI	NORTH AMERICAN-RYAN	North American Navion	Piston	A	I	Fixed-wing	Small
P210	RILEY-CESSNA	Riley Super P210	Piston	A	I	Fixed-wing	Small
P28A	PIPER	Piper Cherokee	Piston	A	I	Fixed-wing	Small
P28B	PIPER	Piper Turbo Dakota	Piston	A	I	Fixed-wing	Small

P28R	PIPER	Cherokee Arrow	Piston	A	I	Fixed-wing	Small
P28T	PIPER	Piper 28T Arrow 4	Piston	A	I	Fixed-wing	Small
P32R	PIPER	Piper PA-32R Lance/ Saratoga SP	Piston	A	I	Fixed-wing	Small
P32T	PIPER	Piper 32T Turbo Lance 2	Piston	A	I	Fixed-wing	Small
P46T	PIPER	Piper Malibu Meridian	Turboprop	A	I	Fixed-wing	Small
P51	NORTH AMERICAN	North American Mustang	Piston	B	I	Fixed-wing	Small
P68	VULCAN-PARTEVANIA	Vulcan Air P68	Piston	A	I	Fixed-wing	Small
P750	PACIFIC AEROSPACE	Pacific Aerospace P-750 Xstol	Turboprop	A	I	Fixed-wing	Small
PA11	PIPER	Piper PA-11 Cub Special	Piston	A	I	Fixed-wing	Small
PA12	PIPER	Piper 12 Supercruiser	Piston	A	I	Fixed-wing	Small
PA16	PIPER	Piper PA-16 Clipper	Piston	A	I	Fixed-wing	Small
PA18	PIPER	Piper 18 Super Cub	Piston	A	I	Fixed-wing	Small
PA20	PIPER	Piper PA-20 Pacer	Piston	A	I	Fixed-wing	Small

PA22	PIPER	Piper 22 Tri-Pacer	Piston	A	I	Fixed-wing	Small
PA23	PIPER	Piper PA-23-150/160 Apache	Piston	A	I	Fixed-wing	Small
PA24	PIPER	Piper PA-24 Comanche	Piston	A	I	Fixed-wing	Small
PA25	PIPER	Piper PA-25 Pawnee	Piston	A	I	Fixed-wing	Small
PA27	PIPER	Piper Aztec	Piston	B	I	Fixed-wing	Small
PA30	PIPER	Piper PA-30 Turbo Twin Comanche/Turbo Twin Comanche	Piston	A	I	Fixed-wing	Small
PA31	PIPER	Piper Navajo PA-31	Piston	B	I	Fixed-wing	Small
PA32	PIPER	Piper Cherokee Six	Piston	A	I	Fixed-wing	Small
PA34	PIPER	Piper PA-34 Seneca	Piston	A	I	Fixed-wing	Small
PA36	PIPER	Piper PA-36 Pawnee Brave	Piston	A	I	Fixed-wing	Small
PA38	PIPER	Piper Tomahawk PA38	Piston	A	I	Fixed-wing	Small
PA44	PIPER	Piper Seminole	Piston	A	I	Fixed-wing	Small

PA46	PIPER	Piper Malibu	Piston	A	I	Fixed-wing	Small
PAT4	PIPER	Piper PA-31T3-500 T-1040	Turboprop	B	I	Fixed-wing	Small
PAY1	PIPER	Piper Cheyenne 1	Piston	B	I	Fixed-wing	Small
PAY2	PIPER	Piper Cheyenne 2	Piston	B	I	Fixed-wing	Small
PAY3	PIPER	Piper PA-42-720 Cheyenne 3	Turboprop	B	I	Fixed-wing	Small
PAY4	PIPER	Piper Cheyenne 400	Turboprop	B	I	Fixed-wing	Small
PRM1	RAYTHEON-HAWKER BEECHCRAFT	Raytheon Premier 1/390 Premier 1	Jet	B	I	Fixed-wing	Small+
RV12	VAN'S	Van's RV-12	Piston	A	I	Fixed-wing	Small
S108	STINSON	Stinson 108 Voyager	Piston	A	I	Fixed-wing	Small
S22T	CIRRUS	Cirrus SR-22 Turbo	Piston	A	I	Fixed-wing	Small
SF50	CIRRUS	Cirrus Vision SF50	Jet	A	I	Fixed-wing	Small
SR20	CIRRUS	Cirrus SR-20	Piston	A	I	Fixed-wing	Small
SR22	CIRRUS	Cirrus SR 22	Piston	A	I	Fixed-wing	Small

T210	CESSNA	Cessna T210 Turbo Centurion	Piston	A	I	Fixed-wing	Small
T28	NORTH AMERICAN	North American T-28 Trojan	Piston	A	I	Fixed-wing	Small
T34P	BEECH	Beech T-34/45 Mentor	Turboprop	A	I	Fixed-wing	Small
T6	NORTH AMERICAN	North American T-6 Texan	Piston	A	I	Fixed-wing	Small
TAYB	TAYLORCRAFT	Taylorcraft BC	Piston	A	I	Fixed-wing	Small
TB20	SOCATA	Socata TB-20 Trinidad	Piston	A	I	Fixed-wing	Small
TBM7	SOCATA	Socata TBM-700/700A	Turboprop	A	I	Fixed-wing	Small
TBM8	SOCATA	Socata TBM-850	Turboprop	A	I	Fixed-wing	Small
TBM9	SOCATA	Socata TBM-900	Turboprop	A	I	Fixed-wing	Small
TEX2	RAYTHEON	Raytheon Texan 2	Turboprop	B	I	Fixed-wing	Small
TOBA	SOCATA	Socata TB-10 Tobago	Piston	A	I	Fixed-wing	Small

[4.2] Appendix C. Airport Noise Footprint Data

dBA (Leq)	AID	Area (mi2)
65	ACV	0.002
60	ACV	0.048
55	ACV	0.420
50	ACV	1.546
45	ACV	4.889
60	APC	0.046
55	APC	0.495
50	APC	1.840
45	APC	4.787
55	BFL	0.259
50	BFL	1.817
45	BFL	5.905
75	BUR	0.000
70	BUR	0.017
65	BUR	0.226
60	BUR	1.114
55	BUR	3.731
65	CCR	0.003
60	CCR	0.070
55	CCR	0.943
50	CCR	3.812
45	CCR	13.063
65	CIC	0.000
60	CIC	0.019
55	CIC	0.287
50	CIC	1.223
45	CIC	4.171
70	CMA	0.000
65	CMA	0.021
60	CMA	0.252
55	CMA	1.064
50	CMA	3.902
65	CNO	0.001
60	CNO	0.248
55	CNO	0.948
75	CRQ	0.000
70	CRQ	0.010
65	CRQ	0.111

60	CRQ	0.521
55	CRQ	1.402
50	CRQ	3.422
45	CRQ	12.336
70	FAT	0.148
65	FAT	0.975
60	FAT	3.076
55	FAT	7.897
50	FAT	18.680
45	FAT	47.839
80	HHR	0.000
75	HHR	0.004
70	HHR	0.012
65	HHR	0.061
60	HHR	0.281
55	HHR	0.960
65	HWD	0.011
60	HWD	0.194
55	HWD	2.792
80	IYK	0.016
75	IYK	0.065
70	IYK	0.195
65	IYK	0.547
60	IYK	1.518
55	IYK	3.498
50	IYK	7.397
45	IYK	18.360
70	LAX	0.099
65	LAX	1.644
60	LAX	5.739
55	LAX	13.986
50	LAX, HHR	23.427
45	LAX, SMO, HHR	56.404
75	LGB	0.001
70	LGB	0.020
65	LGB	0.277
60	LGB	1.050
55	LGB	3.242
50	LGB	9.269
45	LGB	28.054
70	LVK	0.000
65	LVK	0.009
60	LVK	0.115
55	LVK	1.134

50	LVK	3.701
45	LVK	17.091
70	MAE	0.000
65	MAE	0.006
60	MAE	0.017
55	MAE	0.270
50	MAE	1.161
45	MAE	4.373
55	MCC	0.006
50	MCC	0.546
45	MCC	4.475
70	MHR	0.050
65	MHR	0.412
60	MHR	2.257
55	MHR	10.317
50	MHR	17.283
45	MHR	29.154
75	MMH	0.000
70	MMH	0.003
65	MMH	0.029
60	MMH	0.087
55	MMH	0.178
50	MMH	0.406
45	MMH	1.303
80	MOD	0.000
75	MOD	0.002
70	MOD	0.010
65	MOD	0.035
60	MOD	0.075
55	MOD	0.422
50	MOD	1.444
45	MOD	4.233
75	MRY	0.000
70	MRY	0.018
65	MRY	0.179
60	MRY	0.651
55	MRY	1.610
50	MRY	3.322
45	MRY	8.407
75	MYF	0.002
70	MYF	0.038
65	MYF	0.148
60	MYF	0.611
55	MYF	1.957

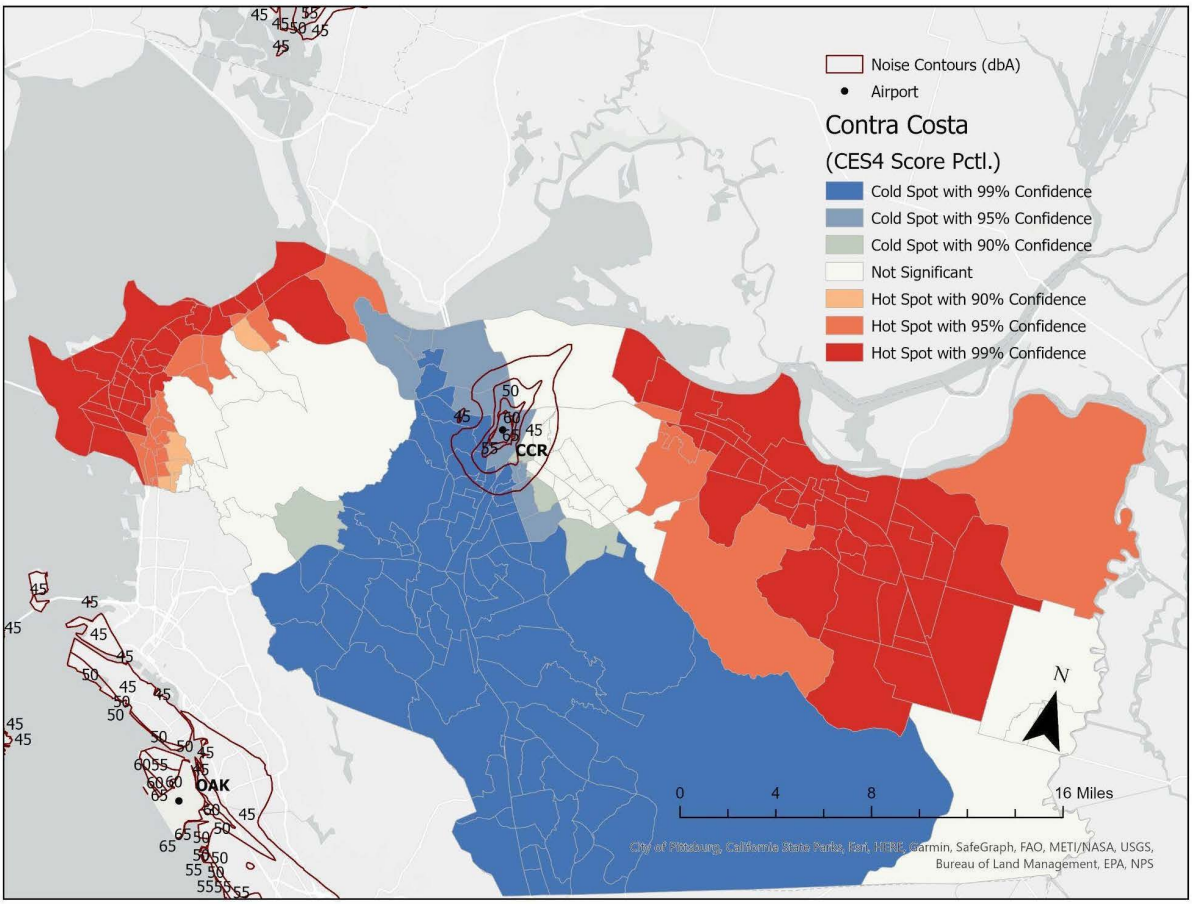
50	MYF	7.133
45	MYF	26.454
55	NUQ	0.346
50	NUQ	1.235
45	NUQ	0.334
70	OAK	0.000
65	OAK	0.063
60	OAK	0.439
55	OAK	1.505
65	ONT	0.004
60	ONT	0.984
55	ONT	4.118
50	ONT, CNO	21.558
45	ONT, CNO	50.432
75	OXR	0.000
70	OXR	0.010
65	OXR	0.047
60	OXR	0.218
55	OXR	0.777
50	OXR	2.221
45	OXR, CMA	29.896
60	PRB	0.005
55	PRB	0.140
50	PRB	0.978
45	PRB	4.716
65	PSP	0.009
60	PSP	0.277
55	PSP	1.497
50	PSP	3.671
45	PSP	9.401
65	RDD	0.002
60	RDD	0.073
55	RDD	0.607
50	RDD	2.445
45	RDD	8.337
65	SAC	0.006
60	SAC	0.113
55	SAC	0.833
50	SAC	2.881
45	SAC	12.170
75	SAN	0.009
70	SAN	0.229
65	SAN	1.163
60	SAN	3.216

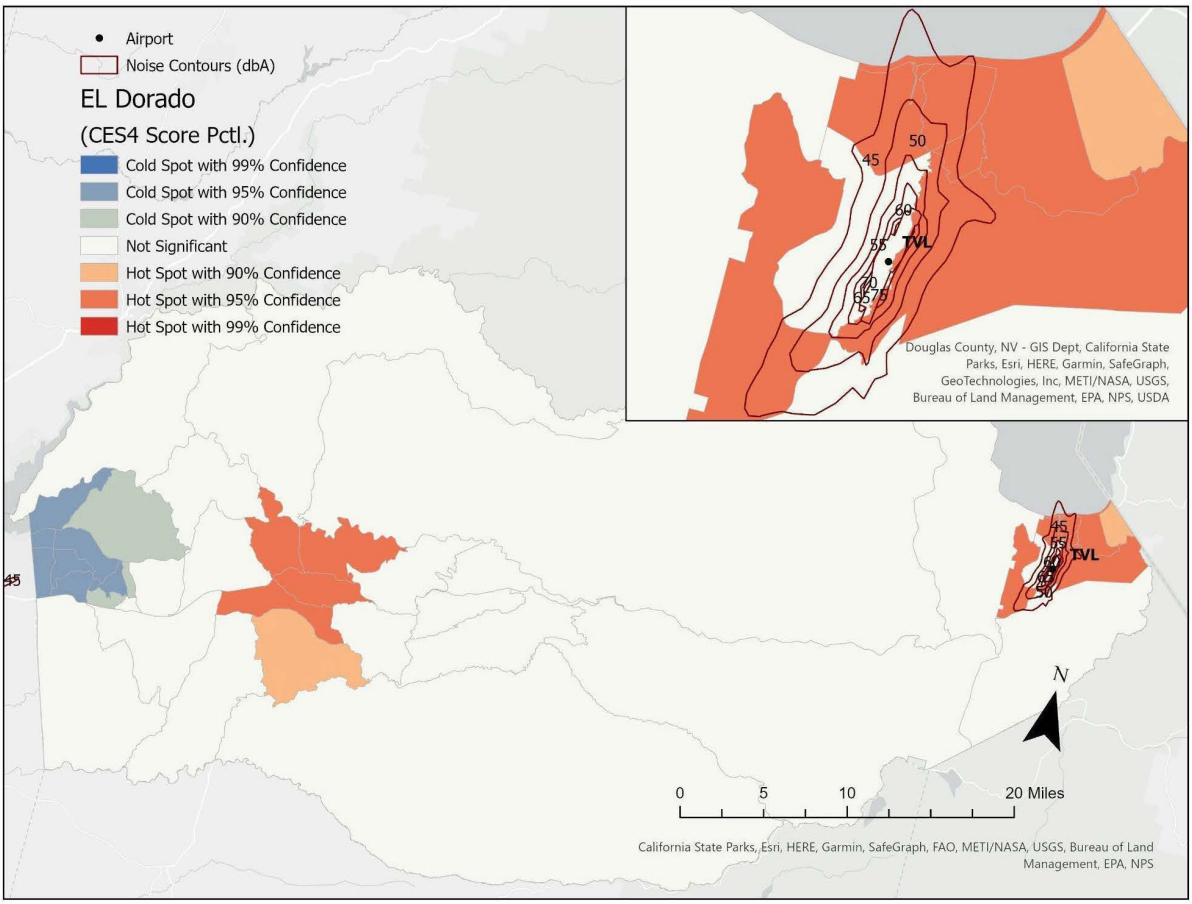
55	SAN	6.084
50	SAN	9.728
45	SAN	16.920
60	SBA	0.121
55	SBA	0.930
50	SBA	2.869
45	SBA	5.551
60	SBD	0.005
55	SBD	0.150
50	SBD	1.372
45	SBD	5.880
75	SBP	0.002
70	SBP	0.012
65	SBP	0.038
60	SBP	0.242
55	SBP	0.990
50	SBP	2.725
45	SBP	10.155
65	SCK	0.119
60	SCK	0.843
55	SCK	4.191
50	SCK	12.380
45	SCK	19.227
75	SDM	0.001
70	SDM	0.081
65	SDM	0.451
60	SDM	1.389
55	SDM	3.199
50	SDM	7.446
45	SDM	19.980
75	SEE	0.003
70	SEE	0.023
65	SEE	0.144
60	SEE	0.657
55	SEE	1.923
50	SEE	6.359
45	SEE	18.461
75	SFO	0.007
70	SFO	0.008
65	SFO	0.100
60	SFO	1.229
55	SFO	5.348
50	SFO, OAK, HWD	27.357
45	SFO, OAK, HWD	82.705

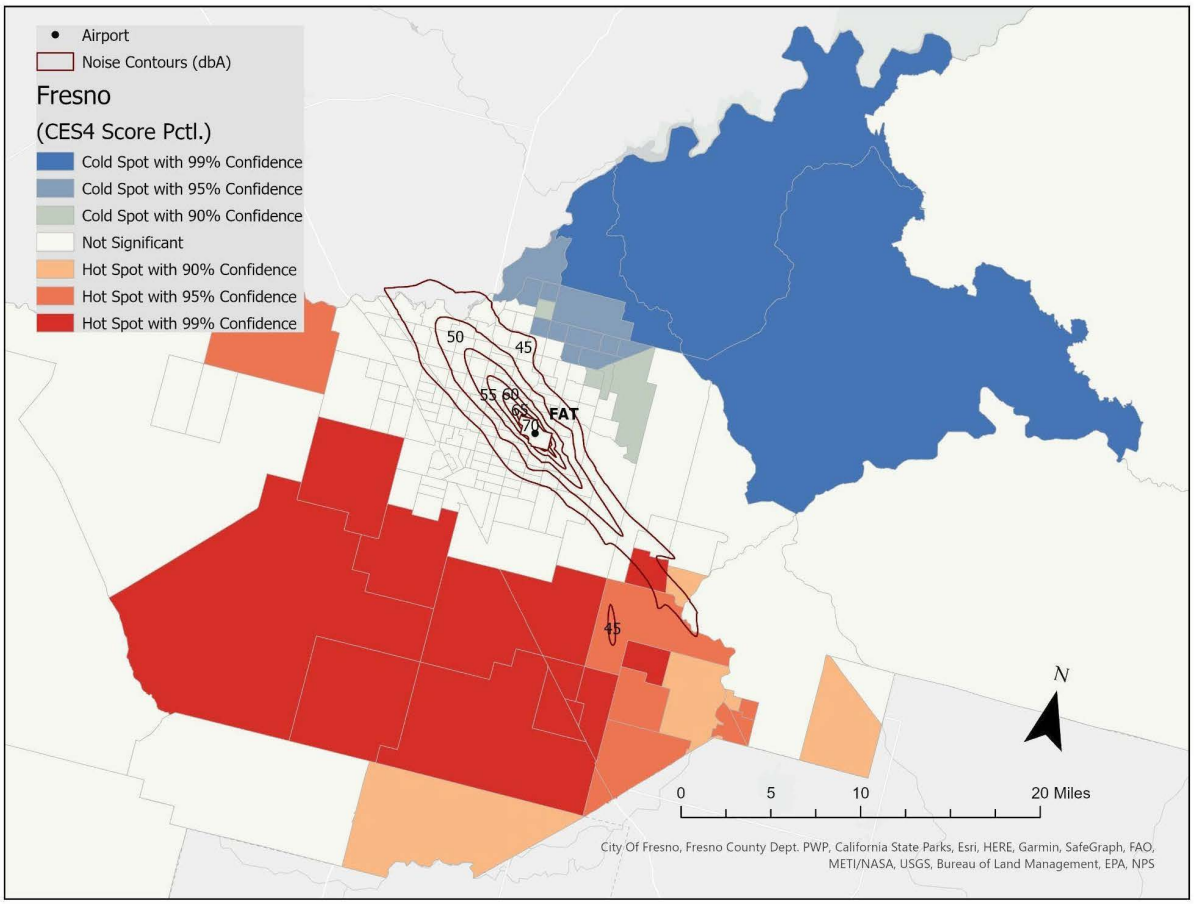
65	SJC	0.516
60	SJC	2.370
55	SJC	7.089
50	SJC	19.785
45	SJC, NUQ	45.688
70	SMF	0.000
65	SMF	0.082
60	SMF	0.982
55	SMF	5.408
50	SMF	15.950
45	SMF	44.581
65	SMO	0.002
60	SMO	0.123
55	SMO	0.700
50	SMO	1.910
65	SMX	0.001
60	SMX	0.127
55	SMX	0.513
50	SMX	1.950
45	SMX	6.114
80	SNA	0.000
75	SNA	0.003
70	SNA	0.072
65	SNA	0.656
60	SNA	1.859
55	SNA	6.019
50	SNA	13.030
45	SNA	24.264
75	SNS	0.000
70	SNS	0.003
65	SNS	0.011
60	SNS	0.193
55	SNS	1.051
50	SNS	3.831
45	SNS	11.917
85	STS	0.000
80	STS	0.001
75	STS	0.001
70	STS	0.004
65	STS	0.017
60	STS	0.170
55	STS	0.831
50	STS	2.978
45	STS	10.867

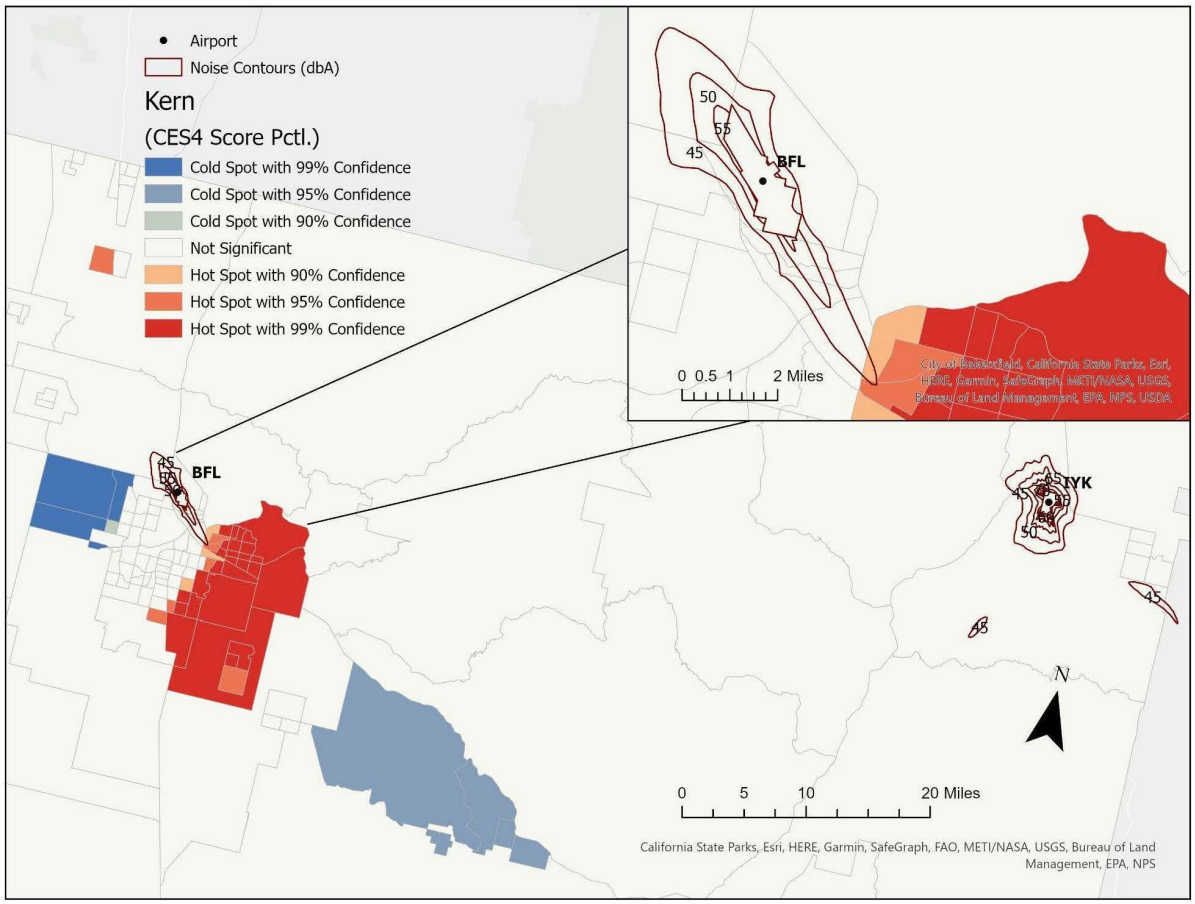
80	TRK	0.000
75	TRK	0.002
70	TRK	0.037
65	TRK	0.138
60	TRK	0.284
55	TRK	0.637
50	TRK	1.985
45	TRK	7.087
60	TRM	0.002
55	TRM	0.245
50	TRM	1.428
45	TRM	6.177
75	TVL	0.000
70	TVL	0.015
65	TVL	0.051
60	TVL	0.334
55	TVL	0.910
50	TVL	2.483
45	TVL	6.068
75	UDD	0.000
70	UDD	0.004
65	UDD	0.015
60	UDD	0.044
55	UDD	0.144
50	UDD	0.412
45	UDD	1.101
65	VCV	0.001
60	VCV	0.045
55	VCV	0.329
50	VCV	1.796
45	VCV	6.899
60	VIS	0.010
55	VIS	0.292
50	VIS	1.462
45	VIS	5.947
65	VNY	0.110
60	VNY	0.727
55	VNY	2.253
50	VNY, BUR	19.825
45	VNY, BUR	50.338

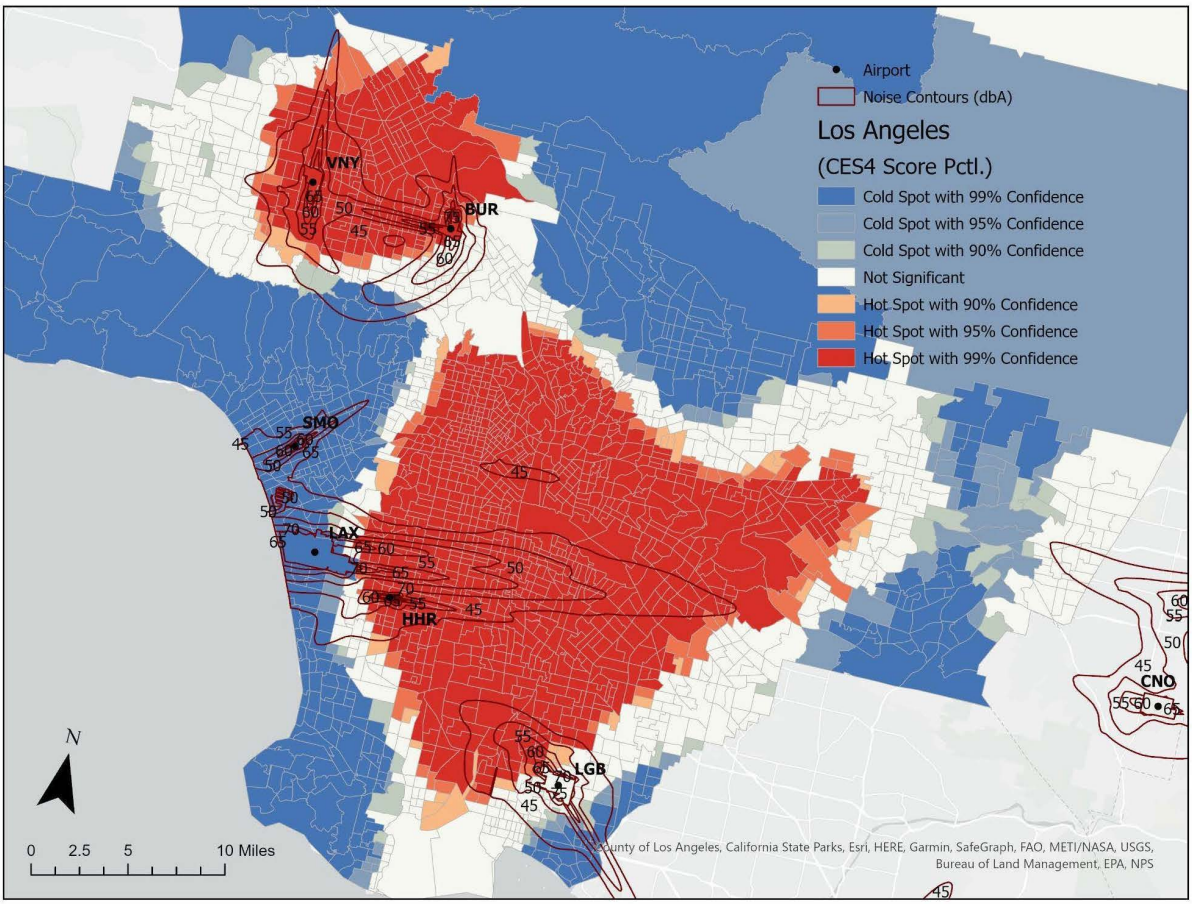
[4.2] Appendix D. County-level Hot-Spot Maps of CES4 Score Percentile and Aviation Noise Contours

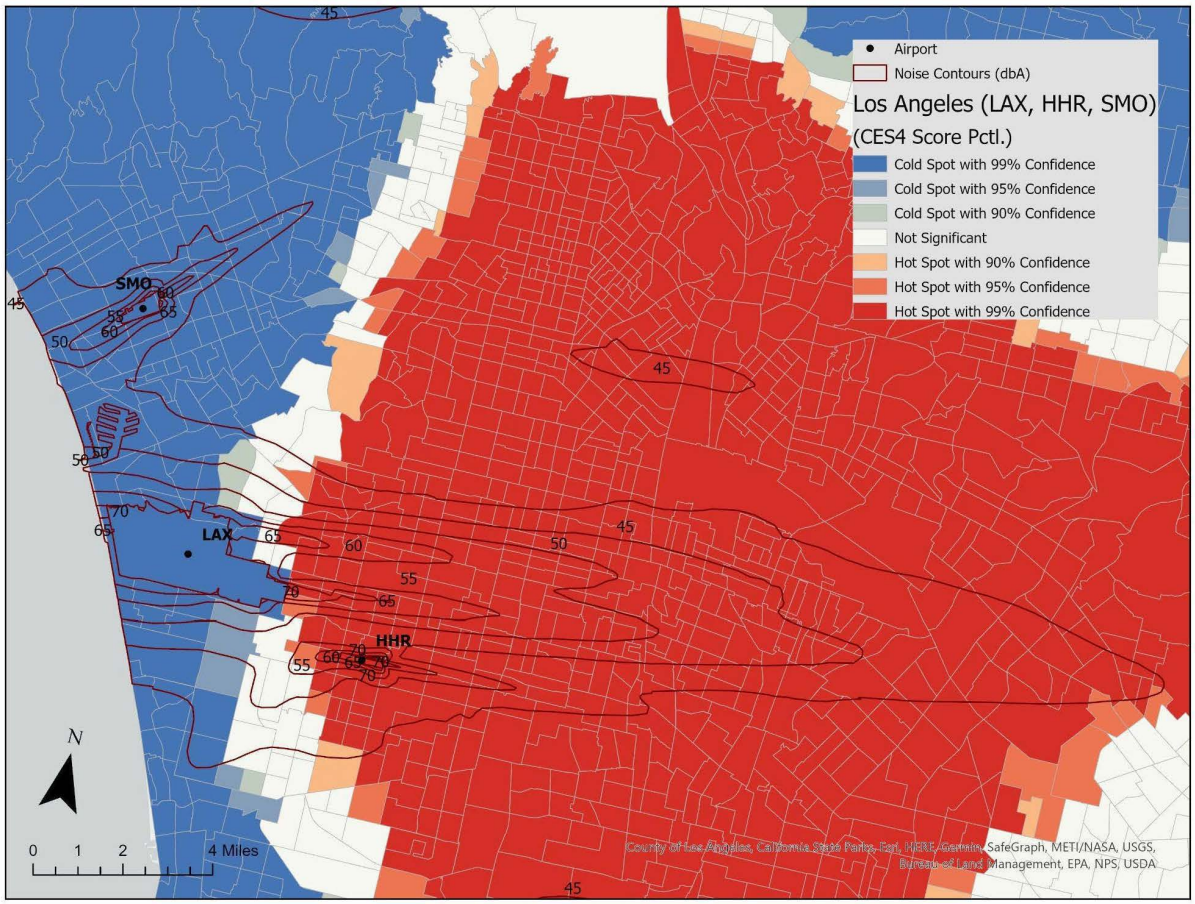

Noise Contours (dbA)
Airport
Contra Costa
(CES4 Score Pctl.)
Cold Spot with 99% Confidence
Cold Spot with 95% Confidence
Cold Spot with 90% Confidence
Not Significant
Hot Spot with 90% Confidence
Hot Spot with 95% Confidence
Hot Spot with 99% Confidence
CCR
OAK
N
0
4
8
16 Miles
City of Pittsburg, California State Parks, Esri, HERE, Garmin, SafeGraph, FAO, METI/NASA, USGS, Bureau of Land Management, EPA, NPS

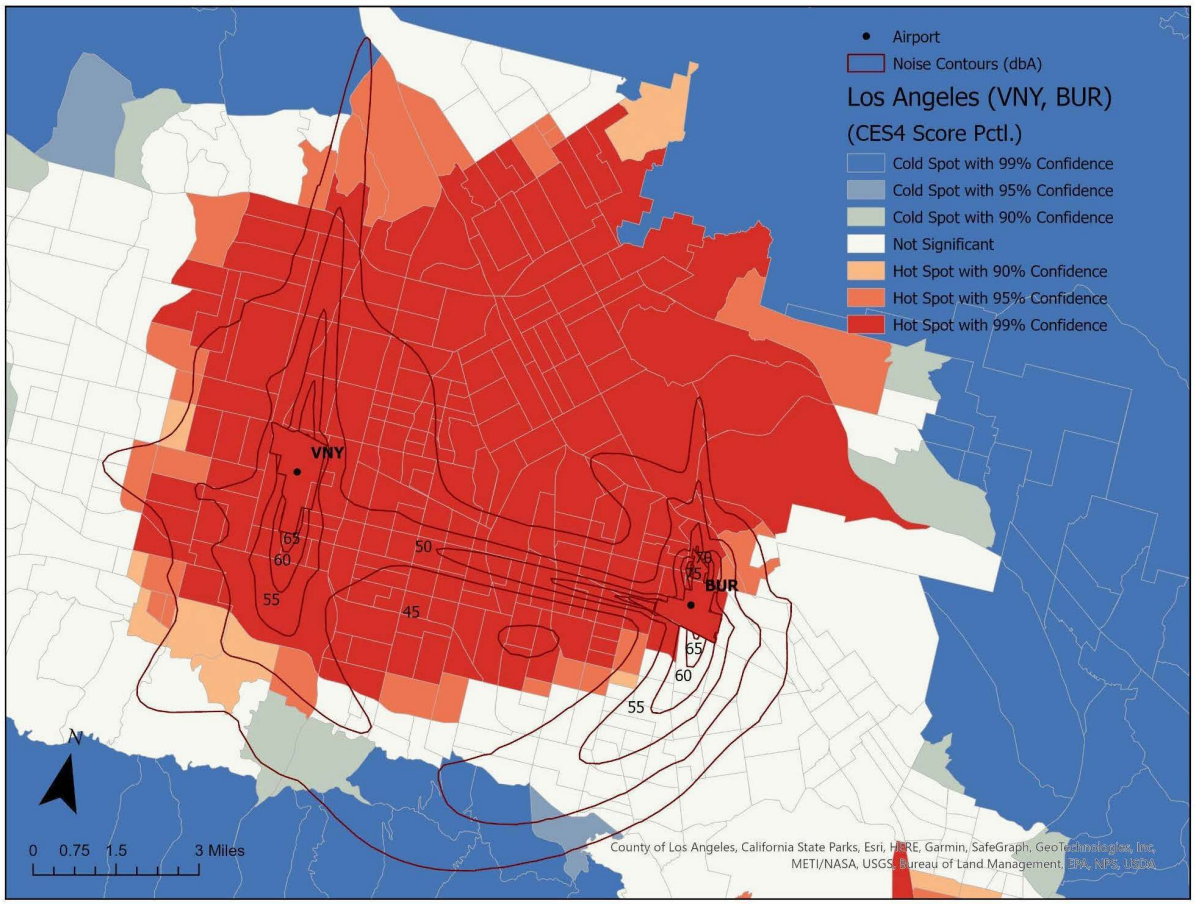

Airport
Noise Contours (dbA)
EL Dorado
(CES4 Score Pctl.)
Cold Spot with 99% Confidence
Cold Spot with 95% Confidence
Cold Spot with 90% Confidence
Not Significant
Hot Spot with 90% Confidence
Hot Spot with 95% Confidence
Hot Spot with 99% Confidence
45
50
55
60
65
70
75
TVL
Douglas County, NV - GIS Dept, California State Parks, Esri, HERE, Garmin, SafeGraph, GeoTechnologies, Inc, METI/NASA, USGS, Bureau of Land Management, EPA, NPS, USDA
N
0
5
10
20 Miles
California State Parks, Esri, HERE, Garmin, SafeGraph, FAO, METI/NASA, USGS, Bureau of Land Management, EPA, NPS

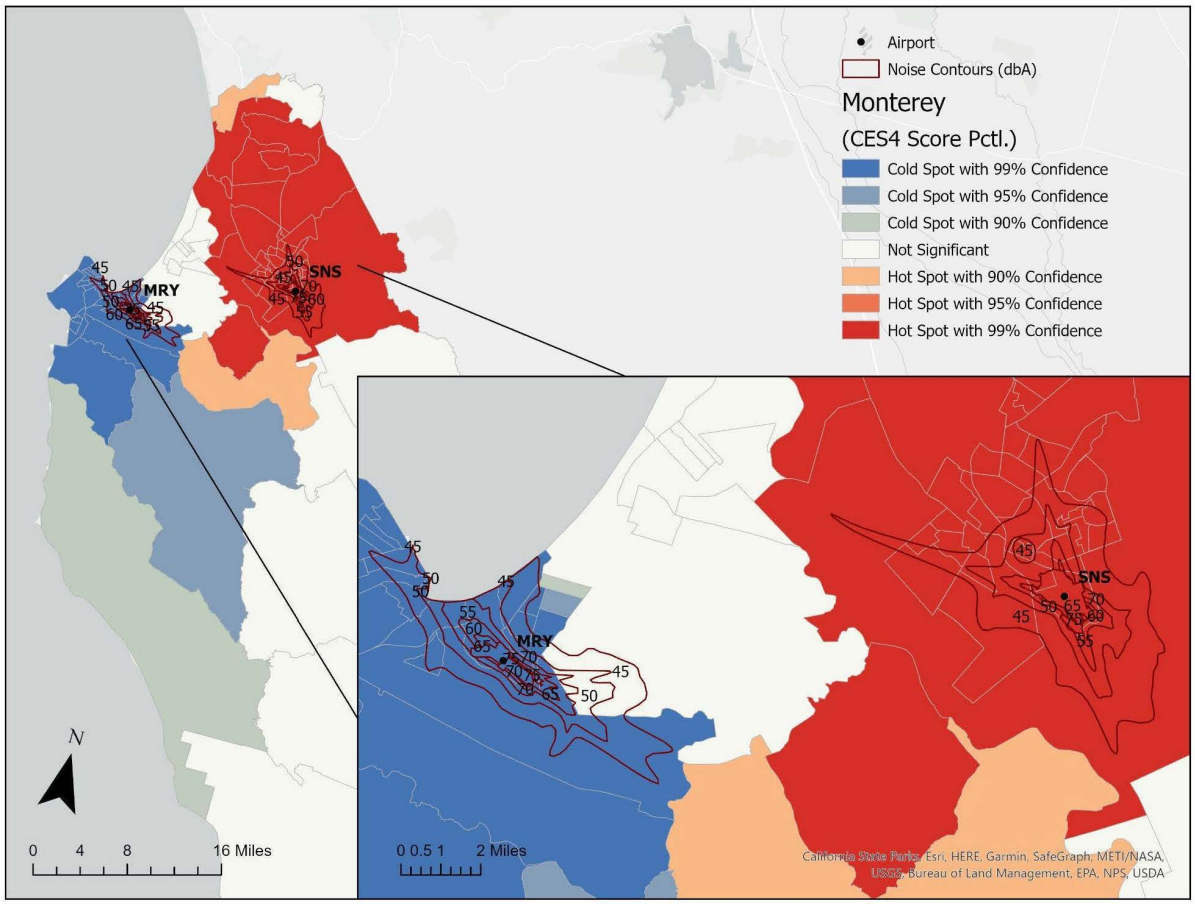

Airport
Noise Contours (dbA)
Fresno
(CES4 Score Pctl.)
Cold Spot with 99% Confidence
Cold Spot with 95% Confidence
Cold Spot with 90% Confidence
Not Significant
Hot Spot with 90% Confidence
Hot Spot with 95% Confidence
Hot Spot with 99% Confidence
50
45
55
60
65
70
FAT
45
N
0
5
10
20 Miles
City Of Fresno, Fresno County Dept. PWP, California State Parks, Esri, HERE, Garmin, SafeGraph, FAO, METI/NASA, USGS, Bureau of Land Management, EPA, NPS

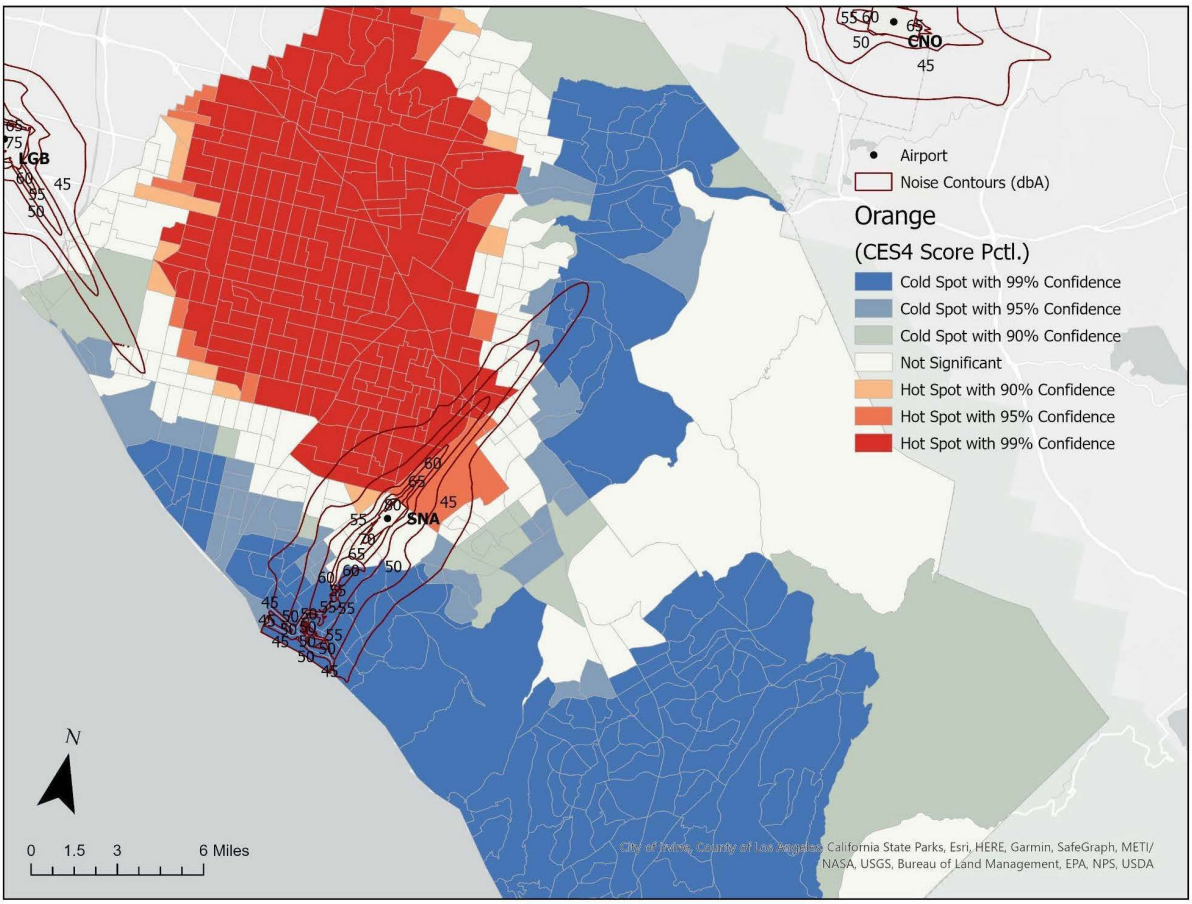

Airport
Noise Contours (dbA)
Kern
(CES4 Score Pctl.)
Cold Spot with 99% Confidence
Cold Spot with 95% Confidence
Cold Spot with 90% Confidence
Not Significant
Hot Spot with 90% Confidence
Hot Spot with 95% Confidence
Hot Spot with 99% Confidence
BFL
50
55
45
0 0.5 1 2 Miles
City of Bakersfield, California State Parks, Esri, HERE, Garmin, SafeGraph, METI/NASA, USGS, Bureau of Land Management, EPA, NPS, USDA
BFL
EYK
N
0 5 10 20 Miles
California State Parks, Esri, HERE, Garmin, SafeGraph, FAO, METI/NASA, USGS, Bureau of Land Management, EPA, NPS

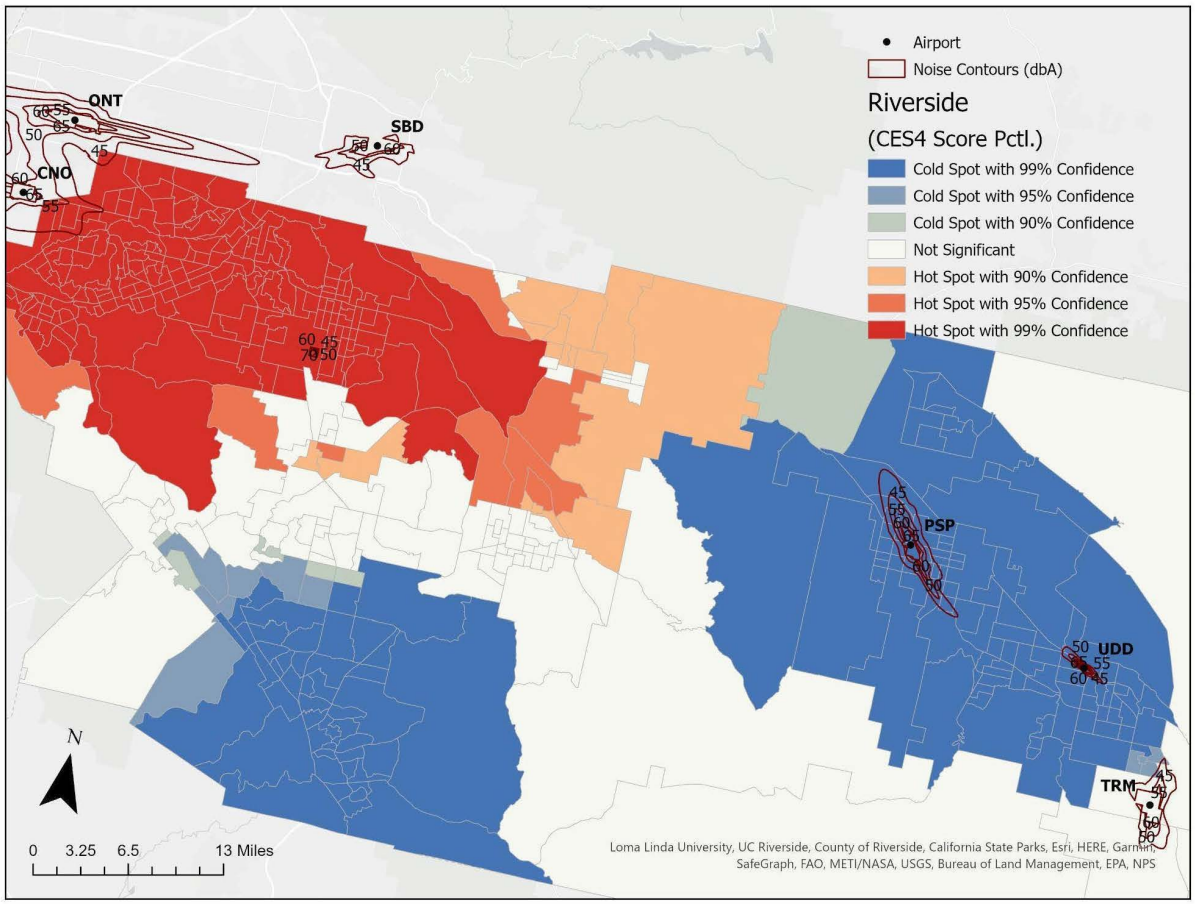

Airport
Noise Contours (dbA)
Los Angeles
(CES4 Score Pctl.)
Cold Spot with 99% Confidence
Cold Spot with 95% Confidence
Cold Spot with 90% Confidence
Not Significant
Hot Spot with 90% Confidence
Hot Spot with 95% Confidence
Hot Spot with 99% Confidence
VNY
BUR
SMO
LAX
HHR
LGB
CNO
N
0 2.5 5 10 Miles
County of Los Angeles, California State Parks, Esri, HERE, Garmin, SafeGraph, FAO, METI/NASA, USGS, Bureau of Land Management, EPA, NPS

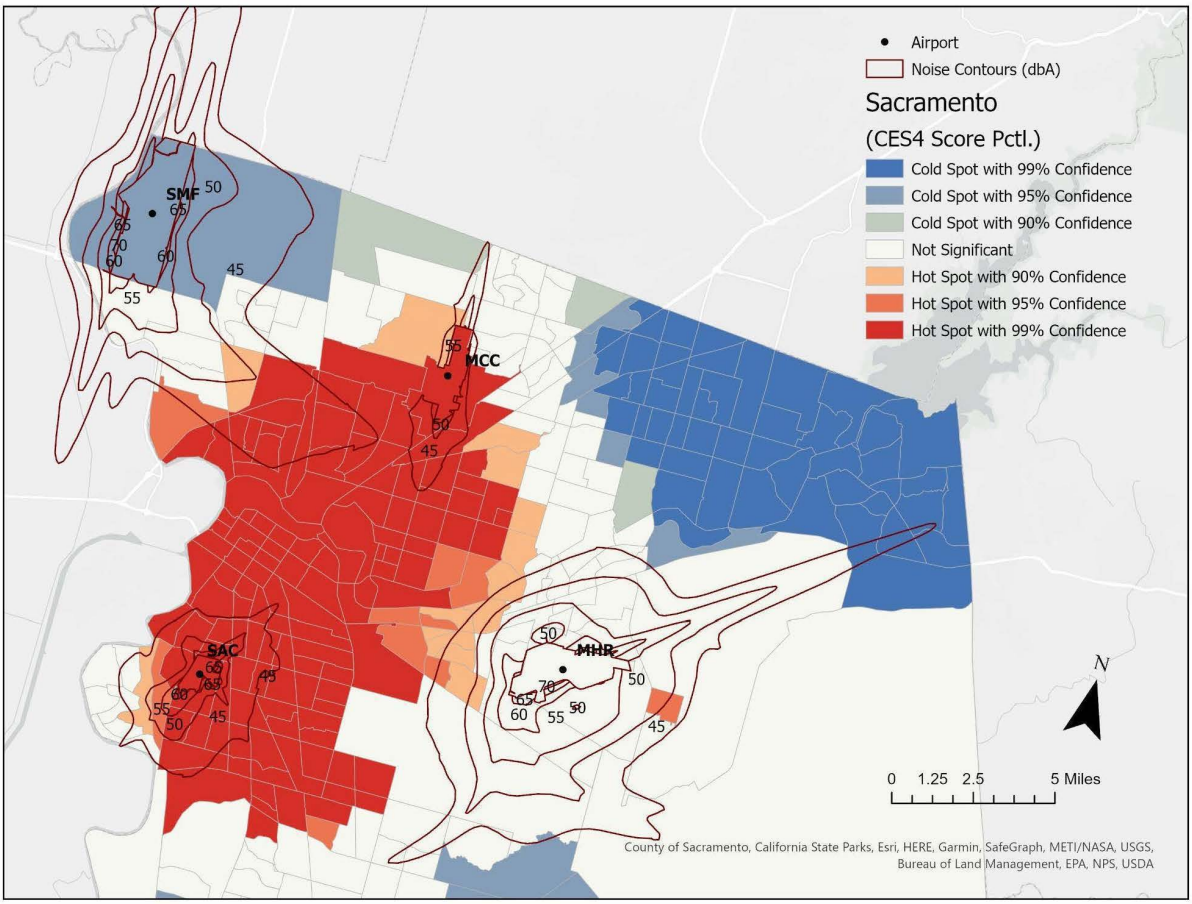

Airport
Noise Contours (dbA)
Los Angeles (LAX, HHR, SMO)
(CES4 Score Pctl.)
Cold Spot with 99% Confidence
Cold Spot with 95% Confidence
Cold Spot with 90% Confidence
Not Significant
Hot Spot with 90% Confidence
Hot Spot with 95% Confidence
Hot Spot with 99% Confidence
SMO
LAX
HHR
N
0 1 2 4 Miles
County of Los Angeles, California State Parks, Esri, HERE, Garmin, SafeGraph, METI/NASA, USGS, Bureau of Land Management, EPA, NPS, USDA

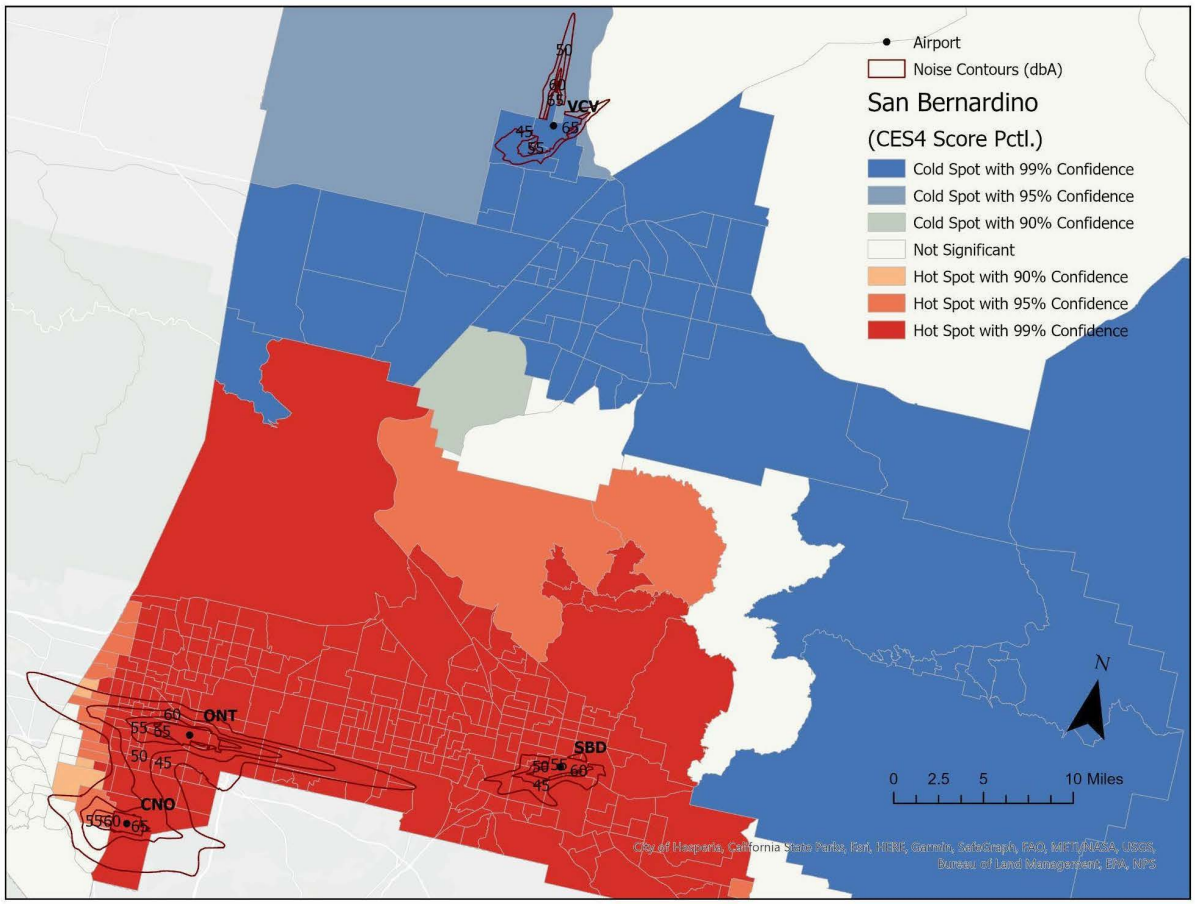

Airport
Noise Contours (dbA)
Los Angeles (VNY, BUR)
(CES4 Score Pctl.)
Cold Spot with 99% Confidence
Cold Spot with 95% Confidence
Cold Spot with 90% Confidence
Not Significant
Hot Spot with 90% Confidence
Hot Spot with 95% Confidence
Hot Spot with 99% Confidence
VNY
BUR
65
60
55
50
45
70
65
60
55
N
0 0.75 1.5 3 Miles
County of Los Angeles, California State Parks, Esri, HERE, Garmin, SafeGraph, GeoTechnologies, Inc, METI/NASA, USGS, Bureau of Land Management, EPA, NPS, USDA

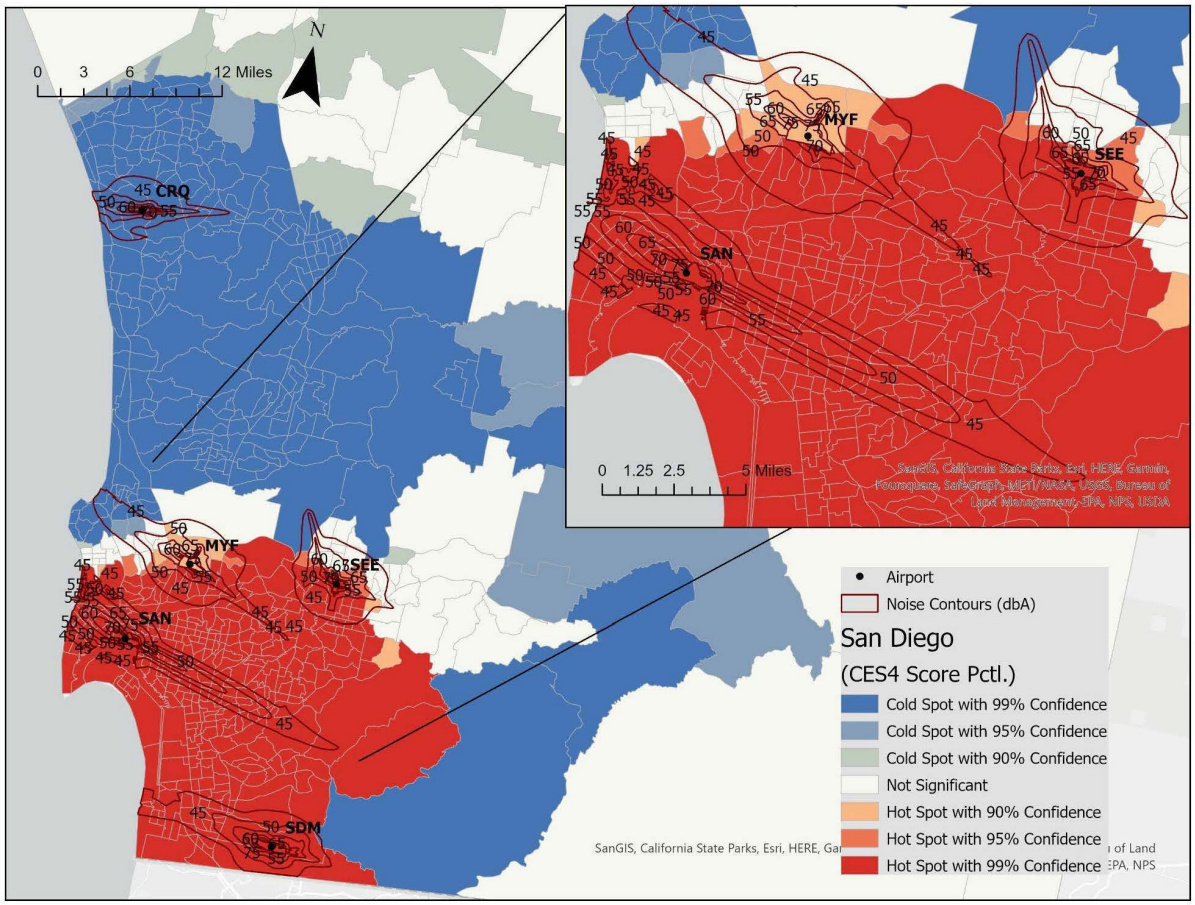

Airport
Noise Contours (dbA)
Monterey
(CES4 Score Pctl.)
Cold Spot with 99% Confidence
Cold Spot with 95% Confidence
Cold Spot with 90% Confidence
Not Significant
Hot Spot with 90% Confidence
Hot Spot with 95% Confidence
Hot Spot with 99% Confidence
MRY
SNS
N
0 4 8 16 Miles
0 0.5 1 2 Miles
California State Parks, Esri, HERE, Garmin, SafeGraph, METI/NASA, USGS, Bureau of Land Management, EPA, NPS, USDA

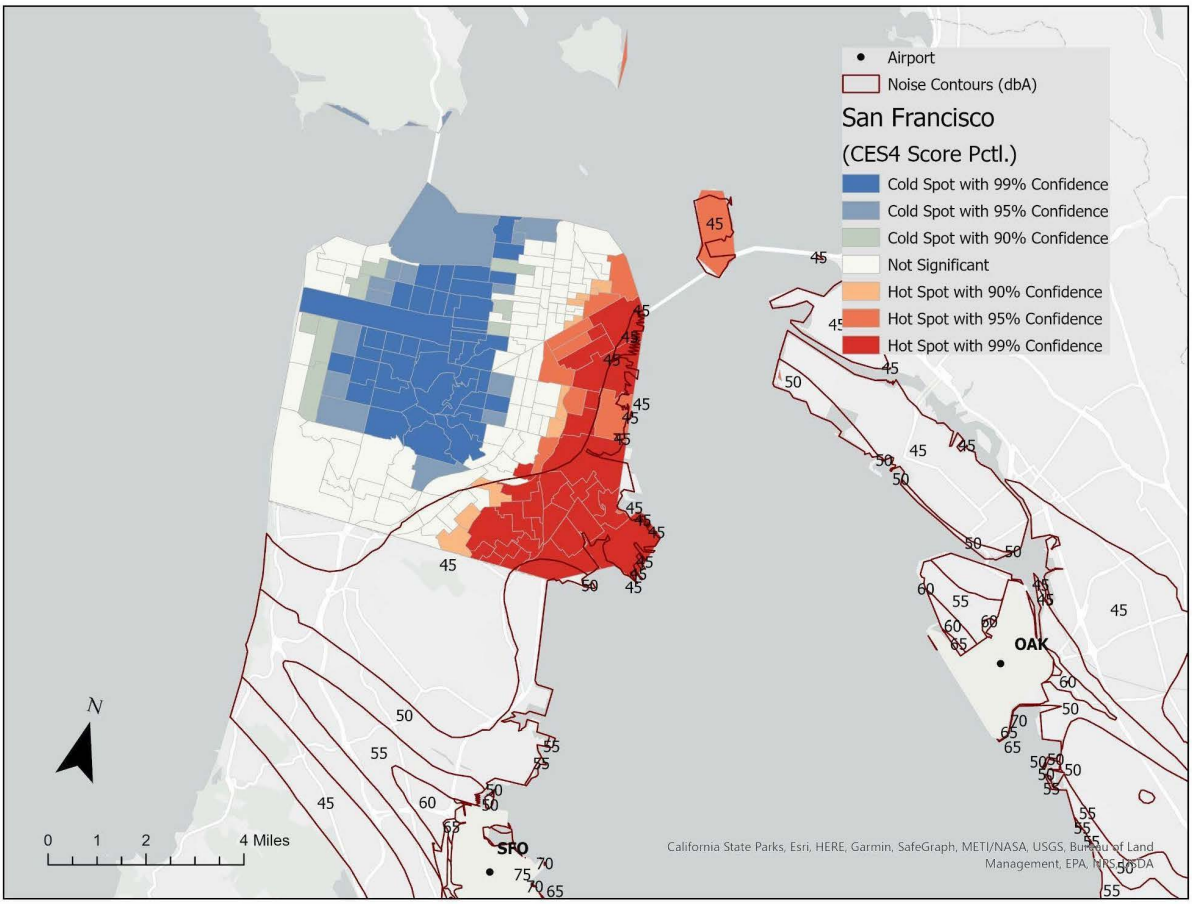

Airport
Noise Contours (dbA)
Orange
(CES4 Score Pctl.)
Cold Spot with 99% Confidence
Cold Spot with 95% Confidence
Cold Spot with 90% Confidence
Not Significant
Hot Spot with 90% Confidence
Hot Spot with 95% Confidence
Hot Spot with 99% Confidence
LGB
SNA
CNO
N
0 1.5 3 6 Miles
City of Irvine, County of Los Angeles, California State Parks, Esri, HERE, Garmin, SafeGraph, METI/ NASA, USGS, Bureau of Land Management, EPA, NPS, USDA

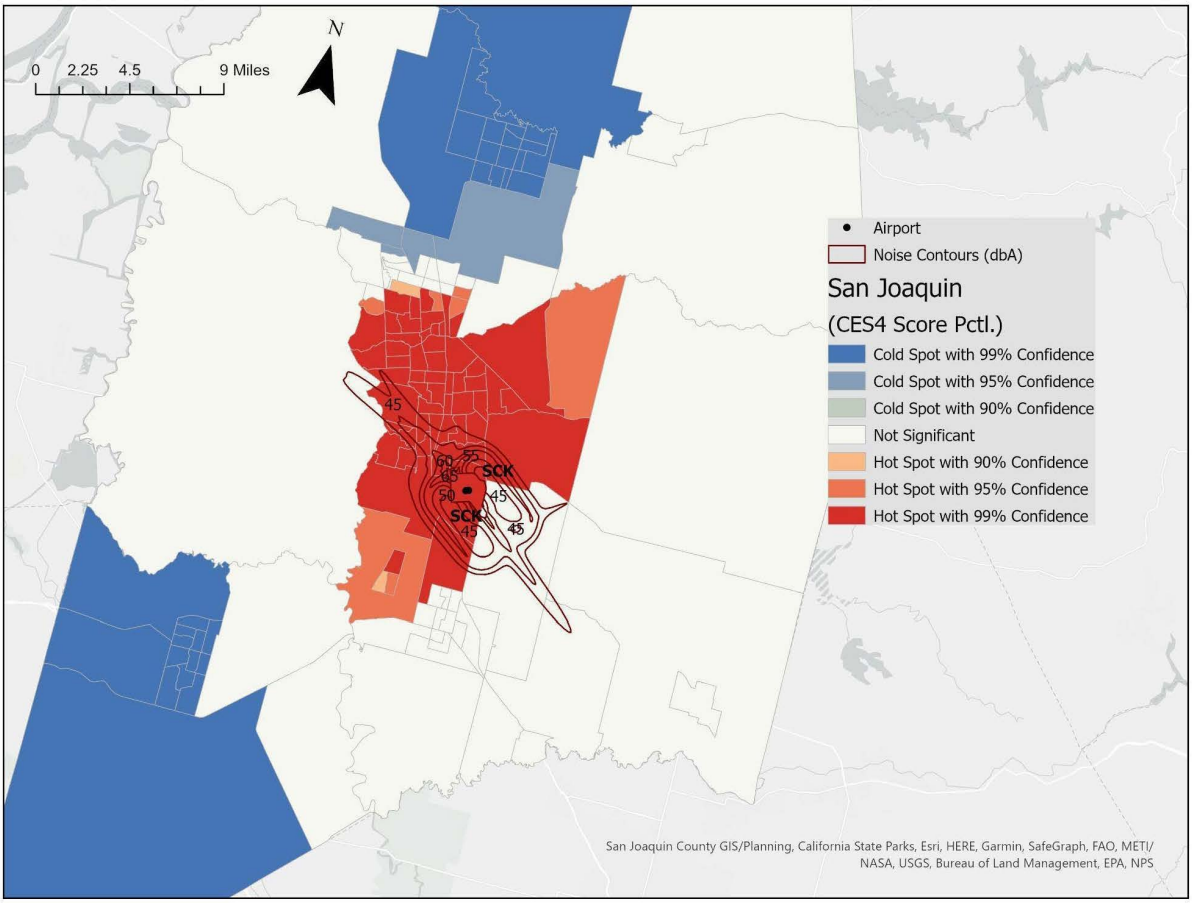

Airport
Noise Contours (dbA)
Riverside
(CES4 Score Pctl.)
Cold Spot with 99% Confidence
Cold Spot with 95% Confidence
Cold Spot with 90% Confidence
Not Significant
Hot Spot with 90% Confidence
Hot Spot with 95% Confidence
Hot Spot with 99% Confidence
ONT
SBD
CNO
PSP
UDD
TRM
N
0 3.25 6.5 13 Miles
Loma Linda University, UC Riverside, County of Riverside, California State Parks, Esri, HERE, Garmin, SafeGraph, FAO, METI/NASA, USGS, Bureau of Land Management, EPA, NPS

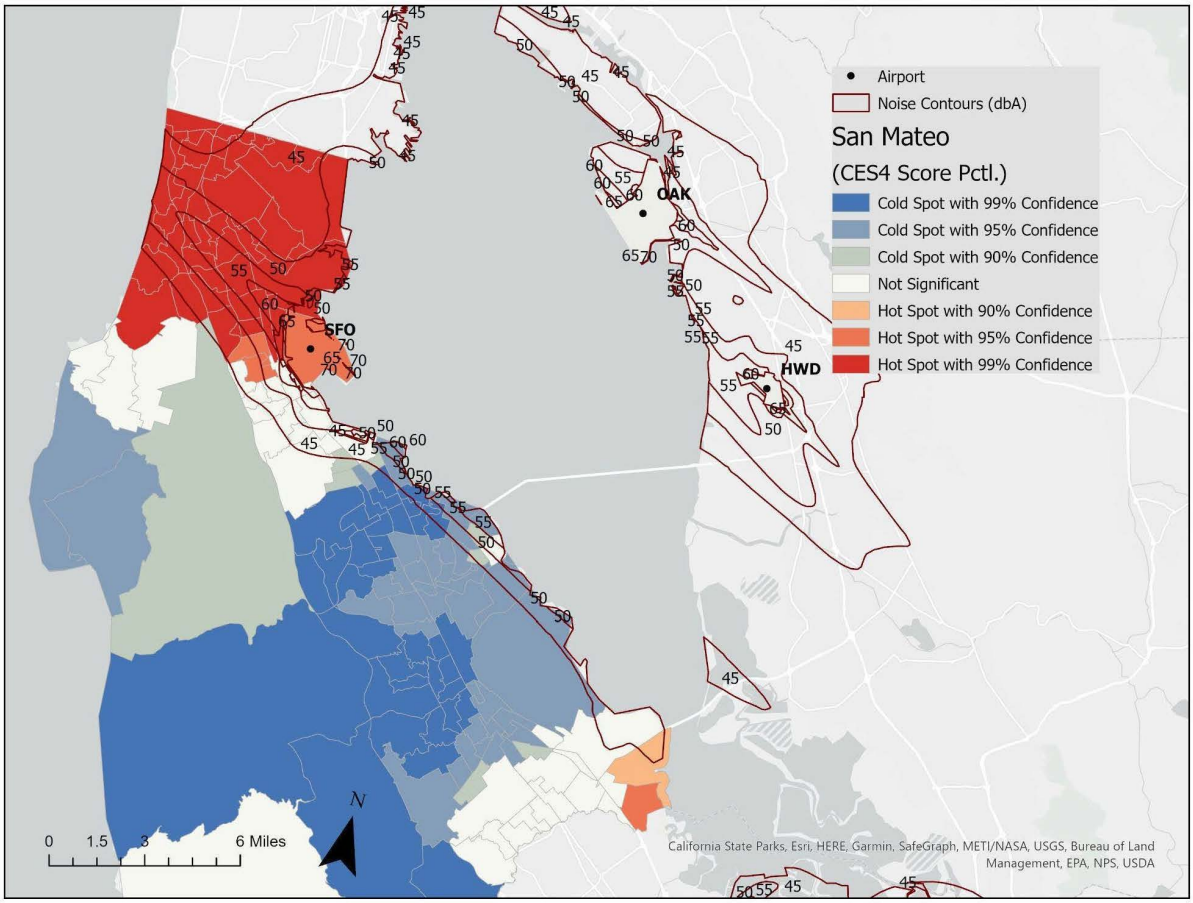

Airport
Noise Contours (dbA)
Sacramento
(CES4 Score Pctl.)
Cold Spot with 99% Confidence
Cold Spot with 95% Confidence
Cold Spot with 90% Confidence
Not Significant
Hot Spot with 90% Confidence
Hot Spot with 95% Confidence
Hot Spot with 99% Confidence
SMF
MCC
SAC
MHR
N
0 1.25 2.5 5 Miles
County of Sacramento, California State Parks, Esri, HERE, Garmin, SafeGraph, METI/NASA, USGS, Bureau of Land Management, EPA, NPS, USDA

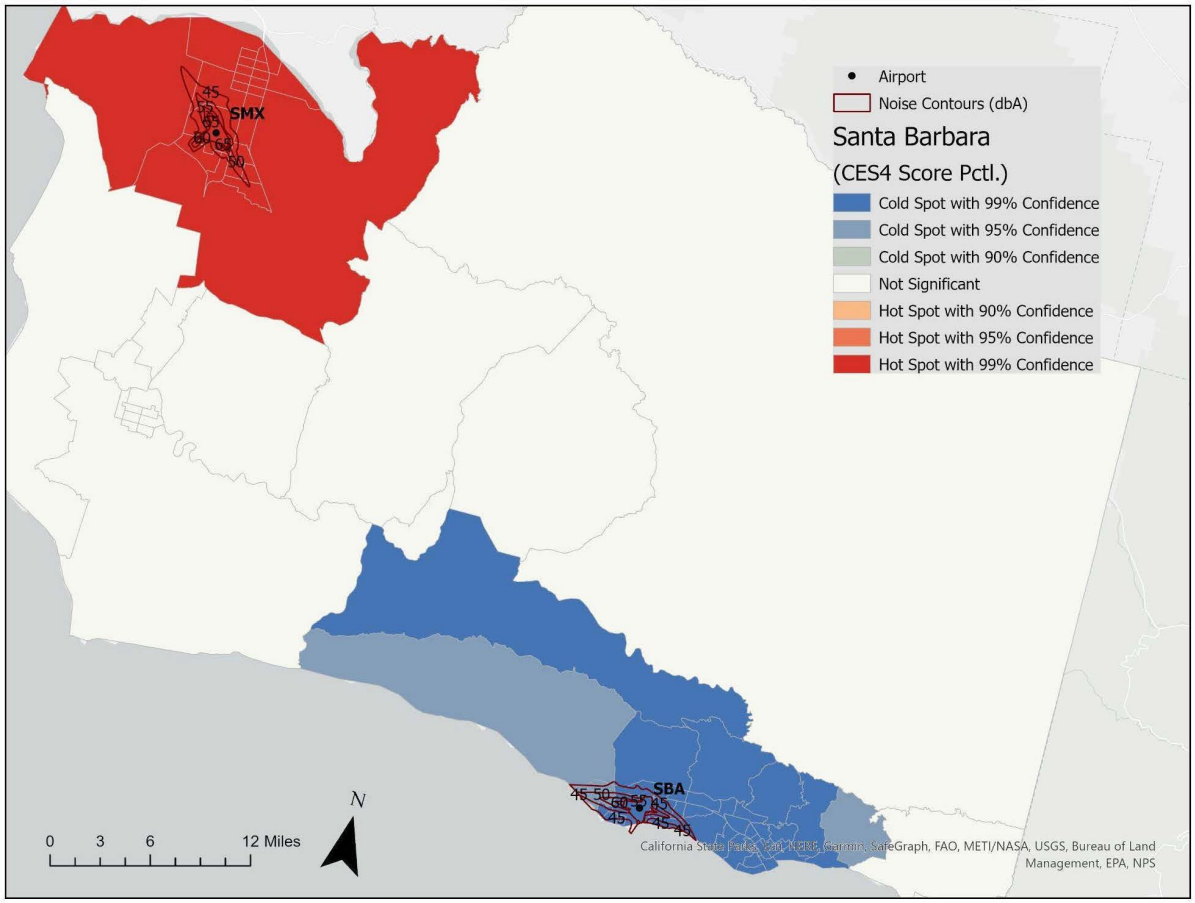

Airport
Noise Contours (dbA)
San Bernardino
(CES4 Score Pctl.)
Cold Spot with 99% Confidence
Cold Spot with 95% Confidence
Cold Spot with 90% Confidence
Not Significant
Hot Spot with 90% Confidence
Hot Spot with 95% Confidence
Hot Spot with 99% Confidence
VCV
ONT
SBD
CNO
N
0 2.5 5 10 Miles

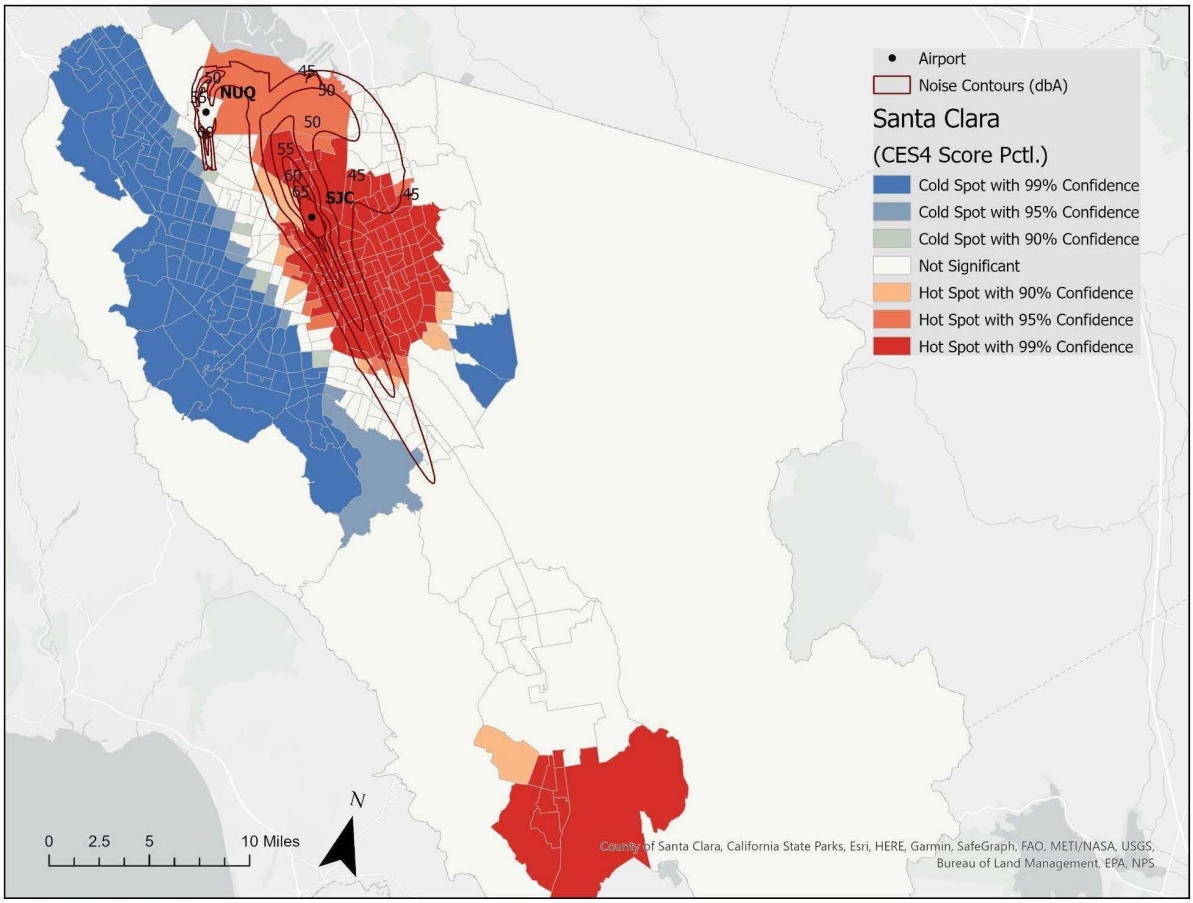

N
0 3 6 12 Miles
CRQ
MYF
SEE
SAN
SDM
0 1.25 2.5 5 Miles
Airport
Noise Contours (dbA)
San Diego
(CES4 Score Pctl.)
Cold Spot with 99% Confidence
Cold Spot with 95% Confidence
Cold Spot with 90% Confidence
Not Significant
Hot Spot with 90% Confidence
Hot Spot with 95% Confidence
Hot Spot with 99% Confidence

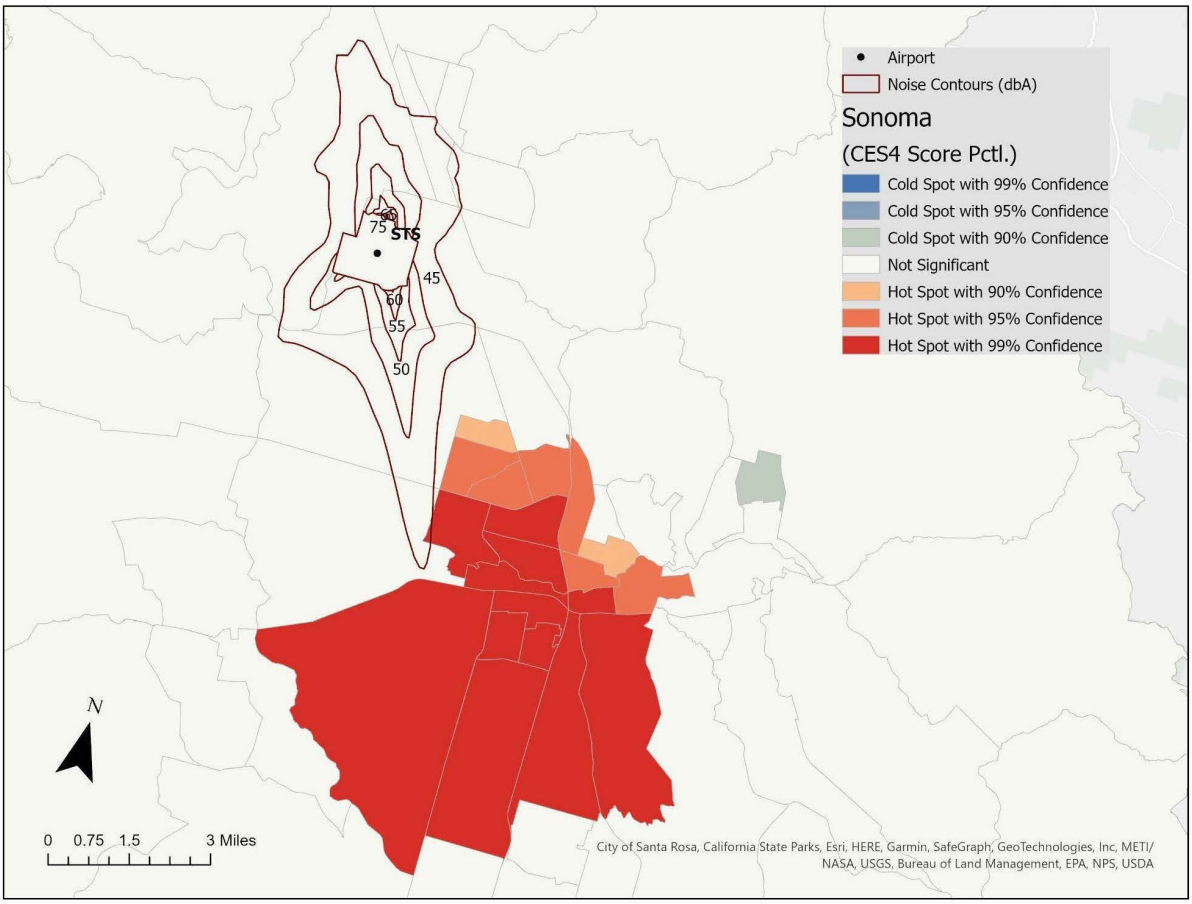

Airport
Noise Contours (dbA)
San Francisco
(CES4 Score Pctl.)
Cold Spot with 99% Confidence
Cold Spot with 95% Confidence
Cold Spot with 90% Confidence
Not Significant
Hot Spot with 90% Confidence
Hot Spot with 95% Confidence
Hot Spot with 99% Confidence
N
0 1 2 4 Miles
SFO
OAK
California State Parks, Esri, HERE, Garmin, SafeGraph, METI/NASA, USGS, Bureau of Land Management, EPA, NPS, USDA

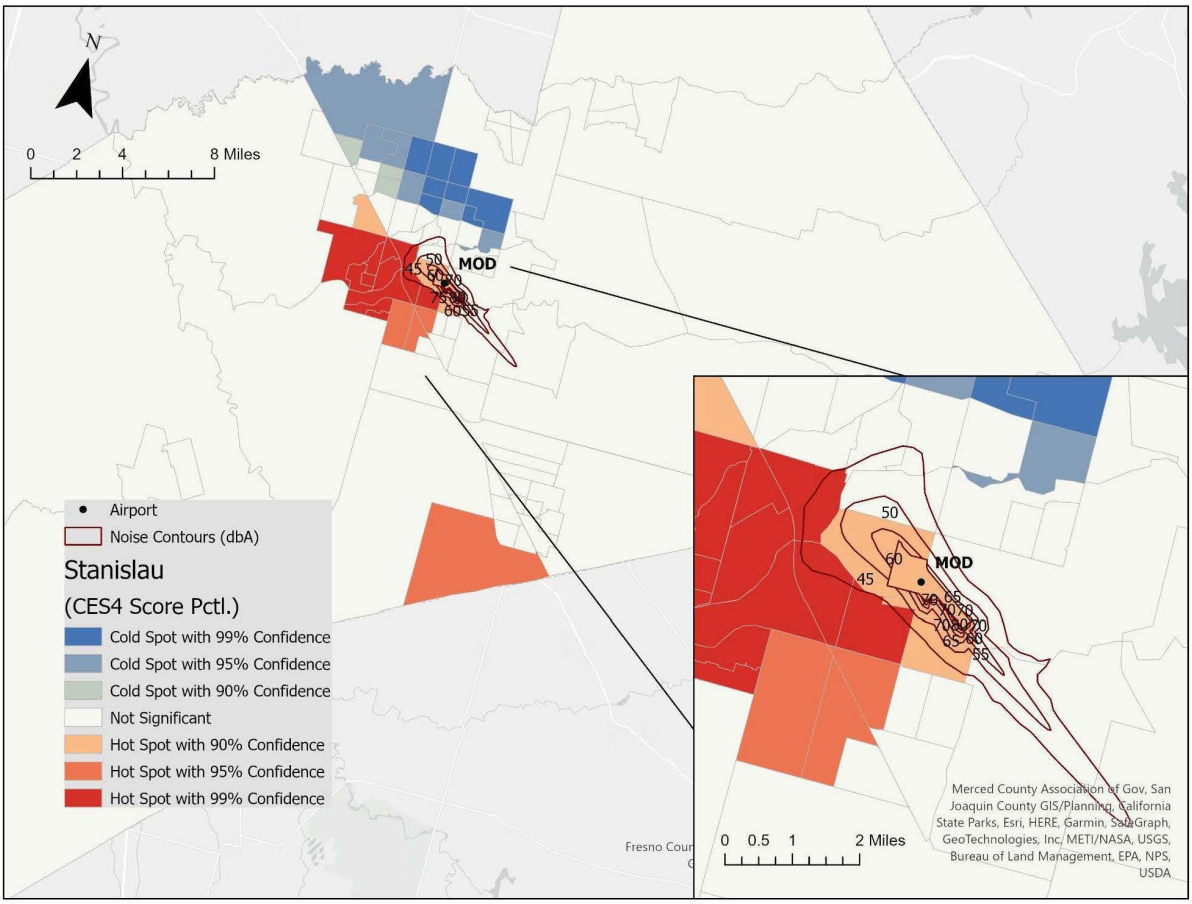

N
0 2.25 4.5 9 Miles
Airport
Noise Contours (dbA)
San Joaquin
(CES4 Score Pctl.)
Cold Spot with 99% Confidence
Cold Spot with 95% Confidence
Cold Spot with 90% Confidence
Not Significant
Hot Spot with 90% Confidence
Hot Spot with 95% Confidence
Hot Spot with 99% Confidence
45
60
55
65
50
SCK
45
SCK
45
45
San Joaquin County GIS/Planning, California State Parks, Esri, HERE, Garmin, SafeGraph, FAO, METI/
NASA, USGS, Bureau of Land Management, EPA, NPS

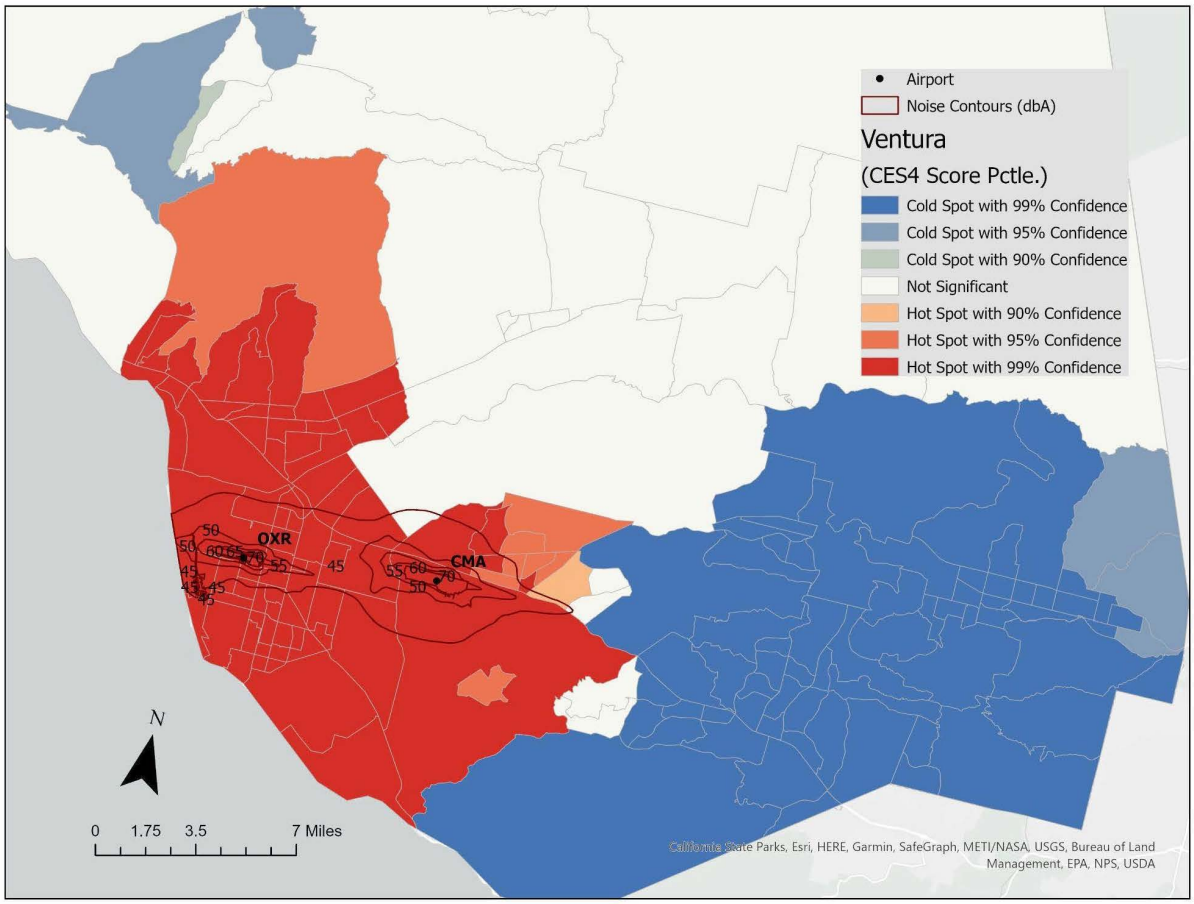

Airport
Noise Contours (dbA)
San Mateo
(CES4 Score Pctl.)
Cold Spot with 99% Confidence
Cold Spot with 95% Confidence
Cold Spot with 90% Confidence
Not Significant
Hot Spot with 90% Confidence
Hot Spot with 95% Confidence
Hot Spot with 99% Confidence
SFO
OAK
HWD
N
0 1.5 3 6 Miles
California State Parks, Esri, HERE, Garmin, SafeGraph, METI/NASA, USGS, Bureau of Land Management, EPA, NPS, USDA

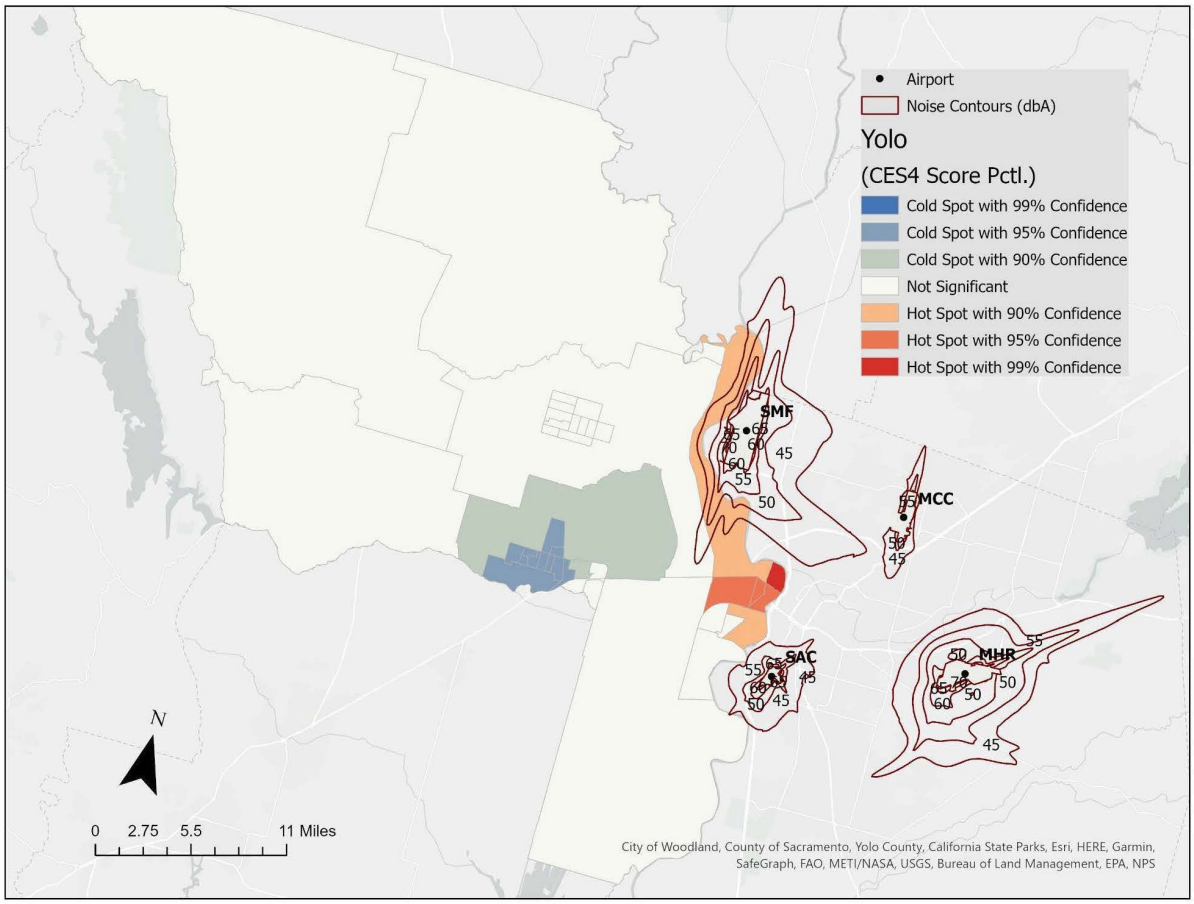

Airport
Noise Contours (dbA)
Santa Barbara
(CES4 Score Pctl.)
Cold Spot with 99% Confidence
Cold Spot with 95% Confidence
Cold Spot with 90% Confidence
Not Significant
Hot Spot with 90% Confidence
Hot Spot with 95% Confidence
Hot Spot with 99% Confidence
SMX
SBA
45
50
55
60
65
70
0
3
6
12 Miles
N
California State Parks, Esri, HERE, Garmin, SafeGraph, FAO, METI/NASA, USGS, Bureau of Land Management, EPA, NPS


Airport
Noise Contours (dbA)
Santa Clara
(CES4 Score Pctl.)
Cold Spot with 99% Confidence
Cold Spot with 95% Confidence
Cold Spot with 90% Confidence
Not Significant
Hot Spot with 90% Confidence
Hot Spot with 95% Confidence
Hot Spot with 99% Confidence
NUQ
SJC
45
50
55
60
65
0
2.5
5
10 Miles
N
County of Santa Clara, California State Parks, Esri, HERE, Garmin, SafeGraph, FAO, METI/NASA, USGS, Bureau of Land Management, EPA, NPS


Airport
Noise Contours (dbA)
Sonoma
(CES4 Score Pctl.)
Cold Spot with 99% Confidence
Cold Spot with 95% Confidence
Cold Spot with 90% Confidence
Not Significant
Hot Spot with 90% Confidence
Hot Spot with 95% Confidence
Hot Spot with 99% Confidence
STS
75
60
45
60
55
50
N
0 0.75 1.5 3 Miles
City of Santa Rosa, California State Parks, Esri, HERE, Garmin, SafeGraph, GeoTechnologies, Inc, METI/ NASA, USGS, Bureau of Land Management, EPA, NPS, USDA


N
0 2 4 8 Miles
MOD
45
50
60
65
70
75
80
55
Airport
Noise Contours (dbA)
Stanislau
(CES4 Score Pctl.)
Cold Spot with 99% Confidence
Cold Spot with 95% Confidence
Cold Spot with 90% Confidence
Not Significant
Hot Spot with 90% Confidence
Hot Spot with 95% Confidence
Hot Spot with 99% Confidence
0 0.5 1 2 Miles
Merced County Association of Gov, San Joaquin County GIS/Planning, California State Parks, Esri, HERE, Garmin, SafeGraph, GeoTechnologies, Inc, METI/NASA, USGS, Bureau of Land Management, EPA, NPS, USDA


Airport
Noise Contours (dbA)
Ventura
(CES4 Score Pctle.)
Cold Spot with 99% Confidence
Cold Spot with 95% Confidence
Cold Spot with 90% Confidence
Not Significant
Hot Spot with 90% Confidence
Hot Spot with 95% Confidence
Hot Spot with 99% Confidence
OXR
CMA
50
60
65
70
55
45
N
0 1.75 3.5 7 Miles
California State Parks, Esri, HERE, Garmin, SafeGraph, METI/NASA, USGS, Bureau of Land Management, EPA, NPS, USDA


Airport
Noise Contours (dbA)
Yolo
(CES4 Score Pctl.)
Cold Spot with 99% Confidence
Cold Spot with 95% Confidence
Cold Spot with 90% Confidence
Not Significant
Hot Spot with 90% Confidence
Hot Spot with 95% Confidence
Hot Spot with 99% Confidence
SMF
MCC
SAC
MHR
N
0 2.75 5.5 11 Miles
City of Woodland, County of Sacramento, Yolo County, California State Parks, Esri, HERE, Garmin, SafeGraph, FAO, METI/NASA, USGS, Bureau of Land Management, EPA, NPS

[4.2] Appendix E.Population Exposed to aviation noise of 45+ dBA and 65+ dBA by County

County	Total Pop.	Exp. 45+dBA	Exp. 50+dBA	Exp. 65+dBA
Alameda	1656754	683466	265552	40968
Butte	225817	53029	28168	6088
Contra Costa	1142251	138292	55638	7430
El Dorado	188563	25950	25950	6828
Fresno	984521	405671	223028	35982
Humboldt	135940	22518	9967	3659
Imperial	180701	2377	0	0
Kern	887641	81033	47504	6015
Los Angeles	10081570	2925753	1565100	168542
Madera	155433	32595	14524	9292
Mono	14310	3697	3697	3697
Monterey	433410	168666	96903	11900
Napa	139623	9601	4404	0
Nevada	99244	14384	11846	5183
Orange	3168044	501272	269675	43609
Placer	385512	22521	1622	1622
Riverside	2411439	234754	133791	14890
Sacramento	1524553	569158	227273	17976
San Bernardino	2149031	438074	238498	31630
San Diego	3316073	1186494	665588	124643
San Francisco	874961	195680	11929	0
San Joaquin	742603	112513	58873	12396
San Luis Obispo	282165	69198	50134	7283

San Mateo	767423	392155	251522	9406
Santa Barbara	444829	136366	81409	6302
Santa Clara	1927470	632493	328688	30480
Shasta	179212	27704	17503	5672
Siskiyou	43468	2787	1711	0
Sonoma	499772	56950	21181	5342
Stanislaus	543194	63548	33089	7047
Sutter	96109	2488	2488	0
Tulare	461898	50924	48388	0
Ventura	847263	221797	78207	15930
Yolo	217352	21769	7729	0

* Data Source: Census 2019 from the CalEnviroScreen Tool v.4

[4.2] Appendix F. Census tract count of the top 25 percentile of CES4, Pollution Burden, and Population Characteristics Exposed to aviation noise of 45+ dBA and 65+ dBA

	Total Census Tracts				**Tracts 25+ percentile Noise exp 45+**				**Tracts 25+ percentile Noise exp 65+**			
	Total	*CES*	*PB*	*PC*	*Total*	*CES*	*PB*	*PC*	*Total*	*CES*	*PB*	*PC*
Alameda	360	35	31	66	136	17	16	40	6	1	2	2
Butte	51	2	1	3	10	0	0	0	1	0	0	0
Contra Costa	207	32	17	41	24	3	4	3	1	1	1	0
El Dorado	42	0	0	0	8	0	0	0	2	0	0	0
Fresno	199	110	73	104	84	39	21	37	8	6	5	6
Humbodlt	30	0	0	4	4	0	0	0	1	0	0	0
Imperial	31	18	7	20	2	0	0	0	0	0	0	0
Kern	151	73	35	78	13	8	4	8	1	1	0	1
LA	2343	1061	1166	853	677	405	414	343	45	28	32	23
Madera	23	14	8	8	4	4	2	0	1	1	1	0
Mono	3	0	0	0	1	0	0	0	1	0	0	0
Monterey	93	2	4	12	38	1	1	6	4	0	0	0
Nevada	20	0	0	0	3	0	0	0	1	0	0	0
Napa	40	0	1	0	3	0	0	0	0	0	0	0
Orange	582	82	185	37	95	10	41	3	5	0	3	0
Placer	84	0	1	0	2	0	0	0	1	0	0	0
Riverside	453	68	61	125	46	3	6	9	4	1	1	1
Sacramento	317	49	23	90	114	25	10	40	5	1	1	1
San Bernardino	369	129	104	152	73	41	47	28	4	3	3	2
San Diego	627	50	41	74	226	21	23	33	23	1	7	1
San Joaquin	139	50	42	70	21	16	15	18	2	2	2	2
San Luis	53	0	3	0	14	0	2	0	2	0	2	0

Obispo												
San Mateo	157	7	13	4	77	4	9	2	3	0	3	0
Santa Barbara	89	2	4	8	25	2	3	2	1	0	1	0
Santa Clara	372	11	21	25	116	4	15	9	5	0	5	0
SF	195	14	19	15	41	12	12	13	0	0	0	0
Shasta	48	0	0	2	7	0	0	0	1	0	0	0
Siskiyou	14	0	0	0	2	0	0	0	0	0	0	0
Sonoma	99	1	1	2	10	0	0	0	1	0	0	0
Stanislau	94	41	42	29	12	6	7	6	2	1	1	1
Sutter	21	5	4	5	1	0	0	0	0	0	0	0
Ventura	173	9	23	10	38	5	10	6	2	0	2	0
Tulare	78	46	36	40	5	2	4	1	0	0	0	0
Yolo	41	4	5	5	3	1	1	1	1	0	0	0

Task 4.3 Wind Analysis for California Airports

Deliverables: A summary report that includes calculations for CA airports for:

(1) probability of crosswind occurrences that include speeds that exceed 10.5 kn on individual runways;

(2) probability of crosswind occurrences that include speeds that are equal to or greater than 10.5 kn at single- and multi-runway airports and demand for each relevant aircraft design group (and aircraft approach speed), and

(3) probability of aircraft incidents during higher (than allowed) crosswind speeds and corresponding aircraft design group (and aircraft approach speed).

Results are displayed on a map for each CA airport.

[4.3] 1. Introduction

Wind conditions affect all aircraft in various ways. In general, the smaller the aircraft, the more it is susceptible to wind, especially crosswind components. Consequently, the design and determination of runway orientation is a result of rigorous historical wind studies that require airports to present landing and takeoff conditions with 95% wind coverage or runway usability (FAA AC 150/5300-13, Appendix 1). California has a large number of public airports, including single-runway general aviation airports and small commercial airports (Figure 1). Because of anticipated changes in future temperature and precipitation in California, a logical question to ask is: will airports in California experience any significant changes in wind direction and speed? This issue is especially important to address at single-runway airports where the occurrence of cross winds exceed 10.5 kn. Under such crosswind conditions, it is not safe for smaller/lighter aircraft to operate (i.e. to land and take off).

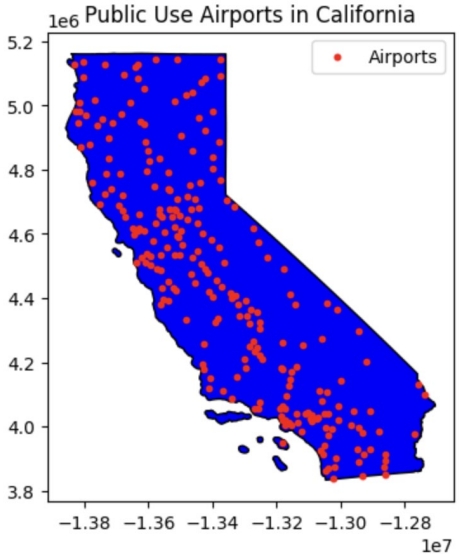


Figure 1. Public Use Airports in California

Conducting wind analyses (by using historical data) to estimate trends in wind speed and direction can provide deeper understanding of safety of operations, and help to create

safer Airport Safety Zones. Because the concept of Regional Air Mobility will focus on operations of smaller aircraft at regional (i.e. smaller) airports, it is anticipated that certain housing developments might occur near such airports, which might overlap with certain Airport Safety Zones. The demand for housing in such locations might increase significantly with the arrival of electric/hybrid fixed-wing aircraft, which will be considerably quieter than current turbo-prop or jet aircraft. Therefore, the objective of this analysis is to determine a level of operational safety across Airport Safety Zones.

In order to ensure safety of arrivals and departures due to wind speed and orientation, the FAA set a minimum value for crosswind design criteria for each aircraft design group (and aircraft approach speed). Because each aircraft has unique maximum demonstrated crosswind characteristics, the following analysis is conducted in this section:

(1) probability of crosswind occurrences that include speeds equal to or greater than 10.5 kn on individual runways,
(2) probability of crosswind occurrences that include speeds equal to or greater than 10.5 kn at single- and multi-runway airports and demand for each relevant aircraft design group and aircraft approach category,
(3) probability of aircraft incidents during higher (than allowed) crosswind speeds for each corresponding aircraft design group and aircraft approach category.

However, before conducting the wind analysis at CA airports, we have to look at this climate-related problem from a much wider perspective. In the following sections we provide background information on wind hazard at the US level, FAA Regional levels, and California level.

1.1. Changing Climate and Wind Hazard Background

Based on available scientific literature, it is expected that the wind speed, direction and frequency of crosswind occurrences will change in the future due to climate change. A previous study, based on observational records, reported dominance of trends toward declining values of the 50th and 90th percentile and annual mean wind speeds over North America during the second half of the 20th century (Pryor et al. 2009). These trends were the result of the reductions in global average surface wind speed, which have been occurring over land since the 1980s, a phenomenon known as global “terrestrial stilling”. Zeng et al. (2019) showed that the stilling reversed around 2010 and that global observed wind speeds over land have recovered. He also showed that these variations in wind speed arise from large-scale atmospheric circulation change, rather than by vegetation growth and/or urbanization as hypothesized previously.

Using CMIP 5 (Coupled Model Intercomparison Project 5) simulations under the forcing level of 8.5W/m2 scenario, Kulkarni et al. (2014) reported increases in wind speed over the large area of the US. In general, wind patterns are projected to change, and wind speeds are projected to increase in some parts of the US and the world. (Zeng et al., 2019).

Using data from the Automated Surface Observing System (ASOS) stations (Iowa State University Environmental Mesonet), Figure 2 displays the variability of prevailing wind direction and average wind speed at north American airports by month, while Figure 3 shows the

variability of prevailing wind direction and average wind speed at north American airports by time of day.

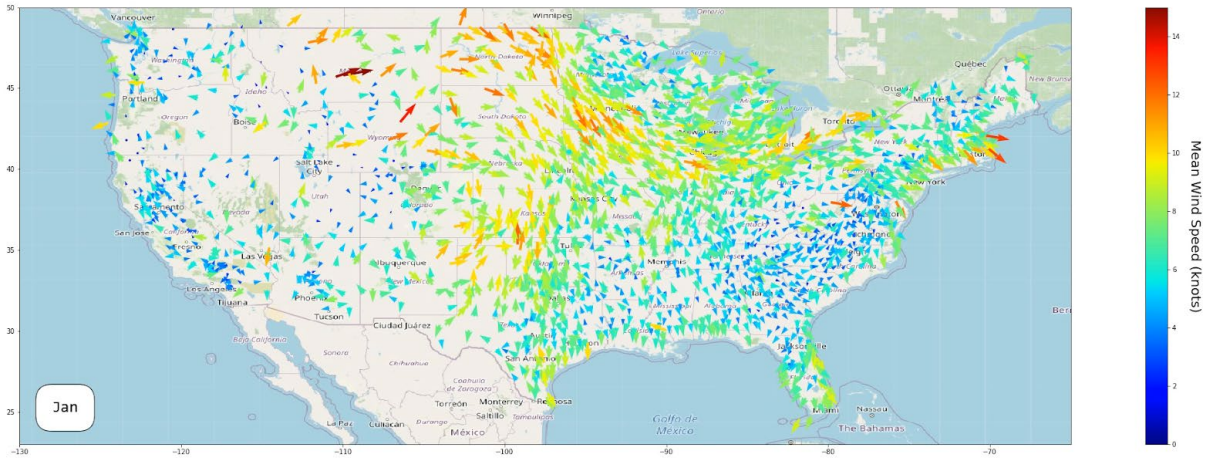


Figure 2. Variability of Prevailing Wind Direction and Average Wind Speed at North American Airports by Month (Ctrl+Click for animation)

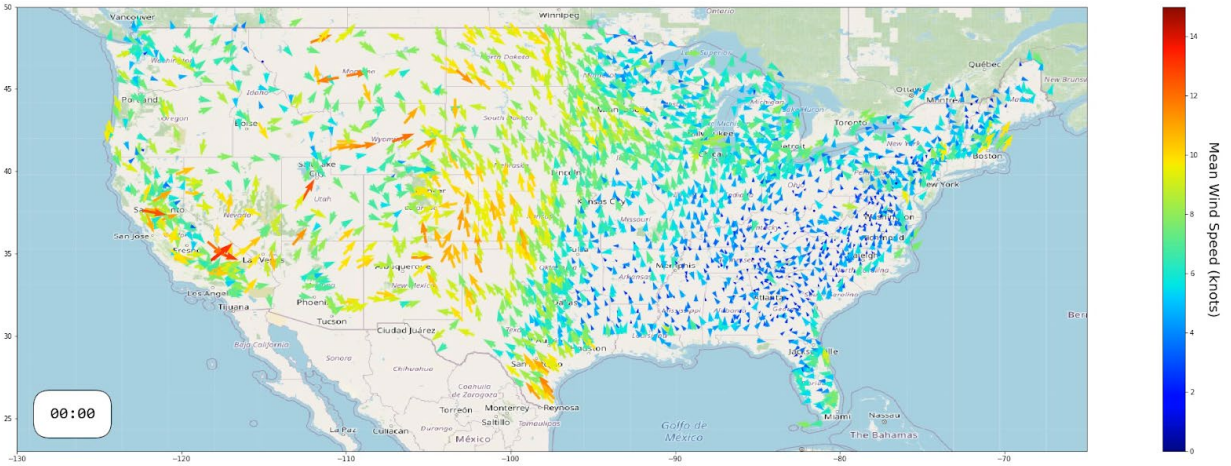


Figure 3. Variability of Prevailing Wind Direction and Average Wind Speed at North American Airports by Time of Day (Ctrl+Click for animation)

1.2. Understanding Runway Sensitivity to Wind Based on Runway and Aircraft Design

Runway length and aircraft size (i.e. critical aircraft) are highly correlated, as larger aircraft require longer runways for take-off and landing. Based on De Neufville and Odoni (2013), preliminary runway length (i.e. aircraft size) can be discussed in terms of the flight range, as indicated in Table 1. In addition, the Airport Reference Code (ARC) depends on the Aircraft Design Group (ADG) and Aircraft Approach Category (AAC) (i.e. approach speed), as indicated

in Table 2. To further illustrate the relations between aircraft types and the ADG, some example aircraft that belong to a specific ADG are listed in Figure 3. Furthermore, to safely operate aircraft, the Allowable Crosswind Component is strictly defined for each aircraft type, i.e. each ARC (and ADG and AAC), as shown in Table 4. Therefore, smaller aircraft, requiring shorter runways (Table 2), are more sensitive to crosswind (Table 4), while larger aircraft, requiring longer runways (Table 2) are less sensitive to crosswind (Table 4)

Table 1. Preliminary Runway Length Determination (De Neufville and Odoni,2013)

Runway Length	**Type of aircraft and range of flight**
7,000 ft	will accommodate regional jets and many short-range flights (up to roughly 1,000-1,500 mi) by narrow-body conventional transport jets
7,500 ft	will accommodate practically all short-to medium-range flights (roughly 2,000 mi), and nearly all landings
8,500-9,000 ft	will accommodate practically all medium-range flights (2,500-3,000 mi)
11,000-14,000 ft	will accommodate all feasible stage lengths in other than extremely high temperatures

Table 2. Airport Reference Code (ARC) Determination (FAA)

Aircraft approach category	Aircraft approach speed (kn)	Airplane design group	Aircraft wingspan (m)
A	<91	I	<15
B	91–<121	II	15–<24
C	121–<141	III	24–<36
D	141–<166	IV	36–<52
E	≥166	V	52–<65
		VI	65–<80

Source: FAA [1989]. Units converted from ft to the most next integer value in m.

Table 3. FAA Aircraft Design Group (ADG) Classification used in Airport Geometric Design and Example Aircraft

Design Group	Wingspan (ft)	Example Aircraft
I	< 49	Cessna 152-210, Beechcraft A36
II	49 - 78	Saab 2000, EMB-120, Saab 340, Canadair RJ-100
III	79 - 117	Boeing 737, MD-80, Airbus A-320
IV	118 - 170	Boeing 757, Boeing 767, Airbus A-300
V	171 - 213	Boeing 747, Boeing 777, MD-11, Airbus A-340
VI	214 - 262	A3XX-200 or VLCA

Table 4. Allowable Crosswind Component per Runway Design Code (RDC) (Source: FAA AC 150/5300-13, p.B-3)

Airport Reference Code or Runway Design Code (RDC)	Allowable Crosswind Component
A-I and B-I *	10.5 knots
A-II and B-II	13 knots
A-III, B-III, C-I through D-III D-I through D-III	16 knots
A-IV and B-IV, C-IV through C-VI D- IV through D-VI	20 knots
E-I through E-VI	20 knots

* Includes A-I and B-I small aircraft.

1.3. Wind Rose and Runway Rose

1.3.1. FAA's Nine Regional Airports Administrative Offices and their Wind and Runway Rose

The FAA divides the country's airports geographically into nine regions, with nine regional administrative offices: Alaskan, Northwest Mountain, Great Lakes, New England, Central, Eastern, Western-Pacific, Southwest and Southern (Figure 4). Each administrative airport office is responsible for overseeing airport development, certification, and safety in its region. Therefore any runway design improvement requires risk management and wind hazard characterization at the regional level .

Using the FAA National Flight Data Center (NFDC) Airport Dataset (https://nfdc.faa.gov), runways across all nine regions were analyzed by their location, orientation and length (Figures 5 -7). Figure 5 shows all runway directions by FAA administrative region. The radius of each bar corresponds to the count of runways in that direction of all paved public-use runways. Figure 6 presents the runway roses of airports included in this study together with the wind roses.

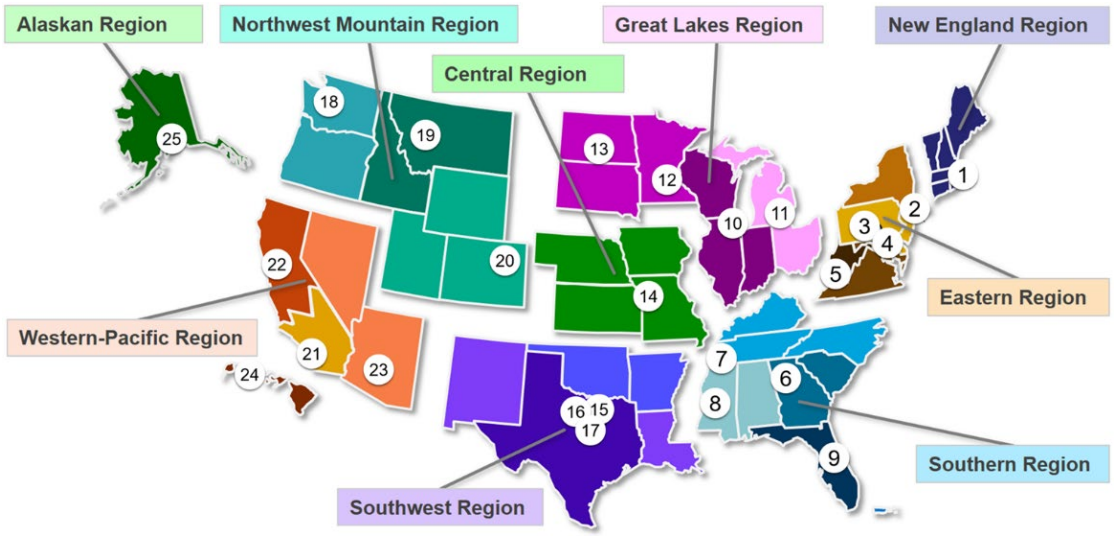


Figure 4. Nine administrative regions of the Federal Aviation Administration (adapted from https://www.faa.gov/airports/regions/)

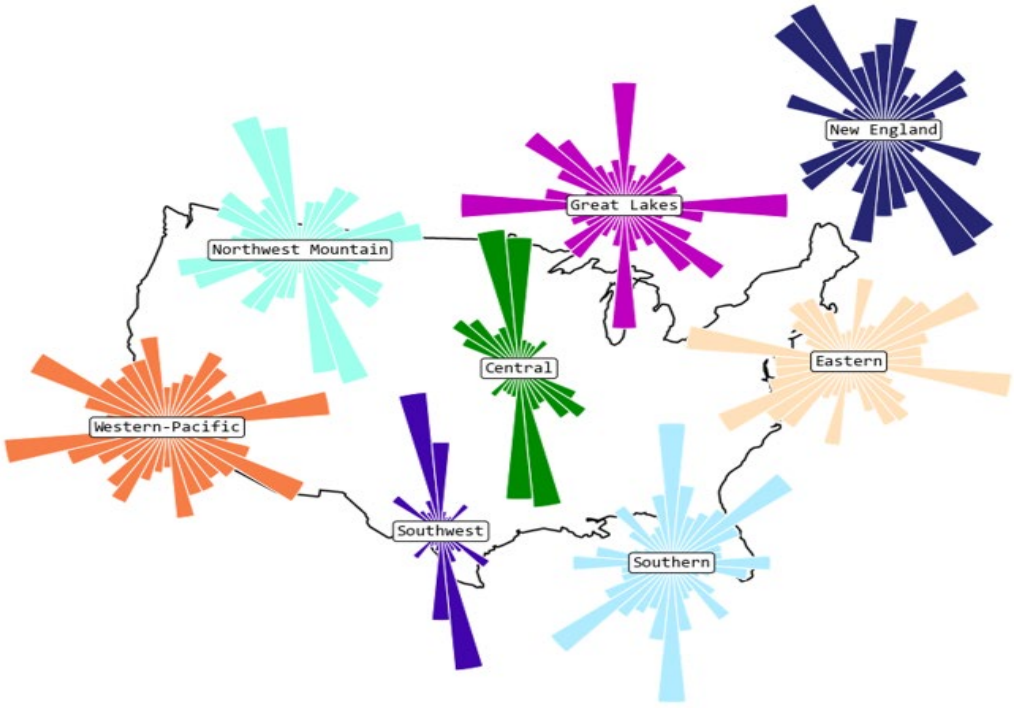


Figure 5. Runway Rose (or Regional direction patterns of most common runway headings). The radius of each bar corresponds to the count of runways in that direction.

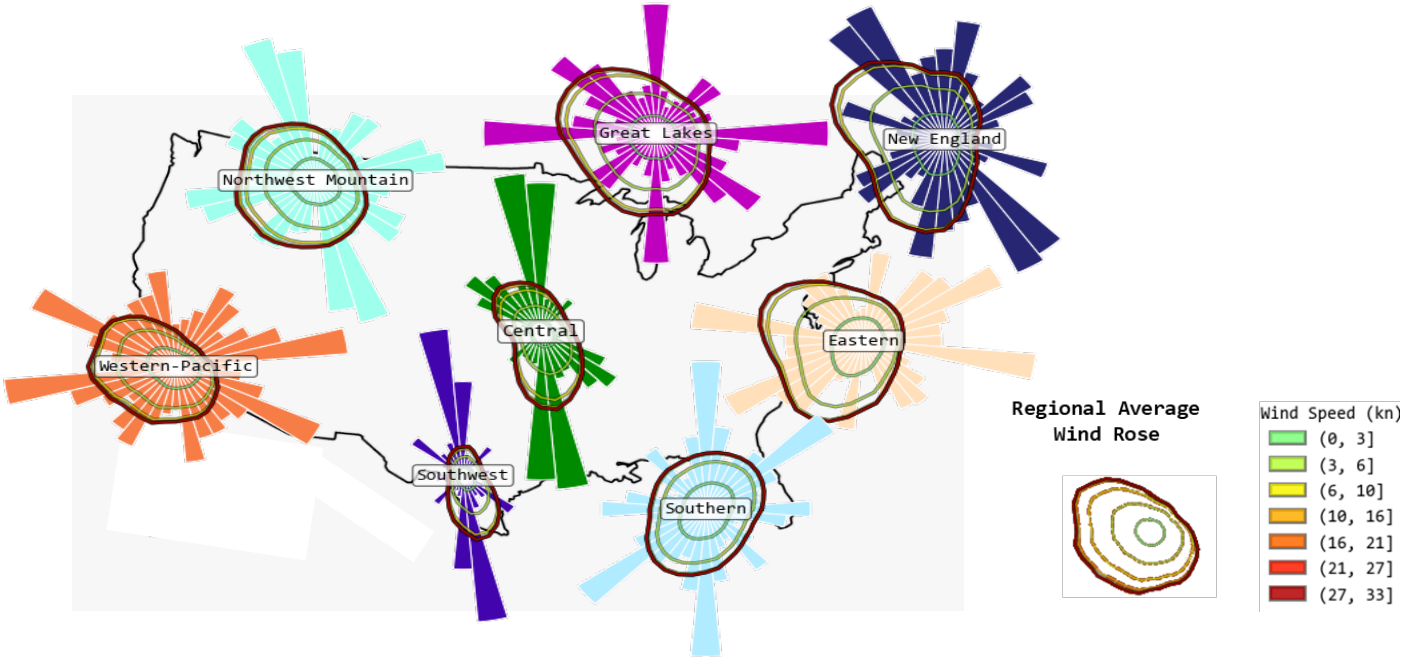


Figure 6. Wind Rose and Runway Rose for all Nine Regions. The contour lines represent the wind rose for different wind speed categories. The radius of each bar for the runway rose corresponds to the count of runways in that direction. USA outline adapted from https://svgsilh.com/image/1674031.html, public-domain CC0 license).

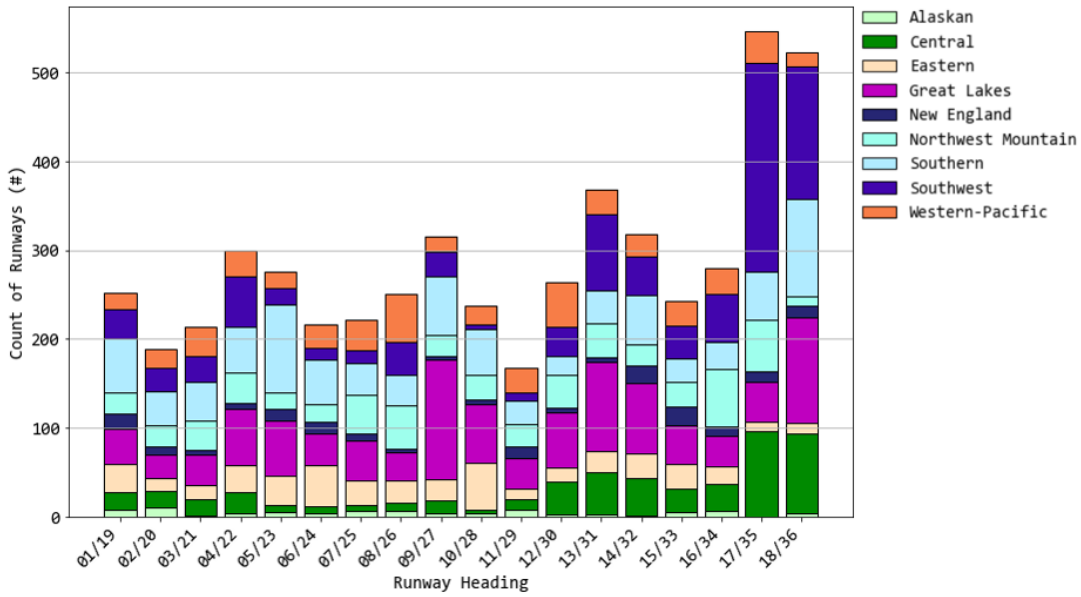


Figure 7. Count of runways categorized by direction, broken down by each FAA Region. North-South is 18/36 and East-West is 09/27

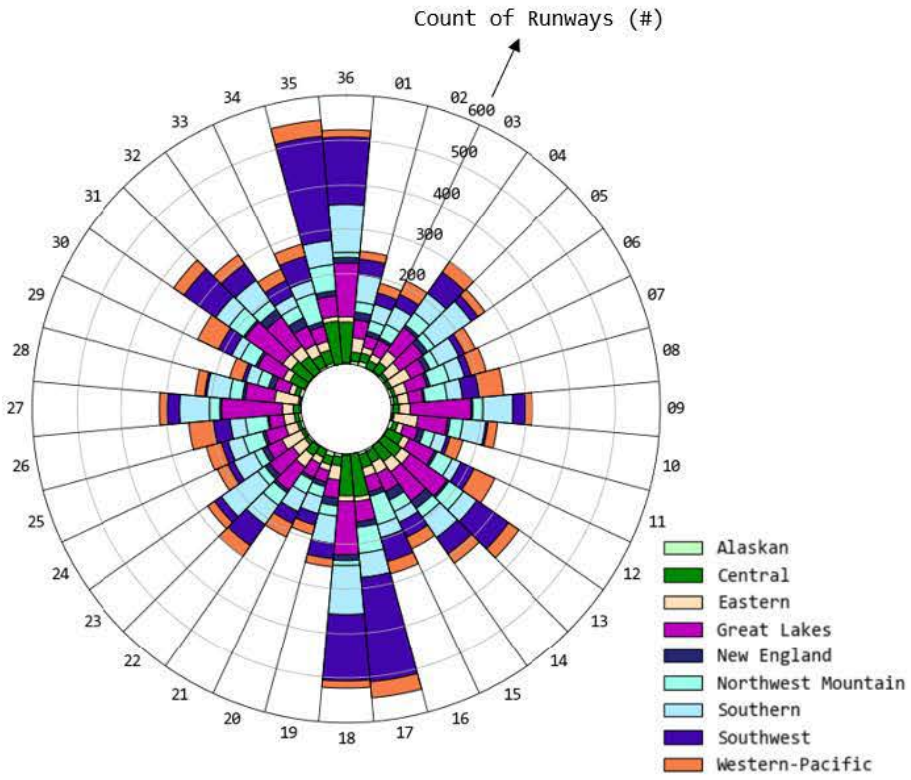


Figure 8. Alternative representation of previous figure showing actual heading of runways. The radius of each bar corresponds to the count of runways in that direction. North-South is 36/18, East-West is 27/09.

1.3.2. FAA's Western-Pacific Region Wind and Runway Rose

The States of Arizona, California, Hawaii, and Nevada make up the Western-Pacific region. Runways in the East-West (08/26) and the North West-South East (12/30) directions are most common in the Western-Pacific region. Number of runways not in the 08/26 and 12/30 directions are spread out relatively evenly across the remaining directions, unlike the other regions.

The median runway length in the Western-Pacific region is 4,805 ft. It is slightly longer than the national average, but has higher variations in length than other regions, with a standard deviation of 2,432 ft. The shortest paved runway in the Western-Pacific region is runway 17/35 at Sonoma Valley Airport (0Q3), CA with a length of 1,513 ft. The longest is runway 17/35 at Southern California Logistics Airport (VCV) in Victorville, CA, with a length of 15,050 ft. In terms of runway lengths, runways in the 13/31 directions appear to be shorter than most other directions. Median runway lengths range from 4,000 to 6,000 ft depending on their orientations (Figure 8a-8c).

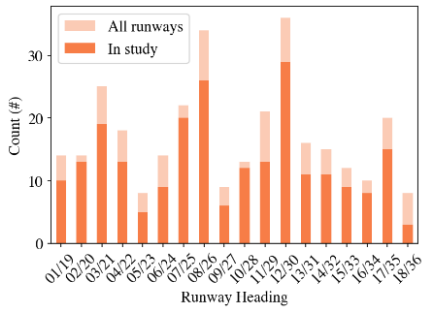






Figure 8a - Runway count histogram

Figure 8b - Runway rose of all runways in region

Figure 8c - Runway rose with wind rose

The overlaying regional (summative) wind roses are generated by adding the wind roses at all airports included in this study for each airport. Airport-level wind roses are generated through 10-year wind records between 2010 and 2020. This overview of the overall wind directions found at airports shows that runway orientations in each region generally correspond to the wind directions at the airports in those regions (Figure 9).

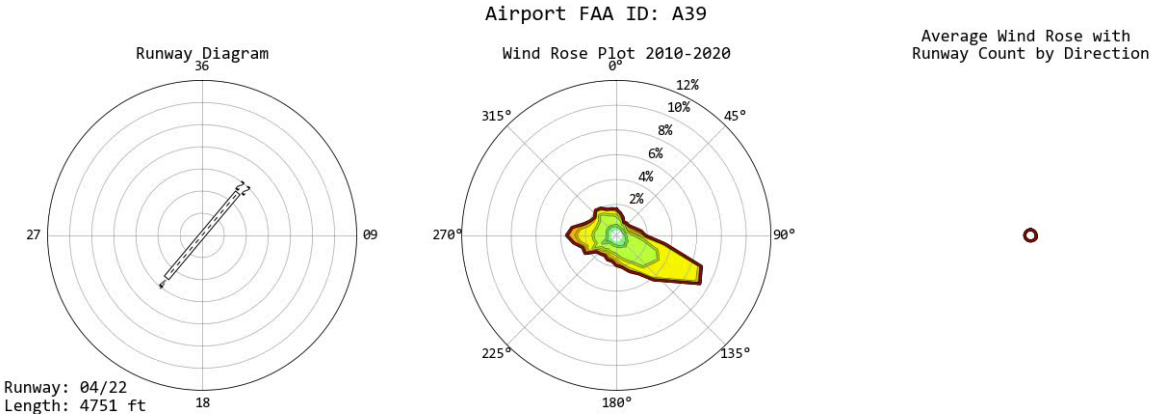


Figure 9. [Wind and Runway Roses Average in the Northern Pacific Region (ctrl click for animation)]

Out of 516 runways in the Western Region, 435 are included in the development of the runway rose, corresponding to a total of 300 out of 367 airports in the region. The studied runways have a median length of 4,884 ft, and a standard deviation of 2,503 ft. A larger portion of the short- to mid-length 2,000- to 7,000-ft runways are not included in the study than longer runways. Both the shortest and longest runways are included in the study (Figures 10a-10b).

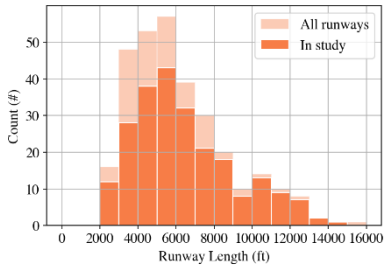


Figure 10a - Runway length distribution histogram

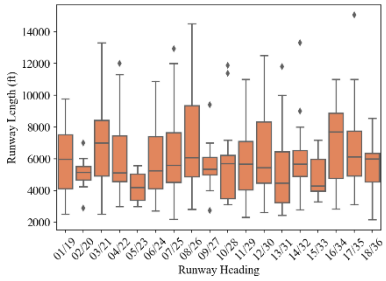


Figure 10b - Runway length by heading boxplot

1.3.3. California Runways

In California, the dominant runway orientation is East-West (10/28 and 9/27) followed by South-East - North West (14/32 and 15/33)(Figure 11), setting the general orientation for the FAA's Western Region runways. The length of the majority of runways is between 3000 and 4000 ft (Figure 12) with interquartile ranges of approximately 3000 and 5500 ft (Figure 13). Independently of the runway orientation, the median runway length tends to be a little above 4,000 feet.

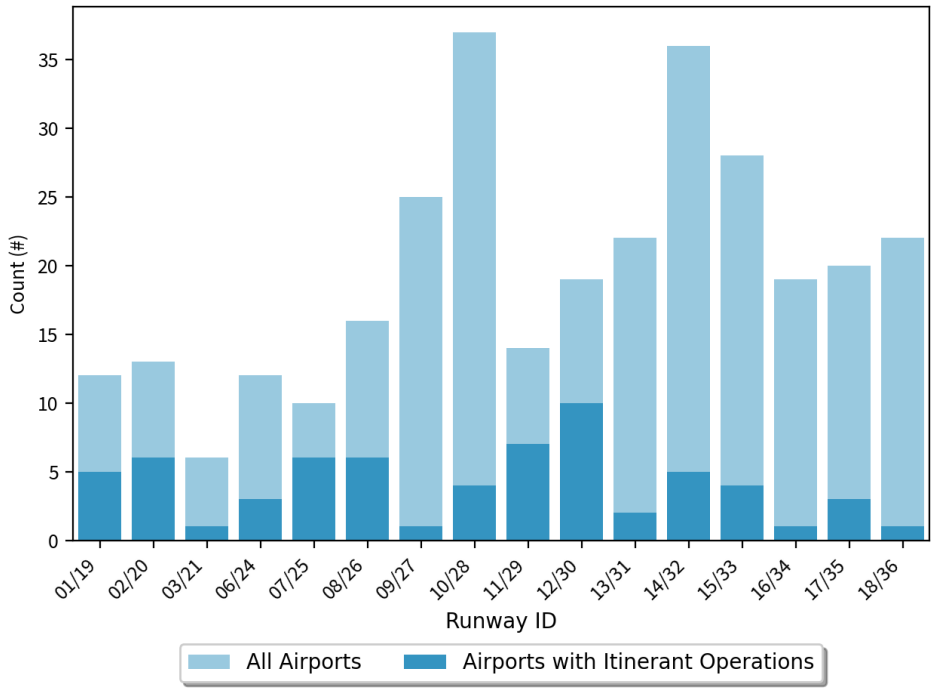


Figure 11. Runway Orientations: all Airports vs. Airports with Itinerant Operations in California

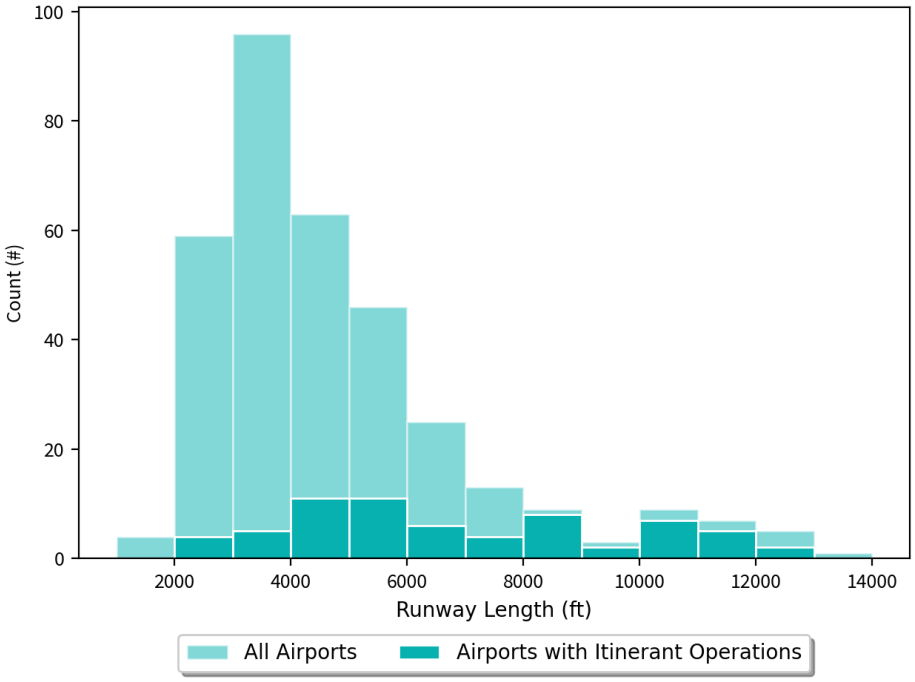


Figure 12. Runway Length: all Airports vs. Airports with Itinerant Operations in California

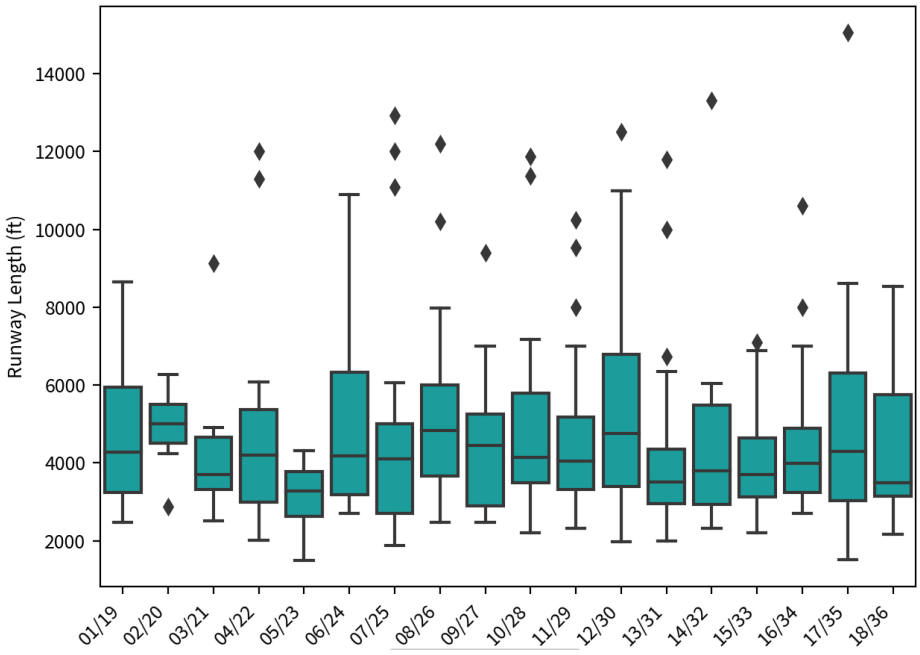


Figure 13. Boxplot of of Runway Length and Orientation across Airports in California

[4.3] 2. Methods

A crosswind hazard in this study is defined as any wind that has a perpendicular component to the runways. Winds that are not parallel to the runway make landings and takeoffs more difficult and susceptible to incidents or accidents. There are multiple allowable crosswind component thresholds where crosswinds become hazardous depending on the fleet mix and runway design. This study focuses only on the lowest threshold of 10.5 kn (Table 4). For subtask (1), the probability of crosswind occurrence is calculated as the percentage of time between 7am and 7pm that crosswind components are equal to or above 10.5 kn. This percentage is calculated for a total of 30 airports, and 65 runways in California (Figure 14) using the 10-year wind dataset from 2010-2020 from the Automated Surface Observing System (ASOS) stations (Iowa State University Environmental Mesonet). The crosswind hazard has then to be put in the context of traffic demand and aircraft type, especially at single-runway airports.

The following steps were taken in order determine subtasks (2) and (3):

> (2) probability of crosswind occurrences that include speeds that are equal to or greater than 10.5 kn for single- and multi-runway airports and demand for each relevant aircraft design group and aircraft approach category (A-I and B-I),
>
> (3) probability of aircraft incidents during higher (than allowed) crosswind speeds for corresponding aircraft design group and aircraft approach category.

First step: 2019 was used as a representative year for analyzing the demand and flights for about 66 CA airports (ASPM database used for this analysis is available in supplementary materials folder “Task4.3.ASPM_CA2019”). Then a fleet mix for those airports/runways was extracted -- i.e. each aircraft type was matched with the correct Aircraft Design Group.

Second step: The Aircraft Design Group (ADG) was determined using the following steps:

1) take the aircraft type field from the *ASPM database*, then
2) match the aircraft type with the aircraft specifications (tail height and wingspan) available in the attached excel file (also available on the FAA website here)
3) assign the ADG roman number (I, II, III, IV...) to aircraft type based on Table 4 (example: https://skybrary.aero/articles/airplane-design-group-adg)

Once ADG is determined for each aircraft, then we can create a fleet mix (i.e. the ADG fleet mix): for example: ADG I is 65%; ADG II is 20%;ADG III is 15%.

The crosswind limitation is then based on the Aircraft Approach Category (i.e. speed) (A, B, C, D..) and Aircraft Design Group (I, II, III..), and subtasks (2) and (3) can be developed. Figure 15 presents the method developed to determine the crosswind occurrences in California.

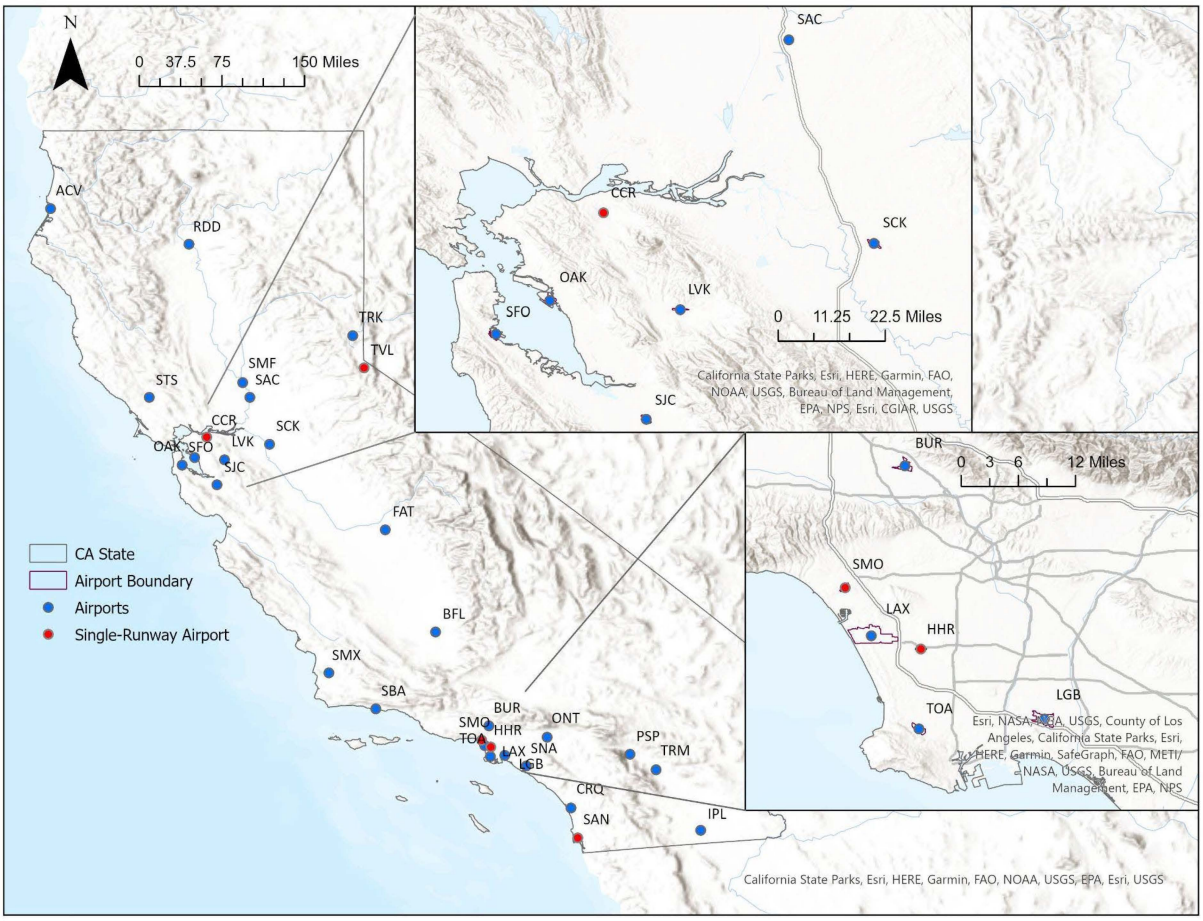


Figure 14. California Airports Represented in the Wind Analysis. Highlighted in Red SIngle-Runway Airports: CRQ, HHR, SAN, SMO, and TVL

The FAA maintains the Aircraft Characteristics Database, which provides basic aircraft characteristics including Aircraft Approach Category (AAC) and Airplane Design Group (ADG), identifiable through the aircraft's ICAO code. AAC and ADG values corresponding to the aircraft model specified by each flight record were looked up in the Aircraft Characteristics Database and matched through the ICAO code. AAC (A, B, C, D, E) and ADG (I through VI) values were combined to arrive at the Airport Reference Code (RDC: A-I, C-IV, etc.). For each airport, yearly fleet mix percentages were calculated by dividing the number of flights served by aircraft in each RDC category by the total number of itinerant flights in 2019, multiplied by 100. Allowable Crosswind Components of each of the airports were then calculated by adding the percentages of RDC categories for each crosswind category, specified by FAA Advisory Circular 150/5300-13B.

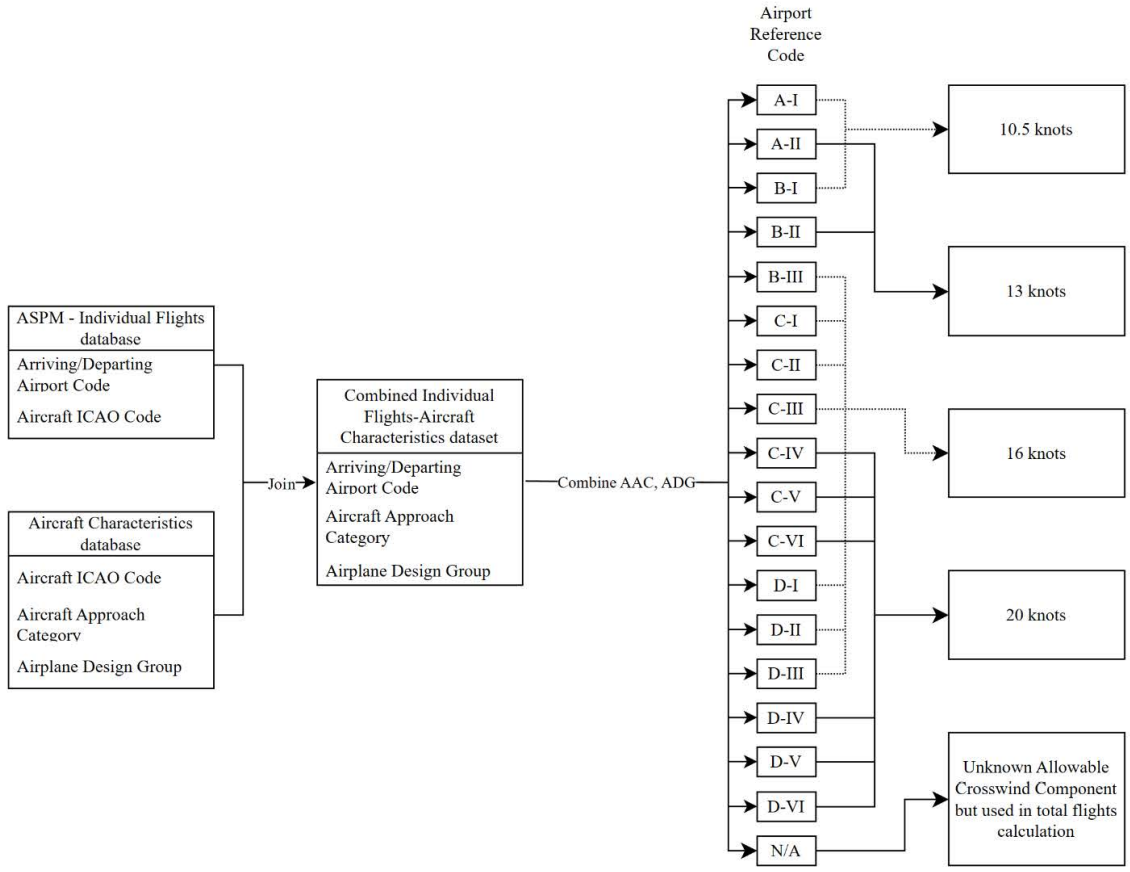


Figure 15. Method for Determining Crosswind Occurrences at California Airports.

[4.3] 3. Wind Analysis Results for California Airports

The probability of crosswind occurrences of speeds equal to or greater than 10.5 kn is presented in Figures 16 and 17. These results are key to understanding California's crosswind hazard exposure at the runway level. The average exposure is 3.14%. Out of 65 runways assessed, 11 have more than 5% of crosswind occurrences, with SFO, SMX and OAK at the top 3 at 21.08; 15.61, and 11.96 % of exposure time to hazardous crosswinds. From the single-runway airports, SAN is at the top with 1.03%, followed by CRQ at 0.17%.

The probability of crosswind incidents at airports with A-I fleet mix is presented on Figures 18 and 19. The average probability is 0.00193. Out of 65 runways assessed, six have probabilities of incident greater than 0.005, with RDD, IPL and TOA at the top 3 with 0.01810; 0.01446; and 01276 respectively. From the single-runway airports, only CRQ and SMO are prone to crosswind incidents given their A-I fleet.

Figures 20 and 21 show that the probability of crosswind incidents at airports with B-I fleet mix is much higher than those for A-I fleet mix. The average probability is 0.41372. Out of 65 runways accessed, 38 runaways have greater than 0.005 incident probability, with SMX, IPL, and RRD

the top 3 with 9.16; 6.48, and 2.55 respectively. All single-runway airports assessed are prone to incidents, with SAN and SMO leading at 0.02209 and 0.00302 probability of incidents given their B-I fleet.

By combining A-I and B-I fleet mix, an overall probability assessment of crosswind incidents (equal to or greater than 10.5 kn) is presented in Figure 22 and Figure 23. A total of 44 runways out of 65 are prone to crosswind incidents given the fleet mix that is susceptible to the lowest allowable crosswind component. The average probability is 0.41565. SMX and IPL airports present a much higher probability than the average, with 9.16 (due only to B-I fleet mix) and 6.49 (due mostly to B-I fleet mix). RDD, IPL, ACV follow the lead with 2.57, 1.58, and 1.17 respectively. From the single-runway airports, SAN is at the top with 0.2209, followed by HHR at 0.00756 probability of crosswind incident at 10.5 kn and sensitive fleet mix.

The result data for subtasks 1-3 used for the figures in this section are available in a table format as a supplementary materials "WindResults_graphData"

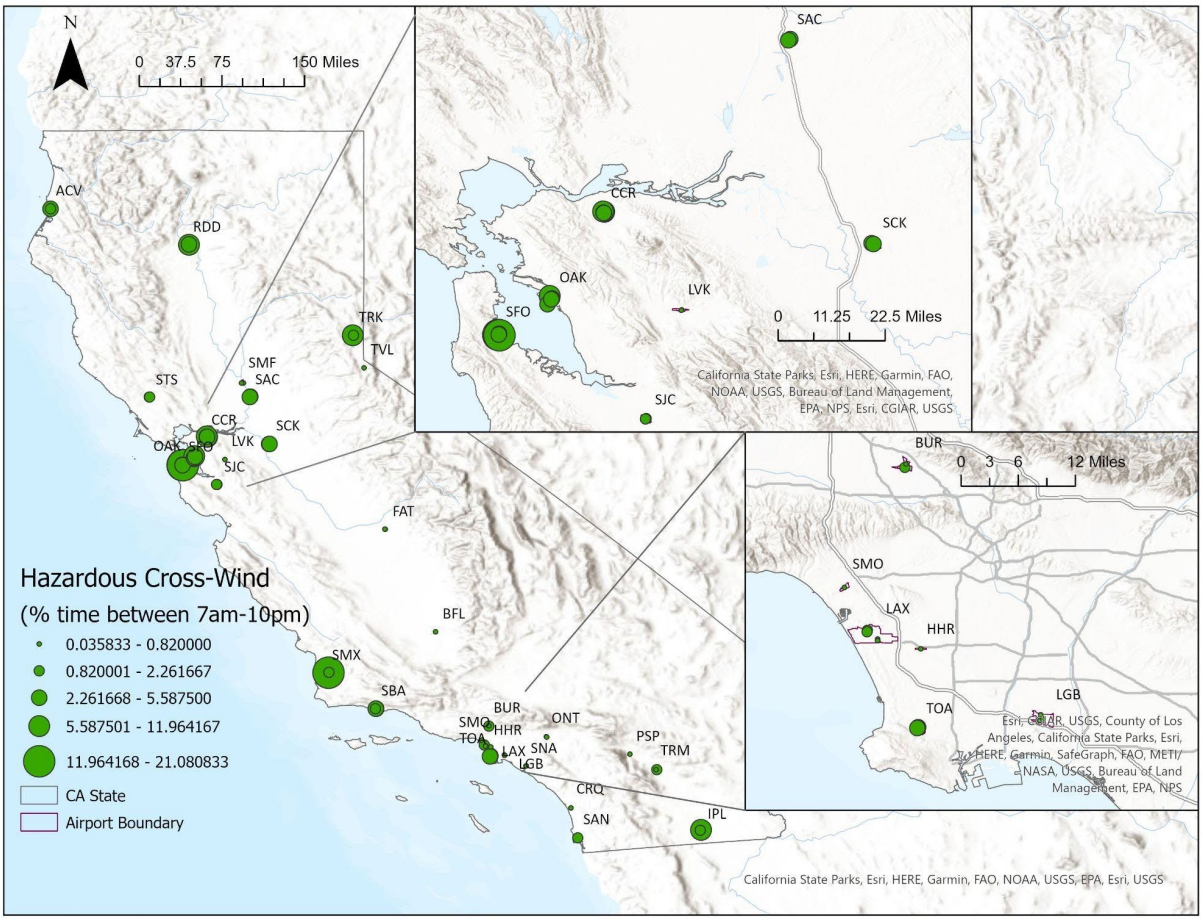


Figure 16. Probability of crosswind occurrences: percentage of time crosswind speed is equal to or greater than 10.5kn (between 7am and 10pm) (Subtask 1).

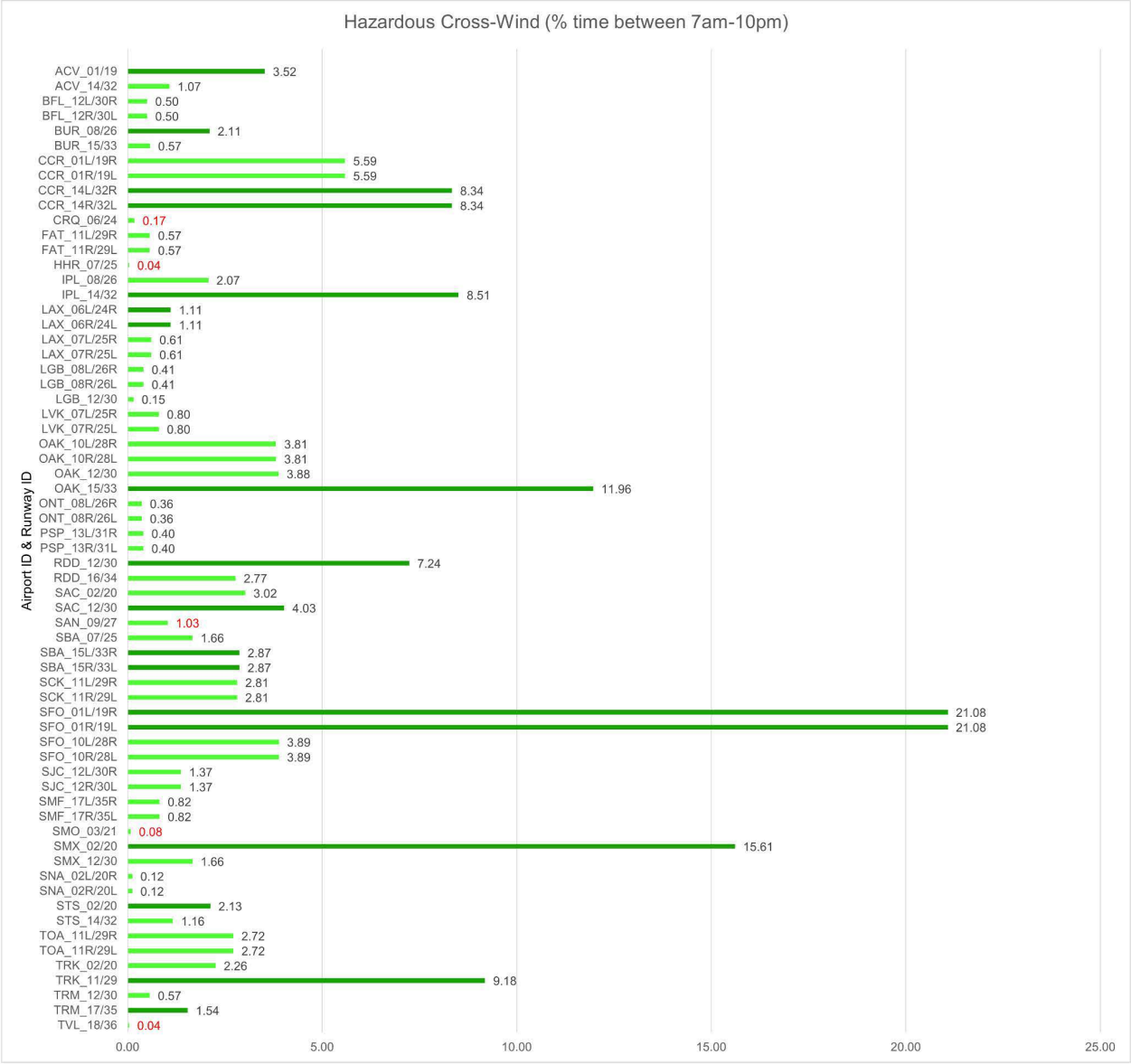


Figure 17. Probability of Crosswind Occurrence with Airport and Runway Detail (Subtask 1). Single-runway airports have their results highlighted in red. Multi-runway airports with different exposure levels have their runways with the highest hazard exposure highlighted in darker

green.

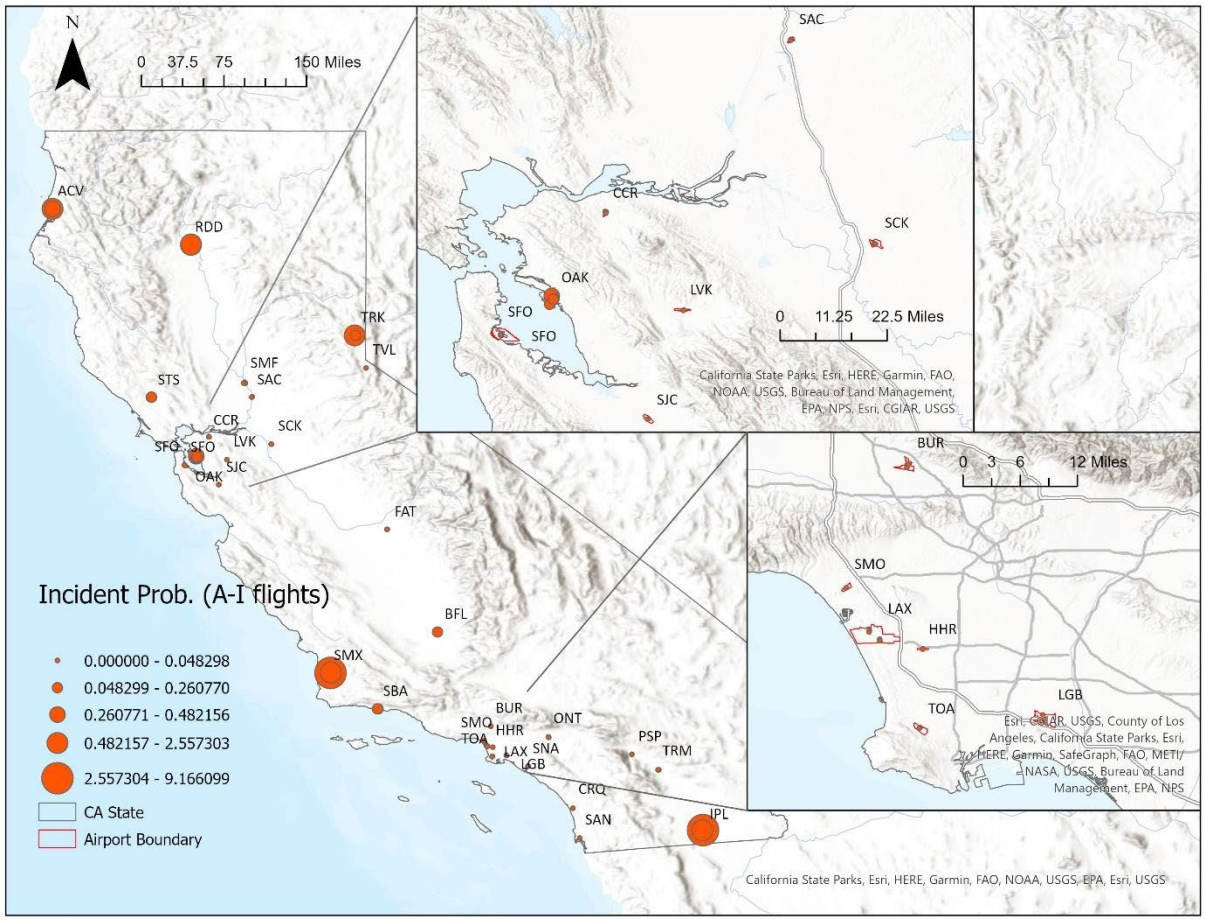


Figure 18. Probability of Crosswind Occurrences on Airports with Demand for A-I Aircraft Design Group and Aircraft Approach Category (Subtask 2).

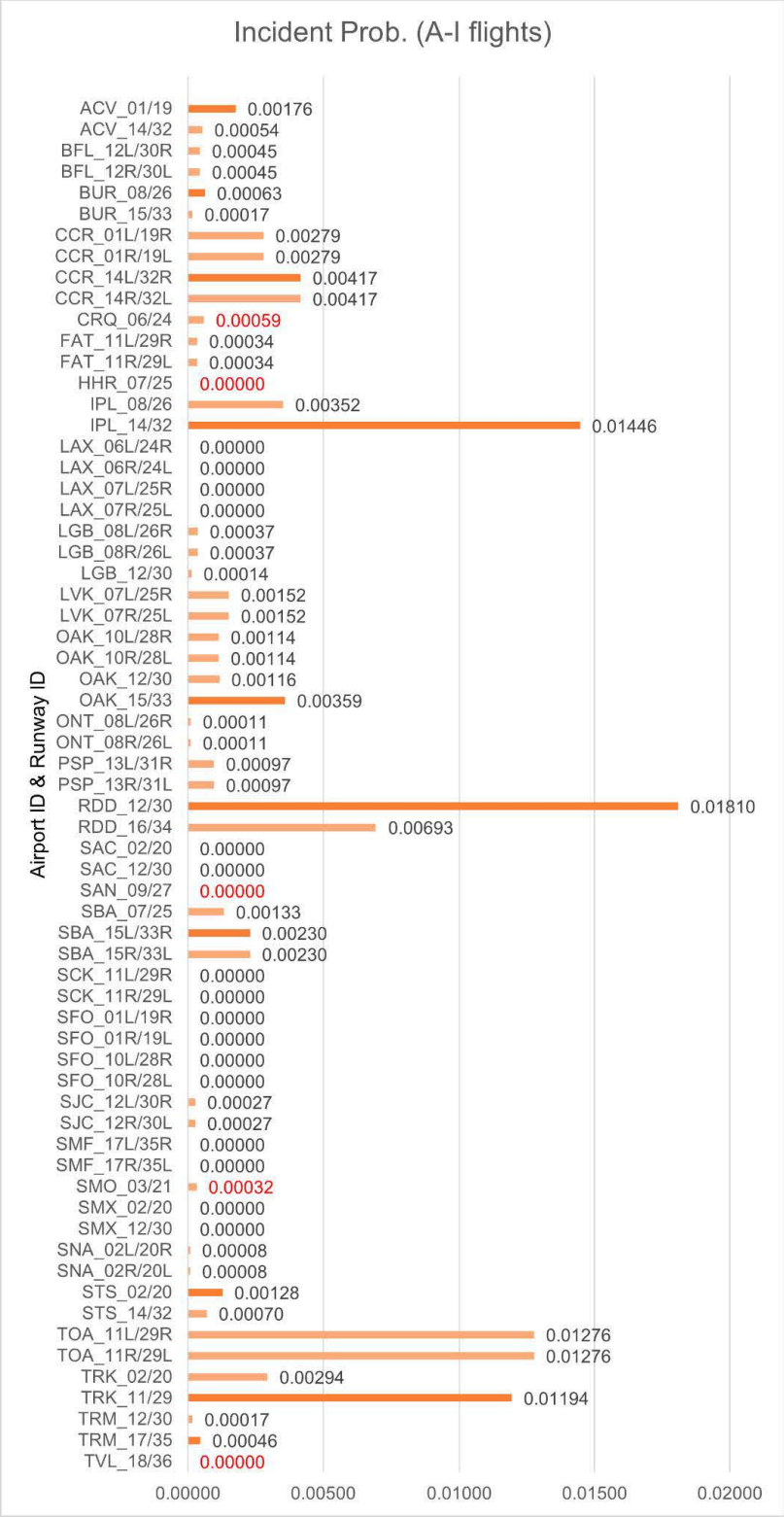


Figure 19. Probability of Crosswind Occurrences on Airports with Demand for A-I Aircraft Design Group and Aircraft Approach Category with Airport and Runway Detail (Subtask 2). Single-runway airports have their results highlighted in red. Multi-runway airports with different probability levels have their runways with the highest probability highlighted in darker orange.

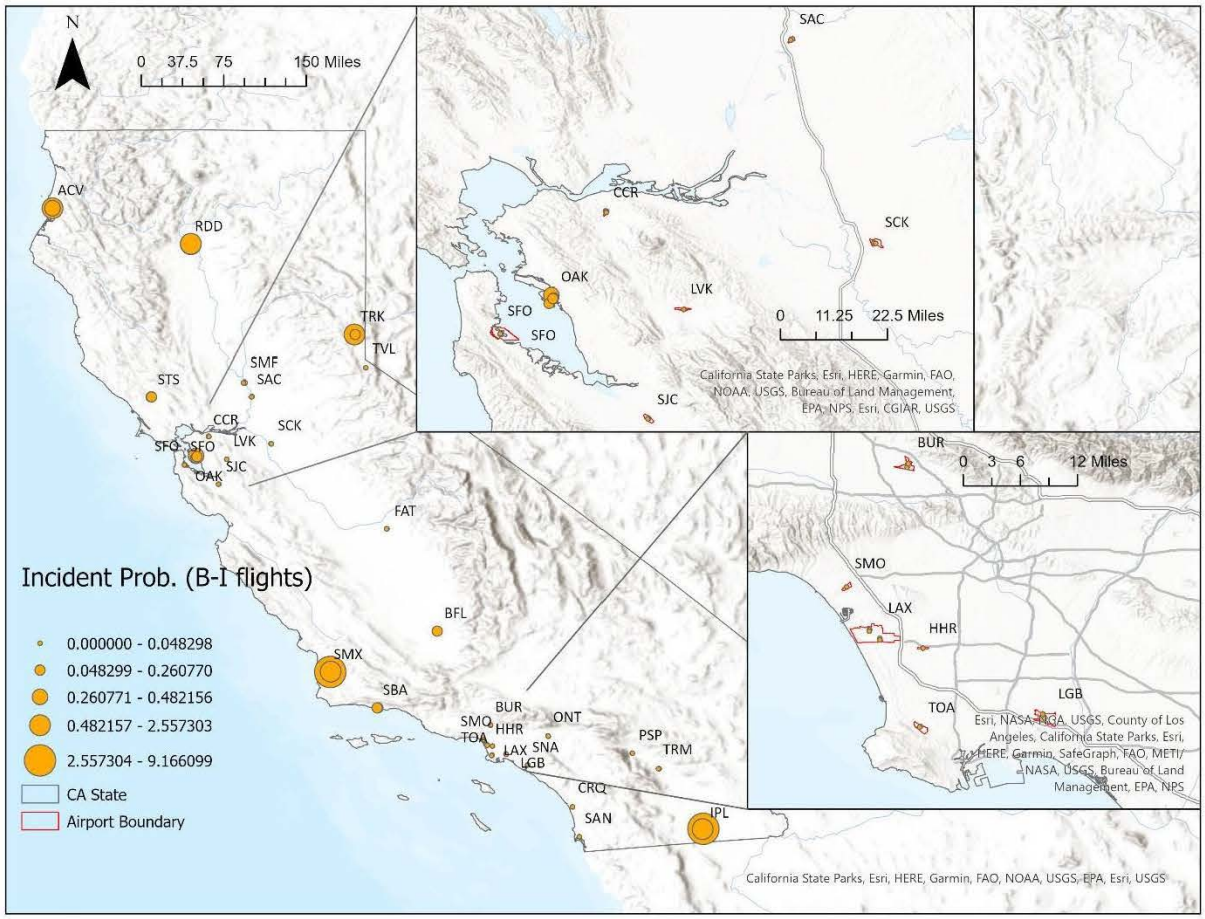


Figure 20. Probability of Crosswind Occurrences at Airports with Demand for B-I Aircraft Design Group and Aircraft Approach Category (Subtask 2).

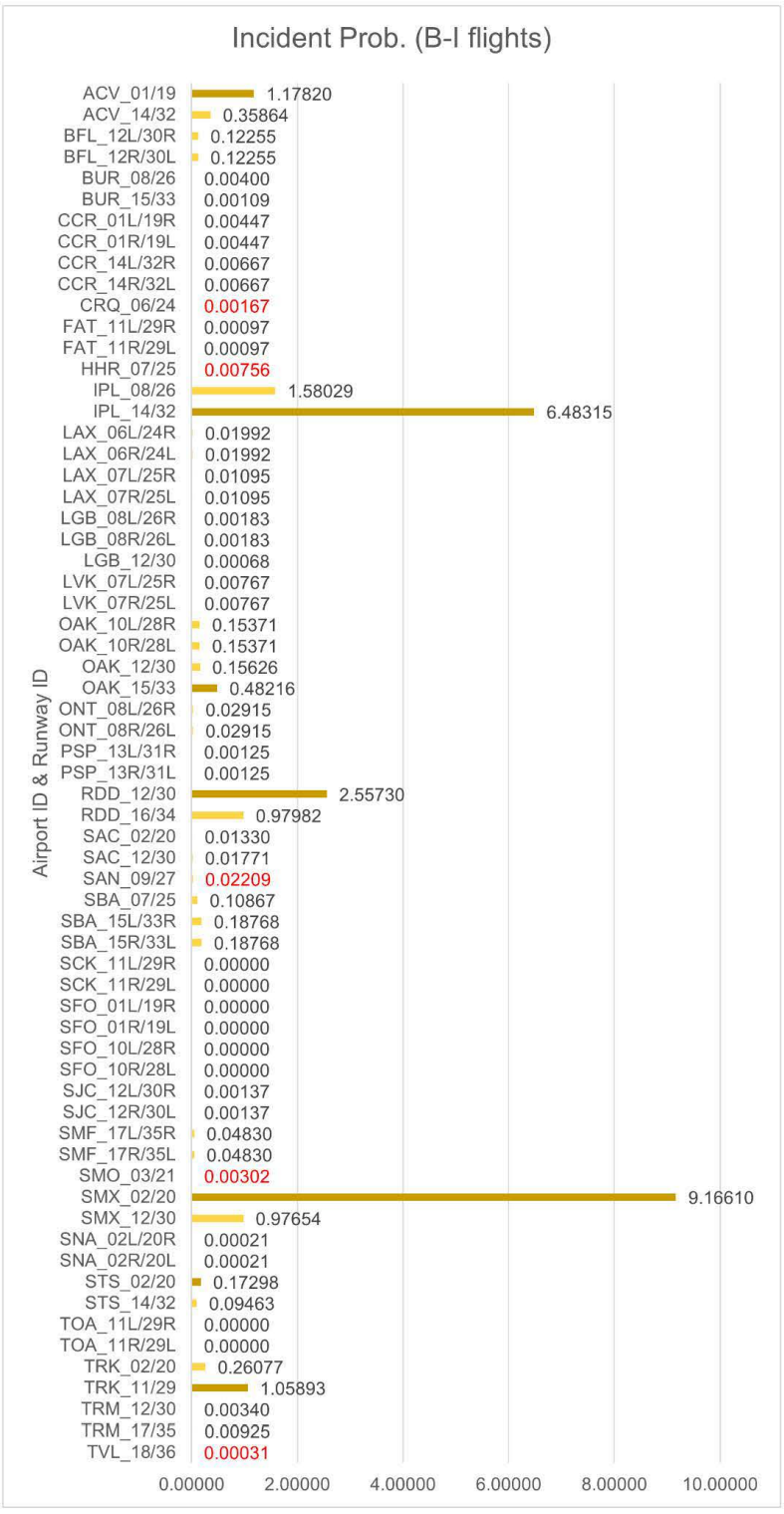


Figure 21. Probability of Crosswind Occurrences at Airports with Demand for B-I Aircraft Design Group and Aircraft Approach Category with Airport and Runway Identification (Subtask 2). Single-runway airports have their results highlighted in red.Multi-runway airports with different incident probability levels have their runways with the highest probability highlighted in darker yellow.

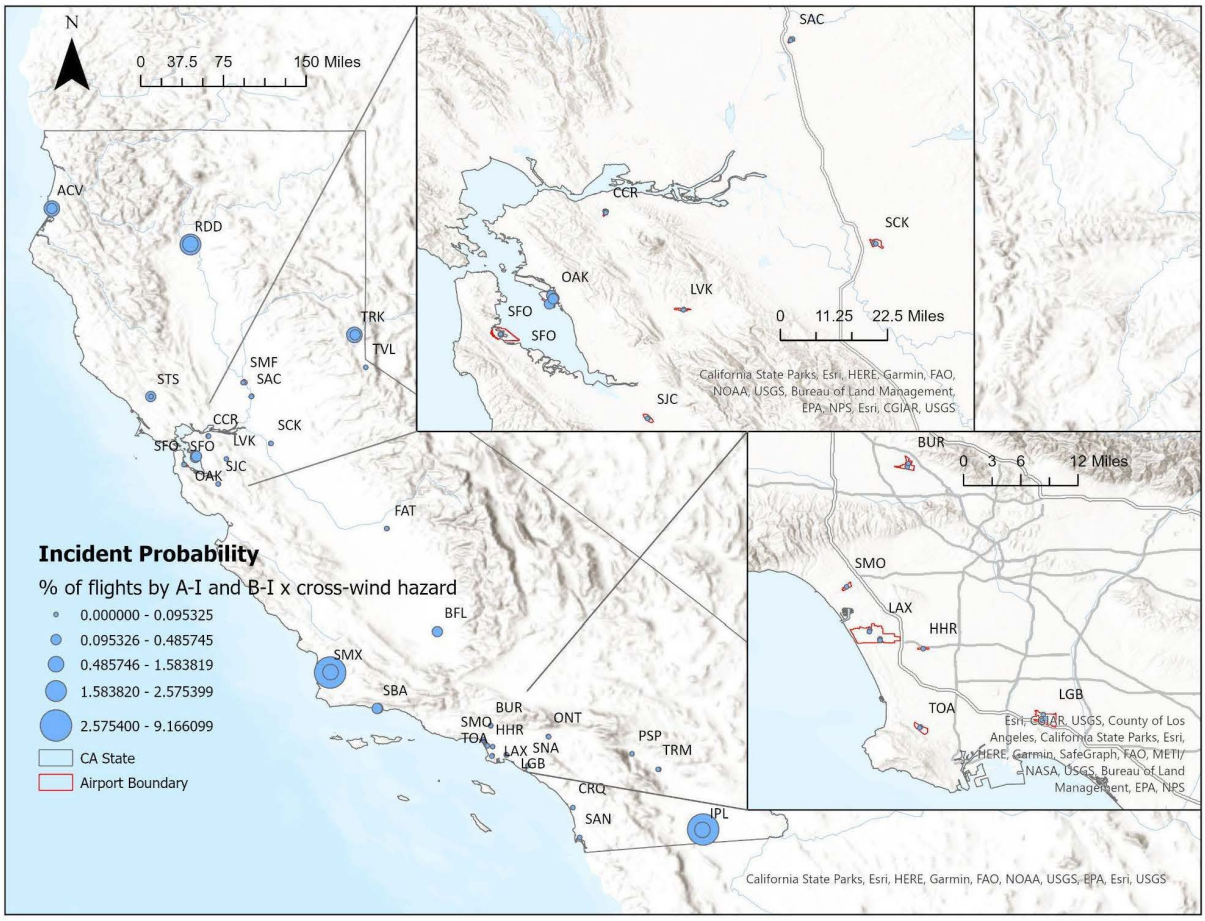


Figure 22. Probability of Aircraft Incidents During Crosswind Speeds Equal than or Greater than 10.5 kn and Corresponding Aircraft Design Group and Aircraft Approach Category (A-I and B-I) (Subtask 3).

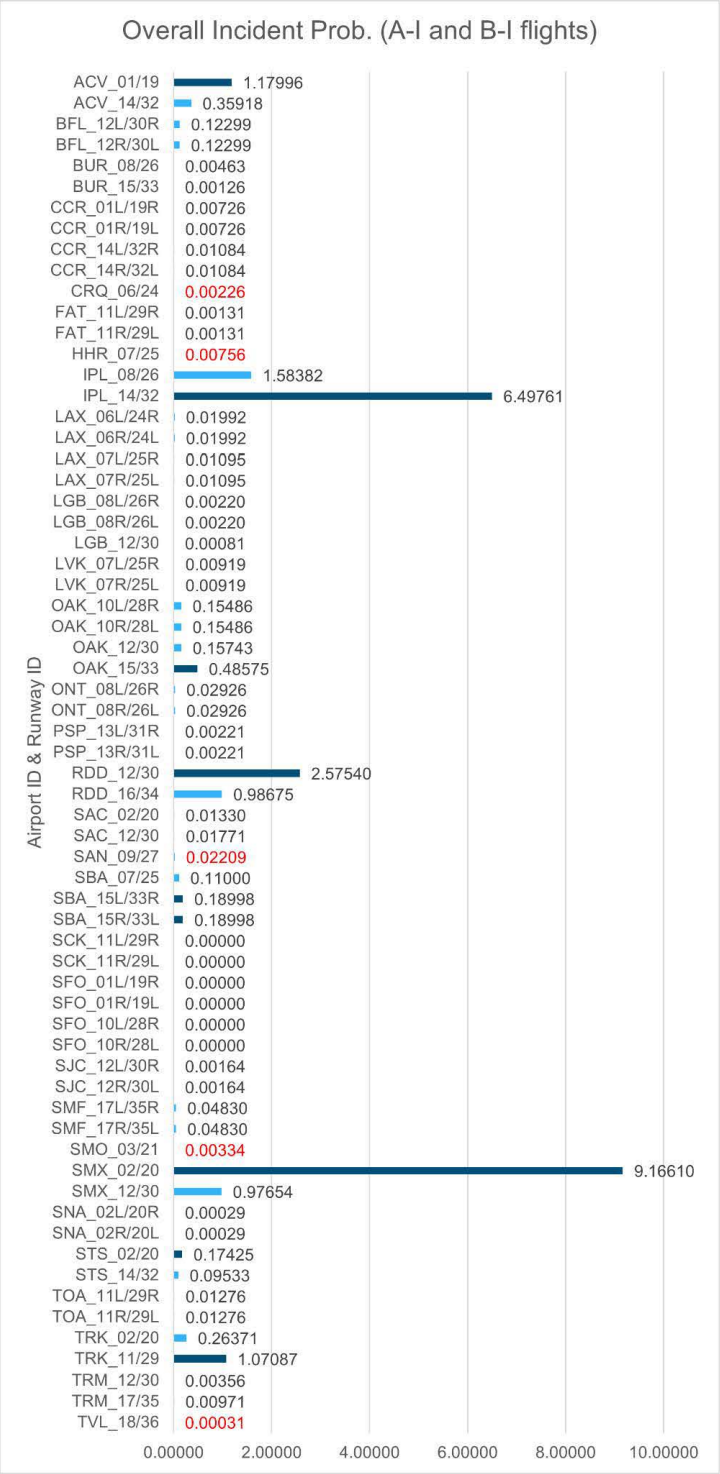


Figure 23. Probability of Aircraft Incidents During Crosswind Speeds Equal to or Greater than 10.5 kn for Corresponding Aircraft Design Group and Aircraft Approach Category (A-I and B-I) (Subtask 3). Single-runway airports have their results highlighted in red. Multi-runway airports with different incident probability levels have their runways with the highest probability highlighted in darker blue.

[4.3] 4. Citations

De Neufville, R. and Odoni, A. Airport Systems –Planning, Design and Management, McGraw-Hill, 2013, 2ndEdition

Kulkarni, S., & Huang, H. P. (2014). Changes in surface wind speed over North America from CMIP5 model projections and implications for wind energy. Advances in Meteorology, 2014.

Pryor, S.C., Barthelmie, R.J., Young, D.T., Takle, E.S., Arritt, R.W., Flory, D., Gutowski Jr, W.J., Nunes, A. and Roads, J., (2009). Wind speed trends over the contiguous United States. Journal of Geophysical Research: Atmospheres, 114(D14).

Zeng, Z., Ziegler, A.D., Searchinger, T., Yang, L., Chen, A., Ju, K., Piao, S., Li, L.Z., Ciais, P., Chen, D. and Liu, J., (2019). A reversal in global terrestrial stilling and its implications for wind energy production. Nature Climate Change, 9(12), pp.979-985.

Task 8. Safety Zones Accident Density & Land Use Compatibility Update

Deliverable: A final report summarizing results from risk and environmental analysis (tasks 4) focusing on how these results might impact current generic Safety Zones geometries and land use recommendations on dwelling densities and intensities (focus on updating tables on pages 4-20 & 4-25 from the 2011 ALUP Handbook)

[8] 1. Introduction

Based on the 2011 ALUP Handbook the following components of risk determine Safety Zones and their land use compatibility: spatial distribution and frequency of accidents as well as potential consequences. The accident component is more directly taken into consideration to determine the shape and size of Safety Zones; and the potential consequences component helps determine land use compatibility criteria (dwelling densities and population intensities) that mitigate the potential for severe consequences in case of an accident.
The handbook underlines that "*The intent of the set of zones […] is that risk levels be relatively uniform across each zone, but distinct from the other zones.*" and that these geometries are "*intended just as a starting place for the development of zones appropriate for a particular airport. In some cases, the zones might be quite suitable, however in most airports, some degree of adjustment of the generic zones is necessary in recognition of the physical and operational characteristics of the airport*." (ALUP Handbook, pp. 3-19 to 3-20). Runway safety zones are created with the goal to maintain "*undeveloped land clear of objects in accordance with FAA standards*" (ALUP 2011 pp.4-31) and is based on the observation that most aircraft accidents occur near runway surfaces and the assumption of decreased risk of damage in case of an accident if open areas are preserved where accidents are observed to occur more regularly. Overall in previous ALUP Handbooks, there is encouragement of low density development in critical Safety Zones 1, 2, and 5; while Zones 3, 4, and 6 have less restrictive land compatibility criteria. The handbook also reminds that safety criteria is largely a function of risk acceptability, and that uses of these Safety Zones, which result in intolerable risk, usually must be prohibited or restricted where risk is significant but tolerable.

This report focuses on assessing the validity of current Safety Zones dimension (from the 2000-2009 published in 2011) based on the updated accident information. It uses the National Transportation Safety Board (NTSB) accident dataset from 2008-2022 and the Federal Aviation Administration Wildlife Strike dataset from 1990 - April 2023. The major innovation in this handbook update is the incorporation of geographic information systems (GIS) to assess the spatial relationship of historical accidents and wildlife strikes with airport Safety Zones (Figure 1). A method was defined to gather raw data from the NTSB website and meticulous data pre-processing for temporal and spatial compatibility. This was possible due to the longer time

series of NTSB accident dataset compared to former handbooks. The 2011 handbook was the first one to cover California accidents exclusively (due to data size limitation the three other handbooks before 2011 assessed accidents across all of the U.S.). Due to the limitation of quality GIS accident data, only 70 out of 1,800 accidents from 2000-2009 were used to develop the safety analysis of the 2011 handbook. The current methodology is uses 8,550 accidents from the 1982-2022 NTSB series, out of which 1,897 are in California (based on a spatial selection) and were further processes through GIS to produce two distinct spatially-relevant databases for this task:

(1) Highest number of spatially-relevant accidents method = total of 1,355 events
(2) Reproduction of 2011 handbook method = total of 495 events (or 298 when removing accidents outside the 5 mi airport buffer).

Another conceptual and methodological innovation of this report is using Land Use and Land Cover (LULC) data from the United States Geological Survey (MLRC, 2023) to assess the potential severity of consequences in case there is an accident. Different from the 2011 Handbook, where risk was measured solely based on accident percentages for each zone, this report defines risk as a function of hazard and exposure. The accident density is used to calculate hazard and the potential consequences (LULC data) are used as a proxy to calculate exposure.

Our main results point to the need to re-assess Safety Zone 5 dimensions due to the discrepant density of accidents as well as a sharp increase of % of accidents in this zone in comparison with what was accounted for in the latest ALUP Handbook. Although the percentage of Zone 5 accidents outside airport boundaries is much smaller than those compared to other zones (24-27%), the density of those accidents remains very high (0.509 to 0.795 accidents per sq mi). Another key result points to reviewing land use compatibility policies for Safety Zone 3 which shows a higher percentage of exposed areas with potential for severe consequences in case of an accident in comparison to other zones (except for zone 6). Zone 3 compatibility revision is however based on LULC data which requires field validation, or a better approximation of developed LULC classes with the ALUP Handbook development characteristics and their associated compatibility criteria. Finally, the risk analysis in section 3.3. reinforces the urgency of increasing the dimensions of the sidelines of Safety Zone 5. Based on a weighted accident risk calculation, we suggest a revision of Zone 6 dimensions and land use compatibility policies to better account for the high concentration of fatal accidents in this zone, as well as the sharp increase in accident percentages when compared to what was accounted for in the 2000-2009 assessment. Based on the general spatial pattern of accidents that concentrate the closer you are to the runway line, we assume that this increase in accident percentage of Zone 6 is likely occurring near the boundaries with Safety Zone 5. Overall, further exploring the spatial pattern of accidents within Zone 5 and Zone 6 is highly recommended to prescribe more specific changes in these zones dimensions and geometries.

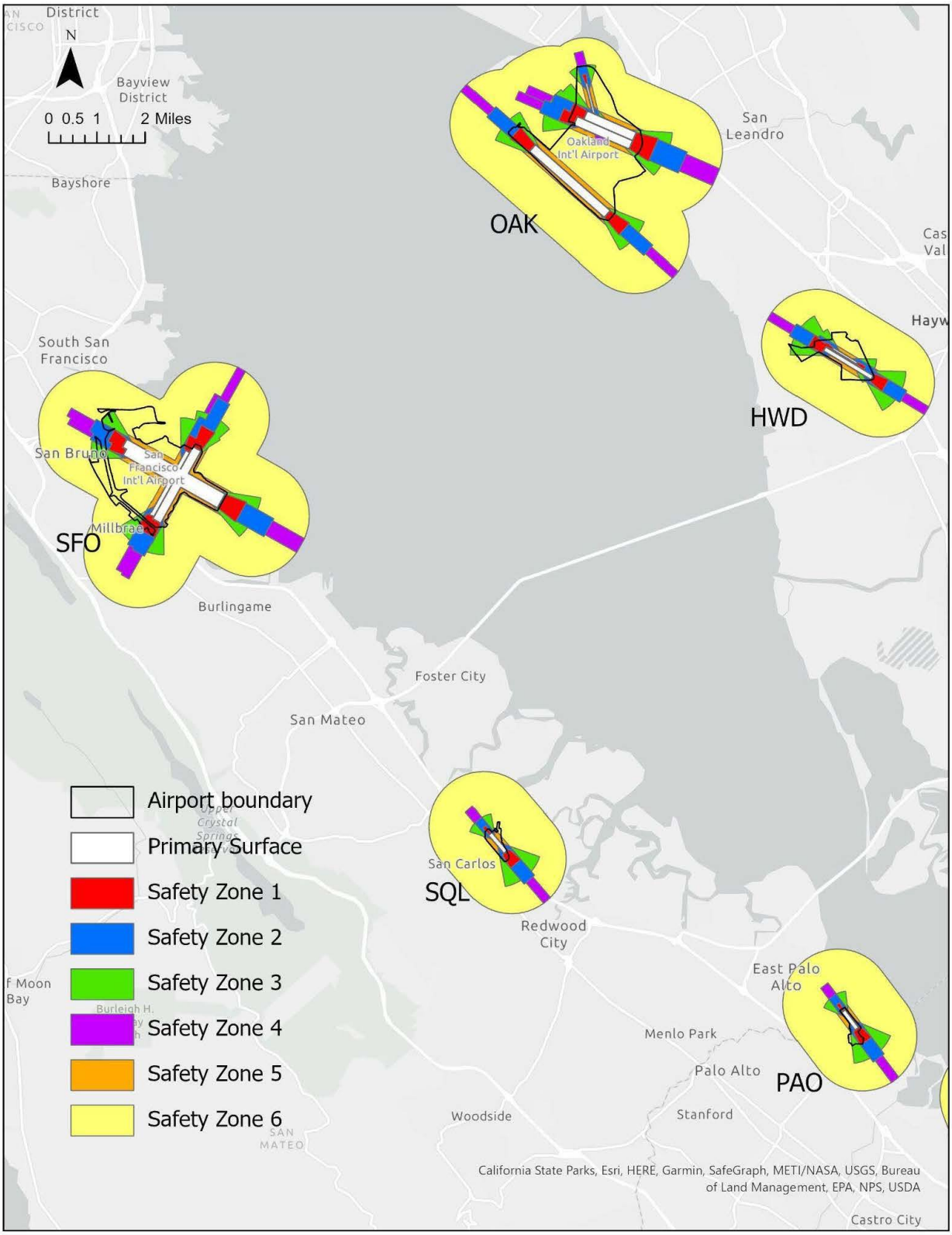


Figure 1. Illustration of generic Safety Zones of the southern San Francisco Bay Area Airports

1.1. Zones Definition

Primary Surface (PS): “The primary surface is longitudinally centereds on a runway and has the same elevation as the elevation of the nearest point on the runway centerline. WHen the runway has a prepared hard surface, the primary surface extends 200 feet beyond each end of that runway. The width of the primary surface ranges from 250-1,000 ft depending on the existing or planned approach type and runway (FAA Part 77). The primary Surface must be clear of all obstructions except those fixed by their function, such as runway edge lights, navigational aids, or airport signage. The majority of primary surface is controlled by runway safety area criteria contained in FAA Advisory Circular 150/5300-13 Airport Design, and almost always lies within airport-controlled property”

Safety Zone 1 (Z1): Runway Protection Zones:
Safety Zone 2 (Z2): Inner Approach/Departure Zone
Safety Zone 3 (Z3): Inner Turning Zone
Safety Zone 4 (Z4): Outer Approach/Departure Zone
Safety Zone 5 (Z5): Runway Sideline
Safety Zone 6 (Z6): Traffic Pattern Zone
Total Safety Zones (Tot SZ): Primary Surface + Zones 1-6

Airport Influence Area (2 miles buffer of airport boundary), hereafter referred as airport vicinity (2mi buff) is considered a default boundary: “an ALUC has not adopted an influence area boundary for a particular airport, then (in accordance with Section 21675.1(b)) the default ‘study area’ includes all land within two miles of the airport boundary[26] (not the runway). Some ALUCs may choose to maintain approximately this boundary when adopting an Airport Land Use Compatibility Plan (ALUCP).” (ALUP Handbook, 2011, p.3-42)

[8] 2. Methods & Data

2.1. Safety Zones and Airport Boundary GIS

The total airport population used in this report is 259 covering civil and general aviation facilities in California with the necessary runway information from the Bureau of Transportation Safety (BTS). The original Caltrans open source GIS dataset provides 221 airport boundaries[27] (parcels), however only 216 airports had the runway data necessary from the BTS[28]. To

[26] Per the Public Utility Commission Section 21675.1(b) this 2 miles vicinity applies to public use airports who fall under ALUC’s jurisdiction.

[27] SCK (Stockton Metropolitan Airport) and SFO (San Francisco International Airport) had conflicting sets of boundaries that needed correction, details available in Appendix B

[28] A total of five airports from Caltrans airport boundary dataset lacked BTS runway data and were therefore excluded from this analysis: KINGDON AIRPARK AIRPORT (O20), LOST HILLS-KERN COUNTY AIRPORT (L84); LODI AIRPARK AIRPORT (L53); RIALTO MUNICIPAL/ART SCHOLL MEMORIAL FIELD AIRPORT (L67); and WOODLAKE AIRPORT (O42).

complete the airport boundary dataset, 43 airport boundaries were digitized manually based on the land use parameters of OpenStreetMap (See section 2.3.1. And Appendix B of Task 4.1.).

To create the runway Safety Zones, different runway open source GIS were examined: Caltrans, FAA Aeronautical Data Delivery Service (ADDS), and the Bureau of Transportation Statistics (BTS) part of the U.S. Department of Transportation (USDOT) National Transportation Atlas Database (NTAD). The BTS runway end table (created on July, 16, 2020) was the most appropriate due to the detailed attribute table with runway end points and the obstruction identification surface codes necessary for determining the runway's primary surfaces according to the Federal Aviation Regulations Part 77 based on runway visibility parameters (i.e. visual runways, non-precision instrument runways, and precision instrument runways) (See section 2.3.2 of Task 4.1.)

After defining the runway's primary surface, the geometries for the 6 generic Safety Zones (civil aviation), were applied based on the BTS runway length, approach visibility minimums, and the type of general aviation or large air carrier runway (see Figures in the 2011 ALUP Handbook p.3-17 to 3-19). Based on the former ALUP handbook, we also considered that where the zones of two or more runways overlap, the lower numbered zone takes over. For runways designed for multiple aircraft operations (i.e., general aviation and large air carriers) the largest critical aircraft zoning is predominant. The intention is to reflect the risk of highest potential consequences and not probability, since the impact of a large commercial airliner would have greater potential damage than that of a single engine aviation aircraft (ALUP, 1983).

The total generic Safety Zones area (including the primary surface and zones 1-6) is 1390.876 sq. mi., out of which 88.59% lies outside the airport boundaries (Tables 1 and 2). The percentage of Safety Zones outside airport boundaries provide the propensity of inappropriate or incompatible land use of each Safety Zone.

Table 1. Characteristics of Primary Runway Zone and Runway Safety Zones (According to FAA Part 77 and ALUP, 2011, pp-4-31, 4-32)

Zone	Jurisdiction	Description	Desirable % of Usable Open Land	% area outside airport boundaries*
Primary Runway Surface (excluded from 2011 Handbook accident analysis)	FAA	A surface longitudinally centered on a runway, dimensioned according to FAA Part 77	100%	1.31%
Runway Safety Zone 1	ALUP/FAA	Runway Protection Zone	Clear of objects in accordance with FAA standards	49.74%

Runway Safety Zone 2	ALUP	Inner Approach/Departure zones	25-30%, especially areas close to the runway extended centerline	79.59%
Runway Safety Zone 3	ALUP	Inner Turning Zone	15-20% minimum	88.39%
Runway Safety Zone 4	ALUP	Outer Approach/Departure Zones	15-20% approximately, with emphasis on areas along the extended runway centerline	97.94%
Runway Safety Zone 5	ALUP	Sideline Zone	25-30% is desirable	26.09%
Runway Safety Zone 6	ALUP	Traffic Pattern Zone	10% approximately every ¼ to ½ mile should be provided	94.64%

*calculated based on the generic Safety Zones dimensions for 259 California airport boundaries modeled in GIS

Table 2. Safety Zones Area (Sq. Miles)

Safety Zone	**Total Area**	**Outside Airp. Boundary**
*PS**	32.54	0.427
Z1	32.116	15.974
Z2	76.193	60.639
Z3	95.403	84.325
Z4	55.108	53.975
Z5	34.742	9.063
Z6	1064.775	1007.748
*Total SZ**	1390.876	1232.151

*PS: Primary Surface; Total SZ: Total Safety Zones (PS + Z1 to Z6)

2.2. NTSB Accident Datasets

To reflect the most accurate spatial data whilst being most efficient with the available data points, two types of spatiotemporal datasets are used in this report (further details on subsection 2.2.3. of Task 4.1.)

(1) Largest number of spatially-relevant accidents (2008-2022):

NTSB Spatial Largest Dataset, total accident events = 1,355
This method benefits the most from spatial accuracy information (GPS measured Latlon data) that became available in 2008 and provides the dataset with the largest number of spatially-relevant events. The tradeoff is the potential APR-colocation error.

(2) Reproduction of 2011 handbook method (2008-2022):

NTSB 2011 Method Dataset, total accident events = 495 (298 when removing those outside 5 mi airport buffer)
This provides the closest reproduction of the 2011 handbook methodology. It removes all accidents within the Primary Surface, and all accidents with the APR-Latlon co-location error in accordance with the 2011 Handbook method. The advantage is that this dataset can be used for comparison purposes, however it does not optimize the use of richer geospatial information available since 2008.

2.3. Wildlife Strike Data

This analysis focuses on wildlife strikes attributed to California state in the original FAA wildlife strike dataset downloaded on April 17th, 2023. The Lat lon information of the incidents refers mostly to airport centroids and therefore could not be used entirely to locate the occurrence of the all wildlife strikes. The geographical information aiding on the location attribution of each incident includes a combination of airport distance (assuming end of runway as the starting point), phase of flight, height, and runway location. The combination of this geographical data with basic assumptions on aircraft landing and departure paths (i.e five miles straight line for arrivals) allowed for the approximate birds strike location. It is important to highlight that the precision of strike distance from airport and height is low (rounded integers).
Although the total number of reported wildlife strikes in the study period was of 20,245, the number of strikes assessed changes in the statistical analysis based on the variable of interest because not all reported incidents have have valid entries for all variables (i.e. phase of flight, height, wildlife species, etc). A total of 19,873 strikes provide Latlon data for the GIS analysis. For more information see section 2 from Task 4.1.2.

2.4. Land Use and Land Cover Data

The 2011 ALUP Handbook associated development characteristics to certain densities and intensities (p.4-18):

- Rural: Areas where the predominant land uses are natural or agricultural; buildings are widely scattered.
- Suburban: Areas characterized by low-rise (1-2 story) development and surface parking lots.
- Urban: Areas characterized by mid-rise (up to 5 stories) development; generally surface vehicle parking, but potentially some parking structures.
- Dense Urban: City core areas characterized by extensive mid- and high-rise buildings, often with 100 percent lot coverage and limited surface parking.

Land use and land cover (LULC) data is employed as a proxy to development characteristics although they are not directly transferable. LULC open-source datasets used in this study are produced by the U.S. federal agency consortium Multi-Resolution Land Characteristics (MRLC). The latest dataset was published in July 2023, providing land cover for 2021; and land use change from 2001-2021, at the national level, at 30 meter spatial resolution. The 2021 LULC has a 16 class legend based on a modified Anderson Level II classification system. From the 16 classes, four classes represent “developed” land use (or urbanized): open space; low intensity, medium intensity and high intensity development (Figures 2 and 3). Within the “developed” LULC class there are growing levels of potential impact severity starting at open space (OS); low intensity, medium intensity and high intensity (Table 3). Table 3 also presents a proxy between the 2011 ALUP Handbook development characteristics itemized above (P.4-18) and the LULC developed classes (detailed in Figure 3). “Developed” and “Urban” classes are synonyms in the National Land Cover Database (MRLC, 2023); these classes refer to “Urban or Built-Up Land” (from Anderson, 1976), representing “areas of intensive use with much of the land covered by structures”. Included in this category are residential areas, strip developments along highways, transportation, power, and communication infrastructure; industrial and commercial complexes and other commercial and service areas. For more information please refer to the MRLC NLCD 2021 Land Cover (CONUS) repository; and the MRLC NLCD Land Cover Change Index (2001-2021) (CONUS) repository.

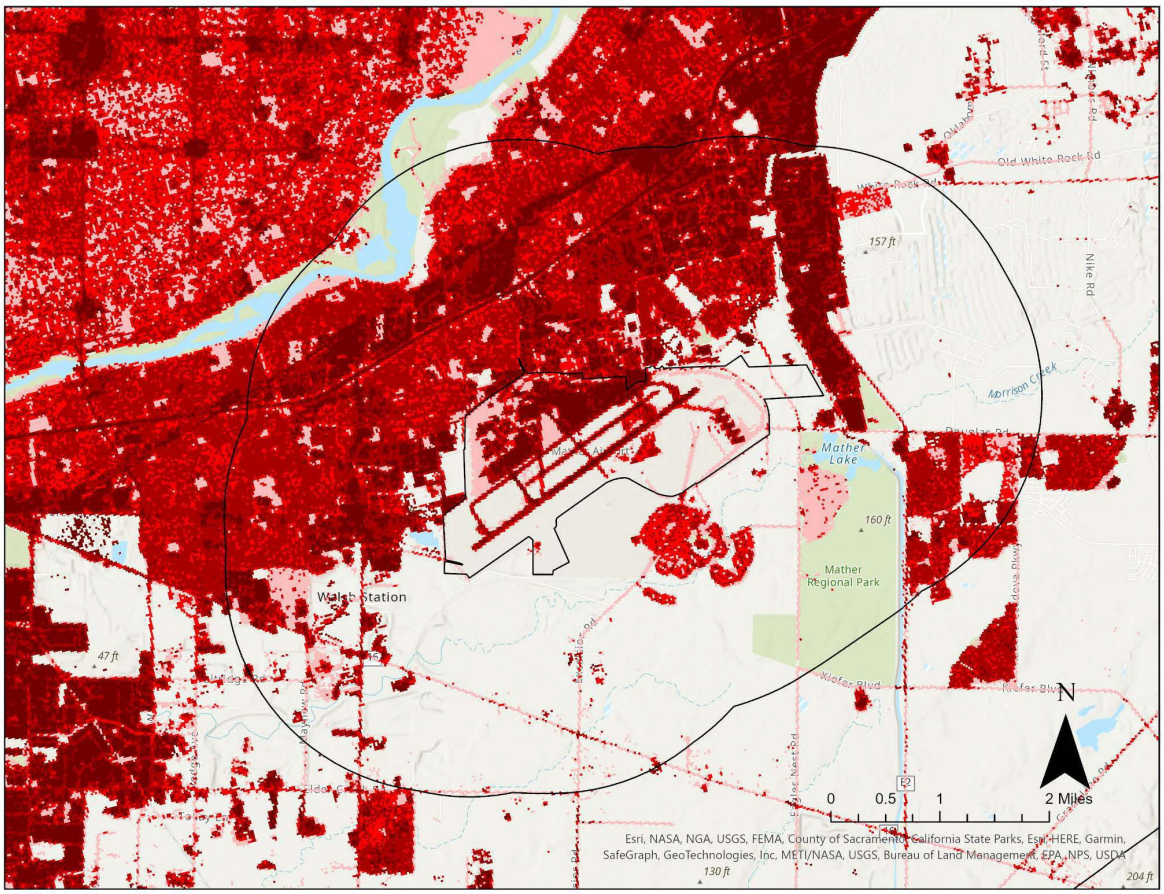


Figure 2. Developed Land Use and Land Cover in 2021, Sacramento Mather Airport (MHR) example with 2 mile buffer around the airport boundary

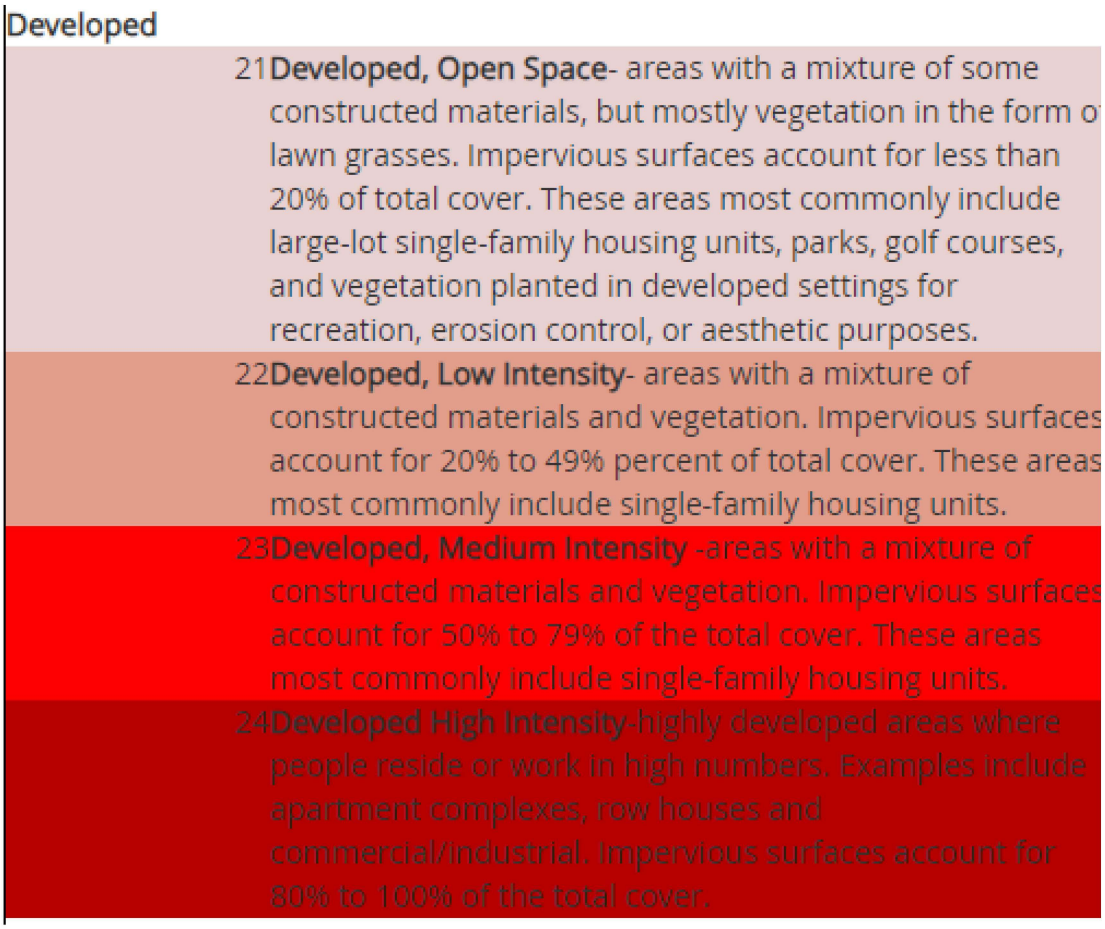


Figure 3. Legend for Developed (Urban) LULC Classification. (Source: MLRC, NLCD 2021, Legend)

Table 3. Potential Impact Severity Based on Developed LULC

Developed LULC Class* (USGS 2021)	**Threshold of impervious surface**	**Typical Development Type**	**Potential Impact Severity**	**Proxy with 2011 ALUP Handbook Development Characteristics**
Developed Open Space	< 20% of impervious surface	Large-lot-single-family housing units, developed setting for recreation (eg. parks, cemeteries)	Low	Rural/Suburban
Developed Low Intensity	20- 49% of impervious surface	Single-family housing units	Medium	Suburban/ Urban
Developed Medium	50- 79% of	Single-family	High	Suburban/ Urban/

Intensity	impervious surface	housing units		Dense Urban
Developed High Intensity	80-100% of impervious surface	Apartment complexes, row houses, and commercial/industrial uses.	Very High	Dense Urban

Class modified by the USGS from Anderson Land Cover Classification (1976)

2.5. Risk Concept and Metrics

The Handbook's conceptual approach to risk, states " Three components of physical risks—spatial distribution, potential consequences, and frequency—provide the conceptual basis for setting safety compatibility policies. Each of these components needs to be considered either in the delineation of safety compatibility zones or in the definition of the criteria applicable within the zones." (ALUP Handbook, 2011 pp. 4-16). However, the risk level for each Safety Zone is based on the percentage of accidents registered between 2000-2009 (ALUP Handbook pp. 4-20 to 4-25). This report proposes a risk metric that is closer to the ALUP Handbook conceptual approach of the three components (accidents spatial distribution and frequency, and the potential consequences), where the accident density provides a metric for hazard and the potential consequences using the LULC data provides a metric for exposure (or potential severity of consequences). Risk is therefore calculated as a function of hazard and exposure using a risk matrix to qualitatively assess risk levels (Figure 4). The risk matrix is based on the FAA Order 8040.4B on Safety Risk Management Policy from (05/02/2017), however the hazard metric is here adapted to focus on the spatial patterns of accidents, instead of the temporal patterns (likelihood) for the purposes of the ALUP Handbook Safety Zones update. The data used for the risk analysis is available as a supplementary material "Task 8. Safety Zones Risk Analysis.xls" and in Appendix A.

Risk Matrix		Exposure Levels			
		Low	Med	High	Very High
Hazard Levels	Very High	Med	High	Very High	Very High
	High	Med	Med	High	Very high
	Med	Low	Med	High	High
	Low	Low	Low	Med	High

Figure 4. Accident Risk Matrix

A simple and a weighted accident risk formulas are proposed to better explore the qualities of the NTSB datasets: (a) simple accident risk; and (b) weighted accident risk. The simple Accident Risk analysis was applied to both the NTSB 2011 method dataset (n= 495) and the

NTSB Largest dataset (n= 1,355), while the weighted accident risk was applied only to the NTSB Largest dataset.

(a) Simple Accident Risk Formula

$$\boldsymbol{Accident\ Risk}_{\boldsymbol{Simple}} = \boldsymbol{Hazard\ Score}_{\boldsymbol{Simple}}\ \boldsymbol{x\ Exposure}_{\boldsymbol{weighted}}$$

Where
$Hazard\ Score_{\boldsymbol{Simple}}\ (Hs)$ is calculated as the spatial density of accidents using rescaling normalization ranging from [-1 to 1] (min-max normalization):

$$Hs = Accident\ n/\ Safety\ Zone\ area\ (sq\ mi)$$
$$\text{Normalized } Hs = Hs - min(Hs)/\ max\ (Hs) - min(Hs)$$

$\boldsymbol{Exposure}_{\boldsymbol{Weighted}}$ $(\boldsymbol{EpW})$ is calculated as percentage of developed (urban) area in each Safety Zone weighted based on the development intensity:

$$Ep = Developed\ area/\ total\ Safety\ Zone\ area\ x\ 100$$
$$EpW = EpOS + (EpLowInt * 2) + (EpMedInt * 3) = (EpHighInt * 4)$$

Where $EpOS$ is the exposure % of LULC for Open Space Development; $EpLowInt$ is for Low Intensity Development; $EpMedInt$ is for Medium Intensity Development and, $EpHighIntx4$ is for High Intensity Development.

(b) Weighted Risk Formula

$$\boldsymbol{Accident\ Risk}_{\boldsymbol{Weighted}} = \boldsymbol{Hazard\ Score}_{\boldsymbol{Weighted}}\ \boldsymbol{x\ Exposure}_{\boldsymbol{Weighted}}$$

Where
$Hazard\ Score_{Weighted}\ (HsW)$ is calculated as the spatial density of accidents weighted based on the highest impact of the event, and normalized using min-max scaling ranging from [-1 to 1]:

$$Hs = Accident\ n/\ Safety\ Zone\ area\ (sq\ mi)$$
$$HsW = HsW\ N_{Inj} + (HsW\ M_{inj} * 2) + (HsW\ S_{inj} * 3) + (HsW\ Finj * 4)$$
$$\text{Normalized } HsW = HsW - min(HsW)/\ max\ (HsW) - min(HsW)$$

Where HsW is the weighted accident density based on the highest level of injury occured in the accident; $HsW\ N_{Inj}$ is for None; $HsW\ M_{inj}$ is for Minor injury; $HsW\ S_{inj}$ is for Serious injury, and $HsW\ Finj * 4$ is for Fatal injury

$\boldsymbol{Exposure}_{\boldsymbol{Weighted}}$ $(\boldsymbol{EpW})$ is calculated as percentage of developed (urban) area in each Safety Zone weighted based on the development intensity:

$$Ep = Developed\ area/\ total\ Safety\ Zone\ area\ x\ 100$$
$$EpW = EpOS + (EpLowInt\ x\ 2) + (EpMedInt\ x\ 3) = (EpHighIntx4)$$

Where $EpOS$ is the exposure percentage of LULC for Open Space Development; $EpLowInt$ is for Low Intensity Development; $EpMedInt$ is for Medium Intensity Development and, $EpHighIntx4$ is for High Intensity Development.

Hs, HsW *and* EpW were then classified into Low, Medium, High, and Very High levels by identifying their scores and percentages quartiles (Table 4 and 5). The quartiles are calculated based on the Hs, HsW *and* EpW result ranges of Safety Zones 1 to 6. The results for the Primary Runway Surface accidents were omitted from the risk analysis to avoid skewing the hazard score ranges of the Safety Zones to relative lower levels when compared to the accident density near the runways. This omission also helps contrast the risk levels amongst the Safety Zones, where Airport Land Use Commission (ALUC) has jurisdiction.

Table 4. Hazard Levels Based on the Score Results (Quartiles)

Percentiles	Hazard Levels	Hs (NTSB 2011 method)	Hs (NTSB Largest)	HsW (NTSB Largest)
0-25th	Low	-1 to -0.027593	-1 to -0.039443	-1 to -0.122476
26-50th	Med	-0.027592 to 0.078481	-0.039442 to 0.0454346	-0.122475 to 0.064854
51-75th	High	0.078482 to 0.463350	0.0454347 to 0.251695	0.064855 to 0.210632
76-100th	Very High	0.463351 to 1	0.251696 to 1	0.210633 to 1

Table 5. Exposure Levels Based on the Percentage Results (Quartiles)

Exposure Classes	*Score*
Low	100 to 101.062818
Med	101.062819 to 107.259964
High	107.259965 to 109.157226
Very High	109.157227 to 141.134396

[8] 3. Results

3.1. Safety Zones Accident Density and Percentage Analysis: NTSB Accidents and Wildlife Strikes

Subsection 3.1.1. presents NTSB accidents and wildlife strikes spatial distribution (density) and percentages relative to all the occurrences within Safety Zones; relative to all the occurrences within the 2 mi buffer of airport boundaries, and relative to all the occurrences in California (Tables 6- 9). The density is calculated based on the accident count per zone divided by the area (in sq mi) of each zone. Figure 5 highlights the higher percentage of accidents through Zones 1 o to 6 relative to accidents within the 2 mile buffer of airport boundaries for the NTSB database that reproduces the 2011 ALUP method. Zone 5 and 6, have 22.04% and 6 31.43% of all accidents within the 2 mile buffer of airport boundaries.This higher percentage is related to the exclusion of primary surface accidents based on the 2011 ALUP Handbook method when compared to the NTSB Spatial Largest dataset. However, Figure 6 shows 2.6 accidents per sq. mi for zone 5, which is slightly discrepant accident density compared to other zones, highlighting the need for revision of the dimensions of Safety Zone 5. Similar to results from previous ALUP Handbooks, the closer to the runway centerline, the higher the concentration of accidents and wildlife strikes. Wildlife strikes are outstandingly high in the primary surface, reaching a density of 345.1 strikes per sq. mi., with another spike in zone 5 (23 strikes per sq. mi) and zone 6 (7.3 strikes per sq. mi). When looking at the broader spatial distribution of accidents, a majority occurs within the Safety Zones with 60.66% and 65.29% within 2 mile buffer of airport boundaries (for NTSB Spatial Largest Dataset).

Subsection 3.1.2 and 3.1.3. focuses on NTSB accidents and wildlife strikes using impact data (Tables 10-17). Figure 7 shows that zone 5 has the highest spatial density of accidents resulting in any type of injury, with 0.896 occurrences per sq. mi. Figure 8 shows that 1.353 wildlife strike occurrences per sq. mi in zone 5 resulted in aircraft damage, followed by 0.459 occurrences per sq. mi for zone 6. There remains a high discrepancy between the accidents and strikes densities and percentages for zones 1 to 6 when compared to the very high levels measured in the primary surface.

Subsection 3.1.4. provides a detailed analysis of the accidents and wildlife strikes in Safety Zones located outside airport boundaries. For the NTSB 2011 Method dataset 57.62% of accidents in Safety Zones are located in areas outside airport boundaries (Table18 and Figure 9 and 10). Zones 1-3 and 6 have nearly 50% or more of accidents located outside airport boundaries, highlighting Zone 6 with 67.15 to 81.82% and Zone 3 with 62.50% to 68.75%. However, Zone 5 has the highest accident density outside airport boundaries (0.509 - 0.795 accidents per sq mi) followed by Zone 1 (0.501 to 0.564). For wildlife strikes inside Safety Zones, 78.68% are located in areas outside airport boundaries (Table 19), highlighting the high percentage of strikes outside airport boundaries for Zone 5 (most adjacent to the PS).

The results dat used to develop the tables and figures of this section are available in supplementary materials “Task8.NTSB_WSdesnity_perct.xls”

3.1.1. Accident Density and Percentage: NTSB & Wildlife Strikes

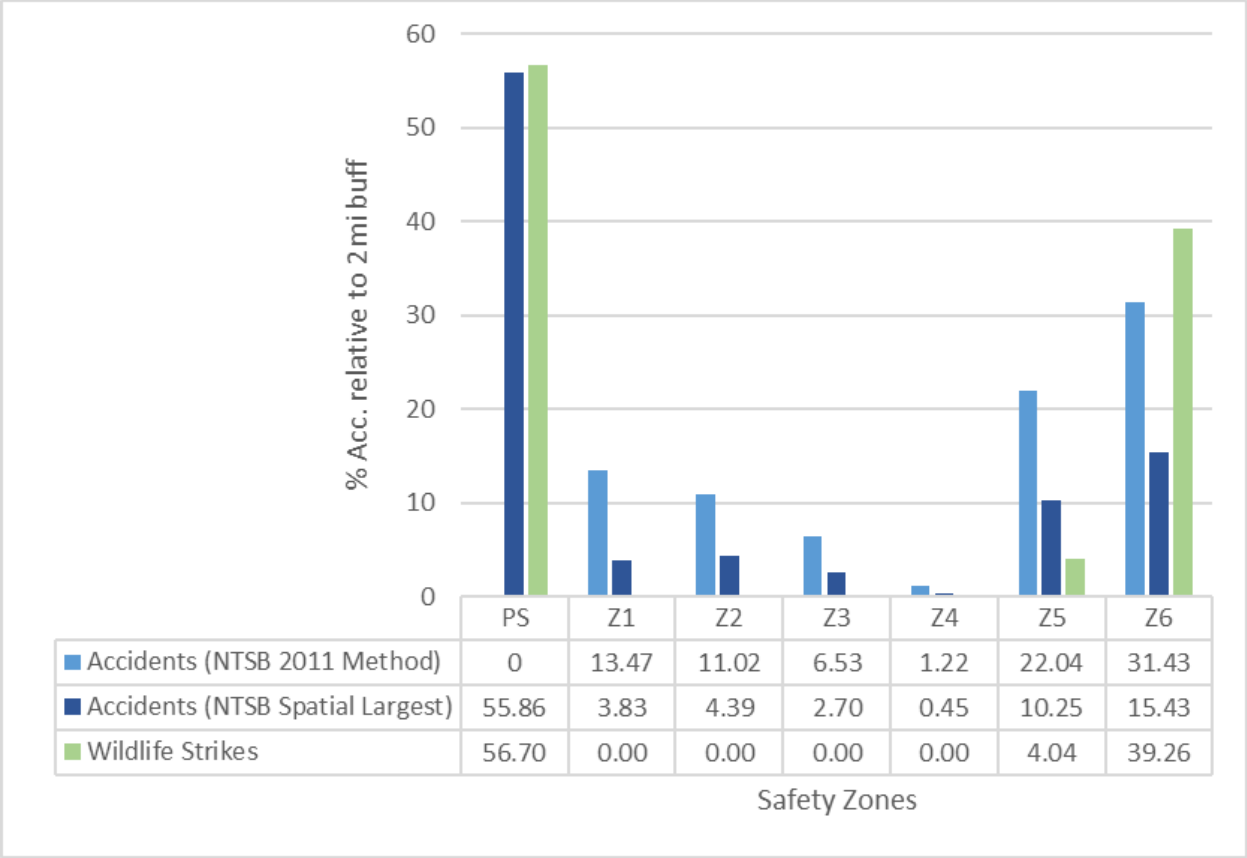


Figure 5. Percentage of Accidents and Wildlife Strikes relative to the Total Accidents and Strikes within 2 mi buffer of Airports Boundaries

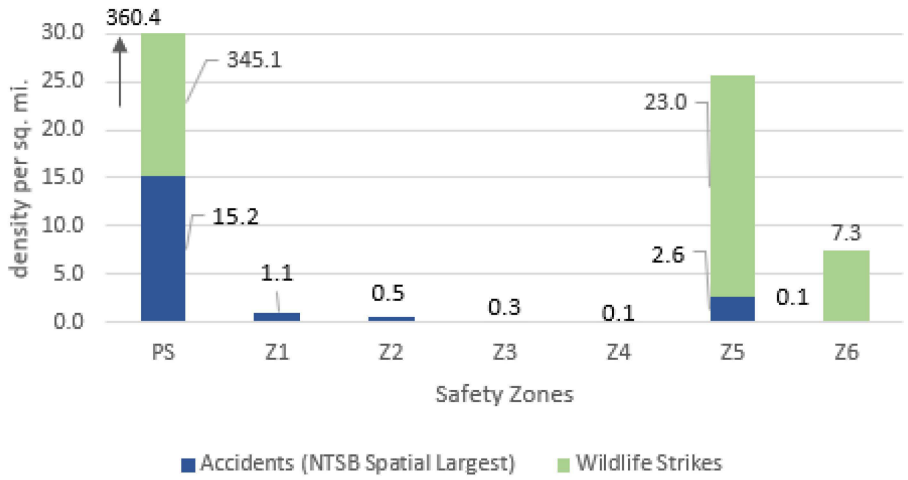


Figure 6. Safety Zone Density of Accidents (NTSB Spatial Largest dataset, 2008-2022) and Wildlife Strikes (1990- April 2023).

Table 6. NTSB 2011 Method Dataset (2008-2022): Accident Density and Percentage

Zone	**Acc. Count**	**Acc. Density per sq mi** (=Count/ Area)	**% Acc. relative to Tot. SZ**	**% Acc. relative to total within 2mi of airp. BND**	**% Acc. relative to total in CA**
PS	N/A	N/A	N/A	N/A	N/A
Z1	33	1.028	15.71	13.47	6.67
Z2	27	0.354	12.86	11.02	5.45
Z3	16	0.168	7.62	6.53	3.23
Z4	3	0.054	1.43	1.22	0.61
Z5	54	1.554	25.71	22.04	10.91
Z6	77	0.072	36.67	31.43	15.56
Tot SZ	210	0.151	100.00	85.71	42.42

2mi buff	245	0.048	N/A	100.00	49.49
CA	495	0.003	N/A	N/A	100.00

*Acc: Accident; PS: Primary Surface; Total SZ: Total Safety Zones (PS + Z1 to Z6); 2mi buff: 2 mi buffer of airport boundary; CA: California State; N/A: Not Applicable

Table 7. NTSB Largest Spatial Dataset (2008-2022): Accident Density and Percentage

Zone	**Acc. Count**	**Acc. Density per sq mi** (=Count/ Area)	**% Acc. relative to Tot. SZ**	**% Acc. relative to total within 2mi of airp. BND**	**% Acc. relative to total in CA**
PS	496	15.243	60.12	55.86	36.47
Z1	34	1.059	4.12	3.83	2.50
Z2	39	0.512	4.73	4.39	2.87
Z3	24	0.252	2.91	2.70	1.76
Z4	4	0.073	0.48	0.45	0.29
Z5	91	2.619	11.03	10.25	6.69
Z6	137	0.129	16.61	15.43	10.07
Tot SZ	825	0.593	100.00	92.91	60.66
2mi buff	888	0.173	N/A	100.00	65.29
CA	1360	0.009	N/A	N/A	100.00

* Acc: Accident; PS: Primary Surface; Total SZ: Total Safety Zones (PS + Z1 to Z6); 2mi buff: 2 mi buffer of airport boundary; CA: California State; N/A: Not Applicable

Table 8. Wildlife Strikes (1990- April 2023): Accident Density and Percentage

Zone	**WS Count**	**WS Density per sq mi** (=Count/ Area)	**% WS relative to Tot. SZ**	**% WS relative to total within 2mi of airp. BND**	**% WS relative to total in CA**
PS	11232	345.180	56.70	56.70	56.52
Z1	0	0.000	0.00	0.00	0.00
Z2	0	0.000	0.00	0.00	0.00
Z3	0	0.000	0.00	0.00	0.00
Z4	0	0.000	0.00	0.00	0.00
Z5	800	23.027	4.04	4.04	4.03
Z6	7777	7.304	39.26	39.26	39.13
Tot SZ	19809	14.242	100.00	100.00	99.68
2mi buff	19809	3.870	N/A	100.00	99.68
CA	19873	0.126	N/A	N/A	100.00

* WS: Wildlife Strikes; PS: Primary Surface; Total SZ: Total Safety Zones (PS + Z1 to Z6); 2mi buff: 2 mi buffer of airport boundary; CA: California State; N/A: Not Applicable

Table 9. Sum of NTSB Accidents (Largest Spatial Dataset: 2008-2022) and Wildlife Strikes (1990- April 2023): Accident Density and Percentage

Zone	**Acc + WS Count**	**Acc + WS Density per sq mi** (=Count/ Area)	**% Acc + WS. relative to total within Tot. SZ**	**% Acc + WS relative to total within 2mi of airp. BND**	**% Acc + WS relative to total in CA**
PS	11728	360.423	56.84	56.67	55.23
Z1	34	1.059	0.16	0.16	0.16

Z2	39	0.512	0.19	0.19	0.18
Z3	24	0.252	0.12	0.12	0.11
Z4	4	0.073	0.02	0.02	0.02
Z5	891	25.646	4.32	4.30	4.20
Z6	7914	7.433	38.35	38.24	37.27
Tot SZ	20634	14.835	100.00	99.70	97.18
2mi buff	20697	4.043		100.00	97.48
CA	21228	0.134			100.00

* Acc: Accidents; WS: Wildlife Strikes; PS: Primary Surface; Total SZ: Total Safety Zones (PS + Z1 to Z6); 2mi buff: 2 mi buffer of airport boundary; CA: California State; N/A: Not Applicable

3.1.2. NTSB Accident Density and Percentage Based on Impact Level (Highest Level of Injury of Accident)

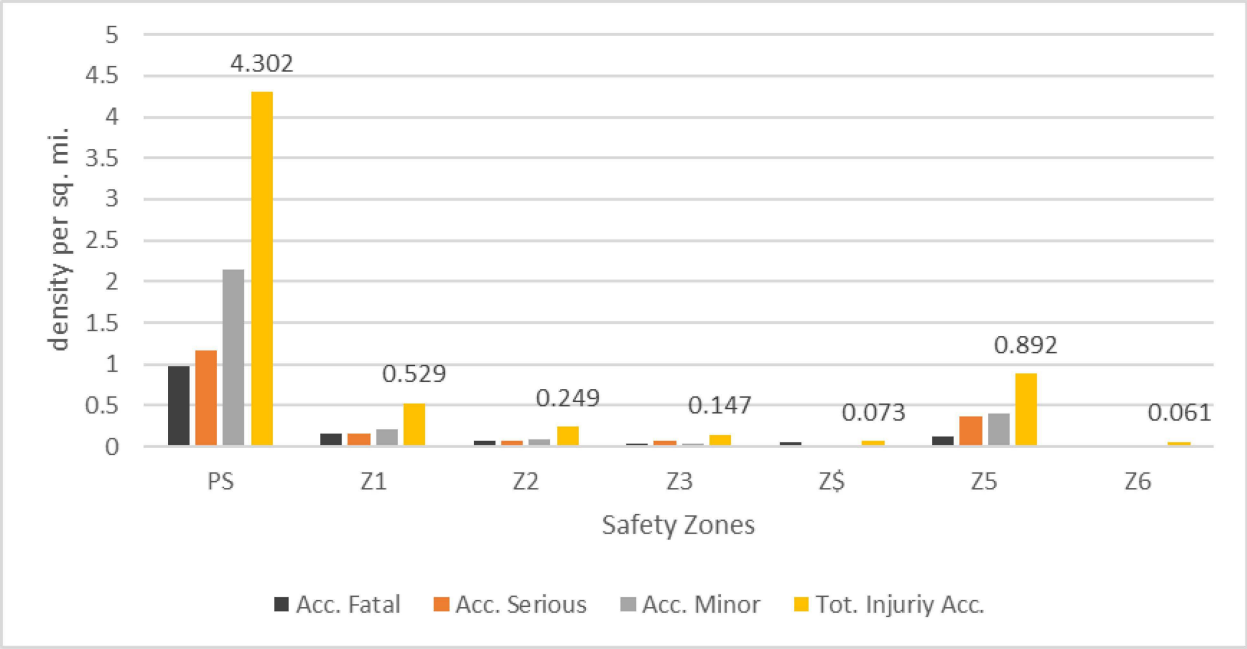


Figure 7. Spatial Density of Accidents Resulting in Injuries (NTSB Spatial Largest 2008-2022 dataset)

Table 10. Fatal Accidents Density and Percentage (NTSB Largest Spatial Dataset, 2008-2022)

Zone	**Fatal Acc. Count**	**Fatal Acc. Density per sq mi** (=Count/ Area)	**% Fatal Acc. relative to total within Tot. SZ**	**%Fatal Acc. relative to total within 2mi of airp. BND**	**% Fatal Acc relative to total in CA**
PS	32	0.983	39.02	34.04	17.02
Z1	5	0.156	6.10	5.32	2.66
Z2	6	0.079	7.32	6.38	3.19
Z3	4	0.042	4.88	4.26	2.13
Z4	3	0.054	3.66	3.19	1.60
Z5	4	0.115	4.88	4.26	2.13
Z6	28	0.026	34.15	29.79	14.89

Tot SZ	82	0.059	100.00	87.23	43.62
2mi buff	94	0.018	N/A	100.00	50.00
CA	188	0.001	N/A	N/A	100.00

*F. Acc.: Fatal Accident; PS: Primary Surface; Total SZ: Total Safety Zones (PS + Z1 to Z6); 2mi buff: 2 mi buffer of airport boundary; CA: California State; N/A: Not Applicable

Table 11. Serious Injury Accidents Density and Percentage (NTSB Largest Spatial Dataset, 2008-2022)

Zone	**Serious Acc. Count**	**Serious Acc. Density per sq mi** (=Count/ Area)	**% Serious Acc. relative to total within Tot. SZ**	**%Serious Acc. relative to total within 2mi of airp. BND**	**% Serious Acc. relative to total in CA**
PS	38	1.168	42.70	37.25	23.03
Z1	5	0.156	5.62	4.90	3.03
Z2	6	0.079	6.74	5.88	3.64
Z3	7	0.073	7.87	6.86	4.24
Z4	1	0.018	1.12	0.98	0.61
Z5	13	0.374	14.61	12.75	7.88
Z6	19	0.018	21.35	18.63	11.52
Tot SZ	89	0.064	100.00	87.25	53.94
2mi buff	102	0.020	N/A	100.00	61.82
CA	165	0.001	N/A	N/A	100.00

*S. Acc.: Serious Injury Accident; PS: Primary Surface; Total SZ: Total Safety Zones (PS + Z1 to Z6); 2mi buff: 2 mi buffer of airport boundary; CA: California State; N/A: Not Applicable

Table 12. Minor Injury Accidents Density and Percentage (NTSB Largest Spatial Dataset, 2008-2022)

Zone	**Minor Acc. Count**	**Minor Acc. Density per sq mi** (=Count/ Area)	**% Minor Acc. relative to total within Tot. SZ**	**%Minor Acc. relative to total within 2mi of airp. BND**	**% Minor Acc. relative to total in CA**
PS	70	2.151	58.82	52.63	29.79
Z1	7	0.218	5.88	5.26	2.98
Z2	7	0.092	5.88	5.26	2.98
Z3	3	0.031	2.52	2.26	1.28
Z4	0	0.000	0.00	0.00	0.00
Z5	14	0.403	11.76	10.53	5.96
Z6	18	0.017	15.13	13.53	7.66
Tot SZ	119	0.086	100.00	89.47	50.64
2mi buff	133	0.026	N/A	100.00	56.60
CA	235	0.001	N/A	N/A	100.00

*M. Acc.: Minor Injury Accident; PS: Primary Surface; Total SZ: Total Safety Zones (PS + Z1 to Z6); 2mi buff: 2 mi buffer of airport boundary; CA: California State; N/A: Not Applicable

Table 13. All Accidents Resulting in Any Injury Level: Density and Percentage (NTSB Largest Spatial Dataset, 2008-2022)

Zone	**All Injury Acc. Count**	**All Injury Acc. Density per sq mi**	**% All Injury Acc. relative to total total**	**% All Injury Acc. relative to total**	**% All Inj. Acc. relative**

		(=Count/ Area)	**within Tot. SZ**	**within 2mi of airp. BND**	**to total in CA**
PS	140	4.302	48.28	42.55	23.81
Z1	17	0.529	5.86	5.17	2.89
Z2	19	0.249	6.55	5.78	3.23
Z3	14	0.147	4.83	4.26	2.38
Z4	4	0.073	1.38	1.22	0.68
Z5	31	0.892	10.69	9.42	5.27
Z6	65	0.061	22.41	19.76	11.05
Tot SZ	290	0.209	100.00	88.15	49.32
2mi buff	329	0.064	N/A	100.00	55.95
CA	588	0.004	N/A	N/A	100.00

*All Inj Acc.: All accidents resulting in injuries (Fatal + Serious + Minor); PS: Primary Surface; Total SZ: Total Safety Zones (PS + Z1 to Z6); 2mi buff: 2 mi buffer of airport boundary; CA: California State; N/A: Not Applicable

3.1.3. Wildlife Strikes Density and Percentage Based on Impact Level (Aircraft Damage Level)

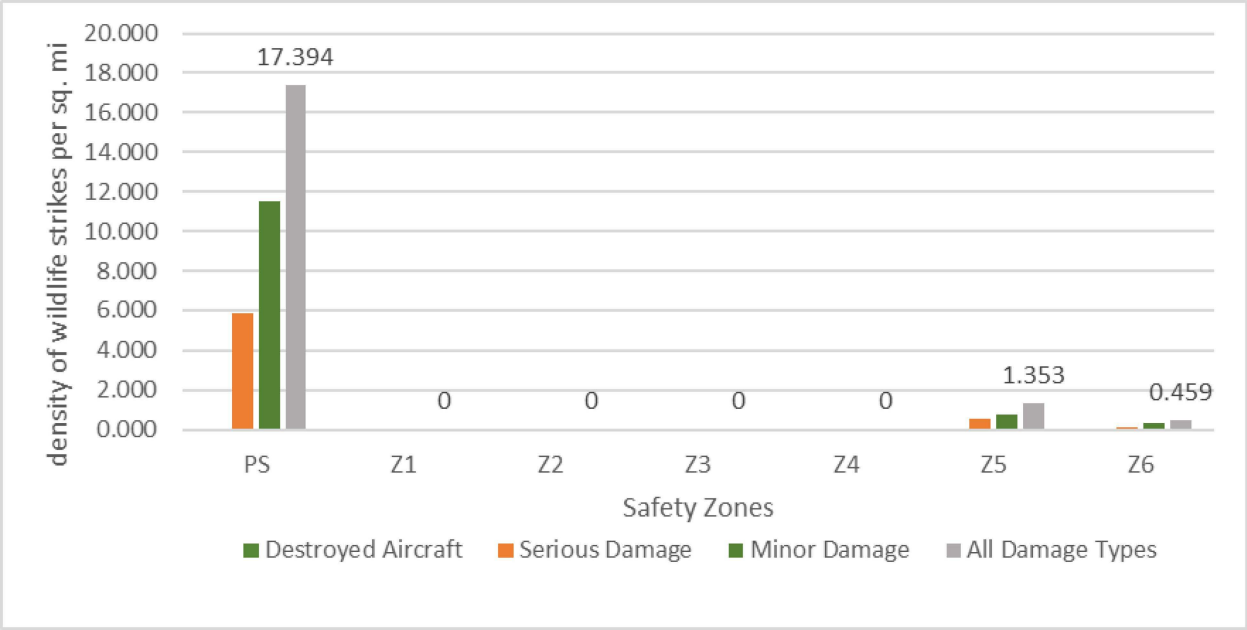


Figure 8. Density of Wildlife Strikes Resulting in Damage in Safety Zones (1990- April 2023)

Table 14. Wildlife Strikes that Resulted in Aircraft Destruction (1990- April 2023)

Zone	**WS Destroyed Damage Count**	**WS D. Dam. Density per sq mi** (=Count/ Area)	**% WS D. Dam. relative to total within Tot. SZ**	**% WS D. Dam. relative to total within 2mi of airp. BND**	**% Total Inj. Acc. relative to total in CA**
PS	2	0.061	66.67	66.67	66.67
Z1	0	0.000	0.00	0.00	0.00
Z2	0	0.000	0.00	0.00	0.00
Z3	0	0.000	0.00	0.00	0.00
Z4	0	0.000	0.00	0.00	0.00
Z5	1	0.029	33.33	33.33	33.33
Z6	0	0.000	0.00	0.00	0.00
Tot SZ	3	0.002	100.00	100.00	100.00

2mi buff	3	0.001	N/A	100.00	100.00
CA	3	0.000	N/A	N/A	100.00

*WS D. Dam: Wildlife Strikes resulting in Destroyed damage level; PS: Primary Surface; Total SZ: Total Safety Zones (PS + Z1 to Z6); 2mi buff: 2 mi buffer of airport boundary; CA: California State; N/A: Not Applicable

Table 15. Wildlife Strikes that Resulted in Serious Damage to Aircraft (1990- April 2023)

Zone	**WS Serious Damage Count**	**WS S. Dam. Density per sq mi** (=Count/ Area)	**% WS S. Dam. relative to total within Tot. SZ**	**% WS S. Dam. relative to total within 2mi of airp. BND**	**% WS S. Dam. relative to total in CA**
PS	190	5.839	51.35	51.35	51.21
Z1	0	0.000	0.00	0.00	0.00
Z2	0	0.000	0.00	0.00	0.00
Z3	0	0.000	0.00	0.00	0.00
Z4	0	0.000	0.00	0.00	0.00
Z5	19	0.547	5.14	5.14	5.12
Z6	161	0.151	43.51	43.51	43.40
Tot SZ	370	0.266	100.00	100.00	99.73
2mi buff	370	0.072	N/A	100.00	99.73
CA	371	0.002	N/A	N/A	100.00

*WS S. Dam: Wildlife Strikes resulting in Serious damage level; PS: Primary Surface; Total SZ: Total Safety Zones (PS + Z1 to Z6); 2mi buff: 2 mi buffer of airport boundary; CA: California State; N/A: Not Applicable

Table 16. Wildlife Strikes that Resulted in Minor Damage to Aircraft (1990- April 2023)

Zone	**WS Minor Damage Count**	**WS M. Dam. Density per sq mi** (=Count/ Area)	**% WS M. Dam. relative to total within Tot. SZ**	**% WS M. Dam. relative to total within 2mi of airp. BND**	**% WS M. Dam. relative to total in CA**
PS	190	5.839	51.35	51.35	51.21
Z1	0	0.000	0.00	0.00	0.00
Z2	0	0.000	0.00	0.00	0.00
Z3	0	0.000	0.00	0.00	0.00
Z4	0	0.000	0.00	0.00	0.00
Z5	19	0.547	5.14	5.14	5.12
Z6	161	0.151	43.51	43.51	43.40
Tot SZ	370	0.266	100.00	100.00	99.73
2mi buff	370	0.072	N/A	100.00	99.73
CA	371	0.002	N/A	N/A	100.00

*WS M. Dam: Wildlife Strikes resulting in Minor damage level; PS: Primary Surface; Total SZ: Total Safety Zones (PS + Z1 to Z6); 2mi buff: 2 mi buffer of airport boundary; CA: California State; N/A: Not Applicable

Table 17. Wildlife Strikes that Resulted in Any Damage to Aircraft (1990- April 2023)

Zone	**WS All Damage Count**	**WS All Dam. Density per sq mi** (=Count/ Area)	**% WS All Dam. relative to total within Tot. SZ**	**% WS All Dam. relative to total within 2mi of airp. BND**	**% WS All Dam. relative to total in CA**
PS	566	17.394	51.36	51.36	51.18
Z1	0	0.000	0.00	0.00	0.00

Z2	0	0.000	0.00	0.00	0.00
Z3	0	0.000	0.00	0.00	0.00
Z4	0	0.000	0.00	0.00	0.00
Z5	47	1.353	4.26	4.26	4.25
Z6	489	0.459	44.37	44.37	44.21
Tot SZ	1102	0.792	100.00	100.00	99.64
2mi buff	1102	0.215	N/A	100.00	99.64
CA	1106	0.007	N/A	N/A	100.00

*WS All Dam.: Wildlife Strikes Resulting Any damage level (Destroyed + Serious + Minor); PS: Primary Surface; Total SZ: Total Safety Zones (PS + Z1 to Z6); 2mi buff: 2 mi buffer of airport boundary; CA: California State; N/A: Not Applicable.

3.1.4. Accidents and Wildlife Strikes in Safety Zones Inside and Outside Airport Boundaries

Table 18. Count of Accidents and Wildlife Strikes of Safety Zones Areas Inside and Outside Airport Boundaries

	NTSB Largest		**NTSB 2011 Method**		**Wildlife Strikes**	
Safety Zone	**IN**	**OUT**	**IN**	**OUT**	**IN**	**OUT**
PS	493	3	N/A	N/A	4229	7003
Z1	16	18	17	16	0	0
Z2	16	23	12	15	0	0
Z3	9	15	5	11	0	0

Z4	0	4	0	3	0	0
Z5	66	25	41	13	7	793
Z6	45	92	14	63	0	7777
SZ Total	645	180	89	121	4236	15573

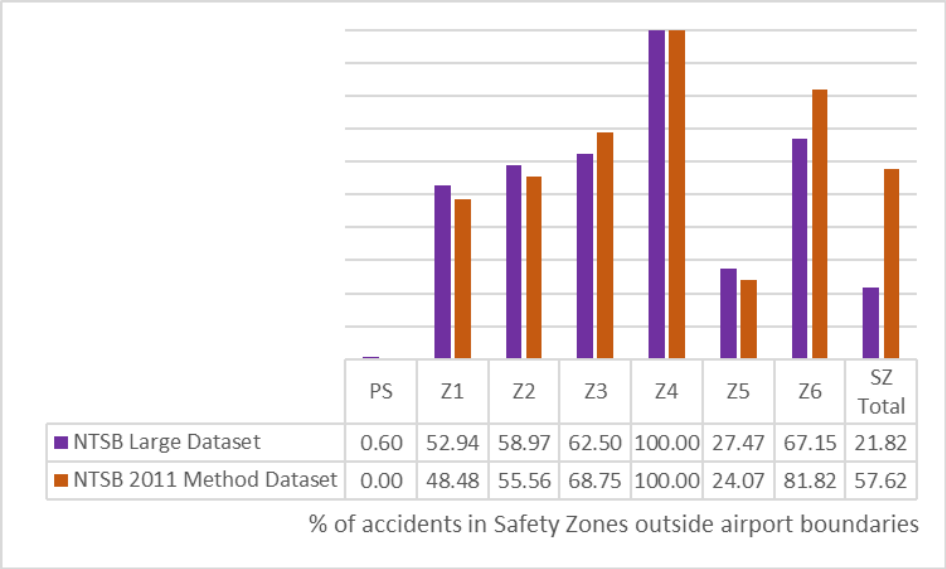


Figure 9. Percentage of Accidents in Safety Zones Outside Airport Boundaries

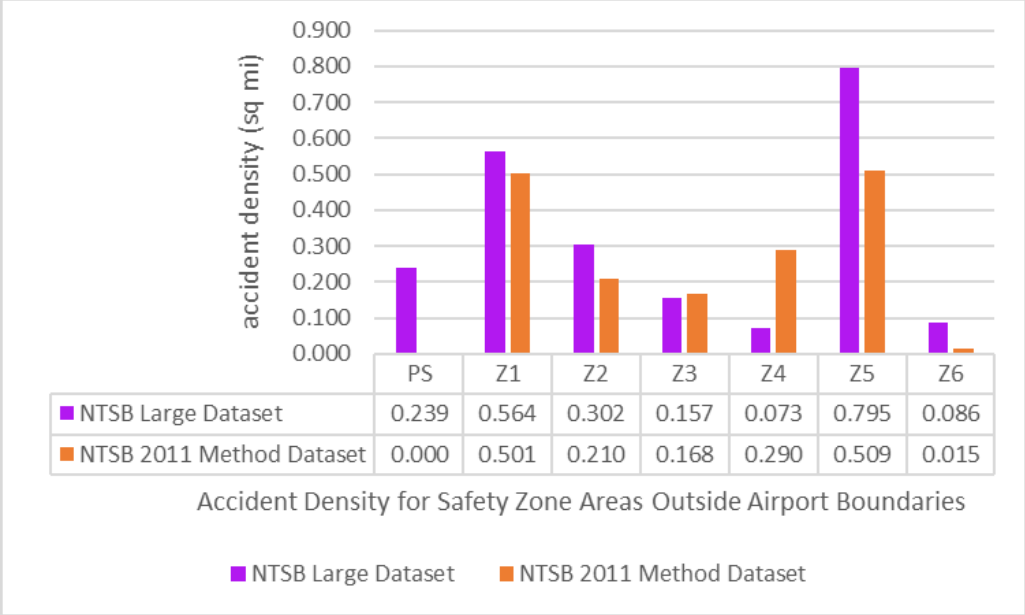


Figure 10. Density of Accidents in Safety Zones Outside Airport Boundaries

Table 19. Percentage and Density of Wildlife Strikes in Safety Zones Areas Outside Airport Boundaries

Safety Zones	**% W. Strikes in SZ Outside Airp. BND**	**Density of W. Strikes in SZ Outside Airp. BND (sq. mi)**
PS	62.35	0.002
Z1	0.00	0.000
Z2	0.00	0.000
Z3	0.00	0.000
Z4	0.00	0.000
Z5	99.13	0.040
Z6	100.00	0.137
SZ Total	78.62	0.088

3.2. Safety Zone Land Use and Land Cover Analysis

3.2.1. Change to Urban Land Use and Land Cover in Safety Zones and Airport Vicinity between 2001-2021: Tracing Increased Exposure and Potential Consequences

Section 3.2.1. provides an overview of how land use and land cover (LULC) has changed between 2001-2021 in Safety Zones, with a focus on change to urban LULC (Tables 20- 24). The assumption is that any change to urban LULC in the past 20 years within runway Safety Zones and airport influence areas (2 mile buffer) represents an increase in exposure to accidents and an increase in the potential consequences in case of accidents. We highlight that land use change of Safety Zones that are majorly inside airport boundaries such as primary surface (98.69% inside) and Safety Zone 5 (73.91% inside) are less relevant to exposure assessment based on LULC change (Figure 11). It is very likely that the high percentages of developed or urban LULC in these areas correspond to impervious surfaces that are functional to airport runways. In opposition, Safety Zones 2, 3, 4, and 6 have respectively 79.59%; 88.39%, 97.94% and 94.64% of their area located outside airport premises, and therefore have higher stakes in ALUP and LULC exposure analysis since their impervious surfaces are more likely to correspond to roads and buildings. Figure 12 to 18 maps Airports with some of the highest percentages of new urban development in their 2 mile buffer zone between 2001 and 2021 (ranging from 8.36 to 36.67%), and Figures 19 and 20 shows two example of airport with

low percentage of urban development for that time period (ranging from 0.68 to 1.14%), one in a high urban intensity setting and the other in a suburban setting for the current LULC. See Appendix B for a rank of all airports in this study based on the percentage of new urban development in their vicinity in the last two decades.

Not surprisingly, urbanization of areas in the vicinity of airports has been proportionately higher than that seen in California. Table 21 shows that 4.46% of Safety Zone areas have changed to urban in the last 20 years in contrast with 2.58% for the 2 mile buffer of airport boundaries,and 0.7 % for all of the State. The percentage of LULC change area (including all classes) varies between 6.63% (PS) to 8.59% (Z6) for the different Safety Zones, and the percentage of the area in each Safety Zone that changed to urban in the last 20 years ranges between 3.64% (Z1) to 5.53% (PS).
Table 22 shows that most areas within the Safety Zones and airport vicinity that did undergo change between 2001-2021 correspond to urbanization changes, thus the increase in exposure and potential consequences in case of accidents. For Safety Zones majorly located outside airport boundaries (Z1-Z4 and Z6) the percentage of land use change attributed to urban development is on average 53%. The percentage of land use change attributed to urban development in Safety Zones and airport vicinities is approximately 10 times higher than that observed in California state.

Table 23 highlights Safety Zone 6 and 3 with a concerning increased level of exposure related to urban development in the last 20 years. Safety Zone 6 has the highest % of urban change (normalized by the total urban change of all Safety Zones, of the 2 mi buffer zone, and California). The discrepancy of Safety Zone 6 exposure can be explained mostly due to its size in comparison with other Safety Zones and that it is 94.64% located outside airport premises. However the increase of urban development on Safety Zone 3 is equally concerning since it covers a smaller area, 88.39% is located outside airport premises, and this zone is more restrictive to land use compatibility than Zone 6. The change to urban LULC over all Safety Zones has occurred in the last two decades approximately 50% inside airport boundaries and 50% outside airport boundaries, with the exception of Zone 5, where only 0.8% change to urban occurred outside airport boundaries relative to all LULC changes in that zone (Table 24). The Primary Surface also registered a higher proportion of change to urban outside airport boundaries relative to all LULC changes of this zone, however this result is skewed due to the very small area of the primary surface located outside airport boundaries. A total of 1.3% of Primary Surface area was computed outside airport boundaries, this small percentage is likely attributed to errors of the generic Safety Zones dimensions when modeled in GIS)

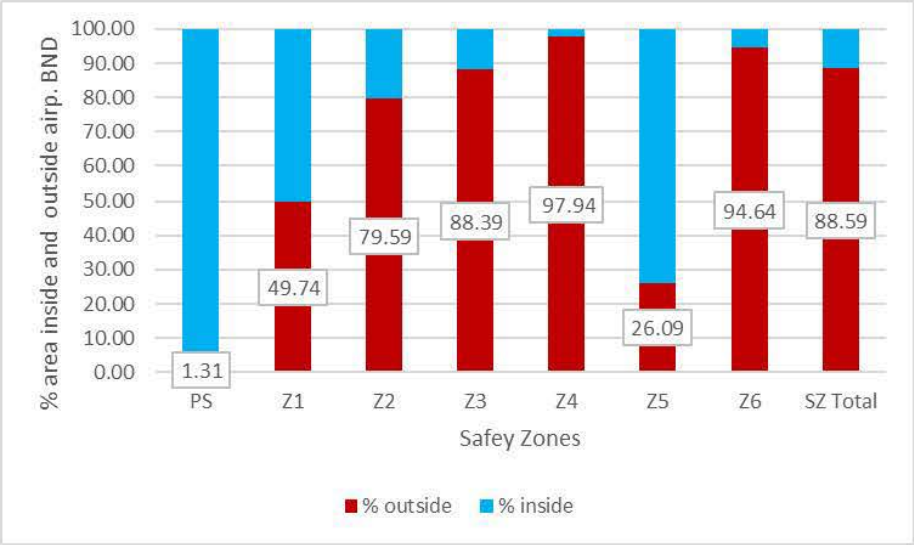


Figure 11. Safety Zones Areas Outside and Inside Airport Boundaries: Relevance of LULC Analysis

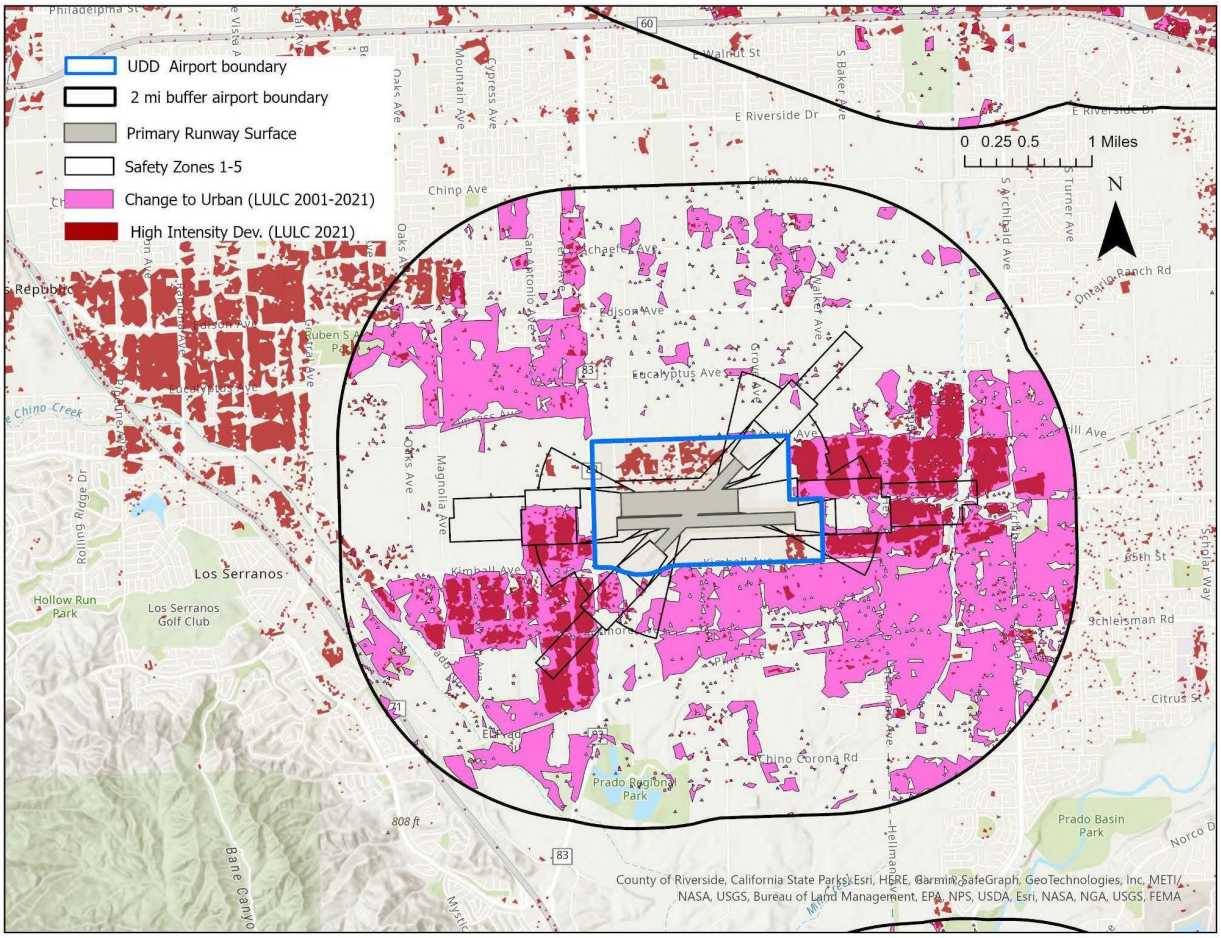


Figure 12. CNO Airport Vicinity New Urban Development from 2001-2021 and Current High Intensity Development. CNO has 39.76 % of new urban development within the 2 mile airport buffer, representing the highest percentage in this study.

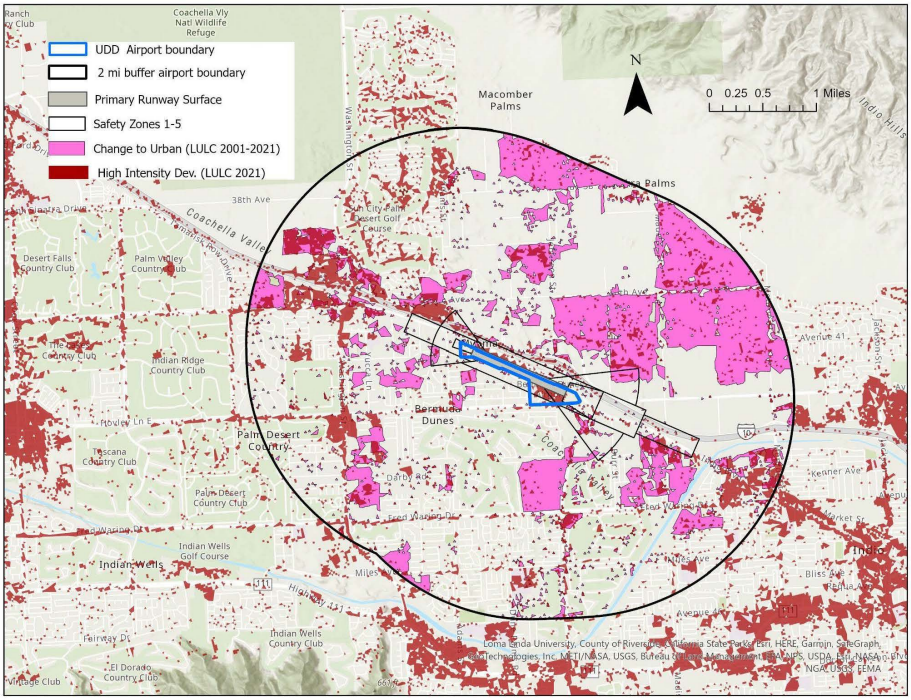


Figure 13. UDD Airport Vicinity New Urban Development from 2001-2021 and Current High Intensity Development. UDD has 22.6 % of new urban development within the 2 mile airport buffer, representing the 4th highest percentage in this study.

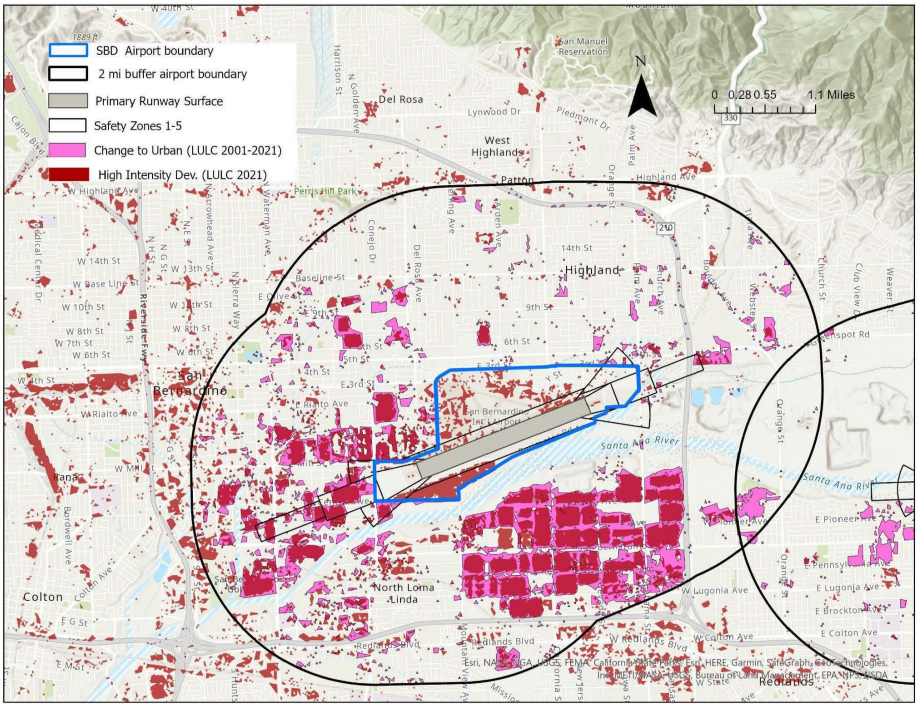


Figure 14. SBD Airport Vicinity New Urban Development from 2001-2021 and Current High Intensity Development. SBD has 17.31 % of new urban development within the 2 mile airport buffer, representing the 6th highest percentage in this study.

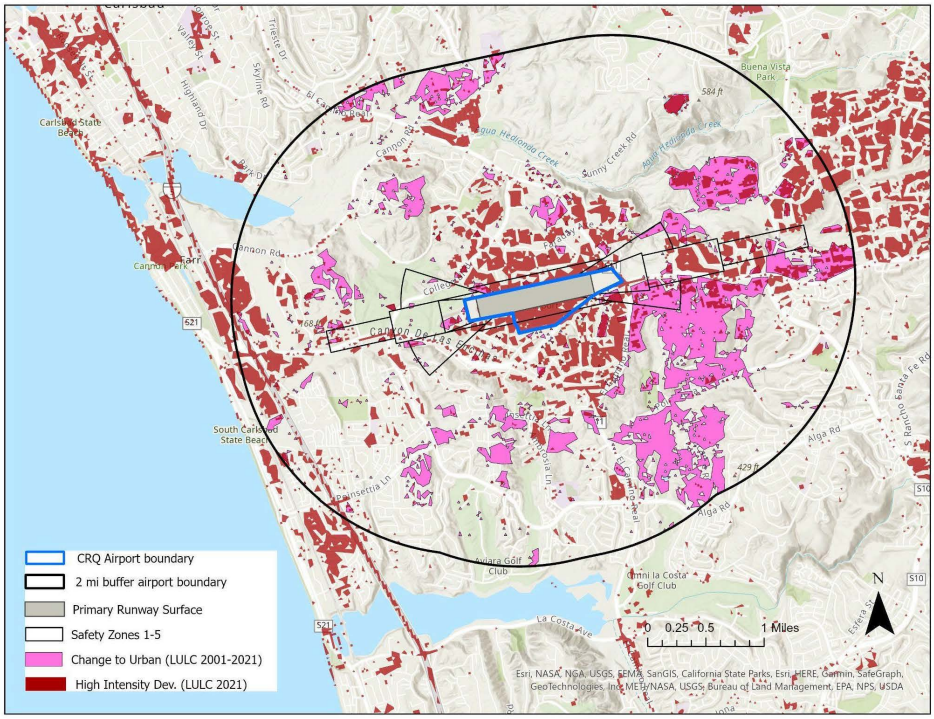


Figure 15. CRQ Airport Vicinity New Urban Development from 2001-2021 and Current High Intensity Development. CRQ has 13.18% of new urban development within the 2 mile airport buffer, representing the 7th highest percentage in this study.

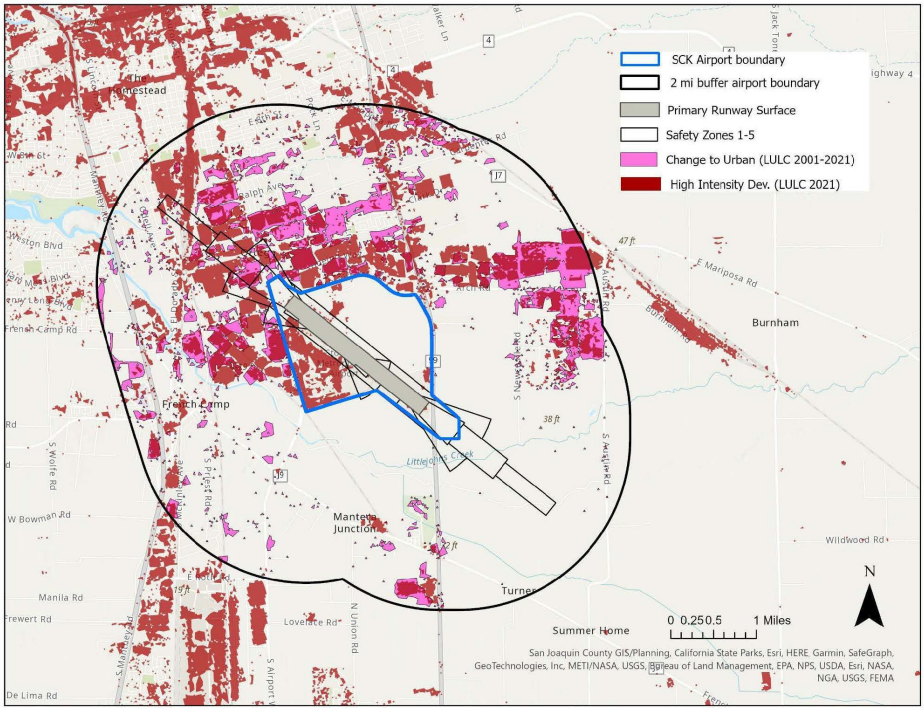


Figure 16. SCK Airport Vicinity New Urban Development from 2001-2021 and Current High Intensity Development. SCK has 13.04 % of new urban development within the 2 mile airport buffer, representing the 8th highest percentage in this study.

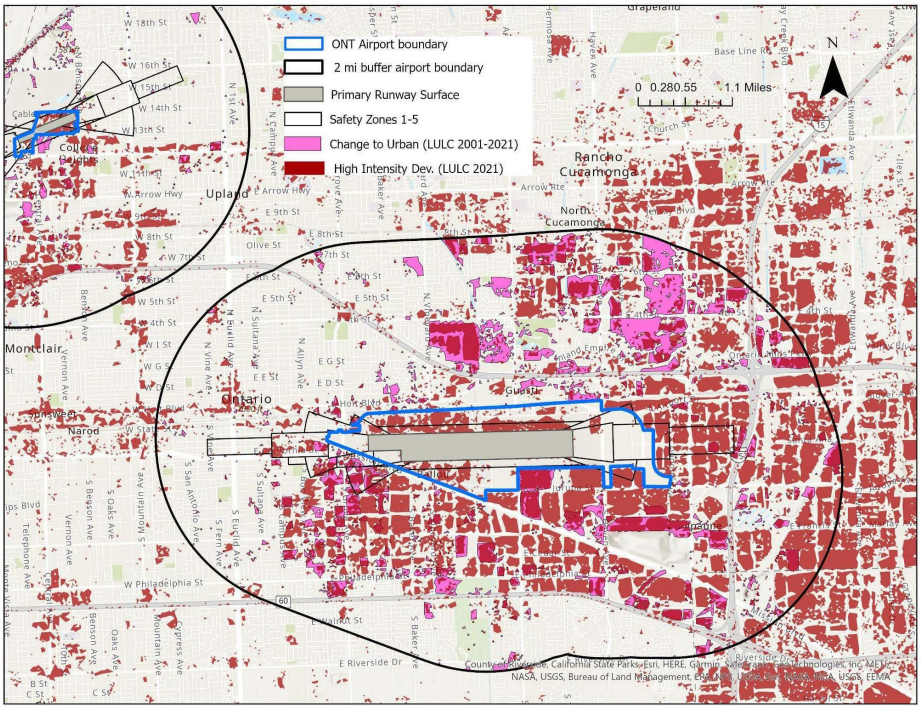


Figure 17. ONT Airport Vicinity New Urban Development from 2001-2021 and Current High Intensity Development. ONT has 12.99 % of new urban development within the 2 mile airport buffer, representing the 9th highest percentage in this study.

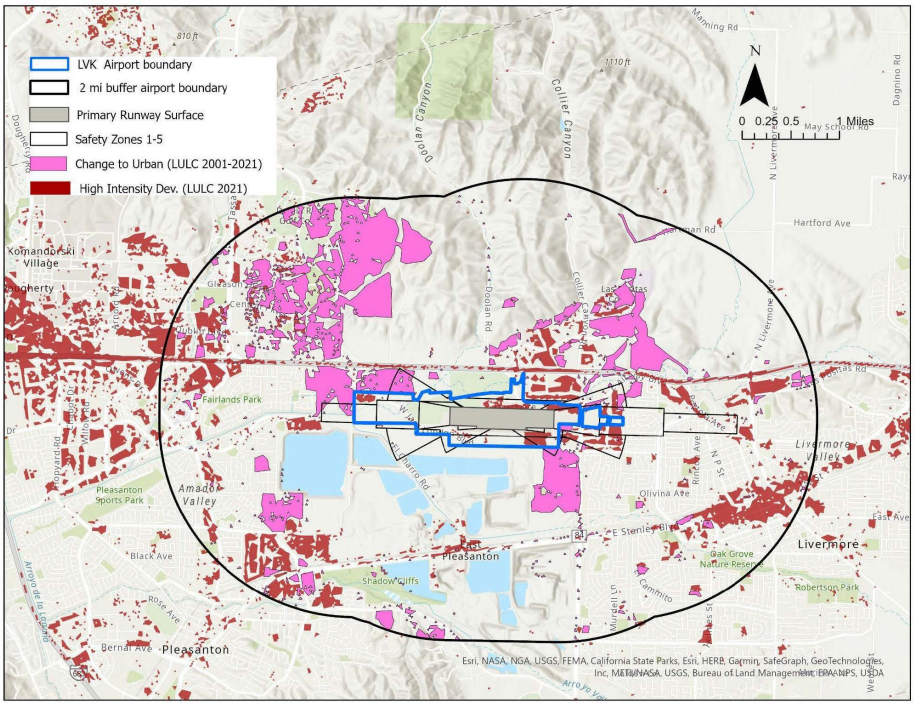


Figure 18. LVK Airport Vicinity New Urban Development from 2001-2021 and Current High Intensity Development. LVK has 10.82 % of new urban development within the 2 mile airport buffer, representing the 12th highest percentage in this study.

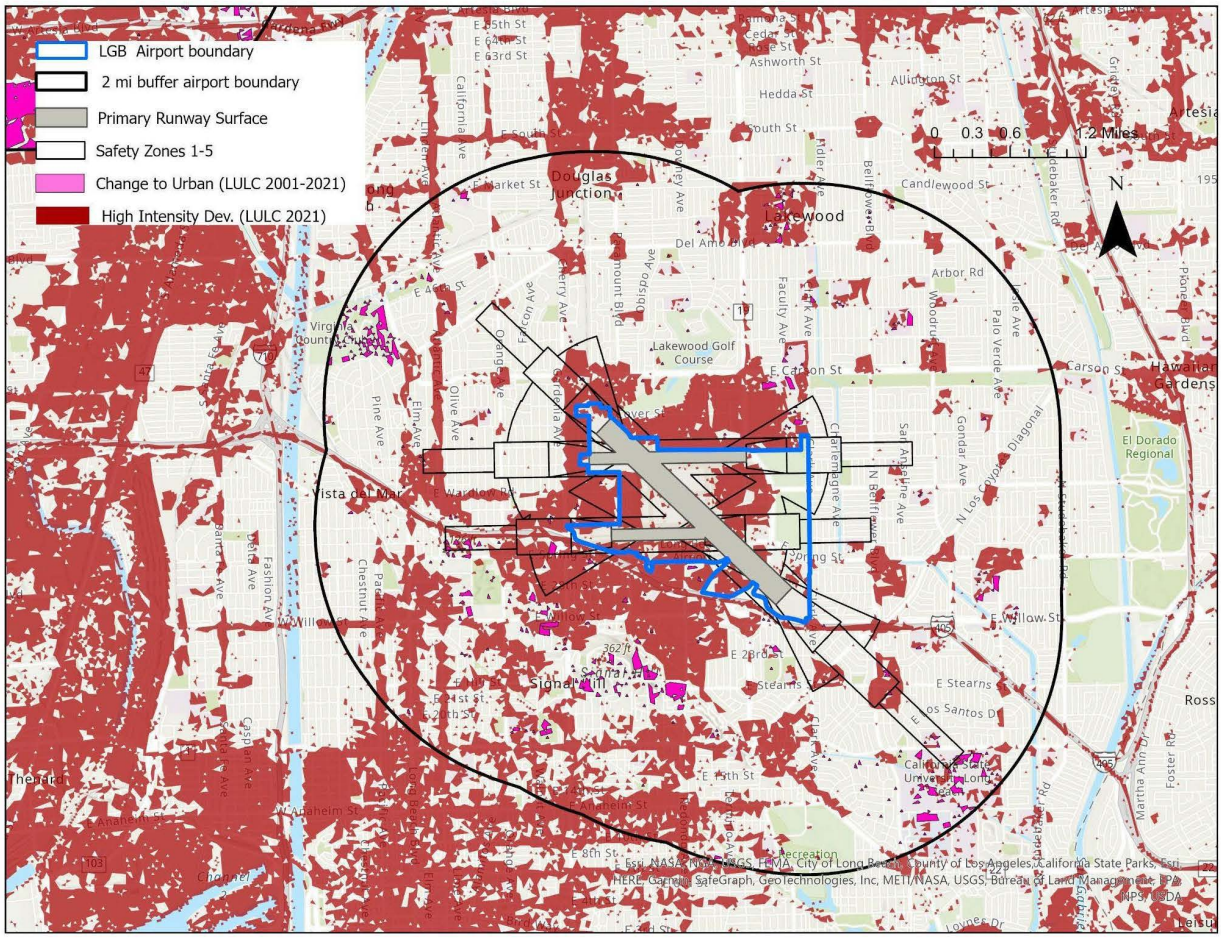


Figure 19. LGB Airport Vicinity New Urban Development from 2001-2021 and Current High Intensity Development. LGB has 1.14 % of new urban development within the 2 mile airport buffer, illustrating areas where there was very low new urban development in a high intensity development setting.

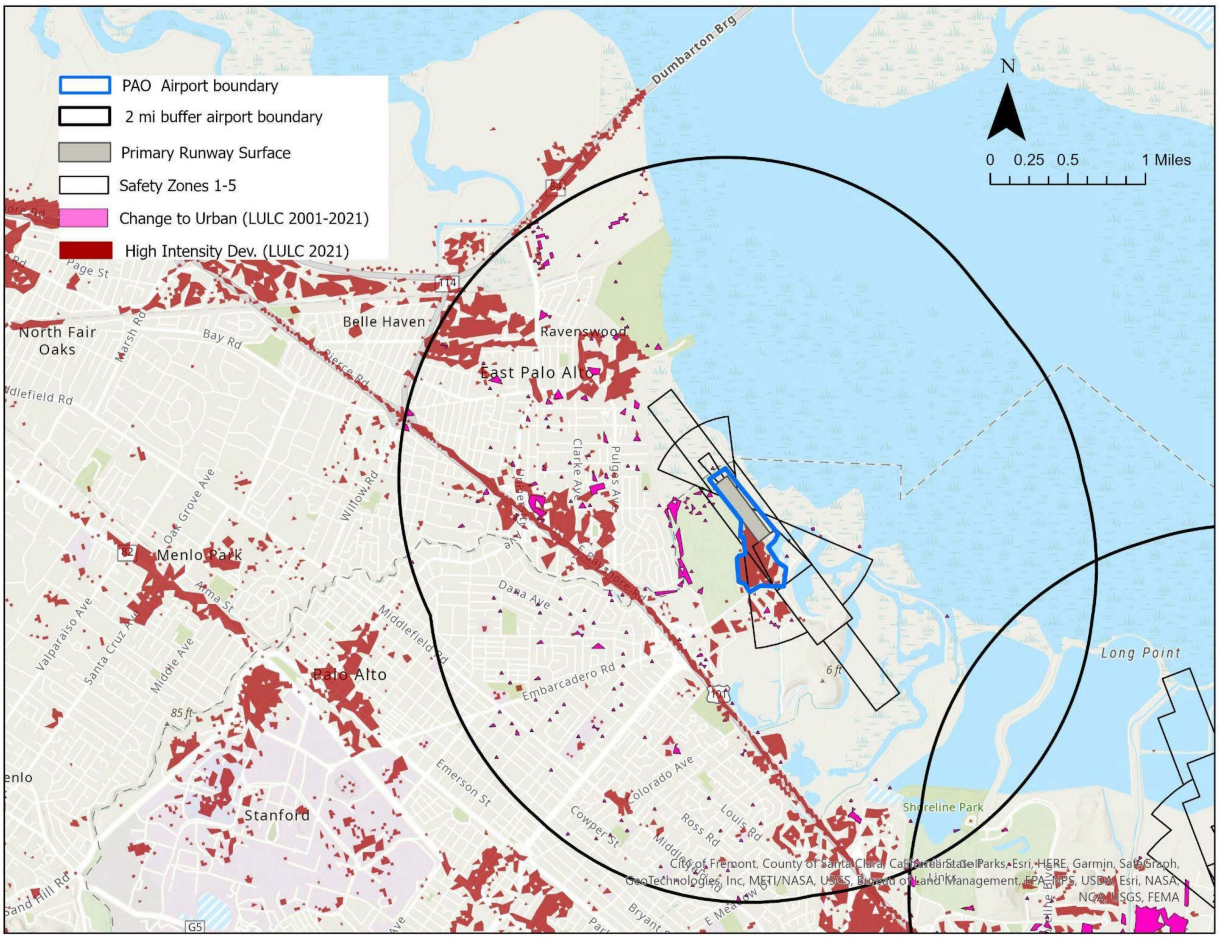


Figure 20. PAO Airport Vicinity New Urban Development from 2001-2021 and Current High Intensity Development. PAO has 0.68 % of new urban development within the 2 mile airport buffer, illustrating airports with very low new urban development, in a suburban setting.

Table 20. Land Use and Land Cover (LULC) Change to Urban (Area in sq. mi)

Zone	**To Urban (sq. mi)**	**Tot LULC Chg (sq. mi)**
PS	1.80	2.16
Z1	1.17	2.18
Z2	3.16	6.05
Z3	4.59	8.19

Z4	2.35	4.56
Z5	1.77	2.47
Z6	47.25	91.33
TotSZ	62.08	116.92
2mibuff	132.11	307.16
CA	1099.21	22598.50

To Urban: Area that changed from another LULC class to urban class; Tot LULC Chg: Total area that changed LULC class; PS: Primary Surface; Total SZ: Total Safety Zones (PS + Z1 to Z6); 2mi buff: 2 mi buffer of airport boundary; CA: California State; N/A: Not Applicable

Table 21. Percentage of LULC Change normalized by the Total Zone Area

Zone	**% chg to Urban relative to total zone area**	**% tot LULC chg**	**Tot Area (sq.mi)**
PS	5.53	6.63	32.54
Z1	3.64	6.77	32.12
Z2	4.15	7.94	76.19
Z3	4.81	8.59	95.40
Z4	4.26	8.27	55.11
Z5	5.10	7.10	34.74
Z6	4.44	8.58	1064.77
TotSZ	4.46	8.41	1390.88

2mibuff	2.58	6.00	5118.74
CA	0.70	14.29	158086.90

* % chg to Urban example: Z1 area that changed to Urban/ Tot Area of Z1 x 100
* % tot LULC chg example: Total Z1 area that changed LULC class / Tot Area of Z1 x 100
*Tot LULC change =(to water+ to urban + to wetland + to herbaceous + to agriculture + to cultivated crop + to hay/pasture + to rangeland herbaceous/ shrub + to barren + to forest)

Table 22. Percentage of LULC Change normalized by the Total LULC Change of each Zone

Zone	**% chg to Urban relative to Tot LULC chg**
PS	83.47
Z1	53.67
Z2	52.27
Z3	55.99
Z4	51.52
Z5	71.82
Z6	51.73
TotSZ	53.10
2mibuff	43.01
CA	4.86

*% of chg to Urban relative to Tot LULC chg example = Z1 area that changed to Urban/ Tot Area of Z1 that has seen LULC change x 100

Table 23. Percentage of LULC Change per Zone normalized by the Total LULC Change of all Safety Zones, of the 2 mi buffer of airport boundaries, and of California

Zone	**% chg to Urban relative to Tot SZ urb chg**	**% chg to Urban relative to 2mi buff urb chg**	**% chg to Urban relative to CA urb chg**
PS	2.90	1.36	0.16
Z1	1.88	0.88	0.11
Z2	5.09	2.39	0.29
Z3	7.39	3.47	0.42
Z4	3.78	1.78	0.21
Z5	2.86	1.34	0.16
Z6	76.10	35.76	4.30
TotSZ	100.00	46.99	5.65
2 mi buff	N/A	100	12.02
CA	N/A	N/A	100

*% chg to Urban relative to Tot SZ urb chg example = Z1 area that changed to urban / total area that changed to urban in all Safety Zones (PS + Z1 to Z6) x 100
*% chg to Urban relative to 2mi buff urb chg example = Z1 area that changed to urban / total area that changed to urban within 2 miles of airport boundaries x 100
*% chg to Urban relative to CA urb chg example = Z1 area that changed to urban / toal area that changed to urban in California x 100

Table 24. Percentage of Change to Urban Outside Airport Boundary (relative to total LULC Change Outside Airport Boundaries

Zone	**% Change outside airp. bnd**
PS	73.20915
Z1	51.29613
Z2	51.42967
Z3	54.82277
Z4	51.14882
Z5	0.824153
Z6	50.42516
TotSZ	50.56377

3.2.2. Developed Areas in Safety Zones and Airport Vicinity: Current Exposure and Potential Consequences

Subsection 3.2.2. Identifies current exposure of Safety Zones based on the percentage of different types of developed LULC areas identified in 2021 based on the data from Table 25. The assumption is that from all the 16 LULC classes the urban class or “developed” represents the exposure to accidents with the highest potential for severe impact, increasing from Developed Open Space, to Developed High Intensity.

Overall the percentage of developed areas is higher for Safety Zones and in airport vicinities than in California. Table 26 shows that while in the state 6.93% of current LULC is classified as developed, 23.66% is classified as developed within 2 miles of airport boundaries and 39.25% is classified as developed in airport Safety Zones. The percentage of medium intensity development is nearly double of other types of development, which correspond to areas that most commonly include single-family housing units.

Figure 21-23 shows the percentage of each developed class relative to the Safety Zone area, relative to the total area of the developed class within airport vicinity, and relative to the total area of the developed class in California. The percentage of total developed area for Safety Zones majorly outside airport boundaries (Z1-4 and Z6) range from 37.14% (Z6) to 46.06% (Z1) (Figure 21). Safety Zone 6 concentrates 36.7% of high intensity developed areas within airport vicinities; followed by zone 3 (4.53%) and zone 2 (3.34%) (Figure 22). When looking at the percentage of developed LULC relative to the total developed area in California, a similar pattern is identified with zone 6 concentrating the highest proportion of high intensity development zones, followed by zones 3 and 2 (Figure 23). Figures 22 and 23 highlight a pattern of high intensity development dominance in comparison to other development types in airport vicinity and Safety Zones. Figure 24 shows the percentage area of each development class located outside airport boundaries, where there is potential for higher land use compatibility issues and ALUCs have jurisdiction. Zone 4 and 6 have the highest portion of developed areas outside of airport boundaries ranging from 99 to 91% respectively; followed by Zones 3 and 2 ranging from 92 to 67% respectively. Zone 5 and 1 present the lowest percentages of developed areas outside airport boundaries ranging from 15 to 52% respectively. Overall these results are closely related to the total percentages of Safety Zones located outside airport boundaries (see Figure 11). These results align with the basic policies for land use compatibility which are more restrictive to urbanization processes in Zones 1, 2 and 5, and less restrictive with Zones 3,4, and 6. Zone 2 should be highlighted because it presents percentages of developed areas outside airport boundaries that are closer to the less restrictive zones (3, 4, and 6) than to the more restrictive Zones 1 and 5.

Overall the 2021 LCLU assessment points to Safety Zone 3 with larger developed areas (sq mi) as well as higher percentage of high intensity development, representing an area of potential severe consequences in case of an accident. Zone 6 presents higher numbers, but considering the size of Zone 3, the percentage outside airport airport boundaries, and its more strict land use compatibility restrictions, it is recommended that land use densities and intensities should be reviewed to mitigate exposure.

Overall, LULC analysis should be complemented with field validation techniques to understand the uncertainty and limitations of remote sensing data. In general this can be done on a case by case basis for engineers, planners and other land use decision makers familiar with the landscape surrounding airports under their jurisdiction or responsibility so that the 2021 NLCD reference data can be evaluated for its reliability or “ground truth”[29].
The data used to develop the tables and figures of this section is available in the supplementary materials “Task8.LULC_analysis”

[29] LULC accuracy assessment for the latest MLRC 2021 NLCD data is 91% (consensus is that the minimum overall accuracy should be at least 85% or more). See https://doi.org/10.1080/15481603.2023.2181143 for the latest accuracy assessment publication. LULC data can be assessed both for thematic accuracy (how well the mapped classes match the actual composition of the landscape?), as well as for positional accuracy (if the mapped classes are in the right location). Thematic accuracy assessment can be done with ground truthing techniques, sampling LULC on the ground with GPS instruments, or using higher quality LULC data from aerial photographs or google maps, and comparing them to the referenced NLCD class. Some of the most usual methods to validate LULC ground truthing are the accuracy assessment statistics ,based on a cross-tabulation matrix to validate LULC maps, and the Kappa Indices (Olmedo et al., 2022)

Table 25. Total Urban Developed Area (sq mi) in 2021

Zone	**Dev OS**	**Dev Low I.**	**Dev Med I.**	**Dev High I.**	**Dev Tot**	**Tot Area**
PS	6.22	5.12	7.69	6.10	25.13	32.54
Z1	4.56	3.19	4.19	2.86	14.79	32.12
Z2	7.05	6.24	10.85	7.13	31.26	76.19
Z3	7.79	7.52	14.26	9.66	39.23	95.40
Z4	3.68	4.19	8.88	4.03	20.79	55.11
Z5	5.49	3.31	4.87	5.58	19.25	34.74
Z6	79.32	80.71	157.25	78.21	395.50	1064.77
TotSZ	114.11	110.29	207.99	113.57	114.11	1390.88
2mibuff	247.75	261.79	488.34	213.14	1211.02	5118.74
CA	4124.96	2432.35	3319.96	1070.40	10947.67	158086.90

*Dev. OS: Developed Open Space; Dev Low, Med, High I: Developed Low, Medium, and High Intensity; Dev Tot = (Dev OS + Dev Low I + Dev Med I +Dev High I); Tot Area: total area of each zone.

Table 26. Percentage of Developed Areas in all Safety Zones, Airport Vicinities, and California

Zone	**% Dev OS Area**	**% Dev Low I Area**	**% Dev Med I Area**	**% Dev High I Area**	**% Dev Tot**
TotSZ	8.20	7.93	14.95	8.17	39.25
2mibuff	4.84	5.11	9.54	4.16	23.66
CA	2.61	1.54	2.10	0.68	6.93

*% Dev OS 2mibuff example = Area classified as Developed Open Space within 2 mile buffer of airport boundaries/ total area of 2 mile buffer of airport boundaries x100

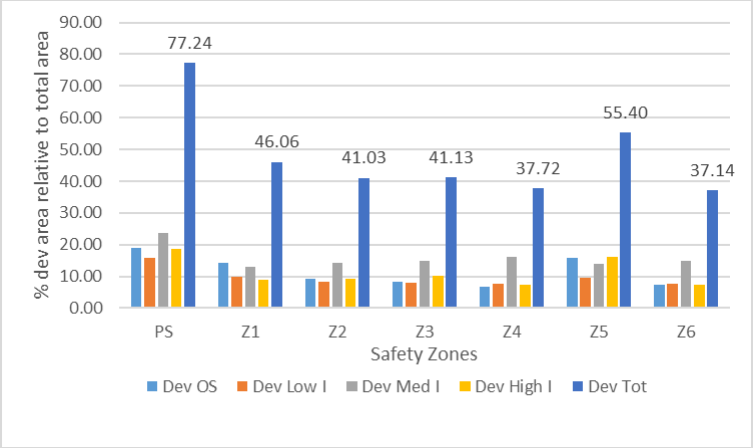


Figure 21. Percentage of Developed Area Normalized by the Area of each Zone (Calculation example: Z1 Dev OS area/ Z1 Area x 100)

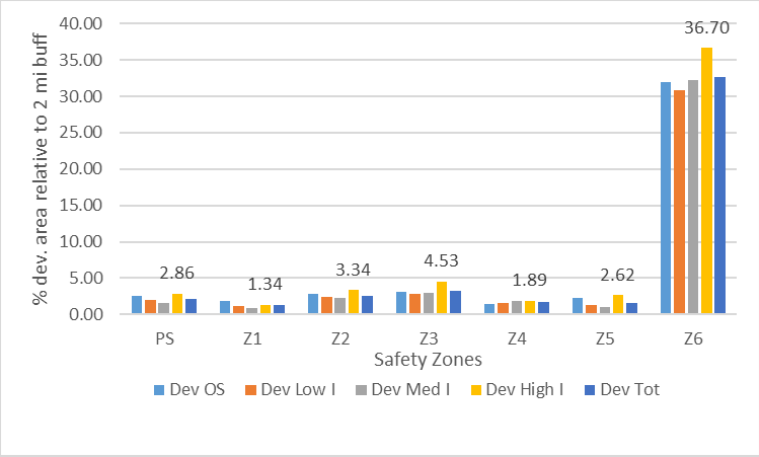


Figure 22. Percentage of Developed Area Normalized by Total Developed Areas within 2 Miles of Airport Boundaries. (Calculation example: Z1 Dev OS area/ 2mi buff Dev OS area x 100)

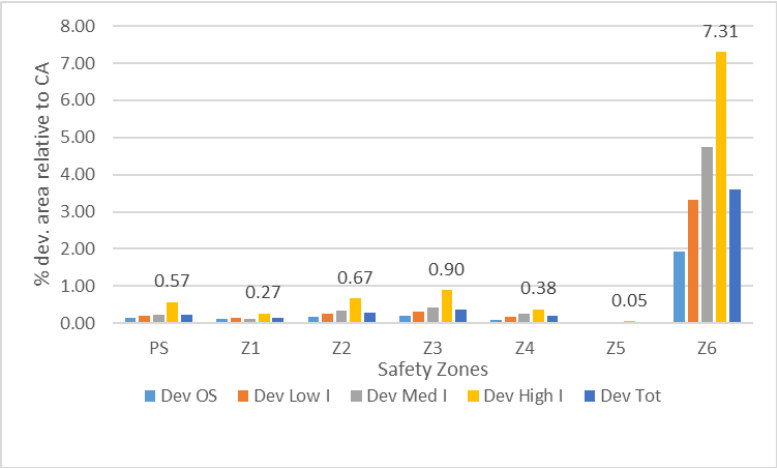
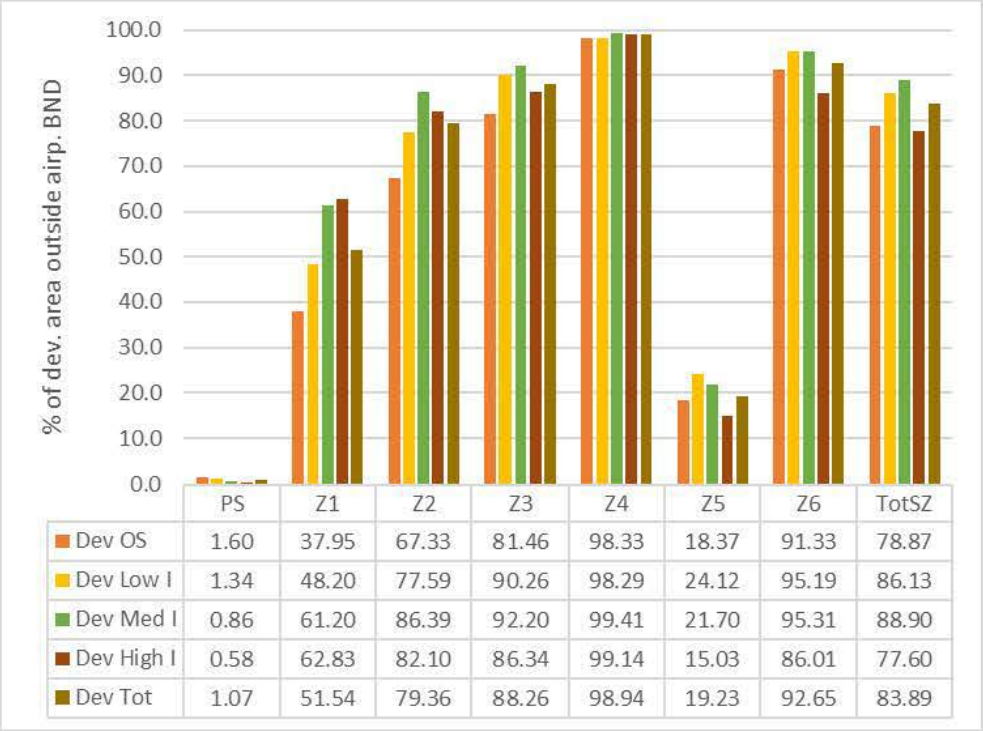


Figure 23. Percentage of Developed Area Normalized by Total Developed Areas in California. (Calculation example: Z1 Dev OS area/ CA Dev OS area x 100)



	PS	Z1	Z2	Z3	Z4	Z5	Z6	TotSZ
Dev OS	1.60	37.95	67.33	81.46	98.33	18.37	91.33	78.87
Dev Low I	1.34	48.20	77.59	90.26	98.29	24.12	95.19	86.13
Dev Med I	0.86	61.20	86.39	92.20	99.41	21.70	95.31	88.90
Dev High I	0.58	62.83	82.10	86.34	99.14	15.03	86.01	77.60
Dev Tot	1.07	51.54	79.36	88.26	98.94	19.23	92.65	83.89

Figure 24. Percentage of Developed Area Outside of Airport Boundaries (Calculation example: Z1 Dev OS area outside irp. Bnd. / Total Z1 area x 100)

3.3. Update of Safety Zone Risk Analysis & Land Use Compatibility Tables (2011 ALUP Handbook p 4-20 to 4-25)

3.3.1. Accident Risk Matrix Results

Tables 27 to 29 present the results of the accident risk analysis using NTSB 2011 method dataset (n=495) and the NTSB Largest dataset (n = 1,355). For the latter dataset a weighted risk formula is applied to better explore the accident impact information.

When using the *Accident Risk*$_{Simple}$ formula, the hazard levels as well as the risk results are similar across the NTSB 2011 method dataset and the NTSB Large Dataset. Zone 5 is considered the most concerning zone, with the highest levels of hazard and exposure, resulting in Very Risk, followed by Safety Zone 1, and Safety Zone 3. Safety Zone 2 is at medium risk, with high exposure level and medium exposure level. Safety Zones 6 and 4 have a low risk level, from low exposure as well as low hazard levels. Safety Zone 6 has a slightly higher hazard and exposure levels than Safety Zone 4.

When using the *Accident Risk*$_{Weighted}$ formula for the NTSB Largest dataset we can observe some changes to the Zone 1 and Zone 6 risk. The most important change concerns Zone 6, that is at medium risk instead of low due to a very high exposure level based on the high concentration of fatal injury accidents relative to the other zones (total of 28 accidents where

the highest level of injury resulted one of more fatalities between 2008-2022), The risk decreases to High for Zone 1 due to a slightly lower concentration of high impact-level accidents relative to other Safety Zones.

Table 27. NTSB 2011 Method Dataset Risk Metrics (*Accident Risk*$_{Simple}$ formula)

Zone	*Acc Den*	*Hazard Score*$_{Simple}$ *(Hs)*	*Hazard Level*	*Exposure (EpW)*	*Exposure Level*	***Risk Class***
Z1	1.028	0.571626	Very High	108.757311	High	**Very High**
Z2	0.354	0.138525	High	105.762618	Med	**Med**
Z3	0.168	0.018438	Med	109.290532	Very High	**High**
Z4	0.054	-0.05444	Low	99.496218	Low	**Low**
Z5	1.554	0.910537	Very High	141.134397	Very High	**Very High**
Z6	0.072	-0.04294	Low	96.297067	Low	**Low**

Table 28. NTSB Large Dataset Risk Metrics (*Accident Risk*$_{Simple}$ formula)

Zone	*Acc Den*	*Hazard Score*$_{Simple}$ *(Hs)*	*Hazard Level*	*Exposure (EpW)*	*Exposure Level*	***Risk Class***
Z1	1.059	0.303886	Very High	108.757311	High	**Very High**
Z2	0.512	0.095122	High	105.762618	Med	**Med**
Z3	0.252	-0.00425	Med	109.290532	Very High	**High**
Z4	0.073	-0.07258	Low	99.496218	Low	**Low**
Z5	2.619	0.899704	Very High	141.134397	Very High	**Very High**

Z6	0.129	-0.05117	Low	96.297067	Low	**Low**

Table 29. NTSB Large Dataset Risk Metrics (*Accident Risk*$_{Weighted}$ formula)

Zone	*Acc Den*	*Hazard Score*$_{Weighted}$ *(HsW)*	*Hazard Level*	*Exposure (EpW)*	*Exposure Level*	***Risk Class***
Z1	2.048	0.147369	High	108.757311	High	**High**
Z2	1.350	-0.01766	Med	105.762618	Med	**Med**
Z3	0.758	-0.15741	Low	109.290532	Very High	**High**
Z4	0.272	-0.27219	Low	99.496218	Low	**Low**
Z5	4.233	0.663504	Very High	141.134397	Very High	**Very High**
Z6	2.405	0.231721	Very High	96.297067	Low	**Med**

3.3.2. Update of Safety Zone Risk and Land Use Compatibility Table (2011 ALUP Handbook p 4-20 to 4-25)

When comparing the risk of Safety Zones from the previous ALUP Handbook of 2011 and the current analysis quantitative and qualitative results of this study need to be taken into consideration :

- Change in percentages of accidents in each Safety Zone
- Hazard levels (densities and percentages from sections 3.1.1 and 3.1.2.)
- Exposure levels (percentages calculated in section 3.2.1. And 3.2.2.). Since the former ALUP handbooks did not incorporate any exposure metrics, the LULC change in the past 20 years can help gauge the need to change land use compatibility to respond to changes in exposure.

- Contrast inside and outside of airport boundaries results because of jurisdiction changes that highly impacts the available strategies for ALUCs to (1) change Safety Zones dimensions for mitigating accident hazard, and/or (2) to modify the land use compatibility criteria for mitigating exposure.
- Risk results aid in qualitatively synthesizing the core accident and potential consequences results.

Key remarks for each zone are described below and further detailed in the synthesis Table 30

Safety Zone 1. Runway Protection Zone: Remains at Very High risk, with a decrease of approximately 6% in the overall percentages of accident compared to what was assessed between 2000-2009 (2011 ALUP Handbook). Zone 1 also presented one of the lowest percentages of change to urban areas between 2001-2021 relative to all LULC changes in Zone 1. From one perspective this reflects the effectiveness of the land use compatibility restrictions and limitations so far, but from another perspective this highlights Zone 1 as most prone to new urban development pressure. Overall there are no suggestions to change Safety Zones geometries or land use compatibility criteria.

Safety Zone 2. Inner Approach/ Departure Zone: Risk remains Medium to High. We highlight the range of accident percentages increase accounted between 2000-2009 (2011 ALUP Handbook) is very high (8 - 22%) making the comparison with the current range mixed: is some aspects there has been a slight increase of 3-4% and in other aspects there has been a decrease of approximately 10%. The current hazard level remains high however, but because the exposure is at a medium level, qualitatively there is a tendency of reducing the overall risk. Overall there are no suggestions to change Safety Zones geometries. We highlight the importance of further investigating the effectiveness of current land use compatibility criteria in mitigating potential consequences of accident since there are relatively high percentages of LULC change to urban change outside the airport perimeter relative to what was accounted for Zone 2 inside the airport boundary.

Safety Zone 3. Inner Turning Zone: Risk remains High. With medium hazard levels and very high exposure levels when applying the Simple Accident Risk formula. When applying the Weighted Accident RIsk formula, the hazard levels are reduced to low, meaning the concentration of accidents in this zone correspond to low or no injury impact types. We highlight that Safety Zone 3 has relatively larger developed areas (in sq mi) as well as a higher percentage of high intensity development, representing an area of potential severe consequences in case of an accident. Zone 3 also has the highest percentage of LULC change to urban outside airport boundaries relative to all LULC change, representing one of the Safety Zone with the highest increase in exposure (relative to its size). A review of land use compatibility policies is highly indicated for Safety Zone 3 together with a LULC classification field validation to verify the accuracy of increased developed areas that corresponds to restricted or limited use.

Safety Zone 4: Outer Approach/Departure Zone: Risk is reduced from Moderate to Low, with consistently low levels of hazard across all datasets and low levels of exposure. Although the percentages of accidents in this zone compared to the 2011 ALUP Handbook assessment whos an increase of approximately a + or - change of 2%, we highlight that Zone 4 has the lowest number of accidents between 2008-2022 with a total of 3 (for the NTSB 2011 method dataset) and 4 (for the NTSB Largest dataset). Zone 4 is almost entirely located outside airport boundaries and has a relatively low developed area compared to the total Zone 4 area (37.72%). Overall Safety Zone can be considered smaller geometries and less strict land use compatibility policies in order to compensate for the need for larger dimensions other zones with high hazard and/or zones needing revision for stricter land use compatibility policies..

Safety Zone 5. Sideline Zone: Risk increases from Low to Very High, with consistently very high hazard and exposure levels through all datasets, including different accident metrics applied throughout this report. Safety Zone 5 needs to be prioritized for dimension revisions and potentially increasing its generic sideline area into Zone 6 areas. The increase in accident percentages compared to the 2000-2009 assessment ranges between 19-22%. Safety Zone 5 is mostly located inside airport boundaries (73.91%) and presents some of the stricter land use compatibility criteria, similar to Zone 1, however the development levels are high both inside and outside airport boundaries. It is likely that field validation of LULC of this zone points to impervious surface areas (parking lots, roads, and other pavement, which corresponds to Open Space Development class), but there are relatively high percentages of low, medium and high intensity development for Zone 5 compared to other more strict zones (1 and 2).
Based on discussions (Taken place in December 2023) between the UC Berkeley Institute of Transportation Studies (ITS) researchers on this project and Caltrans Aeronautics planners, engineers, pilots and others experts of airport safety, suggestions to develop a more detailed Safety Zone 5 dimension change recommendations include:

(a) Airport-level attributes vs. spatiotemporal accident patterns: Assess spatiotemporal accident patterns in each Safety Zone based on airport-level attributes such as airport's runway size, operations capacity, function class, and ownership types. Similar assessments based on density and percentages of accidents in each safety zone can be further categorized based on these airport-level attributes. This information can be found by crossing GIS datasets "AirpBND_Final", and the accident NTSB_spatialLargest dataset by Safety Zones (Acc_within_PS_NTSBLarge; Acc_within_Z1_NTSBLarge…Acc_within_Z6_NTSBLarge) prepared for this study. NTSB Spatial Largest dataset is recommended because it provides the largest possible accident dataset (n = 1,355) which is required for higher statistical significance.

(b) Other accident attributes vs. spatiotemporal accident patterns: Assess spatiotemporal patterns in each Safety Zone based on other NTSB accident attributes such as phase of flight, mid air or ground collision, "sequence of events" which is a dataset from the NTSB that with subject codes used to "identify the individuals, equipment, processes, or phenomena that contributed to the mishap event". This information can be found by crossing NTSB Largest GIS

Dataset, the Safety Zone GIS and “US_NTSB_1948-2023_raw.xls” table where the full NTSB data attributes can be found, and cross referenced with NTSB Spatial Largest dataset based on the “ntsb_no” (unique identifier linking original NTSB accident datasets).

(c) **Explore the position of accidents within each safety zone:** Further assess the spatial distribution of accidents within each safety zone using their relative distance from the runway to better understand if they are concentrating in specific parts of each safety zone, i.e. those in Safety Zone 5 are mostly closer to the primary surface or have they shifted close to the boundary with Safety Zone 6? A dataset has developed for the scatterplots of Task 4.1. Subsection, 3.2.4. called “NTSB_LargestXYplane”. In this accident dataset the accident events were all repositioned in a *X,Y* plane; where x = the distance of the accident perpendicular to the runway; and the y= the distance of the accident parallel to the runway (Example in Figure 25). The NTSB_LargestXYplane data processing is available in Python code under the folder “NTSB_XYplot_py” in Task 9. This analysis can be done by crossing accident NTSB_spatialLargest dataset by Safety Zones (Acc_within_PS_NTSBLarge; Acc_within_Z1_NTSBLarge…Acc_within_Z6_NTSBLarge) with the NTSB_XYplot GIS using “ntsb_no” (unique identifier).

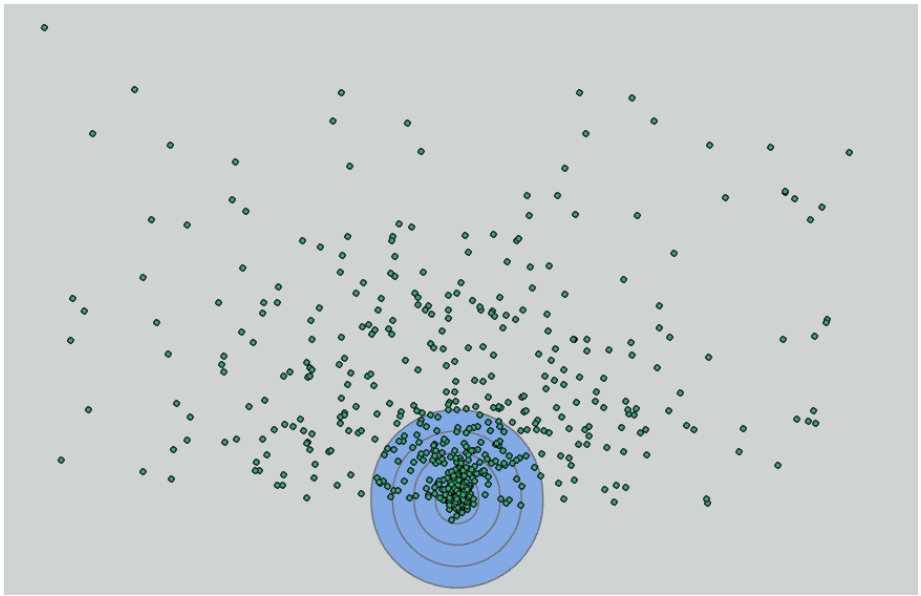
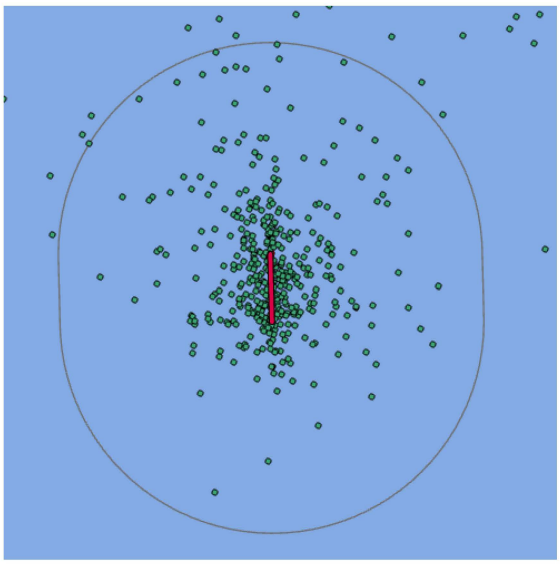


Figure 25. Example of the NTSB Largest



accident dataset (green points) plotted in a XY plane relative to the runway position (red line). The concentric circles represent a 1-5 mile buffer from the runway line.

Safety Zone 6. Traffic Pattern Zone: Risk levels increase from Low to Medium-Low. Based on the *Simple Accident Risk* analysis both hazard and exposure levels remain low, however when applying the *Weighted Accident Risk analysis*, the hazard levels increase from Low to Very High. This is due to the discrepant number of accidents with the highest injury level (fatal). Between 2008-2022 a total of 28 out of 77 accidents in Zone 6 resulted in at least one fatality[30], while other Safety Zones have not registered between 3 and 6. This is probably due to the larger size area that encompasses a higher number of accidents. Zone 6 presents a low accident density, however there was an increase of 7-13% of accidents in this zone when compared to the 2000-2009 assessment. Zone 6 is mostly located outside airport boundaries (94.64%) and is subject to the least restrictive land use compatibility policies, presenting the highest % of urban change (normalized by the total urban change of all Safety Zones, of the 2 mi buffer zone, and California). The discrepancy of Safety Zone 6 exposure can again be explained mostly due to its size in comparison with other Safety Zones. Following the general spatial patterns that concentrate accidents the closer you are to the runway lines, it is likely that the increase of accidents in Zone 6 is closer to the boundaries of Zone 5. An overall revision of accident spatial patterns within Zone 6 is suggested to optimize the need for increasing Zone 5 dimensions, which shares most of its boundary with Zone 6, especially given the increase in

[30] After re-assessing the new zone 6 dimensions (see subsection 3.4.1.) 10 new accidents were included based on the NTSB spatial Largest Dataset, moving the number of accidents with the highest level of Fatal injury from 28 to 31.

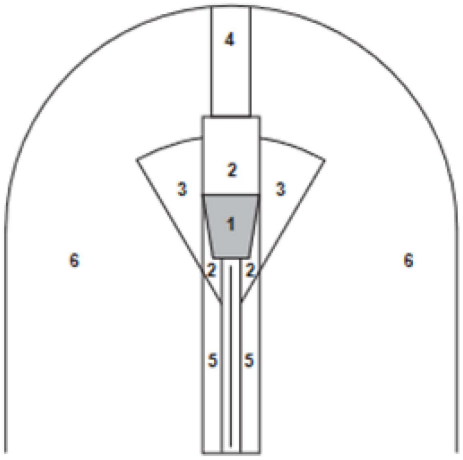
accident percentage in Zone 6 compared to the 2011 Handbook assessment. An overall revision of land use compatibility policies is recommended for increasing restrictions near Zones 5 and 2 or transferring some areas of Zone 6 to Zones 5 and 2.

Table 30. Update of Safety Zone Risk and Land Use Compatibility Table (2011 ALUP Handbook p 4-20 to 4-25)

Safety Zone 1: Runway Protection Zone****	**Accident and Exposure**



SHORT FINAL



Accident Percentage Comparison:
2000-2009: 20-21% of Acc
2008-2022: 13.47-15.71% (excludes Acc in PS)*
2008-2022: 3.83-4.12% (includes Acc in PS)**

Exposure (potential consequences):
2021 LULC:
- 46.06% area developed
- 1.34% of high intensity development (relative to 2 mi buffer)

2001-2021 change to urban:
- 3.64%
- 51.29% of urban change occurred outside airport boundaries relative to total LULC change in Zone 1

2011 risk level: Very High
Current risk levels: High to Very High

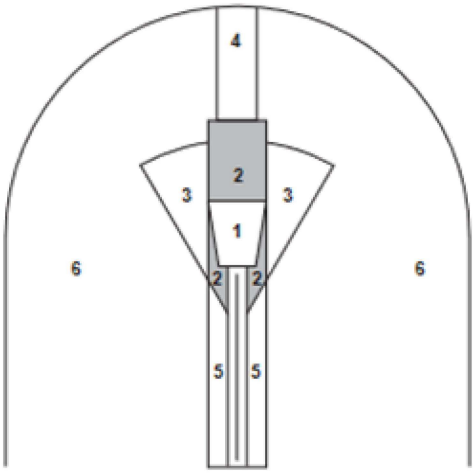
Suggestion for hazard mitigation: None
Suggestion for residential densities and nonresidential intensities: Continue with basic compatibility policies

Basic Compatibility Policies:
Avoid:
-Nonresidential uses except if very low intensity in character and confined to the outer sides
-Parking lots, streets, roads
Prohibit:
-All new structures and residential land uses
Other Factors:
-Airport ownership of property encouraged
-Uses on airport property subject to FAA standards

Safety Zone 2: Inner Approach/ Departure Zone	**Accident and Exposure**



FINAL APPROACH



Accident Percentage Comparison:
2000-2009: 8-22% of Acc
2008-2022: 11.02-12.86% (excludes Acc in PS)*
2008-2022: 4.39- 4.73% (includes Acc in PS)**

Exposure (potential consequences):
2021 LULC:
- 41.03% area developed
- 3.34% of high intensity development (relative to 2 mi buffer)

2001-2021 change to urban:
- 4.15%
- 51.42% of urban change occurred outside airport boundaries relative to total LULC change in Zone 2

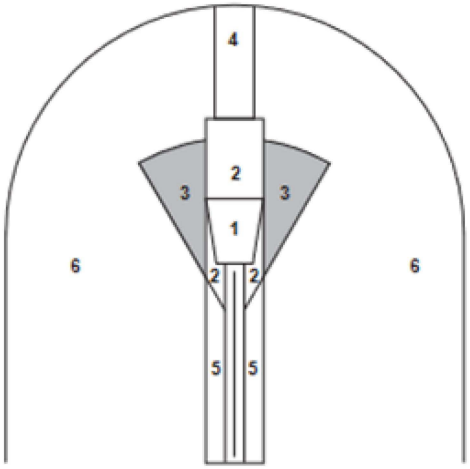
2011 risk level: High
Current risk level: Medium to High
Suggestion for hazard mitigation: None
Suggestion for exposure mitigation: investigate effectiveness of residential and commercial development restrictions outside airport boundaries.

Basic Compatibility Policies
Normally Allow:
-Agriculture; non-group recreational uses -Low-hazard materials storage, warehouses
-Low-intensity light industrial uses; auto, aircraft, marine repair services
Limit:
-Single-story office buildings -Nonresidential uses to activities that attract few people
Avoid:
-All residential uses except as infill in developed areas
-Multi-story uses; uses with high density or intensity
-Shopping centers, most eating establishments
Prohibit:
-Theaters, meeting halls and other assembly uses
-Office buildings greater than 3 stories
-Labor-intensive industrial uses
-Children's schools, large daycare centers, hospitals, nursing homes
-Stadiums, group recreational uses
- Hazardous uses (e.g. above ground bulk fuel storage)

Safety Zone 3: Inner Turning Zone	**Accident and Exposure**



TURNING TO FINAL



Accident Percentage Comparison:
2000-2009: 4-8% of Acc
2008-2022: 6.53-7.62 (excludes Acc in PS)*
2008-2022: 2.70- 2.91% (includes Acc in PS)**

Exposure (potential consequences):
2021 LULC:
- 41.13% area developed
- 4.53% of high intensity development (2 mi buffer)

2001-2021 change to urban:
- 4.81%
- 54.82% of urban change occurred outside airport boundaries relative to total LULC change in Zone 3.

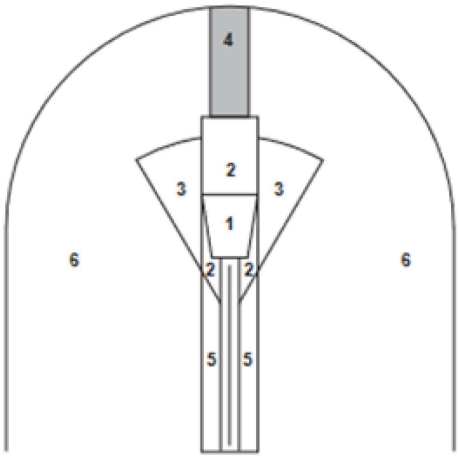
2011 risk level: Moderate to High
Current risk level: Medium to High
Suggestion for hazard mitigation: None
Suggestion of exposure mitigation: Verification of effectiveness of residential and commercial development restrictions outside airport boundaries. Potentially slight increase in development limitations and restriction due to the potential severe consequences in case of accident relative to all other Safety Zones.

Basic Compatibility Policies:
Normally Allow:
-Uses allowed in Zone 2
-Greenhouses, low-hazard materials storage, mini-storage, warehouses
-Light industrial, vehicle repair services
Limit:
-Residential uses to very low densities
-Office and other commercial uses to low intensities
Avoid:
-Commercial and other nonresidential uses having higher usage intensities
-Building with more than 3 aboveground habitable floors
-Hazardous uses (e.g., above ground bulk fuel storage)
Prohibit:
-Major shopping centers, theaters, meeting halls and other assembly facilities
-Children's schools, large daycare centers, hospitals, nursing homes
-Stadiums, group recreational uses

Safety Zone 4: Outer Approach/Departure Zone	**Accident and Exposure**



LONG FINAL



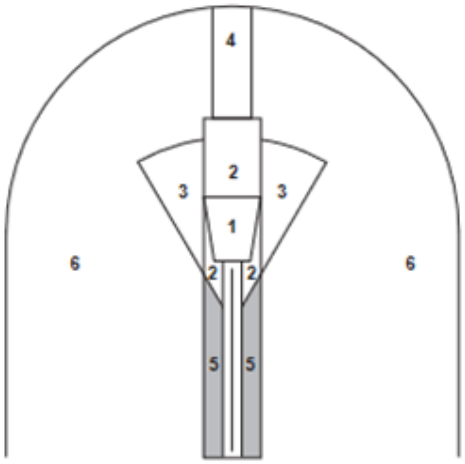
Accident Percentage Comparison
2000-2009: 2-6% of Acc
2008-2022: 1.22-1.43% (excludes Acc in PS)*
2008-2022: 0.45- 0.48% (includes Acc in PS)**

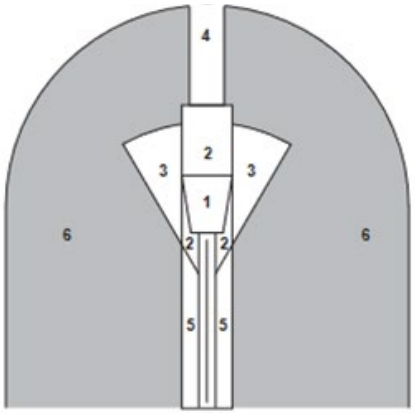
Exposure (potential consequences):
2021 LULC:
- 37.72% area developed
- 1.89% of high intensity development (2 mi buffer)

2001-2021 change to urban:
- 4.26%
- 51.14% of urban change occurred outside airport boundaries relative to total LULC change in Zone 4.

2011 risk level: Moderate
Current risk level:Low
Suggestion for hazard mitigation: None. Potentially reducing geometries to compensate for other zones needing larger dimensions.
Suggestion of exposure mitigation: None. Potentially applying less strict land compatibility policies to compensate for other zones with high exposure levels needing revision for more strict development policies.

Basic Compatibility Policies:
Normally Allow:
-Uses allowed in Zone 3
-Restaurants, retail, industrial
Limit:
-Residential uses to low density
Avoid:
-High-intensity retail or office buildings
Prohibit:
-Children's schools, large daycare centers, hospitals, nursing homes
-Stadiums, group recreational uses
Other Factors:
-Most low to moderate intensity uses are acceptable.
-Restrict assemblages of people
-Consider potential airspace protection hazards of certain
energy/industrial projects

Safety Zone 5: Sideline Zone	Accident and Exposure
 INITIAL LIFT-OFF OR LANDING TOUCHDOWN 	**Accident Percentage Comparison** 2000-2009: 3- 5% of Acc 2008-2022: 22.04- 25.71 % (excludes Acc in PS)* 2008-2022: 10.25- 11.03% (includes Acc in PS)** **Exposure (potential consequences):** 2021 LULC: ● 55.4% area developed ● 2.62% of high intensity development (2 mi buffer) 2001-2021 change to urban: ● 5.10% ● 0.82% of urban change occurred outside airport boundaries relative to total LULC change in Zone 5 2011 risk level: Low to Moderate **Current risk level: Very High** Suggestion for hazard mitigation: Urgent re-dimensioning, potentially increasing the sideline area. Suggestion of exposure mitigation: Maintain all prohibitions. Urgent validation of low to high development intensity classes in this zone, potentially increasing development restrictions closer to basic policies of Zones 1 and 2 due to generalized very high risk levels. **Basic Compatibility Policies** Normally Allow: -Uses allowed in Zone 4 (subject to height limitations for airspace protection) -All common aviation-related activities provided that FAA height-limit criteria are met Limit: -Nonresidential uses similarly to Zone 3 Avoid: -Residential uses unless airport related (noise usually also a factor) -High-intensity nonresidential uses Prohibit: Stadiums, group recreational uses ● Children's schools, large daycare centers, hospitals, nursing homes

Safety Zone 6: Traffic Pattern Zone	Accident and Exposure
 IN TRAFFIC PATTERN  	**Accident Percentage Comparison** 2000-2009: 18- 29% of Acc 2008-2022: 31.43- 36.67 % (excludes Acc in PS)* 2008-2022: 15.43- 16.61% (includes Acc in PS)** **Exposure (potential consequences):** 2021 LULC: ● 37.14% area developed ● 36.70 % of high intensity development (2 mi buffer) 2001-2021 change to urban: ● 4.44% ● 50.42% of urban change occurred outside airport boundaries relative to total LULC change in Zone 6. 2011 risk level: Low **Current risk level: Medium - Low** Suggestion for hazard mitigation: Revision of accident spatial patterns within Zone 6 due to the urgent need of re-dimensioning Zone 5. Optimizing the re-dimensioning of Zone 5 and Zone 6 due to likely concentration of accidents near Zone 5 boundary. Suggestion of exposure mitigation: Revision and validation of low to high development intensity classes in this zone, potentially increasing development restrictions near the boundaries of Zone 5 and Zone 2. **Basic Compatibility Policies:** Normally Allow - Residential uses (however, noise and overflight impacts should be considered where ambient noise levels are low) Limit: -Children's schools, large day care centers, hospitals, and nursing homes -Processing and storage of bulk quantities of highly hazardous materials Avoid: Outdoor stadiums and similar uses with very high intensities:

* Accident range for the 2008-2022 update calculated respectively relative to accidents in 2 mile buffer of airport boundary (2 mi buff) and relative to accidents in all Safety Zones (Tot SZ) using the NTSB 2011 method accident dataset that excludes primary surface accidents.
** Accident range for the 2008-2022 update calculated respectively relative to accidents in 2 mile buffer of airport boundary (2 mi buff) and relative to accidents in all Safety Zones (Tot SZ) using the NTSB Spatial Largest method accident dataset that includes primary surface accidents.

***The 2011 ALUP Handbook outlines qualitative differences in compatibility criteria suitable for each Safety Zone (p.4-18):

- Normally Allow: Typical examples of the use are acceptable.
- Limit: Use is acceptable with limitations on density or intensity.
- Avoid: Use generally should be permitted only if an alternative site outside the zone would not serve intended public function.
- Prohibit: Use should not be permitted under any circumstances.

**** The Safety Zones illustration are from the 2011 ALUP Handbook p. 4-20 to 4-25

3.4. Limitations and Uncertainty of the Safety Zones Risk Analysis and Next Steps

There are two major sources of uncertainty in this analysis, one is related to the spatial accuracy of the safety zones and different GIS layers used in this study, and the second is related to the risk assessment method and the difficulty in establishing continuity between the 2011 Handbook risk method and the current one. These uncertainties are underlined to better understand the limitations of this study's methods, provide a transparent baseline for decision-makers who will use this information for airport safety, and to provide a direction for improving the next generation analysis for safety zones and airport land use planning.

3.4.1. Dissensus between generic zones and real-life boundaries: primary runway surface and airport boundary example

GIS modeling carries uncertainties based on the accuracy of the datasets used and data processing methods. One major source of uncertainty pertains to the generic dimensions of the safety zones, which do not always correspond to the real-world boundaries set for each airport. This limitation was verifiable with the Primary Runway Surface dimensions that when contrasted with the 259 airport boundaries assessed in this study, were found to have 1.31% of their surface outside airport perimeters. Jurisdictionally primary surface zones are not allowed to be outside airport perimeters. This error can come from the airport boundary perimeters that carry their own inaccuracies. The major data source for the airport perimeters do not explain how these were drawn (Caltrans GIS Data: Aviation), and unless they are identified using a global positioning system (GPS), our assumption is that they were digitized based on aerial photography. As detailed in subsection 2.3.1. of Task 4.1The airport boundary GIS was built using 216 polygons from the Caltrans GIS and 43 were manually digitized. Digitization carries its own uncertainties that might also be reflected in this 1,31% error. Different from Safety Zone, Primary Runway Surfaces have more strict prescriptions according to FAA Part 77, based on runway parameters (length, precision instrument), and therefore this error is more easily identifiable. We can assume therefore that other Safety Zones also carry some level of error which comes from the airport specific adjustments to these zones to correspond to natural boundaries (topographic, water bodies, etc) or other location-specific safety and operations prescriptions that require an adaptation of the generic safety zones.

This Primary Surface error was further explored in the supplementary material of Task 4.1. “Primary Surface Boundary Error Exploration”, where examples of :slivers” primary surfaces outside airport perimeters are identified and statistically assessed (Figure 26). We estimate it does not impact the accident hazard results since only 3 accidents (from the NTSB Spatial Largest Dataset - 2008-2022) were found within these slivers. A total of 103 airports have “slivers” of Primary SUrfaces outside airport boundaries that range in area from 0.0041 sq mi, (maximum is for Modesto City-County Airport) to 1.1^{-6} sq mi as a minimum for 24CL airport at



Figure 26. Example of the Modesto City-County Airport (MOD) Primary Surface sliver located outside the airport boundary.

3.4.1. Mitigating errors due to the under-dimensioning of Safety Zone 6 GIS

After the December 2023 discussion between Caltrans engineers and UC Berkeley researchers, a discrepancy was identified in the position of Safety Zone 4 in relation to Zone 6. Zone 6 was under-dimensioned on previous analysis. Figure 27 illustrates the under dimensioned Zone 6 and the corrected Zone 6 with the SFO example. SFO is the airport with the largest under dimensioned area, estimated at 14.45 sq mi followed by OAK with 14.09 sq mi. A total of 247 airports have their zone 6 under dimensioned, and the potential error ranges from 14.45 sq mi for SFO to 0.32 sq mi for 0CL.

The new Zone 6 dimensions indicates that the cumulative Zone 6 area for 259 airports in this study is 1,349.59 sq mi insteal of 1064.77, giving us an under estimate of approximately 21.1% of the generic dimension provided by the ALUP Handbook schematics on p.3-17 to 3-19. This error was identified late in the project process, and therefore it was not possible to re-assess the results from Tasks 4 using the corrected Zone 6 GIS. Zone 6 with its corrected dimension is provided in Task 9 as “z6_dec2023correction” GIS layer.

We highlight that this error does nor significantly impact the accident risk results since only 10 new accidents would be computed to the corrected Zone 6 using NTSB Spatial Largest accident dataset, 5 wold be added using the NTSB Spatial Accuracy dataset, 7 new accidents would be computed for the NTSB 2011 Method dataset, and it did not change the calculations for the wildlife strike incidents within Safety Zone 6. From these 10 new accidents in the corrected Safety Zone 6, 3 events registered fatal injuries as the highest injury type, 1 registered serious injury, 4 registered minor injuries, and one has no injury. Given these added accidents to the corrected zone 6, and due to the discrepancy in size of zone 6 in relation to other safety zones, this error does not significantly impact the accident hazard density or percentage results, and it

does however reinforce the issues concerning the highest concentration of Fatal accidents in this zone when compared to other safety zones (except for the Primary Surface).

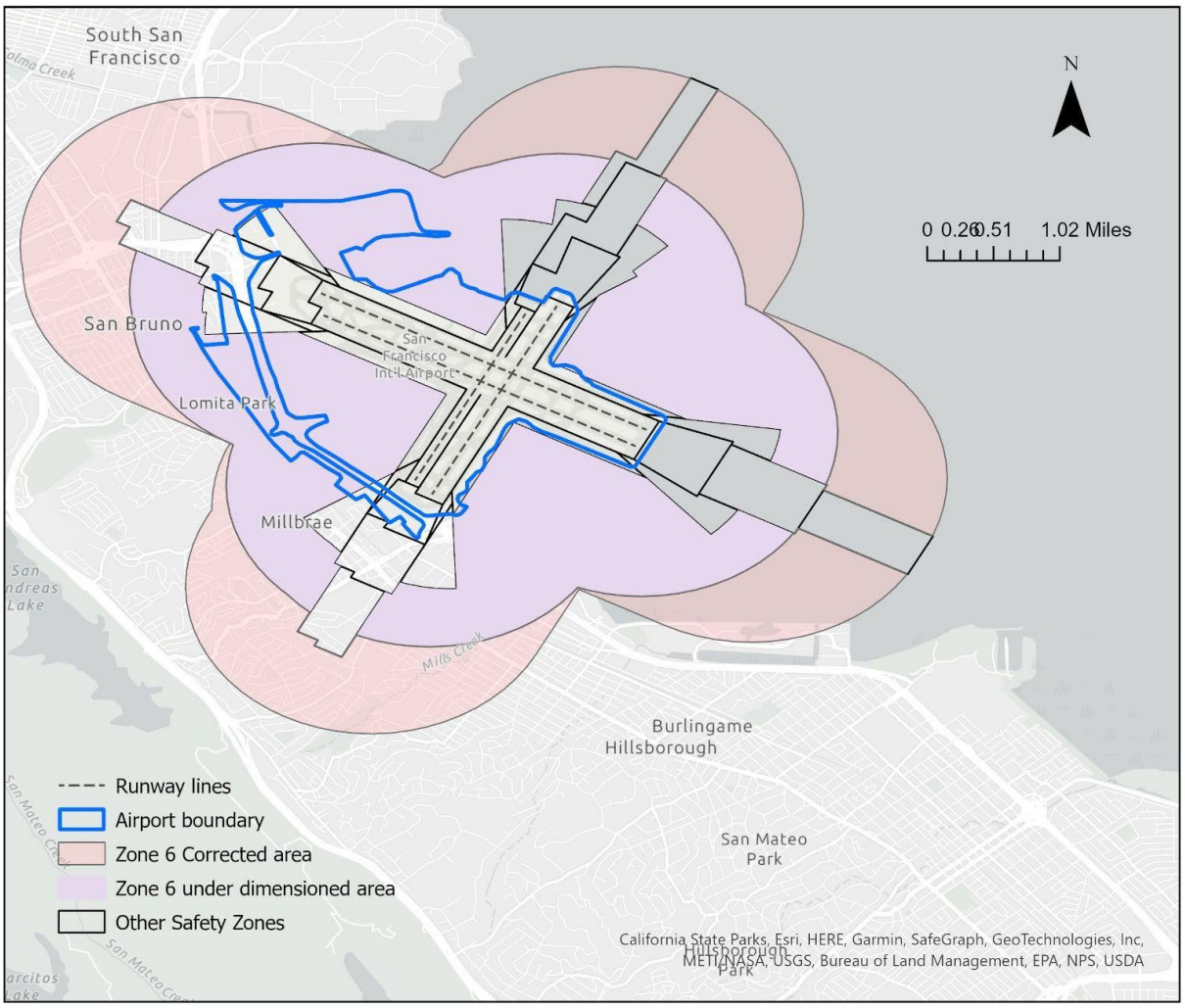


Figure 27. Example of Safety Zone 6 under dimension error for San Francisco International Airport (SFO) (given General Aviation Safety Zones).

3.4.3. Uncertainties Related to the Risk Assessment Method and Discontinuities Between ALUP Handbooks

One of the key advantages of the current methodology employed to assess the NTSB accident and wildlife strike incident data for safety zones is the larger number of incidents with improved geospatial accuracy. As explained before, this allows for a spatially-oriented analysis, where for the first time the generic safety zones are modeled in GIS together with other safety and accident data. The downside of this methodological change is the difficulty in establishing a clear continuity with what was developed in the previous handbook method. These discontinuities occur inherently because of the changes in the way the NTSB accident data has been recorded since 2008, but also because of the unclear calculation of risk levels of each safety zone.

The changes in the NTSB data recording methods, especially where it has increased spatial information and accuracy, could impact the comparative results between the 2000-2009 analysis (2011 Handbook) and the current method (2008-2022) simply due to the higher availability of dataset compared to before. A positive change in the availability of data for longitudinal analysis generally skews the results positively as well, i.e. we would have the impression that there was an increased occurrence of accidents than in reality simply to higher volume of data.

The uncertainties related to the discontinuity in risk levels are related to a lack of clarity of which thresholds were used to determine the different risk classes, and what the accident percentages are relative to based on the land use compatibility tables of the ALUP Handbook, p4-20 to 4-25. It is possible to interpret that the risk levels are associated to the accident percentages within, or close to each safety zone, however the thresholds for low, moderate, high, and very high risk are not described in the 2011 Handbook, nor is a clear description of how these percentages were calculated. We made an assumption that they represent the percentage of accidents within each safety zone relative to all the accidents within the 2 mile buffer (i.e. airport vicinity).

To mitigate discontinuity errors, Tasks 4 and Task 8 have detailed methodology supplementary materials, which are cross referenced with Task 9 dataset (Digitization Strategy Table) so that our methods can be reproduced from scratch with special attention to the safety and noise topics.

Understanding the risk method calculation is very important to trace the limitations of each method. Our method for risk thresholds (low, medium, high, and very high) is based on a combination of hazard metrics (normalized accident density) and exposure metrics (weighted development percentages per zone). One of the limitations of this method is that it reflects risk from cumulative hazard and exposure (cumulative metrics of all safety zones for 259 airports in California) and this does not take into consideration the airport-level hazard and exposure. This means that the hazard and exposure levels are measured within the range of hazard and exposure of the Primary Runway Surface and Safety Zones 1 to 6, but not the range of what is measured for each individual airport. One suggestion to further explore the proposed risk metrics is to calculate risk for each individual airport and their respective safety zones accident density and exposure percentages, then develop hazard and exposure level threshold (low, medium, high and very high) that correspond to the percentiles (quartiles) of what is measured in 259 airports instead of the range within the primary surface and safety zones. This airport-level result is expected to be similar to the cumulative analysis, however it would be enriching to better understand the settings of a high hazard and high exposure airport versus a low hazard and low exposure airport, even if the risk will be very low given the low accident numbers at the airport level for the 15 years assessed (n = 1,355 between 2008-2022). An airport-level risk assessment would also allow to improve risk metrics because it could be associated with the number of operations of each airport, which is key to enrich risk metrics from a probabilistic perspective.

Another key limitation of the current method is the low resolution of the exposure metrics (30m raster cells for LULC urban classes). There are numerous methodologies that can be applied to enrich the exposure metrics. Some examples include using higher resolution land cover data that might be available for specific counties in California; combining land use and aerial photography data with Light Detection and Ranging (lidar) which can be used to create high-resolution models of ground elevation and identifying building footprints; or by adding other GIS layers with critical infrastructure and vulnerable facilities (schools, hospitals) so that these can be weighted differently from other developed structures.

Finally an inherent limitation of the provided risk metrics is that it does not account for risk tolerance that is variable between airport communities, each community and/ or airport operators and owners can develop research to skew the risk thresholds to better reflect the tolerance for accident risk that takes into account the gains and losses of land use compatibility restrictions.

[8] Appendix A. Data Used for the Hazard and Exposure Levels

A.1. Exposure Data (% of LULC Developed classes)

Zone	Dev OS	Dev Low I	Dev Med I	Dev High I	Dev Tot
PS	19.11813	15.73483	23.64483	18.74144	77.23922
Z1	14.20398	9.919757	13.03354	8.903298	46.06058
Z2	9.248576	8.192686	14.24042	9.351854	41.03353
Z3	8.163089	7.887287	14.94649	10.12835	41.12521
Z4	6.681494	7.610763	16.10933	7.316299	37.71789
Z5	15.79729	9.533958	14.011	16.05905	55.40129
Z6	7.449923	7.579644	14.76865	7.345475	37.14369

LULC 2021 Class	Exposure weights
Dev. Open Space	x1
Dev. Low Intensity	x2

Dev. Med Intensity	x3
Dev High Intensity	x4

Zone	*EpW* Results
PS	196.488
Z1	108.7573
Z2	105.7626
Z3	109.2905
Z4	99.49622
Z5	141.1344
Z6	96.29707

A.2. Hazard Data (Accident Count and Densities)

Table A.2.1. NTSB 2011 Method Hazard Data

Zone	Acc. Count	Acc. Den.	Yearly Avr	Faa Likelihood*
Z1	33	1.027532	2.2	Remote
Z2	27	0.354362	1.8	Remote
Z3	16	0.16771	1.066667	Remote
Z4	3	0.054439	0.2	Extremely Remote

Z5	54	1.554301	3.6	Remote
Z6	77	0.072316	5.133333	Remote
Tot SZ	210	0.150984	14	Probable
2mi buff	245	0.047863	16.33333	Probable
CA	495	0.003131	33	Probable

*FAA Likelihood levels are calculated based on the temporal frequency of accidents according to Order 8040.4B on Safety Risk Management Policy from (05/02/2017) (See Figure A.2.1. below)

	Qualitative	Quantitative – Time/Calendar-based Occurrences Domain-wide/System-wide
Frequent A	Expected to occur routinely	Expected to occur more than 100 times per year (or more than approximately 10 times a month)
Probable B	Expected to occur often	Expected to occur between 10 and 100 times per year (or approximately 1-10 times a month)
Remote C	Expected to occur infrequently	Expected to occur one time every 1 month to 1 year
Extremely Remote D	Expected to occur rarely	Expected to occur one time every 1 to 10 years
Extremely Improbable E	Unlikely to occur, but not impossible	Expected to occur less than one time every 10 years

Figure A.2.1. FAA Order 8040.4B Accident Likelihood Definitions for General Aviation Operations/ SMall Aircraft and Rotorcraft

Table A.2.1. NTSB Large Dataset Hazard Data

Zone	Acc count	Acc den.	inj_f_ count	inj_f_d en	inj_s_ count	inj_s_d en	inj_m_ count	inj_m_ den	inj_n_ count	inj_n_den
PS	496	15.243	32	0.983	38	1.168	70	2.151	356	10.941
Z1	34	1.059	5	0.156	5	0.156	7	0.218	17	0.522

Z2	39	0.512	6	0.079	6	0.079	7	0.092	20	0.615
Z3	24	0.252	4	0.042	7	0.073	3	0.031	10	0.307
Z4	4	0.073	3	0.054	1	0.018	0	0.000	0	0.000
Z5	91	2.619	4	0.115	13	0.374	14	0.403	60	1.844
Z6	137	0.129	28	0.026	19	0.018	18	0.017	72	2.213
Tot SZ	825	0.593	82	0.059	89	0.064	119	0.086	535	16.442
2mi buff	888	0.173	94	0.018	102	0.020	133	0.026	559	17.179
CA	1360	0.009	188	0.001	165	0.001	235	0.001	772	23.725

[8] Appendix B. Rank of Airports With Highest Percentage of New Urban Development (To Urban LULC Change from 2001-2021, MLRC, 2023)

Rank	AID	To Urb. (sq mi)	2 mi buff (sq mi)	% to Urb
1	CNO	8.6017	23.3985	36.76

2	F70	6.3268	21.2592	29.76
3	RIV	8.4215	31.2842	26.92
4	UDD	4.0528	17.9321	22.60
5	SDM	3.8273	22.1092	17.31
6	SBD	4.5831	27.3969	16.73
7	CRQ	2.4691	18.7407	13.18
8	SCK	3.5139	26.9408	13.04
9	ONT	3.9959	30.7701	12.99
10	VCB	2.2550	18.9143	11.92
11	HMT	2.2893	19.2190	11.91
12	LVK	2.7190	25.1220	10.82
13	FAT	2.6547	24.7332	10.73
14	BFL	2.8104	26.4455	10.63
15	MYV	2.3159	22.4985	10.29
16	VIS	2.1695	21.1928	10.24
17	A89	1.7246	17.1951	10.03
18	E79	1.5170	15.2590	9.94
19	MHR	2.9865	31.5866	9.45

20	L65	1.6902	18.5079	9.13
21	IPL	1.9082	21.5678	8.85
22	TCY	1.6627	18.8229	8.83
23	SMX	2.0610	23.8765	8.63
24	TRM	2.2583	27.1961	8.30
25	PSP	2.0441	24.7294	8.27
26	N19	1.1218	14.0588	7.98
27	OXR	1.3987	19.3801	7.22
28	LSN	1.2064	16.9528	7.12
29	MAE	1.5270	21.6418	7.06
30	CMA	1.6344	23.4104	6.98
31	CIC	1.4761	21.5318	6.86
32	MOD	1.3735	20.2714	6.78
33	L45	1.1861	18.0737	6.56
34	O88	1.2535	19.7387	6.35
35	APC	1.3612	21.5318	6.32
36	MCE	1.2457	20.0106	6.23
37	O61	1.0626	17.1148	6.21

38	REI	1.0781	17.9804	6.00
39	DLO	1.1890	20.3147	5.85
40	BWC	0.9605	17.0760	5.63
41	2O6	0.9436	17.0057	5.55
42	LHM	1.2901	23.8350	5.41
43	MCC	1.4765	27.9986	5.27
44	SEE	0.9871	19.7662	4.99
45	FCH	0.8236	16.9942	4.85
46	CLR	0.8224	17.2885	4.76
47	O69	0.8367	18.4019	4.55
48	TLR	0.7382	17.6573	4.18
49	CPM	0.6621	16.1517	4.10
50	STS	0.9086	22.2043	4.09
51	O85	0.7172	17.8232	4.02
52	VCV	1.2951	32.2774	4.01
53	HJO	0.7777	19.5146	3.98
54	AJO	0.6816	17.1278	3.98
55	M90	0.6736	17.0811	3.94

56	SBP	0.7724	19.7136	3.92
57	0Q4	0.5987	15.4558	3.87
58	MER	1.1165	28.8469	3.87
59	SMF	1.4240	37.0557	3.84
60	RAL	0.7381	20.2407	3.65
61	TRK	0.7838	21.9604	3.57
62	RDD	0.8025	22.9253	3.50
63	L19	0.5783	16.6329	3.48
64	EDU	0.5627	16.3378	3.44
65	POC	0.6417	18.6831	3.43
66	AUN	0.6487	18.9092	3.43
67	L00	0.5466	15.9517	3.43
68	SAC	0.7082	20.8265	3.40
69	CCB	0.5627	16.8920	3.33
70	TSP	0.5929	17.8124	3.33
71	9CL	0.5024	15.1985	3.31
72	CXL	0.5970	18.6567	3.20
73	LPC	0.5486	17.2003	3.19

74	L35	0.5666	17.8394	3.18
75	N13	0.4716	14.9020	3.16
76	RIR	0.5079	16.2943	3.12
77	WVI	0.6008	19.4539	3.09
78	4CL	0.5410	18.6312	2.90
79	OKB	0.4467	15.8030	2.83
80	PTV	0.5811	21.2772	2.73
81	BNG	0.5059	18.6924	2.71
82	O27	0.4666	17.3645	2.69
83	SNS	0.5985	22.3718	2.68
84	0O4	0.4660	17.4269	2.67
85	RBL	0.5863	21.9636	2.67
86	FUL	0.3994	16.0171	2.49
87	WHP	0.4319	17.8405	2.42
88	L36	0.3630	15.8351	2.29
89	CVH	0.5045	22.3411	2.26
90	CL1	0.3342	14.8199	2.25
91	O37	0.4336	19.3911	2.24

92	MYF	0.4645	21.6914	2.14
93	L08	0.4008	19.0708	2.10
94	A69	0.3329	15.9249	2.09
95	SNA	0.4315	20.6500	2.09
96	E36	0.3701	17.7668	2.08
97	L52	0.3147	15.3703	2.05
98	PVF	0.3903	19.2595	2.03
99	E16	0.3631	18.1381	2.00
100	CA9	0.3130	15.6653	2.00
101	GOO	0.3796	19.1191	1.99
102	BUR	0.4603	23.3005	1.98
103	L18	0.3608	18.2949	1.97
104	SBA	0.4653	23.6162	1.97
105	L17	0.3216	16.3653	1.97
106	PRB	0.4945	25.5330	1.94
107	KIC	0.3221	17.3718	1.85
108	O52	0.3234	17.7051	1.83
109	APV	0.4576	25.2813	1.81

110	FOT	0.3097	17.1942	1.80
111	O60	0.2859	15.9694	1.79
112	F34	0.2830	15.8856	1.78
113	CCR	0.3568	20.1308	1.77
114	O41	0.2862	16.1785	1.77
115	WLW	0.3301	18.6917	1.77
116	OAR	0.3399	19.5600	1.74
117	SZP	0.2605	15.5684	1.67
118	BLH	0.5362	32.1513	1.67
119	TOA	0.3309	20.0234	1.65
120	L22	0.2677	16.3445	1.64
121	RIU	0.2685	16.7178	1.61
122	SJC	0.3708	23.1362	1.60
123	VNY	0.3638	22.9262	1.59
124	L56	0.2381	15.0252	1.58
125	L26	0.2478	15.9615	1.55
126	O63	0.2344	15.1810	1.54
127	BLU	0.2578	17.0129	1.52

128	WJF	0.3551	24.9006	1.43
129	RHV	0.2383	16.8340	1.42
130	O08	0.2296	16.8295	1.36
131	MRY	0.2789	20.8693	1.34
132	ACV	0.2725	20.8008	1.31
133	NUQ	0.2996	23.0800	1.30
134	OVE	0.2933	24.0905	1.22
135	LAX	0.4155	34.5860	1.20
136	OAK	0.3752	31.4300	1.19
137	UKI	0.2190	18.4070	1.19
138	O22	0.2381	20.7583	1.15
139	LGB	0.2956	25.9072	1.14
140	SAN	0.2494	22.1089	1.13
141	0Q9	0.1731	15.3868	1.12
142	JAQ	0.1870	16.8123	1.11
143	AAT	0.1932	17.7486	1.09
144	CEC	0.2248	20.6970	1.09
145	EMT	0.1886	17.3712	1.09

146	1O3	0.1807	17.0648	1.06
147	MHV	0.3218	30.7418	1.05
148	HES	0.1623	15.5967	1.04
149	CA0	0.1628	15.7961	1.03
150	HWD	0.2211	21.6986	1.02
151	O33	0.2154	21.7831	0.99
152	EKA	0.1621	16.4939	0.98
153	1Q1	0.1459	14.8831	0.98
154	BIH	0.2120	22.0209	0.96
155	MPI	0.1571	16.7410	0.94
156	0Q3	0.1663	17.8448	0.93
157	HHR	0.1573	17.0807	0.92
158	MIT	0.2262	25.6882	0.88
159	RNM	0.1661	18.8822	0.88
160	O54	0.1407	17.0562	0.82
161	SQL	0.1370	16.6662	0.82
162	2O1	0.1381	17.1033	0.81
163	1C9	0.1396	17.4902	0.80

164	DVO	0.1387	18.2355	0.76
165	SFO	0.2335	31.0147	0.75
166	D83	0.1089	15.3498	0.71
167	3O1	0.1181	16.8174	0.70
168	PAO	0.1138	16.6576	0.68
169	L70	0.1150	17.4133	0.66
170	D86	0.1108	16.9118	0.66
171	0O2	0.1170	18.1331	0.65
172	O81	0.0953	15.4967	0.61
173	1O2	0.1042	16.9825	0.61
174	F72	0.1169	20.1923	0.58
175	H37	0.0854	15.3582	0.56
176	O32	0.0923	17.3910	0.53
177	TVL	0.1127	21.3627	0.53
178	O09	0.0852	16.6604	0.51
179	36S	0.0821	16.2640	0.50
180	C83	0.1243	25.0148	0.50
181	O21	0.0744	14.9827	0.50

182	IZA	0.0855	17.2423	0.50
183	O26	0.0863	18.1682	0.48
184	0Q5	0.0761	16.0204	0.47
185	O05	0.0992	22.0626	0.45
186	1Q4	0.0848	18.8973	0.45
187	O16	0.0698	15.6394	0.45
188	3O8	0.0731	16.6257	0.44
189	O15	0.0851	19.4049	0.44
190	2O7	0.0723	16.9738	0.43
191	F62	0.0739	17.7889	0.42
192	E45	0.0680	16.6025	0.41
193	A24	0.0676	17.0212	0.40
194	E55	0.0664	16.7158	0.40
195	O28	0.0639	16.4871	0.39
196	SAS	0.0662	17.5865	0.38
197	2O3	0.0637	17.2045	0.37
198	1O5	0.0600	16.8265	0.36
199	SMO	0.0626	17.9390	0.35

200	H47	0.0528	15.5533	0.34
201	O89	0.0674	20.1345	0.33
202	L06	0.0690	20.8434	0.33
203	O02	0.0680	21.0049	0.32
204	HAF	0.0670	21.0407	0.32
205	8CL	0.0581	19.5581	0.30
206	SVE	0.0520	17.5268	0.30
207	CRO	0.0501	17.4360	0.29
208	O57	0.0464	16.5118	0.28
209	O79	0.0436	15.9325	0.27
210	O24	0.0463	17.3212	0.27
211	D63	0.0404	15.3105	0.26
212	L05	0.0440	17.4223	0.25
213	CN2	0.0360	14.9513	0.24
214	L90	0.0456	19.3616	0.24
215	DWA	0.0479	20.7650	0.23
216	L71	0.0433	19.7227	0.22
217	1O6	0.0329	15.7413	0.21

218	L73	0.0396	19.0596	0.21
219	A30	0.0333	16.1357	0.21
220	O86	0.0327	16.1269	0.20
221	SIY	0.0500	24.9381	0.20
222	1Q2	0.0362	18.0847	0.20
223	AVX	0.0295	15.7598	0.19
224	A32	0.0337	18.1658	0.19
225	C80	0.0442	23.8073	0.19
226	L77	0.0384	20.7889	0.18
227	MMH	0.0378	20.7088	0.18
228	LLR	0.0386	21.3341	0.18
229	L78	0.0285	17.0161	0.17
230	0O9	0.0254	15.3287	0.17
231	IYK	0.0376	23.7616	0.16
232	O19	0.0226	14.7363	0.15
233	7CA	0.0239	16.1498	0.15
234	S51	0.0223	15.1993	0.15
235	49X	0.0265	19.1248	0.14

236	L72	0.0230	18.0152	0.13
237	O59	0.0219	17.8390	0.12
238	L62	0.0214	18.2337	0.12
239	DAG	0.0269	23.3555	0.11
240	L88	0.0185	16.3719	0.11
241	A26	0.0169	16.1953	0.10
242	1Q5	0.0160	17.1014	0.09
243	EED	0.0223	23.7780	0.09
244	O55	0.0141	16.6142	0.08
245	TNP	0.0165	21.7253	0.08
246	T42	0.0118	17.5223	0.07
247	L61	0.0105	15.7189	0.07
248	O39	0.0088	15.3077	0.06
249	M45	0.0108	20.0248	0.05
250	O46	0.0109	21.4214	0.05
251	A28	0.0075	15.7376	0.05
252	6CL	0.0068	15.3096	0.04
253	CPU	0.0057	16.8755	0.03

254	L54	0.0054	16.8674	0.03
255	N64	0.0056	18.2044	0.03
256	CL3	0.0013	14.8142	0.01
257	N37	0.0014	17.0419	0.01

[10.A1] APPENDIX 1. Memorandum: Literature Review (based on original Task 2)

Overview of deliverable: The goal of this literature review is to support the set of possible Handbook modifications according to the identification and prioritization of airport land use compatibility topics of interest and concern developed in "Task 1 Acceptance Criteria". The outcome of Task 2 is a "living" document of key literature focusing on specific topics and items that are emerging and/or have significantly changed since the publishing of the 2011 Airport Land Use Handbook. This living document is composed of (I) a Literature Review Repository Table and (II) a "Summary Report" (developed below). Throughout the project, this Literature Review is designed to be modified based on the development of future tasks specific to each topic of concern, and based on feedback from Caltrans and its stakeholders.
Reviewed literature is organized based on topics of interest and concern for airport land use planning and further categorized into international, national, and California policy-levels. For almost all topics, at least one key policy document is provided from policy stakeholders directly involved in airport land use issues at the international, national, and state levels. This multilevel policy approach helps cover baseline standards, leading practices, trends, and opportunities to improve airport land use compatibility planning for each airport land use planning topic:

(a) *International aviation institutions such as the International Civil Aviation Organization (ICAO) or the Airports Council International (ACI), often describe world-wide leading*

practices and trends in airport land use planning, notably environmental concerns (noise and emissions reductions, carbon offset, sustainable fuels, climate resilience, ect)

(b) *National-level policies are covered by Federal Aviation Administration (FAA) Advisory Circulars (ACs) and technical reports, as well as publications from the Airport Cooperative Research Program (ACRP). FAA ACs provide baseline standards and guidance for compliance with 14 Code of Federal Regulations Aeronautics and Space Title. ACRP literature provides applied research on airport's pressing issues, including land use planning, traditional and notably emerging topics. The ACRP's problem identification and problem-solving guidelines are designed to address important cross-agency, collaborative research problems concerning airports that are overlooked in traditional sectoral research. Some of the emerging research topics include advanced air mobility (unmanned aircraft systems, electric aircrafts and hydrogen technologies); climate-induced hazard management (cost-benefit-analysis for airport climate resilience, adaptation planning); and applying Geographic Information Systems (GIS) and collaborative governance to improve land use compatibility planning strategies for airports.*

(c) *California-level policies identify key state regulations or technical and planning reports enforced by state agencies (Caltrans, Environmental Protection Agency,) that further specify environmental or safety thresholds as well as California-specific planning processes and concepts. Some of these include*

Literature on some topics of concern, especially emerging topics, are complemented by scientific articles and aviation business organizations reports.

[10.A1] 1. Literature Review Repository Table

The literature review repository with metadata on key reviewed policy documents, guidelines, standards, scientific articles, and technical reports in a readily retrievable table accessible through this link:
https://docs.google.com/spreadsheets/d/10aE3AYjuKVfMfYiodapw9IK4Vv8u3pgjW29_wepj5ok/edit?usp=sharing
This table is organized based on document type, author, date, target audience, target geography and topic. This literature repository also identifies airport land use compatibility information from each document such as specific environmental or safety metrics, thresholds, and or conceptual information. Asides from supporting development of UC Berkeley teams tasks, one of the potential outcomes of this table is to become an Appendix summarizing the literature review for each key topic of concern for airport land use planning. The goal is to structure the literature and policy so that Caltrans Aeronautics and other stakeholders such as Airport Land Use Commissions can easily access and filter key resources in the topics of their interest.

[10.A1] 2. Literature Review Summary Report

The literature review summary report synthesizes key documents identified in the Literature Review Repository. Section 1 synthesizes current airport land use planning guidelines; Section 2 summarizes key literature on environmental issues (noise, emissions, climate mitigation); Section 3 synthesizes key literature on safety issues (wildlife hazards, drone and laser incidents, climate-induced hazards), and Section 4 is dedicated to all encompassing or emerging topics such as airport economic development, urban development, advanced air mobility and equity.

1. Airport land use planning manuals
    a. International guidelines
    b. FAA standards
    c. California policies

2. Environmental concerns
    2.1. Noise
        a. International guidelines
        b. FAA standards:
            i. Airport operations can create sound levels that produce noise-induced annoyance in communities near airports
                1. Common factors that influence perceived noise impact include:
                    a. Proximity of a land use to an airport's flight patterns;
                    b. Residents/occupants noise sensitivity: noise annoyance and interference
                    to daytime and nighttime activities;
                    c. Building materials used to reduce interior noise levels;
                    d. The surrounding environment ambient noise level;
                    e. Perception and acceptance of the necessity of existing aircraft noise;
                    f. The typical day/night hours of aircraft operations;
                    g. The number and frequency of aircraft operations; and
                    h. The type of aircraft using an airport.
                2. Exterior noise levels at or above Day-Night Average Sound Level (CNEL) 60 decibels (dB) are considered incompatible with residences and some other noise sensitive land uses.
            ii.
        c. California policies
        d. Technical reports and scientific articles:

i. Analysis of the Neighborhood Environmental Survey
FICON curve might be underestimating annoyance levels, so purpose of the study was to update the relationship between aircraft noise exposure and the annoyance of individuals living in airport communities
ii. Relevant to the handbook because most recommendations are based on older dose response levels, so this can change how we view land use and noise exposure, especially in relation to residential neighborhoods

e. The Cost-Effectiveness of Lowering Permissible Noise Levels Around U.S. Airports
i. Analyzes the regulatory levels for noise exposure with respect to cost-benefits (cost of insulation against health benefits)
ii. Relevant due to once again thinking about the regulatory levels and the limitations they possess - we can't really change the regulations but we can recommend something to mitigate impacts

2.2. Emissions & Climate mitigation (emerging topic)
a. International guidelines
b. FAA standards:
i. 2021 Aviation Climate Action Plan
1. FAA document detailing different climate initiatives from different standpoints (airports, aircraft operations, etc.)
2. Useful to see where the policy is heading from a federal standpoint (and then compare to state standards for California)
c. California policies
d. Technical reports and scientific articles:

3. <u>Safety concerns</u>
3.1. Wildlife hazards
a. International guidelines
b. FAA standards:
i. Wildlife
1. Of the wildlife strikes reported to the FAA, the majority happened at or below 500 feet above ground level (AGL).
a. Nearly twice as many strikes occurred during the landing (final approach or landing roll) phase of flight than during takeoff run and climb.
2. Factors that contribute to this increasing wildlife collision threat include:
a. Populations of large bird and mammal species commonly involved in strikes have increased over the last few decades and are adapting to living in urban environments, including airports.

b. Older three and four engine aircraft are being replaced with newer, more efficient two-engine aircraft.
    i. In the event of multiple engine ingestion, aircraft with two engines may have vulnerabilities not shared by three or four engine aircraft
    ii. Newer, quieter engines may not be as easily detected by birds to avoid collision.
3. Minimizing land uses near airports that attract wildlife reduces the likelihood of wildlife strikes.
4. There are typically three categories of attractants: food, shelter/cover, and water.
    a. Common attractants include certain agricultural or aquaculture activities, architectural features, landscaping, surface mining, waste disposal sites, wastewater treatment facilities, and wetlands

c. California policies

3.2. Other hazards to safe navigation (Drones & Lasers) (emerging topic)
a. International guidelines
b. FAA standards
c. California policies

3.3. Climate-induced hazards (emerging topic)
a. International guidelines
b. FAA standards
c. California policies

4. <u>Other topics</u>

4.1. Urban Development
a. International guidelines
b. FAA standards
    i. Development Density
        1. The number of people concentrated in an area near an airport is the land use characteristic tied most closely to the consequences of aircraft accidents.
        2. Limit the maximum number of structures and/or people in areas close to an airport.
        3. Limiting the number of structures around airports may also reduce the severity of an aircraft accident to passengers on board the aircraft.
        4. Limiting the average usage density over a site, coupled with designated areas of open space, reduces the risks associated with either type of accident.

a. In general, the lower the density, the greater the level of compatibility.
b. Maintaining or creating open space within areas of aircraft movement is critical, as it provides clear areas where aircraft can land in the event of an emergency.

5. Types of Land Uses and Risks
    a. Residential Use
        i. As population increases, residential development often encroaches upon what was once open space surrounding airport property.
        ii. There are techniques that can be used to minimize or mitigate the effects of such incompatible development
        iii. Placement of residential structures on the outer edge of a parcel rather than directly underneath a runway's approach or departure path outside of RPZs.
        iv. Disclosing noise impact and discouraging residential development within 60 dB CNEL noise contour.
        v. Decreasing the allowable density in residential uses near an airport.
        vi. Minimizing the development of multi-family residential units
        (apartments, etc.).
        vii. Requiring developers to use sound-insulating building materials to minimize aircraft noise effects.
        viii. Purchasing vacant property within runway noise contours that are under threat of residential development.
    b. Commercial Use
        i. The most common land use compatibility issues with commercial uses are safety impacts to the commercial use, visual interference, and wildlife attractant impacts to aircraft and the airport.
        ii. Commercial uses are specifically discouraged from RPZs due to the density issues that they can pose.
        iii. Considerations when determining compatibility of a commercial use include:
            1. The time of operation and occupancy
            2. The size of the commercial buildings and their lighting, height and facility characteristics
            3. Anticipated occupancy

4. Method of trash containment for large commercial uses
5. Parking lot lighting patterns for large commercial uses
6. Outdoor uses
7. Amount of open space around the structures

c. Industrial or Mining Uses
    i. Industrial development can include materials processing, materials assembly, product manufacturing, and storage of finished products.
    ii. The most common land use compatibility issues with industrial uses are height of structures, visual interferences, and wildlife attractant impacts to aircraft and the airport.
    iii. Industrial/manufacturing uses are specifically discouraged from RPZs due to the assembly of persons/occupancy density issues that they can pose.
    iv. Considerations when determining compatibility of a commercial use include:
        1. Number of employees on site
        2. Hours of operation
        3. Tall towers or stacks that can obstruct flight
        4. The presence of smoke or steam from processing facilities
        5. Thermal plumes that can cause turbulence
        6. Intense lighting around facilities
        7. Dust generation
        8. Storage of flammable materials
        9. Water retention/detention areas.

d. Institutional Uses
    i. Institutional uses include educational facilities (preschool through college), health care facilities and religious assemblies
    ii. Because the majority of these facilities are used by individuals who may not be able to respond to an emergency situation without assistance, they are generally considered to have a lower level of compatibility and are discouraged in proximity to an airport.
    iii. The most common land use compatibility issues are safety and noise impacts to institutional uses
    iv. More sensitive to noise

1. Disruption in a classroom, hospital, or worship environment may be considered an impact to students, patients, and congregations.

e. Infrastructure/Utilities/Energy Production Uses
    i. Infrastructure activities include a variety of land uses such as above ground utilities, cellular communication towers, water towers, water treatment plants, wastewater treatment plants, streets and highways, sanitary landfills, and energy production uses such as wind turbines and solar panels.
    ii. One of the most common land use compatibility issues with infrastructure uses is the height impacts to aircraft
    iii. Some of these uses can be attractive to wildlife.
        1. Could increase the risk of wildlife strikes if placed within the approach or departure corridors or traffic pattern around an airport.
    iv. Electronic interference generated can impact radio aids to navigation and RADAR signals when clustered together in large concentrations.
    v. Industrial uses emitting thermal plumes above their smoke/exhaust stack heights may impact safe flight near airports.
    vi. Transportation infrastructure
        1. Limiting transportation modes within the approach or departure zones can minimize the potential for catastrophic effects should an aircraft incident occur.
        2. Techniques such as down shielding lighting along highways and railroads can help to mitigate some of their impact (visual obstructions)
        3. Adding roadway signage alerting vehicles to the RPZ, or prohibiting stopping and standing in the RPZ is recommended
        4. Avoid locating stoplights near the edge of the RPZ to prevent queues from building into the RPZ

f. Agriculture and Open Spaces
    i. Agriculture and open space activities are most commonly defined as any use related to farming,

including both man-made and naturally occurring water resources.
ii. Most common land use compatibility issues are wildlife attractant impacts to aircraft and the airport
iii. Often perceived as the most compatible of land use types near an airport due to the limited populations associated with them and reduced noise sensitivity.

ii.

c. California policies
d. Technical reports and scientific articles
    i. Analysis and Discussion of California's Housing Shortage, Recent Laws, and Airport Impacts
        1. Substantive overview of the issues relating to the housing crisis in CA and how that impacts the communities around airports
            a. Brings in the legal angle too with the different applicable laws
        2. Written by a member of the Caltrans Aero team and is a very relevant source for equity and land use relationships, especially as they navigate the housing angle

4.3. Advanced Air Mobility (emerging topic)
a. International guidelines
b. FAA standards
c. California policies

4.4. Equity and Environmental Justice (emerging topic)
a. International guidelines
b. FAA standards
c. California policies
d. Technical reports and scientific articles:
    i. Investigation of Environmental Justice Analysis in Airport Planning Practice from 2000 to 2010
        1. Defines a new metric for an airport’s expected level of risk for disproportionate impacts in airport adjacent communities (based on presence of minority and low income groups)
        2. Can be an interesting method to use for equity analysis for the handbook, but even if it is not used, the article is relevant to our discussions of equity and how we view it
    ii. Confronting Transportation Sprawl in Metro Atlanta
        1. While this chapter of the book addresses ATL specifically, I thought it was important to think about the equity implications through this case study (ATL is one of the busiest airports in the

US and CA also is home to some of the highest levels of aviation traffic)

2. It's a great case study because it goes more into the "big picture" with regards to how airports impact these neighboring communities
    a. In addition to equity issues and environmental impacts, it does bring up economic value and more housing implications for the areas as well

[10.A2] APPENDIX 2. Memorandum: Identify emerging transportation modes and technologies and determine their contributions to the ALUP handbook (based on original Task 5)

Deliverable: A memorandum discussing emerging transportation modes and technologies that may be suitable for inclusion into the ALUP handbook.

[10.A2] 1. Introduction

After reviewing the current California Airport Land Use Planning (ALUP) Handbook, it is evident that the content primarily focuses on the first decade of the 21st century aspects of airport land use, including noise impact, safety zones, and aircraft accident characteristics. There is a thorough analysis of factors influencing noise annoyance in communities surrounding airports, measurement of aircraft noise, and detailed studies on aircraft accidents' characteristics and locations relative to the runways.

The handbook was published in 2011, and therefore it does not address today's emerging air transportation modes such as Advanced Air Mobility (AAM) and technologies, such as electric, hybrid, and turboelectric fixed-wing aircraft, electric Vertical Take-Off and Landing (eVTOL) aircraft, and Unmanned Aerial Systems (UASs, a.k.a. drones). These emerging air

transportation modes and technologies, which started to occur after the handbook was published, are crucial for updating the ALUCP handbook, as they represent significant shifts in airside transportation and technology.

Although landside surface technologies and novel surface transportation modes have contributed to overall urban mobility and micro-mobility improvements, they are not covered in this Task as they do not impact the airport airside (and more specifically the Airport Safety Zones). The arrival of automated electric surface vehicles, other green surface vehicles that use hydrogen or hybrid fuels, electric scooters, and other surface vehicles used to enhance micro-mobility have been utilized for personal and shared mobility and micro-mobility. The shared mobility concepts include transportation network companies (TNCs) that provide on-demand services for passengers (individuals or groups), or electric scooters and bicycles for micro-mobility. These concepts are mainly utilized on surface roads, while TNCs are greatly utilized in airports' landside areas (airport access roads, terminal curbsides, and parking garages).

The new aviation-related technologies offer benefits such as reduced emissions, lower operating costs, increased efficiency, and novel propulsion systems. However, they also present challenges, including integration into current regulations and airspace systems, safety concerns, and infrastructure adaptations.

To incorporate these elements into the new ALUP Handbook, it is necessary to discuss the following airside issues: (I) integration of novel aircraft designs, technologies, and systems developments, (II) safety and performance metrics, (III) implications to Airport Safety Zones, and (IV) noise.

[10.A2] 2. Innovations in Aircraft Design, Technology, and Transport Systems

2.1. Recent Innovations and Classification

The last decade has seen significant growth in the research and development of electric aircraft propulsion, hybrid electric aircraft, hydrogen-powered aircraft, as well as eVTOLs, and UASs. This development is primarily driven by the need to reduce the environmental impact of aviation, with electric propulsion (EP) being seen as a key technology in achieving this goal. The primary focus has been on fixed-wing aircraft, encompassing all-electric, hybrid electric, and turboelectric architectures (Brelje & Martins, 2019).

2.2. Classification of Electric Aircraft (fixed wing)

Electric aircraft can be classified based on the degree of hybridization of their power and energy sources. The classification ranges from conventional aircraft with no electric power for propulsion, all-electric aircraft that exclusively use electrical energy and power, hybrid electric aircraft that mix fuel and electrical energy, to turboelectric aircraft that use combustible fuel for energy storage but electric power for propulsion (Isikveren et al., 2014 & Brelje & Martins, 2019b)

2.3. Classification of Hydrogen-Powered Aircraft (fixed wing)

Two types of Hydrogen-Powered Aircraft are classified based on their size and usage: a turboprop for regional markets and a narrow-body turbofan for short and medium-haul flights. When they are compared with current aircraft models like the ATR 72 and Airbus A320neo, they offer a comprehensive view of the technical and economic feasibility of liquid hydrogen (LH2) propulsion in aviation. The emphasis is on the necessity for evolutionary design changes by 2035, rather than revolutionary shifts, highlighting a practical approach to integrating LH2 technology in future aircraft designs.

2.4. Classification of Electric Vertical Takeoff and Landing (eVTOL) Aircraft

Vectored Thrust eVTOLs resemble traditional aircraft but are equipped with rotors or fans that can pivot to provide both vertical and forward thrust. They are used for efficient, longer-distance urban air mobility (Rakas et al., 2021).

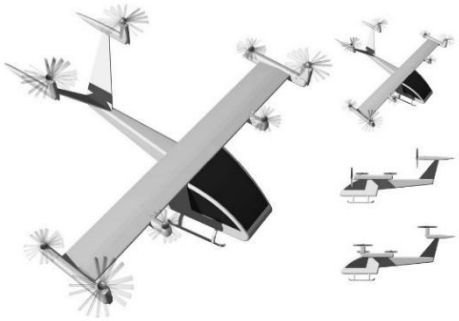


Fig. 1. Vectored Thrust frame schematic (Rakas et al., 2021).

Wingless frame schematic eVTOLS are multirotor air vehicles with large disk actuator surfaces, efficient in hover but lack a wing for efficient cruising. They are suited for short-range operations in cities, such as flying over traffic jams. Examples include the E-Hang 184 and the Volo copter 2X (Rakas et al., 2021).

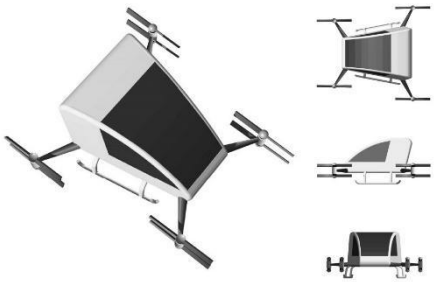


Fig. 2. Wingless frame schematic (Rakas et al., 2021).

Lift+Cruise frame schematic eVTOLs have fixed wings with separate lift and cruise systems, typically rotors for lift and propellers for cruise. They are suitable for longer-range urban air mobility due to their efficient cruise capabilities (Rakas et al., 2021).

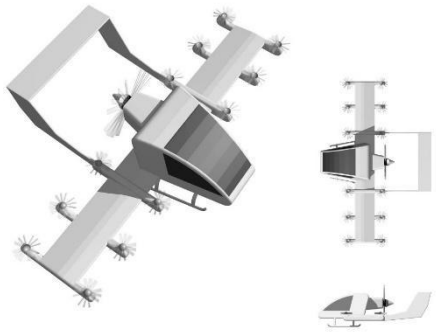


Fig. 3. Lift+Cruise frame schematic (Rakas et al., 2021).

Electric Rotorcraft frame schematic eVTOLs are akin to helicopters, powered by electric motors. They are ideal for vertical takeoff and landing in urban and regional settings (Rakas et al., 2021).

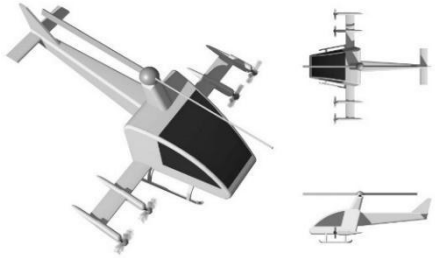


Fig. 4. Electric Rotorcraft frame schematic (Rakas et al., 2021).

2.4.1. Specific Use of eVTOLs

In the early stages of deployment, eVTOLs may utilize existing helicopter routes. As the aerospace structure evolves, separate routes will be developed for eVTOLs, depending on their classification and capabilities (see Task 4.1.1. subtask (1)).

For Unmanned Aerial Systems (UASs), also known as drones, the classifications and airspace regulations are as follows:

2.5. Classification of UASs

Based on Weight and Altitude and Range: This classification is broad and includes various categories based on the UAV's weight and the altitude and range it can cover (Chamola et al., 2021).

2.5.1. Based on Design:

i. Fixed Wing: UAVs with an aeroplane-like design and fixed wings.

ii. Single Rotor: Resemble helicopters with one main rotor and a smaller tail rotor.

iii. Multi-rotor: UAVs with more than one rotor, like quadcopters, hexacopters, etc.

iv. Fixed-Wing Hybrid VTOL: These UAVs combine fixed-wing stability with the ability to hover, take off, and land vertically (Chamola et al., 2021).

2.5.2. Based on Application:

i. Personal: For videography and entertainment.

ii. Commercial: Infrastructure monitoring, product delivery, aerial imaging.

iii. Government and Law Enforcement: Firefighting, patrolling.

iv. Military: Surveillance, combat attacks (Chamola et al., 2021).

2.5.3. Based on Altitude and Range:

Different classes such as NATO, Tactical, MALE, HALE, and Hypersonic UAVs, each defined by specific altitude and range parameters (Chamola et al., 2021).

2.5.4. UAS Airspace Classification:

In the United States, UASs are permitted to operate in Class G airspace, which is uncontrolled and extends up to 700 feet at airports with an Instrument Approach Procedure (IAP) and 1200 feet at those without. Operating in controlled airspace requires explicit authorization from the relevant authorities.

[10.A2] 3. Technological Parameters and Challenges

The feasibility of electric propulsion depends heavily on specific energy (energy per unit mass) and specific power (power per unit mass). Electric aircraft face the challenge of

batteries having significantly lower specific energy compared to liquid fuels, impacting range and payload (Antcliff et al., 2016; Isikveren et al., 2017; Marwa et al., 2017).

Low specific energy of batteries results in heavier takeoff gross weight (TOGW) and higher total energy consumption. Projections suggest specific energy of batteries could reach 400–1000 Whr/kg by 2035 (Jansen et al., 2017; Rheaume & Lents, 2016).

Electrical efficiency is crucial, with improvements leading to better range and reduced waste heat. Theoretically, electric aircraft could surpass combustion engines in efficiency, but the weight of batteries currently negates this advantage for long-range flights (Brelje & Martins, 2019).

[10.A.2] 4. Commercial Developments and Conceptual Studies

a) There have been significant developments in manned electric fixed-wing aircraft, with several models already flown and others expected to fly soon. These include various electric motor gliders and demonstrators like the Pipistrel Alpha Electro, focused on trainer aircraft applications (Karthik et al., 2021; Gierulski & Khandelwal, 2021).

b) The European aviation community has also been active in developing advanced electric propulsion (EP) concepts such as the Airbus-funded VOLTAIR, featuring unique designs such as aft-mounted boundary layer ingestion propulsors and natural laminar flow wings (Brelje & Martins, 2019a)

4.1. Advanced Concept Studies:

a) NASA-funded studies and industry collaborations have resulted in concepts such as the Boeing SUGAR series and Empirical Systems Aerospace's (ESAero) ECO-150, exploring the potential of hybrid electric and turboelectric architectures. These studies show promising fuel burn reductions but also highlight the challenges in balancing technology and design parameters (Brelje & Martins, 2019b)

b) A range of manned electric fixed-wing aircraft and prototypes have been developed, with a focus on scaling up power and exploring new configurations, such as those with higher aspect ratios and different propulsion systems (Kartik et al., 2021). Innovative concepts like NASA's SCEPTOR and LEAPtech aim to reduce drag and increase cruise wing loading through distributed propulsion (Borer et al., 2016).

c) According to the National Business Aviation Association, the construction of vertiports involves considerations such as accommodating multiple aircraft, recharging facilities, parking spaces, and emergency response capabilities.

   As per the Engineering Brief No. 105 on Vertiport Design (FAA, 2022) vertiports are specialized facilities designed for eVTOLs, incorporating both public and private

ports, and even modifications of existing helicopter and airplane landing sites. Key design elements include:

- ❖ Touchdown and Lift Off (TLOF) Area: Central area for eVTOL landing and takeoff.
- ❖ Final Approach and Takeoff Area (FATO): A broader area encompassing the TLOF for safe operation.
- ❖ Safety Area: Surrounding the FATO, it ensures safety during operation.
- ❖ Lighting and Visual Aids: Essential for navigation and operation during different times of the day.

Since eVTOLs are still new, the FAA acknowledges the need for further research to understand eVTOL taxiing, parking needs, and comprehensive vertiport design (FAA, 2022)

[10.A2] 5. Benefits and Risks of Electrification

Electrification can lead to operating cost savings by replacing jet fuel with electricity, especially for shorter flights. It also offers the potential for significant carbon emissions reductions, depending on the electricity source (Greer et al., 2021; Zaporozhets et al., 2020)

All-electric aircraft may have higher theoretical efficiency by eliminating the thermodynamic cycle of combustion engines. Additionally, there is an expectation (though not yet quantitatively backed) that electric motors may incur lower maintenance costs compared to traditional turbofans (Greer et al., 2021; Zaporozhets et al., 2020).

[10.A2] 6. Safety and Performance Metrics

Safety in electric and hybrid aircraft involves ensuring the reliability of these new systems under various operational conditions. Metrics used to assess the performance of electric propulsion include fuel burn, total energy consumption, CO2 emissions, operating costs, and takeoff gross weight. These metrics are influenced by the aircraft's aerodynamic, propulsive, and electrical efficiency, specific energy and power, weight, system reliability, and complexity (Brelje & Martins, 2019).

Additionally, the development of higher-specific energy batteries, improvements in electrical component efficiency, and the utilization of advanced design and simulation tools are crucial for overcoming challenges in electric and hybrid propulsion systems. Rigorous testing and validation within aviation standards are essential for ensuring safety in these new operations. The motivation behind this technological evolution is the potential for reduced environmental impact and operational costs, yet achieving the requisite safety levels is an ongoing, multidisciplinary challenge (Committee on Propulsion and Energy Systems to Reduce Commercial Aviation Carbon Emissions, 2016; Isikveren et al., 2017; Jansen et al., 2017; Rheaume & Lents, 2016).

In the domain of UAS, especially eVTOL aircraft, safety revolves around several key areas. This includes vertiport design and location, where factors like multiple aircraft accommodation,

recharging facilities, and emergency response preparedness, including water availability for electric aircraft fires, are emphasized. Additionally, compliance with evolving FAA standards for vertiports is crucial for ensuring safety (FAA, 2022).

Performance metrics for UASs, particularly eVTOLs, extend to the development of efficient battery systems, payload and range considerations critical for EMS and cargo applications, and operational efficiency, including vertiport turnaround times and the capability to handle multiple aircraft operations (Chamola et al., 2021).

The focus on safety and performance, along with regulatory alignment, environmental considerations, and integration into existing infrastructures, is key for the successful and sustainable development of the advanced air mobility ecosystem. This integrated approach, as supported by various studies and committees, ensures a balanced progression in this innovative aviation field (Rakas et al., 2021; Schunck & Osborne, 2021).

[10.A2 7. Implications for Airport Safety Zones

The integration of new UASs, electric, and hybrid aircraft into airport safety zones under FAA FAR 77 rules presents both challenges and opportunities. It requires a comprehensive re-evaluation of airport design, infrastructure, safety protocols, and operational strategies.

1. Drones operating in and around airports must be strictly regulated to avoid interference with manned aircraft. This includes adherence to Class G airspace restrictions or obtaining special permissions for controlled airspace operations.

2. The introduction of electric and hybrid aircraft necessitates modifications to airport infrastructure. This includes charging/fueling stations, maintenance facilities equipped to handle new technologies, and potentially redesigned taxiways and runways to accommodate different aircraft dimensions and operational needs.

3. Electric and hybrid aircraft, with potentially lower noise levels and emissions, could allow for revised noise and emission control zones around airports, impacting land use planning and community relations.

4. Airports must develop new emergency response strategies and safety protocols tailored to the unique risks associated with electric and hybrid aircraft, including battery fires and electrical system failures.

5. The integration of eVTOLs and Short Takeoff and Landing air vehicles (STOLs), with their unique flight characteristics, requires updates to air traffic management systems to ensure safe and efficient operations within and around airport safety zones. This includes establishing specific flight paths, altitude restrictions, and operational protocols to avoid airspace conflicts with traditional aircrafts.

6. The integration of vertiports into existing airport infrastructure poses challenges in terms of airspace management and safety. The FAA's conservative approach in the interim guidance ensures an acceptable level of safety performance and operation. Coordination with FAA Regional or Airports District Offices is essential for facilities serving non-standard eVTOLs.

Continuous collaboration between industry stakeholders, regulatory bodies, and airports is essential to successfully navigate these changes and realize the potential benefits of these emerging technologies.

[10.A2] 8. Noise

EP has become a crucial research topic, driven by the need to reduce environmental impacts, including noise pollution. This discussion, based on the scholarly and business literature, examines the noise aspect of electric, hybrid electric, and turboelectric fixed-wing aircraft, with a focus on developments since 2000 and their implications for noise reduction (Committee on Propulsion and Energy Systems to Reduce Commercial Aviation Carbon Emissions et al., 2016).

8.1. Development of UASs and eVTOLs

Parallel to the developments described above, there is a growing interest in UASs and eVTOL aircraft. These modern aircraft types are anticipated to produce less noise compared to traditional aircraft. Such a reduction in noise levels is particularly beneficial in the vicinity of airports, where noise pollution is a major concern. The integration of UASs and eVTOLs into aviation systems, therefore, holds promise for alleviating these noise pollution concerns, complementing the efforts in electric propulsion to create a more environmentally friendly and quieter aviation industry (Rakas et al., 2021).

8.2. Development of Electric Aircraft

Since 2000, at least 17 manned electric fixed-wing aircraft have flown (Brelje & Martins, 2019), with three commercially available products. Recent developments have focused on scaling up power, with notable examples like the Pipistrel Alpha Electro and the Siemens Extra 300. These advancements have set new benchmarks for electric propulsion power and efficiency, contributing to noise reduction (Jansen et al., 2017, Yates et al., 2017)

8.3. Direct Benefits of Electrification in Reducing Noise

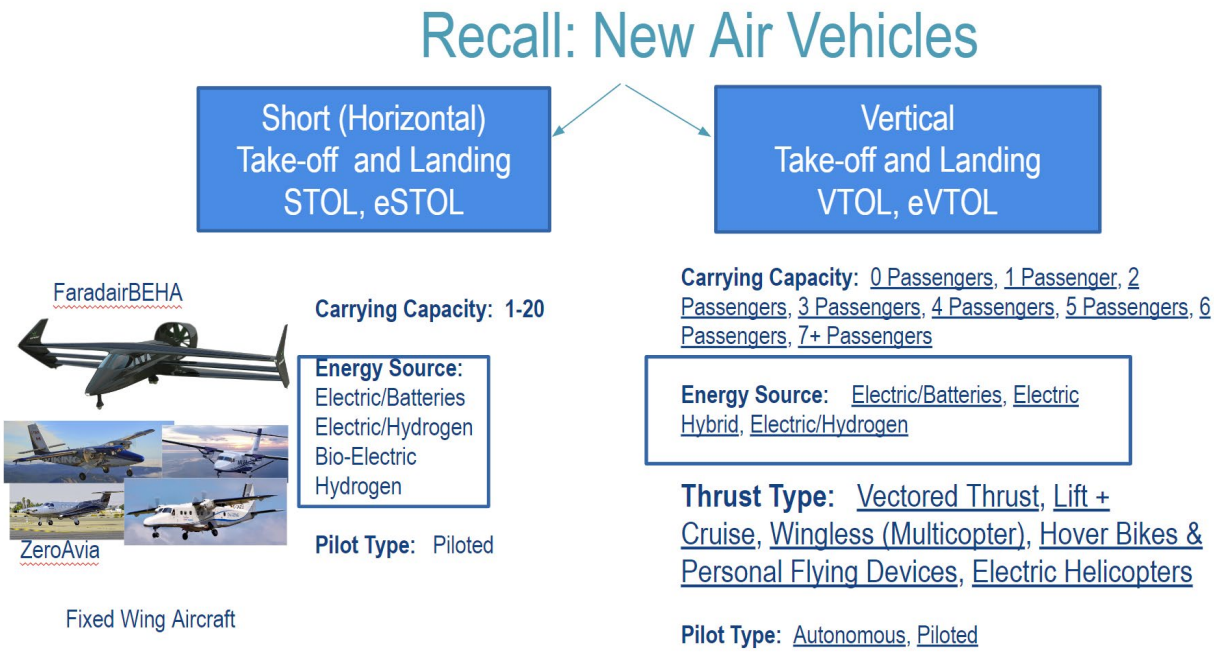
Electrification offers direct benefits in reducing noise, especially for shorter missions. As the specific energy of batteries improves, a larger share of missions can be flown using electric energy, contributing to lower noise levels. Moreover, the theoretical efficiency advantage of electric propulsion over conventional engines, especially if superconducting materials and power electronics are used, further enhances noise reduction (Antcliff et al., 2021).

8.4. Propulsion Effects on Noise

In electric aircraft, the decoupling of fan and turbine speeds allows for operation at optimal points, enhancing efficiency and reducing noise. Turboelectric and series hybrid architectures capture the benefits of reduced fan speed and shaft speed decoupling. Boundary Layer Ingestion (BLI) further increases propulsive efficiency by ingesting slower air, thereby reducing noise. The unique scaling properties of electric motors make BLI more feasible compared to conventional engines (Antcliff et al., 2021).

The integration of these technologies into existing regulatory frameworks, including compliance with noise standards, will be crucial for their widespread adoption and acceptance.

Summary:



[10.A2] 9. Citations

Antcliff, K. R., Guynn, M. D., Marien, T., Wells, D. P., Schneider, S. J., & Tong, M. J. (2016, January 4). Mission Analysis and Aircraft Sizing of a Hybrid-Electric Regional Aircraft. *54th AIAA Aerospace Sciences Meeting*. 54th AIAA Aerospace Sciences Meeting, San Diego, California, USA. https://doi.org/10.2514/6.2016-1028

Antcliff, K., Borer, N., Sartorius, S., Saleh, P., Rose, R., Gariel, M., ... & Oullette, R. (2021). Regional Air Mobility: Leveraging Our National Investments to Energize the American Travel Experience.

Bradley, M.K., Droney, C.K. (2015) Subsonic Ultra green aircraft research: phase II – volume II – hybrid electric design exploration, NASA/CR–2015–218704. doi:2060/20150017039. URL https://ntrs.nasa.gov

Brelje, B. J., & Martins, J. R. R. A. (2019). Electric, hybrid, and turboelectric fixed-wing aircraft: A review of concepts, models, and design approaches. *Progress in Aerospace Sciences*, *104*, 1–19. https://doi.org/10.1016/j.paerosci.2018.06.004

Borer, N. K., Patterson, M. D., Viken, J. K., Moore, M. D., Bevirt, J., Stoll, A. M., & Gibson, A. R. (2016, June 13). Design and Performance of the NASA SCEPTOR Distributed Electric Propulsion Flight Demonstrator. *16th AIAA Aviation Technology, Integration, and Operations Conference*. 16th AIAA Aviation Technology, Integration, and Operations Conference, Washington, D.C. https://doi.org/10.2514/6.2016-3920

Chamola, V., Kotesh, P., Agarwal, A., Naren, Gupta, N., & Guizani, M. (2021). A Comprehensive Review of Unmanned Aerial Vehicle Attacks and Neutralization Techniques. *Ad Hoc Networks*, *111*, 102324. https://doi.org/10.1016/j.adhoc.2020.102324

Committee on Propulsion and Energy Systems to Reduce Commercial Aviation Carbon Emissions, Aeronautics and Space Engineering Board, Division on Engineering and Physical Sciences, & National Academies of Sciences, Engineering, and Medicine. (2016). *Commercial Aircraft Propulsion and Energy Systems Research: Reducing Global Carbon Emissions* (p. 23490). National Academies Press. https://doi.org/10.17226/23490

EADS, VoltAir all-electric transport concept platform, Brochure. URL https:// www.airbusgroup.com/service/mediacenter/download/?uuid=1af7b378-404c- 4345-a243-a13de66a2dbd

FAA (2023). FAADRoneZone https://faadronezone-access.faa.gov/#/

FAA (2022). Engineering Brief #105, Vertiport Design. https://www.faa.gov/sites/faa.gov/files/eb-105-vertiports.pdf

Gierulski, M. P., & Khandelwal, B. (2021). Electric-powered aircraft. In *Aviation Fuels* (pp. 271–296). Elsevier. https://doi.org/10.1016/B978-0-12-818314-4.00009-1

Greer, F., Rakas, J., & Horvath, A. (2021). Reduce aviation's greenhouse gas emissions through immediately feasible and affordable gate electrification. *Environmental Research Letters*, *16*(5), 054039. https://doi.org/10.1088/1748-9326/abf7f1

Isikveren, A. T., Pornet, C., Vratny, P. C., & Schmidt, M. (2017). Optimization of Commercial Aircraft Using Battery-Based Voltaic-Joule/Brayton Propulsion. *Journal of Aircraft*, *54*(1), 246–261. https://doi.org/10.2514/1.C033885

Jansen, R., Bowman, C., Jankovsky, A., Dyson, R., & Felder, J. (2017, July 10). Overview of NASA Electrified Aircraft Propulsion (EAP) Research for Large Subsonic Transports. *53rd AIAA/SAE/ASEE Joint Propulsion Conference*. 53rd AIAA/SAE/ASEE Joint Propulsion Conference, Atlanta, GA. https://doi.org/10.2514/6.2017-4701

Karthik, A., Chiniwar, D. S., Das, M., Pai M, P., Prabhu, P., Mulimani, P. A., Smt Kamala, Sri Venkappa M., Samanth, K., Naik, N. (2021). Electric Propulsion for Fixed Wing Aircraft – A Review on Classifications, Designs, and Challenges. *Engineered Science*. https://doi.org/10.30919/es8d573

Marwa, M., Martos, B., Martin, S. M., & Anderson, R. (2017, January 9). Analytical Forms of the Range Performance of Hybrid and Electric Turboprop Aircraft, for Design Optimization Studies. *55th AIAA Aerospace Sciences Meeting*. 55th AIAA Aerospace Sciences Meeting, Grapevine, Texas. https://doi.org/10.2514/6.2017-0211

Rakas, J., Jeung, J., So, D., Ambrose, P., & Chupina, V. (2021). eVTOL Fleet Selection Method for Vertiport Networks. *2021 IEEE/AIAA 40th Digital Avionics Systems Conference (DASC)*, 1–10. https://doi.org/10.1109/DASC52595.2021.9594309

Rheaume, J. M., & Lents, C. (2016). *Energy Storage for Commercial Hybrid Electric Aircraft*. 2016-01–2014. https://doi.org/10.4271/2016-01-2014

Thomson, R., Sachdeva, M., Nazukin, N. Martinez, N. (2017). Aircraft electrical propulsion – the next chapter of aviation? https://www.rolandberger.com/en/Publications/pub_new_trends_in_electric_aircraft.html.

Schunck, K., & Osborne, C. (2021). Whitepaper Mapping the Advanced Air Mobility (AAM) ecosystem. Lufthansa Innovation Hub.

W.C. Yates, Personal Communication, (2017).

Zaporozhets, O., Isaienko, V., & Synylo, K. (2020). Trends on current and forecasted aircraft hybrid electric architectures and their impact on environment. *Energy*, *211*, 118814. https://doi.org/10.1016/j.energy.2020.118814

[10.A3] APPENDIX 3. Memorandum: Digitization Strategy (original Task 9)

Deliverable: A written memorandum with a digitization strategy that includes:

(1) an organized dataset folder with all the data used for the completion of data-driven tasks of the Handbook Update project, and

(2) a metadata file to help users access and apply this project's dataset in a data platform/ software of their convenience.

[10.A3] 1. Introduction

In this section, a high-level description of the digitization strategy is presented for online resources for future Handbook users. The UCB researchers identified online functionalities that users may find valuable, and proposed an approach to packaging these functionalities on a website or app, as appropriate. Given the existing Web Map tools Caltrans uses from the Environmental Systems Research Institute, Inc. (ESRI), the datasets shared in this Task were mostly converted to GIS formats for readily incorporation if needed to Caltrans Aeronautics Open Source GIS platforms. As with other parts of the project, the aim was to enable Caltrans to include this element in their RFP for the consultant (or an internal office at Caltrans) who will actually update the Handbook. In summary, the UCB overall study and the suggested digitization strategy provide a foundation for creating the ALUP Handbook for the 21st century.

Because the 2011 CA ALUP Handbook has been used successfully by a number of in-state and out-of-state airports, when preparing the digitization strategy for the new 2024 CA ALUP Handbook, it was important to create a more advanced version. The advanced Handbook version would enable aviation/urban planners, and engineers to reproduce the same analysis that were developed in this study, if needed. For example, if one county would like to redo a part of our analysis using their own statistical tools, or more specifically, if they would like to conduct their own analysis of their Safety Zone 5 and 6, they should be able to access the data and methods provided in this study and sucesfully conduct analyses by themselves. This was our goal.

It is important to keep in mind that today's science-policy processes are not just about giving decision-makers one analysis, one figure, or one metric. To the contrary, it is about providing them with the right set of metrics (usually more than one), to help them conduct the study and develop tailored information with clear methods and its limitations for developing critical decision-making. In addition, it is about giving them the tools to conduct reverse-engineering of all our steps and adjust them to their own planning/analysis needs and a different managerial and technical capacities that are often unique to each airport, each Airport Land Use Commission, each County, etc.

As UCB researchers were working with more than 200 California airports and many stakeholders who have different resources that can be applied to airport planning studies, the best way to share information provided in our study is by providing as much access to the steps available to reproduce what we did. Therefore, instead of providing static information, which was a norm to creating previous ALUP Handbooks, we provide a flexible and dynamic method that can help local airports meet their local planning needs.

[10.A3] 2. Strategy

First, the datasets were organized with the objective to help update the Airport Land Use Handbook developed by UC Berkeley for Caltrans Aeronautics. Each tab is organized by topic and each topic corresponds to the data repository folder of Task 9. Our metadata is available in this folder. Most datasets were modified by the UC Berkeley for the Handbook Update project, detailed methodology of data cleaning and processing is described in each Task “Methods” section, which is cross-referenced in the metadata table.

2.1 Metadata File Structure

1. Name: Each dataset is identified by its name, as referenced in both the research report and the data repository. This ensures consistency and ease of identification.

2. Original Source: For each dataset, the original source is documented. This includes not only the name of the organization responsible for developing the data but also a direct link to the dataset, ensuring transparency and ease of access to the primary data source.

3. Data Date: The time period of the data content (i.e. for the accident datasets we have spatial datasets from 2008-2022; for the current exposure metrics using Land Use Land Cover, it covers 2021, etc)

4. Download/ Created Date: This entry specifies the date when the dataset was either downloaded for processing or originally created. It helps in understanding the currency and relevance of the data.

5. Data Type (Data Model if GIS): The type of data (Excel, GIS, CSV, Py etc.) is detailed here. For GIS datasets, the specific data model (point, polyline, polygon, raster) is also indicated, providing users with information about the dataset’s format and potential applications.

6. Original/Modified: This distinction clarifies whether the dataset used is in its original form or has been modified by the UCB team. This is vital for understanding the extent of processing and analysis the data has undergone.

7. Description: A brief description of each dataset is provided, highlighting key characteristics and modifications. For datasets like accident and incident data, a total count of events (N) is also included, offering a quick overview of the dataset's scope.

8. Task Reference: This section links each dataset to the specific task in the project where it was utilized. Detailed methodologies for data cleaning, pre-processing, and processing are described under the "Methods" section of the task, offering a deep dive into the dataset’s application.

9. Notes: Additional notes or observations by the UCB team are included here, providing further insights or caveats about the dataset.

10. Data Dictionary & Other Resources: To assist in the thorough assessment of the datasets, links, and resources related to each dataset are provided. These may include data dictionaries, user guides, technical reports on the datasets, or other relevant materials.

2.2 Metadata Description and Detailed Dataset

1. Safety Zones, Boundaries & Land Use and Land Cover (LULC): They include geospatial data outlining the extents of different safety zones as per FAA Part 77 regulations for the Primary Runway Surface and per the 2011 ALUP guidelines Figure 3-A for the Safety Zones; the airport boundaries; and Land Use Land Cover (LULC) crucial for land use planning and regulatory compliance. Referenced in Task [4.1] *Safety and Risk*, *Safety Zones Accident Density & Land Use Compatibility Update*, Task [8].

2. NTSB - Accidents: This dataset encompasses detailed records of aviation-related incidents and accidents. It was crucial for assessing risk factors and safety concerns around airport vicinities. The data, referenced in Task [4.1] *Safety and Risk*, includes time-stamped events and geolocated information, enabling a comprehensive analysis of safety trends.

3. Wildlife Strikes: Referenced in Task [4.1.2] *Impact of Wildlife Strikes*, this dataset catalogs instances of wildlife strikes, which are critical for assessing and mitigating wildlife hazards in and around airport environments.

4. UAS (Unmanned Aircraft Systems) Incidents: With the increasing use of drones, this dataset {Task [4.1.1. (2)]} *Safety and Risk with Emerging Technologies: Subtask 2: Drone Incidents*, includes incidents involving UAS, essential for understanding and developing regulations for drone operations near airports.

5. Noise Exposure: Task [4.2] *Estimation of Noise and Emissions Exposure*, utilizes this dataset to map noise exposure levels around airports. This is key for community planning and ensuring compliance with noise abatement policies.

6. Wind Results, used in Task [4.3] *Wind Analysis*, informs about prevailing wind patterns essential for runway orientation and airport design. This dataset includes historical wind speed and direction records.

[10.A3] 3. Summary

The following legend summarizes names of datasets, organizations responsible for the development of the original open-source data, and other essential information about each dataset:

Legend	
Name	Name of dataset as described in the report and in the data repository.
Original Source	Organization responsible for developing the original open-source data and link to the dataset.
Download/Created Date	When the data was downloaded for processing or created at the original source.
Data type (data model if	The type of data (excel, GIS, CSV, etc) and the data model if GIS (point, polyline,

GIS)	polygon, raster).
Original/Modified	If the data used is original or modified by the UCB team for the ALUP update purposes.
Description	Short description of the data and key modification. For accident and incident data, N = total number of events.
Task reference	Task where the data is introduced and where detailed methodology on pre-processing and processing are described under the "Methods" section.
Notes	Extra notes if needed.
Data dictionary & other resources	Links and resources to help assess the datasets.

Task 11. Spatial Distribution Analysis of Aircraft Accident in Airport Safety Zones

by
Sarah Lindbergh, Stone Shi, and Jasenka Rakas

The FAA Consortium on Aviation Operations Research (NEXTOR III)
Department of Civil and Environmental Engineering
University of California
Berkeley, CA

May 31, 2024

Abstract

In this study, optimized are visualizations of spatial distribution patterns of aviation accidents across 259 airports in California. Accident data by geographic coordinates are derived from the National Transportation Safety Board (NTSB) for 2008-2022. The accident database is analyzed through Geographic Information Systems (GIS) overlay and point pattern analysis. Results highlight a notable concentration of accidents near the borders between Zones 5 and 6, suggesting potential expansions of Zone 5 into Zone 6. This research contributes to airport land use compatibility strategies by proposing data-driven modifications to safety zones, enhancing their effectiveness in protecting airport vicinities from accidents.

Table of Contents

Abstract 2

1. Introduction 5

2. Background 6

3. Data & Methods 8

3.1 Accident and Safety Zone GIS Data Definition 8

3.2 Data Collection 9

3.3 Geospatial Analysis 10

4. Results 13

4.1. Distance calculation of accidents relative to the nearest boundary of adjacent safety zones 15

4.2 Accident Plots and Distance Histograms: Z5 and Z6 (Datasets from NTSB Largest and Spatial Accuracy) 17

4.2.1 Spatial Analysis Results: Visualizing by Relative Distance 18

4.2.2 Spatial Analysis Results: Relative Distance Histograms with Statistics 25

4.2.3 Spatial Analysis Results: Kernel Density Estimation (KDE) Plots 34

4.2.4 Spatial Analysis Results: Accident Locations in Overlaid Safety Zone Polygons 39

4.2.5 Spatial Analysis Results: Interactive Plots of Accident Distribution in HTML 45

5. Conclusions 46

Appendix 1: Safety Zones Accident Statistics 47

References 49

Table of Figures

Figure 1. ALUP 2011 Handbook Generic Safety Zone Dimensions 7
Figure 2. Illustration of Generic Safety Zones of the Southern San Francisco Bay Area Airports 12
Figure 3. Distance of Accidents in Z5 from the Closest PS Boundary (ft) by Departure and Arrival (NTSB Largest) 19
Figure 4. Distance of Accidents in Z5 from the Closest PS Boundary (ft) by Departure and Arrival (Spatial Accuracy) 20
Figure 5. Distance of Accidents in Z5 from the Closest Z6 Boundary (ft) by Departure and Arrival Accidents (NTSB Largest) 21
Figure 6. Distance of Accidents in Z5 from the Closest Z6 Boundary (ft) by Departure and Arrival (Spatial Accuracy) 22
Figure 7. Distance of Accidents in Z6 from the Closest Z5 Boundary (ft) by Departure and Arrival (Dataset: NTSB Largest) 23
Figure 8. Distance of Accidents in Z6 from the Closest Z5 Boundary (ft) by Departure and Arrival (Data Set: Spatial Accuracy) 24
Figure 9. Histogram of the Distance of Accidents in Z5 from the Closest PS Boundary(ft) (NTSBLargest) 26
Figure 10. Histogram of the Distance of Accidents in Z5 from the Closest PS Boundary(ft) (Spatial Accuracy) 27
Figure 11. Histogram of the Distance of Accidents in Z5 from the Closest Z6 Boundary(ft) (NTSB Largest) 28
Figure 12. Histogram of the Distance of Accidents in Z5 from the Closest Z6 Boundary(ft) (Spatial Accuracy) 29
Figure 13. Histogram of the Distance of Accidents in Z6 from the Closest Z5 Boundary(ft) (NTSBLargest) 31
Figure 14. Histogram of the Distance of Accidents in Z6 from the Closest Z5 Boundary(ft) (Spatial Accuracy) 33
Figure 15. KDE Isoline Plot of the Relative Distance of Accidents in Z5 from the Closest PS Boundary (ft) (Spatial Accuracy) 35
Figure 16. KDE Isoline Plot of the Relative Distance of Accidents in Z5 from the Closest Z6 Boundary (ft) (Spatial Accuracy) 36
Figure 17. KDE Isoline Plot of the Relative Distance of Accidents in Z6 from the Closest Z5 Boundary (ft) (Spatial Accuracy) 37
Figure 18. Overlay of Accidents in Z5 Using the NTSB Largest Dataset 40
Figure 19. Overlay of Accidents in Z5 Using the Spatial Accuracy Dataset 41
Figure 20. Overlay of Accidents in Zone 6 Using the NTSBLargest Dataset 42
Figure 21. Overlay of Accidents in Zone 6 Using the Spatial Accuracy Dataset 43
Figure 22. Interactive Plots with Pop-up Windows HTML Page Preview 45

1. Introduction

In this study, investigated are the changes in risk levels at generic safety compatibility zones near California airports as outlined in Chapter 3.2.3 of the latest Airport Land Use Planning (ALUP) Handbook (Caltrans, 2011). Specifically, the study focuses on safety zones 5 and 6, where accident hazard and risks have escalated since 2008. Aircraft accidents risk increased: (a) in Zone 5 from Low to Very High, and (b) in Zone 6 from Low to Medium-Low. The analysis examines aircraft accident distributions across 259 airports to determine if the boundaries of these zones should be expanded or adjusted to better reflect their new risk profiles. Preliminary findings suggest a concentration of accidents near the border between Zones 5 and 6, potentially warranting an expansion of Zone 5 into Zone 6. This study also revisits the accident density distribution as the future reference that can recommend stricter land use controls near these zones to mitigate risks effectively.

2. Background

The previous studies by Caltrans (Caltrans 1983, 1993, 2002, 2011) emphasize the generic safety zones around California airports and their corresponding land use compatibility based on spatial distribution and frequency of accidents. The ALUP Handbook specifies that safety zones should maintain uniform risk levels within each zone while being distinct from others, adapting to the physical and operational characteristics of each airport. This approach aligns with the goals to preserve open areas near runways, reducing damage in the frequent event of accidents and facilitating lower-density development particularly in critical zones (Figure 1). This study leverages updated accident data from the National Transportation Safety Board (NTSB) for 2008-2022, employing Geographic Information Systems (GIS) to analyze spatial relationships and accident trends within airport safety zones[31].

Our analysis reveals significant shifts in accident patterns and land use characteristics that necessitate adjustments to the dimensions and policies of certain safety zones, notably Zones 5 and 6. Zone 5, despite a low percentage of accidents beyond airport boundaries, exhibits a high density of incidents, suggesting an urgent need to review its safety margins. Meanwhile, Zone 6, characterized by a considerable increase in fatal accidents and overall accident rates, requires a thorough reassessment of its land use compatibility policies. The integration of Land Use and Land Cover (LULC) data from the United States Geological Survey further supports a refined understanding of the potential severity of accidents, advocating for tailored adjustments to safety zones based on actual risk levels and land use dynamics. This comprehensive methodological update aims to refine safety zone delineations and enhance regulatory measures to better protect areas surrounding airports. Appendix 1 presents a more detailed profile of Safety Zones 5 and 6 risk assessment from previous reports (Task 8).

[31] For detailed information please refer to Tasks 4.1. of the project "Re-inventing Airport Land Use Planning in California: A Strategy for Updating the California Airport Land Use Planning Handbook" conducted by NEXTORIII at UC Berkeley, December 2023.

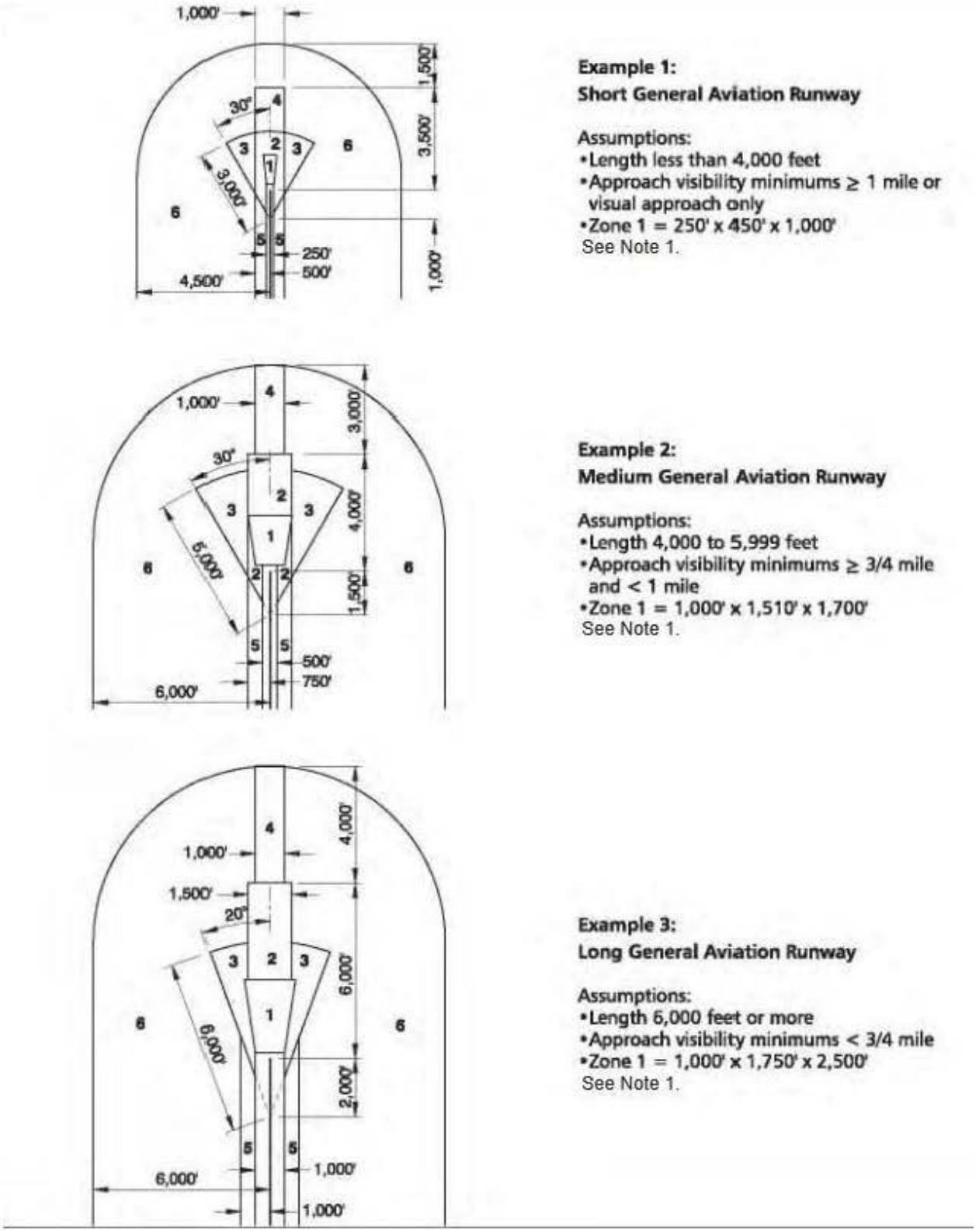


Figure 1. ALUP 2011 Handbook Generic Safety Zone Dimensions

3. Data & Methods

In this section, we present accident and safety zone GIS data definitions, data collection, and geospatial analysis methods based on point pattern analysis.

3.1 Accident and Safety Zone GIS Data Definition

This study utilizes geospatial datasets to analyze the spatial distribution and consequences of aviation accidents in relation to airport safety zones, as outlined in the ALUP Handbook.

Here, we define the safety zones based on FAA regulations and existing safety practices:

Primary Surface (PS): This area extends longitudinally centered on a runway, matching the runway's elevation. It spans 200 ft beyond the runway ends and varies in width from 250 to 1,000 ft depending on the runway and approach type. It must remain clear of all obstructions except for essential fixed objects like runway lights and navigational aids.

There are six Safety Zones (SZ) positioned around a runway, and the Primary Surface (PS):

- Primary Runway Surface (PS): defined by the FAA
- Zone 1 (Z1): Runway Protection Zones
- Zone 2 (Z2): Inner Approach/Departure Zone
- Zone 3 (Z3): Inner Turning Zone
- Zone 4 (Z4): Outer Approach/Departure Zone
- Zone 5 (Z5): Runway Sideline Zone (Safety zone of interest in this report)
- Zone 6 (Z6): Traffic Pattern Zone (Safety zone of interest in this report)

Additional details of each zone are described in Table 1.

Table 1. Basic characteristics of the Primary Surface Zones and Runway Safety Zone Asses

Zone	Jurisdiction	Description	Desirable % of Usable Open Land	% area outside airport boundaries*
PS	FAA	A surface longitudinally centered on a runway, dimensioned according to FAA Part 77	100%	1.31%

Z1	ALUP/FAA	Runway Protection Zone	Clear of objects in accordance with FAA standards	49.74%
Z2	ALUP	Inner Approach/Departure zones	25-30%, especially areas close to the runway extended centerline	79.59%
Z3	ALUP	Inner Turning Zone	15-20% minimum	88.39%
Z4	ALUP	Outer Approach/Departure Zones	15-20% approximately, with emphasis on areas along the extended runway centerline	97.94%
Z5	ALUP	Sideline Zone	25-30% is desirable	26.09%
Z6	ALUP	Traffic Pattern Zone	10% approximately every ¼ to ½ mile should be provided	94.64%

*calculated based on the generic Safety Zones dimensions for 259 California airport boundaries modeled in GIS

3.2 Data Collection

The analysis relies on two primary datasets from the National Transportation Safety Board (NTSB), covering the period 2008-2022, chosen for their spatial relevance and temporal range:

[1] NTSB Spatial Largest Dataset: Comprises 1,355 accident events and utilizes GPS-based latitude and longitude data for high spatial accuracy. This dataset captures the largest number of spatially relevant accidents since 2008, when more precise GPS data became available.

[2] NTSB 2011 Spatial Accuracy Dataset: Contains 495 total accident events (298 excluding those outside a 5-mile airport buffer). This dataset reproduces the methodology of the 2011 handbook, excluding accidents within the primary surface and those with latitude-longitude co-location errors.

These datasets were selected to provide both a broad overview and a detailed reproduction of previous handbook methodologies. The spatial data accuracy is crucial for assessing accident locations in relation to the defined safety zones (See Appendix 1).

3.3 Geospatial Analysis

GIS mapping techniques were employed to create detailed polygons of the Primary Runway Surface and Safety Zones based on the 2011 ALUP Handbook generic dimensions synthesized below (Figure 2).

To create the runway Safety Zones, different runway open source GIS were examined in previous tasks of this project: Caltrans, FAA Aeronautical Data Delivery Service (ADDS), and the Bureau of Transportation Statistics (BTS) part of the U.S. Department of Transportation (USDOT) National Transportation Atlas Database (NTAD). The BTS runway end table (created on July 16, 2020) was the most appropriate due to the detailed attribute table with runway end points and the obstruction identification surface codes necessary for determining the runway's primary surfaces according to the Federal Aviation Regulations Part 77 based on runway visibility parameters (i.e. visual runways, non-precision instrument runways, and precision instrument runways) (See section 2.3.2 of Task 4.1.)

After defining the runway's primary surface, the geometries for the 6 generic Safety Zones (civil aviation), were applied based on the BTS runway length, approach visibility minimums, and the type of general aviation or large air carrier runway (see Figures in the 2011 ALUP Handbook p.3-17 to 3-19). Based on the former ALUP handbook, we also considered that where there is overlap of zones or two or more runways, the lower numbered zone takes precedence. For runways designed for multiple aircraft operations (i.e., general aviation and large air carriers) the largest critical aircraft zoning is predominant. The intention is to reflect the risk of highest potential consequences and not probability, since the impact of a large commercial airliner would have greater potential damage than that of a single engine aviation aircraft (ALUP, 1983).

This spatial framework is essential for overlaying accident data to analyze spatial patterns and assess the effectiveness of current safety zone boundaries. The analysis also considers the proximity of accidents to runway surfaces, where most accidents are observed to occur, underlining the importance of maintaining clear zones as per FAA standards.

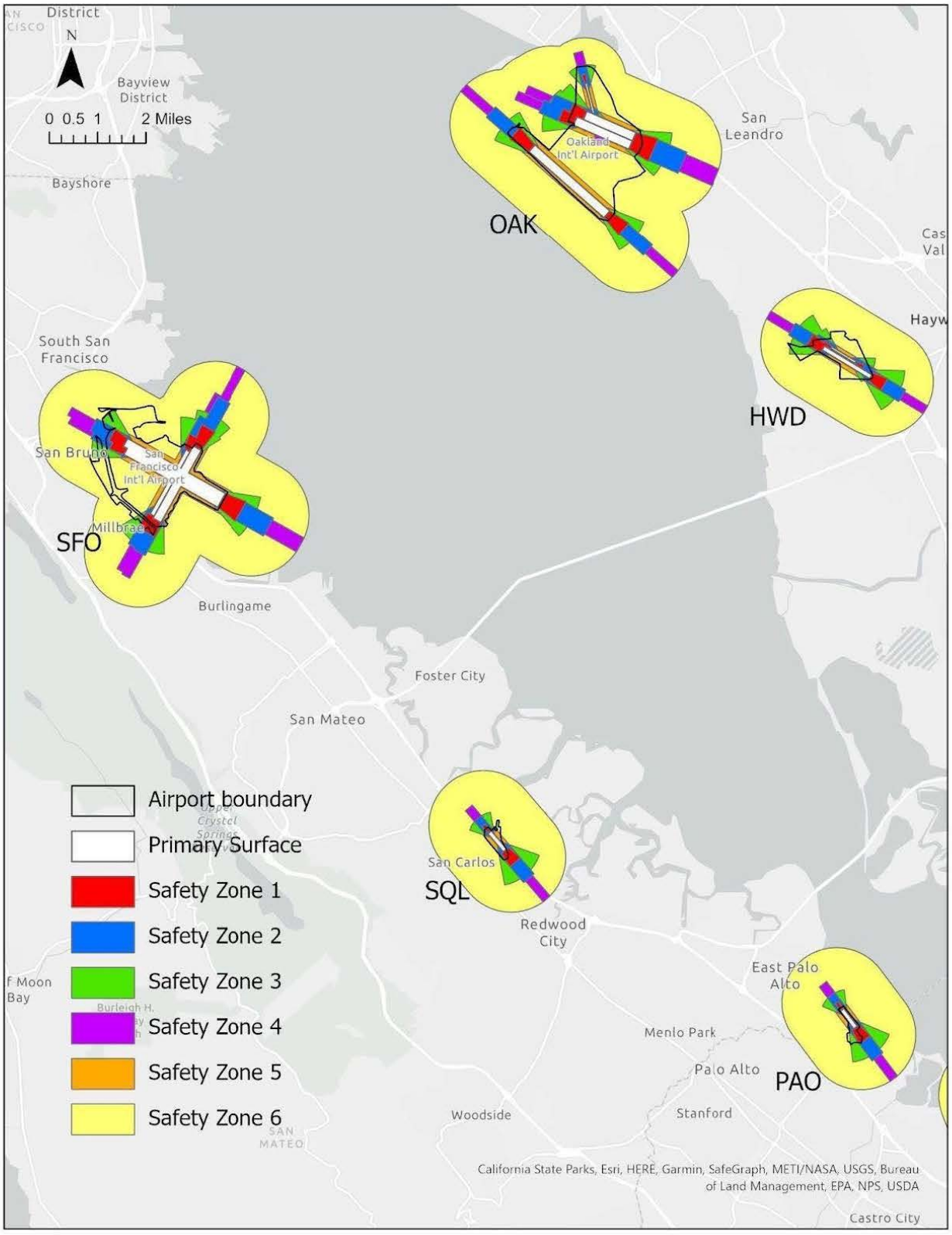


Figure 2. Illustration of Generic Safety Zones of the Southern San Francisco Bay Area Airports

We perform comprehensive geometry calculations to answer the concerns from Caltrans whether the accidents are likely to happen near the boundary of safety zones. Point pattern analysis such as Kernel Density Estimate (KDE) method, and more specifically, a Gaussian KDE function is also applied to spatially visualize the frequency occurrence of accidents.

As one part of the automated programming design of the geospatial analysis, the KDE function has been integrated into the plotting interface that has applied Silverman's Rule (Silverman,1986). We let (x1, x2, ..., xn) be independent and identically distributed samples drawn from some univariate distribution with an unknown density f at any given point x:

$$\widehat{f}_h(x) = \frac{1}{n}\sum_{i=1}^{n} K_h(x - x_i) = \frac{1}{nh}\sum_{i=1}^{n} K\Big(\frac{x - x_i}{h}\Big),$$

Where:

K is kernel, and

h is the bandwidth that has been automatically determined using SciPy package.

By dividing the study into three key tasks, a series of clear geospatial pattern combinations has been developed, which are followed by the following steps:

(1) calculating the relative distances of accidents within Z5 and Z6 in relation to other adjacent safety zones (Table 2);
(2) plotting the relative locations of accidents inside Z5 & Z6; and
(3) creating the point pattern analysis using KDE.

Overall, KDE uses spatial decomposition operations transforming point into polygon patterns to assess accident patterns in geographic space. By combining rigorous GIS analysis with updated NTSB accident data, this study aims to provide a new assessment of airport safety zone effectiveness, and propose necessary modifications based on the latest accident trends and land use developments.

4. Results

In this section, results are organized based on (1) the distance of accidents within each safety zone relative to the nearest adjacent safety zone; (2) Z5 and Z6 accident plots and histograms based on their relative distance to PS, Z5 and Z6; and (3) a density estimation of accidents in Z5 and Z6 relative to their distance to PS, Z5 and Z6.

The plots and data results for all safety zones are retrievable here. For accidents in safety zones of interest, Z5, Z6 and PS, interactive plots were created so that the attributes available in the original NTSB accident data can be viewed by putting the cursor on top of each accident.

4.1. Distance calculation of accidents relative to the nearest boundary of adjacent safety zones

This section focuses on the analysis of accident distances relative to the nearest boundaries of adjacent safety zones for the 259 airports in California. To assess the distance distribution, four key statistical metrics were utilized in Tables 2-5:

1. Median (Med): The middle value of the accident distance data, providing a robust central tendency measure that is less affected by extreme values.
2. Mean: The average distance, offering an overall estimation of accident proximity to zone boundaries but can be influenced by outliers.
3. Minimum (Min): The smallest recorded distance, indicating the closest accident occurrence to a safety zone boundary.
4. Maximum (Max): The largest relative distance observed in a particular zone, highlighting the farthest accident from the closest boundary at a specific safety zone.

Since the mean value is highly sensitive to outliers, the median is also considered to enhance the robustness of the results as part of the comprehensive data explanation. Brief explanations for each table are provided in this section.

The median distances (Table 2) showed mild to moderate variability across the adjacent pairs of safety zones. Notably, the median distance of accidents in Zone 5 (Z5) relative to Zone 6 (Z6) is 447.86 ft; and the median distance of accidents in Z6 relative to Z5 is 1270.6 ft, suggesting different exposure levels between these two zones. Similar to results in Task 4.1. and Task 8, this finding indicates that more focus should be placed on incidents in Zones 5 and 6 in subsequent steps of spatial analysis.

The mean distances between the accidents and the closest boundary of a designated safety zone (Table 3) tend to be larger than the median values, indicating the presence of outliers that are pulling the mean values upwards. Based on this observation and previous discussions, a suggestion for combining the observations from Tables 2 and 3 is proposed.

Table 2. Median accident distances (ft)

	Accidents in Zones	
Relative to	Z5	Z6
PS	164.08	NA*
Z1	NA*	NA*
Z2	865	1643.8
Z3	1439.4	1289.1
Z4	NA*	3419.5
Z5	-	1270.6
Z6	447.86	-

*NA: No adjacency

Table 3. Mean accident distances (ft)

	Accidents in Zones	
Relative to	Z5	Z6
PS	220.6	NA*
Z1	NA*	NA*
Z2	993.6	1867.3
Z3	1414.13	1596.8
Z4	NA	3701.3
Z5	-	2009.1
Z6	505	-

The minimum distances table (Table 4) provides safety insights on how close accidents can occur from other zone boundaries. The smallest distance recorded in Table 4 is 3.73 ft from an accident in Zone 6 relative to Z5 boundary, signaling potential issues in boundary management, especially when the minimum distances of accidents within Z6 relative to other adjacent boundaries are significantly larger. The maximum values (Table 5), such as 11599 ft in Zone 4 relative to Zone 6, is an indicator that accidents within Z4 are closer to this zone's centroid, validating the function of Zone 4. However, a further assessment of other accidents within Z4 relative to its centroid or equidistant line segment would be necessary to fully validate this. The findings from Tables 2-5 can support the need for adjusting and redesigning the safety zone shapes for Caltrans.

Table 4. Minimum accident distances (ft)

Table 5. Maximum accident distances (ft)

	Accidents in Zones	
Relative to	Z5	Z6
PS	23.01	NA*
Z1	NA*	NA*
Z2	7.26	39.3
Z3	15.3	13.57
Z4	NA*	60.91
Z5	-	3.73
Z6	34.47	-

	Accidents in Zones	
Relative to	Z5	Z6
PS	388.7	NA*
Z1	NA*	NA*
Z2	5908.8	8104.4
Z3	3940.2	5131.79
Z4	NA*	11599
Z5	-	8173.4
Z6	1064.6	-

*NA: No adjacency

In summary, section 4.1 provides a detailed quantitative analysis of accident distances relative to the nearest safety zone boundaries across 259 airports in California, utilizing median, mean, minimum, and maximum distance metrics to offer an overview of spatial accident patterns. The analysis highlights significant variability in accident proximity across different zones, with median distances indicating specific zones where safety measures may need to be intensified. The relatively shorter median and minimum distances in certain zones suggest zones of higher accident concentration and potential issues in boundary management.

4.2 Accident Plots and Distance Histograms: Z5 and Z6 (Datasets from NTSB Largest and Spatial Accuracy)

This subsection investigates the spatial analysis of accident distances from safety zone boundaries, specifically focusing on Zones 5 (Z5) and Zone 6 (Z6). We employ three types of analysis and related visualization methods: (1) Kernel Density Estimation (KDE) plots, (2) histograms by frequency, and (3) plots categorized by departure and arrival accident data. These three methods provide a comprehensive view of the spatial distribution and frequency of accidents relative to the nearest boundaries. An Interactive Plot example (Figure 20) with pop-up windows is offered at the end of this section to assist interpreting the relative distance plots.

4.2.1 Spatial Analysis Results: Visualizing by Relative Distance

Figures 3-8 present the accident data, separated into departures or arrivals, providing insights into how accident distributions might differ based on the phase of flight. These figures show the distances of accidents from the nearest boundaries during departures and arrivals. The results reveal variations in accident distances between two datasets (NTSB Largest and Spatial Accuracy), suggesting differences in spatial patterns depending on the phase of flight and data accuracy. A North arrow is added to interpret the cardinal direction trends of accidents relative to its nearest safety zone boundary. For example, the blue "x" mark on the far left of Figure 3 (West), near the "o" horizontal axis, indicates that there is an accident in Zone 5 that occurred during arrival about 500 ft West of the nearest edge of Primary Surface.

Using the NTSB Largest dataset, Figure 3 visualizes the distribution of accident distances from the closest Primary Surface boundary in Zone 5, categorized by whether the accidents occurred during departure or arrival phases. Each point represents an individual accident event, with their spatial relationship depicted relative to the Primary Surface boundary. According to Figure 3, most accidents in Zone 5 are located within 500 ft from the closest Primary Surface boundary. We find that the Departure accidents in Z5 are likely to occur on the North side of the Primary Surface area rather than on the South side.

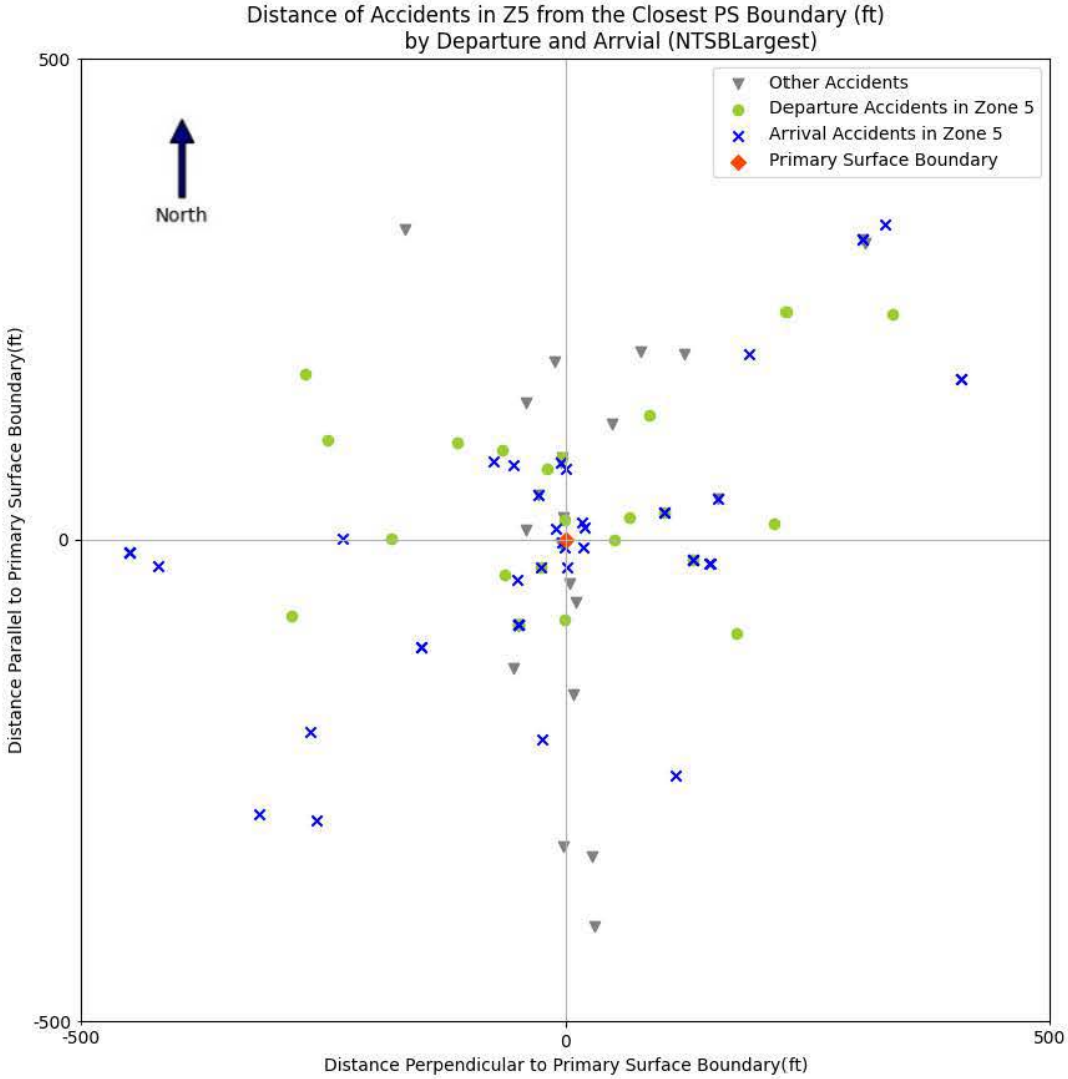


Figure 3. Distance of Accidents in Z5 from the Closest PS Boundary (ft) by Departure and Arrival (NTSB Largest)

Similar to Figure 3, Figure 4 tracks accidents in Zone 5 near the Primary Surface boundary using the Spatial Accuracy dataset. It shows how accident distributions can vary with different data accuracies, highlighting potential discrepancies in spatial patterns across datasets. When analyzing the NTSB Spatial Accuracy dataset, it was found that all the plots using Spatial Accuracy dataset do not contain departure accidents. However, in order to maintain consistency in the analysis and mapping in this section, we still choose to include 'Departure Accidents' in

the legend and in the title of all the plots, regardless of which dataset were used. It is recommended that subsequent research provides corresponding interpretations of this issue in this data set.

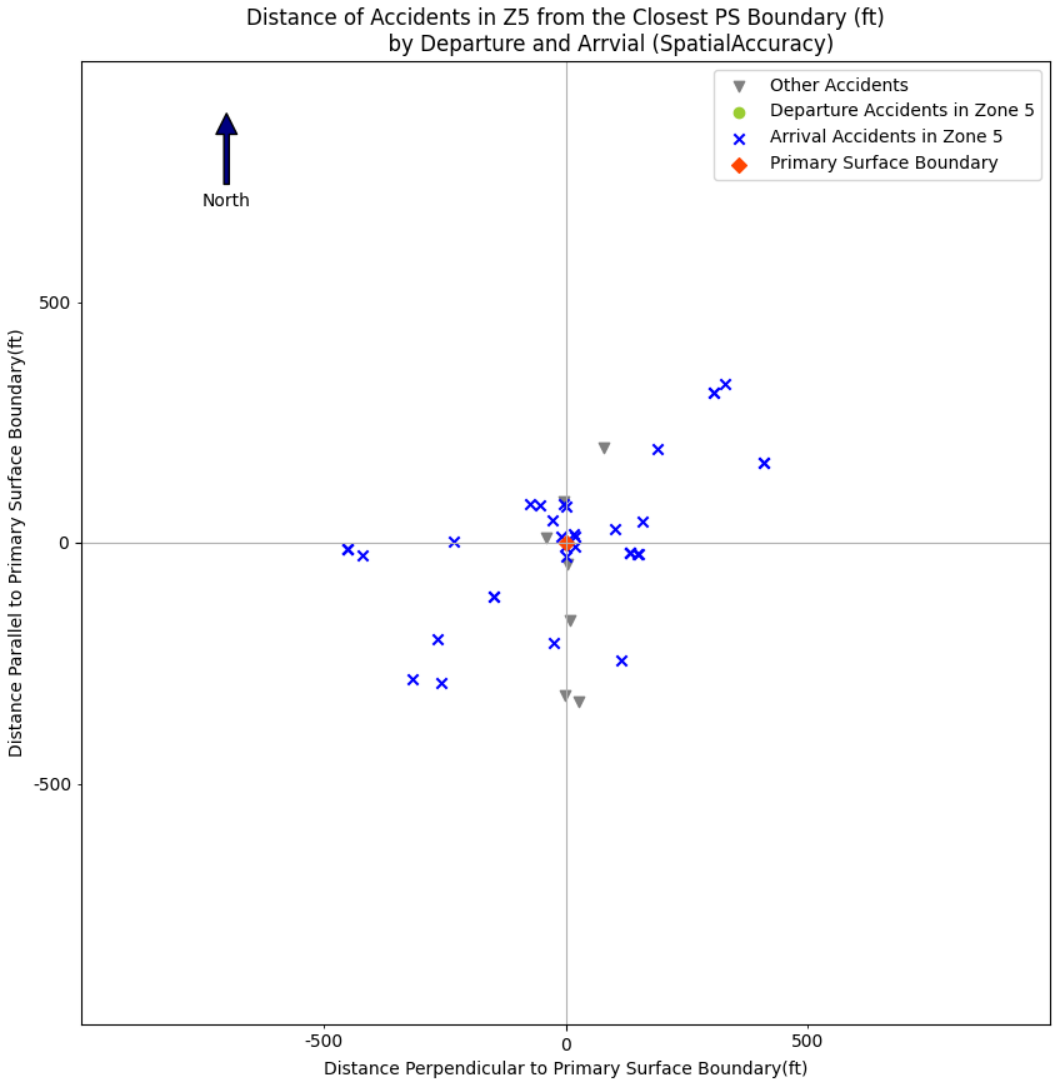


Figure 4. Distance of Accidents in Z5 from the Closest PS Boundary (ft) by Departure and Arrival (Spatial Accuracy)

Figure 5 displays the accidents in Zone 5 relative to the nearest Zone 6 boundary, separated by departures and arrivals. The plot provides insights into the specific high accident areas along the boundary between Zones 5 and 6, indicating where accidents are most likely to

occur during different flight phases using the NTSB Largest dataset. Based on the Figure 5 data display, most accidents are located within the 500 ft buffer zones expanded from Zone 6. However, some outliers at the far East side and Southwest side of Zone 6 are noticeable too.

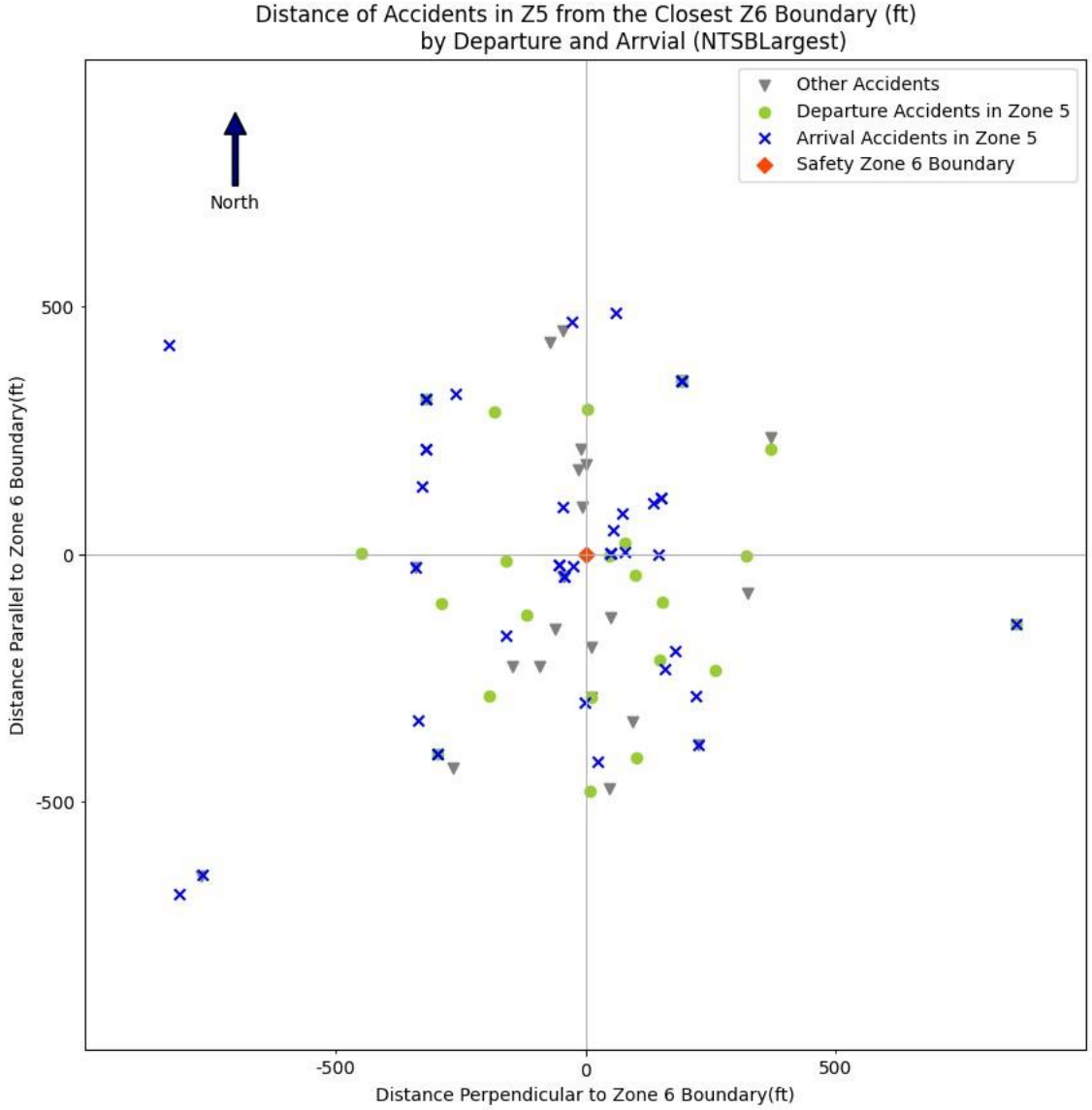


Figure 5. Distance of Accidents in Z5 from the Closest Z6 Boundary (ft) by Departure and Arrival Accidents (NTSB Largest)

Using the Spatial Accuracy dataset, Figure 6 displays the accident distribution in Zone 5 in relation to the nearest Zone 6 boundary. We found that the accidents are likely to occur along the North-South axis, which can be further explored in consequent studies.

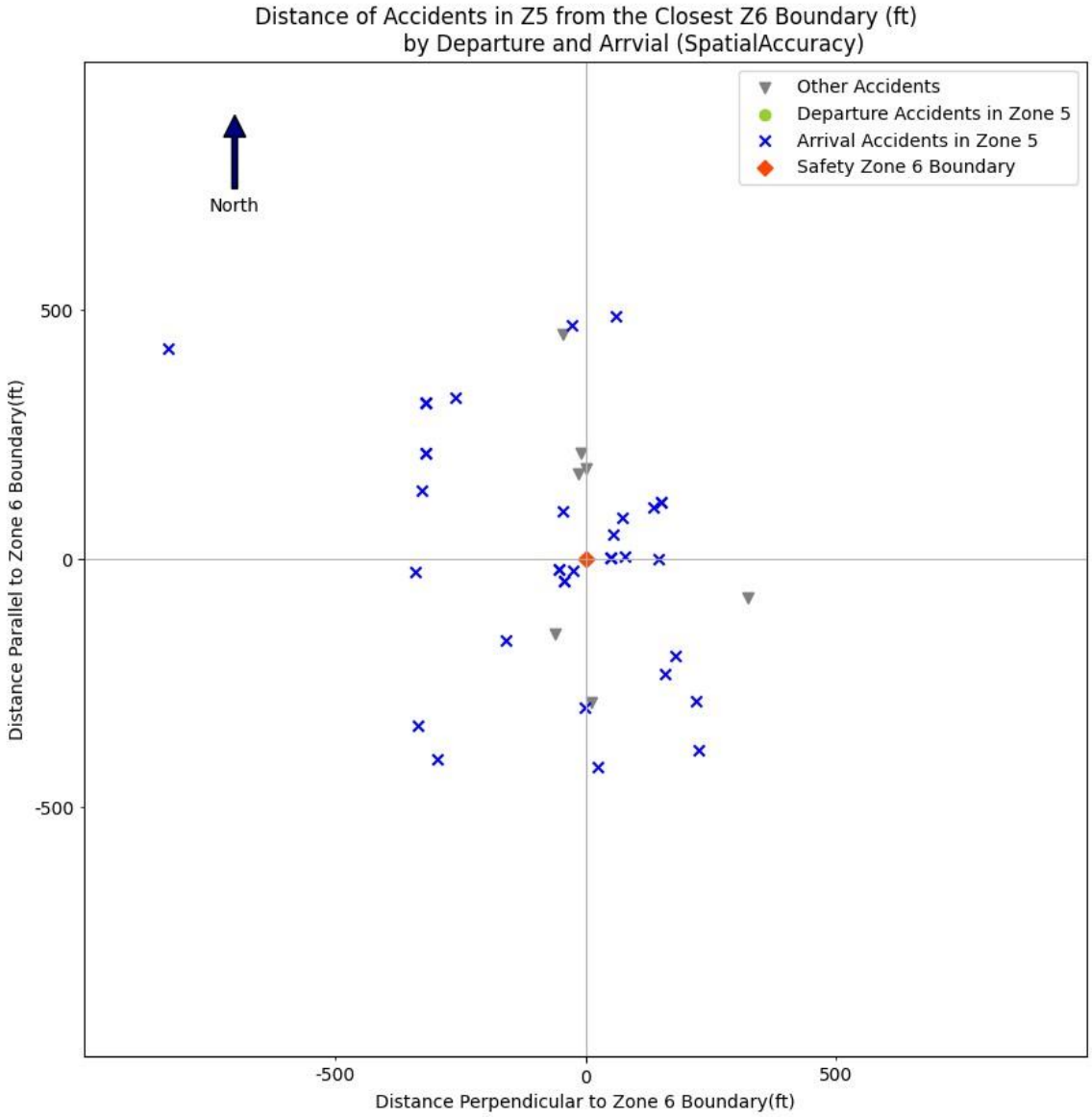


Figure 6. Distance of Accidents in Z5 from the Closest Z6 Boundary (ft) by Departure and Arrival (Spatial Accuracy)

Figure 7 illustrates the accident distances from Zone 6 to the nearest Zone 5 boundary, categorized by the phase of the flight. It shows a higher concentration of accidents in the North side of Zone 6 relative to the closest Z5 boundary.

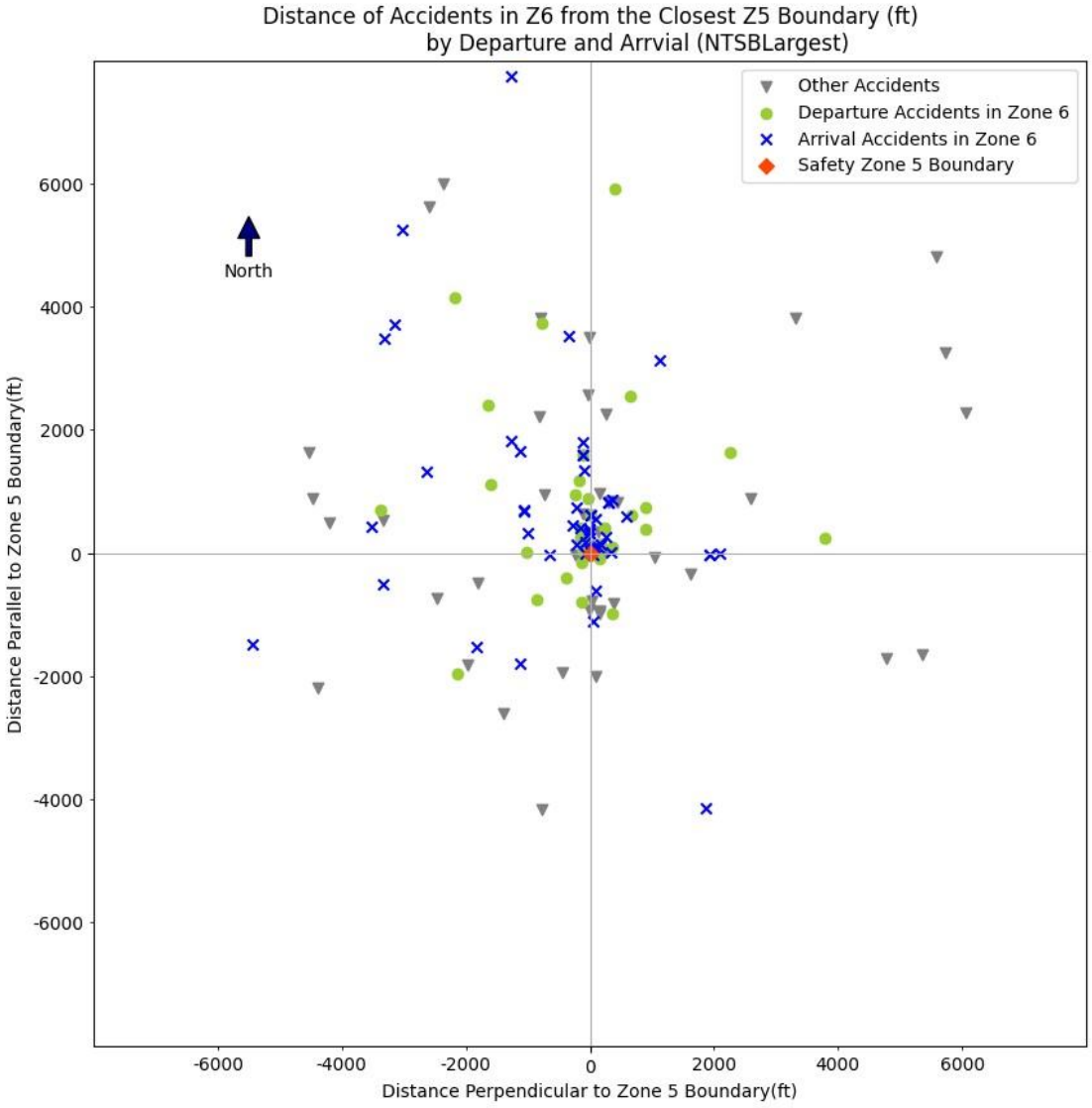


Figure 7. Distance of Accidents in Z6 from the Closest Z5 Boundary (ft) by Departure and Arrival (Dataset: NTSB Largest)

Figure 8 utilizes the Spatial Accuracy dataset to depict accidents in Zone 6 relative to Zone 5. It assesses the spatial accuracy and reliability of accident data, confirming the general trends of accidents concentration on the northern side of Zones 6 relative to Z5 boundary.

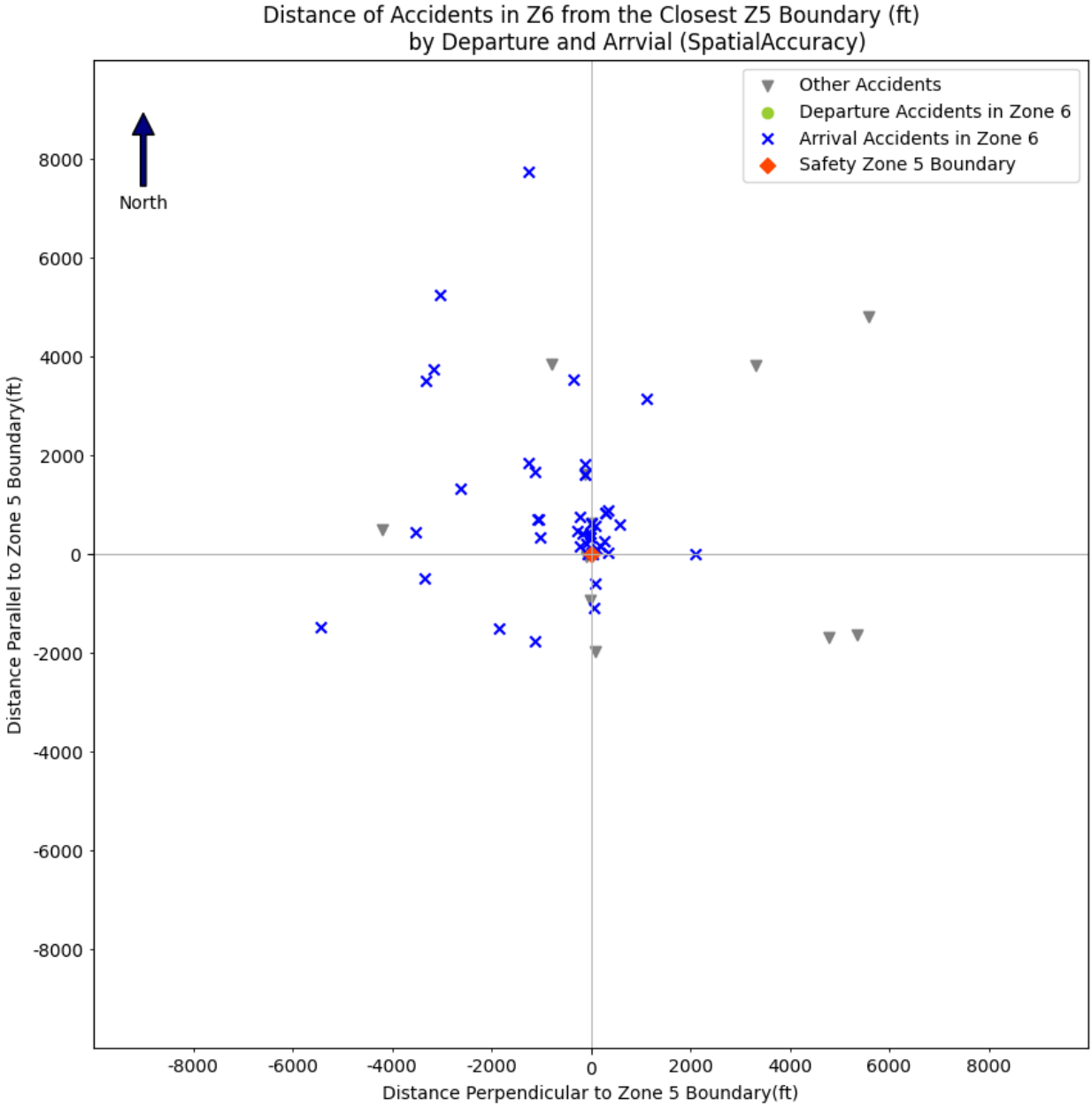


Figure 8. Distance of Accidents in Z6 from the Closest Z5 Boundary (ft) by Departure and Arrival (Data Set: Spatial Accuracy)

Overall, Section 4.2.1, with the relative distance plots (Figures 3-8), effectively illustrates the spatial distribution of accidents in relation to the nearest safety zone boundaries, with a clear

distinction between accidents occurring during departures and arrivals. These visualization methods reveal notable differences in accident distances between the NTSB Largest and Spatial Accuracy datasets, indicating variations in spatial patterns influenced by data accuracy and flight phases (arrivals and departures). The inclusion of cardinal direction provides a deeper understanding of the geographical alignment of these incidents, highlighting trends such as the predominance of accidents within 500 ft of Primary Surface and Z5 boundaries and notable deviations on the north or south sides of the zones.

4.2.2 Spatial Analysis Results: Relative Distance Histograms with Statistics

The histograms display the frequency of accidents at various distances from a specific safety zone boundary, offering a straightforward statistical depiction of the distance data. This method highlights the most common accident distances and the spread of the data (Figures 9-14). The histograms show how accident frequencies vary with distance, providing a clear quantification of proximity trends to safety zone boundaries. Notable findings include the presence of peaks at specific distances, indicating common areas where accidents tend to cluster. The mean and median value of each dataset are labeled in different colors on each diagram for further interpretation.

In Figure 9 we can observe that most of the accidents in Zone 5 are clustered around 120 ft from the Primary Surface (PS). This histogram highlights the concentration of accidents near the Primary Surface boundary in Zone 5 (Z5). Since one bin represents 20 ft, the highest frequency bin occurs between 100 and 120 ft from the boundary, showing the most common distance where accidents happen. This peak frequency emphasizes a specific high-hazard zone very close to the boundary, with the median accident distance at 134.26 ft reinforcing this critical area. The second peak in the histogram occurs between 420-440 ft from the PS boundary. This indicates that there is another cluster of accidents happening at this specific distance from the boundary, suggesting a secondary high hazard zone. Although this peak has a relatively lower frequency than the primary peak, this finding could imply that there is a particular feature or condition in this distance range that contributes to a higher frequency of accidents.

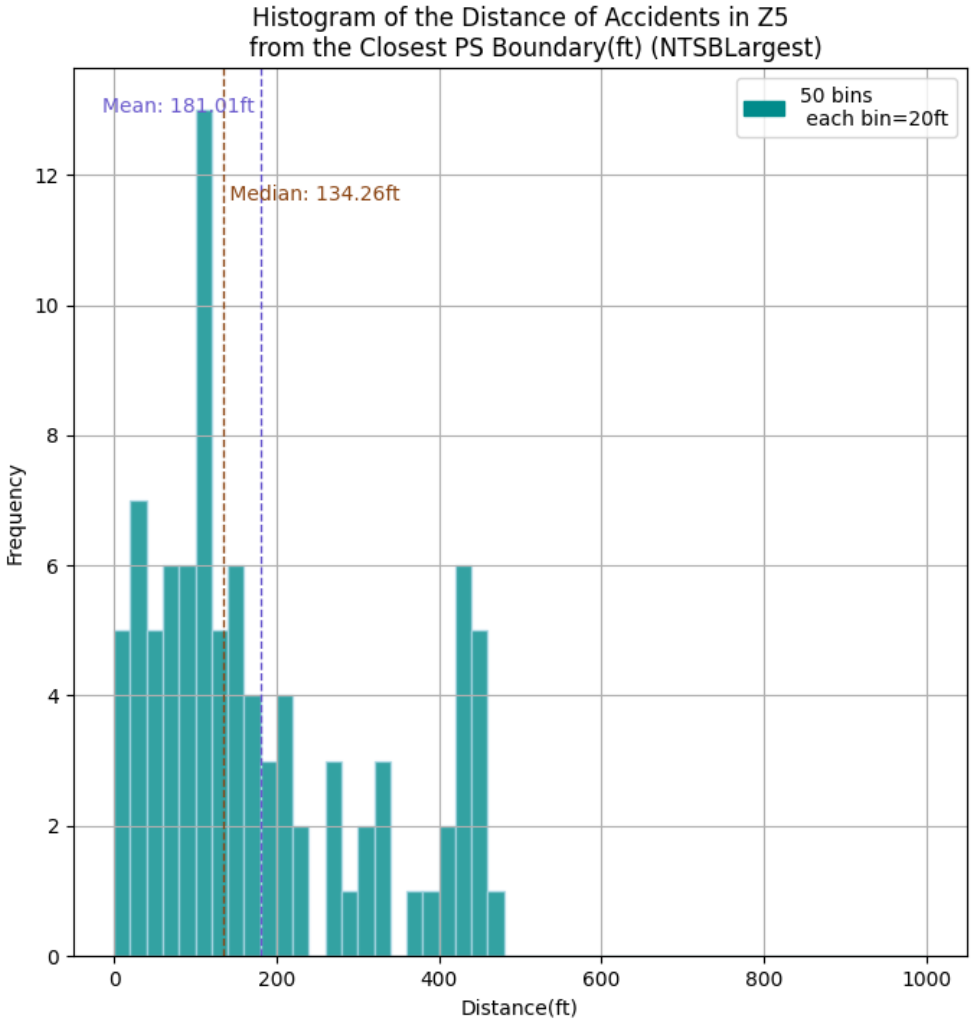


Figure 9. Histogram of the Distance of Accidents in Z5 from the Closest PS Boundary(ft) (NTSBLargest)

In Figure 10, we can observe two clusters. In the first cluster, the value of the highest frequency bin is 3, and it is spread over 0-120 ft. The second peak occurs within 420-440 ft, similar to the position in Figure 9.

Figure 8 and Figure 9 consistently indicate a secondary high hazard zone for accidents. This suggests that there are specific conditions or factors at this distance from the PS boundary contributing to higher accident frequencies. The slight variation between the two datasets could be due to differences in calculation methods mentioned in Section 3.2.

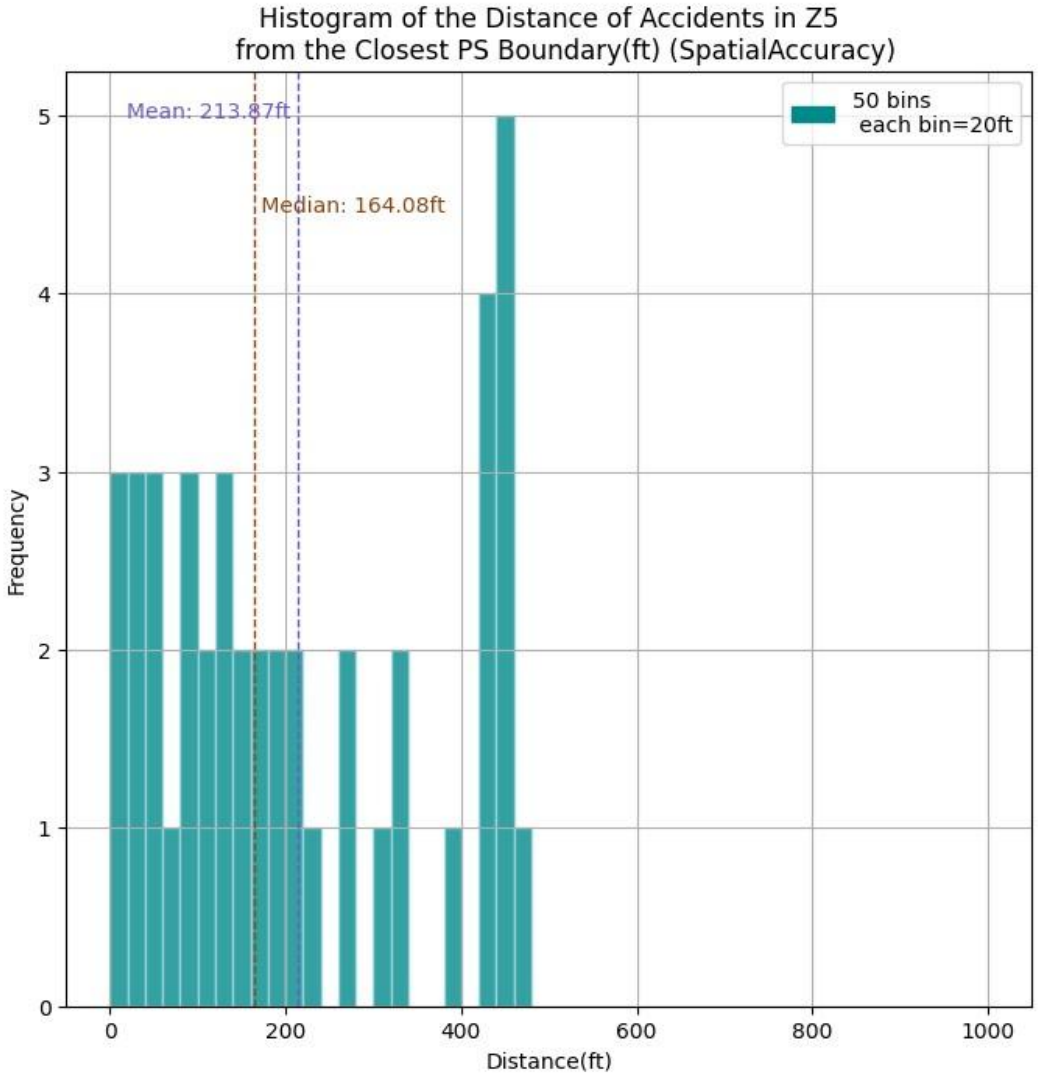


Figure 10. Histogram of the Distance of Accidents in Z5 from the Closest PS Boundary(ft) (Spatial Accuracy)

Figure 11 shows a concentration of accidents around the 380-ft mark from the Zone 6 (Z6) boundary, closely coinciding with the median value of 342.01 ft. This suggests a significant clustering of accidents at this specific distance, marking it as a high-hazard area.

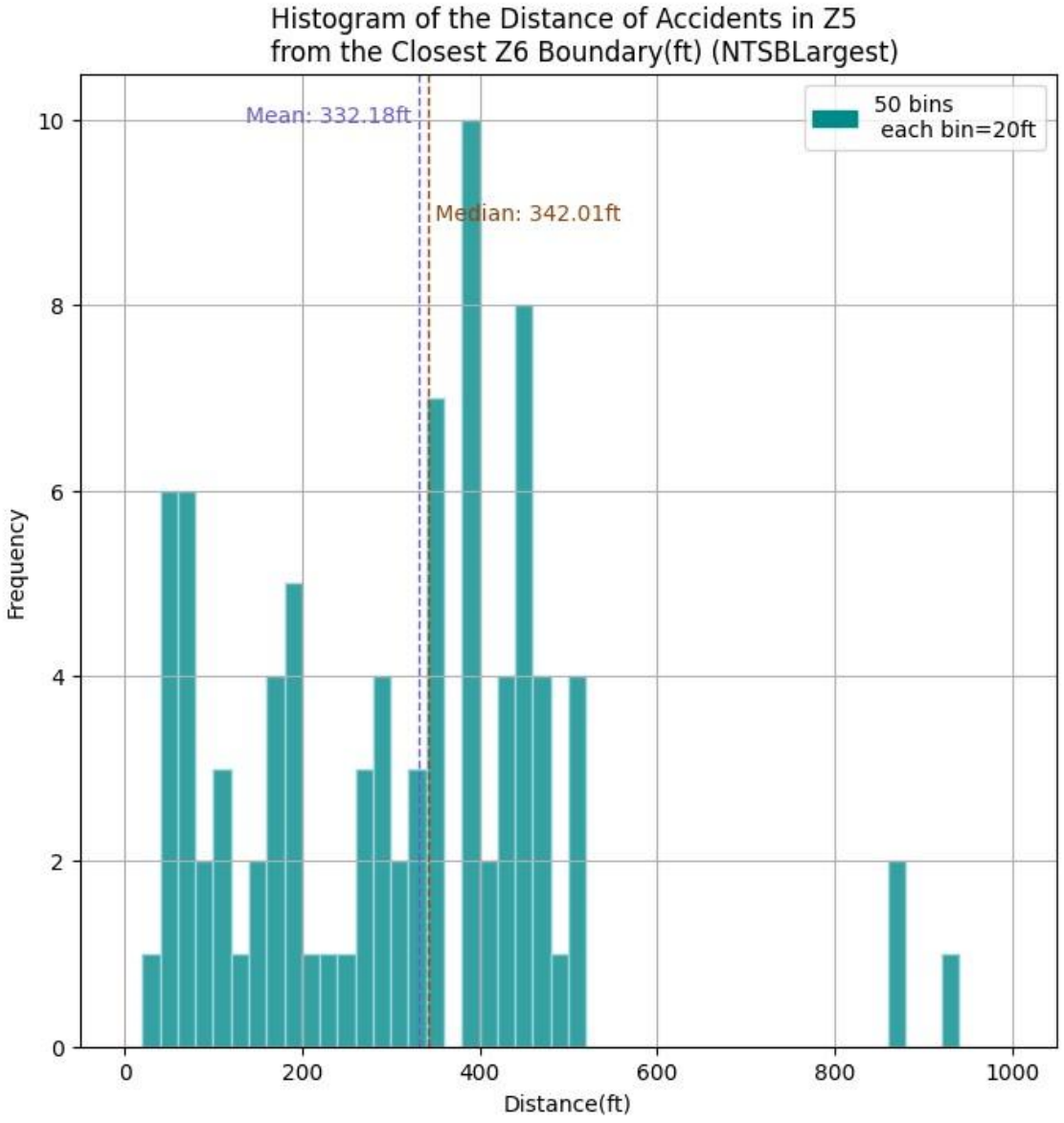


Figure 11. Histogram of the Distance of Accidents in Z5 from the Closest Z6 Boundary(ft) (NTSB Largest)

In Figure 12, accidents recorded in the Spatial Accuracy dataset cluster in a two-peak pattern. The first peak with 4-5 times frequency bin falls between 40 and 60 ft. This distance range appears to be particularly prone to accidents, indicating a critical area for safety measures. The second peak in the histogram occurs between 440 and 460 ft from the Z6 boundary. This suggests that there is another significant cluster of accidents at this distance, indicating a secondary high hazard zone. The consistent presence of this peak across different datasets (Figure 10 and Figure 11) implies that specific conditions or factors contribute to accidents in this range, highlighting the need for targeted safety interventions to address the risks associated with this peak distance interval from the Z6 boundary.

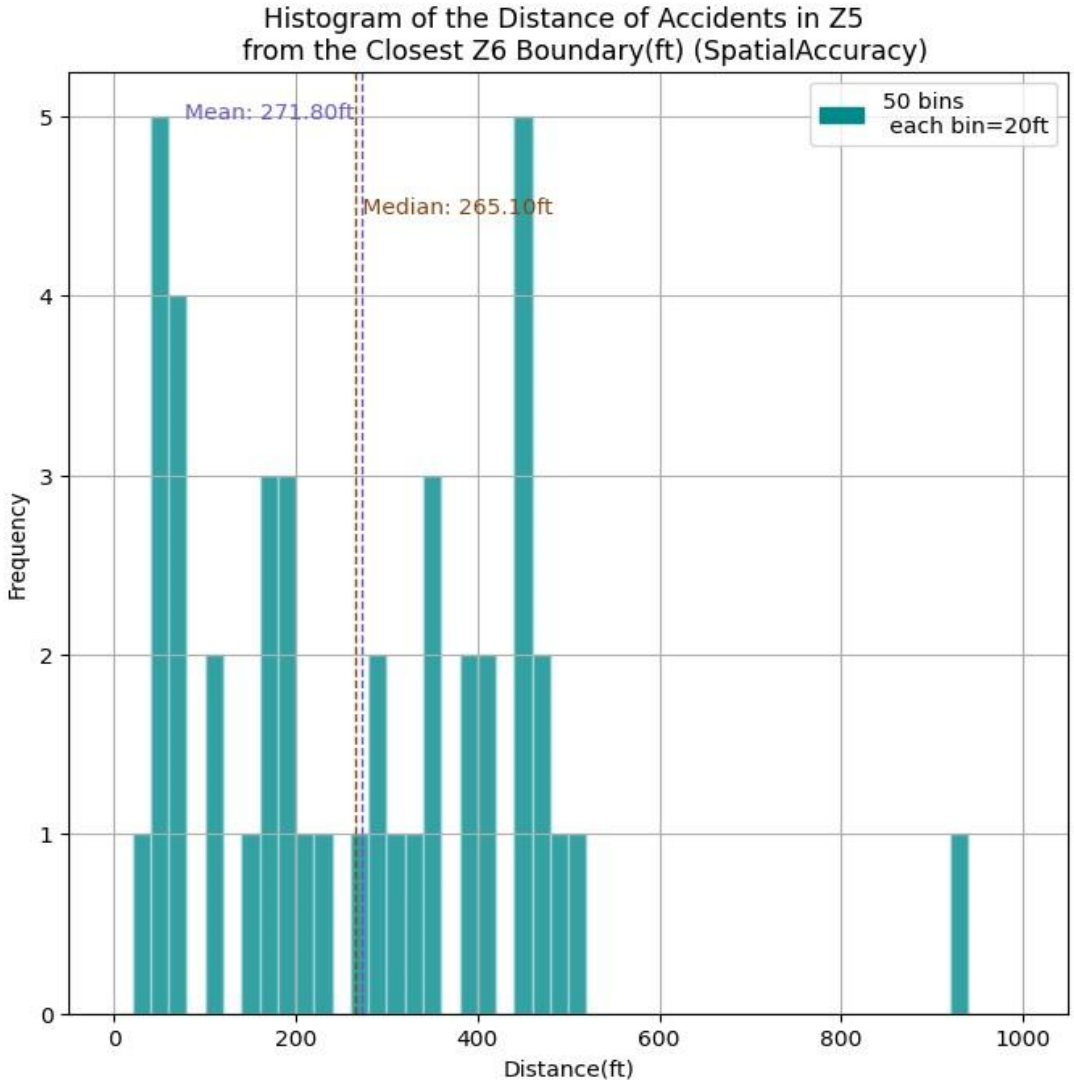


Figure 12. Histogram of the Distance of Accidents in Z5 from the Closest Z6 Boundary(ft) (Spatial Accuracy)

In Figure 13, each bin represents 200 ft in this dataset. We observe a broad spread of accidents, but an outlier is noted between 800 and 1000 ft from the Z5 boundary. Although the mean is much higher, this peak suggests a localized higher hazard close to this specific distance. Since this histogram displays an exponential distribution shape, a fitted curve in blue color is provided in Figure 13. The fitted exponential curve (blue line) closely matches the pattern of the histogram. The probability density function (PDF) for the exponential distribution is given by $f(x|\lambda) = \lambda_e^{-\lambda x}$, where λ is the rate parameter. The curve demonstrates this rapid decay, supporting the exponential nature of the data. Also, the mean distance (1854.12 ft) is higher than the median distance (1003.33 ft), which serves as another indication of a right-skewed distribution typical of an exponential distribution. This difference arises because exponential distributions have a long tail towards higher values. In this case, it suggests that accidents are more likely to occur closer to the Z5 boundary, with the likelihood of accidents decreasing as the distance increases.

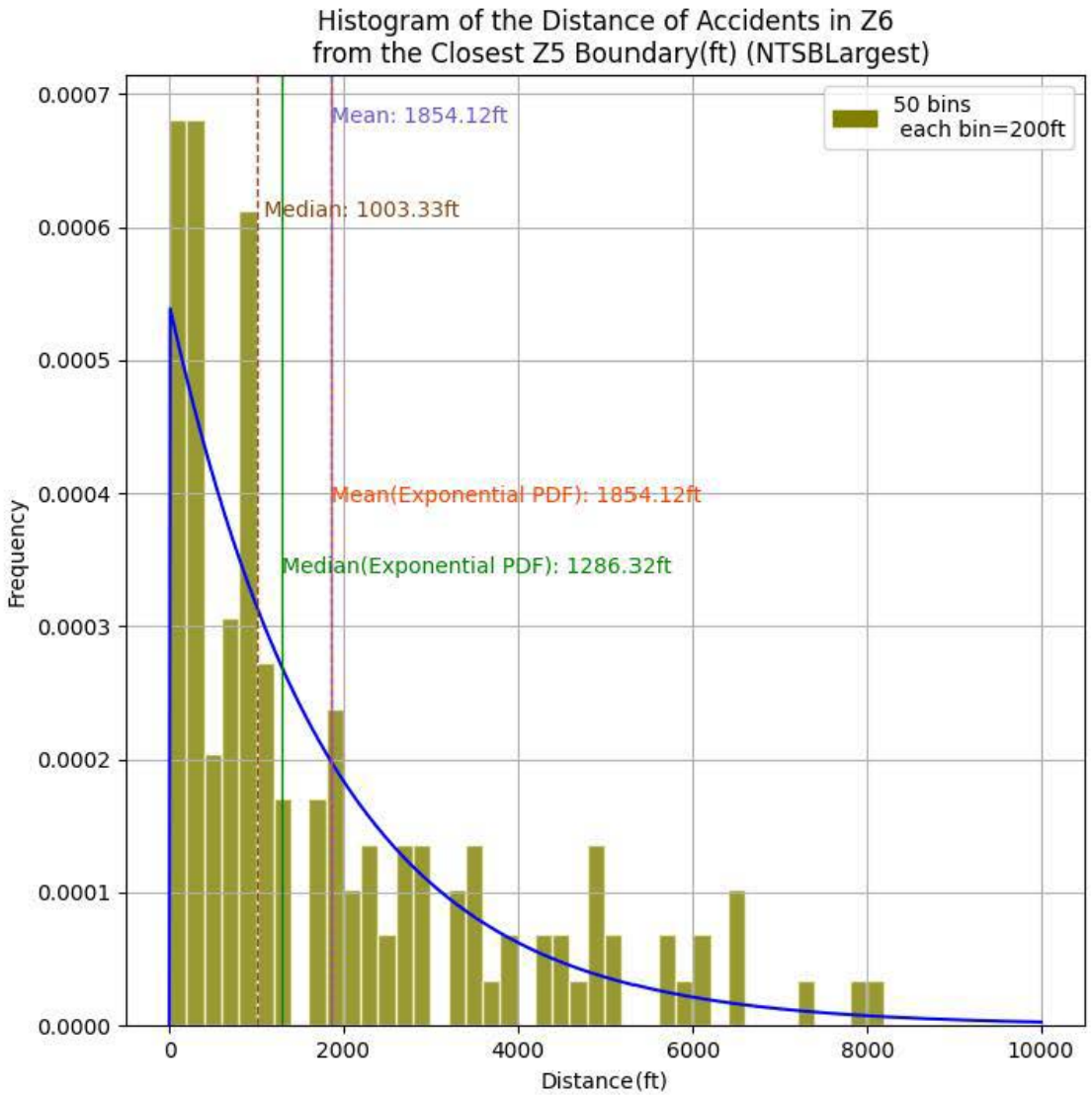


Figure 13. Histogram of the Distance of Accidents in Z6 from the Closest Z5 Boundary(ft) (NTSBLargest)

In Figure 14, the bin size of each bin represents 200 ft in this dataset. The highest frequency bin in this histogram occurs between 200-400 ft, and between 800 and 1000 ft from the Z5 boundary. This indicates a notable concentration of accidents at these ranges, highlighting them as a key area for potential safety interventions. This histogram displays a log-normal distribution, and a fitted curve in blue is provided. The fitted log-normal distribution curve (blue line) matches the pattern of the histogram. The probability density function (PDF) for the log-normal distribution is given by $f(x|\square)=\frac{1}{x\sigma\sqrt{2\pi}}exp\left(-\frac{(lnln\,x-\mu)^2}{2\sigma^2}\right)$, if the natural logarithm of X is normally distributed with mean μ and variance σ. The curve demonstrates this rapid increasing and skewness, supporting the log-normal nature of the data.

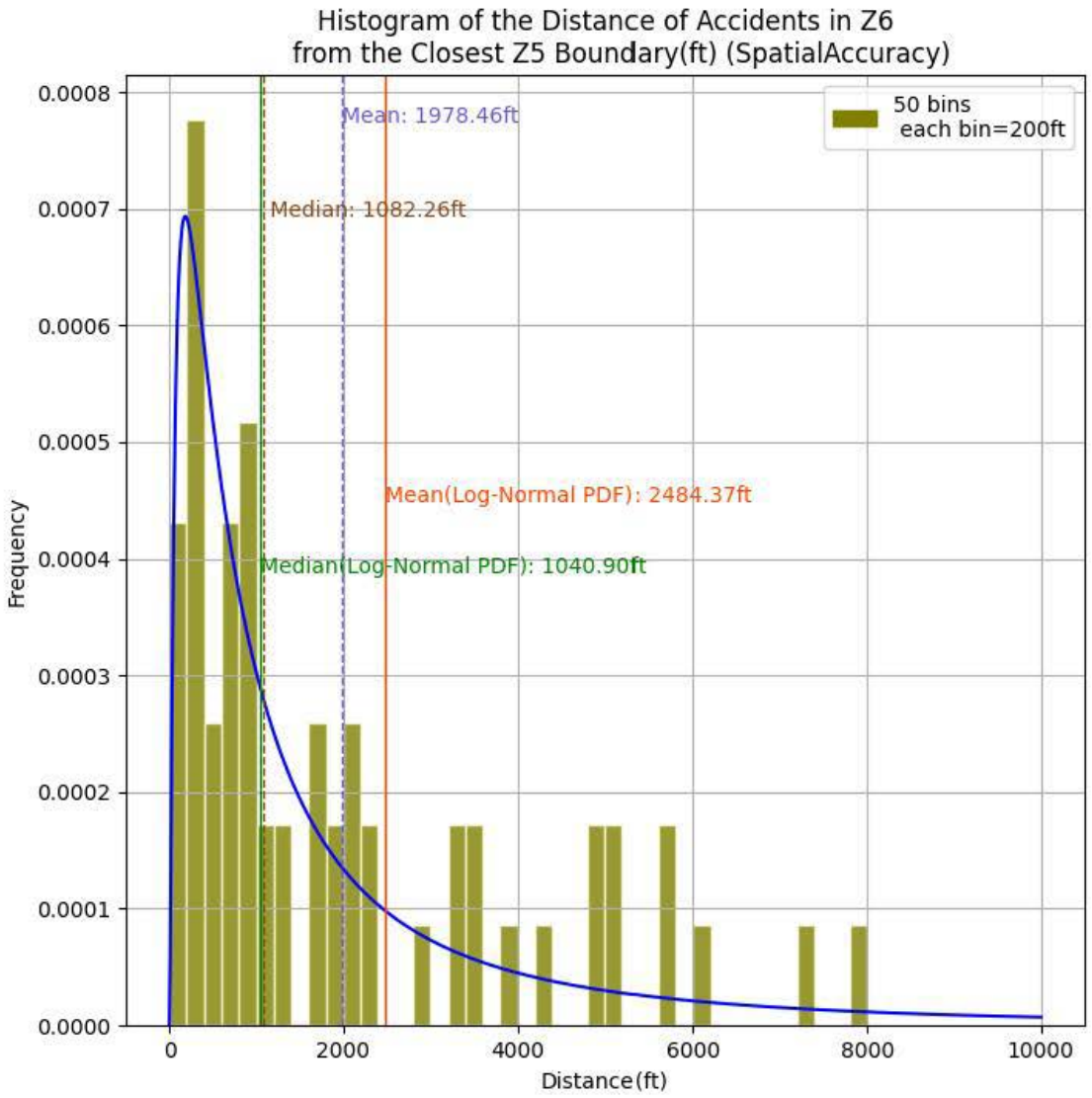


Figure 14. Histogram of the Distance of Accidents in Z6 from the Closest Z5 Boundary(ft) (Spatial Accuracy)

In section 4.2.2, the histograms provide a clear and quantifiable illustration of accident frequencies relative to various safety zone boundaries, using statistical measures to highlight prevalent accident locations and the spread of data across different distances. For instance, notable peaks within specific proximity ranges reveal critical hotspots for accidents, varying slightly between datasets (NTSBLargest and Spatial Accuracy). If any new safety restrictions are to be applied to Z5 boundary with PS, it can take into consideration this clustering of accidents within the first 120-140 ft. Similarly, any new safety restrictions or re-dimensioning of

Z5 and Z6 can take into consideration this optimal distance of 800-1000 ft of Z5 encroachment into Z6. By emphasizing the most common accident distances and examining variations in accident data accuracy, this section provides valuable insights for enhancing safety measures at airport boundaries.

4.2.3 Spatial Analysis Results: Kernel Density Estimation (KDE) Plots

The plots use Kernel Density Estimation (KDE) to estimate the probability density function of the accident distance data. This method helps in identifying the concentration of accidents in relation to zone boundaries, illustrating areas of high accident density and potential hotspots. (Figures 15-17). The KDE plots provide a visual representation of accident density over a range of distances, highlighting spatial frequencies of accidents. The isolines help in visualizing the gradient of accident concentration from zone boundaries. North arrow is labeled on each KDE plot to interpret the cardinal direction of the accident density relative to the nearest safety zone boundary.

Figure 15 visualizes the density of accidents in Z5 relative to the closest PS boundary using the NTSB Spatial Accuracy dataset. The most intense accident concentration appears Northeast and overall North of the boundary, within approximately 200 ft, highlighting a key area for potential safety enhancements.

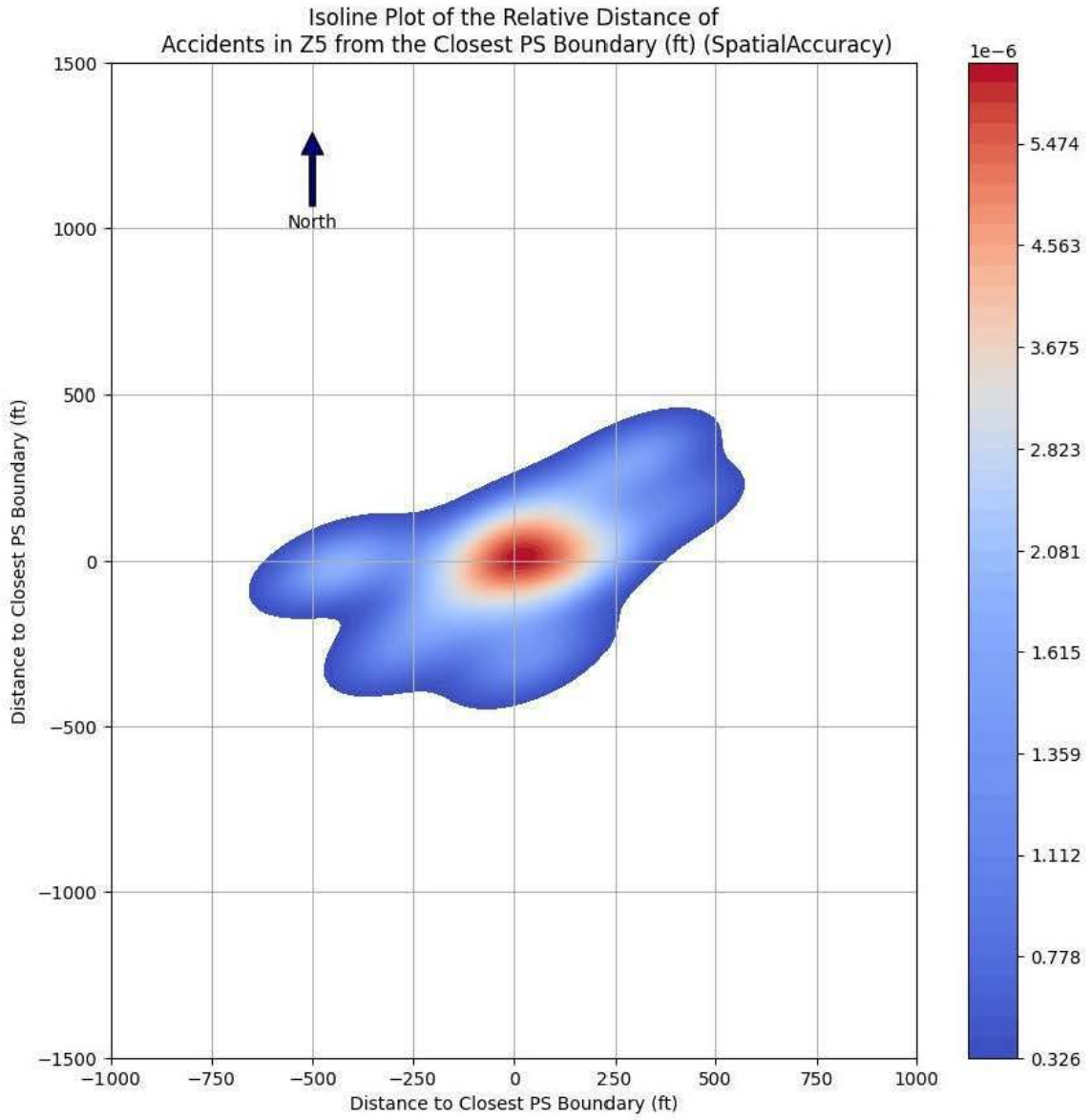


Figure 15. KDE Isoline Plot of the Relative Distance of Accidents in Z5 from the Closest PS Boundary (ft) (Spatial Accuracy)

In Figure 16, the KDE plot shows that the highest density of accidents in Z5 boundary is close to the Z6 boundary. However, this density is spread out, with a clear northward tendency. This means that while accidents are most frequent near the boundary, there is noticeable concentration indicating higher accident occurrence potential in the Northeastern border of Z6 and Z5.

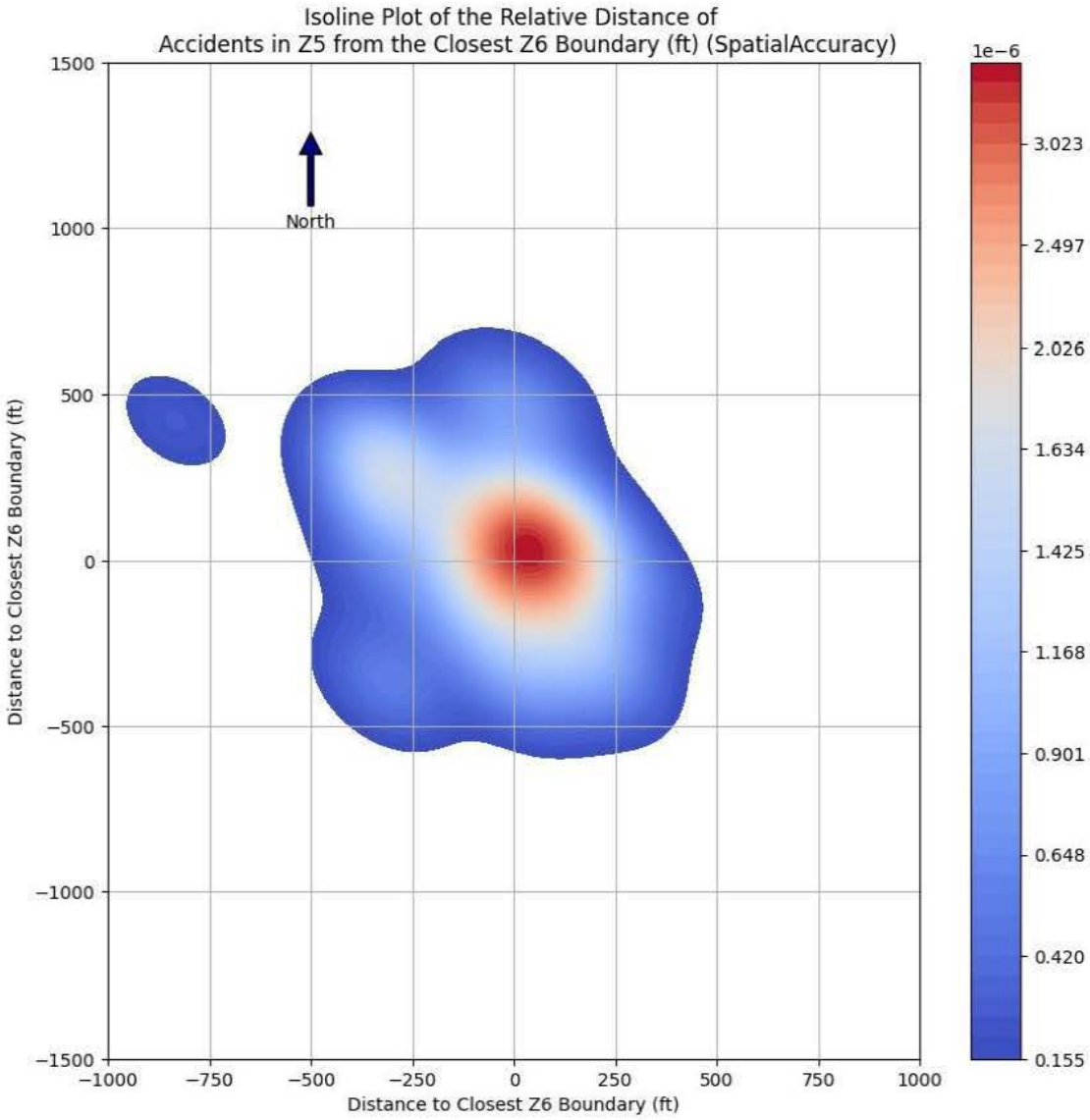


Figure 16. KDE Isoline Plot of the Relative Distance of Accidents in Z5 from the Closest Z6 Boundary (ft) (Spatial Accuracy)

Using the Spatial Accuracy dataset, Figure 17 shows that accidents within Z6 have high density near the Z5 boundary which is clearly skewed to the North. The concentration is highest within about 2500 ft of the boundary, indicating a critical area for accident occurrences and safety focus.

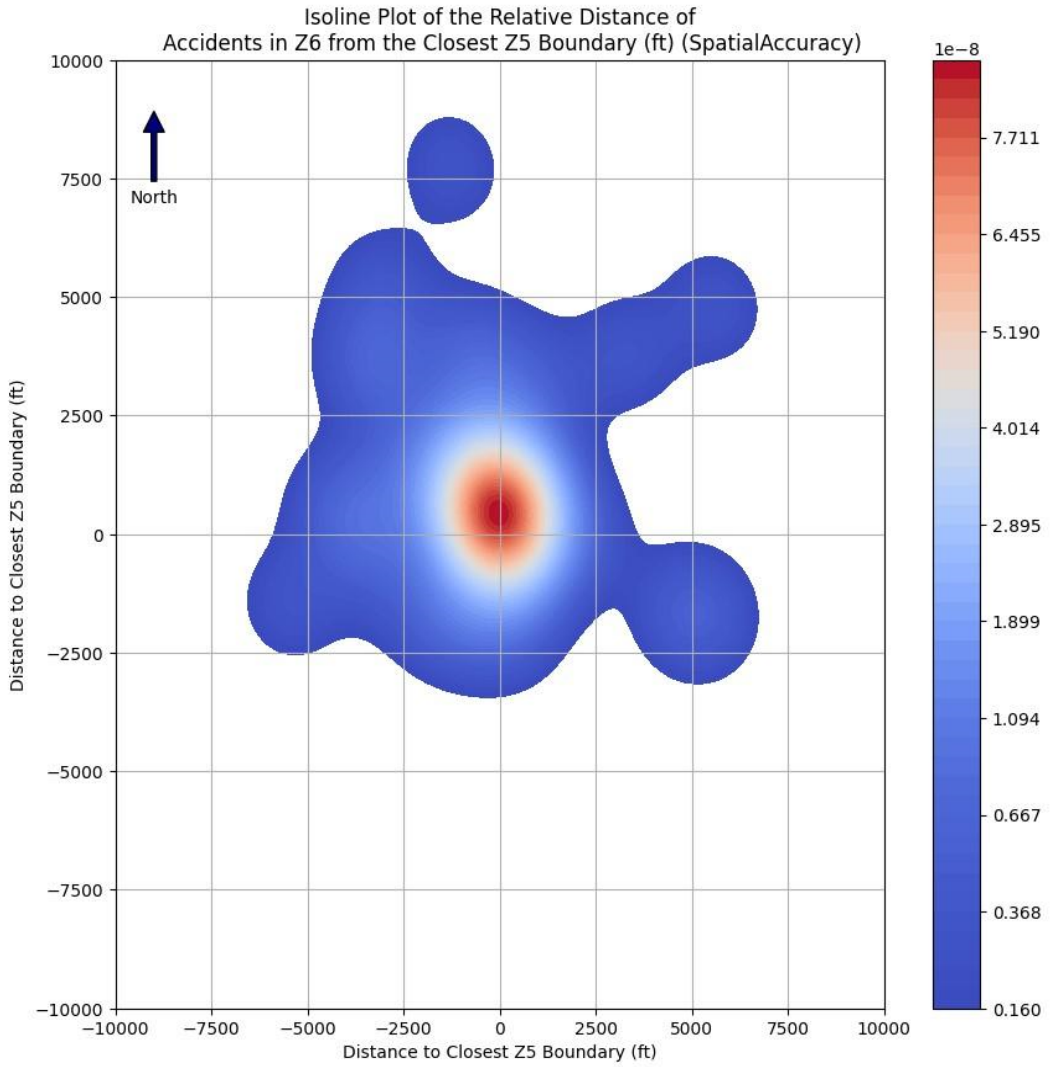


Figure 17. KDE Isoline Plot of the Relative Distance of Accidents in Z6 from the Closest Z5 Boundary (ft) (Spatial Accuracy)

Section 4.2.3 leverages Kernel Density Estimation (KDE) plots to effectively map the distribution of accidents relative to safety zone boundaries, providing a detailed visual representation of accident density across various distances. Figures 15 through 17 underscore areas of heightened accident occurrence, identifying specific high-hazard zones near boundaries. The plots reveal significant patterns, such as the higher accident intensity (1) North of the PS boundary for accidents in Z5, and (2) North/Northeast of Z6 boundary for accidents in Z5; and (3) North of Z5 boundary for accident in Z6, highlighting specific areas requiring targeted safety analysis at the airport level. These cardinal directions can help Airport Land Use Commissioners further assess how the dimensioning of their safety zones can better adapt their airports taking into consideration the orientation of their specific runways. This detailed KDE analysis and accidents cardinal trends is not relevant for the generic safety zones dimensions since they are by default agnostic to geographic particularities of airports (i.e. runway orientations).

4.2.4 Spatial Analysis Results: Accident Locations in Overlaid Safety Zone Polygons

In this analysis, we overlay accident points on normalized and aligned polygon shapes representing safety zones at 259 airports to study the distribution of events within defined safety zones. The following steps were undertaken to achieve this:

1. **Normalization of Polygons:** Each polygon was scaled to a unit diagonal length to ensure uniformity.
2. **Alignment:** Polygons were rotated to align their longer edges pointing to the top of the page.
3. **Transformation of Points:** Accident points were transformed to retain their relative positions within their associated polygons, following the normalization and alignment transformations.
4. **Spatial visualization:** The transformed points are drawn on the transformed polygon and have the original spatial relationship with the airport polygon to which they belong to present the distribution of accidents in the safety zone.

Figures 18-21 present accident visualizations for Safety Z5 and Safety Z6, for two datasets: (1) the NTSB Largest dataset and (2) the Spatial Accuracy dataset. It should be noted that the horizontal and vertical coordinate values in Figures 18-21 do not represent any unit distance or length but are only used as a reference to facilitate positioning in discussion.

In Figure 18, we visualize the transformed accident points overlaid on the normalized and aligned polygons for Safety Z5. The transformed points (in red) are distributed across the safety zone's normalized polygons (in light green). The polygons have been scaled to have a uniform size and rotated to align to the top. Many accidents are concentrated in the center of Z5, corresponding to the vicinity of the runway. The accident distribution shows a diagonal distribution trend from the third quadrant to the first quadrant.

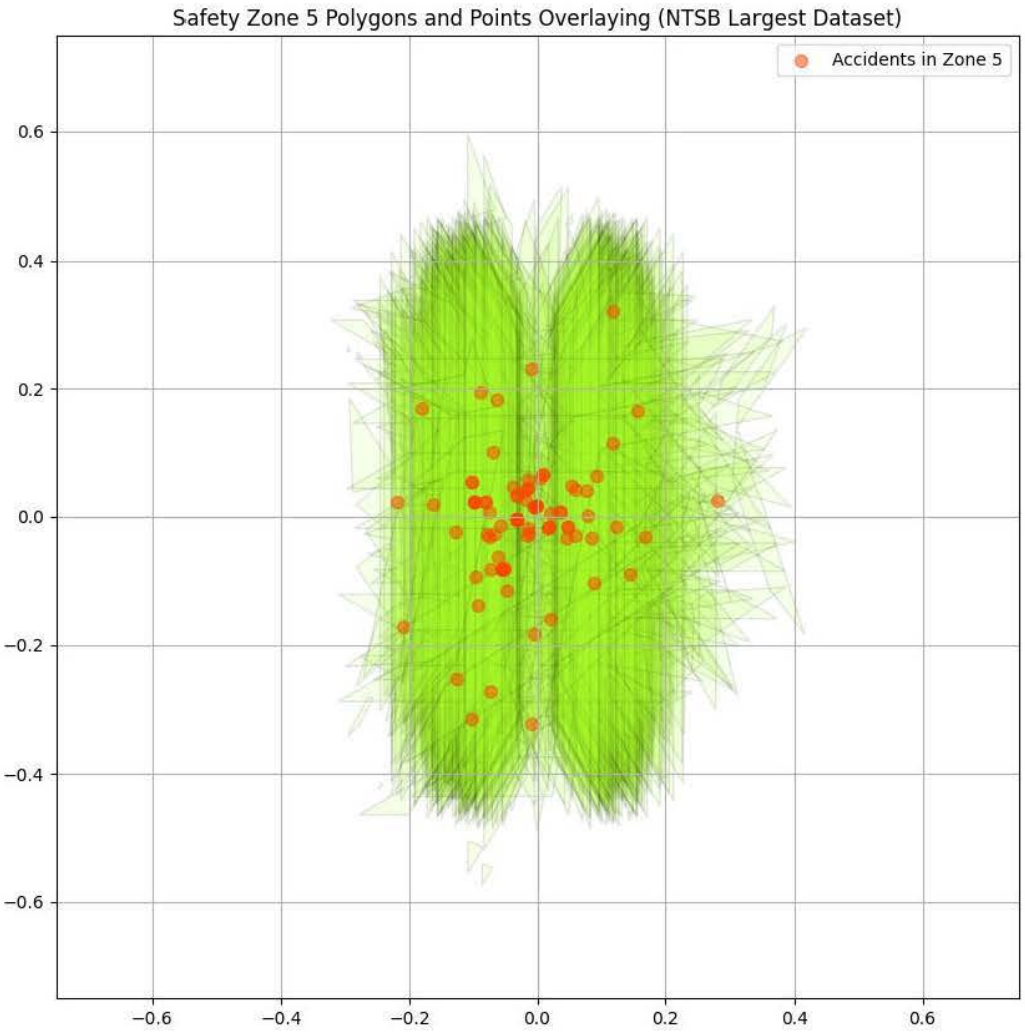


Figure 18. Overlay of Accidents in Z5 Using the NTSB Largest Dataset

Similar to Figure 18, Figure 19 shows the distribution of transformed accident points (in purple) within the normalized and aligned polygons (in peach puff) of Safety Z5. The spatial accuracy dataset provides a more precise representation of the accident locations. Also, most accidents are concentrated in the center of Z5, but there are slightly more accidents above than

below.

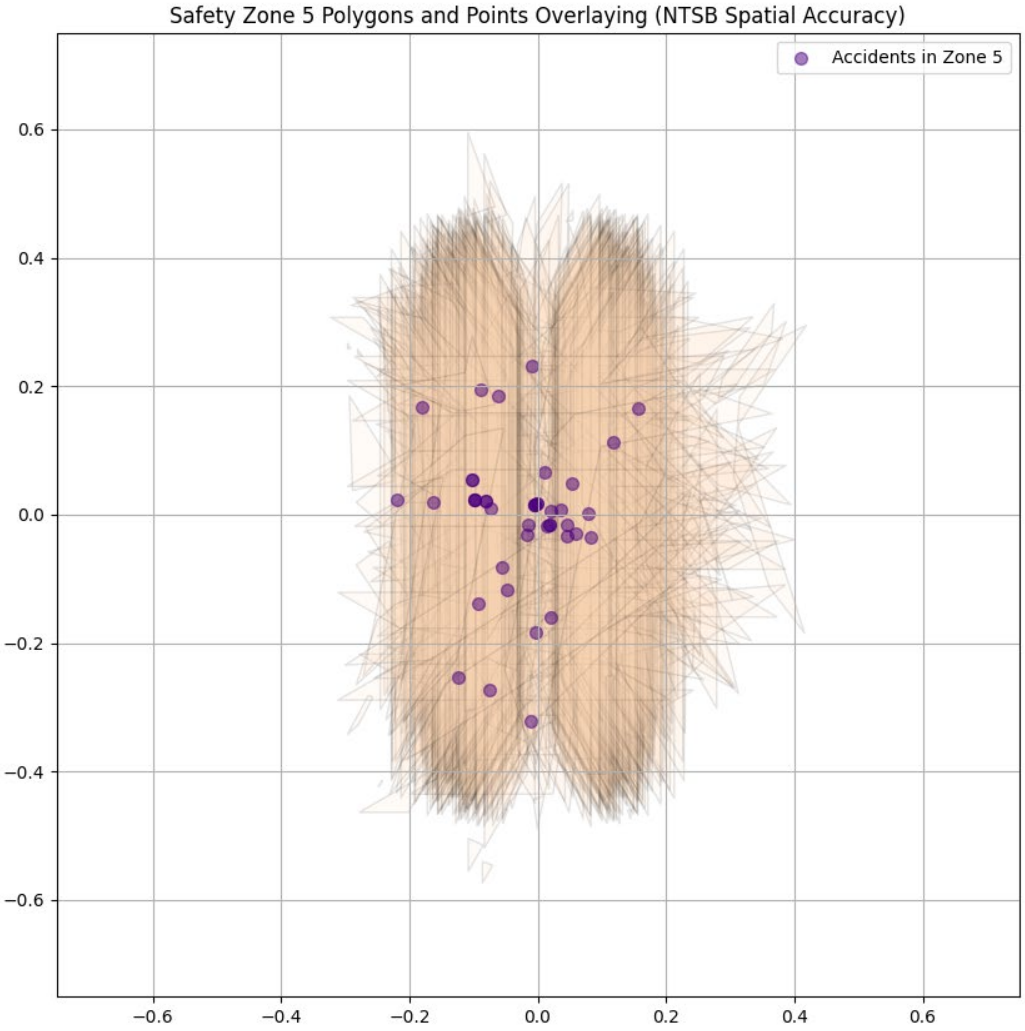


Figure 19. Overlay of Accidents in Z5 Using the Spatial Accuracy Dataset

Figure 20 presents the transformed accident points overlaid on the normalized and aligned polygons for Safety Zone 6. The transformed accident points (in red) are overlaid on the standardized polygons (in light green) for Safety Zone 6. This visualization helps in understanding the spread and concentration of accidents within the normalized safety zone. This image shows that the accident distribution at the polygon edge of Zone 6 shows a relatively clustering trend, especially the outer edge of the third quadrant. In further analysis of the safe zone, this location needs to be focused on.

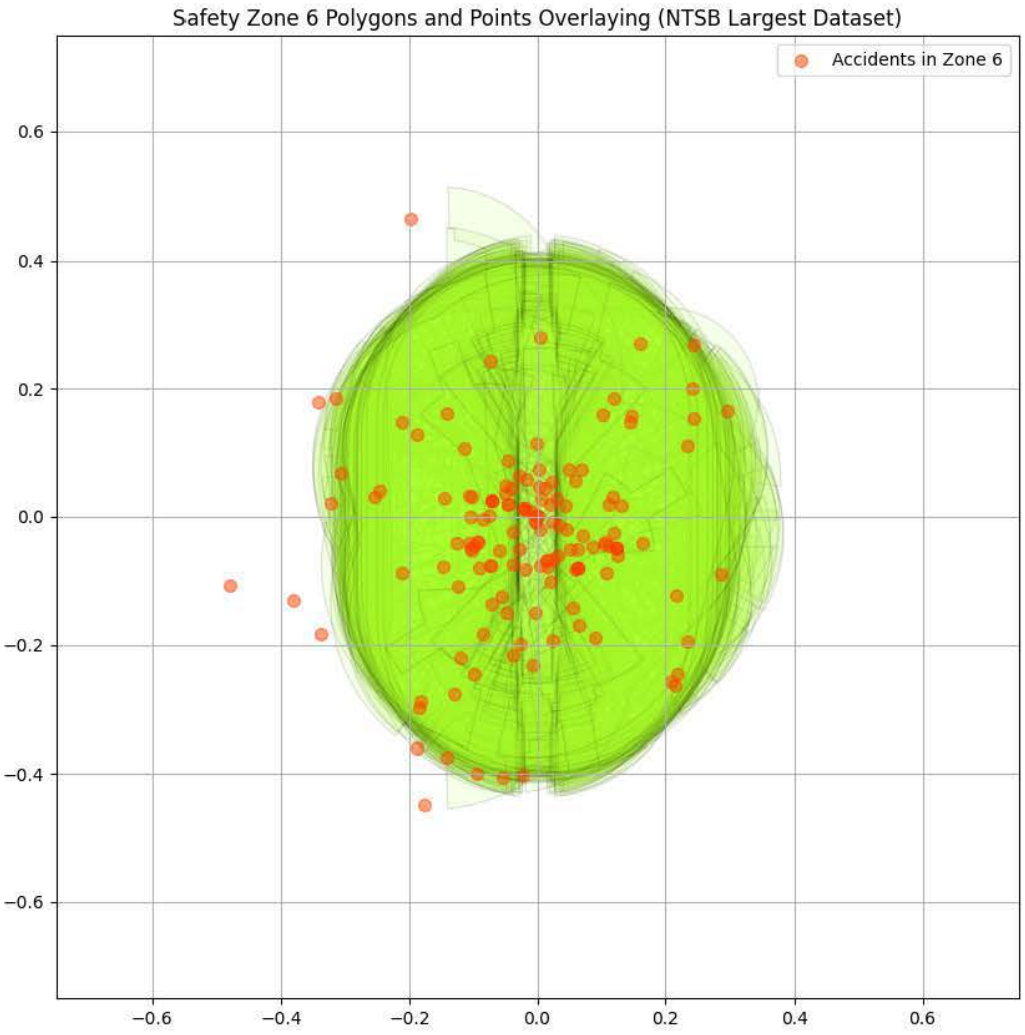


Figure 20. Overlay of Accidents in Zone 6 Using the NTSBLargest Dataset

Figure 21 visualizes the transformed accident points overlaid on the normalized and aligned polygons for Safety Zone 6, using the spatial accuracy dataset. In this visualization, the accident points (in purple) are shown within the normalized polygons (in peach puff) for Safety Zone 6. The spatial accuracy dataset again provides a detailed view of the accident distribution relative to the standardized polygon shapes. The accident locations in Zone 6 present a diagonal distribution from the third quadrant to the first quadrant in this data set, with the center of Zone 6 being concentrated.

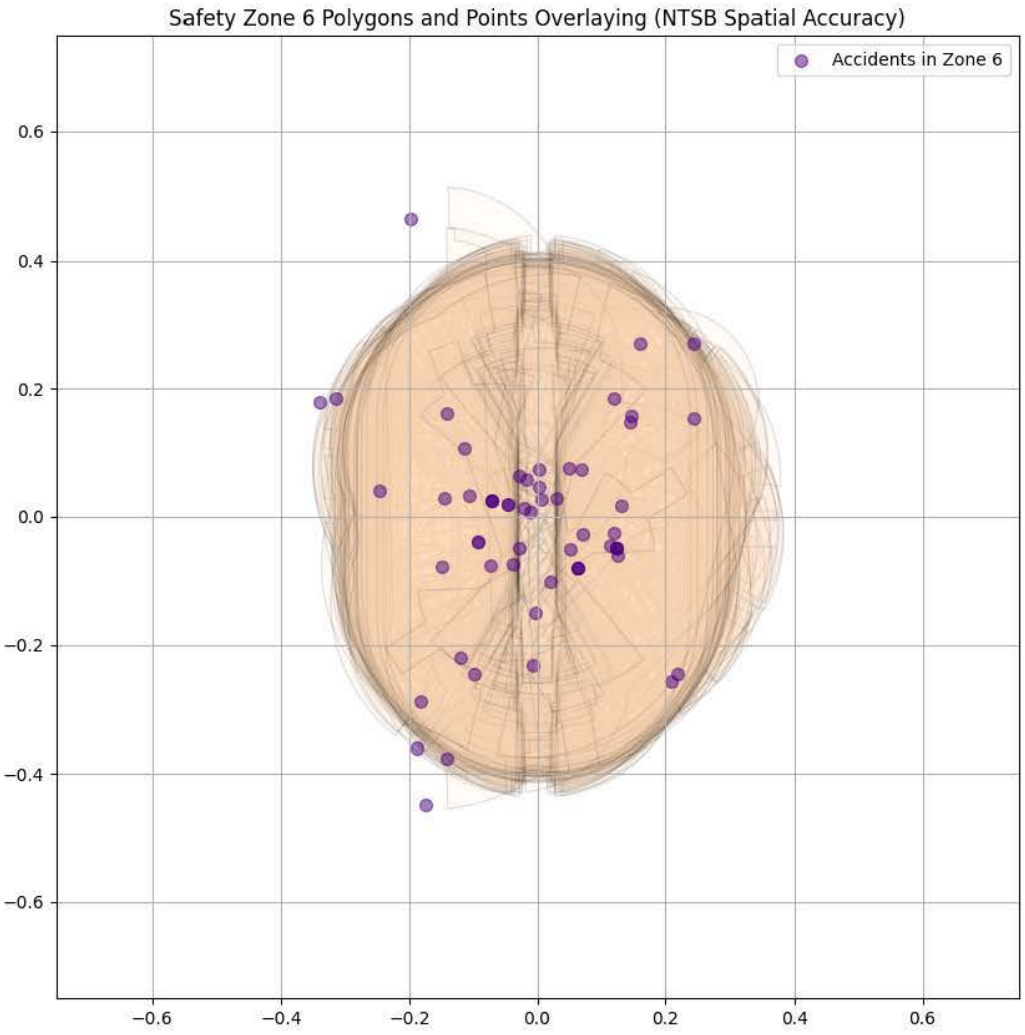


Figure 21. Overlay of Accidents in Zone 6 Using the Spatial Accuracy Dataset

These visualizations offer a comprehensive view of how accidents are distributed within the safety zones, providing insights into patterns and potential areas of concern. However, since the dataset used in the mapping process is ‘Exclusive Polygons’, the shapes of the polygons are not exactly consistent. It is necessary to consider exclusive polygons for the safety zones in the attribution of the accident location otherwise the same accident would be counted multiple times for when the safety zones overlap. Furthermore, the exclusive polygon rule, based on the former ALUP Handbooks, is required to develop land use restrictions that are unique to each

zone, giving prevalence to the most stringent regulations (i.e. if Z1 overlaps with Z5; the land use restrictions of Z1 override those of Z5 to abide to the precautionary rule of safety procedures). It can be noticed that there are still a considerable number of irregular shapes overlapped in Figure 18 as outliers. In subsequent work, it would be interesting to explore 'Non-Exclusive' original safe zone polygons in data visualizations.

4.2.5 Spatial Analysis Results: Interactive Plots of Accident Distribution in HTML

In the last task, Interactive Plots with pop-up windows for each accident-safety zone pair are provided in HTML webpages (Figure 22), offering a dynamic way to explore detailed accident data and insights on an HTML page preview. In the future, analysts and planners can check the basic data of each accident point on the relative distance plot. This function provides a deeper dive into specific accidents and their characteristics.

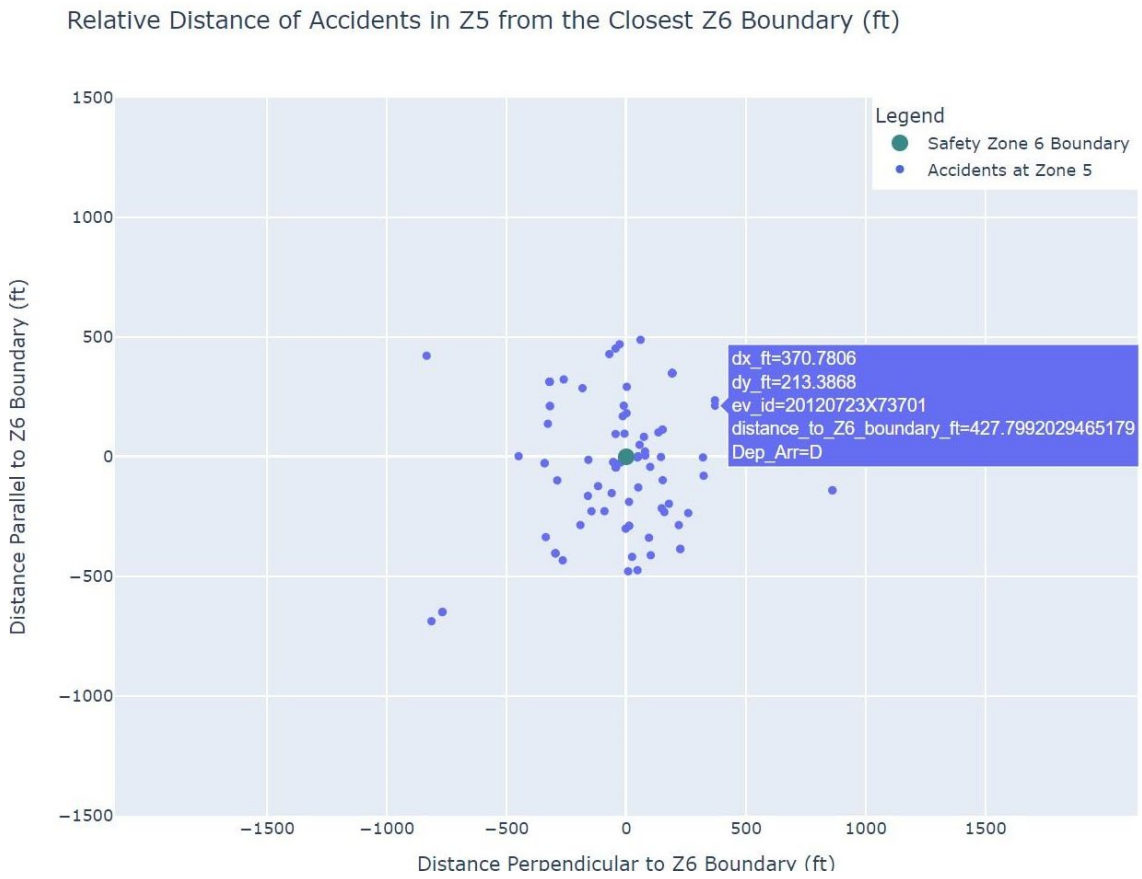


Figure 22. Interactive Plots with Pop-up Windows HTML Page Preview

The analysis across all figures illustrates a notable variance in accident distances relative to different phases of flight and datasets. The use of multiple visualization methods enriches our understanding of the spatial dynamics at play, underlining the importance of zone-specific safety strategies. Additionally, the inclusion of both KDE and histogram plots provides both a macro and micro view of the accident data, highlighting prevalent trends and outlier data points.

5. Conclusions

The findings confirm a noticeable clustering of accidents near the shared boundary of

Zones 5 and 6, suggesting that these areas might benefit from an expansion of Zone 5 into Zone 6 to adequately reflect the heightened risk landscape. This recommendation is supported by the increased accident density and severity within these zones, particularly Zone 5, which shows a significant deviation from expected patterns based on previous safety criteria. The spatial accuracy and relevance of the data allowed for a robust analysis, confirming the need for adjusted safety zone dimensions and enhanced land use compatibility policies.

Moreover, the study emphasizes the necessity of ongoing adjustments to airport safety zones as part of a dynamic process that accommodates new data and evolving risk factors. It highlights the critical role of GIS and advanced spatial analysis in understanding complex patterns and making informed decisions to enhance airport safety effectively. It also highlights some limitations to generic safety zones dimensions that are by design agnostic to geographical specificities of airports and their surroundings. The relevance of this work comes from the aggregation of a rich set of data that allows for the identification of overarching patterns otherwise inaccessible to the assessment of accident patterns in individual airports due to the small number of accidents at that scale. This approach not only aids in immediate risk mitigation but also contributes to the broader field of transportation safety, offering a replicable model for similar assessments at airports globally.

In conclusion, this study underscores the importance of continuous monitoring and data-driven policy-making in airport safety management. The recommendations for modifying safety zone boundaries and policies are geared towards reducing the risk of accidents and enhancing the overall safety of airport vicinities, aligning with the goals of Caltrans and the aviation community at large. The integration of cutting-edge spatial analysis tools with comprehensive accident data sets the stage for future developments in the field, paving the way for more resilient and adaptive safety strategies in airport design and operation.

Appendix 1: Safety Zones Accident Statistics

Background on Safety Zones 5 and 6 risk assessment from Task 8 “Safety Zones & Land Use Compatibility Revision”, UC Berkeley December 2023

Safety Zone 5 “Sideline Zone”: Risk increases from Low to Very High, with consistently very high hazard and exposure levels through all NTSB accident datasets for accident density and hazard score. The increase in accident percentages compared to the 2000-2009 assessment ranges between 19-22% (Caltrans, 2011). Safety Zone 5 is mostly located inside airport boundaries (73.91%) and presents stricter land use compatibility criteria, similar to Zone 1, however the land use development levels are high both inside and outside airport boundaries. It is likely that field validation of LULC of this zone points to impervious surface areas (parking lots, roads, and other pavement, which corresponds to Open Space Development class), but there are relatively high percentages of low, medium, and high intensity development for Zone 5 compared to other stricter zones (1 and 2) which points to a high potential exposure in case of accidents.

Safety Zone 6 “Traffic Pattern Zone”: Risk levels increase from Low to Medium-Low. Based on the Simple Accident Risk analysis both hazard and exposure levels remain low, however when applying the Weighted Accident Risk analysis, the hazard levels increase from Low to Very High. This is due to the discrepant number of accidents with the highest injury level (fatal). Between 2008-2022 a total of 28 out of 77 accidents in Zone 6 resulted in at least one fatality, while other Safety Zones have registered between 3 and 6 fatalities total. This is probably due to the larger size area that encompasses a higher number of accidents and development translating to higher exposure. Zone 6 presents a low accident density, however there was an increase of 7-13% of accidents in this zone when compared to the 2000-2009 assessment (Caltrans, 2011). These accidents are mostly located outside airport boundaries (94.64%) and are subject to the least restrictive land use compatibility policies, presenting the highest % of urban change (normalized by the total urban change of all Safety Zones, of the 2 mi buffer zone, and California). The discrepancy of Safety Zone 6 exposure can again be explained mostly due to its size in comparison with other Safety Zones. Following the general spatial patterns that concentrate accidents the closer you are to the runway lines, it is likely that the increase of accidents in Zone 6 is closer to the boundaries of Zone 5. An overall revision of accident spatial patterns within Zone 6 is suggested to optimize the need for increasing Zone 5

dimensions, which shares most of its boundary with Zone 6, especially given the increase in accident percentage in Zone 6 compared to the 2011 Handbook assessment. An overall revision of land use compatibility policies is recommended for increasing restrictions near Zones 5 and 2 or transferring some areas of Zone 6 to Zones 5 and 2.

Table A1. Overview of Accident Datasets Used in the Spatial Distribution Analysis of Z5 & Z6

	NTSB Spatial Largest Dataset		**NTSB Spatial Accuracy Dataset**	
	# of accidents	# of airports	# of accidents	# of airports
PS	496	157	135	74
Z5	91	49	43	29
Z6	147	88	58	43
Total	1,360	190	466	128[32]

Table A2. Safety Zones Adjacency. The "x"s correspond to existing adjacent polygon boundaries. Highlighted "**x**" s refer to the safety zones of interest as the majority of this study, which are Z5, PS and Z6.

	PS	Z1	Z2	Z3	Z4	**Z5**	**Z6**
PS	-	x	x			**x**	
Z1	x	-	x	x			
Z2	x	x	-	x	x	x	x
Z3		x	x	-		x	x
Z4			x		-		x
Z5	**x**		x	x		-	**x**
Z6			x	x	x	**x**	-

[32] The total number of airports with accident occurrence for each NTSB dataset corresponds to the spatial overlay of accidents and the 2-mile buffer of each airport's boundary.

References

California Department of Transportation (Caltrans) (1983). “Airport Land Use Planning Handbook - A Reference Guide for Local Agencies”.

California Department of Transportation (Caltrans) (1993). “Airport Land Use Planning Handbook”.

California Department of Transportation (Caltrans) (2002). “California Airport Land Use Planning Handbook”. https://www.placer.ca.gov/DocumentCenter/View/8266/Caltrans-2002-California-Airport-Land-Use-Planning-Handbook-PDF

California Department of Transportation (CalTrans) (2011). “California Airport Land Use Planning Handbook”. https://dot.ca.gov/media/dot-media/programs/aeronautics/documents/californiaairportlanduseplanninghandb ook-a11y.pdf

Silverman, B.W. (1986). “Density Estimation for Statistics and Data Analysis”. London: Chapman & Hall/CRC. p. 45. ISBN 978-0-412-24620-3. https://archive.org/details/densityestimatio00silv_0/page/44/mode/2up